The Institute of Paper Chemistry

Appleton, Wisconsin

Doctor's Dissertation

An Investigation of the Vibrational Spectra of the Inositols

Robert Mason Williams

June, 1977

AN INVESTIGATION OF THE VIBRATIONAL SPECTRA OF THE INOSITOLS

A thesis submitted by

Robert Mason Williams

B.A. (Chem.) 1969, Western Washington State College

M.S. (Chem.) 1971, Western Washington State College

M.S. 1973, Lawrence University

in partial fulfillment of the requirements
of The Institute of Paper Chemistry
for the degree of Doctor of Philosophy
from Lawrence University,
Appleton, Wisconsin

June, 1977

TABLE OF CONTENTS

SUMMARY

The vibrational spectra of seven of the inositol isomers were investigated and interpreted based on comprehensive normal coordinate analyses. The inositols investigated included: scyllo-inositol, neo-inositol, myo-inositol, epi-inositol, cis-inositol, L-chiro-inositol, and muco-inositol. The room temperature and liquid nitrogen temperature Raman and infrared spectra of crystalline samples of the seven inositol isomers were recorded. In addition, the room temperature Raman and infrared spectra were recorded for the oxygen deuterated analogues of scyllo-inositol, neo-inositol, myo-inositol, and epi-inositol.

In conjunction with the normal coordinate calculations, a 33-parameter modified valence force field was developed. The force field was optimized for the inositols by refinement of the force constants using the Fletcher-Powell non-linear least-squares algorithm which minimized the least-squares differences between the calculated frequencies and the assigned experimentally observed frequencies. Six molecules, scyllo-inositol, neo-inositol, myo-inositol, epi-inositol, deuterated scyllo-inositol, and deuterated neo-inositol, were included in the force constant refinements. The observed frequencies for these inositols were assigned utilizing their molecular symmetry. For these six inositols, the final force field reproduced the assigned observed frequencies with an overall average error of 10.4 cm^{-1} for two hundred thirty-four assigned frequencies. The good reproduction reflected a sensitivity of the theoretical model to conformational variation and oxygen deuterium substitution. The calculated potential energy distributions showed a majority of the vibrations to be composed of complex atomic motions with extensive coupling of all the different types of motions which occur below 1500 cm^{-1}.

A group of temperature sensitive bands observed in the 750-300 cm^{-1} region of the inositol spectra were interpreted as modes involving the deformations of the hydrogen bonded hydroxyl hydrogens. These bands were not assigned and could

only be reproduced by inclusion of intermolecular potentials in the molecular model.

The validity of the force field was further established by the successful prediction of the vibrational frequencies for cis-inositol, L-chiro-inositol, and muco-inositol, which had not been included in the force constant refinements. The average errors were only slightly higher than those obtained for the other inositols.

An assessment of the degree to which second-order potential effects, such as intermolecular interactions and anharmonic terms in the potential energy, perturb the observed vibrational frequencies was made by an analysis of the factors which could contribute to the errors between the assigned observed and calculated frequencies. The analysis showed that second-order potential effects are the major contributors to the average errors. From the magnitude of the errors it was concluded that, in general, the observed frequencies are perturbed to a relatively minor degree. The results of the analysis also further established the validity of the assumptions made in the theoretical model.

The effects on the Raman solution spectra of several inositols of Group II metal cation complex formation and borate formation were also investigated. Metal ion complex formation, when accompanied by no change in the ligand geometry, resulted in only minor spectral changes, whereas when complex formation occurred with an attendant change in the ligand geometry substantial changes were observed, which were attributed primarily to the structural changes. Reaction between several inositols and borate anions to form tridentate inositol borates resulted in major perturbations of the inositol and borate ion frequencies.

The inositol force field was used to calculate the contribution of vibrational energy to the conformational energy of the inositols. The vibrational

energies were calculated for the preferred and alternate conformations of the inositols and were compared with the conformational energies calculated using nonbonded interaction energies. The difference in vibrational energy between the preferred and alternate conformations was found to contribute less than 1% to the difference in calculated conformational energies.

GENERAL INTRODUCTION

This thesis involves an investigation of the vibrational spectra of the inositols, a unique group of hexahydroxy cyclohexanes. The vibrational spectra were investigated and interpreted by comparing the experimentally observed Raman and infrared vibrational frequencies with theoretical frequencies and associated atomic motions calculated from normal coordinate analyses of models of the inositols.

The thesis is divided into five parts. Part I deals with the development of a thirty-three parameter force field applicable to the inositols. The final force field is presented and the experimental spectra of scyllo-inositol, neo-inositol, myo-inositol, epi-inositol, and oxygen deuterated scyllo-inositol and neo-inositol are compared with the calculated frequencies and interpreted using the calculated potential energy distributions. The application of group theory in the normal coordinate analyses to utilize the symmetry properties of the inositols is explained. Based on an analysis of the average errors, the degree to which second-order potential effects are perturbing the experimentally observed frequencies is estimated. The validity of the assumptions involved in the normal coordinate analyses are then evaluated.

Part II deals with the prediction of the vibrational frequencies for L-chiro-inositol, cis-inositol, and muco-inositol using the final inositol force field. The calculated frequencies are compared with experimentally observed frequencies and the spectra of the three inositols are interpreted.

Parts III and IV examine the observed spectra of several inositols and related compounds in aqueous solutions containing divalent metal cations and borate anions, respectively. The effect of metal cation complex formation and borate formation on the vibrational frequencies of the ligand molecules are investigated.

In Part V, the effect of vibrational energy on the conformational energy of the inositols is investigated.

PART I

AN INVESTIGATION OF THE VIBRATIONAL SPECTRA OF SCYLLO-INOSITOL, NEO-INOSITOL, MYO-INOSITOL, EPI-INOSITOL, OXYGEN DEUTERATED SCYLLO-INOSITOL AND OXYGEN DEUTERATED NEO-INOSITOL

INTRODUCTION

EARLY SPECTRAL INVESTIGATIONS OF CARBOHYDRATES AND THE GROUP FREQUENCY APPROACH

Detailed interpretations of the vibrational dynamics of relatively complex carbohydrate molecules has advanced significantly in recent years. The reasons for the advancement lie in the increased availability and improved technology of spectral instruments and digital computers. The advent of computers quickly expanded the number of molecular systems to which the theoretical normal coordinate analysis treatment, the mathematical methodology used to calculate theoretical vibrational frequencies, was potentially applicable.

Before the availability of computers, carbohydrates were not early choices as subjects of theoretical investigations. Carbohydrates are relatively large and complex molecules and thus do not lend themselves to a ready solution of the lengthy mathematics involved in calculating a theoretical vibrational spectrum. Therefore, extensive experimental investigations, most often infrared investigations, of the vibrational spectra of carbohydrates preceded the application of the normal coordinate analysis treatment.

Initial interpretations of carbohydrate vibrational spectra were based primarily on qualitative spectral comparisons using the group frequency approach. The group frequency approximation assumes that certain atomic groups will vibrate independently of the rest of the atoms in the molecule. In addition, it is assumed that these atomic groups will vibrate at approximately the same frequency throughout a series of structurally similar molecules. The methodology usually

employed involved taking information derived from spectra of simpler molecules, structurally similar to the carbohydrates, and using the information to develop interpretations of more complex carbohydrate spectra. The spectra of a large number of carbohydrates would then be compared to determine which groups had characteristic absorption bands.

The first relevant molecule investigated was cyclohexane, the normal coordinate analysis of which was reported by Beckett, et al. (1) in 1947. Using this work as a basis, Burkett and Badger (2) assigned and interpreted the ring stretching modes and some additional modes of tetrahydropyran. With tetrahydropyran, the effect of having an oxygen in the ring structure was introduced. Shortly thereafter, Kuhn (3) published the infrared spectra of seventy-nine carbohydrates. Only a few prominent characteristics of the spectra were interpreted. In 1954, Barker, et al. (4,5) interpreted the infrared spectra in the region 730-960 cm^{-1} for several pyranose sugars in terms of differentiating between the α- and β-anomers. Barker, et al. (6) also interpreted the same region for several deoxy-compounds.

Additional literature published prior to 1957 has been reviewed by Neely (7). Subsequent investigations strived to further elucidate the effect on group frequencies of the orientation, i.e., axial or equatorial, of a substituent group and its position on the ring. Later comprehensive reviews of the literature on the infrared spectroscopy of carbohydrates have been published by Spedding (8) and Tipson (9). The results of the many investigations illustrated the limited applicability of the group frequency correlations. It was found that specific types of atomic motions could be generally categorized to a frequency range where they would usually occur, but little could be said about the interpretation of a majority of the individual bands. The vibrational motions were more complex than had been initially assumed. The assumption that certain atomic groups would

vibrate independently of the rest of the atoms in a molecule was not sufficiently valid for most regions of the carbohydrate vibrational spectra.

PERTINENT INVESTIGATIONS INVOLVING NORMAL COORDINATE ANALYSES

A mathematical methodology, the normal coordinate analysis, had been available as a means of calculating theoretical vibrational frequencies and the atomic motions associated with each frequency. As stated before, the lengthy calculations involved had restricted its use. A definitive work in the use of digital computers in the application of the normal coordinate analysis treatment was reported by Schachtschneider and Snyder (10,11) in 1963. To aid in analyzing and interpreting the vibrational spectra of the n-paraffins, they developed a method of adjusting a set of force constants, common to a group of molecules, to give the best fit of the calculated frequencies to the observed frequencies. Among the n-paraffins they found good transferability of the force constants used to calculate the theoretical frequencies. Subsequently, Snyder and Schachtschneider (12) extended their work to other saturated hydrocarbons, including cyclohexane. The work of Schachtschneider and Snyder illustrated the applicability of the normal coordinate analysis treatment and its potential usefulness as an aid in interpreting vibrational spectra.

Snyder and Zerbi (13) reported the normal coordinate analyses of several ether compounds, including tetrahydropyran. The force constants were adjusted utilizing the method of Snyder and Schachtschneider (10). For some of the ethers, the results of the normal coordinate analyses were used to assist in establishing the molecular conformations. Pickett and Strauss (14) investigated the ring bending vibrational modes of cyclohexane and three related oxanes utilizing normal coordinate analysis calculations and ring bending potential function calculations.

In a series of publications, workers at Case Western Reserve University have investigated and interpreted the vibrational spectra of some carbohydrates. The normal coordinate analysis of α-D-glucose was reported by Vasko, et al. (15) in 1972. The normal coordinate analysis was done using force constants taken from several literature sources. No force constant refinements were performed. The assignment of the frequencies was based primarily on frequency magnitude. The authors state that an exact one-to-one match of the calculated frequencies with the experimental frequencies was not expected. The results of the normal coordinate analysis provided a more detailed interpretation of the α-D-glucose vibrational modes than had been previously attained. The calculated potential energy distribution illustrated the extensive coupling occurring in a majority of the vibrations. Further work on D-glucose was reported by Cael, et al. (16). A normal coordinate analysis of β-D-glucose enabled the authors to interpret the D-glucose vibrational modes sensitive to anomeric configuration. They then attempted to extend this work to cellulose I, a normal coordinate analysis of which was reported by Cael, et al. (17). However, in their simplified model they employed some assumptions which are not well established.

INVESTIGATIONS OF THE VIBRATIONAL SPECTRA OF CLASSES OF CARBOHYDRATE COMPOUNDS

At The Institute of Paper Chemistry, the vibrational spectra of several classes of carbohydrate model compounds have been investigated and their spectra interpreted based on comprehensive normal coordinate analyses. A methodology of investigating increasingly more complex classes of compounds, in terms of structure and number of vibrational degrees of freedom, has been employed so knowledge gained from each class could be applied to succeeding classes. In this manner, the vibrational dynamics of each individual class of compounds have been characterized and also the accumulated knowledge from all the classes has been used to

better characterize the vibrational spectra of even more complex molecular systems such as the polysaccharides. In chronological order, the classes of compounds studied include the 1,5-anhydropentitols, acyclic alditols, pentoses and the hexoses. The cellodextrins are being studied at this time.

The overall theoretical analysis methodology employed is different from that of the workers at Case Western Reserve University. The primary difference is the adjustment of the force constants, assumed to be quadratic, using a computerized refinement procedure in order to obtain the best fit of the calculated frequencies to the assigned experimentally observed frequencies. The refinement procedure requires a more rigorous assignment of the observed frequencies to the calculated frequencies than when the force constants are not refined.

The 1,5-anhydropentitols, because they are a closer approximation to the saccharides than tetrahydropyran, were the first class of compounds studied. Pitzner (18,19) assigned and interpreted the solid state spectra of 1,5-anhydroxylitol, 1,5-anhydroribitol, and 1,5-anhydro-L-arabinitol. Initially, Pitzner encountered problems with divergence of the force constants during refinements when using the linear least-squares method of Schachtschneider and Snyder (11). To circumvent this, he successfully adapted a nonlinear least-squares technique based on the method of Fletcher and Powell (20) for refining the force constants. The final frequencies calculated for the assumed tetrahedral models satisfactorily reproduced the distributions of bands in the experimental spectra. The results demonstrated that the differences between the experimental spectra of the 1,5-anhydropentitols were primarily due to the variations in the equatorial and axial orientations of the hydroxyl groups. The validity of the force field was supported by frequencies calculated for the alternate conformers of 1,5-anhydroribitol and 1,5-anhydro-L-arabinitol being in fair agreement with 'new' bands

observed in the solution spectra, which were thought to result from the presence of the alternate conformers in solution.

Extending this work to acyclic carbohydrates, Watson (21) investigated the vibrational spectra of several alditols, in particular erythritol, ribitol and xylitol. The force field developed for the normal coordinate analyses of these compounds was used to predict the vibrational spectrum of another pentitol, D-arabinitol, which had not been included in any of the force constant refinements. The agreement of the calculated frequencies with the observed frequencies was comparable to the agreement obtained for the other alditols. This demonstrated the predictive capability of the force field.

The next class of compounds studied was the pentoses, the simplest carbohydrates which would exhibit the effect of the anomeric hydroxyl group on the vibrational spectrum. Edwards (22) refined a set of force constants to the assigned spectra of β-arabinose, β-lyxose and α-xylose using the refinement procedure developed by Pitzner (18). The transferability of the force constants to molecules of similar structure was demonstrated by the prediction of reasonable frequency distributions for α- and β-methyl xylopyranosides. The alternate forms of the pentoses and the different pyranose forms of ribose were also examined. Because of the complexity of the calculated vibrations, no discernable trends between frequency distribution and anomeric hydroxyl group orientation could be detected in the pentoses.

Next in complexity were the hexoses, the vibrational spectra of which were investigated by Wells (23). A forty-six parameter force field was developed using α-D-glucose, β-D-glucose and several deuterated analogues which gave good agreement between the calculated frequencies and the assigned experimental frequencies. The force field was used to successfully predict the vibrational frequencies of

α- and β-galactose and α- and β-mannose. The force field was also used to investigate different hydroxymethylene conformations at the C6 position for glucose, galactose and mannose.

Using the force field developed by Wells, Carlson (95) is now investigating the vibrational spectra of the cellodextrins.

RATIONALE FOR INVESTIGATING THE VIBRATIONAL SPECTRA OF THE INOSITOLS

In the molecular model used in the theoretical analyses at The Institute of Paper Chemistry, several assumptions have been made. It has been assumed that harmonic potentials, i.e., quadratic force constants, could be used to describe the potential energy. In addition, it has been assumed that each molecule could be treated as if it were isolated, that is, all intermolecular interactions are assumed to be negligible. These assumptions have appeared to be valid in the studies just discussed, but their validity has not been critically assessed. Anharmonic terms in the potential energy and intermolecular interactions, such as hydrogen bonding and crystal lattice effects, are present in crystalline carbohydrates and perturb the frequencies of the fundamental vibrational modes to a relatively unquantified extent.

A possible method for assessing the degree to which these second-order potential effects perturb the experimentally observed frequencies is by comparing the fit of the calculated frequencies to the experimental frequencies throughout a series of similar molecules. The sensitivity of this method, however, would be dependent on the number of force constants adjusted in the refinements. The force constants are adjusted in a refinement to optimize the fit of the calculated frequencies to the assigned experimental frequencies, which include any perturbations present. Therefore, inherent in the adjusted force constants would be

compensation for any effect perturbing the experimental frequencies. The greater the number of force constants refined, the more force constants which could be adjusted to compensate for the perturbations. For the 1,5-anhydropentitols, alditols, pentoses, and hexoses, between forty-six and sixty-seven force constants were used to define the respective potential energies. In all cases, almost all the force constants were refined. A molecular system described using a fewer number of force constants would be more sensitive to any second-order potential effects because the fewer constants could not as adequately account for the perturbations in the experimental frequencies. This would manifest itself by increasing the average differences between the calculated and experimental frequencies throughout a series of molecules. To better assess the degree to which second-order potential effects are perturbing the experimental frequencies, it was deemed valuable to examine a molecular system of complexity, in terms of number of degrees of vibrational freedom, comparable to the pentoses and hexoses but which could be described using a fewer number of force constants.

The inositols represent such a molecular system. Closely related to the carbohydrates, the inositols are a unique group of hexahydroxy cyclohexanes. The structures of the nine possible isomers are shown in Fig. 1, as taken from Pigman and Horton (24).

Compared to other classes of carbohydrates of comparable complexity, such as the pentoses or hexoses, the inositols can be described using fewer force constants, at the same level of theoretical approximation, because fewer distinct types of chemical bonds are present in the basic molecular structure of the inositols. The types of chemical bonds associated with the ring oxygen, the anomeric hydroxyl group or methylene hydrogens are not present in the structure of the inositols and thus force constants representing these types of chemical bonds need not be defined. A primary objective of this thesis is to utilize

the simplified force field to more closely assess the extent to which second-order potential effects perturb the experimentally observed frequencies of the fundamental modes of vibration. Concurrently, this would also permit a more critical evaluation of the assumptions involved in doing a normal coordinate analysis of molecules having approximately the same number of vibrational degrees of freedom as the inositols.

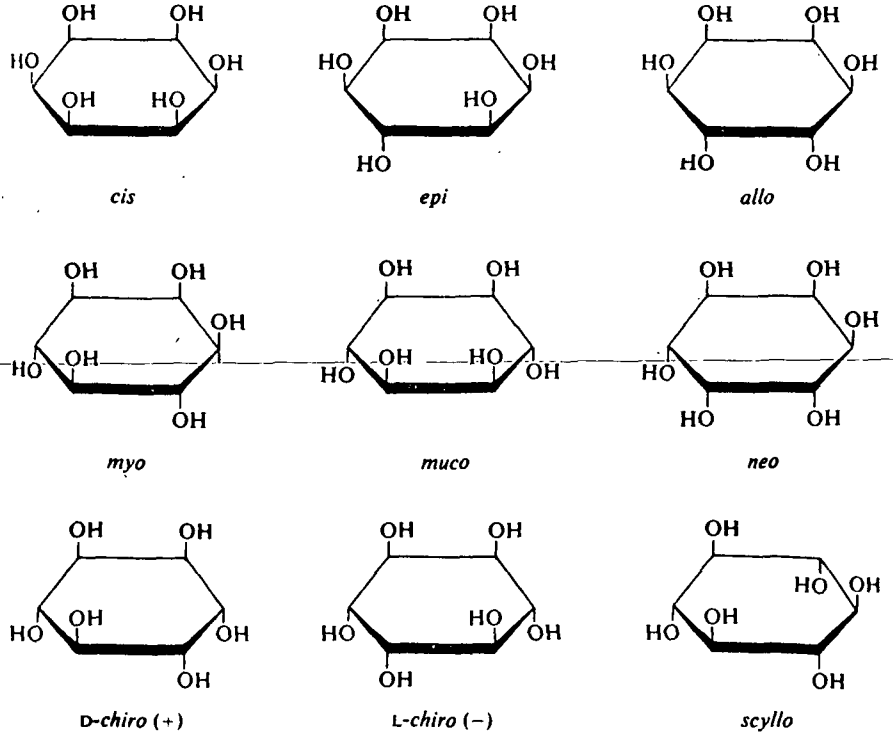

Figure 1. The Nine Inositol Isomers (24)

A second objective of this thesis is to assign and interpret the vibrational spectra of seven of the inositol isomers in the crystalline state. The seven include: scyllo-inositol, neo-inositol, myo-inositol, epi-inositol, cis-inositol, L-chiro-inositol and muco-inositol. The selection of only these seven was based primarily on the availability of samples. The structures of these seven inositols exhibit distinct variations in hydroxyl configurations, as shown in Fig. 1, so the effects of major hydroxyl group configuration differences will be observed,

both experimentally and theoretically. The interpretation of the molecular vibrations will be based on normal coordinate analyses of these inositols. Crucial to this objective is the development of a force field capable of satisfactorily reproducing the experimentally observed vibrational frequencies and reasonable associated atomic motions. Also vitally important is the correct assignment of the experimentally observed frequencies to the calculated frequencies. The inositols represent a departure from the carbohydrate norm in that all but one of the inositol isomers theoretically contain at least one element of symmetry and several contain additional symmetry elements. The molecular symmetry, through the application of the vibrational selection rules, can be used to assist in the assignment of the observed frequencies to the calculated frequencies. For carbohydrates having no symmetry, such as the hexoses or pentoses, the assignments are based primarily on frequency magnitude, where the experimentally observed frequencies are assigned to the calculated frequency of closest magnitude. The vibrational selection rules would provide criteria other than frequency magnitude as a basis for making the assignments. This investigation, then, will also allow an appraisement of the degree to which the group theory analysis and vibrational selection rules may be applied to the molecules of this class.

Until this time, only limited interest has been shown in the vibrational spectra of the inositols. Kuhn (3) and Shay, et al. (25) have reported the infrared spectrum of myo-inositol. Barker, et al. (6) recorded the infrared spectra of scyllo-inositol, myo-inositol, muco-inositol, and D- and L-chiro-inositols. The spectra were used for comparative purposes in characterizing the C-methyl and methylene rocking modes of other carbohydrate compounds.

EXPERIMENTAL

SAMPLE PREPARATION

myo-Inositol was obtained commercially from Pfanstiehl Laboratories, Inc. and was not purified further. The following compounds were obtained from Dr. Laurens Anderson of the University of Wisconsin at Madison: epi-inositol, an impure sample of neo-inositol and an impure sample of penta-O-acetyl myo-inosose-2. The epi -inositol was not further purified.

Preparation of scyllo-Inositol

Penta-O-acetyl myo-inosose-2, shown in Fig. 2, is an intermediate in the synthesis of scyllo-inositol. Approximately 2 g of this compound were obtained. The myo-inosose-2 derivative had sat for some time prior to being received and had turned brown in color. Thin-layer chromatography, using ethyl acetate, acetone and methanol as developing solvents, showed two and possibly three different compounds present. To recover what penta-O-acetyl myo-inosose-2 remained, the brown solid was again acetylated.

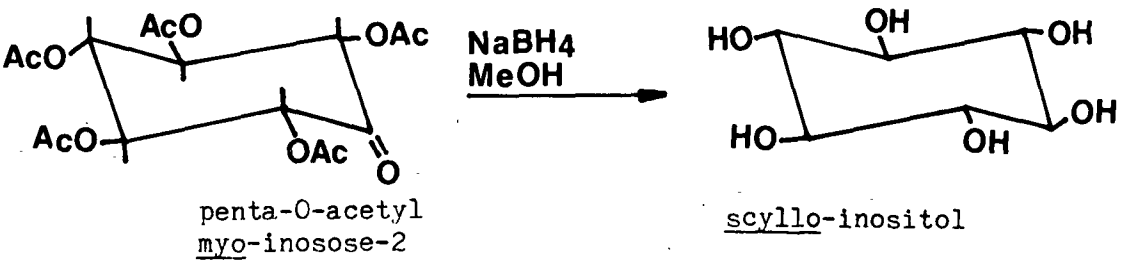

penta-O-acetyl myo-inosose-2

scyllo-inositol

Figure 2. The Reaction of Penta-O-acetyl myo-Inosose-2 to scyllo-Inositol

Reacetylation of Penta-O-acetyl myo-Inosose-2

The acetylation was done according to the method of Posternak (26). Approximately 1 g of the brown material was dissolved in 6 ml of a 1:19 sulfuric acid-acetic anhydride solution which had been heated to 120°C. The solution was filtered while hot and allowed to stand at room temperature for 2 hours. A

white precipitate formed and was collected on a sintered glass filter. The precipitate was washed four times with glacial acetic acid and then three times with ethyl ether. The resulting 0.39 g of product had a melting point of 208-211°C. The reported melting point of penta-O-acetyl myo-inosose-2 is 211-212°C (26). The above sequence was repeated with the remaining 1.04 g of the inosose. This reaction yielded 0.52 g of product which had a melting point of 206-211°C. An additional 0.08 g of product was crystallized from the combined reaction mixtures.

scyllo-Inositol

The penta-O-acetyl myo-inosose-2 was reduced with sodium borohydride and deacetylated in a single step using the procedure of Stancev and Kates (27). The reaction is shown in Fig. 2. The reaction was run in two batches. In each case, 0.49 g of penta-O-acetyl myo-inosose-2 was suspended in 13 ml of methanol. To each suspension was added 0.075 g sodium borohydride dissolved in 13 ml of methanol. The solution was stirred for thirty minutes. As the penta-O-acetyl myo-inosose-2 reacted it dissolved in the solution. The resulting light orange solution was acidified with 2N HCl, evaporated in vacuo to about 5 ml and placed in the refrigerator. Approximately 150 mg of lightly colored crystals were isolated from one batch. The compound was recrystallized from distilled water. The melting point of the crystals was 354-356°C. The reported melting point of scyllo-inositol is 355-356°C (27). The second batch was not properly neutralized and heating of the reduced volume resulted in degradation of the scyllo-inositol. The solution was neutralized and a minor amount of scyllo-inositol was obtained from this batch.

Purification of neo-Inositol

The neo-inositol sample was estimated by Dr. Anderson to be of 80% purity. Several batches were dissolved in hot distilled water. The neo-inositol readily crystallized upon cooling of the solution. The melting point of the crystals, repeated three times, was 324-326°C. Reported melting point is 315°C (28).

MEASUREMENT OF THE RAMAN AND INFRARED SPECTRA OF THE INOSITOLS

Measurement of the Room Temperature and Liquid Nitrogen Temperature Raman Spectra of the Inositols in the Crystalline State

The Raman spectra were measured with a SPEX 1401 Raman Spectrometer (3/4 meter-Czerny-Turner double monochrometer spectrometer) with photoelectric recording. The radiation source was a Coherent Radiation Model 52A argon ion laser. A laser wavelength of 514.5 nm (green) was used. The slit widths were set for a minimum resolution of 5 cm^{-1}. A more detailed description of the instrumental conditions is given in Appendix I.

For measuring the room temperature spectra, pressed powder pellets of the compounds were placed in a 180° backscattering platform. In some cases the pellets were set on a cover slip and placed on the platform.

For the low temperature spectra, part of the pellet was glued onto a wire sample holder. The sample holder was placed inside a Harney-Miller temperature control cell. The sample was tilted at a 45° angle with respect to the incident beam to maximize the scattered radiation, the scattered radiation then being viewed at 90° to the incident beam. Nitrogen was boiled off from a large Dewar flask filled with liquid nitrogen and passed through the cell to cool the sample. The flow of nitrogen, and thus the temperature, was regulated by a rheostatically controlled heater immersed in the Dewar flask. To monitor the sample temperature, a thermocouple was inserted into the cell next to the sample. The thermocouple was connected to a Bailey Cryo-thermometer which measures temperatures down to -200°C. The low temperature Raman spectra were recorded in the temperature range from -175 to -182°C.

The temperatures at which the low temperature Raman and infrared spectra were recorded are not actually at the temperature of liquid nitrogen but approximately 15-20°C higher. However, for convenience the low temperature spectra will be referred to as liquid nitrogen temperature spectra.

Measurement of the Room Temperature and Liquid Nitrogen Temperature Infrared Spectra of the Inositols in the Crystalline State

The infrared spectra were recorded on a Perkin-Elmer Model 621 Grating Infrared Spectrophotometer.

The crystalline samples were well ground and then prepared as Fluorolube and Nujol mulls. A capillary thickness of the Fluorolube and Nujol mulls was spread between calcium fluoride and cesium iodide plates, respectively. The Fluorolube mull was used to record the sample spectrum from 3900 cm^{-1} to $\sim$1350 cm^{-1} and the Nujol mull from $\sim$1350 cm^{-1} to 200 cm^{-1}.

The spectra at liquid nitrogen temperature were recorded using a low temperature cell constructued at The Institute of Paper Chemistry by Henry Wells. The mulls were used to record the spectra. The sample temperature was not directly monitored.

To obtain better frequency resolution for both the room temperature and low temperature spectra, the frequency axis was expanded by four times and the spectra recorded at a lower speed.

Almost all samples were recovered from the mulls by extracting the mulling agent with chloroform. The samples were then recrystallized from an appropriate solvent.

The infrared spectra of scyllo-inositol, neo-inositol, myo-inositol and epi-inositol were also recorded in the form of KBr pellets.

Oxygen Deuteration (COD) of scyllo-Inositol, neo-Inositol, myo-Inositol and epi-Inositol

The deuteration of the samples was done in a dry box. A dry environment was attained by passing air from an air line through a drop-out flask, through two tubes filled with calcium chloride diluted slightly with indicating Drierite and then through a tube filled with sodium hydroxide pellets and into the dry box. The approximate dimensions of all three tubes were 50 cm in length and 3 cm in diameter. When the indicating Drierite showed that the first tube was nearing its limit of water absorption, the calcium chloride in this tube was replaced. The first tube was used to remove the majority of the water from the air. A partial overhauling of the dry box, mainly replacing a fractured glass top, substantially reduced the amount of air needed to maintain a positive pressure inside the dry box. The dry box was purged for at least two hours before any work was done inside.

The solvent used to exchange the hydroxyl groups was 99.9% D_2O. The D_2O was removed from the bottle by inserting a syringe through a rubber septum placed, under dry conditions, over the bottle top. The D_2O and syringe were stored in a vacuum desiccator inside the dry box. Approximately 30 mg of myo-inositol and epi-inositol were dissolved in 2-3 ml of D_2O. Approximately 25 mg of scyllo-inositol and 20 mg of neo-inositol were dissolved in an amount of D_2O needed to completely dissolve the sample, 3-6 ml. In the latter two cases, sample dissolution was facilitated by heating the sample and D_2O on a hot plate placed inside the dry box. To enhance evaporation of the D_2O, the solutions were evaporated in a vacuum oven which had been placed inside the dry box. For myo-inositol, epi-inositol and scyllo-inositol the above procedure was repeated three times and for neo-inositol twice because of its extreme insolubility in the D_2O.

Measurement of the Room Temperature Raman and Infrared Spectra of Oxygen Deuterated scyllo-Inositol, neo-Inositol, myo-Inositol, and epi-Inositol

For recording the Raman spectra, powdered samples of the deuterated compounds were pressed into 2-mm diameter pellets inside the dry box. The pellets were placed on a cover slip and sealed from the atmosphere by inverting a 10-mm diameter Raman solution cell over the pellet and sealing the cell to the cover slip with a small amount of stopcock grease. The Raman spectra were then recorded by placing the cover slip and sealed sample on the 180° platform.

The four sealed samples were returned to the dry box, dissolved in D_2O and evaporated to dryness in the vacuum oven. For recording the infrared spectra, two mulls, a Fluorolube mull and a Nujol mull, of each sample were made inside the dry box. The infrared spectra were then recorded using the same procedure described earlier. All the deuterated spectra were recorded at room temperature only.

Measurement of the Water Solution Spectra of the Inositols

The Raman spectra of saturated or near-saturated water solutions of the inositols were recorded. The solution spectrum of neo-inositol could not be measured because of its low solubility in water. The solution spectra were recorded with the solutions in capillary tubes. The capillary tubes were placed in a holder with the scattered radiation viewed at 90° to the incident beam. The capillary tubes were sealed to prevent evaporation losses.

DEPOLARIZATION RATIO MEASUREMENTS FOR AQUEOUS SOLUTIONS OF scyllo-INOSITOL, myo-INOSITOL AND epi-INOSITOL

Important in the experimental determination of depolarization ratios is the instrumental arrangement chosen. Various arrangements have been discussed and evaluated by Allemand (29). For optimum results he recommends that the polarization of the laser beam be kept constant and a polarization analyzer be placed after the

sample. To minimize the effects of the instrument functions, Allemand (29) and Rahn, et al. (30) suggest placing a polarization scrambler between the analyzer and the entrance slit.

The arrangement just described with the polarization analyzer and polarization scrambler placed between the sample and the entrance slit was employed in this work. Depolarization measurements were made for aqueous solutions of scyllo-inositol, myo-inositol, and epi-inositol. The sample spectra were first recorded with the plane of polarization of the analyzer set parallel to the plane of polarization of the incident beam. The spectra were then recorded with the analyzer rotated 90° so that the plane of polarization of the analyzer was perpendicular to the plane of polarization of the incident beam.

The depolarization ratios were calculated by dividing the height of each band where the analyzer was in the perpendicular position by the band height where the analyzer is in the parallel position. This was done assuming the intensity of the symmetric bands was proportional to the band heights.

The instrumental arrangement was checked using carbon tetrachloride as a standard.

EXPERIMENTAL RESULTS

ROOM TEMPERATURE AND LIQUID NITROGEN TEMPERATURE RAMAN AND INFRARED SPECTRA OF scyllo-INOSITOL, neo-INOSITOL, myo-INOSITOL, AND epi-INOSITOL IN THE CRYSTALLINE STATE

scyllo-Inositol

The Raman and infrared spectra are shown in Fig. 3 and 4, respectively. The frequencies of the bands are tabulated in Table I.

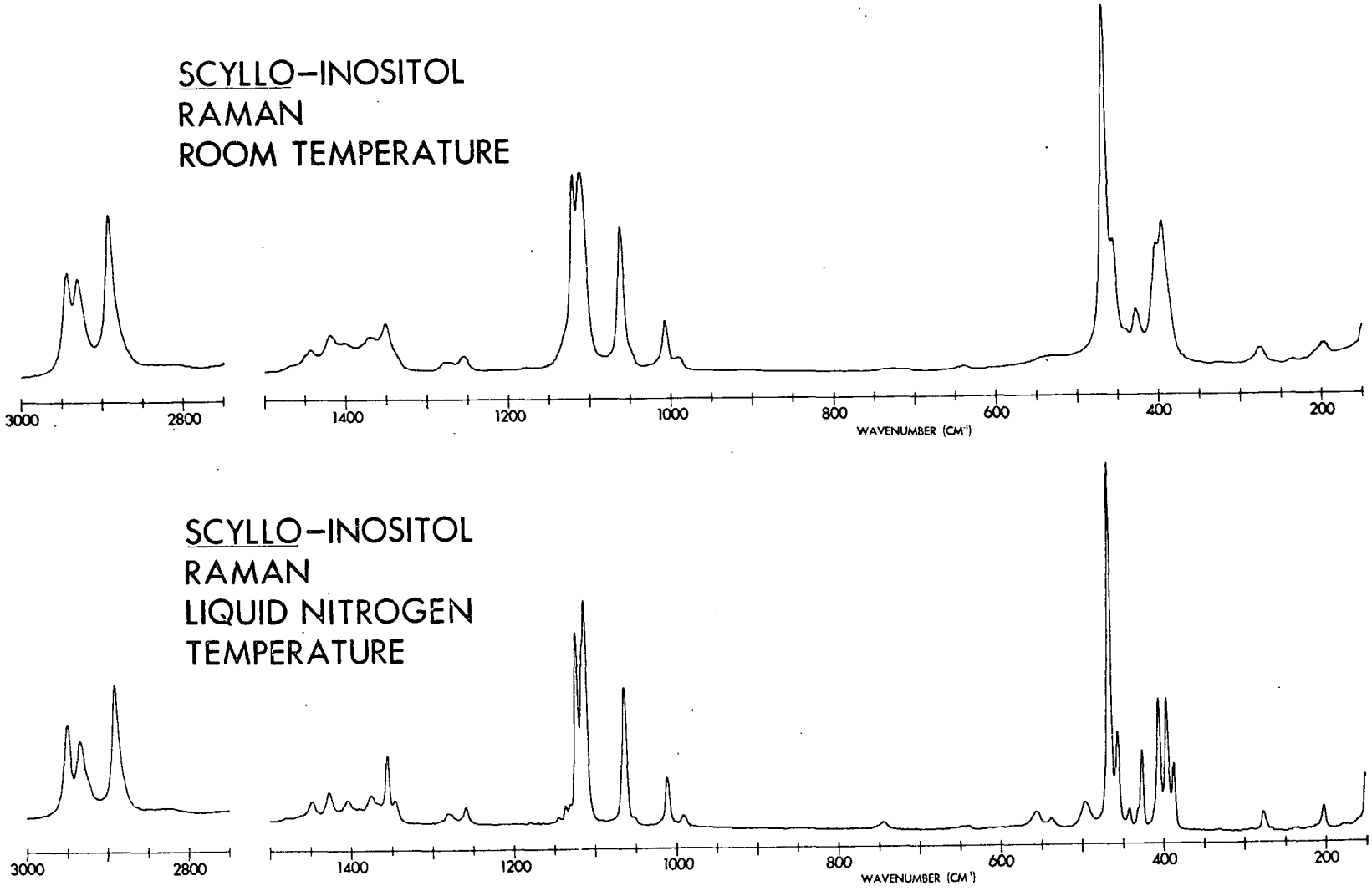

Figure 3. The Room Temperature and Liquid Nitrogen Temperature Raman Spectra of Crystalline scyllo-Inositol

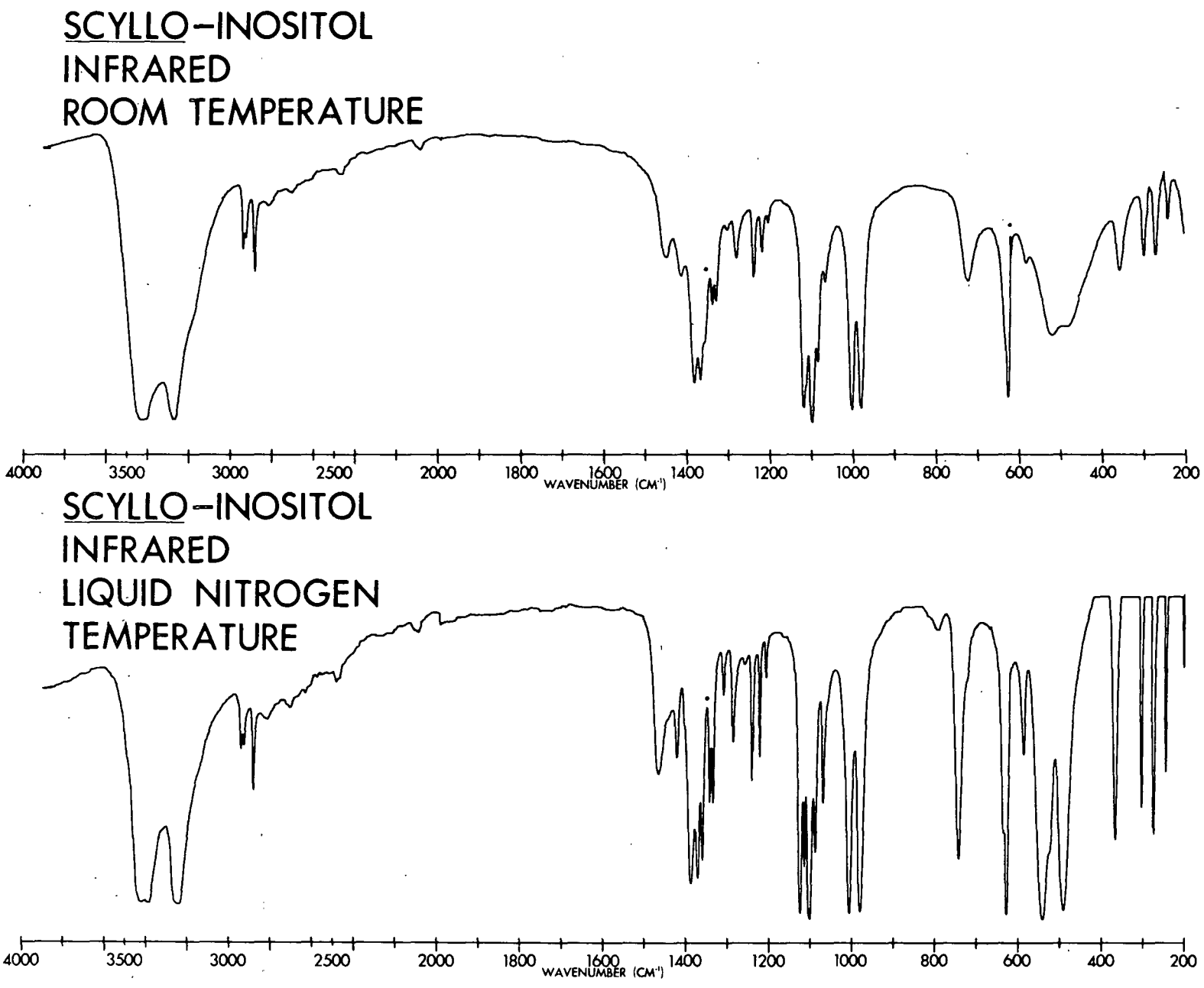

Figure 4. The Room Temperature and Liquid Nitrogen Temperature Infrared Spectra of Crystalline scyllo-Inositol

TABLE I

TABULATED FREQUENCIES FOR THE ROOM TEMPERATURE AND LIQUID NITROGEN TEMPERATURE RAMAN AND INFRARED SPECTRA OF scyllo-INOSITOL

RAMAN		INFRARED		RAMAN		INFRARED	
ROOM TEMPERATURE (cm^{-1})	LIQUID NITROGEN TEMPERATURE (cm^{-1})	ROOM TEMPERATURE (cm^{-1})	LIQUID NITROGEN TEMPERATURE (cm^{-1})	ROOM TEMPERATURE (cm^{-1})	LIQUID NITROGEN TEMPERATURE (cm^{-1})	ROOM TEMPERATURE (cm^{-1})	LIQUID NITROGEN TEMPERATURE (cm^{-1})
		3430 (vs)	3425 (s)	1058 (m)	1060 (m)		
			3390 (s)	1004 (w)	1007 (w)	1002 (s)	1006 (vs)
		3275 (vs)	3250 (s)	987 (vw)	986 (vw)		
2942 (m)	2948 (m)	2940 (m)	2945 (m)			981 (s)	979 (vs)
2929 (m)	2932 (m)	2930 (m)	2935 (m)				796 (w)
2890 (m)	2889 (m)	2885 (m)	2885 (m)		737 (vvw)		
		1454 (m)	1468 (m)			724 (m,b)	744 (s)
1442 (w)	1442 (w)		~1441 (w,sh)				~723 (sh)
1416 (w)	1421 (w)	1416 (m)	1422 (m)	~637 (vvw)	~634 (vvw)	~635 (sh)	636 (sh)
			~1405 (sh)			627 (s)	628 (vs)
1398 (w)	1398 (w)					585 (w)	587 (m)
		1383 (s)	1387 (s)		551 (w)		
1367 (w)	1370 (w)	1369 (s)	1370 (s)		532 (vw)		542 (vs)
		~1357 (sh)	1359 (s)			~522 (m,b)	~525 (sh)
1348 (w)	1350 (m)				490 (w)	~485 (m,b)	492 (vs)
	1340 (w,sh)	1341 (m)	1344 (m)	464 (vs)	463 (vs)		
		1331 (m)	1335 (m)	452 (sh)	451 (m)		
		1305 (w)	1310 (w)		437 (w)		
		1282 (m)	1286 (m)	424 (w)	420 (m)		
1277 (vvw)	1275 (vw)			399 (m,sh)	400 (m)		
1253 (vw)	1254 (w)		1258 (vw)	391 (m)	391 (m)		
		1240 (m)	1241 (m)		382 (m)		
		1220 (m)	1222 (m)			360 (m)	370 (s)
		1206 (w)	1207 (w)			302 (m)	307 (s)
		1119 (s)	1124 (vs)	271 (w)	272 (w)	273 (m)	277 (s)
1116 (m)	1119 (s)				263 (vw)		
		~1112 (sh)	1113 (s)			244 (m)	247 (s)
1107 (m)	1108 (s)			231 (w)	229 (vw)		
		1099 (vs)	1101 (vs)		214 (vvw)		
		1085 (m)	1087 (s)	196 (w,b)	198 (w)		
		1067 (w)	1068 (m)		181 (vvw)		
				168 (vw)			

Conventional symbolism indicating relative intensity: s = strong, m = medium, w = weak, sh = shoulder, b = broad, v = very.

neo-Inositol

The Raman and infrared spectra are shown in Fig. 5 and 6, respectively. The frequencies of the bands are tabulated in Table II.

myo-Inositol

The Raman and infrared spectra are shown in Fig. 7 and 8, respectively. The frequencies of the bands are tabulated in Table III.

epi-Inositol

The Raman and infrared spectra are shown in Fig. 9 and 10, respectively. The frequencies of the bands are tabulated in Table IV.

The dots (•) which appear in some of the infrared spectra at approximately 1350 cm^{-1} indicate where the mulls were changed. The dots which appear in some of the infrared spectra at 625 cm^{-1} indicate the noticeable manifestation of a grating change.

The spectra shown in all the figures are photoreductions of actual spectra. None of the spectra have been retraced.

The symbol '$\sim$' which appears in the tables of tabulated bands means 'approximately' and indicates that the frequency could not be determined with the precision attained for the other bands.

ROOM TEMPERATURE RAMAN AND INFRARED SPECTRA OF OXYGEN DEUTERATED (COD) scyllo-INOSITOL, neo-INOSITOL, myo-INOSITOL, AND epi-INOSITOL IN THE CRYSTALLINE STATE

Oxygen Deuterated scyllo-Inositol

The Raman and infrared spectra are shown in Fig. 11. The frequencies of the bands are tabulated in Table V.

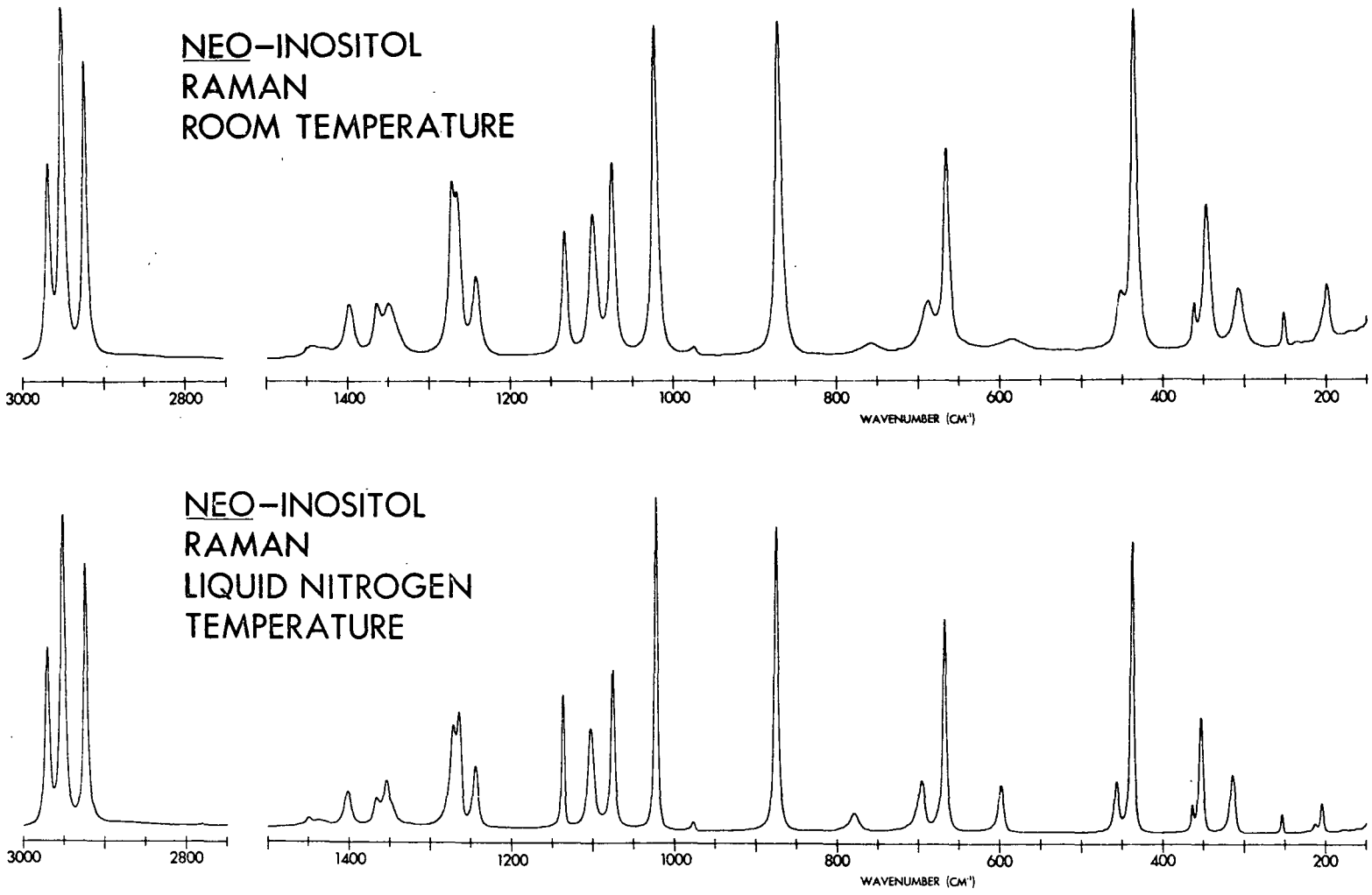

Figure 5. The Room Temperature and Liquid Nitrogen Temperature Raman Spectra of Crystalline neo-Inositol

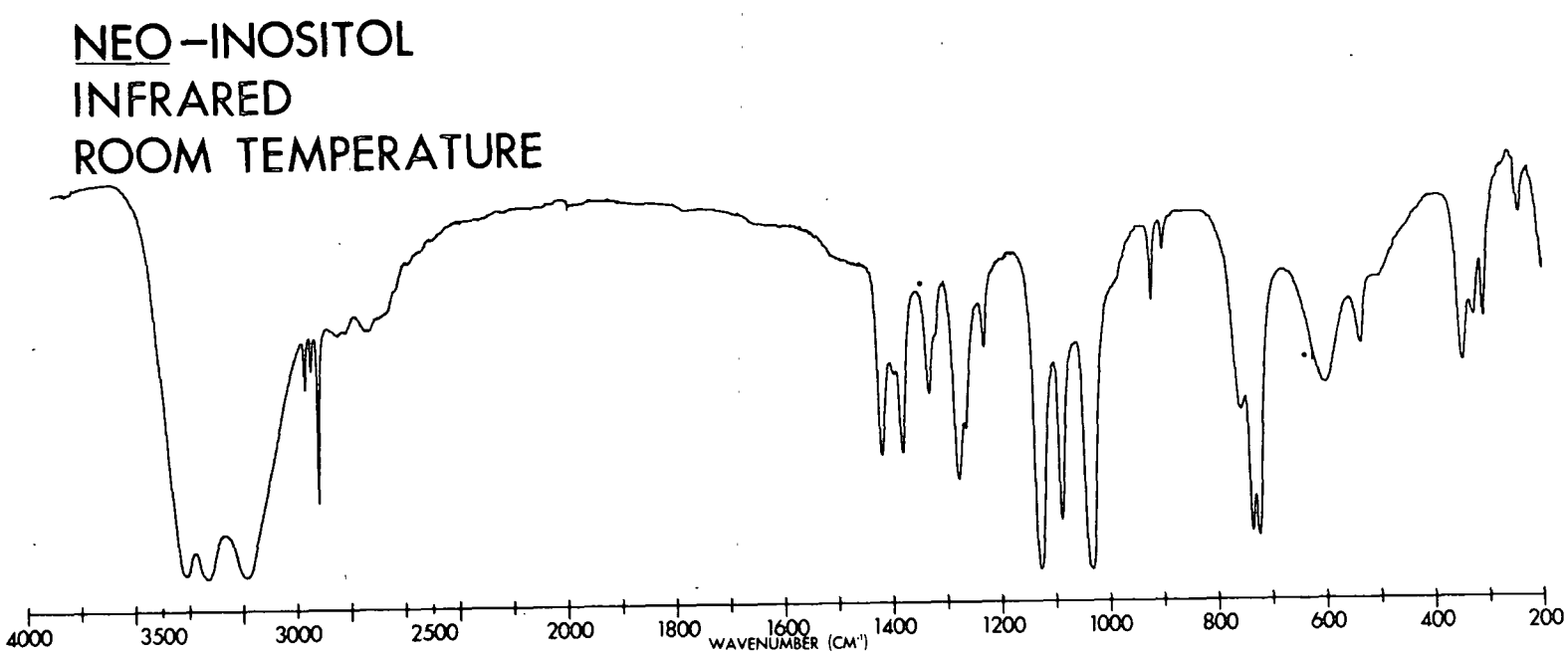

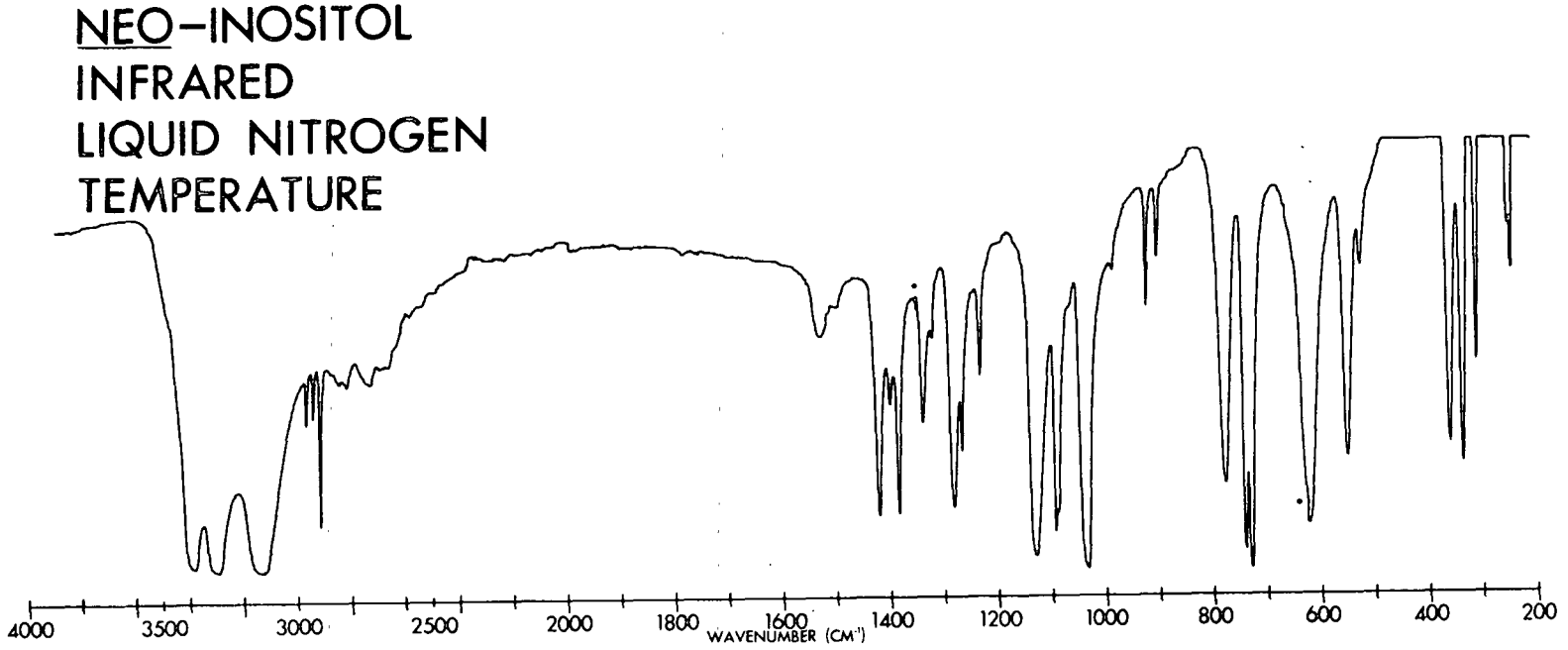

Figure 6. The Room Temperature and Liquid Nitrogen Temperature Infrared Spectra of Crystalline neo-Inositol

TABLE II

TABULATED FREQUENCIES FOR THE ROOM TEMPERATURE AND LIQUID NITROGEN TEMPERATURE RAMAN AND INFRARED SPECTRA OF neo-INOSITOL

RAMAN		INFRARED		RAMAN		INFRARED	
ROOM TEMPERATURE (cm^{-1})	LIQUID NITROGEN TEMPERATURE (cm^{-1})	ROOM TEMPERATURE (cm^{-1})	LIQUID NITROGEN TEMPERATURE (cm^{-1})	ROOM TEMPERATURE (cm^{-1})	LIQUID NITROGEN TEMPERATURE (cm^{-1})	ROOM TEMPERATURE (cm^{-1})	LIQUID NITROGEN TEMPERATURE (cm^{-1})
		3410 (vs)	3390 (vs)	1023 (vs)	1021 (vs)		
		3330 (vs)	3305 (vs)				1013 (vvw,sh)
		3190 (vs)	3140 (vs)			987 (vvw,sh)	988 (vw)
2968 (vs)	2969 (m)	2965 (w)	2970 (w)	974 (vw)	975 (w)		
2951 (vs)	2950 (s)					922 (w)	924 (m)
		2942 (w)	2945 (w)			901 (w)	904 (w)
2923 (vs)	2922 (s)	2920 (m)	2920 (m)	872 (vs)	874 (vs)		
1449 (vw,sh)	1449 (w)			758 (vw,b)	776 (w,b)	758 (m)	778 (s)
1443 (vw)	~1445 (sh)					738 (s)	740 (vs)
	~1435 (sh)					726 (s)	729 (vs)
~1425 (vvw)	1430 (vw)			688 (m)	694 (m)		
		1425 (m)	1424 (s)	665 (s)	668 (s)		
1397 (m)	1401 (m)					604 (m,b)	622 (s,b)
		1401 (w)	1404 (m)	584 (vw,b)	597 (m)		
			~1400 (sh)			538 (m)	552 (m)
		1386 (m)	1387 (s)			~500 (w,sh)	527 (w)
1353 (m)	1365 (m)						469 (vvw)
1348 (m)	1354 (m)			451 (m)	454 (m)		
	~1346 (sh)			435 (vs)	437 (vs)		
		1335 (m)	1338 (m)		386 (vvw,b)		
		1323 (sh)	1322 (w)	362 (w)	362 (w)		
		1281 (m)	1282 (s)			349 (m)	363 (m)
1271 (s)	1270 (s)			345 (m)	352 (s)		
		1267 (m)	1267 (m)			329 (m)	338 (m)
1265 (s)	1264 (s)					310 (m)	313 (m)
1241 (m)	1243 (m)			307 (m)	312 (m)		
		1232 (w)	1233 (m)		265 (w)		
		~1194 (vvw)	~1194 (vvw)	250 (w)	251 (w)		
1132 (s)	1135 (s)					250 (sh)	254 (m,sh)
		1130 (vs)	1132 (vs)			245 (w)	248 (m)
			~1126 (sh)	232 (vvw)	230 (vw)		
1098 (s)	1102 (s)				218 (vvw,sh)		
		1091 (s)	1094 (s)		~208 (vw,sh)		
			1089 (s)	198 (m)	202 (m)		
1074 (s)	1074 (s)				183 (vvw)		
			1068 (vvw,sh)	172 (vvw)	~169 (vvw)		
1037 (vs)	1037 (vs)						

Conventional symbolism indicating relative intensity: s = strong, m = medium, w = weak, sh = shoulder, b = broad, v = very

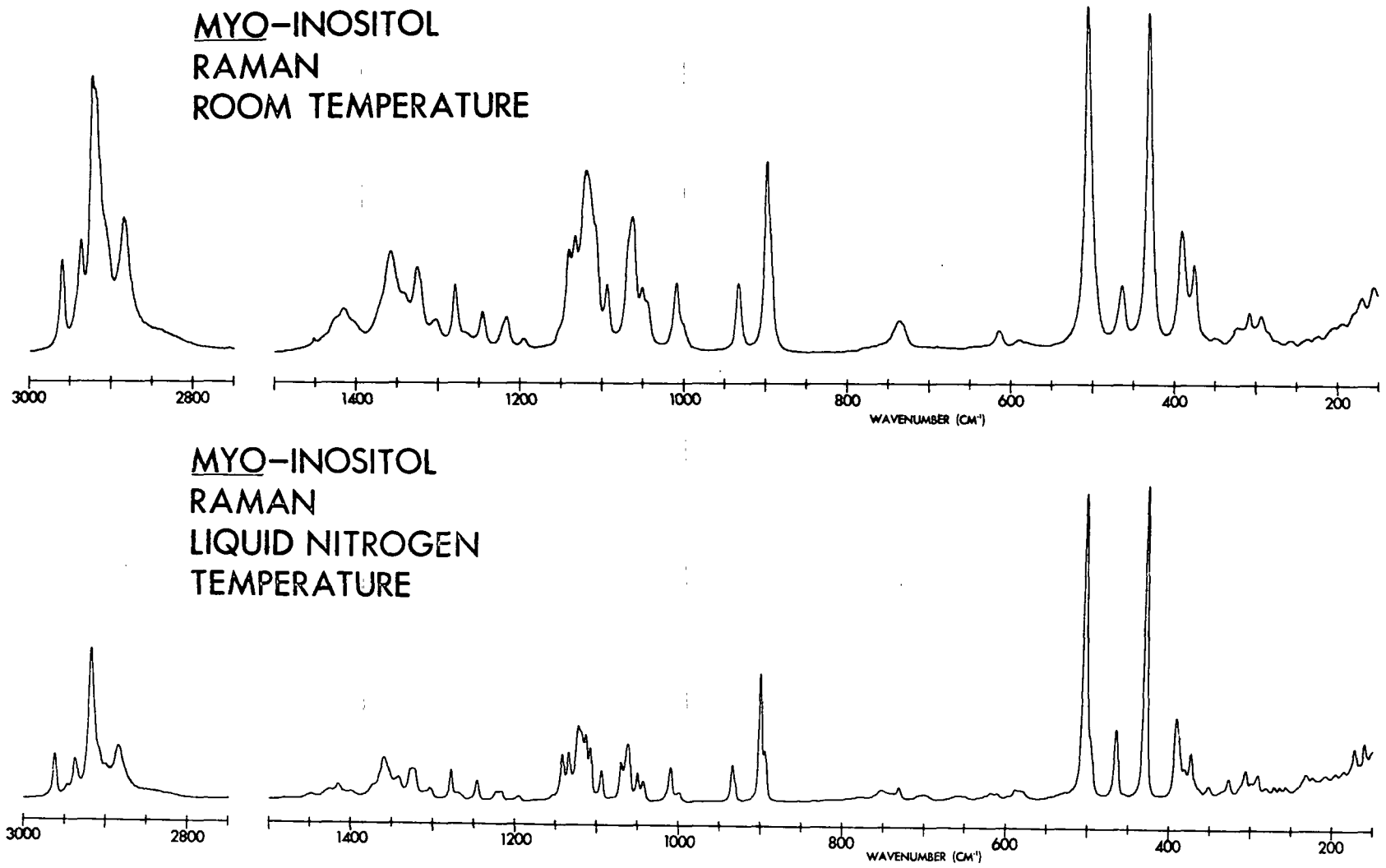

Figure 7. The Room Temperature and Liquid Nitrogen Temperature Raman Spectra of Crystalline myo-Inositol

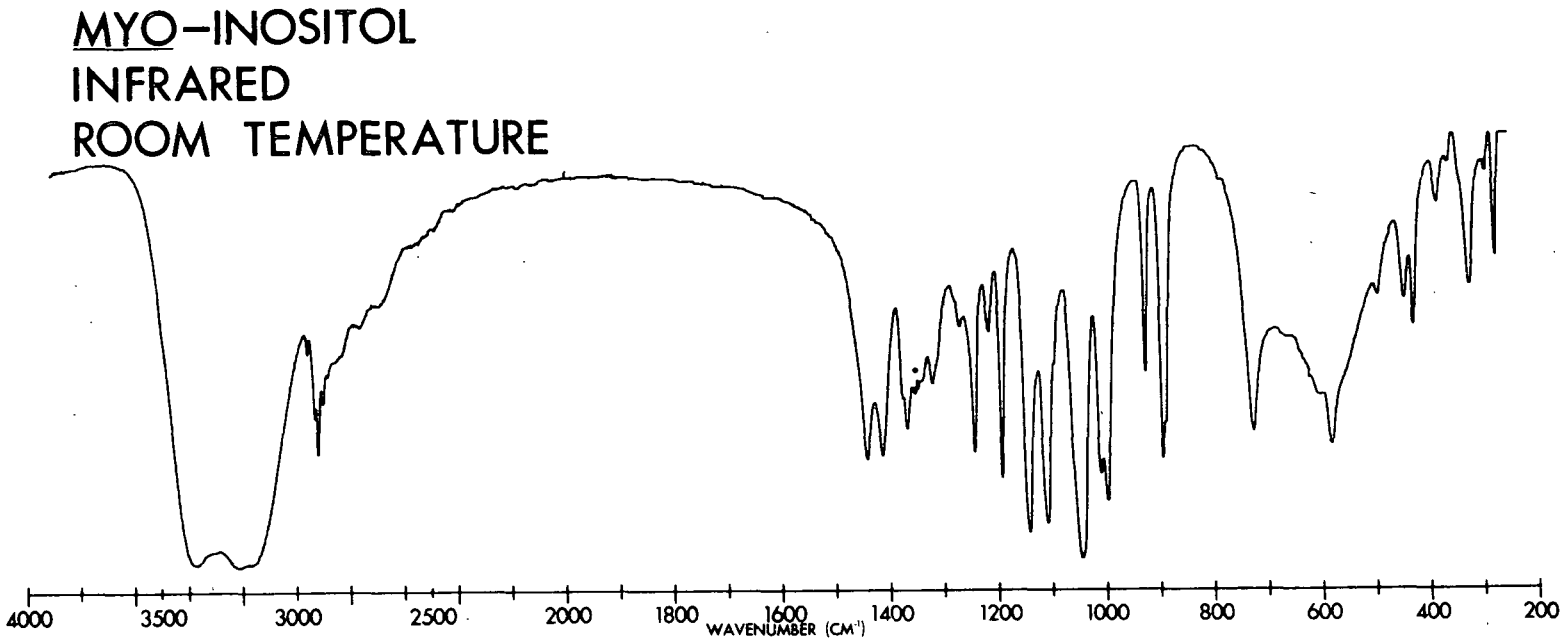

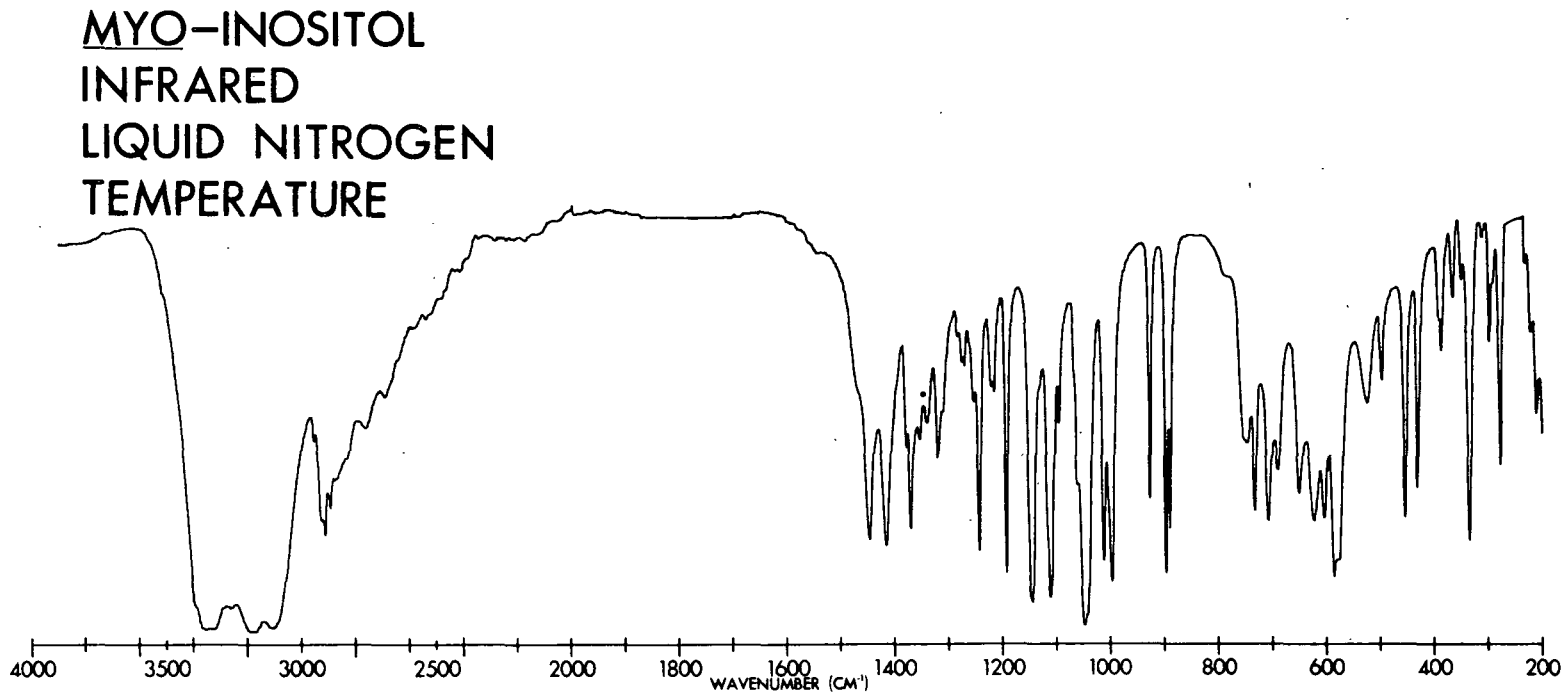

Figure 8. The Room Temperature and Liquid Nitrogen Temperature Infrared Spectra of Crystalline myo-Inositol

TABLE III

TABULATED FREQUENCIES FOR THE ROOM TEMPERATURE AND LIQUID NITROGEN TEMPERATURE RAMAN AND INFRARED SPECTRA OF myo-INOSITOL

RAMAN		INFRARED		RAMAN		INFRARED	
ROOM TEMPERATURE (cm^{-1})	LIQUID NITROGEN TEMPERATURE (cm^{-1})	ROOM TEMPERATURE (cm^{-1})	LIQUID NITROGEN TEMPERATURE (cm^{-1})	ROOM TEMPERATURE (cm^{-1})	LIQUID NITROGEN TEMPERATURE (cm^{-1})	ROOM TEMPERATURE (cm^{-1})	LIQUID NITROGEN TEMPERATURE (cm^{-1})
			3400 (sh)	902 (s)	900 (s)	896 (m)	900 (s)
		3380 (vs)	3360 (vs)		894 (sh)	890 (m,sh)	893 (m)
			3330 (vs)				~885 (vw,sh)
		3220 (vs)	3265 (vs)			~790 (vw,sh)	~790 (w,sh)
		3170 (vs)	3180 (vs)		~750 (w,b)		754 (m)
			3110 (vs)	738 (w)	729 (w)	730 (m)	736 (m)
2964 (m)	2963 (m)						711 (m)
	2947 (sh)	2955 (w)	2958 (w)		700 (vw,b)		694 (m)
2940 (m)	2938 (m)	2935 (w)	2935 (sh)		~660 (vvw,b)	~665 (w,b)	
2925 (vs)	2920 (vs)	2920 (m)	2917 (m)				654 (m)
	2900 (sh)	2900 (w)	2895 (w)				626 (m)
2887 (m)	2885 (m)	2880 (vw)	2880 (sh)	617 (w)	~615 (vvw,b)	608 (w,sh)	607 (m)
1454 (vvw)	1453 (vw)			~593 (vw)	~585 (vw,b)	584 (m)	589 (s)
	1447 (vw)	1445 (m)	1451 (m)	~575 (vvw)			581 (m,sh)
~1427 (vw,sh)	~1425 (vw)					557 (sh)	
1418 (w)	1414 (w)	1416 (m)	1420 (m)		529 (vvw)		529 (w,b)
~1406 (sh)	1397 (vw)		~1398 (sh)	509 (vs)	505 (vs)	500 (w)	~505 (sh)
		1379 (w,sh)	1382 (w)		~497 (sh)		500 (w)
1373 (sh)	1373 (w,sh)	1371 (m)	1373 (m)	467 (m)	465 (m)		
1360 (m)	1358 (m)	1355 (w)	1357 (w)			450 (w)	457 (m)
1344 (w)	1341 (w)	1343 (w)	1346 (w)	435 (vs)	430 (vs)	432 (m)	435 (m)
1328 (m)	1326 (m)	1323 (w)	1325 (m)				~431 (sh)
	1322 (m)				392 (m)	~391 (sh)	395 (sh)
1305 (w)	1303 (w)	~1312 (sh)	~1315 (sh)	393 (m)	~389 (sh)	387 (w)	390 (m)
			1288 (vw)		382 (vw)		
1282 (m)	1277 (m)	~1281 (vw,sh)	1279 (w)	378 (m)	374 (w)	367 (vw)	369 (w)
~1268 (vw)	1266 (w,sh)	1271 (w)	1274 (w)		~370 (vvw,sh)		
			~1266 (vw,sh)		364 (vvw)		
	~1251 (vvw,sh)		1258 (w)		352 (vw)		
1248 (w)	1245 (w)	1245 (m)	1247 (m)	~352 (vw)	343 (vvw)	344 (sh)	354 (w)
	1222 (w)	1222 (sh)	1225 (w)		333 (vvw)	329 (m)	338 (m)
1220 (w)	1216 (w)	1217 (w)	1220 (w)	~325 (w)	327 (w)		
1198 (vw)	1195 (vw)	1194 (m)	1197 (s)		314 (vvw)		316 (vw)
~1150 (vvw,sh)	~1153 (vvw,sh)		1150 (s)	312 (w)	306 (w)		
1143 (m)	1140 (m)	1145 (s)	1147 (s)		300 (vvw)	299 (vw)	302 (m)
1131 (m)	1132 (m)		~1133 (vw,sh)	296 (w)	292 (w)	~294 (sh)	295 (sh)
1122 (s)	1122 (s)		~1120 (sh)	~289 (vw,sh)	281 (vvw)	280 (m)	281 (m)
	1119 (sh)			277 (vvw)	271 (sh)	~275 (sh)	~276 (sh)
~1112 (sh)	1112 (s)	1111 (s)	~1112 (s)?		264 (vvw)		267 (vw)
	1107 (m)		~1107 (sh)	260 (vw)			245 (sh)
1097 (m)	1094 (m)	~1096 (sh)	1099 (w)	241 (vvw)		~229 (vw,sh)	237 (w)
	1070 (m)		~1071 (sh)	227 (vvw)		~221 (vw,sh)	226 (w)
1066 (s)	1061 (s)	~1063 (sh)	1065 (m,sh)			~208 (vw,sh)	215 (w)
1053 (m)	1049 (w)		1050 (vs)	210 (vw)		~200 (vw,sh)	203 (w)
~1048 (sh)	1042 (w)	1047 (vs)	1045 (vs)	~198 (vvw)			
1012 (m)	1009 (m)	1012 (m)	1016 (s)	~188 (vw)			
~1003 (sh)	999 (w)	999 (s)	1001 (s)	~171 (vw)			
936 (m)	933 (m)	927 (m)	930 (m)	160 (w)			

Conventional symbolism indicating relative intensity: s = strong, m = medium w = weak, sh = shoulder, b = broad, v = very

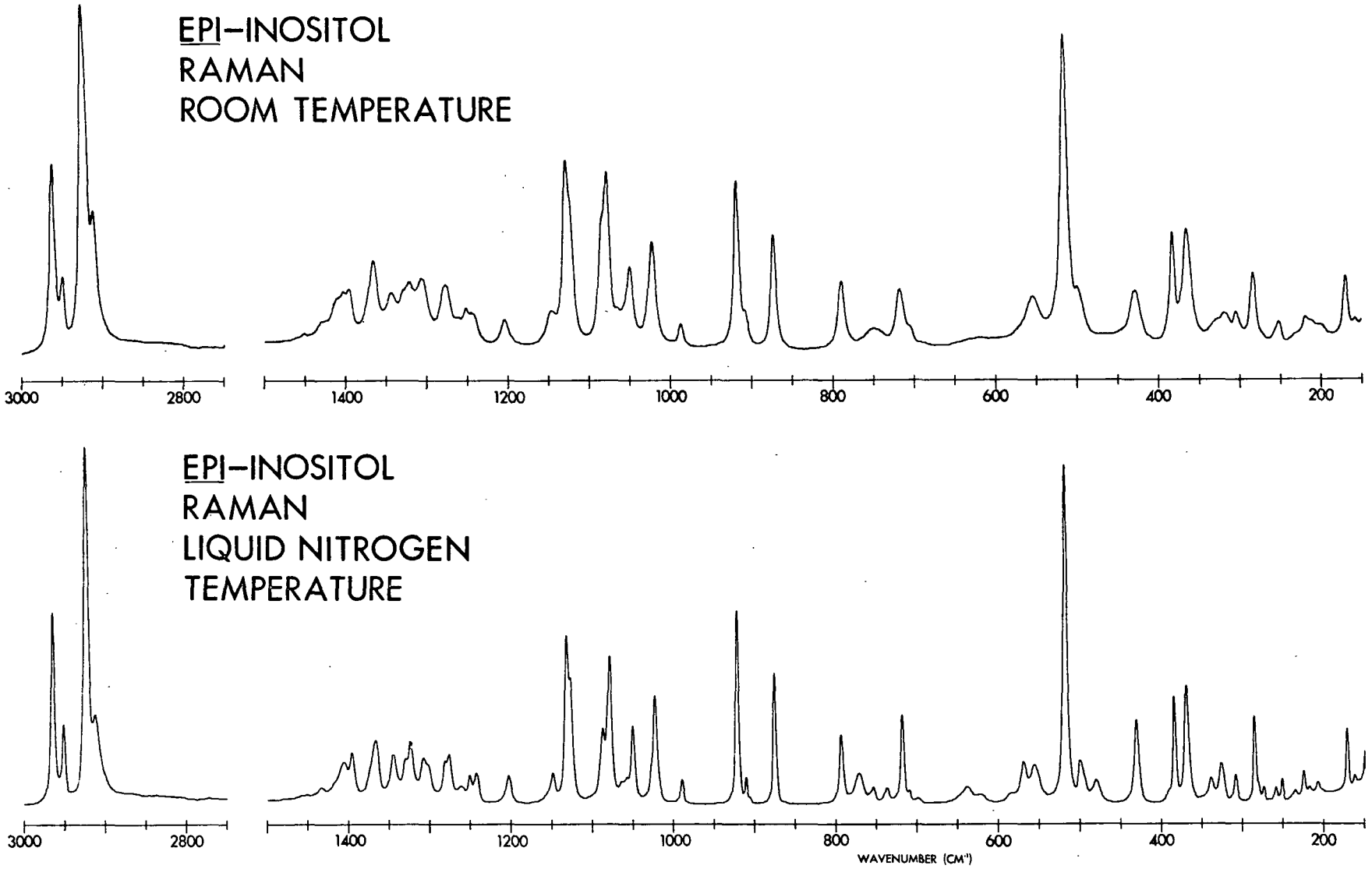

Figure 9. The Room Temperature and Liquid Nitrogen Temperature Raman Spectra of Crystalline epi-Inositol

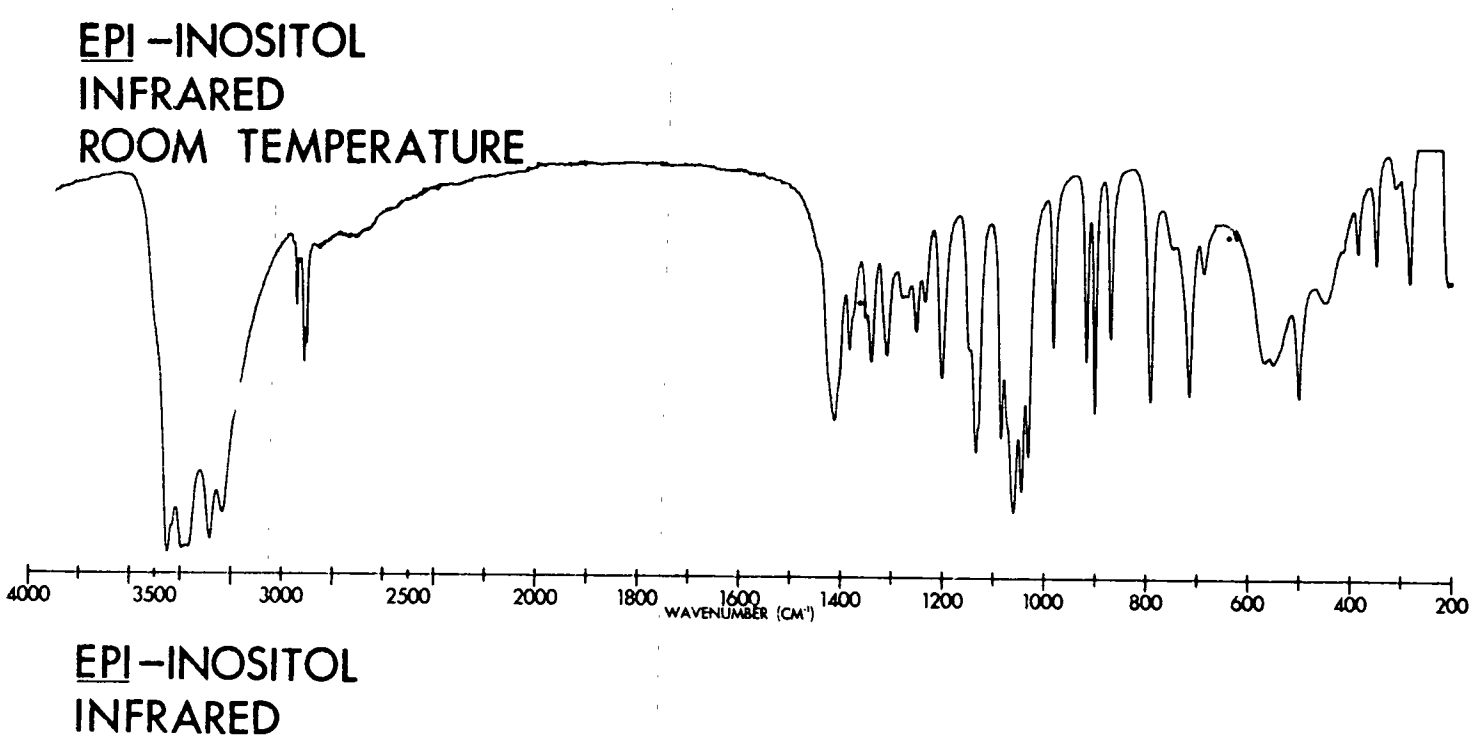

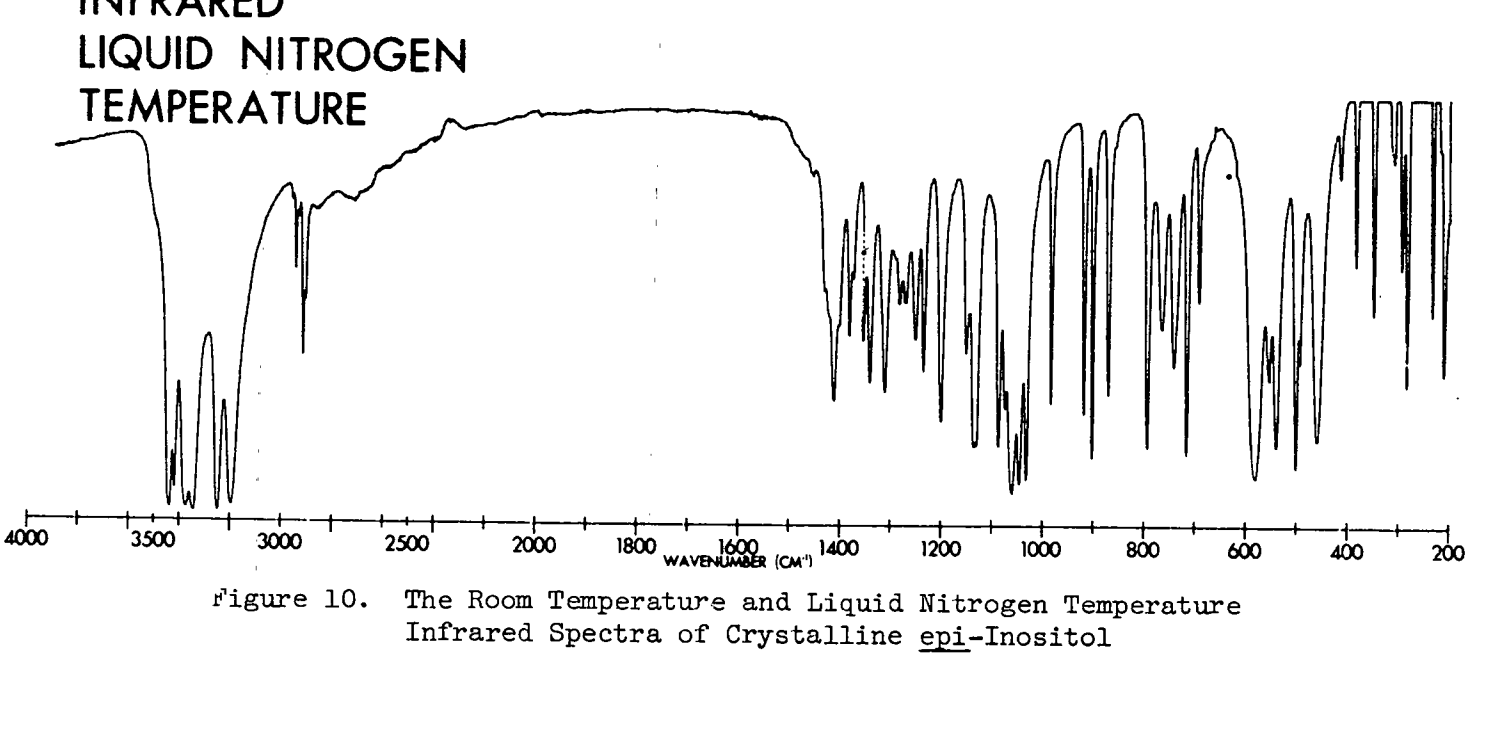

Figure 10. The Room Temperature and Liquid Nitrogen Temperature Infrared Spectra of Crystalline epi-Inositol

TABLE IV

TABULATED FREQUENCIES FOR THE ROOM TEMPERATURE AND LIQUID NITROGEN TEMPERATURE RAMAN AND INFRARED SPECTRA OF epi-INOSITOL

RAMAN		INFRARED		RAMAN		INFRARED	
ROOM TEMPERATURE (cm^{-1})	LIQUID NITROGEN TEMPERATURE (cm^{-1})	ROOM TEMPERATURE (cm^{-1})	LIQUID NITROGEN TEMPERATURE (cm^{-1})	ROOM TEMPERATURE (cm^{-1})	LIQUID NITROGEN TEMPERATURE (cm^{-1})	ROOM TEMPERATURE (cm^{-1})	LIQUID NITROGEN TEMPERATURE (cm^{-1})
		3450 (vs)	3440 (vs)	910 (w)	908 (w)	902 (s)	905 (s)
		3435 (sh)	3420 (vs)	874 (m)	874 (m)	872 (m)	874 (m)
		3390 (vs)	3380 (vs)			~858 (vw,sh)	~860 (vw,sh)
		3370 (vs)	3350 (vs)				843 (vvw)
		3285 (vs)	3250 (vs)	791 (m)	791 (m)	793 (s)	798 (s)
		3235 (vs)	3200 (vs)		770 (w)		770 (m)
2964 (s)	2964 (s)	2960 (sh)	2960 (vw)	750 (w,b)	753 (w)	749 (w)	746 (m)
2951 (m)	2949 (m)				736 (w)		
		2942 (w)	2942 (w)	718 (m)	716 (m)	716 (s)	720 (s)
2928 (vs)	2922 (vs)	2930 (vw)	2930 (vw)	706 (w,sh)	708 (vw,sh)		
		2918 (m)	2918 (m)	695 (vvw)	695 (vvw)	689 (w)	697 (m)
2913 (m)	2911 (m)	2905 (m)	2905 (sh)	625 (vw,vb)	636 (w,b)		
1450 (vw)	1450 (vw)				619 (vw)		
			1438 (m)		582 (vw)		585 (vs,b)
~1428 (w,sh)	1431 (w)	~1433 (sh)	1429 (sh)		567 (m)	569 (m)	
		1418 (m)	1418 (m)	556 (m)	553 (m)	552 (m)	558 (m)
~1410 (sh)	~1414 (sh)	~1407 (sh)	1407 (sh)				543 (s)
1403 (m)	1403 (m)			518 (vs)	515 (vs)		
1395 (m)	1393 (m)	1386 (m)	1387 (m)	501 (m,sh)	496 (m)	501 (s)	504 (s)
	1373 (sh)	1377 (w,sh)	1379 (w)			~493 (sh)	497 (m)
1366 (m)	1364 (m)				477 (w)		
		1352 (m)	1357 (m)			452 (m,b)	463 (m,b)
1344 (w)	1343 (m)	1341 (m)	1343 (m)	431 (m)	427 (m)		
1328 (sh)	1329 (sh)					417 (w)	419 (w)
1322 (m)	1321 (m)		1321 (sh)		388 (vvw,sh)		
1306 (m)	1306 (m)	1310 (m)	1313 (m)	385 (m)	381 (m)	386 (m)	391 (m)
	1301 (sh)		1293 (vw)	367 (m)	366 (m)		
	1279 (sh)	1280 (w)	1284 (w)			350 (m)	356 (m)
1276 (m)	1275 (m)	1271 (w)	1271 (w)	330 (w,sh)	336 (w)		341 (w)
~1258 (w)	1258 (vw)			321 (w)	323 (m)	313 (w)	321 (w)
1252 (w)	1249 (w)	1251 (m)	1252 (m)				316 (w)
1243 (w,sh)	1240 (w)	1234 (w)	1236 (m)	306 (w)	305 (w)	~295 (sh)	302 (m)
1204 (w)	1201 (w)	1202 (m)	1202 (s)	285 (m)	282 (m)	285 (m)	290 (m)
1147 (w)	1147 (w)	1149 (m,sh)	1153 (m)	~275 (vvw,sh)	~270 (w)	~275 (sh)	~277 (vvw)
1130 (s)	1129 (s)	1136 (s)	1138 (s)		263 (vvw)		259 (vw)
1125 (sh)	1125 (sh)	1131 (s,sh)	1132 (s)		255 (vw)		
			~1105 (vvw,sh)	252 (w)	247 (w)	243 (sh)	249 (w)
1085 (sh)	1085 (m)	1086 (s)	1090 (s)	234 (vw,sh)	231 (vvw)	236 (m)	241 (m)
1079 (s)	1077 (s)	1076 (sh)	1076 (m)	220 (vw)	221 (w)		226 (sh)
1066 (vvw)	1063 (vw,sh)	1062 (vs)	1062 (vs)	214 (vw)	214 (vvw)	211 (m)	218 (m)
~1056 (sh)	1056 (vw,sh)		1058 (sh)	201 (vw)	203 (vw)		
1050 (m)	1048 (m)	1047 (vs)	1048 (vs)		193 (vvw)		
		1033 (s)	1034 (vs)		182 (vvw)		
1023 (m)	1020 (m)		~1015 (vw,sh)	171 (m)	169 (m)		
988 (w)	988 (w)	984 (m)	987 (m)	158 (vw)	159 (vw)		
919 (s)	919 (s)	919 (m)	922 (m)				

Conventional symbolism indicating relative intensity: s = strong, m = medium, w = weak, sh = shoulder, b = broad, v = very

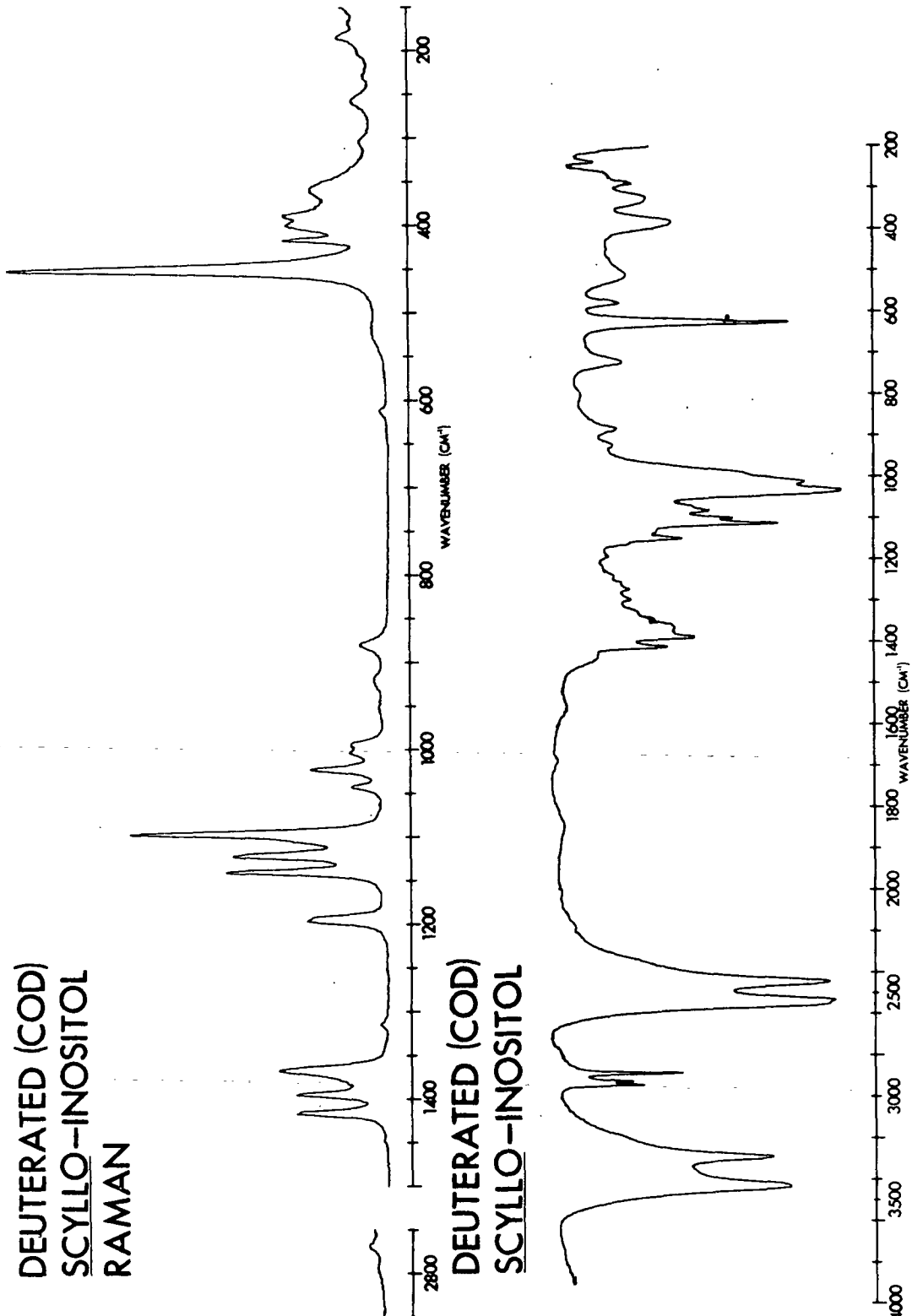

Figure 11. The Room Temperature Raman and Infrared Spectra of Crystalline Oxygen Deuterated scyllo-Inositol

TABLE V

TABULATED FREQUENCIES FOR THE RAMAN AND INFRARED SPECTRA OF DEUTERATED (COD) scyllo-INOSITOL

RAMAN (cm^{-1})	INFRARED (cm^{-1})	RAMAN (cm^{-1})	INFRARED (cm^{-1})
1416 (m)	1416 (m)	994 (w)	990 (sh)
1394 (m)	1392 (m)	952 (vw)	
1366 (m)	1367 (w,sh)		926 (w)
	1345 (vw,sh)	921 (vw)	
	1328 (vw)	880 (w)	885 (w)
1315 (vw)			724 (m)
	1298 (w)		627 (s)
	1273 (w)	613 (vw)	
	1256 (vw)		582 (m)
	1242 (vw)	525 (vw)	
1194 (m)	1195 (vw)		513 (m)
	1167 (vw,sh)	451 (vs)	
	1151 (m)	417 (m)	
1139 (m)	1133 (vw,sh)	400 (m)	
1121 (m)		389 (m)	387 (m)
	1114 (s)	360 (m,b)	
1106 (sh)	1102 (m)		329 (m)
1096 (s)		305 (vw)	
	1083 (m)	292 (w)	292 (w)
	1072 (w,sh)		265 (vw,sh)
1042 (w)			251 (vw)
	1034 (vs)		240 (w)
1023 (m)		231 (vw)	
	1013 (vs)	185 (w)	
1003 (w)			

Conventional symbolism indicating relative intensity: vs = very strong, s = strong, m = medium, w = weak, vw = very weak, sh = shoulder, b = broad.

Oxygen Deuterated neo-Inositol

The Raman and infrared spectra are shown in Fig. 12. The frequencies of the bands are tabulated in Table VI.

Oxygen Deuterated myo-Inositol

The Raman and infrared spectra are shown in Fig. 13. The frequencies of the bands are tabulated in Table VII.

Oxygen Deuterated epi-Inositol

The Raman and infrared spectra are shown in Fig. 14. The frequencies of the bands are tabulated in Table VIII.

The percentage deuteration, as estimated from the relative intensities of the O-H and O-D stretching bands, was approximately 70% for scyllo-inositol, neo-inositol and myo-inositol and 80% for epi-inositol.

The dots (•) which appear in the infrared spectra at approximately 1350 cm^{-1} indicate where the mulls were changed. The dots which appear in some of the infrared spectra at 625 cm^{-1} indicate the noticeable manifestation of a grating change.

RAMAN SPECTRA OF scyllo-INOSITOL, myo-INOSITOL AND epi-INOSITOL IN WATER SOLUTION

scyllo-Inositol

The Raman spectrum of scyllo-inositol in water solution is shown in Fig. 15. The frequencies of the bands are tabulated in Table IX.

myo-Inositol

The Raman spectrum of myo-inositol in water solution is shown in Fig. 15 also. The frequencies of the bands are tabulated in Table X.

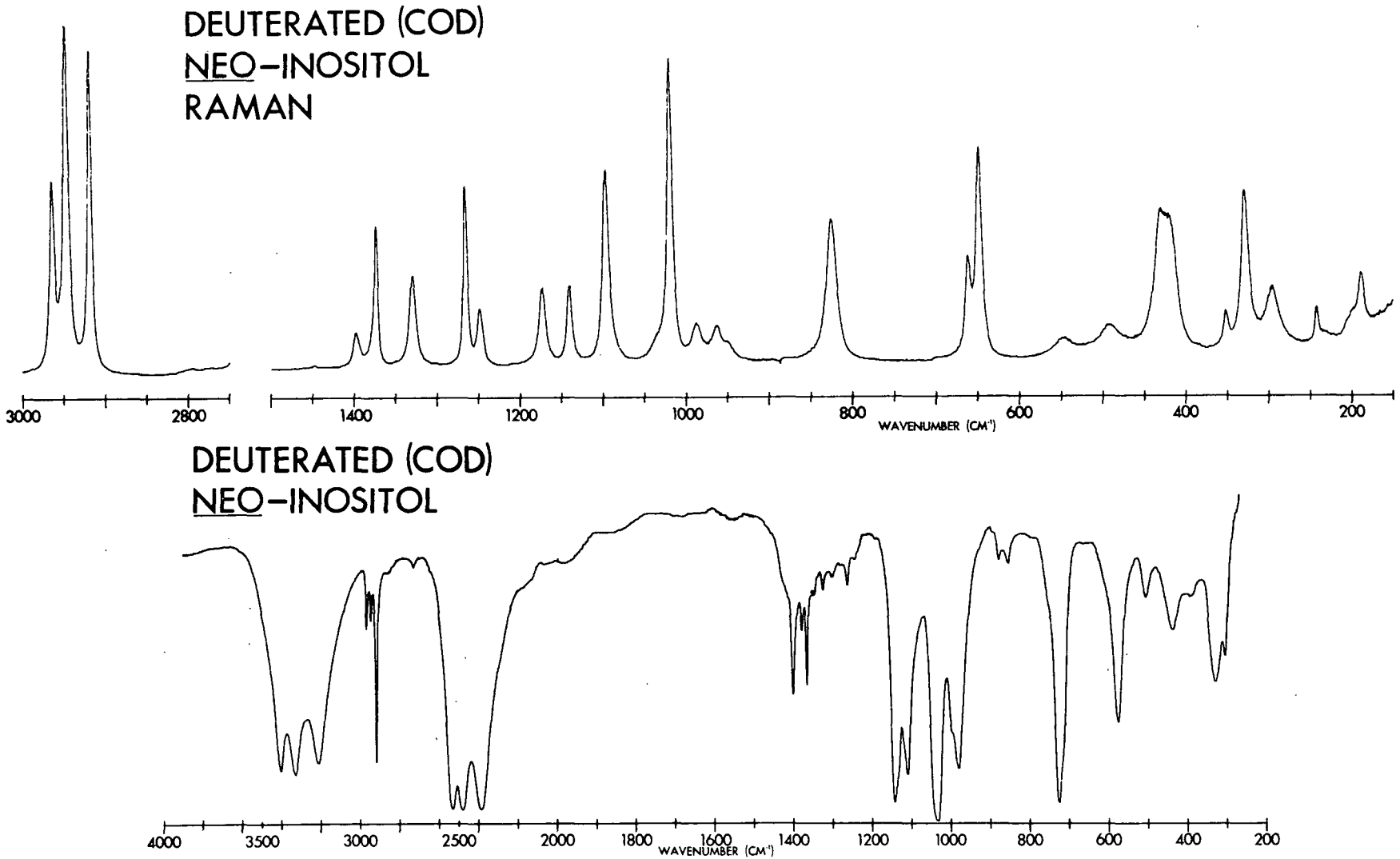

Figure 12. The Room Temperature Raman and Infrared Spectra of Crystalline Oxygen Deuterated neo-Inositol

TABLE VI

TABULATED FREQUENCIES FOR THE RAMAN AND INFRARED SPECTRA OF DEUTERATED (COD) neo-INOSITOL

RAMAN (cm^{-1})	INFRARED (cm^{-1})	RAMAN (cm^{-1})	INFRARED (cm^{-1})
	1405 (m)		880 (w)
1396 (m)			856 (w)
	1381 (w)	824 (s)	
1373 (s)			755 (sh)
	1368 (m)		727 (vs)
	1347 (vw)		712 (sh)
1329 (m)		660 (m)	
	1326 (w)	646 (s)	
	1303 (vw)		577 (s)
1265 (s)	1264 (w)	542 (w,b)	
1246 (m)	1246 (vw)		507 (m)
1172 (m)		490 (w,b)	
	1145 (vs)		438 (m)
1138 (m)	1133 (sh)	423 (m,b)	
	1120 (sh)		393 (w)
	1112 (s)	349 (w)	
1095 (s)			330 (m)
	1037 (vs)	326 (m)	
1018 (vs)			306 (m)
	999 (sh)	294 (m)	
986 (m)	987 (s)	239 (w)	
961 (m)		187 (m)	
948 (w)			

Conventional symbolism indicating relative intensity: vs = very strong, s = strong, m = medium, w = weak, vw = very weak, sh = shoulder, b = broad

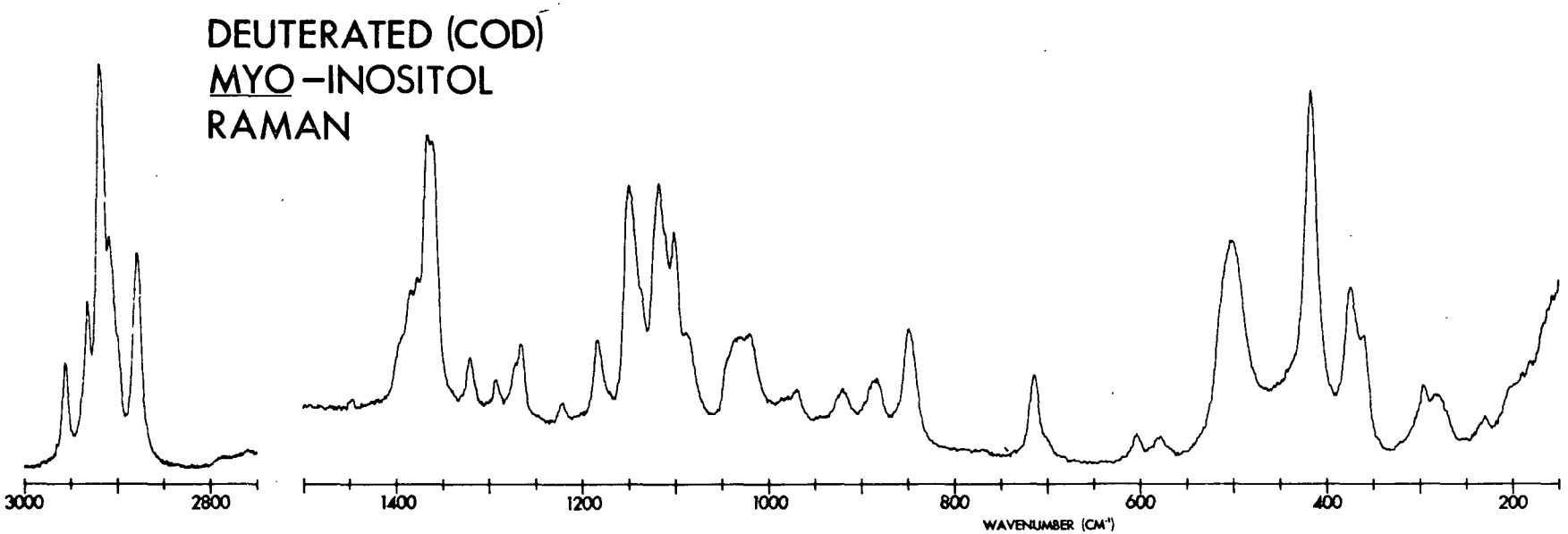

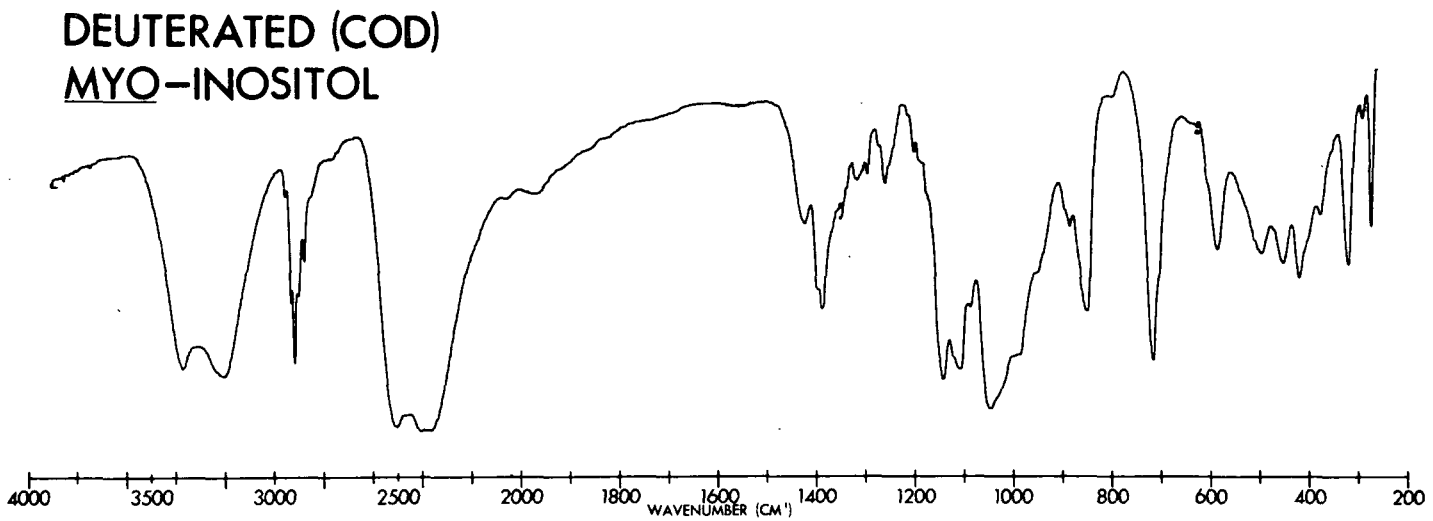

Figure 13. The Room Temperature Raman and Infrared Spectra of Crystalline Oxygen Deuterated myo-Inositol

TABLE VII

TABULATED FREQUENCIES FOR THE RAMAN AND INFRARED SPECTRA OF DEUTERATED (COD) myo-INOSITOL

RAMAN (cm^{-1})	INFRARED (cm^{-1})	RAMAN (cm^{-1})	INFRARED (cm^{-1})
	1427 (m)	988 (sh)	986 (vs)
1400 (sh)	1398 (s,sh)	972 (w)	
1387 (m)	1390 (s)		949 (s,sh)
1379 (m)		923 (w)	
1368 (s)	1372 (sh)	887 (w)	886 (w)
1362 (s)		854 (m)	851 (s)
1323 (w)	1319 (w)	716 (m)	716 (vs)
1296 (w)	1297 (w)	704 (vw,sh)	703 (sh)
1274 (w,sh)	1276 (vw)	605 (w)	607 (sh)
1268 (m)	1261 (w)	583 (w)	587 (m)
1225 (vw)		500 (s,b)	497 (m)
	1203 (vw)		452 (m)
1187 (m)	1187 (vw,sh)	417 (vs)	420 (m)
	1175 (vw,sh)	375 (s)	377 (w)
1151 (s)	1153 (sh)	362 (m)	354 (vvw)
1140 (w,sh)	1144 (vs)		320 (m)
1119 (s)	1123 (vs)	298 (w)	292 (vw)
1103 (s)	1109 (vs)	282 (w)	
1089 (m)	1087 (s)		274 (m)
1048 (sh)	1049 (vs)		250 (w)
1035 (m)	1030 (vs)	233 (vw)	
1024 (m)		162 (vw)	

Conventional symbolism indicating relative intensity: vs = very strong, s = strong, m = medium, w = weak, vw = very weak, sh = shoulder, b = broad

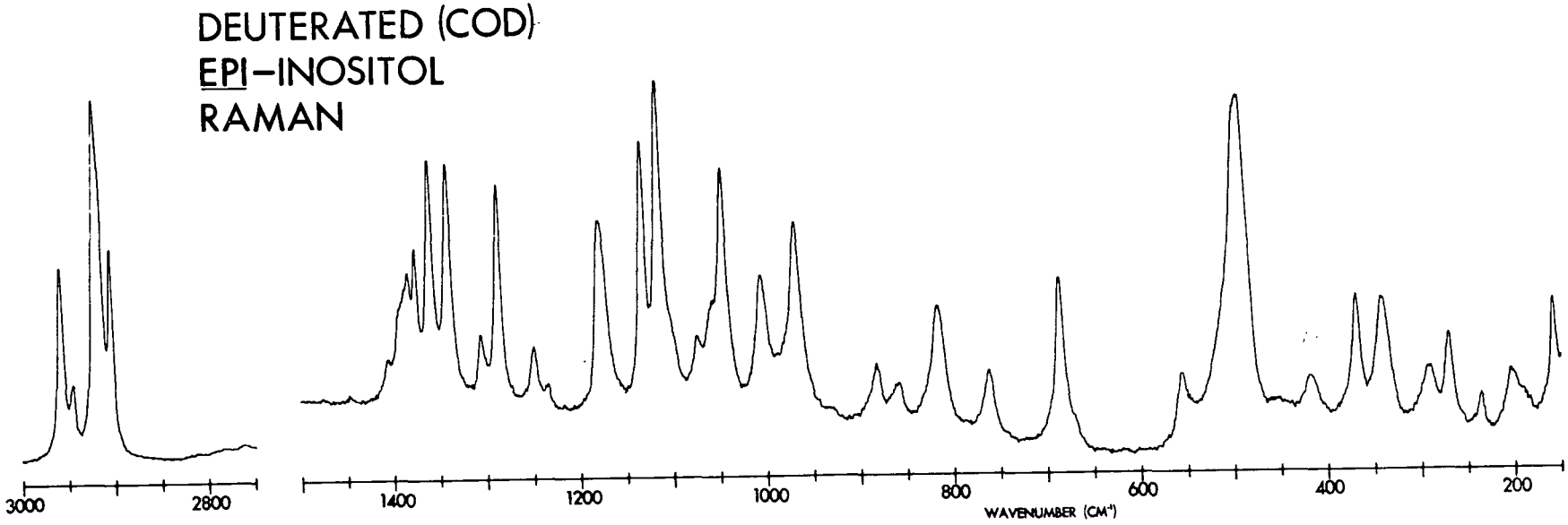

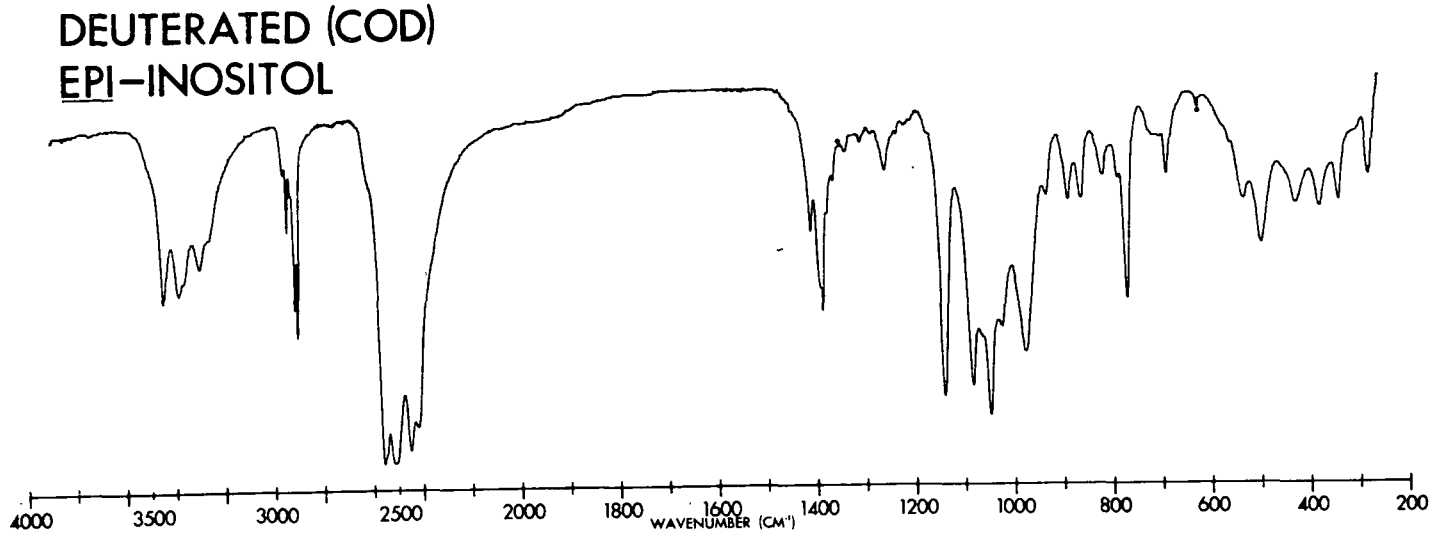

Figure 14. The Room Temperature Raman and Infrared Spectra of Crystalline Oxygen Deuterated epi-Inositol

TABLE VIII

TABULATED FREQUENCIES FOR THE RAMAN AND INFRARED SPECTRA OF DEUTERATED (COD) epi-INOSITOL

RAMAN (cm^{-1})	INFRARED (cm^{-1})	RAMAN (cm^{-1})	INFRARED (cm^{-1})
	1415 (m)		934 (m)
1407 (w,sh)		882 (w)	889 (m)
	1395 (m)	860 (w)	863 (m)
1389 (sh)	1390 (s)	817 (m)	819 (w)
1383 (m)	1381 (sh)		788 (w)
1375 (m)			771 (s)
1361 (s)	1367 (w)	763 (w)	
1341 (s)	1344 (vw)		713 (w,b)
1306 (m)	1311 (vw)	686 (m)	688 (w)
1287 (s)	1291 (vw)	555 (w)	562 (vw,sh)
	1261 (w)		533 (m)
1250 (w)		494 (vs)	498 (m)
1235 (w)	1238 (vw)		427 (m)
	1223 (vw)	418 (w)	
1177 (m)	1175 (vw,sh)		380 (m)
	1142 (vs)	368 (m)	
1134 (s)		340 (m)	341 (m)
1115 (vs)			308 (vw)
	1085 (vs)	289 (w)	
1071 (m)	1065 (sh)		280 (m)
1058 (m,sh)		271 (w)	
1046 (s)	1049 (vs)	236 (vw)	
	1025 (s)	200 (w)	
1005 (m)		158 (w)	
	977 (s)		
969 (m)			

Conventional symbolism indicating relative intensity: vs = very strong, s = strong, m = medium, w = weak, vw = very weak, sh = shoulder, b = broad

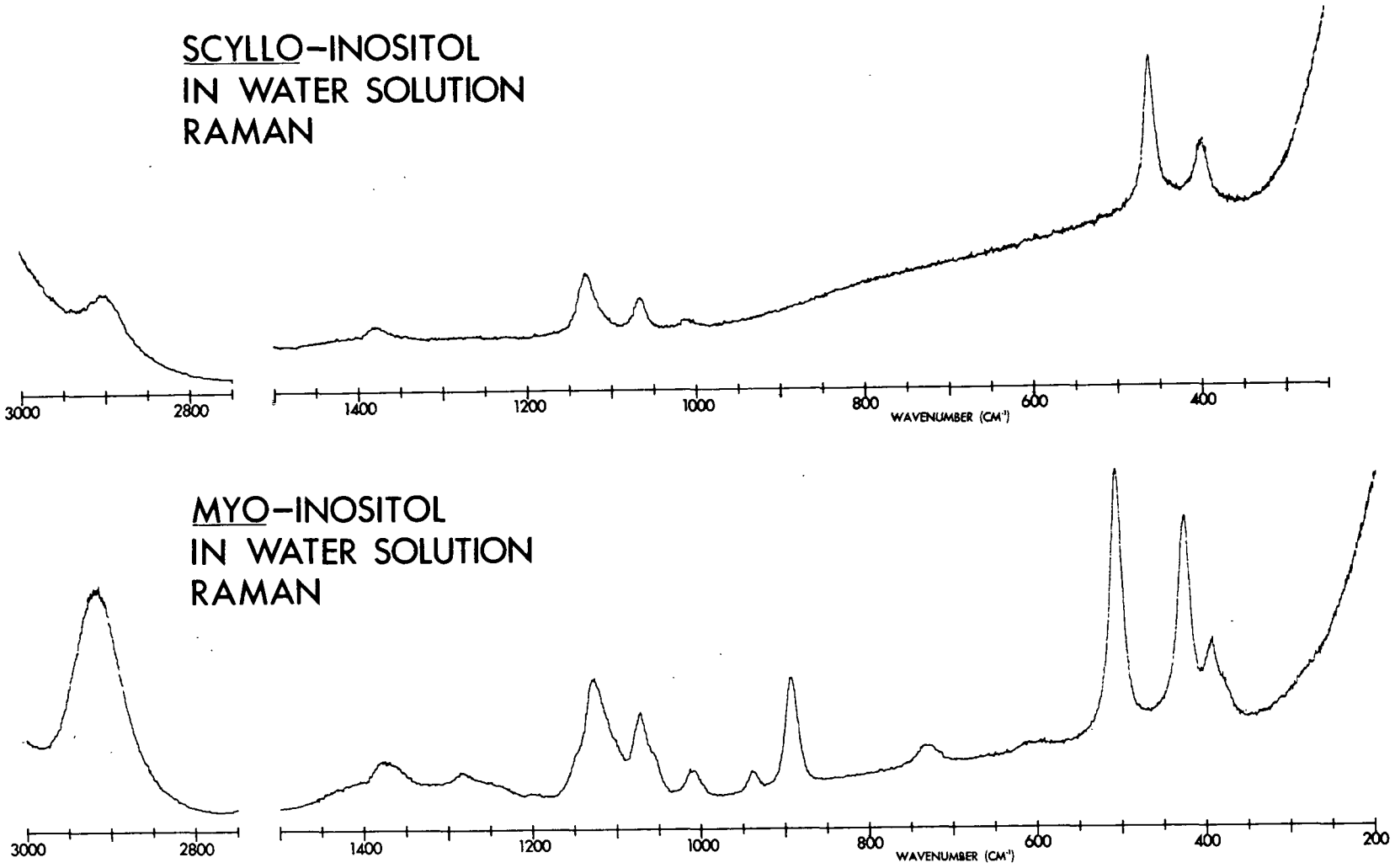

Figure 15. The Raman Spectra of the Water Solutions of scyllo-Inositol and myo-Inositol

TABLE IX

TABULATED FREQUENCIES FOR THE RAMAN WATER SOLUTION SPECTRUM OF scyllo-INOSITOL

RAMAN FREQUENCIES (cm^{-1})
1379 (vw)
1127 (m)
1063 (m)
456 (s)
396 (m)

See footnote below.

TABLE X

TABULATED FREQUENCIES FOR THE RAMAN WATER SOLUTION SPECTRUM OF myo-INOSITOL

RAMAN FREQUENCIES (cm^{-1})	RAMAN FREQUENCIES (cm^{-1})
1371 (w,vb)	936 (w)
1283 (w,b)	889 (m)
1145 (sh)	729 (w)
1125 (m)	504 (vs)
1070 (m)	423 (s)
1050 (sh)	390 (m)
1008 (w)	375 (sh)

Conventional symbolism indicating relative intensity: vs = very strong, s = strong, m = medium, w = weak, vw = very weak, sh = shoulder, b = broad.

epi-Inositol

The Raman spectrum of epi-inositol in water solution is shown in Fig. 16. The frequencies of the bands are tabulated in Table XI.

TABLE XI

TABULATED FREQUENCIES FOR THE RAMAN WATER SOLUTION SPECTRUM OF epi-INOSITOL

RAMAN FREQUENCIES (cm^{-1})	RAMAN FREQUENCIES (cm^{-1})
1400 (w,vb)	869 (m)
1285 (w,b)	808 (m)
1131 (m)	731 (w)
1080 (m)	568 (vw)
1046 (m)	506 (vs)
980 (vw)	428 (m)
915 (m)	397 (m)
894 (w,sh)	360 (w)

Conventional symbolism indicating relative intensity:
vs = very strong, s = strong, m = medium, w = weak,
vw = very weak, sh = shoulder, b = broad.

MEASURED DEPOLARIZATION RATIOS FOR WATER SOLUTIONS OF scyllo-INOSITOL, myo-INOSITOL AND epi-INOSITOL

Depolarization ratios were calculated for the vibrational bands observed in the water solution spectra of scyllo-inositol, myo-inositol and epi-inositol. The depolarization ratios are listed in Tables XII through XIV, respectively. The depolarization ratios for some of the bands are questionable either because the bands are weak or because they overlap with adjacent bands. The bands in question are noted in the tables. Bands above 1150 cm^{-1} were not considered because their broadness, overlapping and weak intensity prohibited resolution and identification of individual bands.

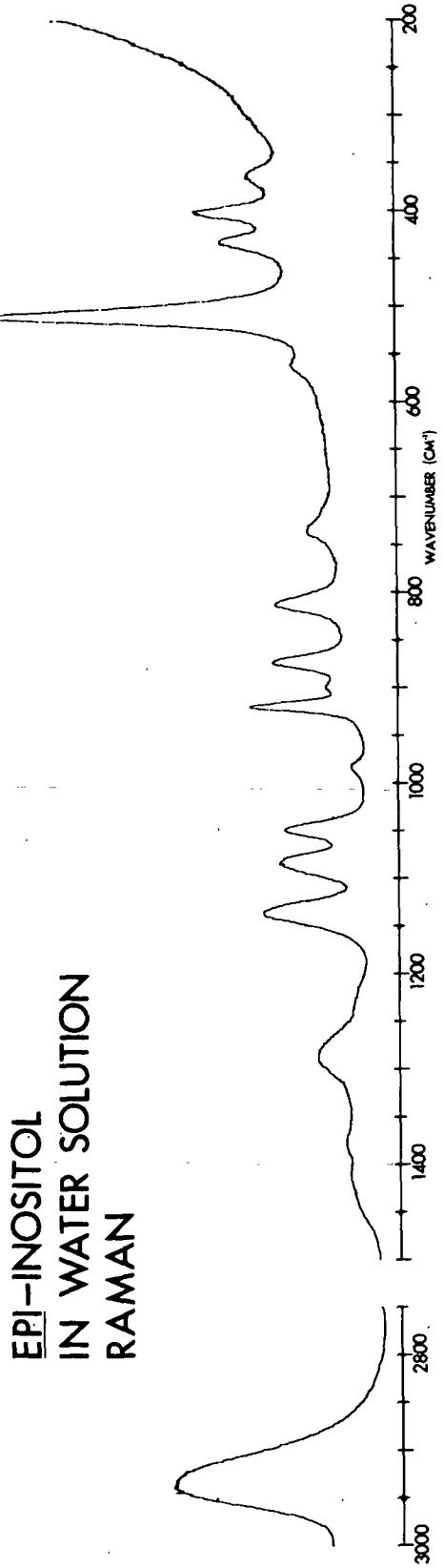

Figure 16. The Raman Spectrum of the Water Solution of epi-Inositol

TABLE XII

MEASURED DEPOLARIZATION RATIOS FOR A WATER SOLUTION OF scyllo-INOSITOL

RAMAN FREQUENCIES (cm^{-1})	ρ^a, H_2O
1127	0.53
1063	0.07
456	0.07
396	0.76

[a] ρ designates the depolarization ratio.

TABLE XIII

MEASURED DEPOLARIZATION RATIOS FOR A WATER SOLUTION OF myo-INOSITOL

RAMAN FREQUENCIES (cm^{-1})	ρ^a, H_2O	RAMAN FREQUENCIES (cm^{-1})	ρ^a, H_2O
1145[b]	--	889[c]	0.06
1125[b]	0.42	729[c]	0.50
1070[b]	0.26	504	0.07
1050[b]	--	423	0.16
1008	0.58	390[c]	0.79
936[c]	0.75	375[c]	--

[a] ρ designates the depolarization ratio.

[b] Measured depolarization ratio is questionable because band is overlapped with neighboring bands.

[c] Measured depolarization ratio is questionable because band is weak.

TABLE XIV

MEASURED DEPOLARIZATION RATIOS FOR A WATER SOLUTION OF epi-INOSITOL

RAMAN FREQUENCIES (cm^{-1})	ρ^a, H_2O	RAMAN FREQUENCIES (cm^{-1})	ρ^a, H_2O
1131	0.27	808	0.13
1080	0.62	731[b]	0.27
1046[b]	0.72	568[b]	--
980[b]	--	506	0.08
915[b]	0.22	428	0.07
894[b]	--	397	0.44
869	0.07	360	0.69

[a] ρ designates the depolarization ratio.

[b] Measured depolarization ratio is questionable because band is weak.

The instrumental arrangement was checked for accuracy using carbon tetrachloride as a standard. The Raman spectrum of carbon tetrachloride has two bands at 219 cm^{-1} and 316 cm^{-1} which are not polarized and a band at 459 cm^{-1} which is highly polarized. The depolarization ratios for these bands are shown in Table XV.

TABLE XV

MEASURED DEPOLARIZATION RATIOS FOR CCl_4

RAMAN FREQUENCIES (cm^{-1})	ρ^a, CCl_4
459	0.004
316	0.76
219	0.77

[a] ρ designates the depolarization ratio.

VIBRATIONAL ANALYSES

MOLECULAR MODEL AND NORMAL COORDINATE ANALYSIS TREATMENT

The normal coordinate analysis treatment is a mathematical simulation of molecular vibrations which allows calculation of theoretical fundamental vibrational frequencies and their associated atomic motions for a molecule. In this section, the assumptions made in constructing the molecular model and the information needed to perform the normal coordinate analyses of the inositols will be surveyed. The equations shown will be the result of the mathematical derivation. A more explicit and complete treatment of the mathematical development is given in Wilson, et al. (31).

The basis for the normal coordinate analysis is an assumed simplified molecular model. The model employed is described in detail in Wilson, et al. (31). In the model, particles representing the atoms of a molecule are assumed to have their mass concentrated at a point. For this investigation, the bonds which hold the particles together are assumed to be like weightless springs which obey Hooke's law. The intramolecular forces represent the response of the springs to small displacement of the atoms from an equilibrium configuration. This model is used in both the classical treatment and quantum mechanical treatment of molecular vibrations. The model is specified such that it is consistent with the laws of quantum mechanics.

In the molecular model, the kinetic and potential energies associated with the atomic displacements are defined in terms of a suitable set of coordinates. A commonly used set of coordinates, called internal coordinates, were utilized in this work. Internal coordinates constitute a complete set which describe all the possible deformations of the internal configuration of a molecule but are unaffected by translations or rotations of the molecule as a whole. In addition, internal

coordinates allow the potential energy of a molecule to be described in a physically meaningful manner.

Seventy-eight internal coordinates were defined for the inositols. As an illustration, the internal coordinates defined for scyllo-inositol are shown in Table XVI. Twenty-four bond stretching, forty-two angle bending and twelve torsion coordinates were defined. The bond stretching and valence angle bending coordinates are identically defined for all the inositols. The torsion coordinates around the C-C and C-O bonds were defined using the procedure described by Hilderbrandt (32). The C-C ring torsions were defined in terms of the atoms in the anti-configuration, i.e., $A\text{-}C\text{-}C\text{-}B$, around each C-C bond. For each C-C bond there are three such four-atom trans-groups. Each C-C torsion was defined by taking a normalized linear combination of the three trans-groups. The C-O torsions were defined in a similar manner except the three groups are not all defined in the anti-configuration because only a single atom is attached to the oxygen. As illustrations, the C-C and C-O torsion definitions for scyllo-inositol are listed in Table XVI. The normalization constant 1/3, calculated by Hilderbrandt for normalizing the linear combinations of the three groups, was used in defining both the C-C and C-O torsions. The internal coordinate definitions for the other inositols are listed in Appendix II.

While seventy-eight internal coordinates were defined, the inositols have only sixty-six (3N-6, where N = 24 atoms for the inositols) degrees of vibrational freedom. There are, then, twelve redundancies. Six of these are local around each carbon and can be removed, whereas the six others are due to the cylic nature of the molecules and are not removable. All twelve were retained to facilitate the construction of the force field and the symmetry coordinates, which will be discussed later in this section.

TABLE XVI

INTERNAL COORDINATE DEFINITIONS FOR scyllo-INOSITOL

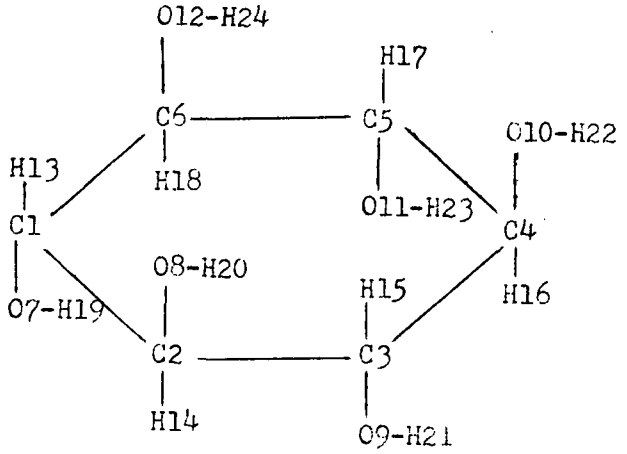

Valence Bond Coordinates

1. C1-C2	7. C1-O7	13. C1-H13	19. O7-H19
2. C2-C3	8. C2-O8	14. C2-H14	20. O8-H20
3. C3-C4	9. C3-O9	15. C3-H15	21. O9-H21
4. C4-C5	10. C4-O10	16. C4-H16	22. O10-H22
5. C5-C6	11. C5-O11	17. C5-H17	23. O11-H23
6. C6-C1	12. C6-O12	18. C6-H18	24. O12-H24

Valence Bond Angle Coordinates

25. C1-C2-C3	36. O9-C3-C4	47. H15-C3-C2	57. H15-C3-O9
26. C2-C3-C4	37. O10-C4-C3	48. H15-C3-C4	58. H16-C4-O10
27. C3-C4-C5	38. O10-C4-C5	49. H16-C4-C3	59. H17-C5-O11
28. C4-C5-C6	39. O11-C5-C4	50. H16-C4-C5	60. H18-C6-O12
29. C5-C6-C1	40. O11-C5-C6	51. H17-C5-C4	61. C1-O7-H19
30. C6-C1-C2	41. O12-C6-C5	52. H17-C5-C6	62. C2-O8-H20
31. O7-C1-C6	42. O12-C6-C1	53. H18-C6-C5	63. C3-O9-H21
32. O7-C1-C2	43. H13-C1-C6	54. H18-C6-C1	64. C4-O10-H22
33. O8-C2-C1	44. H13-C1-C2	55. H13-C1-O7	65. C5-O11-H23
34. O8-C2-C3	45. H14-C2-C1	56. H14-C2-O8	66. C6-O12-H24
35. O9-C2-C3	46. H14-C2-C3		

Valence Bond Angle Torsion Coordinates

67. C6-C1-C2-O8 H13-C1-C2-H14 O7-C1-C2-C3	70. C3-C4-C5-O11 O10-C4-C5-C6 H16-C4-C5-H17	73. H19-O7-C1-H13 H19-O7-C1-C6 H19-O7-C1-C2	76. H22-O10-C4-H16 H22-O10-C4-C3 H22-O10-C4-C5
68. C1-C2-C3-O9 O8-C2-C3-C4 H14-C2-C3-H15	71. C4-C5-C6-O12 O11-C5-C6-C1 H17-C5-C6-H18	74. H20-O8-C2-H14 H20-O8-C2-C1 H20-O8-C2-C3	77. H23-O11-C5-H17 H23-O11-C5-C4 H23-O11-C5-C6
69. C2-C3-C4-O10 O9-C3-C4-C5 H15-C3-C4-H16	72. C5-C6-C1-O7 O12-C6-C1-C2 O18-C6-C1-H13	**75. H21-O9-C3-H15** **H21-O9-C3-C2** **H21-O9-C3-C4**	78. H24-O12-C6-H18 H24-O12-C6-C5 H24-O12-C6-C1

Once constructed, the kinetic and potential energies are substituted into the equations of motion and a solution to the equations assumed. A set of algebraic equations results, which are shown as matrices in terms of internal coordinates in Equation (1):

$$(\underset{\sim}{GF} - \lambda_k E)\, l_k = 0 \qquad k = 1,\ldots,78 \qquad (1)$$

where $\underset{\sim}{G}$ = inverse kinetic energy matrix

$\underset{\sim}{F}$ = force constant matrix

λ_k = frequency parameter = $4\pi^2 \nu_k^2$, where ν_k is the frequency of the kth fundamental vibration

l_k = column vector of the amplitudes of the displacement coordinates of the kth vibration

In this equation, k would go from one through seventy-eight. However, twelve of the λ_k values would be zero, i.e., no net internal motion of the molecule, representing the frequencies resulting from the redundant internal coordinates.

The condition that nonzero l_k vectors, the displacement coordinates, exist is that the matrix resulting from the part of Equation (1) in parentheses, $(\underset{\sim}{GF} - \lambda_k E)$, has no inverse (33). This will be true when

$$|\underset{\sim}{GF} - \lambda_k E| = 0 \qquad (2)$$

Only certain values of λ_k, the eigenvalues, will satisfy this determinental equation. For each λ_k, the corresponding motions of the internal coordinates are at the same frequency and phase but the amplitudes usually are different. A vibrational mode having these characteristics is called a normal mode of vibration and the corresponding frequency is a fundamental, or normal, frequency of vibration. It is the solution of this determinental equation, the vibrational secular equation, which is the heart of the normal coordinate analysis. Numerical solution of the vibrational secular equation to obtain the fundamental vibrational

frequencies calculated from the λ_k, and the atomic motions ($\underline{l}_k$) of a molecule requires that an explicit form be given to the $\underline{G}$ and $\underline{F}$ matrices in Equation (1).

$\underline{G}$ MATRIX

The molecular model geometry is specified by calculating the relative positions, in cartesian coordinates, of the 'atoms' in the model. In practice, the $\underline{G}$ matrix is calculated by determining a transformation, the $\underline{B}$ matrix, from cartesian coordinates to internal coordinates. This transformation and the masses of the 'atoms' are then used to calculate the $\underline{G}$ matrix. In Equation (1), the $\underline{G}$ matrix is in terms of the internal coordinates. The dimension of the $\underline{G}$ matrix is equal to the number of internal coordinates defined, seventy-eight for the inositols.

In this study, molecular geometries based on both assumed tetrahedral models and x-ray crystal structures were used to construct $\underline{G}$ matrices. Tetrahedral geometry models were assumed for all the inositols and $\underline{G}$ matrices were constructed based on these models. In the tetrahedral models, the six-membered rings were defined in the most stable chair conformations. The ring torsional (dihedral) angles were set equal to 60°. All the bond angles were assumed to be tetrahedral. Common bond types were assigned the same bond length. The bond lengths used in the inositol models are listed in Table XVII. The hydroxyl groups were oriented so the symmetry of the molecule was maintained and yet the steric interactions were minimized. 'Ball-and-stick' drawings of the tetrahedral models for scyllo-inositol, neo-inositol, myo-inositol, and epi-inositol are shown in Fig. 17. The atom numbering sequences used for defining the relative atom positions and internal coordinates are also shown.

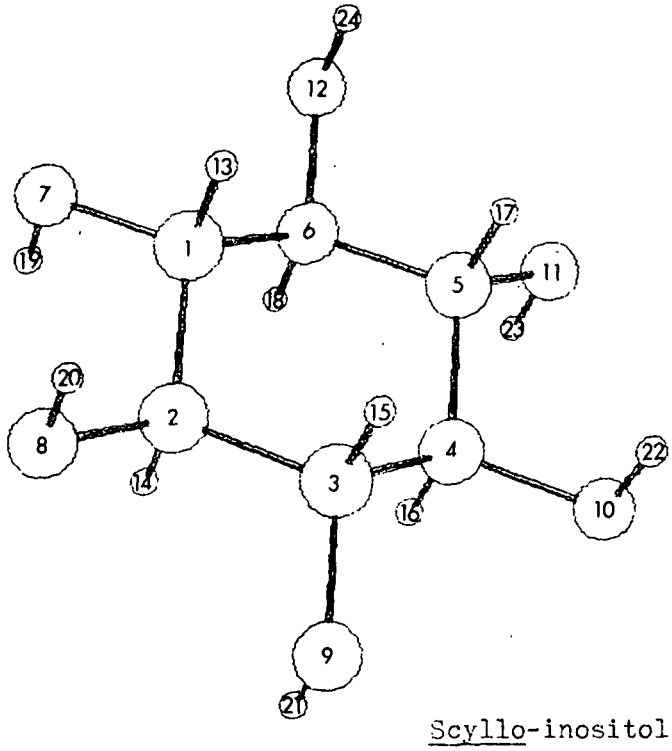

Scyllo-inositol

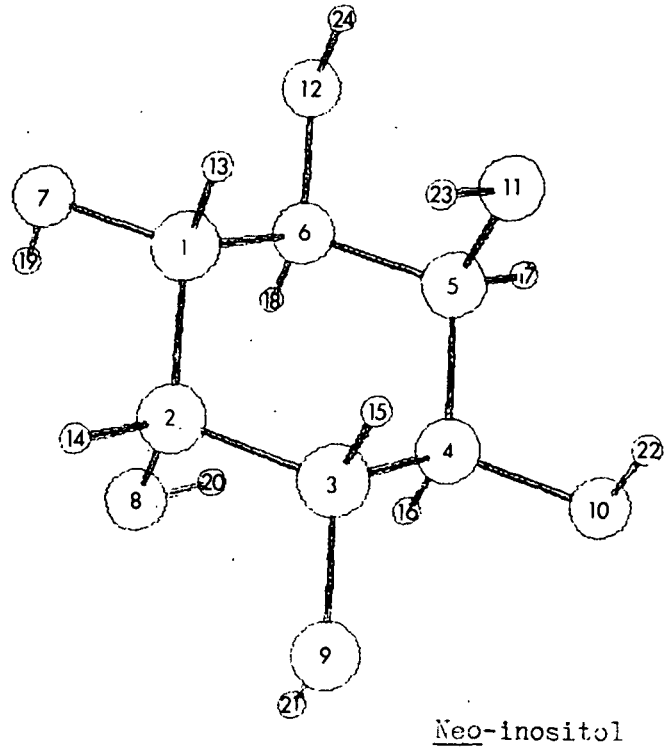

Neo-inositol

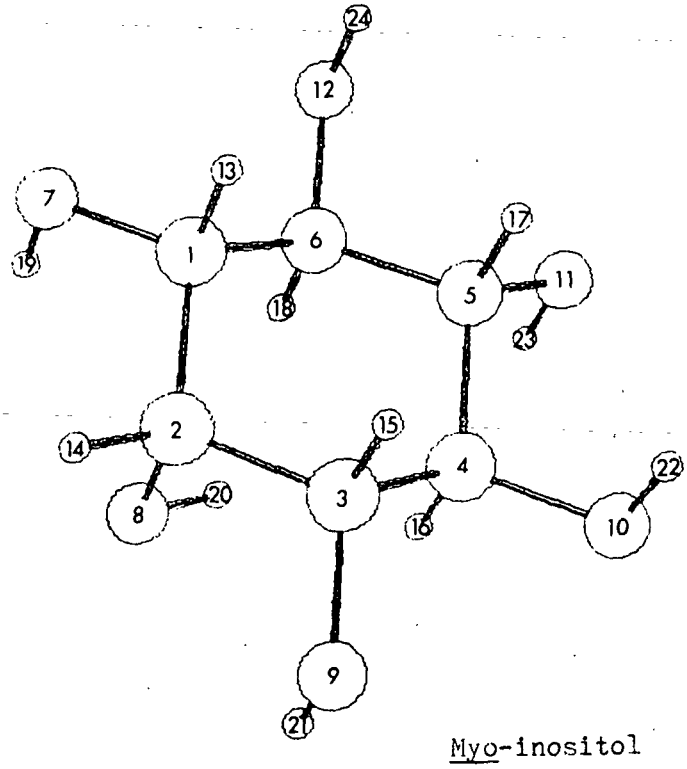

Myo-inositol

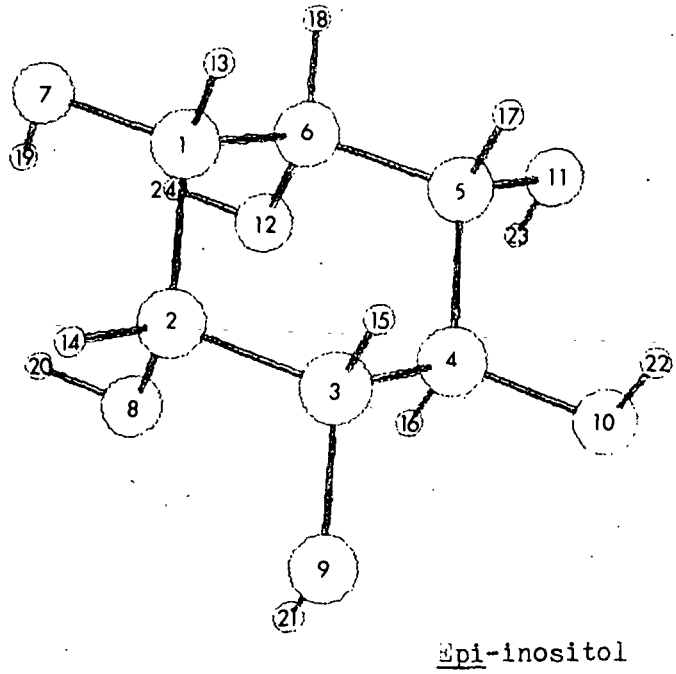

Epi-inositol

Figure 17. Representations of the Tetrahedral Models for scyllo-Inositol, neo-Inositol, myo-Inositol and epi-Inositol

TABLE XVII

BOND LENGTHS USED IN THE INOSITOL TETRAHEDRAL MODELS

C-C	1.545 A
C-O	1.425
C-H	1.100
O-H	0.970

Calculation of G matrices based on the x-ray determined crystal structures of myo-inositol and epi-inositol were also done. The x-ray crystal structure for myo-inositol has been determined by Rabinowitz and Kraut (34). Jeffrey and Kim (35) determined the x-ray crystal structure of epi-inositol and have compared the structure with that of myo-inositol (36). Because of the generally observed large uncertainty in the positions of the hydrogens in x-ray work, for the construction of the G matrices the O-H and C-H bond lengths were set equal to those bond lengths used in the tetrahedral models. Nothing else was altered from the crystal structure data.

MATHEMATICAL FORM OF THE POTENTIAL ENERGY — THE FORCE CONSTANTS, F MATRIX AND Z MATRIX

An integral part of the normal coordinate analysis of a molecule is the mathematical form chosen to express the potential energy. In this study, the intramolecular potential forces were expressed in terms of quadratic force constants. The potential energy can be expressed in the form

$$2V = \sum_{k,l=1}^{78} F_{kl} R_k R_l \qquad (3)$$

where F_{kl} = quadratic force constants

R = internal coordinates

The upper limit of the summation is the number of internal coordinates defined because of the inclusion of the redundant internal coordinates. To obtain the potential form shown in Equation (3), the potential is assumed to be harmonic and it is assumed that the atomic displacements occurring in the vibrations are of small amplitude. The quadratic force constants are defined as:

$$F_{kl} = \frac{\partial^2 V}{\partial R_k \, \partial R_l} \tag{4}$$

The F_{kl} terms can be expressed as a matrix, the $\underset{\sim}{F}$ matrix. The dimension of the $\underset{\sim}{F}$ matrix is the number of internal coordinates defined. Two classes of force constants can be distinguished in the $\underset{\sim}{F}$ matrix. The 'diagonal' force constants, when $k = l$ in the F_{kl} terms, occupy the diagonal positions in the $\underset{\sim}{F}$ matrix. The diagonal constants include the stretching, bending or torsion of a single internal coordinate. The off-diagonal elements of the $\underset{\sim}{F}$ matrix, when $k \neq l$, are called 'interaction' constants. They represent the interactions between two different internal coordinates. In the most general form, the general quadratic force field, a force constant would be defined for every element of the $\underset{\sim}{F}$ matrix. It should be noted that, as defined, the $\underset{\sim}{F}$ matrix is symmetric, that is, $F_{kl} = F_{lk}$.

To reduce the number of individual force constants, it was assumed that all stretch-stretch interactions which do not have one common atom between the two interacting stretching internal coordinates and all bend-bend interactions which do not have two common atoms between the two interacting bending internal coordinates are negligible. These interaction constants were assigned zero values.

In addition, it was assumed that all internal coordinates of a common type, for example all twelve of the HCC bending coordinates, could be described with a single force constant. This is done by defining a transformation matrix, the Z matrix as follows:

$$F_{kl} = Z_{klm}\,\phi_m \qquad (5)$$

where F_{kl} = force constants, the elements of the F matrix

ϕ_m = numerical values of the force constants

The Z matrix is the transformation from the numerical force constant values to the F matrix. The Z matrix is a mathematical formalism which is defined as a convenience for the numerical computations. In the computer programs, to be discussed later in this section, the Z matrix is defined as four 1 x 78 column vectors, in which are sequentially stored the row number, column number, force constant number and weighting factor for each Z matrix element.

An F matrix constructed on the basis of the assumptions just stated is called a Simplified Valence Quadratic Force Field (SVQFF) after Pitzner (18). It is to be noted that implicit in this type of force field is the assumption that the forces acting between molecules in the crystal environment, the intermolecular forces, are negligible. The F and G matrices have been constructed for an individual molecule of each inositol. Each molecule is treated as if it were vibrating independently of the other molecules in the crystal. This is termed the isolated molecule approximation.

The Z matrices constructed for the different inositols are listed in Appendix III. The force constants defined for the inositols will be presented later in this section.

REFINEMENT OF THE FORCE CONSTANTS

Given the molecular structural information, the atomic masses and the force constants, it is a relatively straightforward problem to calculate the vibrational frequencies and related atomic motions. However, for molecules with the complexity of the inositols, the force constants are not exactly known, they can only be

approximated. To optimize the force constant approximations, a procedure for refining the force constants was employed which utilized the experimentally observed vibrational frequencies, the only source of direct molecular information available for determining the force constants.

The refinement technique used in this work was a nonlinear least-squares method developed by Fletcher and Powell (20) and adapted to the vibrational problem for large molecules by Pitzner (18,19). Gans (37-39) has also employed the Fletcher-Powell method. For a refinement, the experimental frequencies were manually assigned to previously calculated frequencies and initial approximations to the force constants were made. Using a computer program, the force constants were then successively adjusted by the Fletcher-Powell algorithm to minimize the least-squares difference between the assigned experimentally observed frequencies and the calculated frequencies. The refinement of the force constants would continue until certain specified termination criteria were met. Actual refinements averaged approximately fifteen perturbations before termination, with the Fletcher-Powell algorithm calculating at least two adjustments to the force constants per perturbation. A refinement could include either a single molecule or several molecules. When several molecules were refined together, it was assumed that the same force field could be used to describe the potential energies of the different molecules. In effect, this is assuming transferability of the force constants between molecules of similar structure. The number of force constants refined was also flexible. Any of the constants could be refined individually or any number could be refined simultaneously.

In calculating the adjustments to the force constants, the Fletcher-Powell algorithm uses an approximation to the Hessian matrix, which is an attempt to use second-order information. It is the inclusion of the second-order information

which gives the method its convergence power from an ill-defined initial set of force constants.

Originally, Pitzner (18) had attempted to use the linear least-squares refinement technique employed by Schachtschneider and Snyder (10). This method utilizes only gradient, or first-order information, in calculating the corrections to the force constants. The refinements attempted by Pitzner (18) using the linear least-squares technique failed to converge. In all cases, the refinements ended with the least-squares difference between the experimental and calculated frequencies getting larger and larger. Because of the divergence problems, no attempt was made to use the linear least-squares method in this work.

SYMMETRY PROPERTIES OF THE INOSITOLS AND THE APPLICATION OF GROUP THEORY TO MOLECULAR VIBRATIONAL ANALYSIS

The symmetry of a molecule can be utilized to obtain information concerning the symmetry properties and the infrared and Raman activities of the normal modes of vibration and also to optimize the numerical solution of the vibrational secular equation. This is accomplished by the application of group theory to the analysis of molecular vibrations. The interested reader is referred to several standard texts which cover this topic in detail (31,40-42). Because space considerations prohibit a complete derivation of the application of group theory to molecular vibrations, only the areas pertinent to this study will be briefly discussed in this section.

The symmetry of a molecule is described by listing the symmetry elements the molecule possesses. For a complete description of a molecule's symmetry, four kinds of symmetry elements need be considered: 1) plane of symmetry, σ; 2) center of symmetry or center of inversion, i; 3) proper axis of rotation, C_N; and 4) improper axis of rotation, S_N. The elements of symmetry possessed by the

nine inositol isomers are illustrated in Fig. 18 as taken from Stoddard (43). All the inositols except allo-inositol have at least one element of symmetry. scyllo-Inositol possesses the most elements of symmetry and thus is the inositol of highest symmetry.

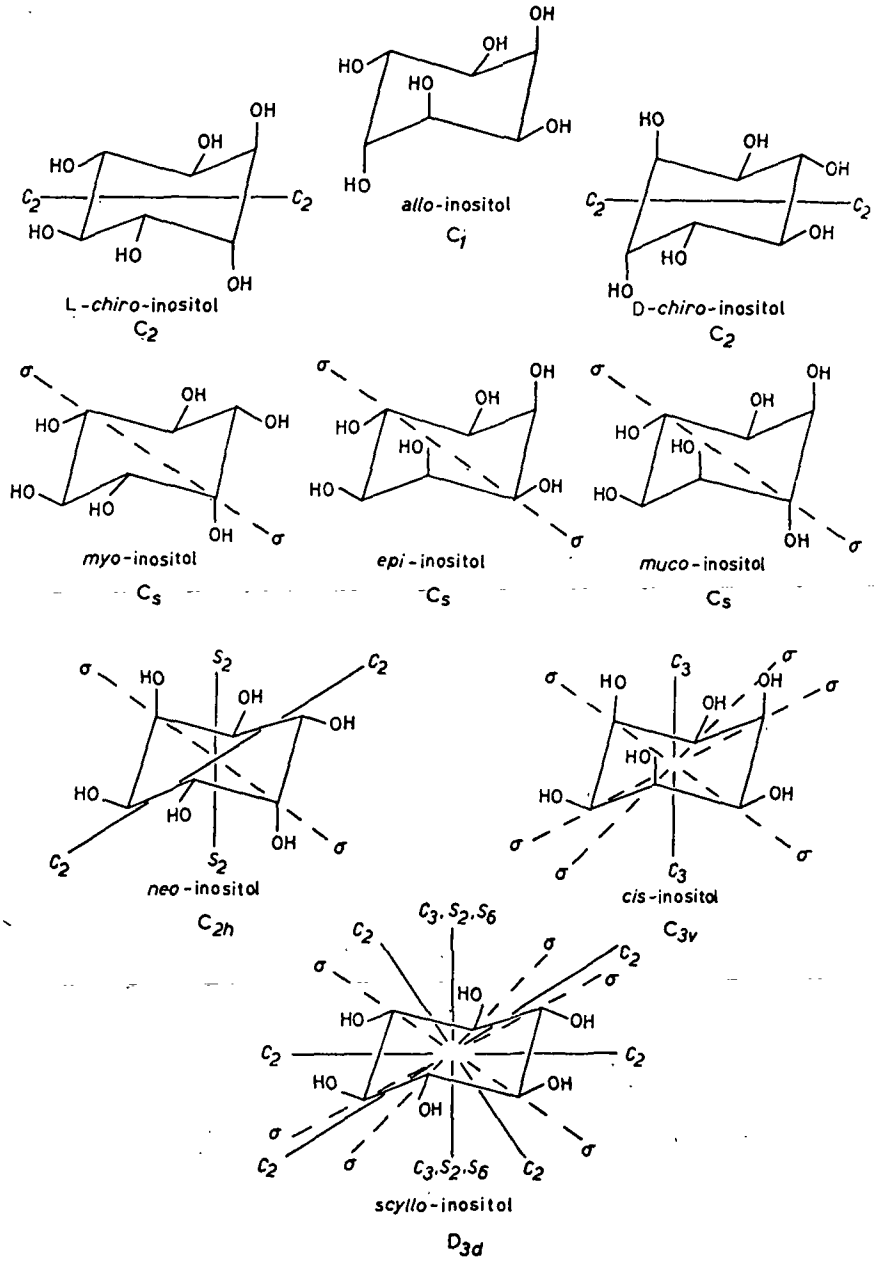

Figure 18. The Symmetry Properties of the Inositols (43)

"A symmetry element is a geometrical entity such as a line, a plane, or a point, with respect to which one or more symmetry operations may be carried out. A symmetry operation is a movement of a body such that, after the movement has been carried out, every point of the body is coincident with an equivalent point (or perhaps the same point) of the body in its original orientation. In other words, if we note the position and orientation of a body before and after a movement is carried out, that movement is a symmetry operation if these two positions and orientations are indistinguishable" (41). The effect of a symmetry operation is to take a body, such as a molecule, into an equivalent configuration. For example, the model of myo-inositol shown in Fig. 17 has a plane of symmetry which passes through the atoms O8-C2-C5-O11. The symmetry operation of reflecting the myo-inositol atoms through the plane of symmetry would result in C1 being exchanged with C3, O7 with O9, H19 with H21, etc. After the reflection of all the atoms have been made, the resulting structure would be indistinguishable from the original, except for the arbitrary numbers placed on the atoms.

Molecules such as the inositols which possess elements of symmetry, and thus the symmetry operations generated by each of these elements, can be classified according to their particular symmetry operations into molecular point groups. Each point group has its own characteristic symmetry operations. The point groups for the inositols are shown in Fig. 18. The symmetry operations characteristic to each point group can be found in any of the texts cited earlier in this section.

In the example of myo-inositol, the atoms C1 and C3, for example, are said to be symmetrically equivalent atoms because they can be exchanged by the reflection symmetry operation. The atoms symmetrically equivalent to any arbitrarily selected atom in a molecule are all the atoms into which the chosen atom can be sent by the symmetry operations of the point group. The exchangeable atoms then constitute a symmetrically equivalent set. In scyllo-inositol, all six carbons

are symmetrically equivalent because any carbon can be sent into all the others by the symmetry operations of the scyllo-inositol D_{3d} point group. The concept of symmetrically equivalent atoms will be used later when the symmetry properties of the calculated normal modes are discussed.

When a molecule contains elements of symmetry, the normal modes of vibration of the molecule also have certain symmetry properties. If all the normal modes of a molecule were examined, it would be found that they could be classified according to their symmetry properties. A fundamental theorem of group theory states that there are only a definite small number of these classes, or symmetry species as they are commonly called, for each point group. The symmetry species for the point groups of the inositols and the number of vibrational modes of each symmetry type are listed in Table XVIII. Among the important properties derivable about the vibrational modes in the different symmetry species are their infrared and Raman activities. The infrared and Raman activities for the symmetry species present in the point groups of the inositols are also shown in Table XVIII. The activities are listed such that a '+' indicates activity and a '-' no activity. For scyllo-inositol and neo-inositol it can be seen that the vibrational modes are either active in the Raman or active in the infrared but none are active in both. This is termed mutual exclusion and occurs when a center of inversion is present as a symmetry element, as it is in both scyllo-inositol and neo-inositol. scyllo-Inositol and cis-inositol both have symmetry species, the A_{2g} and A_{1u} species for scyllo-inositol and the A_2 species for cis-inositol, which are inactive in both the Raman and the infrared. scyllo-Inositol and cis-inositol also have doubly degenerate symmetry species, the E_g and E_u species for scyllo-inositol and the E species for cis-inositol, which result from the presence of a 3-fold rotation axis symmetry element.

TABLE XVIII

THE POINT GROUPS, SYMMETRY SPECIES, AND RAMAN AND INFRARED VIBRATIONAL ACTIVITIES OF THE INOSITOLS

	POINT GROUP	SYMMETRY SPECIES	RAMAN ACTIVITY	INFRARED ACTIVITY	NO. NORMAL MODES
scyllo-Inositol	D_{3d}	A_{1g}	+	-	8
		A_{2g}	-	-	3
		E_g	+	-	22
		A_{1u}	-	-	4
		A_{2u}	-	+	7
		E_u	-	+	22
cis-Inositol	C_{3v}	A_1	+	+	15
		A_2	-	-	7
		E	+	+	44
neo-Inositol	C_{2h}	A_g	+	-	19
		B_g	+	-	14
		A_u	-	+	15
		B_u	-	+	18
myo-Inositol	C_s	A'	+	+	37
		A''	+	+	29
epi-Inositol	C_s	A'	+	+	37
		A''	+	+	29
muco-Inositol	C_s	A'	+	+	37
		A''	+	+	29
L-chiro-Inositol	C_2	A	+	+	34
		B	+	+	32
D-chiro-Inositol	C_2	A	+	+	34
		B	+	+	32
allo-Inositol	C_1		+	+	66

An additional piece of information which can be gained from the symmetry analysis concerns the depolarization ratios. It can be shown (31) that, for the case when the incident beam is plane polarized, vibrations which are totally symmetric, i.e., symmetric with respect to all the symmetry operations, have a theoretical depolarization ratio less than 0.75, while vibrations which are not totally symmetric have a depolarization ratio of 0.75. Therefore, observed bands which have a measured depolarization ratio of less than 0.75 can be assigned to calculated bands which belong to the totally-symmetric symmetry species for a particular point group.

The group theory analysis also provides a method for dividing the $\underset{\sim}{G}$ and $\underset{\sim}{F}$ matrices into a number of submatrices, where each submatrix corresponds to a symmetry species of the particular point group. This reduction of the matrices, often termed factoring, is effected by changing the coordinates from internal coordinates to symmetry coordinates. It can be shown (44) that when symmetry coordinates are used, no cross terms will occur in either the kinetic or potential energies between two symmetry coordinates of different symmetry species. Since the $\underset{\sim}{G}$ and $\underset{\sim}{F}$ matrices are factored into equivalent blocks, the $\underset{\sim}{GF}$ product will be factored in the same fashion and thus the vibrational problem for each symmetry species may be treated independently. The factoring of either a $\underset{\sim}{G}$ or $\underset{\sim}{F}$ matrix into symmetry blocks can be represented as shown in Fig. 19, where, after factoring, all the nonvanishing elements fall in the shaded areas.

The symmetry coordinates were constructed by taking suitable linear combinations of the internal coordinates such that each symmetry coordinate belonged to one of the symmetry species. The coordinate transformation from internal coordinates to symmetry coordinates can be written in matrix form as

$$\underset{\sim}{S} = \underset{\sim}{UR} \tag{6}$$

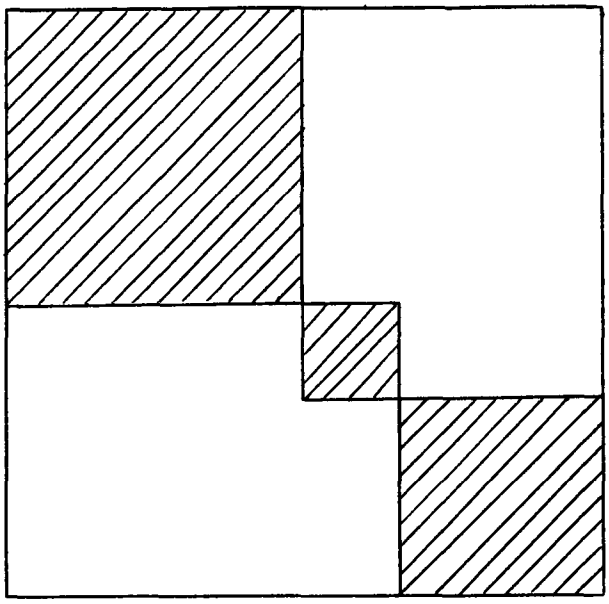

Figure 19. Representation of a Factored Matrix

where $\underset{\sim}{R}$ = the internal coordinates

$\underset{\sim}{S}$ = the symmetry coordinates

$\underset{\sim}{U}$ = the transformation between the internal and symmetry coordinates

In the case of the inositols, the $\underset{\sim}{U}$ matrix would be a 78 x 78 matrix and the $\underset{\sim}{S}$ and $\underset{\sim}{R}$ matrices 1 x 78 column vectors.

The symmetry coordinates, symmetry-adapted linear combinations of internal coordinates, were generated using an operator termed a projection operator. The projection operator for a given symmetry species, when applied to an internal coordinate, will generate a symmetry coordinate as a linear combination of internal coordinates if the symmetry coordinate belongs in the given symmetry species. If the symmetry coordinate does not belong in the symmetry species, the internal coordinate combinations will cancel each other out and no symmetry coordinate will be generated. In effect, the projection operator provides a method for determining

the coefficients in the $\underset{\sim}{U}$ transformation matrix. The projection operator can be written as follows (45):

$$P^{(\mu)} = \sum_{R} X^{(\mu)}(R)\, O_R \qquad (7)$$

where $P^{(\mu)}$ is the projection operator for a given symmetry species, $\Gamma\mu$. The summation is over all the symmetry operations, R, of the point group of the molecule. The coefficient $X^{(\mu)}(R)$ of each O_R, where O_R represents the operators of the symmetry operations, is the character of R in the symmetry species, $\Gamma\mu$, which can be found in tabulated character tables (31,40-42). The symmetry coordinates were generated by applying the projection operator for a given symmetry species to each internal coordinate. Using this projection operator technique, the unnormalized symmetry coordinates were constructed for scyllo-inositol, neo-inositol, myo-inositol, epi-inositol, cis-inositol, L-chiro-inositol, and muco-inositol. The symmetry coordinates defined for these molecules appear in Appendix VI. The generated symmetry coordinates were used to set up the unnormalized $\underset{\sim}{U}$ matrices which were in turn normalized and then used to factor the $\underset{\sim}{G}$ and $\underset{\sim}{Z}$ matrices.

The $\underset{\sim}{U}$ matrix is a matrix representation of the transformation which gives all normalized linear combinations of internal coordinations needed to generate the normalized symmetry coordinates for a molecule. The $\underset{\sim}{U}$ matrix is constructed such that the symmetry coordinate number corresponds to the $\underset{\sim}{U}$ matrix row number, the internal coordinate number to the $\underset{\sim}{U}$ matrix column number and the coefficients of the internal coordinates to the matrix elements. As constructed, the $\underset{\sim}{U}$ matrix represents a linear, orthogonal transformation. Because the $\underset{\sim}{U}$ matrix is an orthogonal matrix, the inverse of the $\underset{\sim}{U}$ matrix is simply its transpose, $\underset{\sim}{U}'$. Utilizing this property of orthogonal matrices, the following simple matrix transformation can be derived for transforming the $\underset{\sim}{F}$ matrix into the factored $\underset{\sim}{\tilde{F}}$ matrix (46):

$$\hat{F} = UFU' \tag{8}$$

This transformation represents a change from a coordinate system based on internal coordinates to a coordinate system based on symmetry coordinates. In practice, the Z matrix and the U matrix are combined according to the equation

$$\hat{Z} = UZU' \tag{9}$$

The factored F matrix, $\hat{F}$, is then computed from the factored Z matrix, $\hat{Z}$, from

$$\hat{F} = \hat{Z}\phi \tag{10}$$

where ϕ represents a column matrix of the force constants.

The G matrix is factored by a procedure analogous to that used for the F matrix. The following equation was used to transform the G matrix into the factored G matrix, $\hat{G}$:

$$\hat{G} = UGU' \tag{11}$$

To insure that the F and G matrices had been factored correctly, frequencies were calculated, without refinement, using both the symmetrized and unsymmetrized forms of the matrices. The calculated frequencies for the two cases were compared and were found to be the same for all cases.

It was stated earlier that factoring the secular equation optimizes the numerical solution. It takes approximately 8-1/2 minutes to calculate the frequencies for unsymmetrized scyllo-inositol. The frequency calculations for the six scyllo-inositol symmetry blocks takes only 2-1/2 minutes. The much shorter time is primarily due to the difference in time required to diagonalize six small matrices, the largest of which is 13 x 13, versus one large 78 x 78 matrix.

In the refinements where several molecules were involved, this represented a substantial savings in time. In all the refinements, the calculations were based on the symmetrized forms of the matrices.

NUMERICAL SOLUTION OF THE VIBRATIONAL PROBLEM

The form of the vibrational secular equation shown in Equation (2) is often called the Wilson 'GF' form. Numerical solution of the vibrational secular equation in this form was programmed for computer by Schachtschneider (47,48). The computer program package developed by Schachtschneider also includes programs for setting up the G and F matrices. The computer programs, obtained from Schachtschneider, were adapted by Pitzner (18) for use on the IBM Model 360/44 computer available at The Institute of Paper Chemistry. The programs employed in this work will be only briefly discussed. Copies of the programs and instructions for their use have been provided by Pitzner (18).

The Fletcher-Powell algorithm, obtained from IBM (49), was incorporated by Pitzner (18) into the refinement program written by Schachtschneider (48). The program name is FLPO and this program was used for all the refinements performed in this work.

Two programs were used to solve the vibrational secular equation and to obtain potential energy distributions associated with the molecular normal modes. The program EIGV was used to calculate the vibrational frequencies and to calculate a potential energy distribution in terms of the internal coordinates. A second program, MASORT, would read the potential energy distribution data, arrange it in decreasing order and label each internal coordinate contribution with a four character code. The program NFAD also solved the vibrational secular equation but calculated a potential energy distribution in terms of the contributions of

the different force constants. This data was then ordered and labelled by the program PESORT.

In the matrix setup programs, the program CART was used to calculate the cartesian coordinates from the selected molecular geometry. The geometries were visually checked by drawing 'ball-and-stick' representations of the molecules with the drawing program PAMOLE. This program was written by Cole and Adamson (50) and modified by Pitzner (18). The program CARTSET (23) was used to calculate input data for CART from the fractional atomic coordinates determined from the x-ray crystal data. The cartesian coordinates along with the atomic masses and the internal coordinate definitions were used as input for the program GMAT which calculated the B matrix, the transformation from cartesian coordinates to internal coordinates, and then the G matrix. The U matrix could also be entered into GMAT which normalizes the U matrix and then generates the G matrix in symmetry block form. The program UBZM was used to construct the first few Z matrices while the others were constructed from those already generated. The U matrix and the Z matrix were entered into the program ZSYM which normalizes the U matrix and then factors the Z matrix into symmetry blocks.

The input data for all the inositols for the programs CART, PAMOLE and GMAT are listed in Appendix II. The input data for the program CARTSET for myo-inositol and epi-inositol, taken from the x-ray crystal structure data, are listed in Appendix IV.

FINAL INOSITOL FORCE FIELD AND CALCULATED RESULTS

The force constants defined for the inositol models and the final force constant values resulting from the refinements are shown in Table XIX. Thirty-three force constants were defined in the final field, eleven diagonal constants, twenty-one interaction constants and a single dummy constant. A diagonal constant was

TABLE XIX

SVQFF FORCE CONSTANT PARAMETERS FOR THE INOSITOL MODELS

FORCE CONSTANT NUMBER	GROUP	COORDINATES INVOLVED	COMMON ATOMS	FINAL VALUE	WELLS (HEXOSES)	EDWARDS (PENTOSES)	PITZNER (1,5-AHP's)	SNYDER and ZERBI
			STRETCHING CONSTANTS			(mdyn./A)		
1	C-OH	C-O	--	5.144	5.120	5.122	5.103	5.090
2	C-C	C-C	--	4.193	4.215	4.183	4.247	4.261
3	H-C-OH	C-H	--	4.690	4.650	4.694	4.589	4.688
4	O-H	O-H	--	6.283	5.500	6.283	6.283	-----
			BENDING CONSTANTS			(mdyn.A/(rad.)^2)		
5	C-C(H)-OH	HCC	--	0.728	0.671	0.698	0.725	0.718
6	H-C-OH	HCO	--	0.969	0.861	0.980	0.963	0.961
7	C-O-H	COH	--	0.923	0.950	0.871	0.734	-----
8	C-C-OH	CCO	--	1.205	1.332	1.137	1.180	1.182
9	C-C-C	CCC	--	1.044	1.028	1.112	1.056	1.071
			STRETCH-STRETCH INTERACTION CONSTANTS			(mdyn./A)		
10	C-C-OH	C-C,C-O	C	0.302	0.351	0.127	0.107	0.101
11	C-C-C	C-C,C-C	C	0.043	0.112	0.117	0.107	0.101
			STRETCH-BEND INTERACTION CONSTANTS			(mdyn./rad.)		
12	H-C-OH	C-O,HCO	CO	0.360	0.502	0.452	0.388	0.387
13	C-O-H	C-O,COH	CO	0.425	0.430	0.342	0.357	-----
14	C-C-OH	C-O,CCO	CO	0.707	0.522	0.657	0.664	0.618
15	C-C(H)-OH	C-C,HCC	CC	0.329	0.330	0.518	0.481	0.478
16	C-C-OH	C-C,CCO	CC	0.495	0.443	0.408	0.381	0.403
17	C-C-C	C-C,CCC	CC	0.482	0.467	0.271	0.485	0.417
			BEND-BEND INTERACTION CONSTANTS			(mdyn.A/(rad.)^2)		
18	C-C(H)-OH	HCO,HCC	CH	0.140	0.035	0.157	0.135	0.115
19	C-C(H)-OH C-C(H)-C C-C(H)-OH	HCC,CCO HCC,CCC HCO,CCO	CC CC CO	-0.076	-0.076	-0.067 -0.012 -0.067	-0.044	-0.031
20	C-C(OH)-C C-C(OH)-C	CCO,CCO CCO,CCC	CO CC	0.017	0.090	0.074 0.133	0.052	-0.041
21	C-C-C-OH HO-C-C-OH C-C-C-C	CCC,CCO CCO,CCO CCC,CCC	(C)C-C(O) gauche (O)C-C(O) gauche (C)C-C(C) gauche	0.008	0.017	0.018 0.074 0.031	-0.024	0.011
22	C-C-C-OH HO-C-C-OH	CCC,CCO CCO,CCO	(C)C-C(O) trans (O)C-C(O) trans	0.048	-0.007	-0.002 0.004	-0.014	-0.011
23	H-C-C-OH	CCO,HCC	(H)C-C(O) gauche	-0.230	-0.198	-0.164	-0.238	-0.113
24	H-C-C-OH	CCO,HCC	(H)C-C(O) trans	-0.084	0.126	-0.008	0.037	0.028
25	H-C-C-C	CCC,HCC	(C)C-C(H) gauche	-0.111	0.017	-0.179	-0.106	-0.052
26	H-C-C-C	CCC,HCC	(C)C-C(H) trans	0.087	0.126	-0.155	-0.047	0.040
27	H-C-C-H	HCC,HCC	(H_a)C-C(H_b) gauche	0.018	-0.032	-0.004	-0.002	0.004
28	H-C-C-H	HCC,HCC	(H_a)C-C(H_b) trans	0.095	0.147	0.057	0.049	0.121
29	H-C-OH H-C-OH	COH,HCO COH,HCO	(H)O-C(H) gauche (H)O-C(H) trans	0.059	0.043	0.117 0.132	0.0 0.016	-----
30	C-C-OH C-C-OH	CCO,COH CCO,COH	(C)C-O(H) gauche (C)C-O(H) trans	0.115	-0.068 -0.165	0.151	0.010	-----
			TORSION CONSTANTS					
31	C-C	C-C	--	0.100	0.100	0.023	0.027	0.024
32	C-OH	C-O	--	0.015	0.025	0.059	0.028	0.026
33	ALL FORCE CONSTANTS ASSIGNED A ZERO VALUE							

defined for each type of stretching, bending and torsion internal coordinate. In the calculations, the $\underset{\sim}{F}$ matrix was obtained by multiplying these force constants, which are the elements of the column matrix $\underset{\sim}{\phi}$ in Equation (5), times the $\underset{\sim}{Z}$ matrix elements as defined in Equation (5). The final refinement from which the force constant values in Table XIX were obtained included: scyllo-inositol, neo-inositol, myo-inositol, epi-inositol, deuterated scyllo-inositol and deuterated neo-inositol. The rationale for the inclusion of these inositols in the final refinement and the exclusion of deuterated myo-inositol, deuterated epi-inositol and the other inositols will be discussed in a later section.

The final calculated frequencies and potential energy distributions for scyllo-inositol, neo-inositol, myo-inositol and epi-inositol are presented in Tables XLV through XLVIII in Appendix V and for deuterated scyllo-inositol, deuterated neo-inositol, deuterated myo-inositol and deuterated epi-inositol in Tables LII through LV, respectively. Shown in these tables are the room temperature Raman and infrared observed frequencies, the frequencies assigned in the final refinement, the frequencies calculated using the force constants presented in Table XIX and the calculated symmetry species for each frequency. The potential energy distributions are given in two forms, in terms of internal coordinates and in terms of the force constants.

Calculations were also done for myo-inositol and epi-inositol using the x-ray crystal structures as a basis for the $\underset{\sim}{G}$ matrices. The calculated frequencies and potential energy distributions are given in Tables LVI and LVII, respectively, in Appendix V.

DISCUSSION OF RESULTS

At the inception of the normal coordinate calculations, there were several attributes which were desired in the final inositol force field and calculated

results, i.e., the frequencies and the potential energy distributions. These attributes were:

1. Correct assignment of the experimental frequencies to the calculated frequencies.
2. Optimum agreement between the refined calculated frequencies and the assigned experimentally observed frequencies.
3. Reasonable values of the force constants.
4. A minimum number of force constants in the force field.
5. Satisfactory predictive capabilities of the force field.
6. Reasonable potential energy distributions.

The degree to which these attributes were attained in the final force field and calculated results is a measure of the success of the normal coordinate analyses. The key to the success of the normal coordinate calculations is the development of a satisfactory force field. The frequencies and potential energy distributions are dependent on the force constants used in the calculations. But, crucial to the development of a satisfactory force field is the correct assignment of the experimentally observed frequencies to the calculated frequencies for the refinement of the force constants. Thus, the information utilized in making the frequency assignments will be presented first in this section. Because of the determining role played by the force field, it will be discussed next. The final force field will be examined in terms of its development using the refinement technique, the factors which affect the determination of the force constants and how the force field compares with other force fields in the literature. The results of the calculations, the frequencies and the potential energy distributions, will then be examined. The fit of the calculated frequencies to the assigned experimental frequencies will be evaluated and the assigned spectra of scyllo-inositol, neo-inositol, myo-inositol, epi-inositol, deuterated

scyllo-inositol and deuterated neo-inositol will be interpreted. The remaining unassigned observed bands will be examined and a specific group of the unassigned bands will be discussed. Lastly, the degree to which second-order potential effects perturb the experimentally observed frequencies will be appraised by analyzing the average errors between the calculated and assigned experimental frequencies. This will also include an evaluation of the assumptions made in doing the normal coordinate analyses of the inositols.

INFORMATION UTILIZED IN THE ASSIGNMENT OF THE EXPERIMENTALLY OBSERVED FREQUENCIES TO THE CALCULATED FREQUENCIES

Of primary importance when the force constants are to be adjusted using a refinement technique is the correct assignment of the calculated frequencies to the observed frequencies. Several sources of information were utilized in making the frequency assignments for the inositols. Because the most valuable information came from the symmetry analyses, the use of this information will be discussed first.

The frequencies assigned for the inositol refinements were those observed below 1500 cm^{-1}. The O-H and C-H stretching modes were not assigned for the refinements.

As stated earlier, the presence of the center of inversion symmetry element in the tetrahedral structures of scyllo-inositol and neo-inositol will result in mutual exclusion, where the active vibrational modes will be active either in the Raman or the infrared but not in both. For scyllo-inositol, neo-inositol and their oxygen deuterated analogues, this information was utilized by assigning the observed Raman frequencies only to frequencies calculated in the Raman active symmetry species. The observed infrared frequencies were assigned in the same manner. But inherent in the assignments for these molecules based on the symmetry analyses are the assumptions that the molecules in the crystalline

environment do, in fact, possess a center of inversion, and if so, that the vibrational selection rules are being obeyed in the assumption of treating the inositols as isolated molecules. If the selection rules are being obeyed, the result would be exhibited by observance of mutual exclusion in the vibrational spectra. Figure 20 is a bar graph representation of the room temperature experimental frequencies for scyllo-inositol and neo-inositol. The figure compares the Raman active frequencies and the infrared active frequencies for both molecules. For many of the frequencies, there is clearly no Raman or infrared counterpart. For some frequencies, however, it would appear that the band is occurring in both the Raman and the infrared. For example, the two bands around 1000 cm^{-1} in the spectra of scyllo-inositol appear to occur in both the Raman and the infrared. However, in the cases where an experimental frequency appears in both spectra, it was found that both a Raman active frequency and an infrared active frequency were calculated for the corresponding observed frequency. Although the experimental bands are observed at nearly the same frequency, they are calculated to be two different vibrational modes, one Raman active and one infrared active. When two different vibrational modes are observed at approximately the same frequency, it is termed 'accidental' degeneracy. Thus, when substantiated by the calculated frequencies, the observance of Raman and infrared bands at approximately the same frequency in the spectra of scyllo-inositol and neo-inositol were interpreted as cases of accidental degeneracy. Another type of accidental degeneracy encountered was where two bands, both Raman (or infrared) active were found to occur at the same frequency. This type of accidental degeneracy will be discussed more completely in a later section when the calculated frequencies are compared with the assigned experimentally observed frequencies.

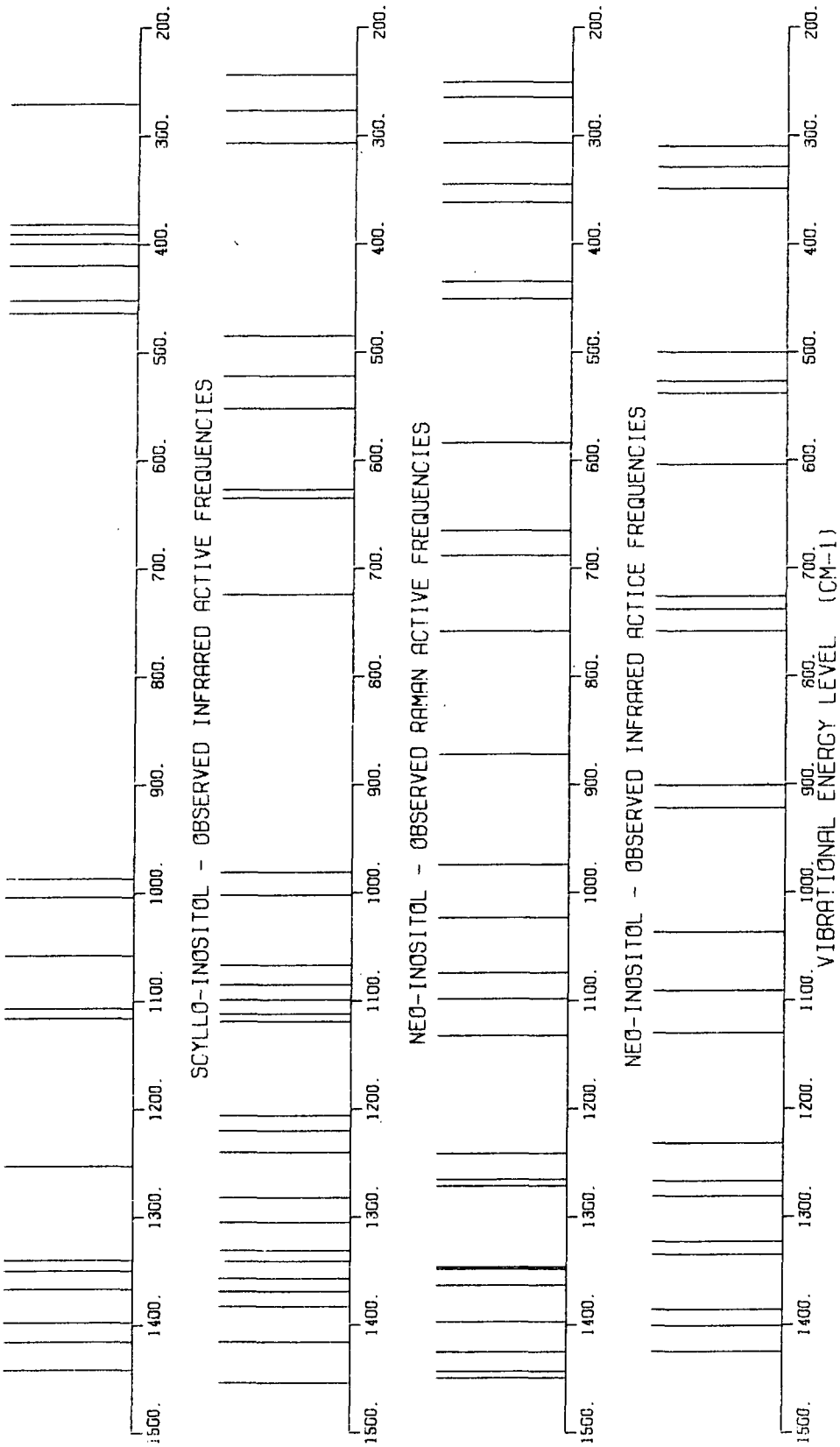

Figure 20. Bar Graph Representations of the Experimentally Observed Room Temperature Raman and Infrared Frequencies for scyllo-Inositol and neo-Inositol

In addition to the occurrence of accidental degeneracies, it can be seen in Fig. 20 that above 1000 cm^{-1} there are more bands observed in the infrared spectrum of scyllo-inositol than in the Raman. It was noted when the first attempts were made to assign the infrared spectrum of scyllo-inositol that more bands were being observed than were calculated. The correct melting point for scyllo-inositol had been obtained indicating no substantial amounts of impurities were present. The scyllo-inositol was recrystallized and the infrared spectrum again recorded. The second spectrum was different from the first but only in terms of relative intensities of some of the bands. The types of changes observed are shown in Fig. 21. This is a comparison of the 1500-200 cm^{-1} region for two scyllo-inositol infrared spectra. The bottom spectrum, Spectrum B, is the one presented earlier in the Experimental Results section. Changes can be observed in the relative intensities of the bands at 992, 1067, 1112, and 1331 cm^{-1}. The only difference between the samples was hypothesized to be the amount of water present. To further explore this hypothesis, a finely ground sample of scyllo-inositol was dried at 105°C for forty-eight hours and the infrared spectrum then recorded. The resulting spectrum is Spectrum B in Fig. 21. As a result of drying, the band at 992 cm^{-1} in Spectrum A, where the ground scyllo-inositol sample was not dried, is not observed in Spectrum B, the band at 1112 cm^{-1} is reduced to a shoulder, the band at 1067 cm^{-1} is greatly reduced in intensity while the bands at 1206 cm^{-1} and 1331 cm^{-1} are somewhat less reduced in intensity. Differences are also noted in the band at 1305 cm^{-1} and in the region 425-400 cm^{-1}. The changes observed after drying the scyllo-inositol suggest that partial dehydration of the scyllo-inositol crystals is the phenomenon occurring. This was further supported by an observation made earlier in this work that the scyllo-inositol crystals obtained from aqueous recrystallization were clear but when the crystals were stored in a vacuum desiccator over Drierite, they turned white and became

opaque. This observation could also be readily explained by progressive dehydration of the crystals.

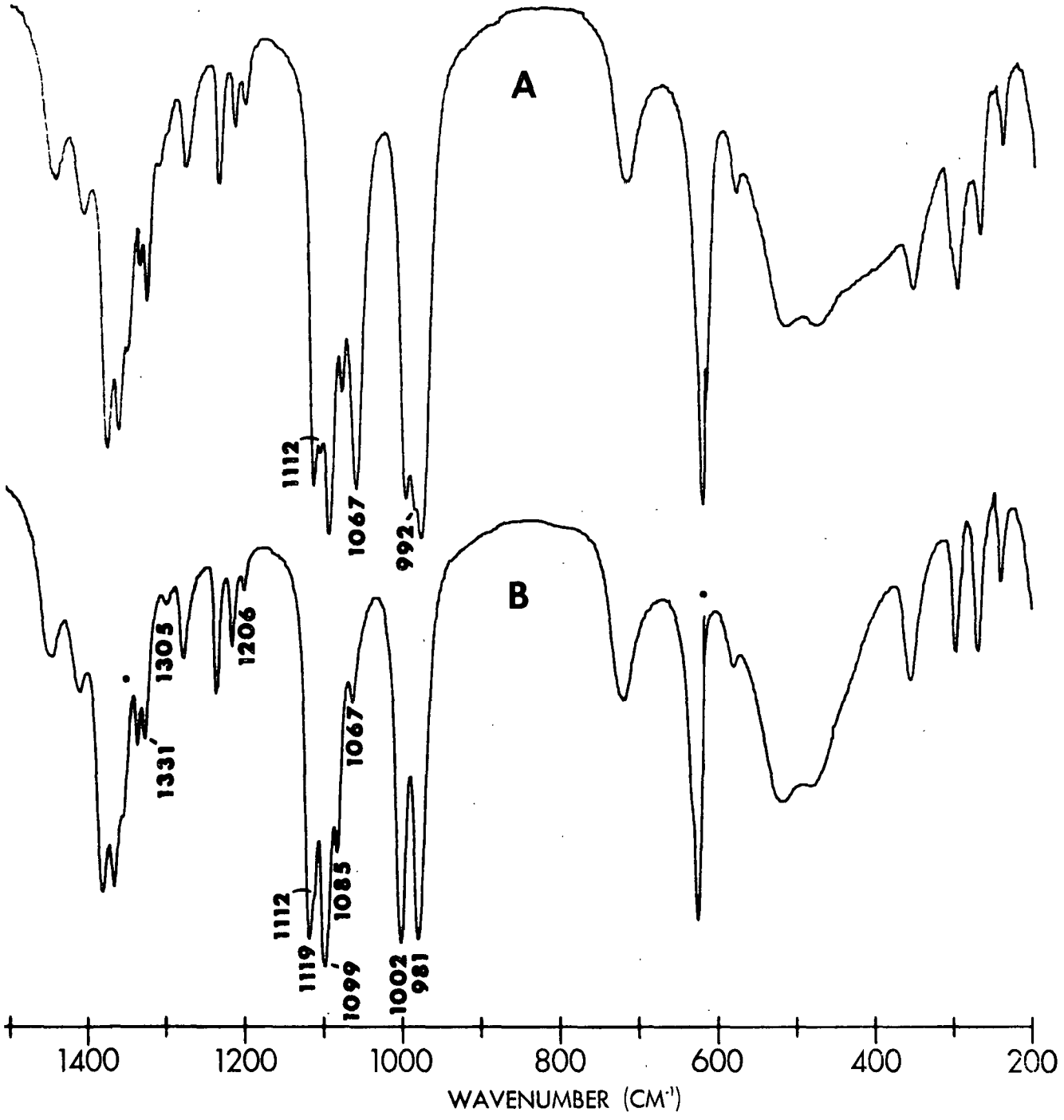

Figure 21. Comparison of the Room Temperature Infrared Spectra of: (A) Undried scyllo-Inositol and (B) scyllo-Inositol Dried at 105°C

As a result of the changes observed in the infrared spectra after sample drying, the bands observed at 992, 1067, 1112, 1206, 1305 and 1331 cm^{-1} in Fig. 21(A) were not assigned as fundamentals in the refinements. These bands were associated with the presence of water in the crystals. Their origin is not certain, but they may be due to perturbed fundamentals, combination bands or overtones. The observed bands at 981, 1002, 1085, 1099, and 1119 cm^{-1} in Fig. 21(B) were assigned as fundamentals in the refinements. After another scyllo-inositol sample was dried, the Raman spectrum was also rerecorded. The observed changes in the Raman were not as profound. Two shoulders at 1128 and 1049 cm^{-1} disappeared and thus were not assigned as fundamentals.

When the cases of accidental degeneracy and the extra bands in the infrared spectrum of scyllo-inositol are taken into account, the experimental and calculated spectra for scyllo-inositol and neo-inositol support the idea that mutual exclusion is being observed. This also supports the assumption that the calculated frequencies of these molecules can be assigned to the experimentally observed frequencies according to symmetry species.

One further note of interest concerns the effect of oxygen deuteration on the vibrational selection rules. If the centrosymmetric symmetry of a molecule, including the positions of the hydroxyl hydrogens, must be maintained for the selection rules to be obeyed, then partial deuteration of the hydroxyl groups, which should destroy the centrosymmetric symmetry in a majority of the molecules, would result in a breakdown of the selection rules and the mutual exclusion. This was not found to be the case with deuterated scyllo-inositol or deuterated neo-inositol. The degree of deuteration in both cases was approximately 70%. A comparison of the Raman active and infrared active observed frequencies for deuterated scyllo-inositol and deuterated neo-inositol is shown in Fig. 22. It can be seen in both cases that the majority of the frequencies still have no

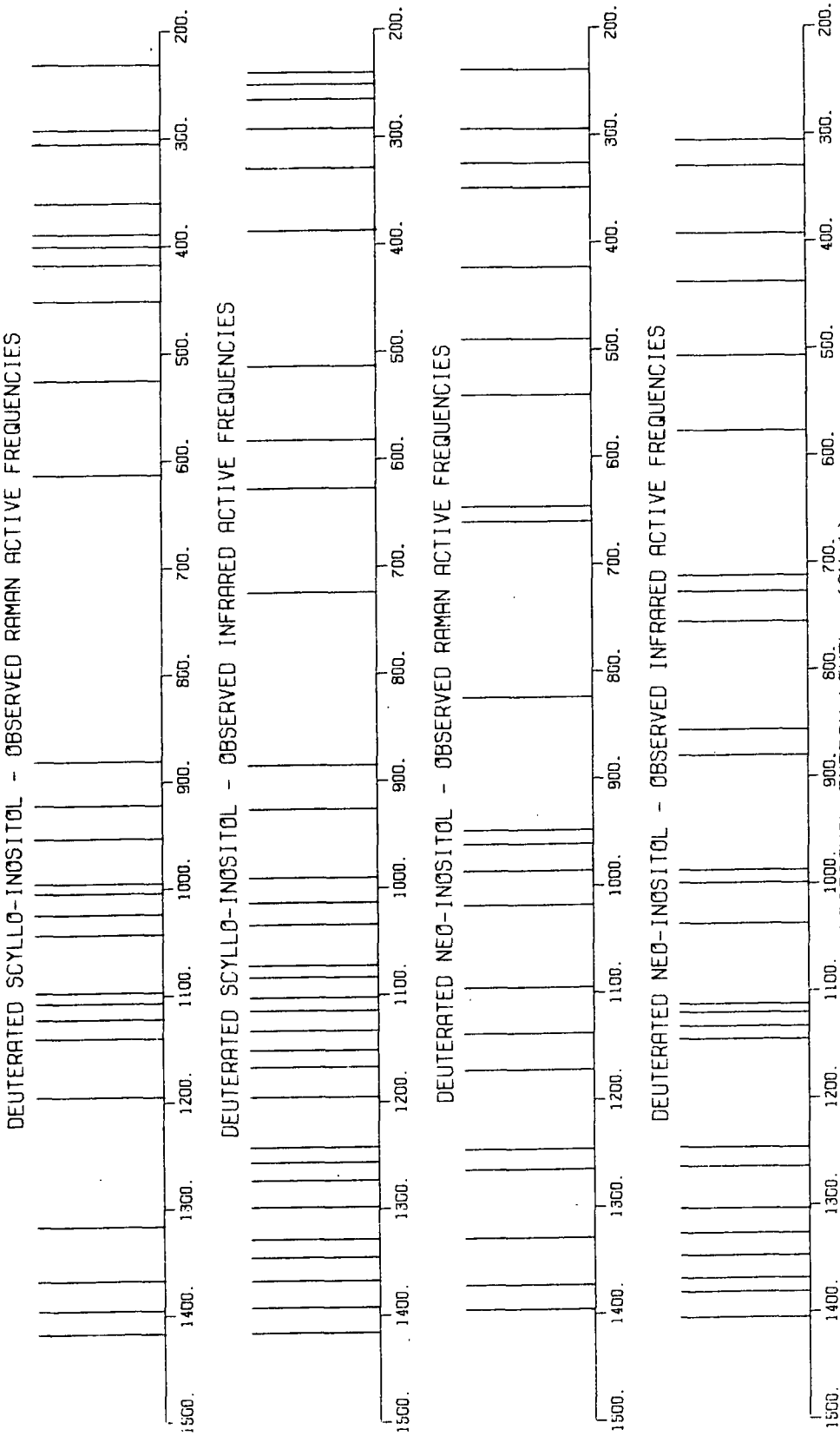

Figure 22. Bar Graph Representations of the Experimentally Observed Room Temperature Raman and Infrared Frequencies for Deuterated scyllo-Inositol and Deuterated neo-Inositol

apparent counterparts. The calculations confirm cases of accidental degeneracy where the Raman and infrared frequencies are nearly the same. Again, it is noted that above 1000 cm^{-1} in the infrared spectrum of deuterated scyllo-inositol there are many more frequencies observed than in the Raman. Several are weak bands which correspond to frequencies present in the undeuterated scyllo-inositol spectrum. This suggests these bands are likely contaminant bands from partially deuterated species. The mutual exclusion has apparently not broken down as a result of the partial deuteration. This suggests that the selection rules are governed primarily by the symmetry of the carbon-oxygen skeleton and perhaps the methine hydrogens but are not significantly affected by the hydroxyl hydrogens.

Another important aid derivable from the symmetry analyses used in the frequency assignments of scyllo-inositol, myo-inositol, and epi-inositol were the depolarization ratios. As stated earlier, the depolarization ratios for vibrational modes belonging to the totally-symmetric symmetry species are less than 0.75. The depolarization ratios measured for the inositols clearly identified several bands as belonging to the totally-symmetric species. These bands were then assigned to bands calculated in the totally-symmetric species.

A primary advantage of having the information from the symmetry analysis is that once several bands in a spectrum have been definitely assigned, the number of ways the remaining bands can be assigned is greatly reduced. This increases the validity of the assignments because they can be substantiated using the symmetry information.

One of the objectives of this thesis was to determine if the group theory analysis and vibrational selection rules could be applied to the inositols. The experimental spectra of scyllo-inositol and neo-inositol strongly suggest that the vibrational selection rules, resulting in mutual exclusion of the vibrational

modes, are being obeyed. The successful assignment of the experimental frequencies to the calculated frequencies according to symmetry species demonstrates that the symmetry analysis is applicable to the inositols. This will be more clearly illustrated when the frequency distributions comparing the assigned experimental frequencies and the calculated frequencies are presented in a later section.

Two additional sources of information, not related to the molecular symmetry, were also used in establishing the assignments. The first was the characteristic 'gaps' which occur in the experimental spectra below 1500 cm^{-1}. In general, three gaps were used to help categorize the frequencies: the first source between 1200 and 1150 cm^{-1}, the second between 975 and 930 cm^{-1} and the third between 870 and 800 cm^{-1}. These characteristic gaps were also used by Watson (21) and Edwards (22). The other sources of information made use of were the liquid nitrogen temperature Raman and infrared spectra. There were several instances where individual bands could not be resolved out of a broad band at room temperature, but where the individual bands were clearly resolved at low temperature. This helped greatly in the assignment of frequencies where several bands were calculated within a narrow frequency range.

Even with the use of all the information available, there is still some question as to the accuracy of some of the assignments. The errors involved in the initial assignments left a number of the assignments in doubt. The regions where difficulty in making the assignments occurred were from 1380 to 1250 cm^{-1} and from 1150 to 1050 cm^{-1} primarily in the spectra of myo-inositol and epi-inositol. Part of the reason for the difficulty was the occurrence of more observed frequencies, especially when the liquid nitrogen temperature spectra were considered, than there were calculated frequencies. Some difficulty was encountered in determining whether frequencies resolved at the low temperature were additional fundamentals or the result of fundamentals splitting into multiple bands. The

experimental frequencies not assigned will be discussed when the interpretation of the spectra is presented.

The frequency assignments were examined after almost every refinement to determine if improvements could be made. This process continued right up through the final refinement to insure that the assignments were as correct as could be attained.

SUMMARY OF THE DEVELOPMENT OF THE FINAL INOSITOL FORCE FIELD

Equally important as the final force constant values in a force field is some knowledge of how the final values were arrived at. An idea of the constraints and factors influencing the force constant values and of the methodologies employed in the force constant refinements is necessary in placing a force field in perspective with respect to evaluating the results obtained using the force field and in comparing the field to other force fields in the literature. For these reasons, the development of the force field for the inositols, the major problems encountered in the development, the methodologies employed in the refinements and the factors which affect the values of the force constants will be summarized. The strategy of the refinements and the difficulties which were encountered are closely related and will be discussed concurrently in chronological order.

The six qualities listed at the beginning of the Discussion of Results section were employed as general guidelines throughout the development of the force field. Each change made was in an attempt to improve on one or more of these qualities. The force field was developed using primarily neo-inositol, myo-inositol and epi-inositol. scyllo-Inositol, deuterated scyllo-inositol and deuterated neo-inositol were included in several refinements, particularly at

the later stages. scyllo-Inositol was not included in all the refinements because of problems in correctly assigning the infrared bands due to the extra bands observed in the infrared, as previously discussed. Primarily two reasons were used in deciding to include these inositols in the development of the force field and not the others, i.e., L-chiro-inositol, cis-inositol, muco-inositol, deuterated myo-inositol and deuterated epi-inositol. First, scyllo-inositol and neo-inositol were included because of their relatively high degrees of symmetry which could aid in the frequency assignments. cis-Inositol, which also has a relatively high degree of symmetry, was not included because of uncertainties as to whether a tetrahedral structure was a valid approximation to the actual crystal structure. Because of the 1:3:5 triaxial arrangement of the cis-inositol hydroxyl groups, it was felt that substantial distortion from the tetrahedral structure could be occurring. At the time this decision was made it was not known that the cis-inositol x-ray crystal structure had been previously determined. The structure of cis-inositol will be discussed further in Part II. Second, myo-inositol and epi-inositol were chosen over muco-inositol and L-chiro-inositol, all of which have a single element of symmetry, because their crystal structures had been determined. As will be discussed later in this section, deuterated scyllo-inositol and deuterated neo-inositol were included in refinements because their higher symmetry permitted greater accuracy in the assignments of the frequencies than in the cases of deuterated myo-inositol and deuterated epi-inositol.

Initial calculations were made for scyllo-inositol, neo-inositol, myo-inositol and epi-inositol using force constants from the final force fields of Pitzner (18) and Edwards (22). The forty-six force constants defined initially for the inositols are listed in Table XX. Several dummy parameters were included in the field so additional constants could be added if necessary.

TABLE XX

THE SIXTY PARAMETER INOSITOL FORCE FIELD AND THE FORCE CONSTANTS FROM REFINEMENT #28

FORCE CONSTANT NUMBER	GROUP	COORDINATES INVOLVED	COMMON ATOMS	FINAL VALUE REF. #28
		STRETCHING CONSTANTS		
1	C-OH	C-O		5.118
2	H-C-OH	C-H		4.690
3	C-C	C-C		4.194
4	O-H	O-H		6.283
5	Dummy			0.0
		BENDING CONSTANTS		
6	C-C(H)-OH	HCC		0.734
7	Dummy			0.0
8	C-C-OH	CCO		1.200
9	C-O-H	COH		0.940
10	C-C-C	CCC		1.077
11	H-C-OH	HCO		0.877
12	Dummy			0.0
		STRETCH-STRETCH INTERACTION CONSTANTS		
13	Dummy			0.0
14	C-C-OH	C-C,C-O	C	0.278
15	C-C-C	C-C,C-C	C	0.050
16	H-C-OH	C-C,C-H	C	0.0
17	C-C(H)-OH	C-C,C-H	C	0.0
18	C-O-H	C-O,O-H	O	0.0
19	Dummy			0.0
		STRETCH-BEND INTERACTION CONSTANTS		
20	H-C-OH	C-O,HCO	CO	0.359
21	Dummy			0.0
22	C-C-OH	C-O,CCO	CO	0.679
23	Dummy			0.0
24	C-C-OH	C-C,CCO	CC	0.492
25	C-C(H)-OH	C-C,HCC	CC	0.372
26	C-C-C	C-C,CCC	CC	0.502
27	C-C(H)-OH	C-H,HCC	CH	0.0
28	C-C(H)-OH	C-H,HCC	CH	0.0
29	C-C-H	C-C,COH	CC	0.441
30	C-C-H	C-H,COH	CH	0.0
31	Dummy			0.0
32	Dummy			0.0
		BEND-BEND INTERACTION CONSTANTS		
33	C-C(H)-OH	HCO,HCC	CH	0.098
34	C-C(H)-OH	HCC,CCO	CC	-0.018
35	C-C(H)-C	HCC,CCC	CC	-0.084
36	C-C(H)-OH	CCO,HCO	CO	-0.118
37	C-C(H)-C	HCC,HCC	CH	0.0
38	C-C(OH)-C	CCO,CCO	CC	0.021
39	C-C(OH)-C	CCO,CCC	CC	0.014
40	C-C-C-OH	CCC,CCO	(C)C-C(O) gauche	-0.069
41	HO-C-C-OH	CCO,CCO	(O)C-C(O) gauche	-0.025
42	C-C-C-C	CCC,CCC	(C)C-C(C) gauche	0.074
43	C-C-C-OH	CCC,CCO	(C)C-C(C) trans	0.063
44	HO-C-C-OH	CCO,CCO	(O)C-C(O) trans	0.007
45	Dummy			0.0
46	H-C-C-OH	CCO,HCC	(H)C-C(O) gauche	-0.163
47	H-C-C-OH	CCO,HCC	(H)C-C(O) trans	-0.102
48	H-C-OH	COH,HCO	(H)O-C(H) gauche	0.043
49	H-C-OH	COH,HCO	(H)O-C(H) trans	0.057
50	H-C-C-H	HCC,HCC	$(H_a)C-C(H_b)$ gauche	0.025
51	H-C-C-H	HCC,HCC	$(H_a)C-C(H_b)$ trans	0.097
52	H-C-C-C	CCC,HCC	(C)C-C(H) gauche	-0.140
53	H-C-C-C	CCC,HCC	(C)C-C(H) trans	0.112
54	C-C-OH	CCO,COH	(C)C-O(H) g and t	0.130
55	Dummy			0.0
56	Dummy			0.0
57	Dummy			0.0
58	Dummy			0.0
		TORSION CONSTANTS		
59	C-C			0.100
60	C-O			0.015

It was noted in the spectra calculated using Edwards' field that the C-O torsions were occurring in the region 380-300 cm^{-1}. For the deuterated inositols, these bands were calculated to shift down to 300-210 cm^{-1}. But the bands observed experimentally in the region 400-250 cm^{-1}, especially the Raman bands, did not shift significantly upon oxygen deuteration. This suggested that the C-O torsion contributions were being predicted at frequencies too high in the spectra. At this time, the C-O and C-C torsions were redefined using the method of Hilderbrandt (32). Using Edwards' field and the C-O torsion constant from the force field of Snyder and Zerbi (13), the calculations were repeated. The major C-O torsion contributions were now predicted between 235 and 205 cm^{-1}, which at the time was considered more reasonable.

The initial assignments were made using a field composed primarily from Edwards' final force constants. The average errors for the initial assignments were: neo-inositol 25.5 cm^{-1} with forty-one bands assigned, myo-inositol 20.7 cm^{-1} with forty-three bands assigned, and epi-inositol 35.0 cm^{-1} with forty-two bands assigned.

Through approximately the first eleven refinements two tasks were being dealt with simultaneously: the correct assignment of the frequencies and the adjustment of the force constants. As expected, the refinements were found to be very sensitive to the frequency assignments. Using the information described in the previous part of this section, the necessary assignment changes were made as needed.

The second task being dealt with was the adjustment of the force constants. Throughout the development of the force field the magnitudes of the force constants resulting from the refinements were closely monitored. This quickly led to the question of what constitutes reasonable values of the force constants.

How much deviation in magnitude from previous values could be tolerated, that is, what range of values are acceptable? It was found that what constitutes reasonable values of the force constants is almost exclusively a matter of judgment. In general, the basis for the judgment was the comparison of each constant with values from previous work and evaluating whether the magnitude of the constant was consistent with what would be expected physically for the particular bonds in a real molecule.

The force fields resulting from many of the refinements, especially the early refinements, did contain force constants which had grown to magnitudes which were judged to be unreasonable. It was hypothesized that two possible causes of a force constant growing during a refinement to unreasonable magnitudes were wrong assignments or the correlations known to exist between the force constants.

The type of force constants used in this thesis are not a linearly independent set. The inclusion of redundant internal coordinates in defining the molecular models results in the definition of redundant force constants (31,51,52). The redundant force constants belong to smaller dependent sets. The force constants in these sets cannot be uniquely determined. Consequently, the values of some of the force constants are dependent on the values of other constants, i.e., the values of the constants are correlated with each other. Within each dependent set of constants, the indeterminacy of a unique solution results in a large number of combinations of values being possible solutions. The unknown factor is: to what extent do these correlations affect the force constant values when they are refined using the Fletcher-Powell nonlinear method? It has proved very difficult to estimate to what extent the Fletcher-Powell method is just generating different combinations of values within the dependent sets. The redundant force constants and resulting correlations were hypothesized as the reason the linear refinements failed to converge for Pitzner (18). The Fletcher-Powell method

converged in all the refinements conducted. Apparently, the inclusion of second derivative information by the Fletcher-Powell method in determining the changes to be made in the individual force constants gives the method its power of convergence.

Because the redundancies cannot be removed from the inositol internal coordinates, a unique force field cannot be determined for the inositols using the normal coordinate methodology employed. But it was not the purpose of this thesis to develop a unique, 'absolute' set of force constants for the inositols. It was desired to develop a force field which optimized the qualities listed at the beginning of this section. The force field was developed acknowledging that the redundancy condition existed and that the correlations between the force constants were a factor in the refinement process and the final force constant values. The force constants developed in this work are viewed as semiempirical parameters. They are not absolute, but they retain a close similarity to force constants calculated directly for smaller molecules and can be used to interpret the potential energy in a semiquantitative manner. In addition, other sets of force constants developed using the Fletcher-Powell method have been shown to possess the ability to predict the vibrational frequencies and related atomic motions for molecules not involved in the development of the force field (21-23). The predictive capabilities of the inositol force field will be discussed in Part II.

Because the force constants developed for the inositols cannot be uniquely determined, an analysis of the force constant errors will not be discussed. In addition, the error figures obtained from the Fletcher-Powell method are subject to limitations, as they are good approximations only if the number of perturbations in the refinement approaches the number of force constants refined (18) and this was only rarely the case.

Once a problem, such as a large force constant value, was observed it had to then be decided what corrective action would be taken. However, from an examination of the force constants and frequencies resulting from a refinement, it was difficult to decipher what the cause of the problem was. Most often, the corrective action was based on trial and error.

In dealing with the problem of unreasonable force constant magnitudes, two primary methodologies were used in the refinements. If a force constant reached what was deemed an unacceptable value, this constant would be set at a reasonable value and fixed in the next refinement. The other constants would then be refined. This would adjust the field around the fixed constant. It was hoped that when the fixed constant was again refined with the others it would stay within smaller limits and not grow unreasonably large. This method worked in some cases but not always. The method was used as a means of directing the refinements in the direction of the desired force field. The second method employed was to refine the force constants in groups representing the different types of constants (stretches, stretch-bend interactions, etc.) or in groups organized to minimize the correlations between the constants. This method was tried several times, but never worked successfully. In almost all cases where a few force constants were refined, one or more of the constants would grow to an unreasonable value. The 'best' force fields were obtained when all the constants which could be refined were allowed to refine. This is the case of fitting the frequencies with the maximum number of adjustable parameters.

After eleven refinements, the force field developed yielded the most satisfactory results to date. The average errors resulting from Refinement No. 11 were: neo-inositol 10.2 cm^{-1} with thirty-nine bands assigned, myo-inositol 8.6 cm^{-1} with thirty-seven bands assigned, and epi-inositol 6.8 cm^{-1} with thirty-

eight bands assigned. The potential energy distributions agreed adequately with previous results.

The following refinement, Refinement No. 12, was an experiment to determine whether refining the inositols in symmetry block form was acting as a constraint on the refinements. neo-Inositol was refined using C_s symmetry, only a plane of symmetry, instead of the normal C_{2h} symmetry. The C_s symmetry results in two symmetry blocks and the C_{2h} in four symmetry blocks. The initial conditions for Refinement No. 12 were identical to those used in Refinement No. 11 where neo-inositol was refined using C_{2h} symmetry. Several differences were noted between the two refinements. The origin of the differences involved the switching of assignments in one of the two symmetry blocks of neo-inositol. The eigenvalues, proportional to the frequencies, are arranged in order of decreasing magnitude after they are calculated from the '$\underset{\sim}{GF}$' product diagonalization. If, during a refinement, one calculated frequency becomes higher than another, its position in the ordering will then change. This, in effect, assigns the frequency to a new, different experimental frequency. In the case of neo-inositol, the reduced C_s symmetry placed fewer constraints on the assignments. With a greater number of frequencies in each of the two C_s symmetry blocks, the frequencies were closer together and consequently more assignment changes from the frequency ordering could and did take place. The assignments for only two pairs of frequencies were changed, but the average error for neo-inositol dropped over 1 cm^{-1} from the average error of Refinement No. 11. Refinement No. 12 ran fourteen perturbations while Refinement No. 11 ran seven perturbations. The resulting force fields were substantially different in terms of force constant magnitudes. The comparison of these two refinements clearly illustrates that the refining of a molecule in symmetry block form is acting as a constraint on the assignments and the refinement results by permitting fewer assignment changes than would occur if the molecule were refined in unsymmetrized form.

This finding reinforced the previous decision to refine the molecules in their symmetrized form versus the unsymmetrized form. Refinement in the unsymmetrized form could likely result in, for example, an assignment change which would assign a calculated Raman active mode to an observed infrared active band. Thus the advantage in the assignment of the inositols gained from the symmetry analysis information would be lost.

After Refinements No. 11 and 12, a major turning point was reached in the development of the inositol force field. The primary innovation involved changing the value of the COH bending constant, Constant 7 in Table XIX, and subsequently fixing the constant. Calculations by Wells (23) on β-arabinose C-d_6 indicated that a value of approximately 0.95 was needed for the COH bending constant to adequately reproduce the experimental COH bending frequencies. Up until this time, a COH bending constant of approximately 0.87 had been used. Even though a satisfactory force field had been developed, it was decided that this change could potentially result in improvements. For the subsequent refinement, the COH bending constant was started at 0.95. During the course of the refinement, the COH constant dropped to 0.84, a value considered unsatisfactorily low. To prevent this undesired drop, the COH constant was then fixed at 0.95. The next several refinements involved readjusting the other constants in the field. The adjustments concentrated on the stretch-bend interaction constants, Constants 12 through 17 in Table XIX, which are the most influential of the interaction force constants.

After several refinements, renewed attempts were made to assign the experimental frequencies of deuterated neo-inositol and deuterated scyllo-inositol. Previous attempts had shown that substantial errors, around 50 cm^{-1} for assignments in the region 1250-1350 cm^{-1}, would be involved in assigning the deuterated neo-inositol spectrum. It was believed that the final inositol force field

should be able to satisfactorily predict the deuterated spectra. The inability of previous fields to satisfactorily predict the deuterated spectra was viewed as an inadequacy in the fields which would be reflected in the potential energy distributions of all the inositols. The fit of the frequencies for deuterated neo-inositol was now definitely improved. It could be seen where errors in assigning the deuterated neo-inositol frequencies had been made earlier, the previous fits were actually poorer than had been suspected. The potential energy distributions were believed to now be more representative than those previously obtained.

Based on the improved results with the new COH bending constant, it was decided that the assigned deuterated scyllo-inositol and deuterated neo-inositol should be added as a constraint in the refinements to help optimize the force field and the potential energy distributions. It was felt that deuterated scyllo-inositol and deuterated neo-inositol were quite unique for deuterated carbohydrates in that they could be quite accurately assigned using the vibrational selection rules. In the case of the less symmetric myo-inositol and epi-inositol, the deuterated spectra could not be as accurately assigned. Because of the larger number of bands occurring in both the Raman and infrared, the resolution of the bands in the partially deuterated spectra was not as clear. In addition, when the four inositols were recrystallized from D_2O, the crystals obtained from the scyllo-inositol and neo-inositol solutions were noticeably better formed than the crystals from the myo-inositol and epi-inositol solutions. The quality of the crystals is reflected in the better clarity and band resolution observed in the Raman and infrared spectra of deuterated scyllo-inositol and deuterated neo-inositol versus the spectra of deuterated myo-inositol and deuterated epi-inositol as illustrated in Fig. 11 through 14. For these reasons, deuterated myo-inositol and deuterated epi-inositol were not included in the refinements.

Fourteen refinements after the COH bending constant had been changed, it was again thought that a satisfactory force field had been developed. The force field from Refinement No. 28-2 was the final sixty parameter field. The force constant values from Refinement No. 28-2 are listed in Table XX. The average errors resulting from Refinement No. 28-2 were: scyllo-inositol 10.8 cm^{-1} with twenty-two bands assigned, neo-inositol 9.3 cm^{-1} with forty-two bands assigned, myo-inositol 9.9 cm^{-1} with forty bands assigned, epi-inositol 9.9 cm^{-1} with forty-three assigned, deuterated scyllo-inositol 9.5 cm^{-1} with eighteen bands assigned, deuterated neo-inositol 11.2 cm^{-1} with thirty-nine bands assigned and L-chiro-inositol 9.8 cm^{-1} with thirty-eight bands assigned. scyllo-Inositol and deuterated scyllo-inositol have fewer assigned frequencies because there are two symmetry species in the scyllo-inositol D_{3d} point group which are inactive in both the Raman and the infrared and frequencies calculated in these species were not observed and thus were not assigned. Also, only one frequency of the doubly degenerate pairs was assigned. If two frequencies were observed, they were averaged and assigned to one of the degenerate calculated frequencies. The potential energy distributions from Refinement No. 28-2 were in agreement with previous work. An additional validation of the force field was the inclusion of the deuterated spectra in the refinement. The predictive capability of the force field was demonstrated by the successful incorporation of L-chiro-inositol into the refinement for the first time.

During the development of the force field, there was some confusion as to the status of the smaller magnitude bend-bend interaction force constants. Initially, it was not known which interaction constants were essential and which, if any, were just meaningless factors used to fit the frequencies. At first it was thought that all the small magnitude bend-bend interaction constants could be zeroed and fixed. But through experience it was found that even though many were of small magnitude, they provided important coupling between the atomic

motions. After Refinement No. 28-2, it was decided to group those bend-bend interaction constants which were physically indistinguishable under single constants. This served to minimize the number of constants but also preserve their necessary contributions. The final force constant definitions and groupings are as shown in Table XIX.

After the force field was condensed, two additional refinements were run to adjust the force constants. L-chiro-Inositol was removed from the second refinement because the frequency assignments were not as certain as for the other molecules. It was decided that the final force field would be developed using molecules where the frequency assignments were as correct as possible.

For the previous sixteen refinements, the COH bending constant had been held fixed. It was known that this was a definite constraint on the ability of the force field to fit the frequencies. Since the force field had been fitted around this constant many times, it was decided that the constant was not so special that it should not be allowed to refine. The results of the refinement would be checked to see if the COH constant had dropped in magnitude as it had done previously and if the potential energy distributions remained reasonable. During the refinement, the COH bending constant dropped only to 0.923. None of the other constants changed significantly. After close examination of the frequency assignments, the force constant values and the calculated results, it was decided that the attributes listed at the beginning of the Discussion of Results section had been satisfactorily optimized at this point. Thus the force field from this refinement represents the final inositol force field which is presented in Table XIX and was used to calculate the final results of the theoretical model which will be discussed later.

If each refinement conducted were examined individually, the sequence of refinements to this final inositol force field would appear even more haphazard than it does in this summary. Part of the purpose of this summary was to illustrate that the development of a force field for a group of compounds involves subjective judgments based primarily on experience, many false starts and a few lucky breaks.

At the beginning of this section, the attributes desired in the final force field and calculated results were listed. The degree to which some of these attributes were attained can now be evaluated. The first quality desired was the correct assignment of the calculated frequencies to the experimental frequencies. The several sources of information utilized in making the frequency assignments have already been discussed. The frequency assignments were examined and corrected repeatedly throughout the sequence of refinements. Several times wrong assignments were pointed out by the results of the refinements. By the final refinement, it was felt that a large majority of the assignments were sound and as correct as could be attained with the information available. The other attributes desired in the final force field were reasonable values of the force constants and a minimum number of force constants in the force field. In the judgment of the author, the values of the force constants listed in Table XIX are all reasonable. The number of force constants defined in the field could not be minimized further without jeopardizing the quality of the results. It is believed that these three attributes were optimized in the final results.

The other three attributes will be examined in later sections.

FACTORS INFLUENCING THE FORCE CONSTANT VALUES OBTAINED FROM A NONLINEAR LEAST-SQUARES REFINEMENT AND SOME CONVERGENCE PROPERTIES OF THE FLETCHER-POWELL METHOD

Experience has shown that a multiplicity of factors influence the force constants resulting from a refinement. Several of these factors have already been

discussed. Following is a list of factors which are known to affect the values of the force constants obtained from a refinement:

1. The frequency assignments.
2. The correlations between the force constants.
3. The number and groupings of the force constants defined in the force field.
4. The initial force field in the refinement.
5. Which force constants were held fixed during a refinement.
6. Whether the molecules were refined in symmetry block form or unsymmetrized.
7. The number and type of molecules included in the refinement, i.e., if any deuterated analogues were included.
8. The molecular geometry used in defining the molecules.
9. The variation in the strengths of the hydrogen bonds present in a molecule or series of compounds.

All these factors must be kept in perspective when force fields of the type used in this thesis (SVQFF) are compared with other force fields of a similar nature. This makes a direct comparison of force fields difficult. In Table XIX, the final inositol field is compared numerically with the force constants developed by Wells (23) for the hexoses, Edwards (22) for the pentose sugars, Pitzner (18) for the 1,5-anhydropentitols and Snyder and Zerbi (13) for the ethers. Without additional information, little can be said in comparing the fields except that they are numerically similar.

Because the factors listed above affect the values of the force constants, they also affect the transferability of a set of force constants from one molecular system to another. Each force field is developed under its own unique

conditions. One then cannot expect direct transferability to different molecular systems of the type of force constants developed for the inositols. However, transferability can be expected to molecules of similar structure. This was one of the attributes desired in the inositol force field, satisfactory predictive capabilities, i.e., transferability of the force field to inositols not included in the refinements. This aspect will be dealt with in Part II.

After the final inositol force field was developed, two experimental refinements were conducted in order to gain some additional information concerning the convergence properties of the Fletcher-Powell refinement method. In a normal refinement, where experimentally observed frequencies are assigned to calculated frequencies, it is very difficult to discern whether the least-squares difference between the assigned and calculated frequencies has been minimized to the lowest possible value or whether the refinement has settled into a higher 'false' minimum and terminated at this point. To test the convergence power of the Fletcher-Powell method, an experiment was set up whereby calculated frequencies were substituted as the observed frequencies. In this way, the Fletcher-Powell method was given a case where a harmonic solution, the harmonic force field used to calculate the frequencies, was known. The least-squares difference theoretically could be reduced to nearly zero (not exactly zero because the calculated frequencies, used as the observed frequencies, were entered into the program less precisely than they were calculated). This type of experiment was conducted to not only see if the Fletcher-Powell method would converge at the lowest minimum, but also to see if it would converge to the same force field used to calculate the 'observed' frequencies.

In the first experiment, the initial average error between the 'observed' frequencies and the starting calculated frequencies was 4.5 cm^{-1}. The largest individual error was 22.0 cm^{-1}. Twenty-eight force constants were refined to

two-hundred twelve frequencies assigned for scyllo-inositol, neo-inositol, myo-inositol, epi-inositol, deuterated scyllo-inositol and deuterated neo-inositol. After twenty-four perturbations the refinement terminated because all the adjustments made in the force constants were less than 0.0001. The final average error was 0.22 cm^{-1}. The largest remaining individual error was 1.1 cm^{-1}. The initial field, final field, changes in the force constants, the reference force field, and the difference between the reference constants and the final constants are listed in Table XXI. The reference force field is the field used to calculate the frequencies used as observed frequencies. The force constant numbers in Table XXI correspond to the force constants defined in Table XIX. It can be seen that most of the final force constants converged quite close to the reference force constant values. The average difference between the reference field values and the final field constants was 0.003. The largest differences were 0.011 for Constants No. 1 (C-O stretch) and No. 16 (C-C,CCO stretch-bend interaction).

In the second experiment, the initial conditions were chosen such that there was a substantially greater difference between the initial starting force field and the reference field. The initial average between the 'observed' frequencies and the initial calculated frequencies was 11.1 cm^{-1}, with the largest individual error being 30.8 cm^{-1}. One-hundred nineteen frequencies were assigned for scyllo-inositol, neo-inositol, myo-inositol, and epi-inositol. Thirty-four force constants were refined. The refinement terminated after sixty-two perturbations when all the adjustments to the force constants became less than 0.0001. The final average error was 0.46 cm^{-1} with the largest remaining individual error being 3.8 cm^{-1}. The results of the refinement are shown in Table XXII. The force constant numbers correspond to the force constants defined in Table XX. In this case, many of the final constants did not converge as closely to their counterparts in the reference field. The average difference between the reference field

TABLE XXI

TABULATED RESULTS FROM EXPERIMENTAL REFINEMENT NO. 1

	INITIAL FIELD	FINAL FIELD	CHANGE	REFERENCE FIELD	DIFFERENCE FROM FINAL FIELD
1	5.135527	5.133189	0.002337	5.144029	0.010839
2	4.184429	4.189668	-0.005239	4.193250	0.003582
3	4.690000	4.690000	0.0	4.690000	0.0
4	6.283000	6.283000	0.0	6.283000	0.0
5	0.739160	0.727932	0.011228	0.727881	-0.000051
6	0.942694	0.964967	-0.022273	0.969146	0.004179
7	0.940000	0.922869	0.017131	0.923119	0.000250
8	1.188845	1.202576	-0.013731	1.204652	0.002076
9	1.048650	1.046455	0.002194	1.043774	-0.002682
10	0.260000	0.299392	-0.039392	0.301909	0.002517
11	0.039984	0.048569	-0.008585	0.042947	-0.005622
12	0.361417	0.365272	-0.003855	0.360495	-0.004777
13	0.460426	0.424970	0.035456	0.425304	0.000334
14	0.665000	0.703009	-0.038009	0.706657	0.003648
15	0.329581	0.325991	0.003590	0.329380	0.003389
16	0.501295	0.484427	0.016868	0.495089	0.010662
17	0.483179	0.482689	0.000490	0.481679	-0.001010
18	0.130489	0.138119	-0.007630	0.140437	0.002318
19	-0.086110	-0.075456	-0.010654	-0.075703	-0.000247
20	0.029006	0.019965	0.009041	0.016806	-0.003159
21	0.038063	0.004250	0.033813	0.008313	0.004063
22	0.048988	0.044912	0.004076	0.047686	0.002774
23	-0.150000	-0.228918	0.078918	-0.230225	-0.001307
24	-0.096977	-0.087160	-0.009817	-0.084390	0.002770
25	-0.102251	-0.112838	0.010587	-0.110675	0.002163
26	0.103721	0.084597	0.019124	0.087413	0.002816
27	0.013615	0.017971	-0.004356	0.018065	0.000094
28	0.085641	0.094223	-0.008582	0.094882	0.000659
29	0.057695	0.059710	-0.002015	0.059368	-0.000342
30	0.139251	0.115199	0.024052	0.115445	0.000246
31	0.100000	0.100000	0.0	0.100000	0.0
32	0.015000	0.015000	0.0	0.015000	0.0
33	0.0	0.0	0.0	0.0	0.0

TABLE XXII

TABULATED RESULTS FROM EXPERIMENTAL REFINEMENT #2

	INITIAL FIELD	FINAL FIELD	CHANGE	REFERENCE FIELD	DIFFERENCE FROM FINAL FIELD		INITIAL FIELD	FINAL FIELD	CHANGE	REFERENCE FIELD	DIFFERENCE FROM FINAL FIELD
1	5.107855	5.124616	-0.016761	5.101148	-0.023468	31	0.0	0.0	0.0	0.0	0.0
2	4.690000	4.690000	0.0	4.690000	0.0	32	0.0	0.0	0.0	0.0	0.0
3	4.188583	4.148924	0.039660	4.187780	0.038857	33	0.078378	0.094104	-0.015726	0.073624	-0.020480
4	6.283000	6.283000	0.0	6.283000	0.0	34	-0.069287	0.005553	-0.074840	0.008949	0.003396
5	0.0	0.0	0.0	0.0	0.0	35	-0.162714	-0.116319	-0.046395	-0.104224	0.012095
6	0.747173	0.725302	0.021871	0.726543	0.001241	36	-0.027954	-0.039437	0.011483	-0.059121	-0.019684
7	0.0	0.0	0.0	0.0	0.0	37	0.0	0.0	0.0	0.0	0.0
8	1.246827	1.240165	0.006662	1.225677	-0.014488	38	0.046773	0.014070	0.032703	0.019607	0.005537
9	0.866440	0.940971	-0.074531	0.940000	-0.000971	39	0.040279	-0.004499	0.044778	0.024341	0.028840
10	1.126422	1.092910	0.033512	1.082369	-0.010541	40	0.000000	-0.012547	0.012547	-0.016625	-0.004078
11	0.936464	0.901693	0.034771	0.860828	-0.040865	41	0.012687	-0.025961	0.038648	-0.036444	-0.010483
12	0.0	0.0	0.0	0.0	0.0	42	0.029000	0.110189	-0.081189	0.094821	-0.015368
13	0.0	0.0	0.0	0.0	0.0	43	0.000000	0.038001	-0.038001	0.056688	0.018687
14	0.104087	0.259623	-0.155536	0.263445	0.003822	44	0.0	0.0	0.0	0.0	0.0
15	0.108831	0.144907	-0.036076	0.157699	0.012792	45	0.0	0.0	0.0	0.0	0.0
16	0.0	0.0	0.0	0.0	0.0	46	-0.147043	-0.139953	-0.007090	-0.128926	0.011027
17	0.0	0.0	0.0	0.0	0.0	47	0.036467	-0.044852	0.081319	-0.047600	-0.002748
18	0.0	0.0	0.0	0.0	0.0	48	0.077535	0.030265	0.047270	0.029335	-0.000930
19	0.0	0.0	0.0	0.0	0.0	49	0.092275	0.069003	0.023272	0.069338	0.000335
20	0.384100	0.401055	-0.016955	0.404214	0.003159	50	0.000000	0.028970	-0.028970	0.026991	-0.001979
21	0.0	0.0	0.0	0.0	0.0	51	0.046247	0.086798	-0.040551	0.084632	-0.002166
22	0.770521	0.675626	0.094895	0.665772	-0.009854	52	-0.055498	-0.081916	0.026418	-0.086599	-0.004683
23	0.0	0.0	0.0	0.0	0.0	53	-0.155345	0.116104	-0.271449	0.118775	0.002671
24	0.432664	0.431968	0.000696	0.439401	0.007433	54	0.140990	0.109218	0.031772	0.106396	-0.002822
25	0.506924	0.363396	0.143528	0.360974	-0.002422	55	0.0	0.0	0.0	0.0	0.0
26	0.373897	0.486378	-0.112481	0.486506	0.000128	56	0.0	0.0	0.0	0.0	0.0
27	0.0	0.0	0.0	0.0	0.0	57	0.0	0.0	0.0	0.0	0.0
28	0.0	0.0	0.0	0.0	0.0	58	0.0	0.0	0.0	0.0	0.0
29	0.349091	0.457232	-0.108141	0.450611	-0.006621	59	0.100000	0.100000	0.0	0.100000	0.0
30	0.0	0.0	0.0	0.0	0.0	60	0.015000	0.015000	0.0	0.015000	0.0

constants and the final field constants was 0.01. Several of the constants, No. 1 (C-O stretch), No. 3 (C-C stretch), and No. 11 (HCO bend), are distinctly different from their counterparts in the reference field. But some constants, such as No. 9 (COH bend) and No. 14 (C-C,C-O stretch-stretch interaction), changed substantially in value during the refinement and came close to the corresponding values in the reference field.

The results of these two refinements suggest that the Fletcher-Powell algorithm does reduce the least-squares difference to the lowest minimum, even from quite ill-defined initial conditions as was the case in the second experiment. This result clearly indicates that the average errors between the assigned and calculated frequencies are not the result of the Fletcher-Powell algorithm terminating at a minimum other than the lowest minimum. This result will be discussed more fully in a later section when contributions to the average errors are analyzed. Both refinements, especially the second, suggest that the minumum can be attained with a force field different in varying degrees from the reference field used to calculate the 'observed' frequencies. This is illustrated by the differences between the final constants and the reference constants. Additional conclusions or interpretations concerning the meaning of the results cannot be justified. Further work would have to be done on the properties of the Fletcher-Powell method before additional conclusions could be made.

COMPARISON OF THE ASSIGNED EXPERIMENTALLY OBSERVED FREQUENCIES AND THE CALCULATED FREQUENCIES FOR *scyllo*-INOSITOL, *neo*-INOSITOL, *myo*-INOSITOL, *epi*-INOSITOL, DEUTERATED *scyllo*-INOSITOL, AND DEUTERATED *neo*-INOSITOL

In order to accurately interpret the vibrational spectra of the inositols, the normal coordinate calculations had to be able to satisfactorily reproduce the experimentally observed frequencies. In this section, the calculated frequencies

will be compared with the assigned experimental frequencies for scyllo-inositol, neo-inositol, myo-inositol, epi-inositol, deuterated scyllo-inositol, and deuterated neo-inositol. The assigned experimentally observed frequencies will than be interpreted using the calculated potential energy distributions.

When the initial frequency assignments were made, it was found that the calculations were not reproducing the entire observed spectra. In all cases, there were fewer calculated frequencies than observed frequencies. Some observed frequencies, then, were not assigned. Following the interpretation of the assigned frequencies, the unassigned bands will be examined.

To visually illustrate the agreement between the calculated and assigned frequencies, bar graph representations of the assigned experimental frequencies and the calculated frequencies will be presented. The frequency assignments will not be explicitly indicated on the graphs, but in most cases the assignments are apparent from the one-to-one correspondence. The frequency assignments used in the final refinement are given in the potential energy distribution tables in Appendix V.

The bar graph representation of the assigned experimental frequencies and calculated frequencies for scyllo-inositol is shown in Fig. 23. To more clearly illustrate the reproducibility of the assigned frequencies by the calculated frequencies, the frequencies are presented in two groups, the Raman frequencies and the infrared frequencies. The frequencies labelled with a 'D' are calculated to be doubly degenerate frequencies. The experimental frequencies to which the degenerate frequencies were assigned are indicated in the figure. In most cases, two experimental bands were observed for each calculated degenerate mode. In these instances the degeneracy has broken down and the vibrations are occurring at two different frequencies. In general, the band pairs observed in the infrared

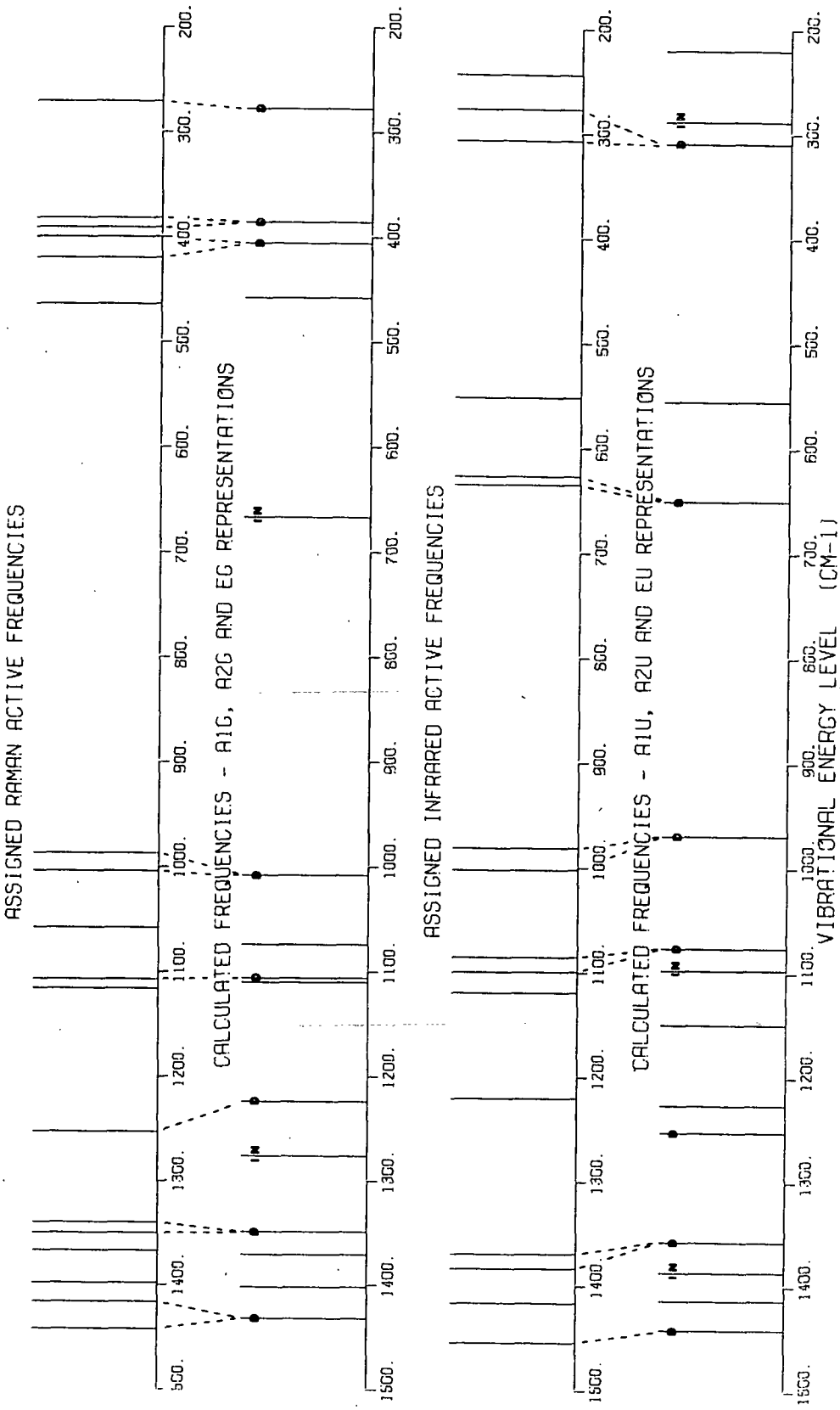

Figure 23. Bar Graph Representations of the Assigned Experimentally Observed Frequencies and Calculated Frequencies for scyllo-Inositol

were of approximately the same intensity while those observed in the Raman were not. The observed split between the observed bands assigned to degenerate modes ranged from 30 to 8 cm^{-1}. Assuming each of the calculated degenerate frequencies is assigned to one of the observed pair, then thirty-five frequencies were assigned for scyllo-inositol with an average error of 13.3 cm^{-1}. This is relatively poor agreement compared to the other inositols.

The frequencies labelled with an 'IN' in Fig. 23 are calculated to be inactive in both the Raman and infrared. These bands were not assigned, but some question remains as to whether these bands are observed in the infrared because of the presence of the extra bands cited earlier. The A_{1u} species modes, inactive in the infrared, calculated at 1359 and 1097 cm^{-1} were not assigned. The mode at 1097 cm^{-1} did not appear to be present and for the 1359 cm^{-1} mode it was uncertain. An infrared active degenerate mode calculated at 1252 cm^{-1} was not assigned because of the uncertainty as to which of the bands in the region were fundamentals. Neither of the A_{2g} species modes, inactive in the Raman, calculated at 1275 and 667 cm^{-1} were observed in the Raman spectrum.

The Raman and infrared spectra of neo-inositol, shown in Fig. 5 and 6, were easily the most straightforward to assign. The majority of the bands are spaced apart and easily distinguished. Forty-two frequencies were assigned for neo-inositol with an average error of 8.8 cm^{-1}. The assigned experimental and calculated frequencies are shown in Fig. 24. The spectra have again been separated into the Raman and infrared groups. Frequencies belonging to the A_g and B_g symmetry species are Raman active and infrared inactive and the frequencies belonging to the A_u and B_u symmetry species are infrared active and Raman inactive. The figure shows that the calculated frequencies reproduce the assigned frequencies well. In neo-inositol there occurred two Raman modes which were accidently degenerate and two infrared modes which were accidently degenerate.

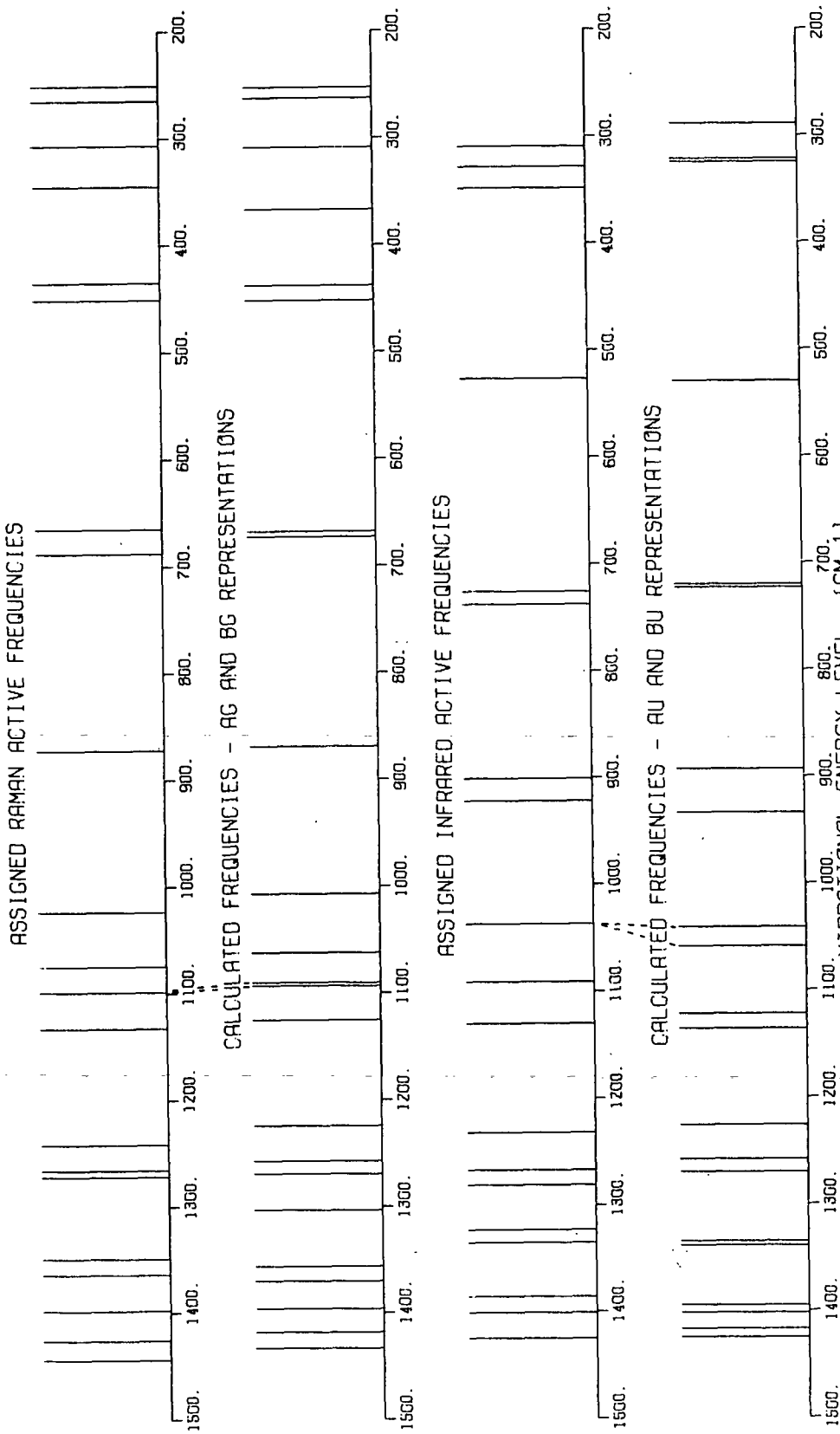

Figure 24. Bar Graph Representations of the Assigned Experimentally Observed Frequencies and Calculated Frequencies for neo-Inositol

The Raman band observed at 1098 cm^{-1} was concluded to be two accidently degenerate frequencies because two Raman active frequencies were calculated in close proximity at 1090 and 1092 cm^{-1}. After several different assignment schemes were tried, the only combination which gave satisfactory results was when both calculated frequencies were assigned to the single observed band at 1098 cm^{-1}. The infrared band at 1037 cm^{-1} was also concluded to be two accidently degenerate frequencies. The two calculated frequencies, at 1041 and 1059 cm^{-1}, assigned to the observed 1037 cm^{-1} band are not as close in frequency as in the previous case. But several different assignment combinations were tried and satisfactory results were only obtained when the two calculated frequencies were assigned to the 1037 cm^{-1} band. The 1037 cm^{-1} band does split slightly at liquid nitrogen temperature providing further support for the assignment. The two calculated frequencies and the single experimental frequency to which they were assigned are indicated for both cases by the dotted lines in Fig. 24.

The assigned experimental and calculated frequencies for myo-inositol are shown in Fig. 25. The frequencies have been divided into the A' and A'' symmetry species of the myo-inositol C_s point group. Both species are active in both the Raman and infrared. The agreement between the assigned frequencies and the calculated frequencies is again seen to be quite good. Forty-two bands were assigned for myo-inositol with an average error of 9.7 cm^{-1}.

For epi-inositol, forty-four bands were assigned with an average error of 8.5 cm^{-1}. The assigned frequencies and the calculated frequencies for the A' and A'' species are shown in Fig. 26. The agreement is probably the best attained for any of the inositols.

A discussion of deuterated scyllo-inositol and deuterated neo-inositol will be included in this section and in the next section when the assigned frequencies

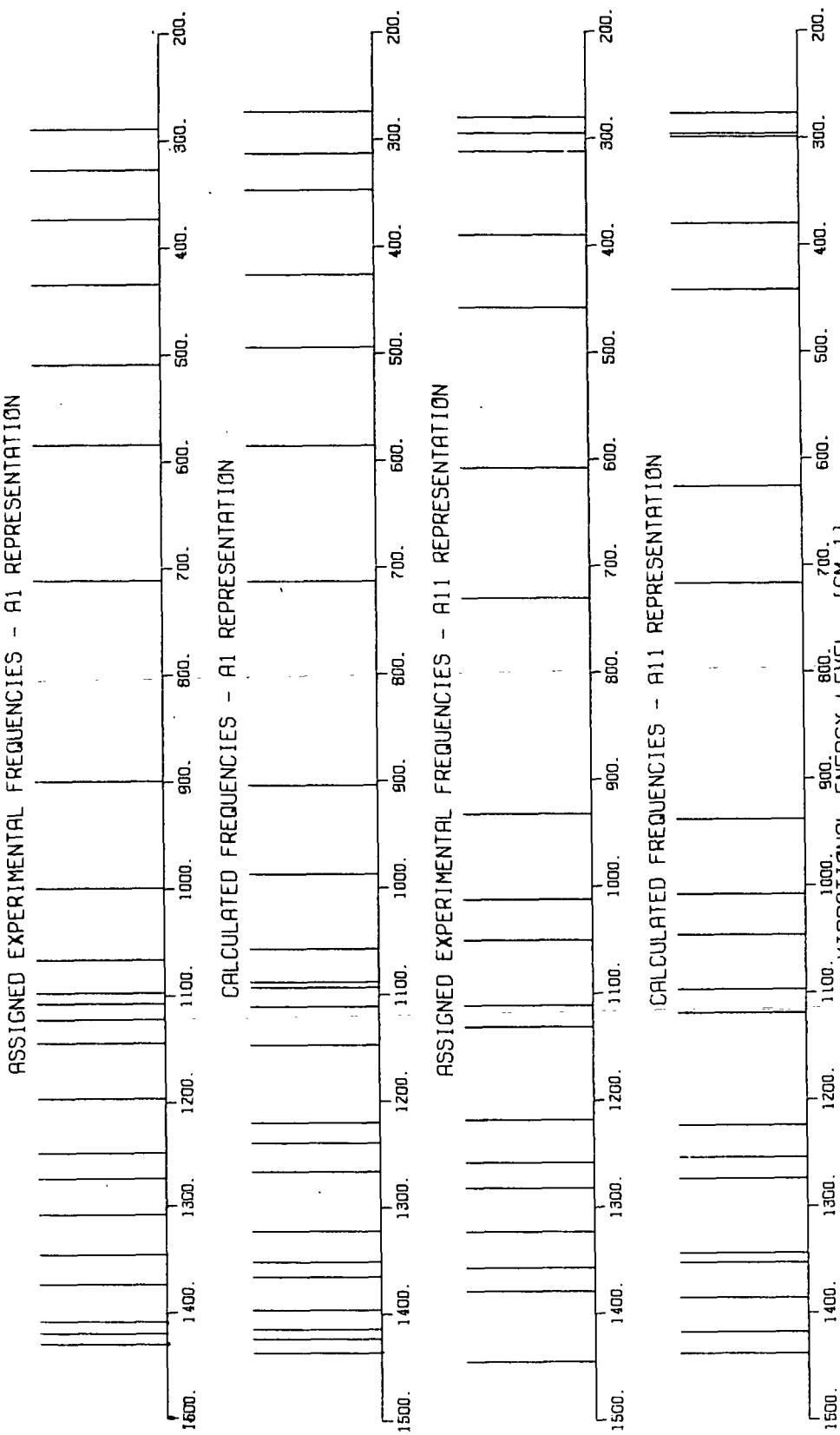

Figure 25. Bar Graph Representations of the Assigned Experimentally Observed Frequencies and Calculated Frequencies for myo-Inositol

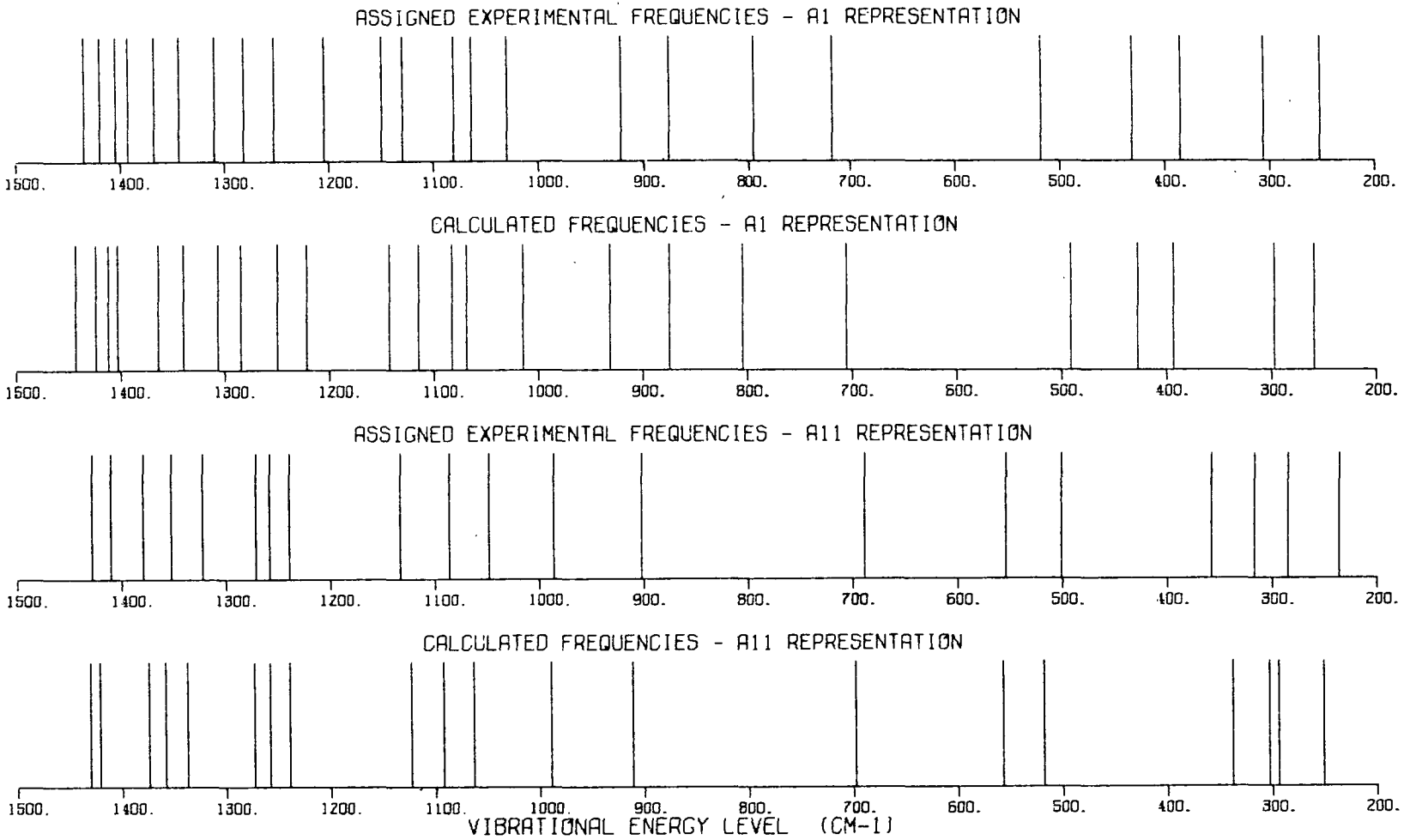

Figure 26. Bar Graph Representations of the Assigned Experimentally Observed Frequencies and Calculated Frequencies for epi-Inositol

are interpreted. These deuterated compounds provided an important constraint on the refinements. The satisfactory reproduction of the observed frequencies for deuterated scyllo-inositol and deuterated neo-inositol and the successful prediction of observed band shifts upon deuteration further establishes the validity of the force field and the calculated potential energy distributions.

The assigned frequencies for deuterated scyllo-inositol and the calculated frequencies are illustrated in Fig. 27. Thirty bands were assigned and were reproduced with an average error of 12.1 cm^{-1}. There was some difficulty in completely assigning the spectrum of deuterated scyllo-inositol, particularly in the infrared. This was primarily because of an excess number of observed bands. The origin of the extra bands will be discussed shortly. Several bands were left unassigned because of difficulty in some regions in identifying the deuterated scyllo-inositol fundamentals. The calculated frequencies were left unassigned rather than introduce uncertain assignments into the refinements. The doubly degenerate modes are labelled in the figure with a 'D' and the calculated inactive modes are labelled with an 'IN'. The A_{2g} modes, inactive in the Raman, were not observed in the Raman spectrum. The A_{1u} modes, inactive in the infrared, were not assigned but some question remains as to whether they are observed because of the extra observed infrared bands.

The assigned and calculated frequencies for deuterated neo-inositol are shown in Fig. 28. The frequencies have been divided into the Raman and infrared groups. The deuterated neo-inositol spectra were more completely assigned than the deuterated scyllo-inositol spectra and the agreement in Fig. 28 is seen to be almost as good as that attained for the undeuterated inositols. Forty-one bands were assigned with an average error of 10.9 cm^{-1}. Four cases of accidental degeneracy occurred and are indicated by the dotted lines in Fig. 28. The interpretation of the Raman bands observed at 1265 and 1095 cm^{-1} and the infrared

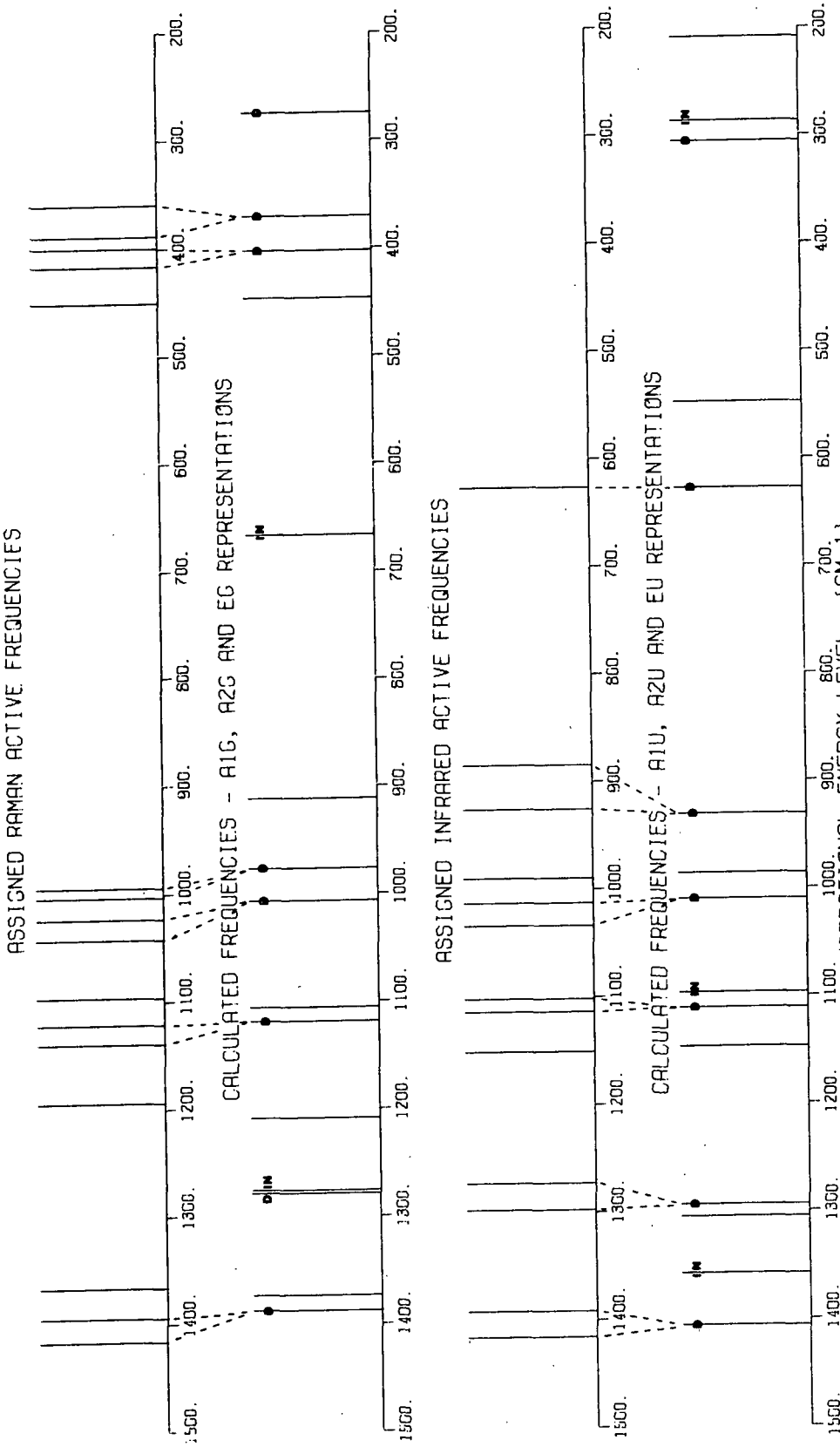

Figure 27. Bar Graph Representations of the Assigned Experimentally Observed Frequencies and Calculated Frequencies for Deuterated scyllo-Inositol

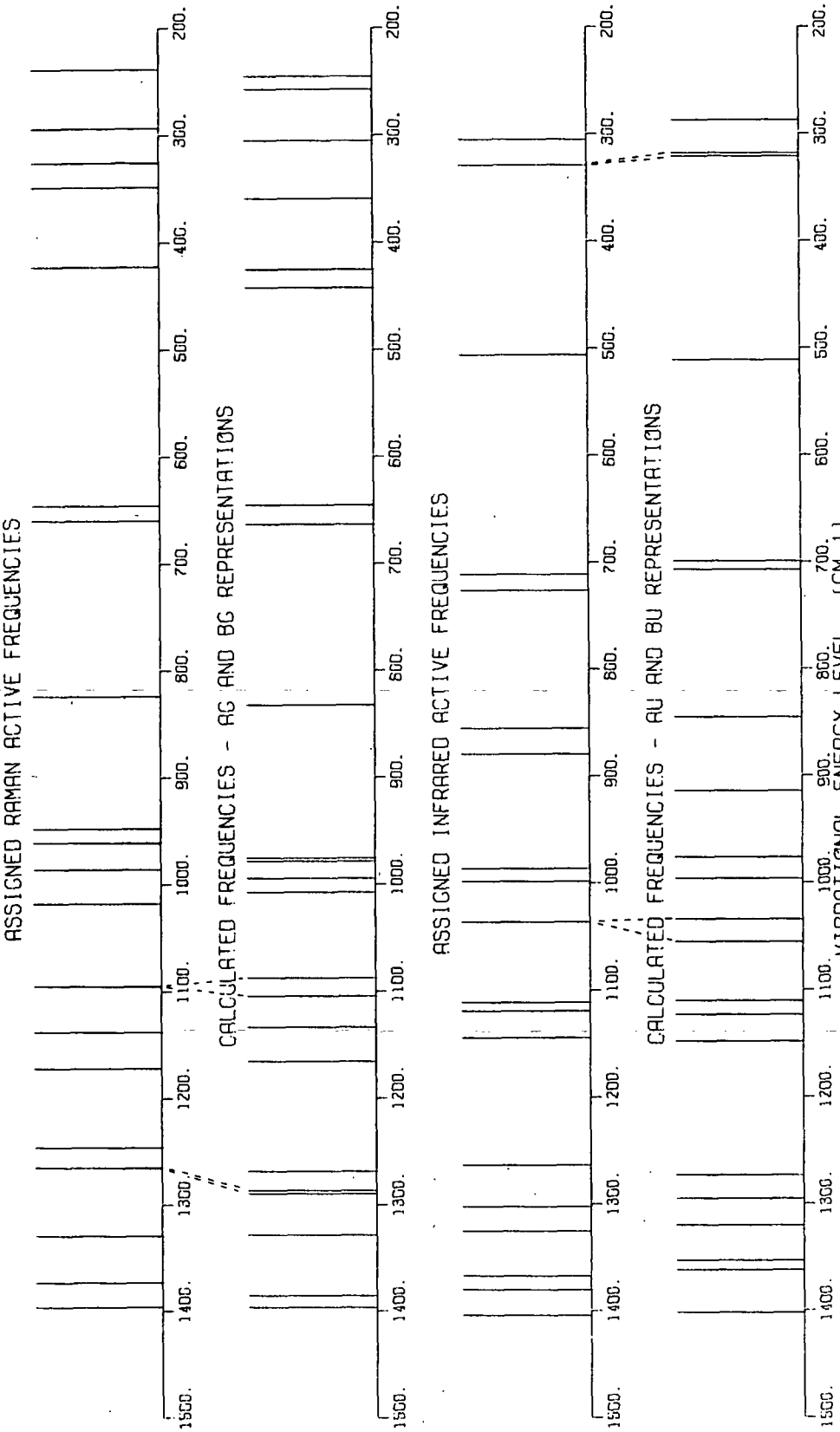

Figure 28. Bar Graph Representations of the Assigned Experimentally Observed Frequencies and Calculated Frequencies for Deuterated neo-Inositol

bands at 1037 and 330 cm^{-1} as two accidently degenerate frequencies was based on two frequencies being calculated at close proximity and/or the results of trying several assignment schemes.

The generally successful assignment of the deuterated scyllo-inositol and neo-inositol species validates an assumption implicit in their assignment. It was assumed that frequencies calculated using completely deuterated (d-6) molecules in the molecular model could be assigned to the observed frequencies resulting from molecules which are only approximately 70% deuterated. At 70% deuteration, assuming random deuteration, in fact only 12% of the molecules are calculated to be completely deuterated, whereas 30% are deuterated at five positions (d-5), 22% d-4, 19% d-3, 6% d-2, 1% d-1, and 0.07% d-0. The fact that the experimental spectra could be assigned using a completely deuterated model raises an interesting observation. There are 2^6 or 64 possible species ranging from no deuteration to complete deuteration present in the deuterated samples. Yet, the clarity and sharpness of the bands in the experimental deuterated scyllo-inositol and neo-inositol spectra, shown in Fig. 11 and 12, respectively, suggest that a large number of contributing species are not being observed. This is especially true in the Raman spectra. A large number of contributing species would be expected to broaden the bands and/or result in the observance of many weaker intensity bands. This latter phenomena may be what is being observed in the deuterated scyllo-inositol infrared spectrum, where extra weak intensity bands were observed. To more completely explain the clarity of the spectra at only 70% deuteration would require, and deserves, additional experimental attention, including better verification of the percent deuteration, which may well be a contributing factor in this case.

Considering the constraints of the small number of force constants, the refinement of the molecules in symmetrized form and the inclusion of the deuterated

compounds in the refinements, it is felt that the agreement for the six molecules of the calculated frequencies with the assigned experimental frequencies is quite good. Overall, two-hundred thirty-four experimentally observed frequencies assigned to the six inositols were reproduced with an average error of 10.4 cm^{-1}. One of the qualities desired in the final analysis was the optimum agreement between the refined calculated frequencies and the assigned experimental frequencies. Overall it is believed this objective has been achieved.

INTERPRETATION OF THE ASSIGNED EXPERIMENTALLY OBSERVED FREQUENCIES FOR CRYSTALLINE scyllo-INOSITOL, neo-INOSITOL, myo-INOSITOL, epi-INOSITOL, DEUTERATED scyllo-INOSITOL, AND DEUTERATED neo-INOSITOL

An important result of doing the normal coordinate analyses of the inositols is the calculated potential energy distributions. The potential energy distributions are the basis for interpreting the observed vibrational spectra in terms of atomic motions. Reasonable potential energy distributions was one of the qualities desired in the final inositol calculations. In this section, the interpretation of the assigned observed frequencies for scyllo-inositol, neo-inositol, myo-inositol, epi-inositol, deuterated scyllo-inositol and deuterated neo-inositol will be discussed. Length prohibits an interpretation of each individual band. For a detailed interpretation of any individual frequency or compound, the interested reader is referred to the potential energy distributions presented for each of the above compounds in Tables XLV through XLVIII, respectively, and Tables LII and LIII for the deuterated inositols, in Appendix V. For discussion purposes, a general outline of what types of motions are occurring in what regions of the inositol spectra will be presented. Following this, the symmetry properties of the molecular vibrations of the different inositols will be discussed.

The inositol spectra can be conveniently divided into five regions for discussion of the vibrational modes. The region 3450-2350 cm^{-1} encompases the OH

stretches, CH stretches and the OD stretches. The second region from 1460-1160 cm^{-1} is dominated almost exclusively by the in-plane (HCO internal coordinates) and out-of-plane (HCC internal coordinates) bending motions of the methine hydrogens and the in-plane bending motions of the COH groups. The bands in this region of the deuterated spectra involve only the methine bending modes. The C-O and C-C stretches predominate in the third region from 1160-850 cm^{-1} with some contributions from the methine bending and heavy atom bending (CCO and CCC bending) motions. The deuterated spectra in this region also contain the COD in-plane bending motions. The bands in the fourth region, between 850-250 cm^{-1} are characterized primarily by the CCO bending and CCC bending motions with minor methine bending and C-O and C-C stretching contributions also calculated. Below 250 cm^{-1}, additional ring bending, the ring torsions and the OH out-of-plane bending (C-O torsions) are calculated. In this study the terms 'CCC bending' and 'ring bending' are used synonymously. The division of the spectra into five regions is not meant to be a rigorous categorization of the different types of atomic motions. As the spectral regions are discussed, the extensive coupling between the different types of motions and the complexity of a majority of the vibrational modes will become apparent.

Region I: 3450-2350 cm^{-1}

The region 3450-2350 cm^{-1} contains the bands arising from the OH stretching, CH stretching, and OD stretching modes. These modes were not dealt with extensively in this work. The frequencies were not assigned for the refinements. The force constants used to calculate the OH and CH stretching frequencies were taken from Pitzner (18). These constants were not refined further.

The OH and OD stretching modes are observed in the regions 3450-3100 cm^{-1} and 2600-2350 cm^{-1}, respectively. They were observed in the infrared spectra and were not recorded in the Raman. The OH and OD stretching modes are strong,

somewhat broad bands in the infrared. Most of the OH stretching bands were observed to shift down in frequency, by up to 50 cm^{-1}, at liquid nitrogen temperature. The broad range, approximately 350 cm^{-1}, over which these modes are observed is indicative of the effect of hydrogen bonding. All the calculated OH stretching modes are predicted at a single frequency. Because the OH stretching modes were not recorded in the Raman, it could not be determined whether these modes obeyed mutual exclusion in the spectra of scyllo-inositol and neo-inositol. For both molecules, only three OH stretching modes are infrared active and in both cases only three bands were observed in the infrared. In the spectra of myo-inositol and epi-inositol, where there is no center of inversion, more than three OH stretching modes were observed in the infrared. The observance of only three bands for scyllo-inositol and neo-inositol suggests that the unit cells also possess a center of inversion. This cannot be verified, however, because the crystal structures of scyllo-inositol and neo-inositol have not been determined.

The methine CH stretching modes were observed in the region 2970-2880 cm^{-1} and were recorded in both the Raman and the infrared. In the Raman, the CH stretching bands were often very intense bands. In contrast, they were fairly weak intensity bands in the infrared. For scyllo-inositol and neo-inositol three CH stretching modes were calculated to be Raman active and three infrared active and three modes were observed in each the Raman and the infrared.

Region II: 1460-1160 cm^{-1}

The potential energy distributions are shown in this region to be dominated by motions of the methine hydrogens, both in-plane (HCO) and out-of-plane (HCC), and the COH in-plane bending motions. Only the motions of the methine hydrogens are present in this region of the deuterated compounds. This is illustrated in Fig. 29 and 30 which show bar graph representations of the potential energy

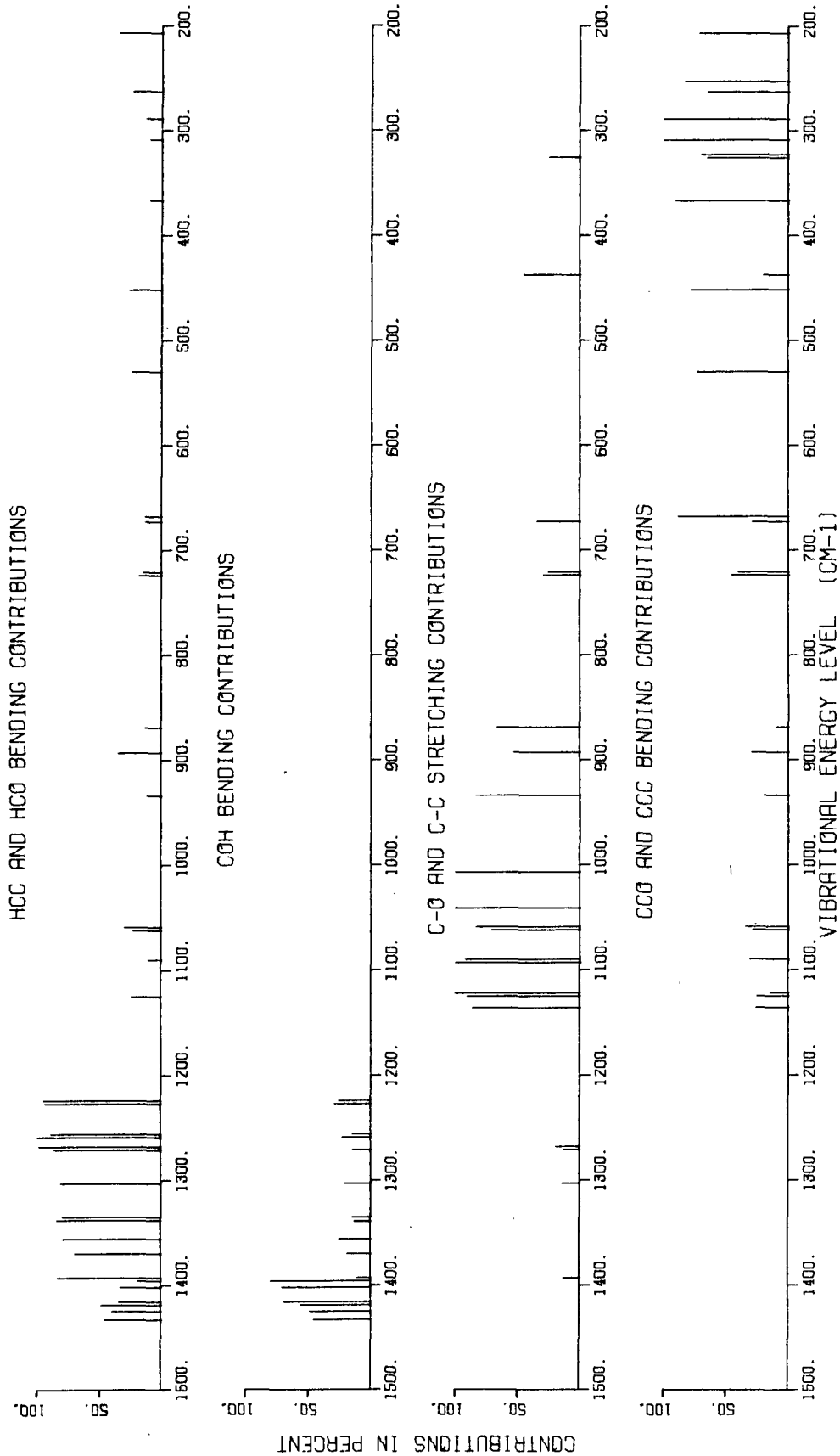

Figure 29. Bar Graph Representation of the Internal Coordinate Potential Energy Distribution for neo-Inositol

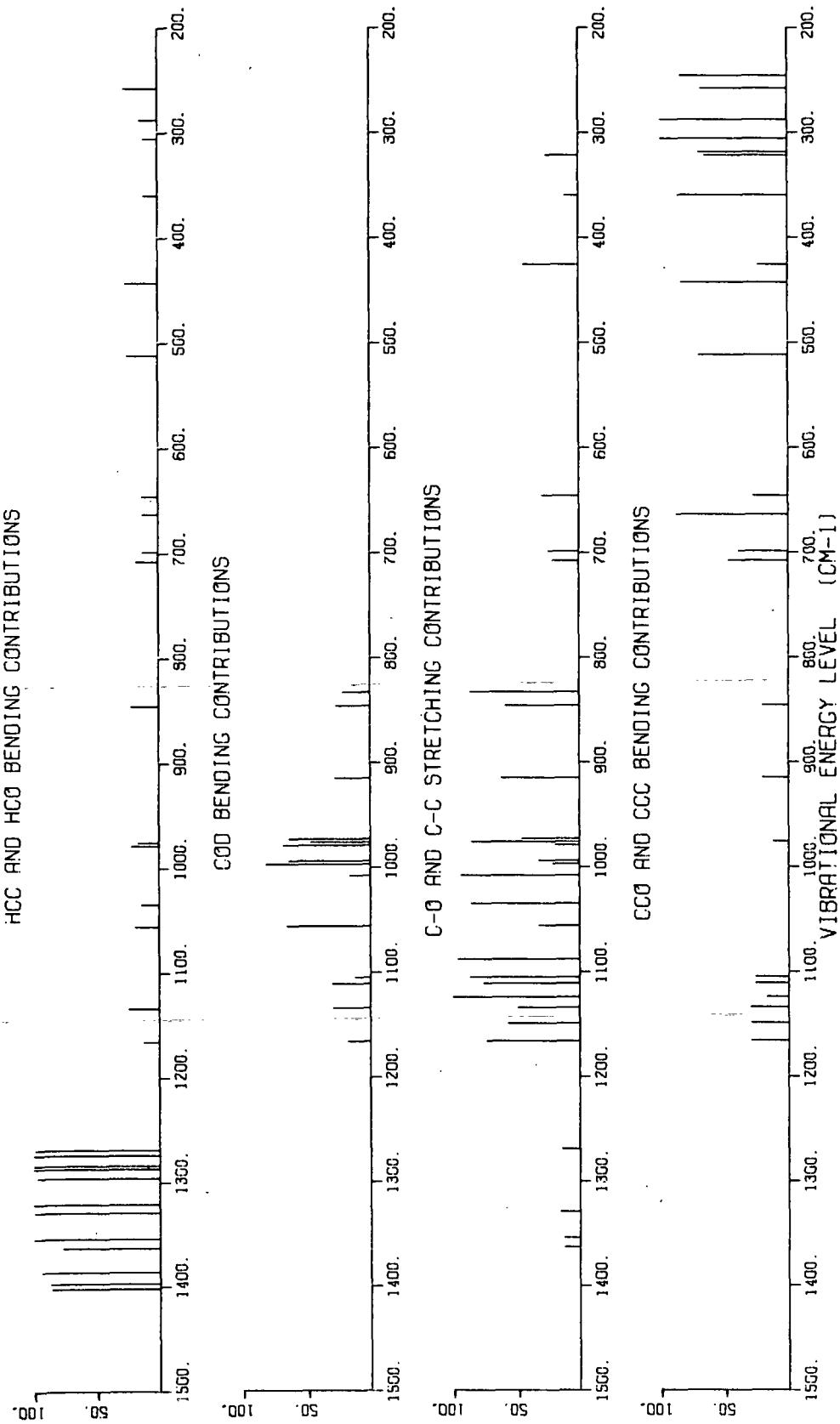

Figure 30. Bar Graph Representation of the Internal Coordinate Potential Energy Distribution for Oxygen Deuterated neo-Inositol

distributions of neo-inositol and deuterated neo-inositol, respectively. The different types of internal coordinates have been divided into four groups. The percent contribution of each group to the calculated neo-inositol and deuterated neo-inositol frequencies is represented on the ordinate axis. Only contributions greater than 10% were considered. These graphs provide a visual illustration of where, in general, the different groups of motions are making their major contributions in the spectral region from 1500-200 cm^{-1}. neo-Inositol and deuterated neo-inositol were chosen as having representative potential energy distributions for the inositols and deuterated inositols, but minor variations in the potential energy distributions of each inositol are present.

Figure 29 shows the methine bending and the COH bending deformations contribute extensively throughout Region II. The highest contributions of COH bending are centered around and above 1400 cm^{-1}, whereas the methine bending motions make their largest contributions starting just below 1400 cm^{-1}. The methine in-plane and out-of-plane bending deformations are highly mixed, but there is a noticeable tendency for the in-plane deformations to concentrate below approximately 1270 cm^{-1} and the out-of-plane deformations above 1270 cm^{-1}. A representative mode illustrating the methine and COH bending motions is shown in Fig. 31(A). In the figure, the smallest circles depict the relative motions of the atoms. The motions of the carbon and oxygen atoms were multiplied by a scaling factor in order to more clearly illustrate their small motions. The vibration illustrated in Fig. 31(A) is the 1355 cm^{-1} mode of neo-inositol which contains contributions from the methine in-plane and out-of-plane motions and the COH bending motions.

The methine bending deformations were observed to be relatively weak to medium intensity broad bands in the Raman, while the bands interpreted as primarily COH bending modes were quite weak, sometimes almost indiscernable. The 1460-1160 cm^{-1}

region in the Raman was often substantially clarified at liquid nitrogen temperature. The bands in this region of the infrared were generally of medium intensity.

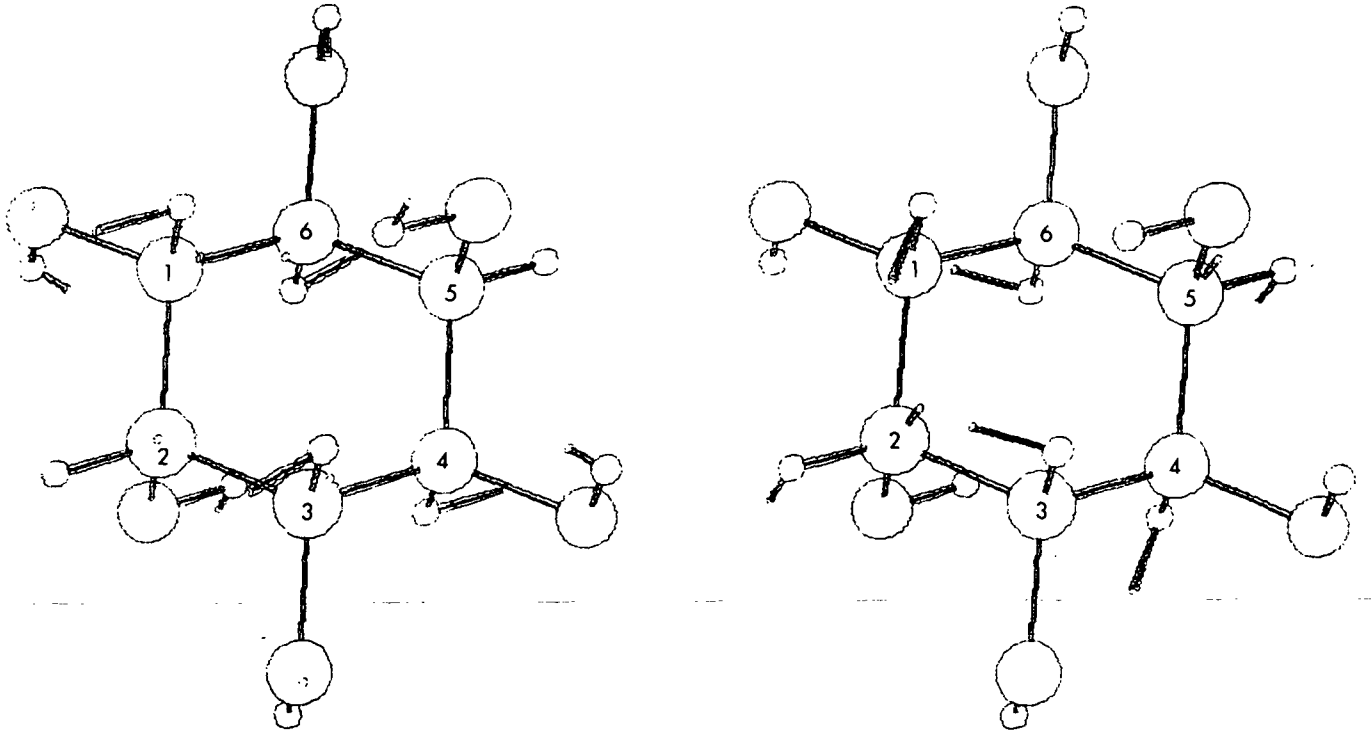

(A) neo-Inositol Mode at 1355 cm^{-1}

(B) Deuterated neo-Inositol Mode at 1354 cm^{-1}

Figure 31. Representative Vibrational Modes in Region II

Oxygen deuteration of the inositols shifts the COH bending deformations to lower frequencies leaving only the methine bending deformations in Region II. This is shown in Fig. 30. The methine in-plane and out-of-plane modes are still highly mixed, with the in-plane deformations again tending to concentrate in a lower region, below approximately 1350 cm^{-1}, than the out-of-plane deformations, above 1350 cm^{-1}. An example of a mode in Region II of the deuterated spectra is shown in Fig. 31(B). The mode is the 1354 cm^{-1} vibration of deuterated neo-inositol and shows only methine hydrogen motion with some heavy atom motion, but no hydroxyl hydrogen motion. The bands observed in Region II of the Raman

deuterated spectra were, in general, substantially more intense than in the undeuterated spectra.

Region III: 1160-850 cm^{-1}

Figure 29 shows that the C-O and C-C stretches are predominant in this region, but significant hydrogen bending and heavy atom bending (CCO and CCC bending) contributions are also present. The presence of several types of deformations in this region is indicative of the complexity of the vibrational modes. The presence of several interaction force constants in the force constant potential energy distributions confirms that the C-O and C-C stretches couple extensively with each other and also with the bending deformations, both the methine hydrogen bending and heavy atom bending deformations. An example of the complexity of the modes in Region III is shown in Fig. 32(A). This mode, the 1062 cm^{-1} band of neo-inositol, contains C-C and C-O stretching, methine bending, CCO and CCC bending and COH in-plane bending contributions. As a result, it can be seen that almost every atom in the molecule in Fig. 32(A) is in motion.

The observed Raman bands in Region III were usually of medium to strong intensity. On the average, they were substantially more intense than the proton bending modes in Region II. A majority of the observed infrared bands were among the most intense bands in the spectra. In several cases, a weaker Raman or infrared band would have a substantially more intense counterpart in the infrared or Raman. In the low temperature spectra the band clarity in both the Raman and the infrared was improved.

Figure 30 shows that the 1160-850 cm^{-1} region of the deuterated inositols contains all the types of motions just described, but in addition, the coupling is further complicated by the presence of the COD in-plane bending deformations. The C-O and C-C stretches are still predominant throughout the region, but the

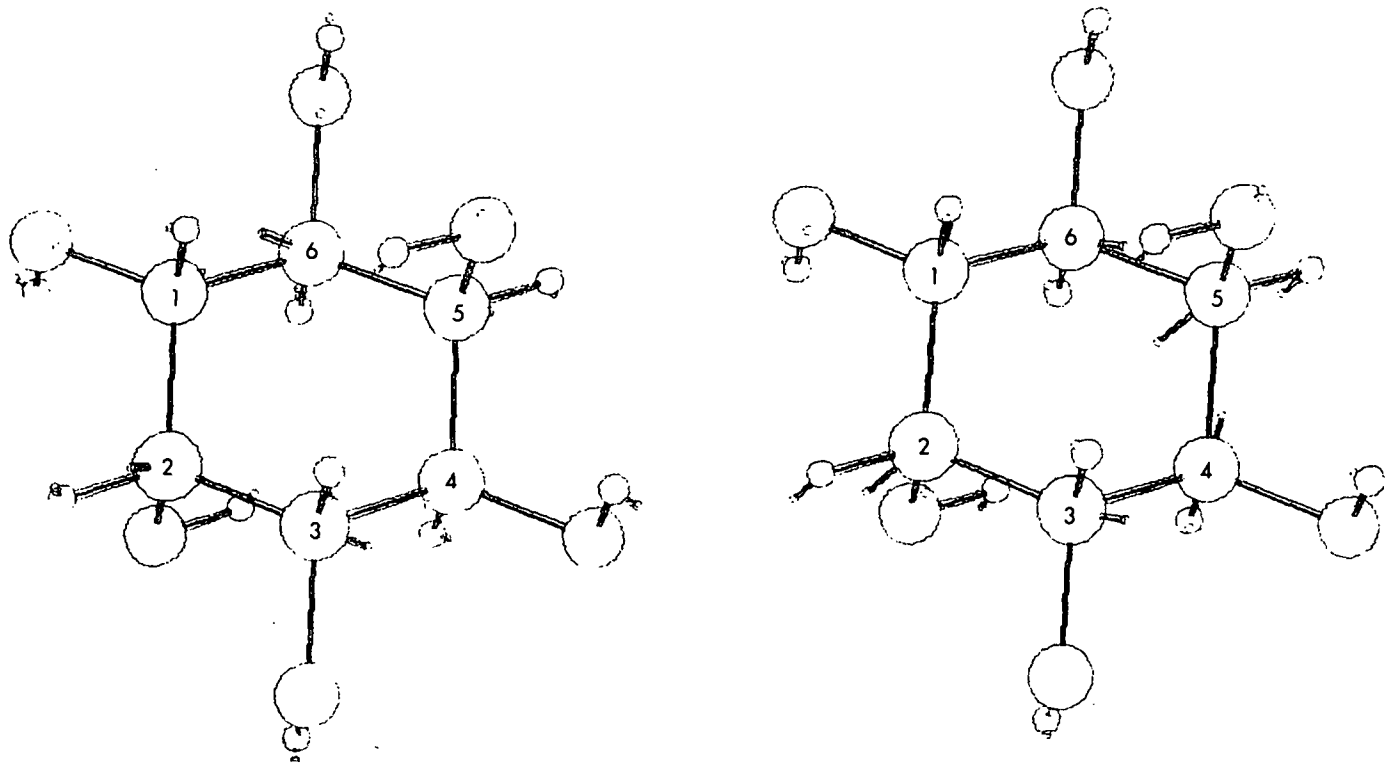

(A) neo-Inositol Mode at 1062 cm^{-1}

(B) Deuterated neo-Inositol Mode at 1111 cm^{-1}

Figure 32. Representative Vibrational Modes in Region III

COD bending deformations contribute heavily to several of the modes. Figure 32(B) illustrates one of the deuterated modes in Region III. The mode is the 1111 cm^{-1} deuterated neo-inositol mode which contains substantial COD bending, C-C and C-O stretching and CCO bending contributions. The observed Raman and infrared bands containing large COD bend contributions were weaker in intensity and broader than those consisting predominantly of the C-O and C-C stretches.

Region IV: 850-250 cm^{-1}

The 850-250 cm^{-1} region in Fig. 29 is seen to be dominated by the CCO and CCC bending contributions but with some significant contributions from the C-O and C-C stretches and the methine out-of-plane bending deformations. The force constant potential energy distributions demonstrate that extensive coupling between the heavy atom bending, the C-O and C-C stretches and the methine out-of-

plane bending deformations is occurring. Region IV also contains observed bands in several of the spectra which were not assigned. These bands will be discussed in a later section.

The bands observed in Region IV cover a broad range of relative intensities in both the Raman and infrared. Some of the Raman bands are sharp and among the most intense in the spectra. In scyllo-inositol, a very intense band in the Raman spectrum occurs at 464 cm^{-1}. In the Raman spectrum of neo-inositol an intense band occurs at 435 cm^{-1}, in myo-inositol two intense Raman bands occur at 509 cm^{-1} and 434 cm^{-1}, and in epi-inositol the most intense band below 1500 cm^{-1} occurs at 518 cm^{-1}. In all cases, these bands are highly polarized and were assigned to calculated frequencies belonging to the totally symmetric species. The potential energy distributions of these bands show that they represent the totally symmetric ring-breathing modes. The scyllo-inositol mode calculated at 458 cm^{-1} and assigned to the 464 cm^{-1} band is illustrated in Fig. 33(A). The mode is predominantly C-C stretch (51%) and C-O stretch (16%). The 438 cm^{-1} neo-inositol calculated A_g mode, assigned to the 435 cm^{-1} observed band, is illustrated in Fig. 33(B). The mode is predominantly C-C (35%) and C-O (11%) stretch but with some CCC (12%) and CCO (9%) heavy atom bending also present. The myo-inositol frequencies calculated at 494 and 426 cm^{-1}, assigned to the 509 and 434 cm^{-1} bands, respectively, are illustrated in Fig. 33(C) and 33(D), respectively. The 494 cm^{-1} mode is composed of C-C stretch (30%), C-O stretch (16%), CCC bend (17%) and CCO bend (14%) while the 426 cm^{-1} band is CCO bend (23%), C-C stretch (22%), CCC bend (21%) and C-O stretch (8%). The 491 cm^{-1} epi-inositol band, assigned to the 518 cm^{-1} band, is also primarily C-C (34%) and C-O (17%) stretch with some CCC (13%) and CCO (12%) bend. This mode is illustated in Fig. 33(E).

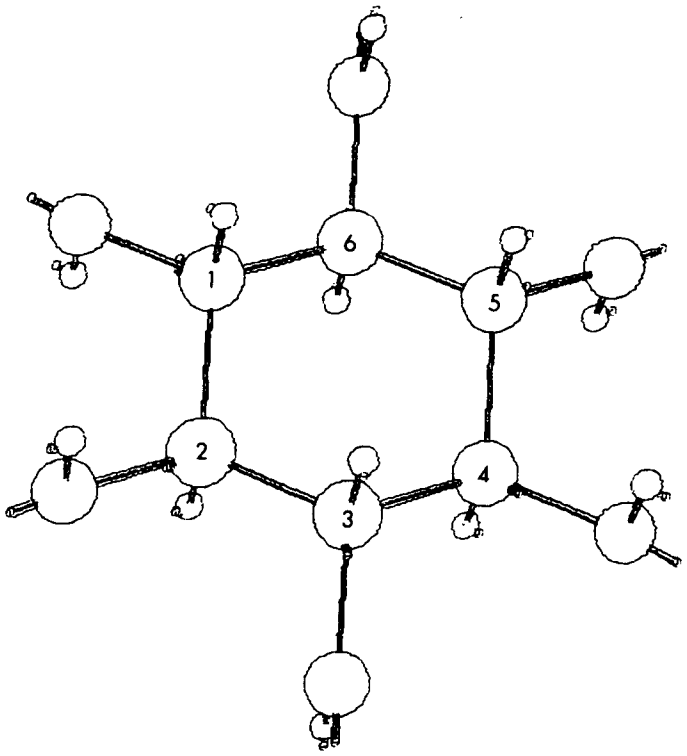

(A) scyllo-Inositol Mode at 458 cm^{-1}

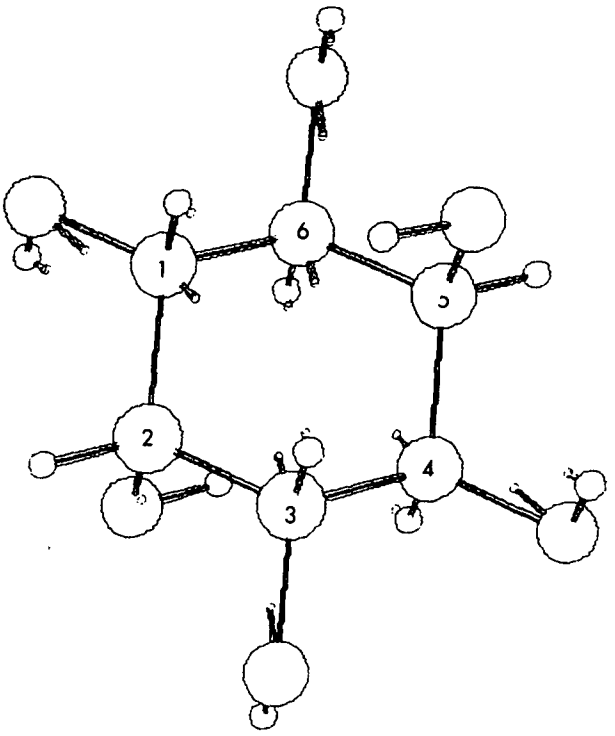

(B) neo-Inositol Mode at 438 cm^{-1}

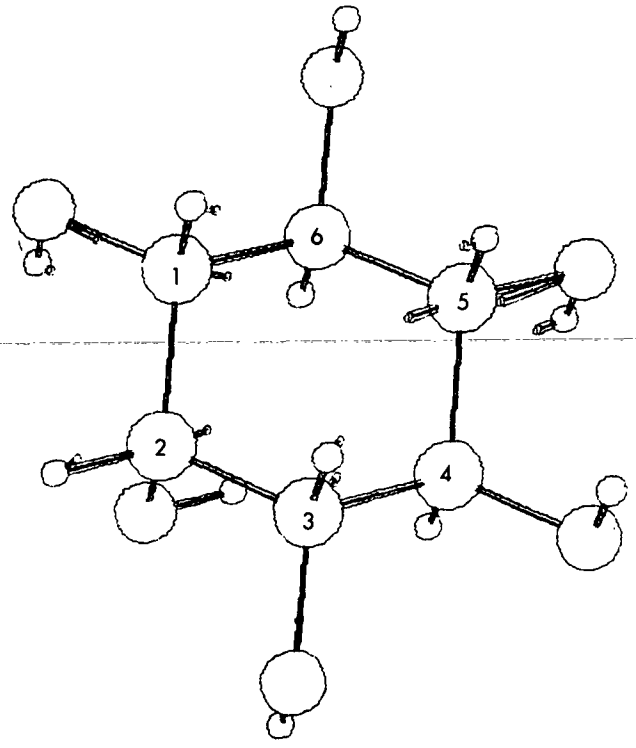

(C) myo-Inositol Mode at 494 cm^{-1}

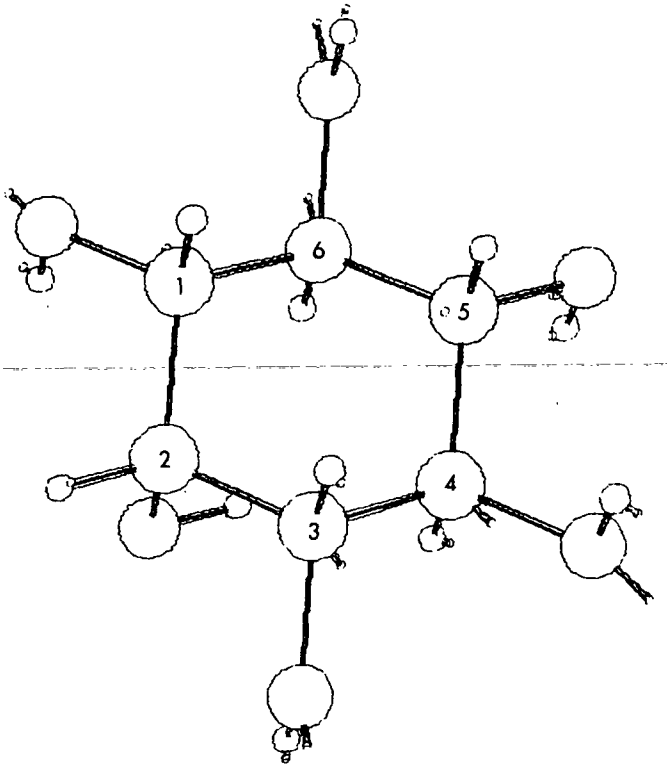

(D) myo-Inositol Mode at 426 cm^{-1}

Figure 33. Symmetric Ring-Breathing Modes from Region IV

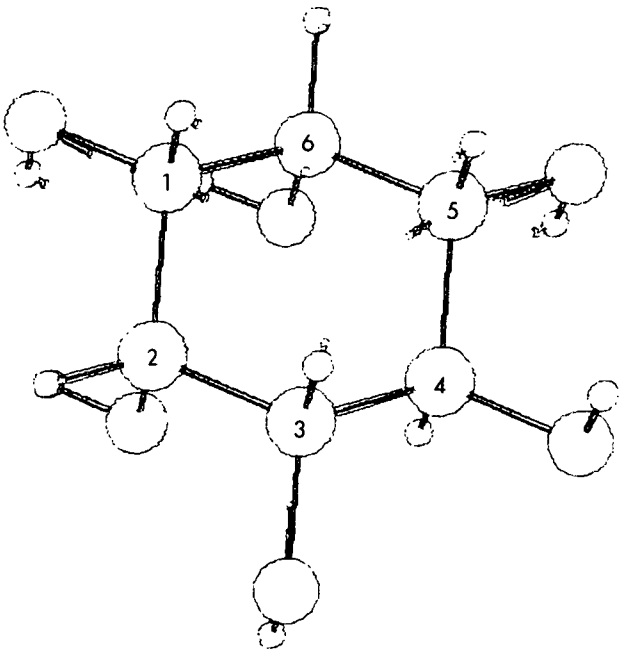

(E) epi-Inositol Mode at 491 cm^{-1}

Figure 33 (cont'd). Symmetric Ring-Breathing Modes from Region IV

The spectral changes observed upon going to liquid nitrogen temperature are the most pronounced in Region IV, especially in the infrared. Band shifts are observed and increases in relative band intensities at low temperature are common.

Figure 30 shows the composition of the Region IV bands in the deuterated spectra to be very similar to the bands just discussed in the undeuterated spectra. The heavy atom bending deformations dominate with contributions from the C-O and C-C stretches and the methine out-of-plane bending deformations also calculated.

Region V: Below 250 cm^{-1}

Below 250 cm^{-1}, the two predominant types of deformation predicted are the C-O torsions (OH out-of-plane bending) and the C-C torsions (ring torsions). Significant contributions from the CCO and CCC heavy atom bending motions and the methine out-of-plane bending motions are also present in some of the bands. Almost none of the bands calculated in Region V were assigned for the refinements.

There was too much uncertainty as to which of the observed bands in Region V corresponded to the C-O and C-C torsional modes. The calculated C-O torsion modes were deuteration sensitive, shifting from around 170 down to 120 cm^{-1} upon deuteration. But the calculated shifts were not observed in the experimental spectra where few bands in Region V exhibited significant shifts upon deuteration. Further experimental and theoretical work needs to be done to more rigorously interpret the bands observed in Region V. In addition to the torsional modes, other types of modes, such as lattice vibrations, are also expected in this region.

From an examination of the calculated potential energy distributions and the vibrational mode drawings, it can be concluded that many of the inositol vibrational modes are quite complex, involving motion of many of the atoms in the molecules. This would be expected for molecules of this size. It can also be concluded that all the different types of motions which occur below 1500 cm^{-1} couple extensively together. The methine hydrogen bending deformations, COH bending deformations, C-O and C-C stretches, the CCO and CCC heavy atom bending deformations and to a lesser extent the C-C and C-O torsions all couple extensively with one another.

SYMMETRY PROPERTIES OF THE CALCULATED VIBRATIONAL MODES OF THE INOSITOLS

It was stated earlier that when a molecule contains elements of symmetry, the normal modes of vibration of the molecule will also have certain symmetry properties. In this section, the symmetry properties of the normal modes calculated in the different symmetry species of the inositol point groups will be discussed. Also the effect of the degree of molecular symmetry on the localization of the normal modes will be examined.

In the earlier section, where the symmetry of the inositols was discussed, only the symmetry of the undistorted molecules, where all the atoms are in their

equilibrium positions, was considered. However, when molecular vibrations are being studied it is the distorted molecule, where all the atoms are not in their equilibrium positions, which is of interest. An important result of the group theory analysis of the distorted vibrating molecule is that: "Nondegenerate normal modes of vibration are always either symmetrical (unaltered) or antisymmetical (changed in sign) with respect to a given symmetry operation of the undistorted molecule (53)." Further, all the normal modes of vibration belonging to a particular symmetry species will behave in an identical fashion, being either symmetric or antisymmetric, under the symmetry operations of the point group. Whether the atomic displacements of a vibration belonging to a particular symmetry species will be symmetric or antisymmetric under the different symmetry operations of a point group can be determined from the character table of the point group.

The character table for the point group C_{2h}, to which neo-inositol belongs, is shown in Table XXIII. Across the top of the table are the four symmetry operations of the point group: the identity operation, E; the C_2 axis of rotation; the center of inversion, i; and the plane of symmetry, σ_h. The four symmetry species are listed down the side. The sign of the characters in Table XXIII indicates whether a vibration will be symmetric (a positive sign) or antisymmetric (a negative sign) with respect to a given symmetry operation. This will be illustrated by examining representative normal mode drawings for each symmetry species of neo-inositol. Table XXIII shows the vibrations belonging to the A_g symmetry species will be symmetric with respect to all the symmetry operations. A neo-inositol mode belonging to the A_g species is shown in Fig. 34(A). The carbon skeleton has been numbered to aid the following discussion. Again the smallest circles represent the atomic displacement vectors. When examining the symmetry properties of the vibrations, it is convenient to transform just the

TABLE XXIII

CHARACTER TABLE FOR THE POINT GROUP C_{2h}

C_{2h}	E	C_2	i	σ_h
A_g	1	1	1	1
B_g	1	-1	1	-1
A_u	1	1	-1	-1
B_u	1	-1	-1	1

displacement vectors with the symmetry operations without permuting the atoms themselves. The vibration shown in Fig. 34(A) is symmetric with respect to the center of inversion, located in the center of the ring, and the C_2 rotation axis which bisects the C3-C4 and C6-C1 bonds as depicted by the dotted line in the figure. A different view of the same mode is shown in Fig. 34(B). The plane of symmetry passes through C2-O8 and C5-O11. All the atomic displacements are symmetric with respect to the symmetry plane. When a vibration is symmetric with respect to a symmetry operation, then if all the displacement vectors are interchanged and transformed according to the symmetry operation the resulting displacements will be indistinguishable from the original displacements. This can be further illustrated with the C_2 axis of rotation shown in Fig. 34(A). If the displacements of the methine hydrogens attached to C2 and C5 are rotated 180° around the C_2 axis, the rotated displacements would be indistinguishable from the original displacements. According to Table XXIII, vibrations belonging to the B_g species are antisymmetric with respect to the C_2 axis and the plane of symmetry. When a vibration is antisymmetric with respect to a symmetry operation, then if all the displacement vectors are transformed according to the symmetry operation, the resulting displacements will be the negative of the original displacements, i.e., the motions are of the same magnitude but changed in sign, representing a 180° phase change. Figures 34(C)

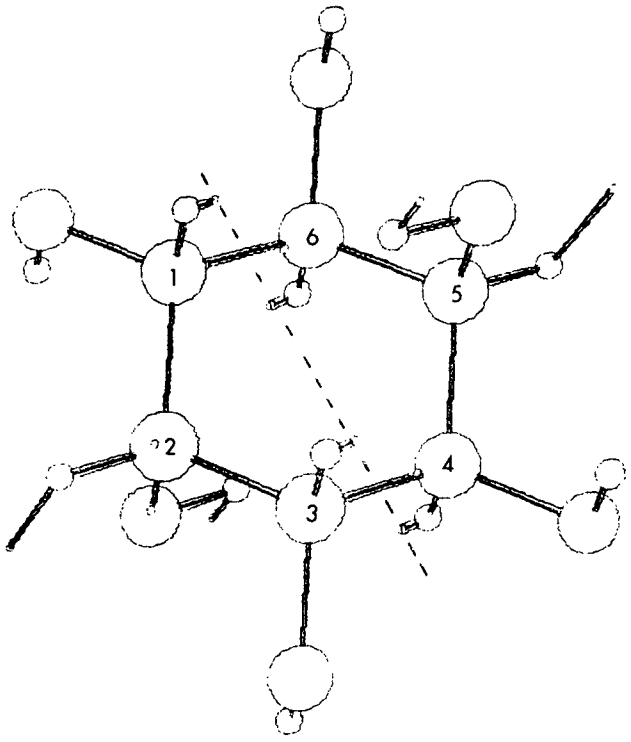

(A) neo-Inositol Mode at 1257 cm^{-1}
A_g Representation

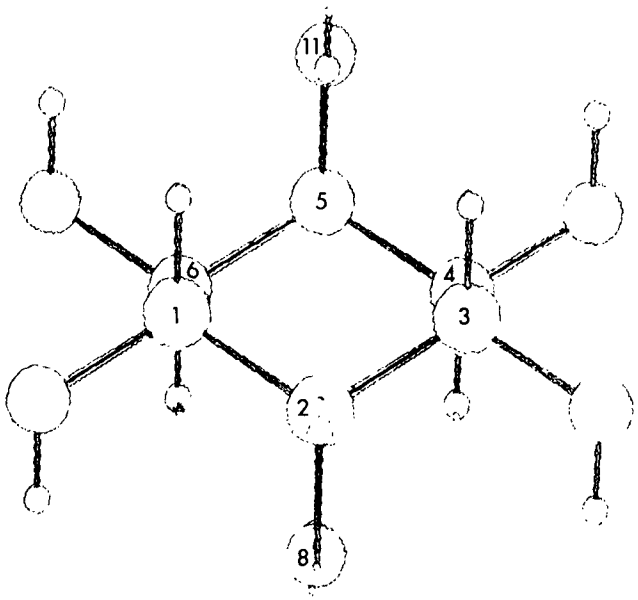

(B) neo-Inositol Mode at 1257 cm^{-1}
A_g Representation

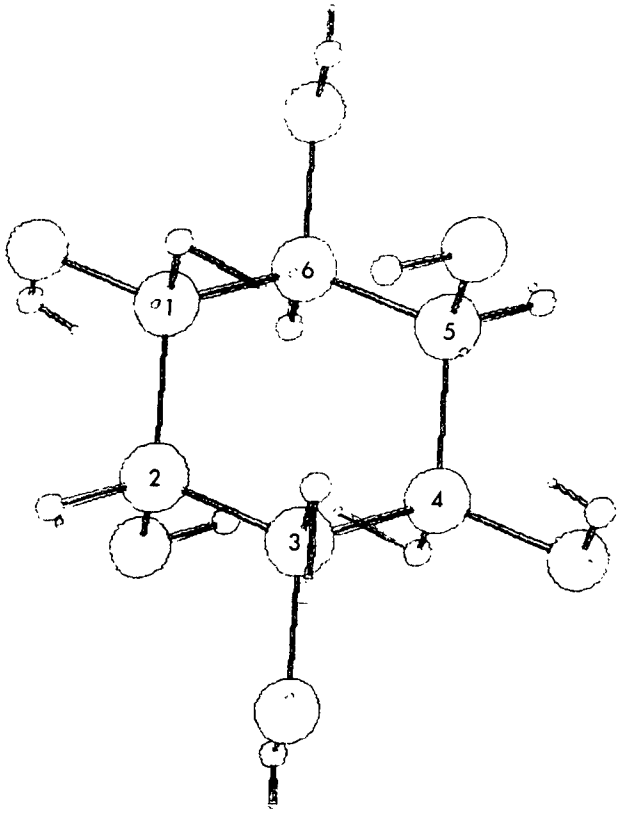

(C) neo-Inositol Mode at 1224 cm^{-1}
B_g Represenation

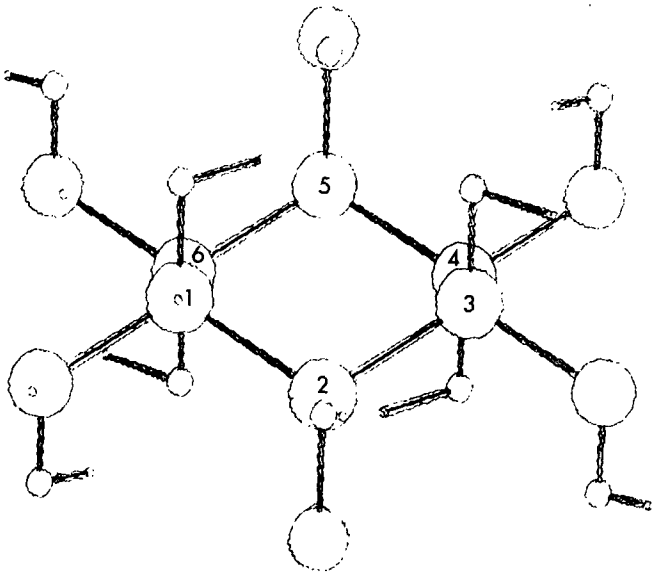

(D) neo-Inositol Mode at 1224 cm^{-1}
B_g Representation

Figure 34. Representative Vibrational Modes from the neo-Inositol Symmetry Representations

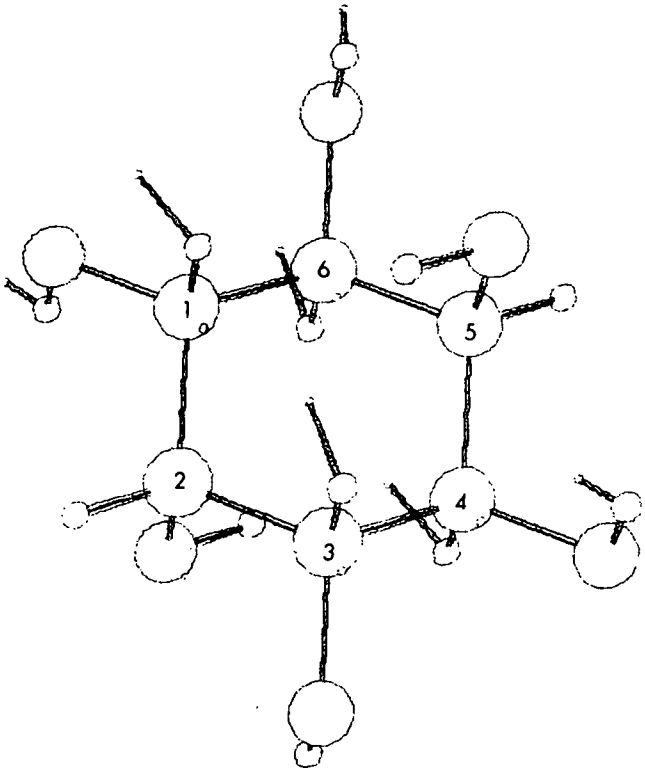

(E) neo-Inositol Mode at 1258 cm^{-1}
A_u Representation

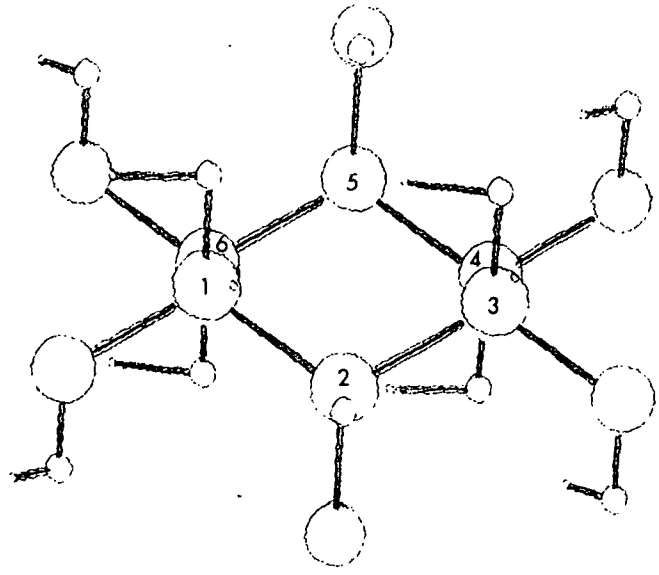

(F) neo-Inositol Mode at 1258 cm^{-1}
A_u Representation

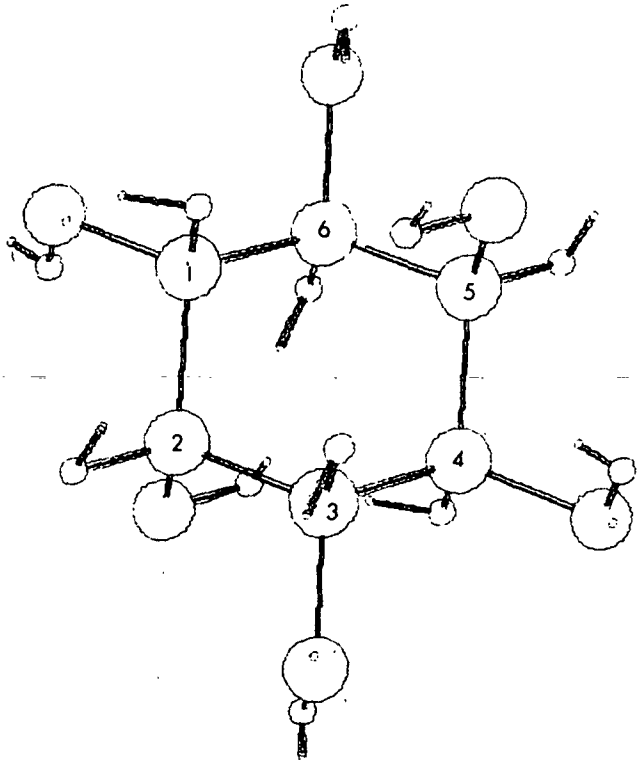

(G) neo-Inositol Mode at 1226 cm^{-1}
B_u Representation

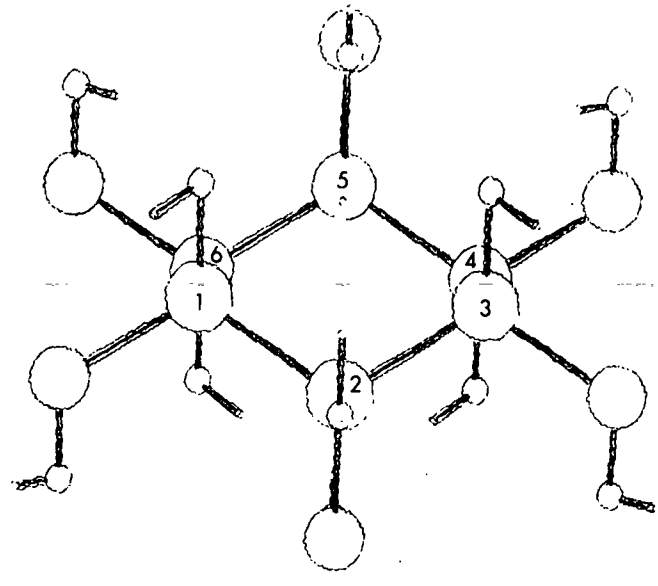

(H) neo-Inositol Mode at 1226 cm^{-1}
B_u Representation

Figure 34 (cont'd). Representative Vibrational Modes from the neo-Inositol Symmetry Representations

and 34(D) illustrate a neo-inositol mode belonging to the B_g species. Figure 34(D) clearly shows the mode is antisymmetric with respect to the plane of symmetry. If the displacements of the methine hydrogen attached to C1 and C3 are reflected through the plane of symmetry, the resulting displacements are the negative of the original displacements. Figure 34(C) shows the mode to be antisymmetric with respect to the C_2 axis but symmetric with respect to the center of inversion. Modes belonging to the A_u symmetry species are symmetric with respect to the rotation axis and antisymmetric with respect to the center of inversion and the symmetry plane. This is illustated in Fig. 34(E) and 34(F) for a neo-inositol A_u mode. Modes belonging to the B_u symmetry species are symmetric with respect to the symmetry plane and antisymmetric with respect to the C_2 axis and the center of inversion. A B_u species neo-inositol mode is illustrated in Fig. 34(G) and 34(H). Figure 34(G) shows the mode is antisymmetric with respect to the C_2 axis and the center of inversion and Fig. 34(H) shows the mode is symmetric with respect to the plane of symmetry.

The character table for the scyllo-inositol D_{3d} point group is shown in Table XXIV. The symmetry operations of the point group are listed across the top of the character table. The symmetry elements from which the symmetry operations arise are shown in Fig. 18. For the nondegenerate symmetry species, A_{1g}, A_{2g}, A_{1u} and A_{2u}, the sign of the characters in Table XXIV shows whether the vibrations in each of these species will be symmetric or antisymmetric with respect to the different symmetry operations. Representative vibrations for the A_{1g}, A_{2g}, A_{1u}, and A_{2u} symmetry species are illustrated in Fig. 35(A), 35(B), 35(E), and 35(F), respectively. The symmetry of these calculated vibrations conform with the information from the character table.

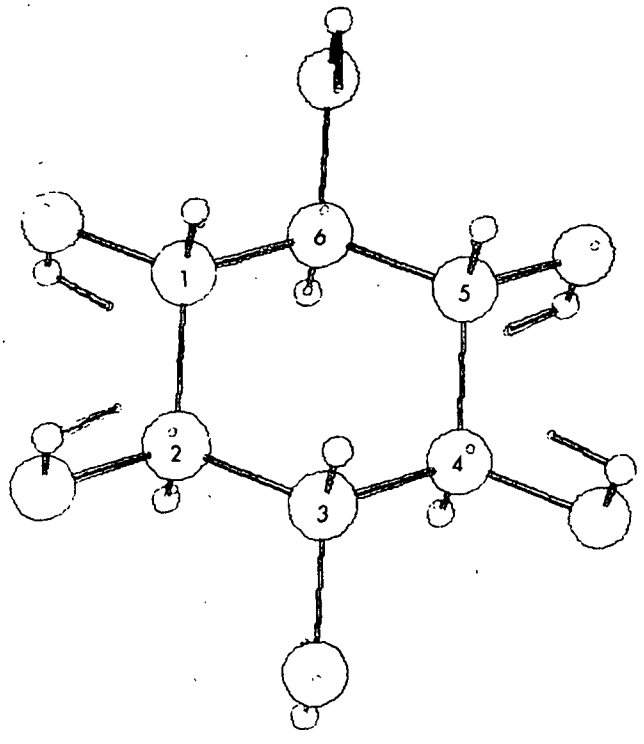

(A) scyllo-Inositol Mode at 1402 cm^{-1}
A_{1g} Representation

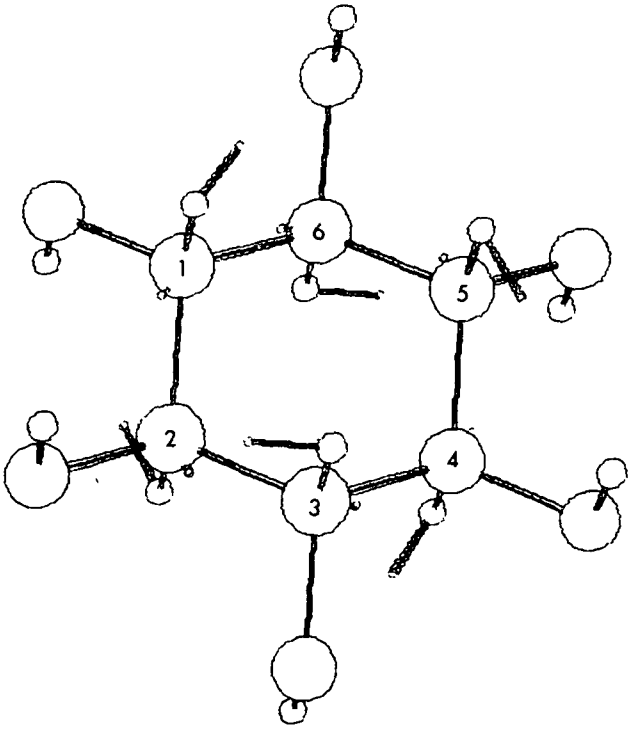

(B) scyllo-Inositol Mode at 1276 cm^{-1}
A_{2g} Representation

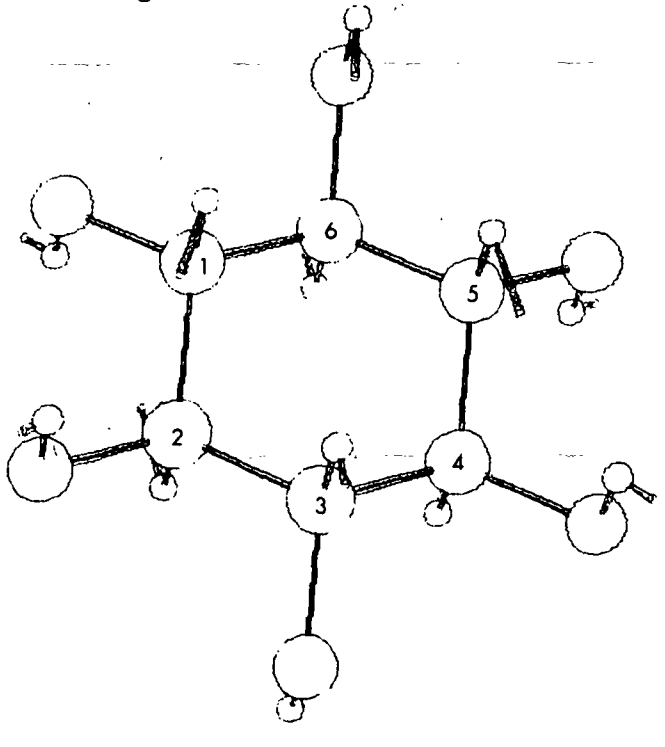

(C) scyllo-Inositol Mode at 1349 cm^{-1}
E_g Representation

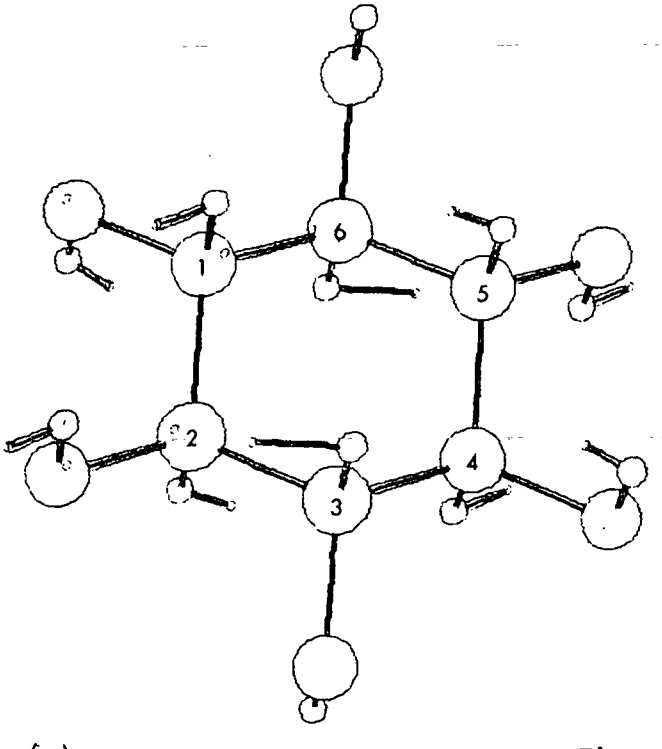

(D) scyllo-Inositol Mode at 1349 cm^{-1}
E_g Representation

Figure 35. Representative Vibrational Modes from the scyllo-Inositol Symmetry Representations

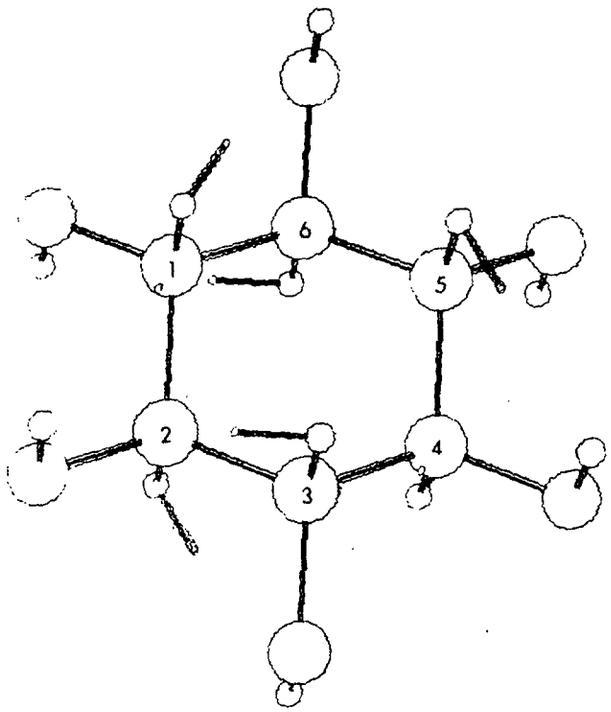

(E) scyllo-Inositol Mode at 1358 cm^{-1}
A_{1u} Representation

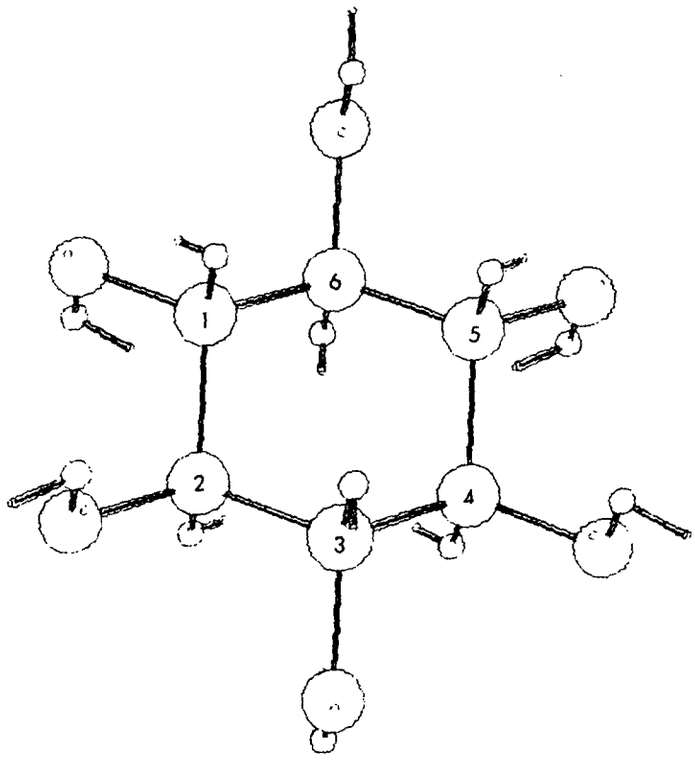

(F) scyllo-Inositol Mode at 1413 cm^{-1}
A_{2u} Representation

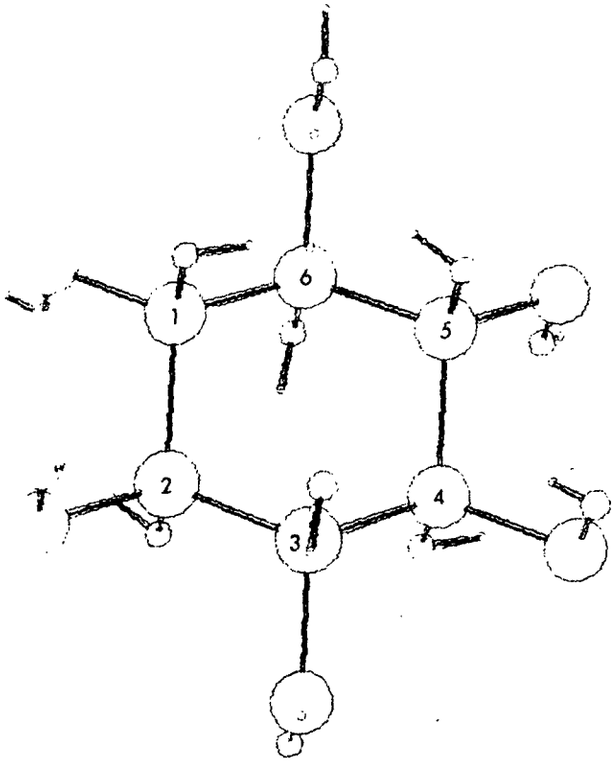

(G) scyllo-Inositol Mode at 1357 cm^{-1}
E_u Representation

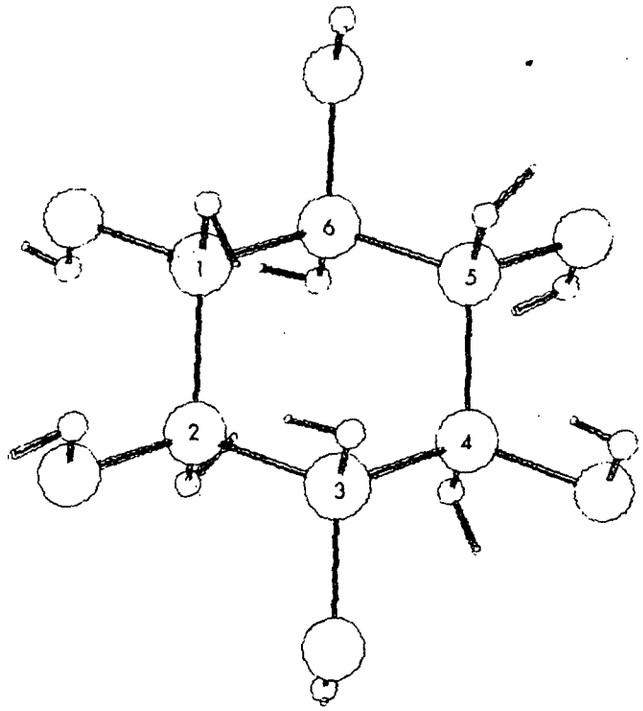

(H) scyllo-Inositol Mode at 1357 cm^{-1}
E_u Representation

Figure 35 (cont'd). Representative Vibrational Modes from the scyllo-Inositol Symmetry Representations

TABLE XXIV

CHARACTER TABLE FOR THE POINT GROUP D_{3d}

D_{3d}	E	$2C_3$	$3C_2$	i	$2S_6$	$3\sigma_d$
A_{1g}	1	1	1	1	1	1
A_{2g}	1	1	-1	1	1	-1
E_g	2	-1	0	2	-1	0
A_{1u}	1	1	1	-1	-1	-1
A_{2u}	1	1	-1	-1	-1	1
E_u	2	-1	0	-2	1	0

As stated earlier, the scyllo-inositol D_{3d} point group also contains doubly degenerate symmetry species, the E_g and E_u species. The symmetry properties of the doubly degenerate vibrations with respect to the different symmetry operations of the point group is not as easily analyzed as for the nondegenerate vibrations. "A symmetry operation of the molecule will transform a member of a degenerate set of vibrations into a linear combination of the members of the degenerate set (53)." Examples of doubly degenerate vibrations belonging to the Raman active E_g symmetry species are shown in Fig. 35(C) and 35(D). The atomic motions for the two degenerate vibrations are seen to be quite different. Examples of doubly degenerate vibrations belonging to the infrared active E_u symmetry species are shown in Fig. 35(G) and 35(H). Again, the motions of the two degenerate modes are distinctly different.

Two of the inositols dealt with thus far, myo-inositol and epi-inositol, possess only a single element of symmetry, a plane of symmetry. These inositols belong to the C_s point group. The simple character table for this point group is shown in Table XXV. The vibrational modes for myo-inositol and epi-inositol are either symmetric with respect to the plane of symmetry, the A' symmetry

species, or antisymmetrical with respect to the plane of symmetry, the A'' symmetry species. Myo-inositol modes belonging to the two symmetry species are illustrated in Fig. 36. Figures 36(A) and 36(B) are two views of a mode belonging to the A' species. It is easily seen that this mode is symmetric with respect to the plane of symmetry which passes through C2 and C5. Figures 36(C) and 36(D) are drawings of a mode belonging to the A'' symmetry species. This mode is seen to be antisymmetric with respect to the symmetry plane.

TABLE XXV

CHARACTER TABLE FOR THE POINT GROUP C_s

C_s	E	σ_h
A'	1	1
A''	1	-1

In the earlier section dealing with the symmetry of the inositols, the concept of symmetrically equivalent sets of atoms was introduced. A symmetrically equivalent set was defined as all the atoms of a molecule which could be sent into one another by all the symmetry operations of the point group. For example, any carbon atom of scyllo-inositol can be sent into all the other carbon atoms by the symmetry operations of the D_{3d} point group. Thus, all six of the carbons of scyllo-inositol are symmetrically equivalent, as are the oxygens, etc. For the vibrational modes belonging to each of the symmetry species just discussed, it was the atomic displacement vectors which were permuted by the symmetry operations. For nondegenerate vibrations the displacement vectors were found to be either symmetric or antisymmetric with respect to each of the symmetry operations of the point group. The displacement vector of any chosen atom, then, can be permuted by the symmetry operations into the displacement vectors, whether it be symmetric or antisymmetric, of all the atoms symmetrically equivalent to the

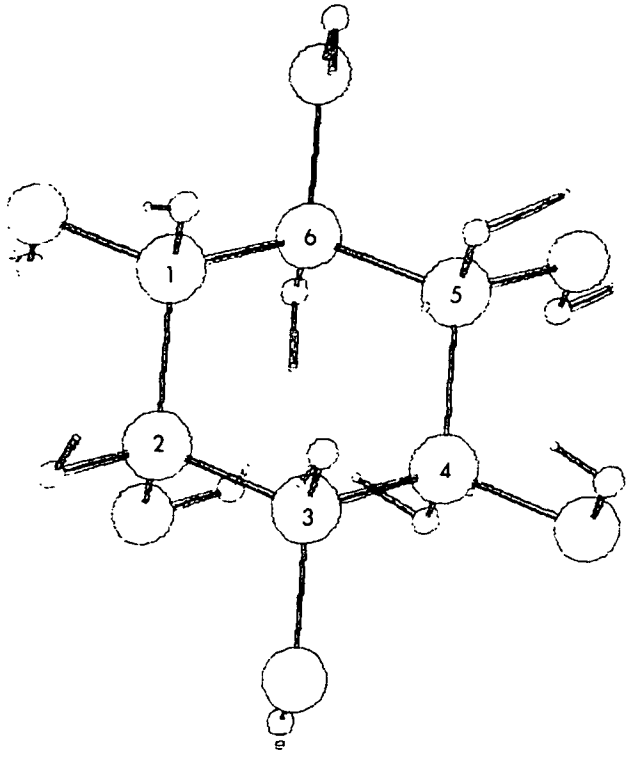

(A) myo-Inositol Mode at 1220 cm^{-1}
A' Representation

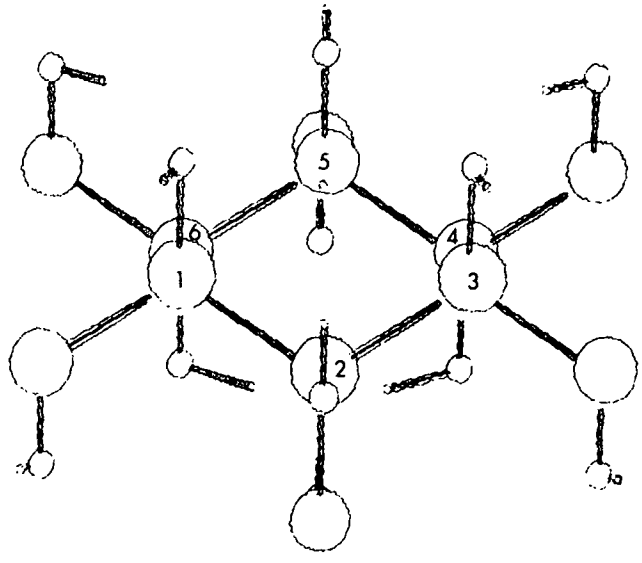

(B) myo-Inositol Mode at 1220 cm^{-1}
A' Representation

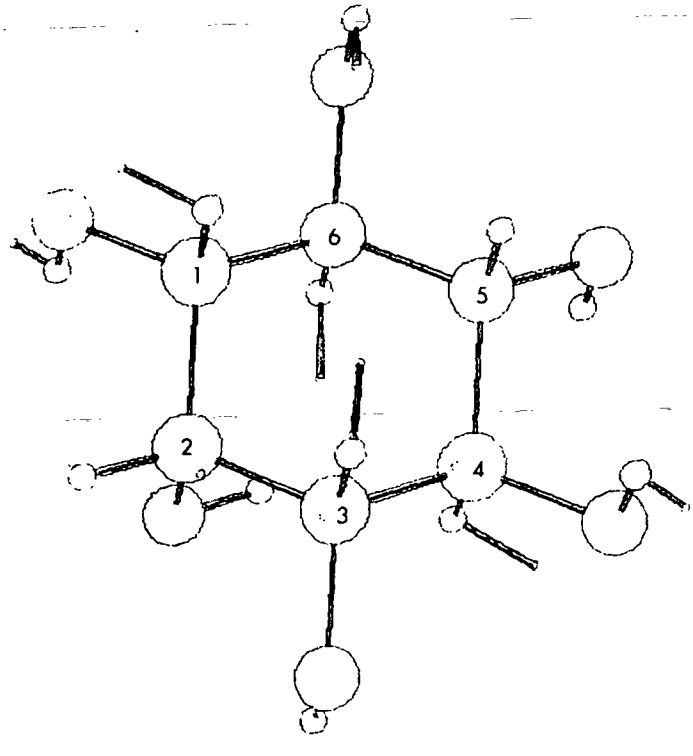

(C) myo-Inositol Mode at 1224 cm^{-1}
A'' Representation

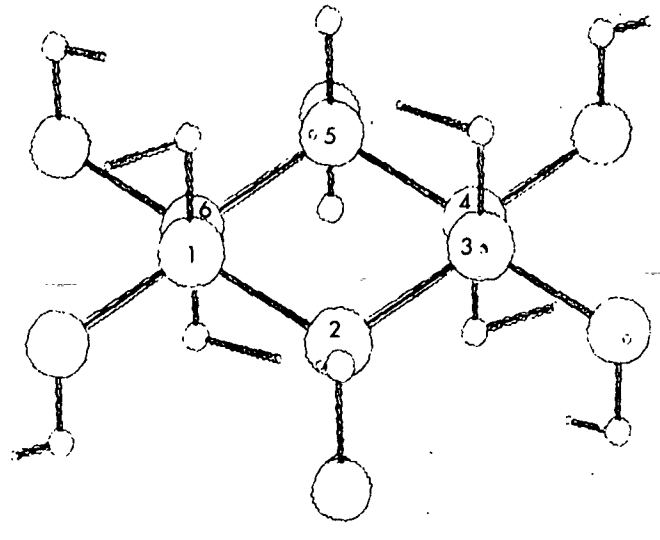

(D) myo-Inositol Mode at 1224 cm^{-1}
A'' Representation

Figure 36. Representative Vibrational Modes from the myo-Inositol Symmetry Representations

chosen atom. For nondegenerate vibrations, if one of the atoms of a symmetrically equivalent set is in motion all the other atoms in the set must also be in motion. The displacements of the other atoms in the set will either be the equivalent of the chosen displacement or the negative of the displacement, depending on the symmetry class of the vibration.

This concept can be demonstrated in the normal mode drawings presented earlier. Figure 35(A) is a drawing of a totally-symmetric A_{1g} mode of scyllo-inositol. It can be seen that the displacements of the six hydroxyl hydrogens, which constitute a symmetrically equivalent set, are all of the same magnitude and are all directed back along the C-O bonds. In the internal coordinate potential energy distribution, the contributions from all the hydroxyl groups are of the same magnitude. In Fig. 35(F), a scyllo-inositol A_{2u} mode, the displacements of the hydroxyl hydrogens associated with C1, C3 and C5 are of the same magnitude but in the opposite direction of the displacements of the hydroxyl hydrogens associated with C2, C4, and C6. The potential energy distribution again shows the contributions of all the hydroxyl group internal coordinates to be of the same magnitude. Because all six symmetrically equivalent hydroxyl groups must be in motion to satisfy the symmetry requirements, this delocalizes the hydroxyl motion in this particular mode all around the ring. The hydroxyl motion cannot concentrate at one or two sites because the resulting atomic displacements would not meet the symmetry requirements. For the scyllo-inositol degenerate modes, where the analysis is not as simple, the motions of the symmetrically equivalent atoms do not have to be the same magnitude.

In neo-inositol the six carbons are not all symmetrically equivalent as was the case with scyllo-inositol. Taking C3 in Fig. 34(A), for example, and permuting it using the symmetry operations of the C_{2h} point group, it is found that C1, C3, C4, and C6 are symmetrically equivalent and C2 and C5 form a second

symmetrically equivalent set. The displacement of an atom within either set necessitates the displacement of the other atoms in the set. The magnitudes of the internal coordinate contributions associated with sites at C1, C3, C4, and C6 are always the same. For example, the neo-inositol frequency calculated at 1092 cm^{-1}, shown in Table XLVI in Appendix V, has equal 17% stretching contributions from the four symmetrically equivalent C-O bonds at C1, C3, C4, and C6. This is also true of the internal coordinate contributions at the C2 and C5 sites. The displacements in a vibration can involve the members of only one symmetrically equivalent set or several sets. For example, the displacements in a neo-inositol vibration might only involve the hydroxyl groups associated with C2 and C5. The resulting motion would be more localized, at only two sites, than in the case of scyllo-inositol where the motion was delocalized over all six sites. The lower symmetry of neo-inositol dictates less delocalization of the different types of motions around the ring. In this context, the term delocalization is not meant to imply a symmetry restriction on the number of different types of internal coordinate displacements (i.e., C-O stretch, HCO bending, C-C torsion, etc.) which may contribute to a particular vibration. A vibration may consist of a single type of displacement or contributions from several types.

For myo-inositol, shown in Fig. 36(A) and 36(B), reflection through the symmetry plane exchanges C1 and C3, C4 and C6 and leaves C2 and C5 unchanged. There are then, four symmetrically equivalent sets for myo-inositol, and thus for epi-inositol which has the same symmetry. A particular myo-inositol vibration, for example, could be entirely localized at C5. The C_s symmetry places even fewer restrictions on the localization of the atomic displacements.

The differing degrees of symmetry of the inositols have been shown to affect the degree of delocalization of the different types of atomic displacements

around the ring. As the molecular symmetry increases, there is more delocalization of the atomic motions around the ring.

UNASSIGNED EXPERIMENTALLY OBSERVED FREQUENCIES

As stated earlier, not all the frequencies were assigned to calculated frequencies. The unassigned frequencies for scyllo-inositol, neo-inositol, myo-inositol, and epi-inositol are represented in Fig. 37. The frequencies labelled with an 'R' appear in the Raman and those labelled with an 'IR' appear in the infrared. These unassigned bands will be discussed in this section. Attention will be focused on a group of bands observed in the region 750-390 cm^{-1} whose frequencies were found to be sensitive to temperature. Such temperature sensitive bands have been previously observed. Following the discussion and characterization of the unassigned bands, the literature concerning the temperature sensitive bands observed in the spectra of other carbohydrates will be briefly reviewed. The literature will be compared with the features observed in the inositol spectra and then an interpretation of the temperature sensitive bands with supporting calculations will be presented.

It can be seen in Fig. 37 for scyllo-inositol that there are several unassigned frequencies, especially in the infrared above 1000 cm^{-1}. Most of these bands, including those at 1331, 1305, 1206, 1112, and 1067 cm^{-1}, were earlier shown to result from the presence of water in the scyllo-inositol crystals. The region 800-400 cm^{-1} of the Raman and infrared spectra of scyllo-inositol is shown in Fig. 38. The room temperature infrared bands at 724, 522, and 485 cm^{-1} were not assigned to calculated fundamentals. Figure 38 shows that all three bands shift to higher frequencies, 744, 542, and 492 cm^{-1}, respectively, at liquid nitrogen temperature. The infrared bands assigned as fundamentals at 635, 627, and 585 cm^{-1} did not shift appreciably at liquid nitrogen temperature. In

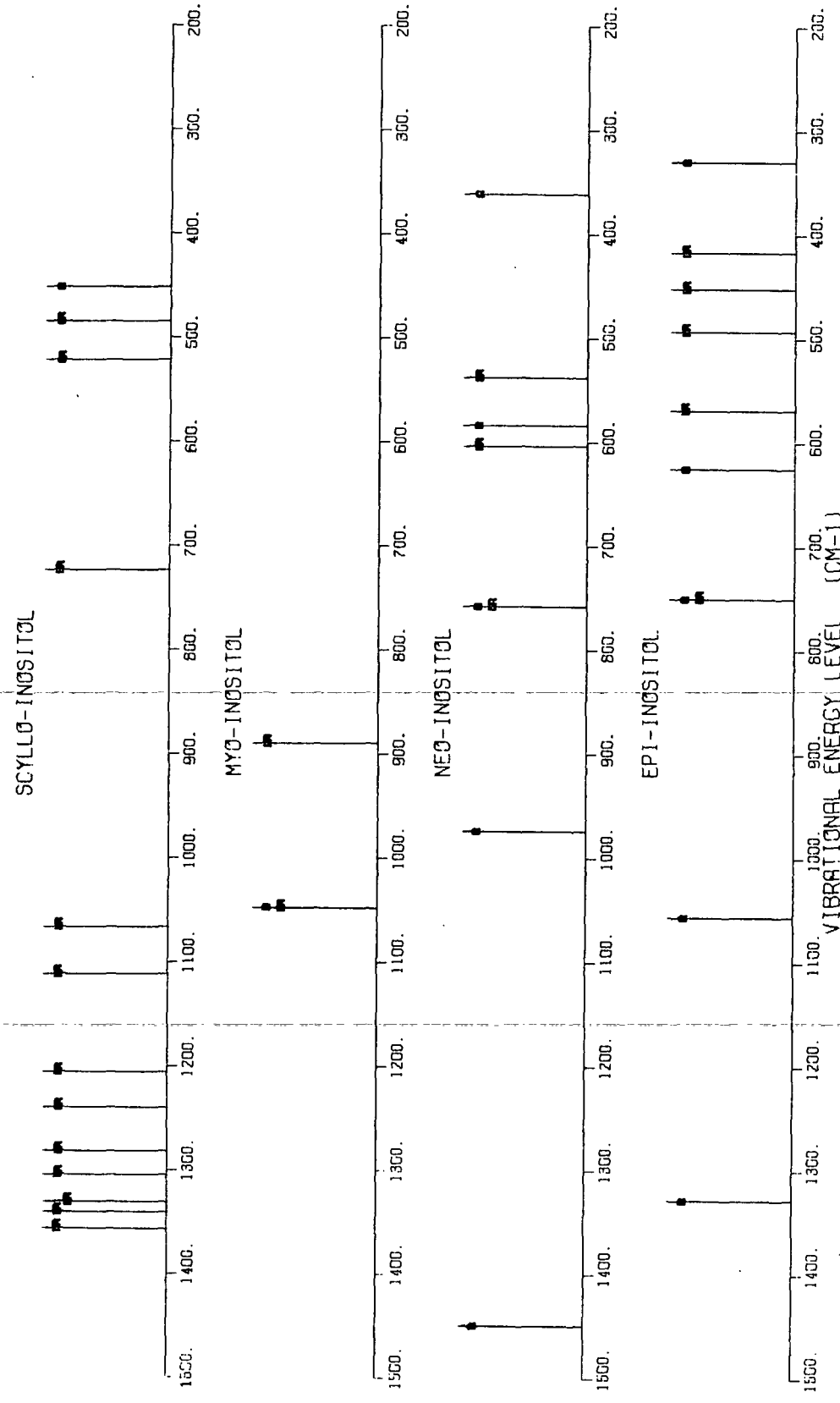

Figure 37. The Unassigned Observed Raman and Infrared Frequencies for scyllo-Inositol, neo-Inositol, myo-Inositol and epi-Inositol

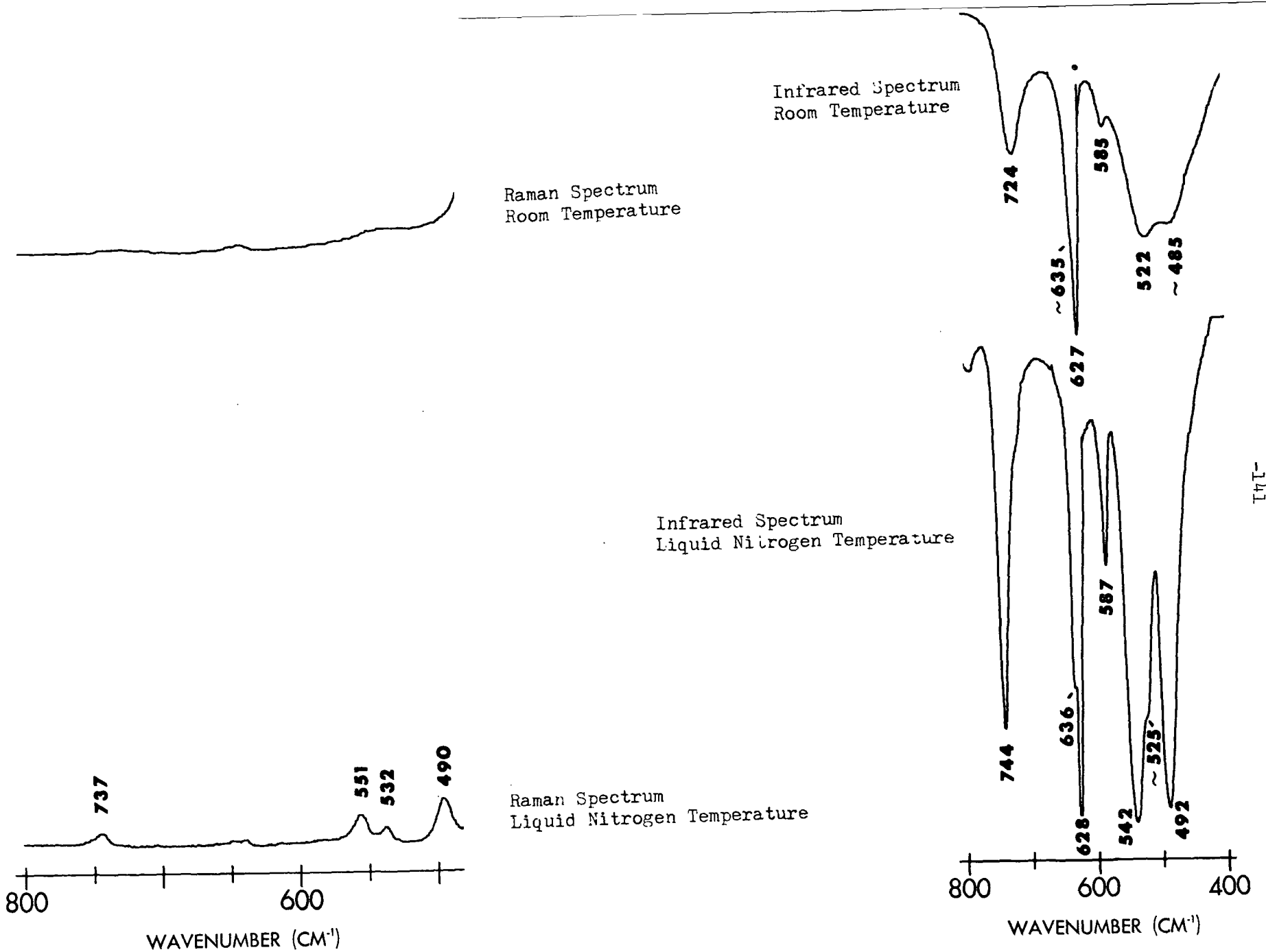

Figure 38. The 800-400 cm^{-1} Region of the Room Temperature and Liquid Nitrogen Temperature Raman and Infrared Spectra of scyllo-Inositol

the Raman spectrum, where no bands are readily distinguishable at room temperature in the region 800-500 cm^{-1}, four weak bands appear at liquid nitrogen temperature.

Seven neo-inositol bands were left unassigned. Two Raman bands at 1449 and 974 cm^{-1} are very weak in intensity. A Raman band observed at 362 cm^{-1}, which is adjacent to a more intense band, was not assigned because only one fundamental was calculated in the region. Several of the remaining unassigned bands again occur in the region 800-500 cm^{-1}. The room temperature and liquid nitrogen temperature Raman and infrared spectra for this region are shown in Fig. 39. The unassigned Raman bands at 758 and 584 cm^{-1} are seen to be very weak and broad at room temperature but shift to 776 and 597 cm^{-1} at liquid nitrogen temperature and become more intense. The bands at 665 and 688 cm^{-1}, assigned as fundamental modes, do not shift as appreciably. The unassigned infrared bands at 758 and 604 cm^{-1} shift up to 777 and 622 cm^{-1}, respectively, and are substantially increased in relative intensity. The room temperature infrared band at 538 cm^{-1} appears to shift up to 552 cm^{-1} at liquid nitrogen temperature leaving another band at 527 cm^{-1}. An infrared active band was calculated at 531 cm^{-1}. It was assigned to the band at 527 cm^{-1} which is more likely the fundamental than the band at 552 cm^{-1}. The infrared bands at 638 and 726 cm^{-1} were also assigned as fundamentals.

Figure 37 shows that only two room temperature bands for myo-inositol were left unassigned. Both bands are part of a single band which has split into two bands. Distinct changes were also observed in the region 750-500 cm^{-1} in the low temperature spectra, especially in the infrared, of myo-inositol.

For epi-inositol, four of the unassigned bands, at 1328, 1056, 493, and 330 cm^{-1}, are weak shoulders on more intense bands. The 800-550 cm^{-1} region of the

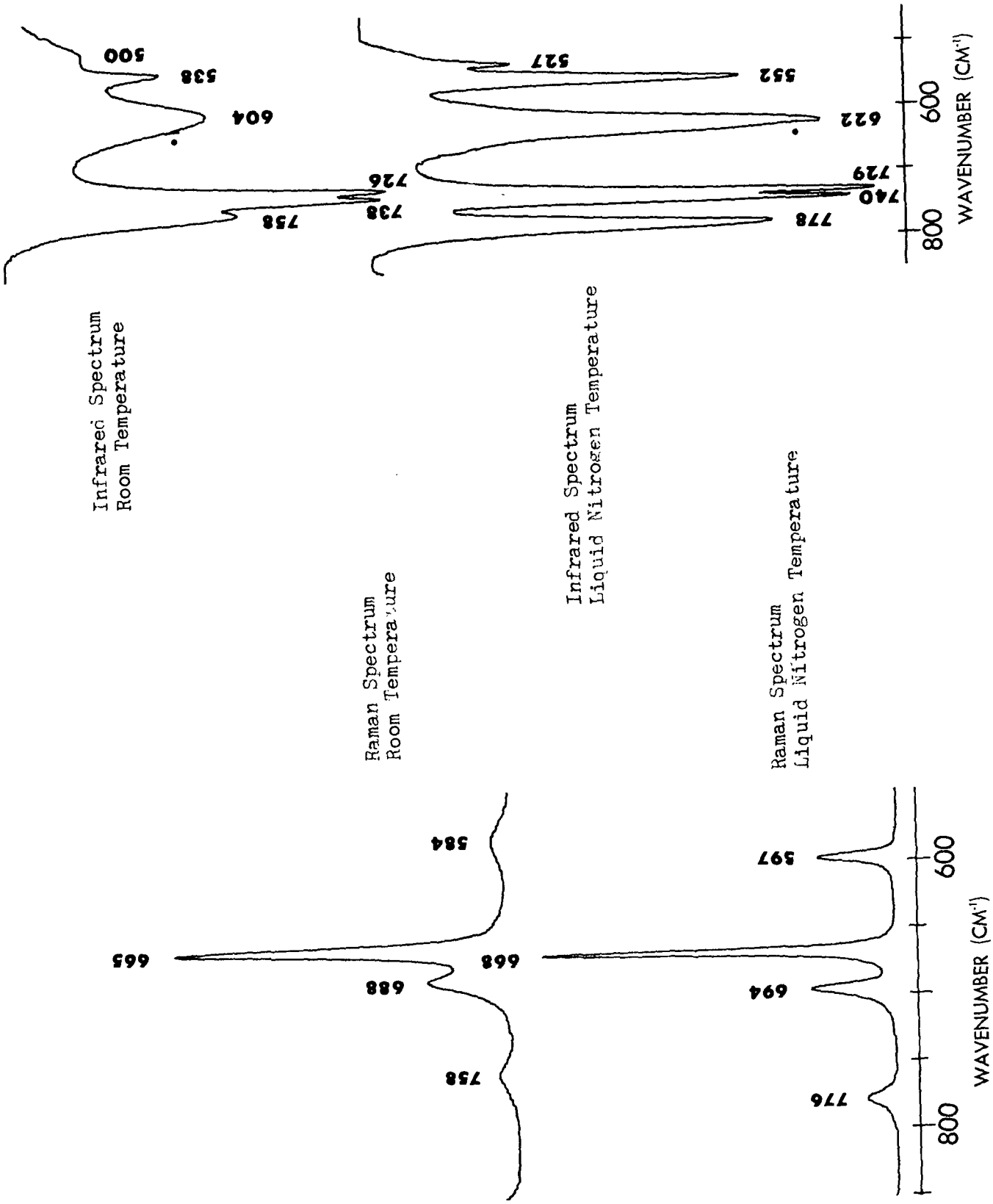

Figure 39. The 800-500 cm^{-1} Region of the Room Temperature and Liquid Nitrogen Temperature Raman and Infrared Spectra of neo-Inositol

Raman spectrum and the 800-400 cm^{-1} region of the infrared spectrum for epi-inositol, where several unassigned bands were observed, are shown in Fig. 40. The unassigned weak Raman bands at 750 and 625 cm^{-1} are seen to split into multiple bands at liquid nitrogen temperature. Correspondingly, the room temperature infrared band at 749 cm^{-1} also splits, but into two bands at 770 and 746 cm^{-1}. The unassigned infrared bands at 569 and 452 cm^{-1} appear to shift to 585 and 463 cm^{-1}, respectively, at liquid nitrogen temperature. The bands at 791, 718, 689, 556, and 501 cm^{-1} were assigned as fundamentals and do not shift appreciably at low temperature.

As stated in the previous section, several deuterated scyllo-inositol bands were left unassigned. Many of the unassigned bands are weak in intensity and occur at frequencies where bands are observed in the undeuterated spectra. Liquid nitrogen temperature spectra were not obtained for deuterated scyllo-inositol and consequently the shifting properties of the bands were not observed. This inhibited the assignment of bands in the lower region of the infrared.

The spectra of deuterated neo-inositol were more clearly assigned. All the unassigned bands, except for two weak shoulders at 1246 and 755 cm^{-1}, occurred in the region 580-390 cm^{-1}. The 755 cm^{-1} shoulder is likely a residual undeuterated band observed at 758 cm^{-1}. Two weak, broad bands at 542 and 490 cm^{-1} were left unassigned. Three infrared bands at 577, 438, and 393 cm^{-1} were also left unassigned. Again the liquid nitrogen temperature spectra were not recorded so the shifting characteristics of these bands were not observed.

If the bands suspected to arise from contaminant species, i.e., the scyllo-inositol hydrate and the incompletely deuterated species, are excluded, relatively few experimentally observed bands could not be assigned. The major group of

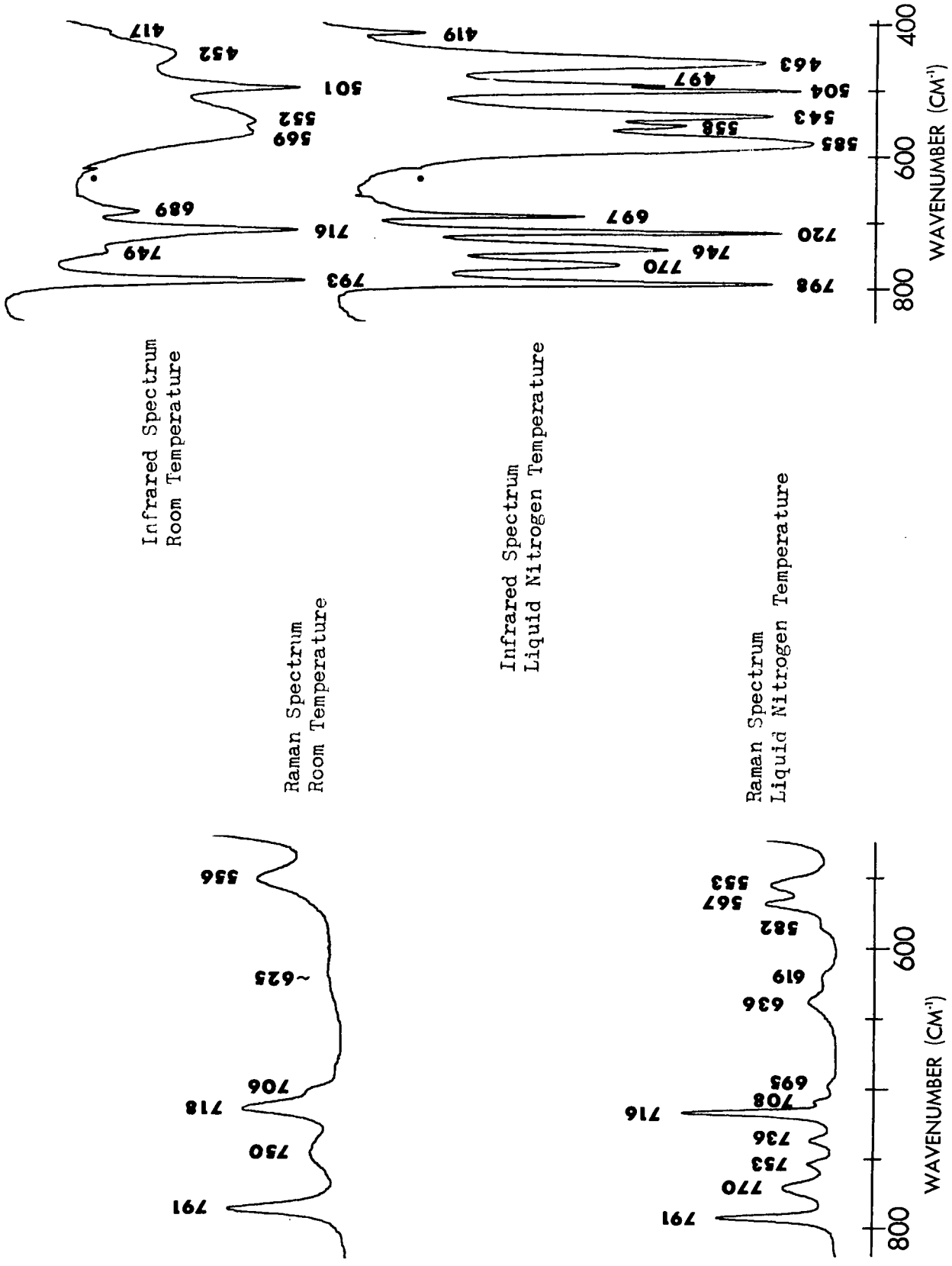

Figure 40. The 800-400 cm^{-1} Region of the Room Temperature and Liquid Nitrogen Temperature Raman and Infrared Spectra of epi-Inositol

bands which could not be accounted for by the calculated frequencies were observed in the region 750-300 cm^{-1}. In the figures just discussed, the unassigned bands observed in the spectra of scyllo-inositol, neo-inositol, and epi-inositol in this region characteristically shifted to higher frequencies by an average of approximately 16 cm^{-1} when the spectra were recorded at liquid nitrogen temperature. The bands in the 750-300 cm^{-1} region assigned to calculated fundamentals did not shift appreciably when the spectra were recorded at the lower temperature. The observation and interpretation of temperature sensitive bands by other authors will now be reviewed and compared with the observations made in the inositol spectra.

INTERPRETATION OF THE TEMPERATURE SENSITIVE VIBRATIONAL BANDS OBSERVED IN THE REGION 750-300 CM^{-1}

In 1967, Katon, et al. (54,55) reported observing distinctive changes in the infrared spectra of carbohydrates when the spectra were recorded at low temperature, near the temperature of liquid nitrogen. They found the observed changes, including the shifting of observed bands and the appearance of new spectral features, occurred to a much greater degree with compounds that could undergo hydrogen bonding. They noted a satisfactory explanation of the observed phenomenon was not available at that time. A possible explanation, they suggested, involved the internal rotation of the various hydroxyl groups around the C-O bonds. At room temperature, the hydroxyl hydrogens would be generally disordered. The ordering of the hydroxyl hydrogens and their resulting spectral features would be dependent on the temperature of the crystal.

At the same time, Michell (56,57) was investigating the low temperature infrared spectra of several carbohydrates including: methyl β-D-glucopyranoside, cellobiose, cellotriose, cellotetraose, and cellulose II. He also reported improved spectral clarity and resolution, the narrowing of band widths and frequency

shifts to higher or lower frequencies in the low temperature spectra. He concurred with Katon, et al. (54,55) that the "marked increase in definition in carbohydrate spectra found on cooling occurs only for highly ordered compounds having hydroxyl groups involved in strong intermolecular hydrogen bonds (57)." In the case of methyl β-D-glucopyranoside, Michell cited three bands in the liquid nitrogen temperature spectra at 812, 698, and 658 cm^{-1} which were temperature sensitive. He observed these bands were weakened or removed by oxygen deuteration.

In 1970, Dempster and Zerbi (58) published an investigation of hydrogen bonding in crystalline methanol. They studied the vibrational dynamics of crystalline methanol and oxygen deuterated methanol by comparing experimental infrared spectra with normal coordinate analysis calculations performed using a hydrogen bonded methanol chain model. In their model, they defined internal coordinates and valence-type force constants for motions involving the hydrogen bonded hydroxyl group. They assigned the experimentally observed infrared frequencies to the calculated frequencies and refined the force constants using a linear least-squares refinement. For methanol, they calculated bands at 758 and 679 cm^{-1} which the potential energy distributions showed to be a combination of the O-H•••O out-of-plane bending deformation and the C-O torsion. In their notation, the dots in the H•••O designation represent the hydrogen bond where the C-O•••H-O plane defines the plane for the out-of-plane motion. A band consisting predominantly of the O•••H stretching vibration was calculated at 347 cm^{-1}. Lower energy bands contained contributions from the O-H•••O in-plane bending, O•••H stretching and C-O•••H bending deformations. For oxygen deuterated methanol, the modes calculated to be a mixture of O-D•••O bending and C-O torsion deformations shifted down to 577 and 492 cm^{-1}. The O•••D stretching vibration shifted only slightly to 333 cm^{-1}. The calculated bands just described all closely reproduced the experimentally observed frequencies to which they were assigned. Dempster and Zerbi, then, successfully identified the observed vibrational modes resulting

from the atomic motions involving the hydrogen bonded hydroxyl group and reproduced and interpreted these modes with the aid of normal coordinate calculations.

Kogan, et al. (59) studied the hydrogen bonds in several monosaccharides including: methyl α-D-glucopyranoside, methyl α-D-mannopyranoside, methyl α-D-galactopyranoside, methyl β-D-xylopyranoside, and 1,2,3,4,6-penta-O-acetyl-α-D-glucopyranose. Part of their investigation centered on finding the region where the out-of-plane hydroxyl bending vibrations were occurring. To do this, they examined the room temperature and low temperature infrared spectra of the above compounds and the room temperature infrared spectra of oxygen deuterated methyl α-D-gluco-, methyl α-D-manno- and methyl α-D-galactopyranosides. A comparison of the room temperature and low temperature undeuterated spectra revealed bands in the region 750-400 cm^{-1} which shifted substantially, up to 25 cm^{-1}, and the appearance of new bands. Differences in the room temperature undeuterated and deuterated spectra were also observed in the 750-400 cm^{-1} region. For example, a band at 693 cm^{-1} in the room temperature spectrum of methyl α-D-glucopyranoside shifted up to 724 cm^{-1} at low temperature. The 693 cm^{-1} band, however, was absent in the spectrum of oxygen deuterated methyl α-D-glucopyranoside. But, new bands were observed in the 500-400 cm^{-1} region. The absence of the 693 cm^{-1} band in the deuterated spectrum suggested the band involved the hydroxyl out-of-plane bending deformation. From evidence of this type, Kogan, et al., concluded that the hydroxyl out-of-plane bending vibrations were sensitive to change in temperature. For the molecules they examined, the hydroxyl out-of-plane bending vibrations were assigned to the regions 750-600 and 500-400 cm^{-1}. To further substantiate their conclusions, they examined the room temperature and low temperature spectra of 1,2,3,4,6-penta-O-acetyl-α-D-glucopyranose. This fully acetylated compound is unable to form hydrogen bonds. No changes, such as large band shifts, were observed in the low temperature spectrum, only some

changes in band intensities and decreases in band half-widths. For the unsubstituted compounds, from smaller band shifts observed in the region below 200 cm^{-1}, Kogan, et al., concluded this region contained the bands arising from the O•••H stretching vibrations.

The experimental observations of Kogan, et al. (59) are in accordance with the findings of Dempster and Zerbi (58). Kogan, et al., observed the hydroxyl out-of-plane bending vibrations in the same region these vibrations were observed and calculated for methanol. In deuterated methanol, the OD out-of-plane bending vibrations were observed to shift and calculated to shift to lower frequencies, between 580 and 490 cm^{-1}. Kogan, et al., noted the appearance of new bands in the 500-400 cm^{-1} region of the deuterated carbohydrates.

Almost identical findings were reported by Michell (60). He examined the room temperature, low temperature, and oxygen deuterated room temperature infrared spectra of methyl α-D-altropyranoside, methyl α-D-mannopyranoside, methyl α-D-glucopyranoside, and methyl α-D-galactopyranoside. The logic of his investigation was very similar to that of Kogan, et al. (59), comparison of the room temperature, low temperature, and oxygen deuterated spectra. For methyl α-D-altropyranoside, Michell observed bands at 730, 623, 525, and 490 cm^{-1} in the low temperature spectra. On deuteration, the bands at 730 and 623 cm^{-1} disappeared with new bands appearing at 538 and 460 cm^{-1}. Michell states, "Since the ratios 730/538 and 623/460 are both close to $\sqrt{2}$, the value predicted by simple theory for the exchange of deuterium for hydrogen, it seems likely that these bands arise from OH out-of-plane bending vibrations (60)." Bands in the spectra of the other molecules were identified as being out-of-plane bending modes using the same argument. Michell noted that theoretical calculations (16) for α-D-glucopyranose show almost no OH out-of-plane bending contributions to the frequencies calculated in the region 750-400 cm^{-1}.

The experimental findings of these authors are very similar to the phenomena observed in the inositols spectra. They observed temperature sensitive bands in the region 750-400 cm^{-1}. In the previous section, several temperature sensitive bands were identified in the region 760-450 cm^{-1} for scyllo-inositol, neo-inositol, and epi-inositol. To further characterize the temperature sensitive bands, Michell (57,60) and Kogan, et al. (59) compared the room temperature and low temperature infrared spectra with the room temperature oxygen deuterated spectra. They observed the disappearance of many of the temperature sensitive bands and the appearance of new bands lower in the spectrum. The room temperature, liquid nitrogen temperature and room temperature oxygen deuterated Raman and infrared spectra in the 800-400 cm^{-1} region for neo-inositol are shown in Fig. 41. Earlier, the Raman bands at 758 and 584 cm^{-1} were seen to be temperature sensitive. These bands are not present in the deuterated spectrum, but two new bands appear at 542 and 490 cm^{-1}. The infrared bands at 758, 604, and 538 cm^{-1} are also temperature-sensitive. Again, these bands are not present in the deuterated spectrum, except a shoulder remnant of the undeuterated band at 755 cm^{-1}. But new bands appear in the deuterated infrared spectrum at 577, 438, and 393 cm^{-1}. This pattern of band shifts is the same as observed by the other authors. Of the new bands appearing in the deuterated neo-inositol spectrum at 542 and 490 cm^{-1} in the Raman and 577, 438, and 393 cm^{-1} in the infrared, none were assigned as fundamentals to calculated frequencies for refinements. The conclusion reached by the other authors that the temperature sensitive bands represent the O-H•••O out-of-plane bending deformations is also the logical interpretation of the temperature sensitive bands observed in the inositols. It is felt that the term O-H•••O out-of-plane bending after Dempster and Zerbi (58) is a more accurate description than the terms OH or hydroxyl out-of-plane bending. The latter terms imply the hydroxyl groups are free and unbonded. In reality, nearly all the inositol hydroxyl groups are involved in hydrogen bonds.

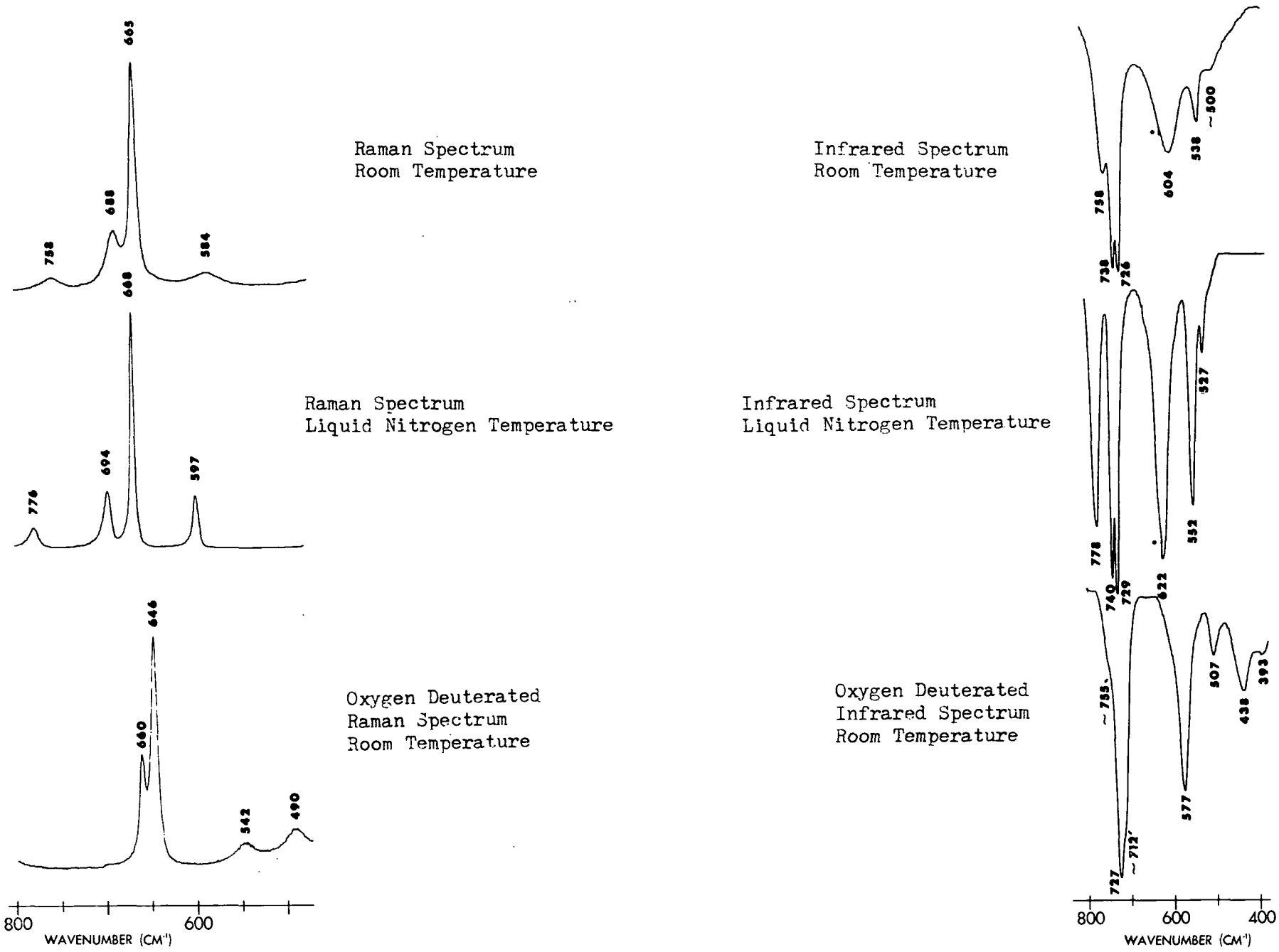

Figure 41. The 800-400 cm^{-1} Region of the Room Temperature, Liquid Nitrogen Temperature and Room Temperature Oxygen Deuterated Raman and Infrared Spectra of neo-Inositol

To further investigate the interpretation of the temperature sensitive bands, a simple molecular model was constructed for neo-inositol which included a single hydrogen bond for each hydroxyl group. A drawing of the model is shown in Fig. 42. The carbons in the neo-inositol ring are numbered to put the molecule in perspective. A rigid carbon-oxygen combination, labelled with C's and O's, respectively, in the drawing, was defined in conjunction with each hydroxyl group to simulate a hydrogen bonding situation. The hydrogen bonds are indicated in the figure by the broken lines. The geometry of the hydrogen bonds was the same as used by Dempster and Zerbi (58) in their model of methanol. The O•••O distance was defined as 2.65 A and the C-O•••O angle as 104° 40'. The C-O-H•••O-C atoms all lie in a plane. This model was not meant to simulate the complete hydrogen bonding scheme of the neo-inositol molecules in the crystalline environment, but represents a very simple approximation to the crystalline environment.

To describe the motions involving the hydrogen bond, four additional types of internal coordinates were defined. In-plane and out-of-plane bending motions of the O-H•••H group were defined. The in-plane and out-of-plane bending motions are illustrated on the hydroxyl hydrogen on C1 in Fig. 42. Hydrogen bond stretching coordinates (H•••O stretch) and H•••O-C bending coordinates were also defined. The force constants for these four types of internal coordinates were also taken from Dempster and Zerbi (58).

The calculations based on the neo-inositol hydrogen bonding model resulted in two types of deformations involving the hydrogen bonds being predicted in the 750-300 cm^{-1} region of interest. The O-H•••O out-of-plane bending deformations were predicted between 617 and 605 cm^{-1}, which is indeed in the region of the observed temperature sensitive bands. There was some mixing of the C-O torsions with the O-H•••O out-of-plane bending deformations. But in addition to the O-H•••O out-of-plane bending deformations being calculated in the region 750-300

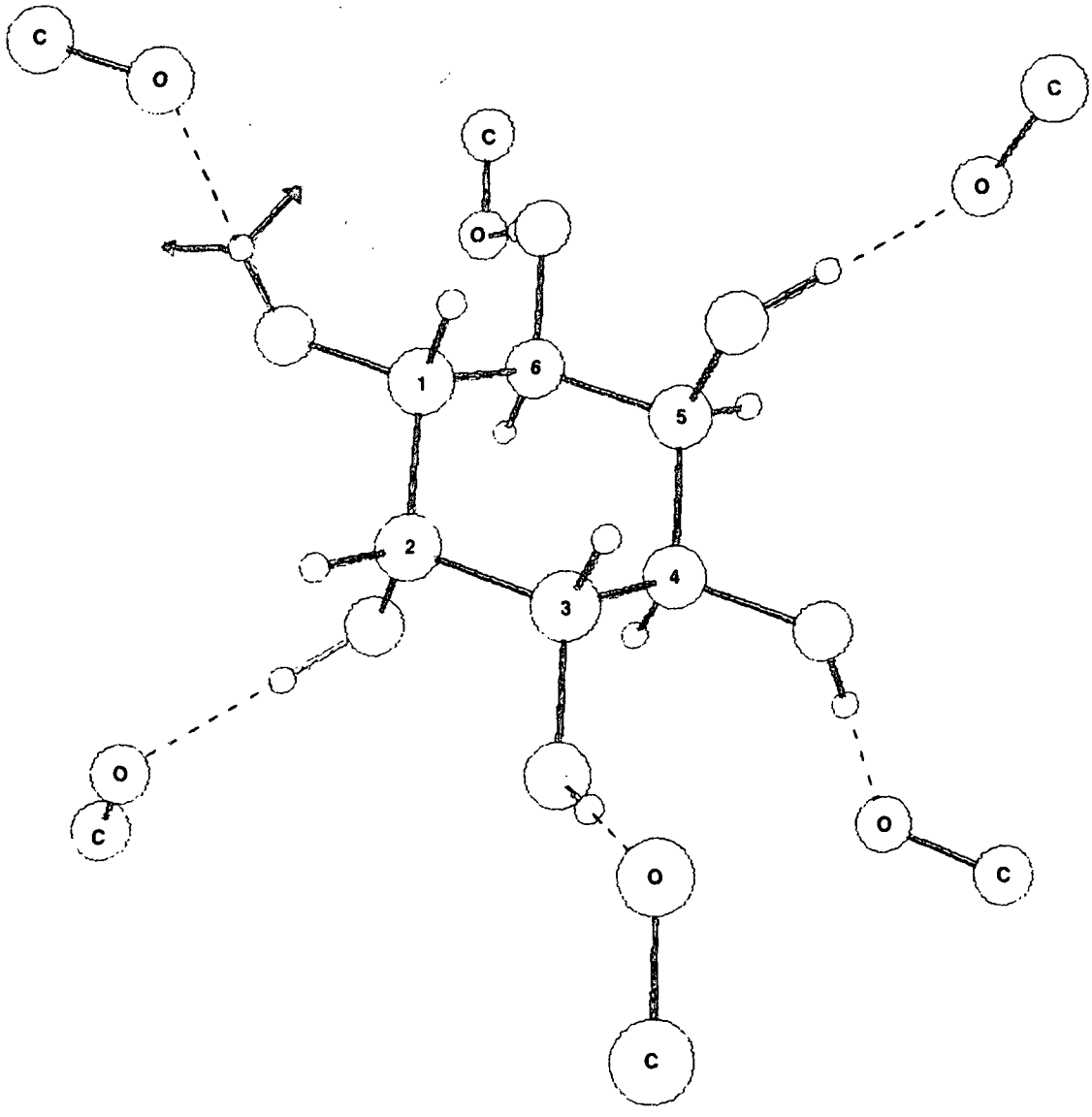

Figure 42. Representation of the neo-Inositol Hydrogen Bonding Model

cm^{-1}, the H•••O stretching modes were calculated between 767 and 762 cm^{-1}. In methanol, the same type of mode was predicted at 347 cm^{-1}. The difference in the calculated frequencies of the H•••O stretching modes may be due to the inclusion of the hydroxyl hydrogen on the added C-O combination or the definition of several additional types of internal coordinates in the methanol model. The O-H•••O in-plane and H•••O-C bending deformations were calculated below 130 cm^{-1} and were highly mixed with other motions. When deuterium was exchanged for the hydroxyl hydrogens in the model, both the O-D•••O out-of-plane bending and D•••O stretching

deformations shifted to lower frequencies, to 453-430 and 559-550 cm^{-1}, respectively. This is the general region where new bands were observed in the deuterated spectra, as illustrated in the case of neo-inositol in Fig. 41. The calculated results, then, closely parallels the behavior of the observed temperature sensitive bands.

Many of the original neo-inositol fundamental modes were perturbed to varying degrees in the hydrogen bonding models calculations. This is illustrated in Table XXVI which compares the original neo-inositol frequencies and the frequencies calculated using the hydrogen bonding model. The differences in the frequencies are caused primarily by contributions to the fundamentals from the O-H•••O in-plane bending coordinates. Table XXVI shows that the COH bending modes around 1400 cm^{-1} were perturbed significantly. Although the O-H•••O in-plane bending contributions to the COH bending modes were relatively small, approximately 5% or less, 5% of 1400 cm^{-1} is 70 cm^{-1} which results in a significant change in the frequencies. Small contributions from the H•••O stretching coordinates (less than 0.5%) and the H•••O-C bending coordinates (less than 0.3%) were also observed in the region around 1400 cm^{-1}. The frequencies below 1150 cm^{-1} were not, in general, perturbed to as great a degree. The perturbations below 1150 cm^{-1} arise from O-H•••O in-plane bending and H•••O stretching contributions. Aside from the perturbing contributions, usually totalling less than 4%, the potential energies of the bands calculated from the hydrogen bonding model were almost identical to the original neo-inositol potential energy distribution.

The results of the hydrogen bonding model calculations are not taken as conclusive, that is, the observed temperature sensitive bands cannot be rigorously interpreted from the calculated potential energy distribution. But, the model, which was based on the simpler system of solid methanol, does predict motions of the hydrogen bonded hydroxyl hydrogens in the region of the observed temperature

sensitive bands and the model calculations closely approximate the observed behavior upon deuteration. This reinforces the interpretation of the temperature sensitive bands in the inositol spectra as vibrations involving the deformations, including the O-H•••O out-of-plane deformations, of the hydrogen bonds.

TABLE XXVI

COMPARISON OF THE neo-INOSITOL AND THE neo-INOSITOL HYDROGEN BONDING MODEL CALCULATED FREQUENCIES

neo-INOSITOL (cm^{-1})	neo-INOSITOL H BONDING MODEL (cm^{-1})	CHANGE (cm^{-1})	neo-INOSITOL (cm^{-1})	neo-INOSITOL H BONDING MODEL (cm^{-1})	CHANGE (cm^{-1})
1433	1499	66	1090	1094	4
1425	1499	74	1063	1081	18
1418	1468	50	1059	1070	11
1417	1467	50	1041	1045	4
1402	1457	55	1007	1011	4
1396	1454	58	935	939	4
1395	1399	4	894	917	23
1370	1380	10	869	884	15
1356	1372	16	721	737	15
1339	1346	7	673	701	28
1335	1338	3	723	731	8
1303	1325	22	668	680	12
1270	1294	24	531	554	23
1269	1285	16	452	465	13
1258	1274	16	438	447	9
1257	1271	14	367	371	4
1226	1262	36	324	321	3
1224	1261	37	323	319	4
1136	1145	9	309	309	0
1125	1135	10	263	261	2
1123	1124	1	253	252	1
1092	1095	3			

The results of the calculations also suggest that the manner in which the OH out-of-plane bending deformations, the C-O torsions, were originally defined is not adequate in the case of a hydrogen bonded system. Originally, the C-O torsions were defined as if the hydroxyl groups were free and not hydrogen bonded. The hydrogen bonding model calculations demonstrate that this is not an adequate description of the potential involved in the OH out-of-plane deformations. To calculate the OH out-of-plane modes in the 600 cm^{-1} region using the original simple torsion definition, the C-O torsion force constant would have to be so large it would have a pronounced effect on the frequencies of a large number of the other calculated frequencies. Thus, to provide a satisfactory description of the O-H•••O out-of-plane potential, the hydrogen bonds have to be taken into account.

It can also be noted that the major nonideality associated with the hydrogen bonded hydroxyl groups, which is clearly an anhormonicity, is much more pronounced in the infrared than in the Raman. This provides further support for observations (18,96) that the vibrational selection rules, i.e., overtones and combination bands, are more strictly adhered to in the Raman than in the infrared.

This completes the interpretation of the observed vibrational spectra of scyllo-inositol, neo-inositol, myo-inositol, epi-inositol, deuterated scyllo-inositol, and deuterated neo-inositol. The prominent spectral features have been examined and interpreted. These results will now be compared to previous interpretations.

COMPARISON OF THE INTERPRETATION OF THE INOSITOL VIBRATIONAL SPECTRA WITH PREVIOUS CARBOHYDRATE SPECTRAL INTERPRETATIONS

The types of internal coordinates defined for the inositols also occur in the hexoses, pentoses, 1,5-anhydropentitols, and the alditols. In addition, internal

coordinates involving the methylene hydrogens and in the cases of the hexoses, pentoses, and 1,5-anhydropentitols, the ring oxygen were also defined for these other carbohydrates. The presence of additional internal coordinate types will affect the vibrational coupling patterns in these compounds. Even so, this does not preclude a comparison of the regions in which the common types of internal coordinates contribute. Figure 43 shows a bar graph representation of the internal coordinate contributions for β-D-glucopyranose as taken from Wells (23). Contributions from the methylene HCC and HCO bending and the ring oxygen stretching deformations are included, but contributions involving the heavy atom bending deformations of the ring oxygen are not shown. Comparison of Fig. 43 with Fig. 29 of neo-inositol shows the regions of contributions for the types of motions illustrated to be quite similar. Similar types of motions are calculated to occur in the same regions in both molecules. The inositol results were also quite similar to the results calculated for the pentoses (22). A difference was noted in the calculated COH bending contributions between the inositols and the 1,5-anhydropentitols and alditols. The COH bending contributions in the inositols were in general calculated in a higher frequency range than for the 1,5-anhydropentitols and the alditols.

AN EVALUATION OF THE ASSUMPTIONS USED IN THE NORMAL COORDINATE ANALYSIS MODEL AND AN ASSESSMENT OF THE DEGREE TO WHICH SECOND-ORDER POTENTIAL EFFECTS PERTURB THE EXPERIMENTALLY OBSERVED VIBRATIONAL FREQUENCIES

In the Introduction, a primary objective of this thesis was stated to be, "to more closely assess the extent to which second-order potential effects perturb the experimentally observed frequencies of the fundamental modes of vibration. Concurrently, this would also permit a more critical evaluation of the assumptions involved in doing a normal coordinate analysis of molecules having approximately the same number of vibrational degrees of freedom as the inositols." In this

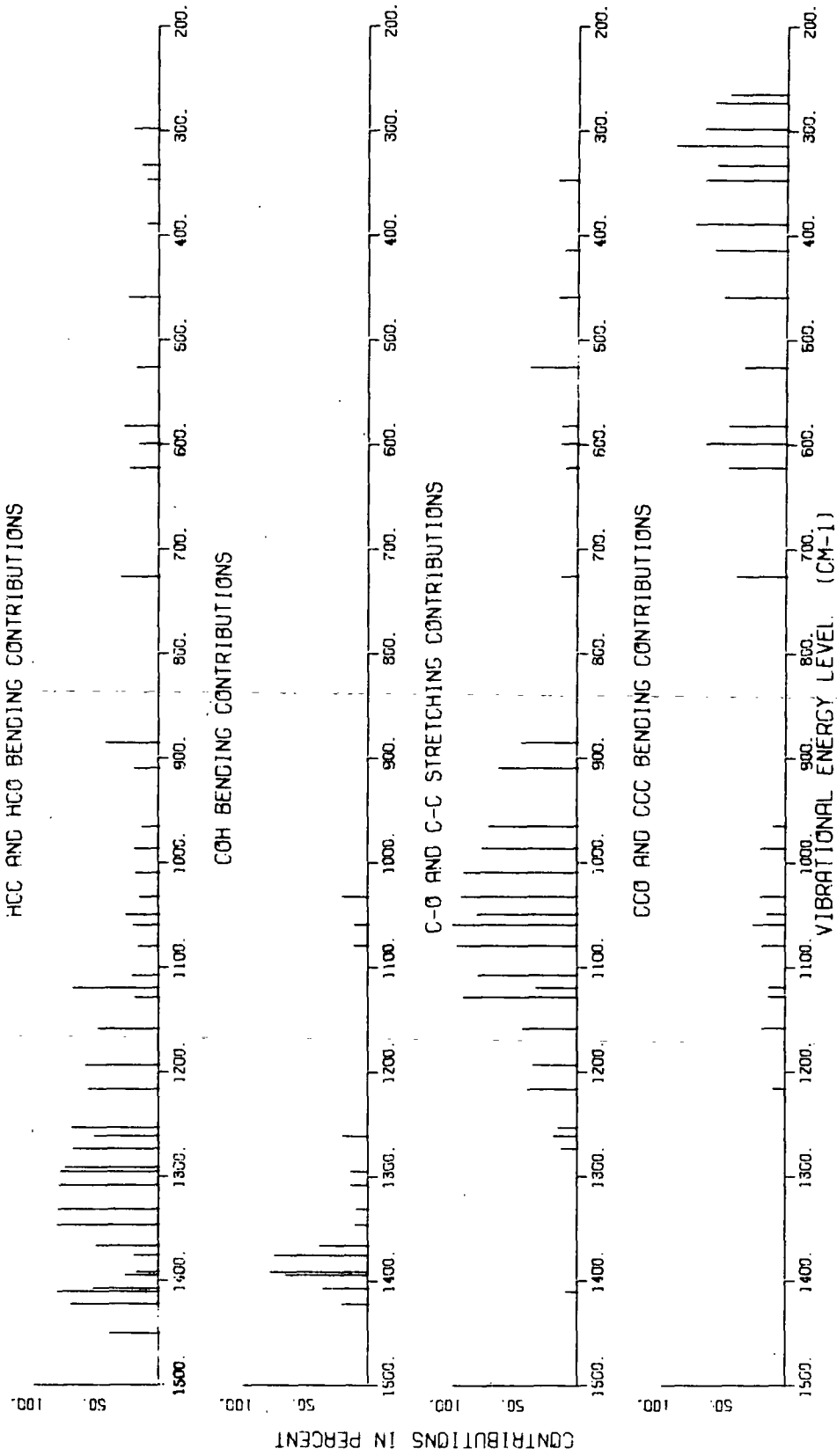

Figure 43. Bar Graph Representation of the Internal Coordinate Potential Energy Distribution for β-D-Glucose

section, both aspects of this objective will be examined. First, the assumptions made in defining the molecular model will be reviewed. The validity of the assumptions will then be evaluated in conjunction with an appraisal of the extent to which second-order potential effects perturb the observed frequencies.

In defining the potential energy, four individual assumptions were made. First, it was assumed that all the internal coordinate deformations and the interactions between different types of internal coordinates could be described using harmonic potentials. This was the harmonic oscillator approximation. Second, all intermolecular interactions were assumed to be negligible. Each molecule was treated as if it were vibrating independently of the other molecules in the crystal. Third, it was assumed that the same force constant could be used to describe the deformations of all internal coordinates of a common type and between internal coordinate interactions of a similar type. This third assumption was actually invoked twice. Within each molecule it was assumed that all internal coordinates and internal coordinate interactions of a common type could be described with a single force constant. For the refinements, it was assumed that the same force field could be used for a series of molecules of similar structure. This assumes transferability of the force constants between molecules which contain common types of internal coordinates and interactions. A fourth assumption was implicit in the definition of the inositol force field. No distinction was made in the definition of the diagonal force constants between the axial and equatorial orientations. For example, the same C-O stretch constant was used for both orientations. The only conformation dependent force constants, which take into account the difference between the axial and equatorial orientations, are eight of the bend-bend interaction constants. In applying the force field as defined to the inositols, it is assumed that the difference in the positions of the vibrational frequencies between the inositols are

primarily a $\underset{\sim}{G}$ matrix effect rather than a potential effect. That is, the differences in the band positions can be primarily accounted for by differences in the $\underset{\sim}{G}$ matrices.

The only assumption made in generating the $\underset{\sim}{G}$ matrices for the inositols was the assumption of tetrahedral geometries for the molecular structures.

The validity of the assumptions just cited will be reflected in the ability of the normal coordinate calculations to reproduce the experimentally observed frequencies. The decreasing validity of any one or all of the assumptions would be expected to result in a relatively poorer agreement between the calculated and observed frequencies. In the Introduction, it was hypothesized that the fewer the number of force constants used to describe the potential energy, the less adequately the force constants could account for second-order potential effects perturbing the experimentally observed frequencies in a series of structurally similar molecules. Inherent in this original hypothesis was the assumption that a major part of the average error results from second-order potential effects perturbing the observed frequencies. It was thought, then, that because the inositols were described using substantially fewer force constants, a comparison of the overall average errors for the inositols with other classes of carbohydrates would provide some measure of the degree to which the experimentally observed frequencies are perturbed.

In the final inositol calculations, two-hundred thirty-four experimental frequencies, assigned to six molecules, were reproduced with an average error of 10.4 cm^{-1} using a thirty-three parameter force field. Earlier, the frequency distributions were examined for the six molecules involved in the last refinements, Fig. 23 through 28, and the fits of the calculated frequencies to the assigned experimentally observed frequencies were seen to be quite good. Pitzner

(18,19) attained an overall average error of 6.3 cm^{-1} for the 1,5-anhydropentitols using a fifty-six parameter force field, Watson (21) an overall average error of 9.1 cm^{-1} for the alditols, ribitol, xylitol and erythritol using a fifty-nine parameter force field, Edwards (22) an overall average error of 7.4 cm^{-1} for the three pentoses, β-arabinose, β-lyxose and α-xylose using a seventy-four parameter force field, and Wells (23) an overall average error of 6.4 cm^{-1} for α-D-glucose, β-D-glucose and seven carbon-deuterated analogues using a forty-six parameter force field. Thus, the overall average error for the inositols is somewhat higher than those previously attained. But there are two significant differences between the inositols and the other studies which have already been shown to affect the average errors. First, there is the refinement of the inositols in symmetrized form and second, the inclusion of the deuterated species in the refinements. Both acted as additional constraints on the refinements and therefore tended to raise the average errors. The presence and resulting effect on the average errors of these added constraints makes a direct comparison of the inositols' overall average error and the overall average errors of the other classes of carbohydrates difficult to interpret. While the overall average error for the inositols is somewhat higher, an average of 3 cm^{-1} higher than the other studies, in light of the additional constraints the difference is not great enough to permit conclusions to be drawn. The hypothesis proposed originally, that the fewer the number of force constants the less adequately the force constants could account for perturbations in the experimental frequencies which would result in higher average errors, is not applicable to the extent originally anticipated. In other words, the fit of the inositols attained is better than had been originally expected.

Because little information can be gained by comparison with other molecular systems, the validity of the assumptions and the degree to which the experimental

frequencies are perturbed will be investigated by evaluating the factors which contribute to the errors between the assigned experimental frequencies and the calculated frequencies for the inositols. There are several factors which could potentially contribute to the average errors: (1) the perturbation of the experimentally observed frequencies by what has been referred to as second-order potential effects, meaning specifically effects such as intermolecular interactions, for example hydrogen bonding, and anharmonic terms, the higher order terms, in the Taylor series expansion of the potential energy; (2) $\underset{\sim}{G}$ matrix effects resulting from the assumed tetrahedral geometries being only an approximation to the real molecular structures could contribute to the average errors; (3) the potential inability of the Fletcher-Powell method to find the lowest minimum achievable could result in residual errors. The latter two factors have been investigated individually and their relative contributions to the average errors can be estimated.

In the generation of the $\underset{\sim}{G}$ matrices, tetrahedral geometry models for the inositols were assumed. To evaluate the validity of this assumption, $\underset{\sim}{G}$ matrices were calculated for myo-inositol and epi-inositol based on the molecular geometries determined for the x-ray investigations (34-36). The only alteration from the determined x-ray crystal structures was that the O-H and C-H bond lengths were set at 0.97 and 1.10 A, respectively. This was done because the positions of the hydrogens are not accurately determined in x-ray studies. The frequencies calculated using the x-ray crystal structure geometry are compared with the frequencies calculated using the tetrahedral geometry and the assigned observed frequencies for myo-inositol and epi-inositol in Fig. 44 and 45, respectively. In both cases, the differences between the calculated frequencies based on the x-ray structure and the tetrahedral structure are relatively minor. For myo-inositol, the average error of the assigned frequencies was 10.2 cm^{-1} for the

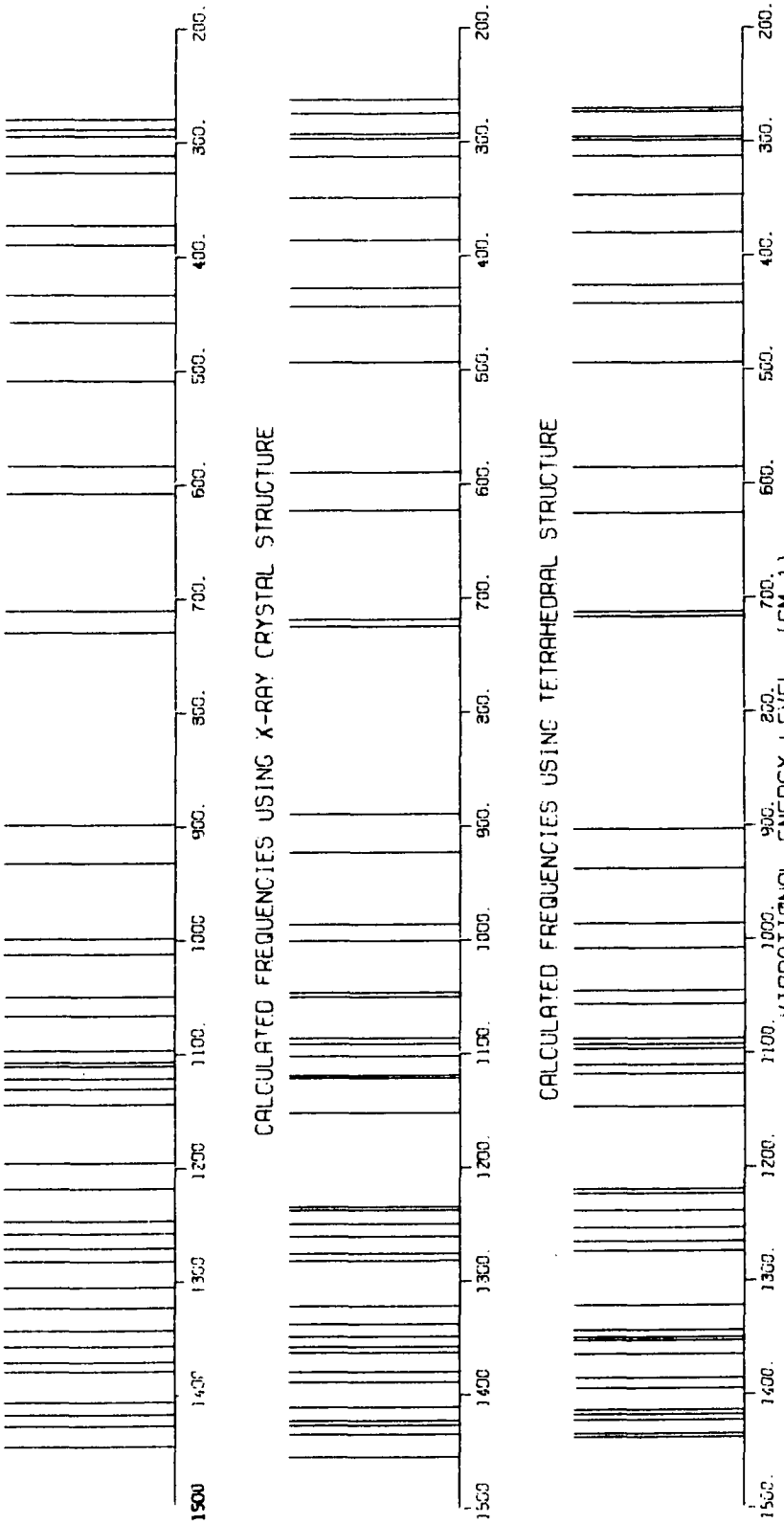

Figure 44. Bar Graph Representation of the Frequencies Calculated Using the X-ray Crystal Structure and the Tetrahedral Structure and the Assigned Experimental Frequencies for myo-Inositol

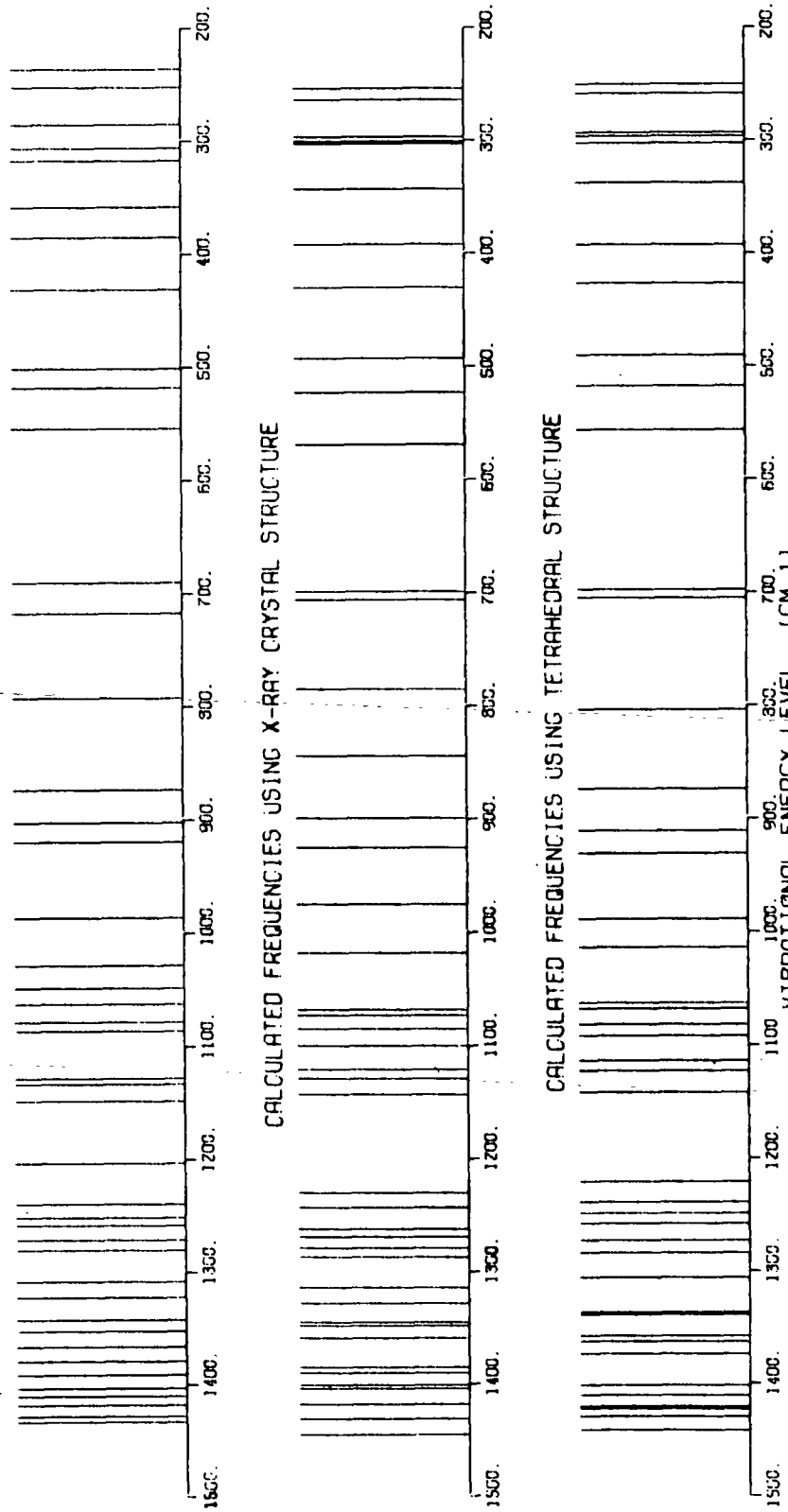

Figure 45. Bar Graph Representation of the Frequencies Calculated Using the X-ray Crystal Structure and the Tetrahedral Structure and the Assigned Experimental Frequencies for epi-Inositol

x-ray crystal structure and 9.7 cm^{-1} for the tetrahedral structure. For epi-inositol, the average error of the assigned frequencies was 9.7 cm^{-1} for the x-ray crystal structure and 8.5 cm^{-1} for the tetrahedral structure. Above 1200 cm^{-1} the differences between the two structures arise primarily from the sensitivity of the calculated frequencies to the orientation of the hydroxyl groups. The assumed hydroxyl group orientation was almost always different from the x-ray determined orientation. A close examination of individual frequency errors in the region around 1400 cm^{-1}, where the COH bending modes primarily occur, shows no inordinately large errors resulting from the hydroxyl group orientation effect.

The comparison of the x-ray and tetrahedral structures is further illustrative in the case of epi-inositol. Whereas the crystal structure of myo-inositol shows only minor deviations from the tetrahedral geometry, there are major deviations in the case of epi-inositol. epi-Inositol has two axial hydroxyl groups, at O2 and O6, in 1:3 relative positions on the ring. This is illustrated in Fig. 46 as taken from Jeffrey and Kim (35). The figure illustrates a representation of the tetrahedral model and the determined x-ray crystal structure. The tetrahedral model reflects no 1:3-diaxial interaction between the two hydroxyl groups. The x-ray structure, however, clearly illustrates that such an interaction is present, substantially distorting the structure from tetrahedral. The most obvious effect of the 1:3-diaxial interaction is to increase the O2-O6 distance from 2.50 A in the tetrahedral model to 2.96 A in the crystal structure. This results in a slight flattening of the ring at C1 and an opening of the C2-C1-C6 angle to 114.7°. The flattening of the ring at C1 also tilts O1 from an equatorial position into a quasi-axial position. In light of these substantial distortions from the tetrahedral geometry, in addition to the variation in bond lengths, bond angles and hydroxyl group orientations, a greater difference between

the frequencies calculated using the x-ray structure and the tetrahedral structure was expected. The relatively minor differences demonstrate that the assumption of a tetrahedral geometry for a molecular model is a reasonable and valid assumption. Thus, contributions to the average errors resulting from the assumed tetrahedral geometries are present but could not account for a major part of the average errors.

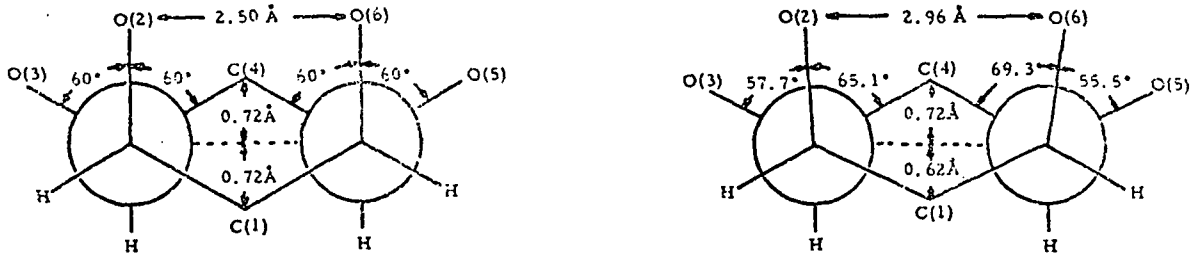

Tetrahedral Model

epi-Inositol

Figure 46. Representations of the Tetrahedral Model and the X-ray Crystal Structure for epi-Inositol (35)

Earlier, two experimental refinements were discussed which dealt with the convergence properties of the Fletcher-Powell method. If the Fletcher-Powell method can settle into false minima and then terminate a refinement at this point, a residual error between the assigned observed and calculated frequencies produced by the inability of the refinement method to find the lowest minimum could result. This residual error would then contribute to the average errors. In the two experimental refinements discussed earlier, frequencies calculated with a known force field were assigned as observed frequencies. The initial average errors in the two refinements were 4.5 and 11.1 cm^{-1}. The final average errors were 0.22 and 0.46 cm^{-1}, respectively. In both cases the Fletcher-Powell algorithm reduced the average errors by greater than 95%. These results suggest that the Fletcher-Powell method does fully minimize the least-squares difference between the assigned and calculated frequencies and will not terminate a refinement at a

higher false minimum. The residual error remaining at the termination of the two experimental refinements was finite but quite small when compared to the average errors being dealt with in the inositols. So the results of the two experimental refinements demonstrate that the residual error in the least-squares difference resulting from the inability of the Fletcher-Powell method to find the lowest possible minimum is not a major contributing factor in the average errors of the inositols.

It has been concluded that neither the assumption of tetrahedral geometries or the residual errors from a refinement can account for a major portion of the average errors of the inositols. This points to the perturbation of the experimentally observed frequencies by the second-order potential effects, the intermolecular interactions and/or the anharmonic terms in the potential energy, as the major contributors to the average errors of the inositols. The perturbations present in the experimental frequencies of the six inositols used in the final refinements cannot be completely compensated for by the force constants and consequently are the major cause of the errors observed between the assigned experimental frequencies and the calculated frequencies. Based on this conclusion, the degree to which the second-order potential effects perturb the observed frequencies can be roughly estimated from the magnitudes of the average errors.

The average percent error for the assigned frequencies of the six inositols involved in the final refinement is approximately 1.4% with an overall average error of 10.4 cm^{-1}. The largest individual frequency percent error is 13.0% for a scyllo-inositol band. The small average percent error suggests that the observed frequencies are, in general, perturbed to a relatively minor degree. This is not meant to exclude the likely possibility of individual frequencies which are perturbed to a greater degree due to local conditions in the crystalline environment, or individual frequencies whose error is primarily a $\underset{\sim}{G}$ matrix

effect from the assumption of the tetrahedral geometry or residual refinement error. For example, the COH bending modes are likely perturbed by the hydrogen bonding of the hydrogen but also part of the errors of these modes result from the assumed hydroxyl group orientation being different from the actual orientation. An exceptional case discussed earlier of a type of deformation perturbed to an inordinate degree were the hydroxyl torsions. These modes were perturbed to the extent where the torsional definition normally employed to describe the deformations could not be used to predict where in the vibrational spectrum the hydroxyl torsions would occur. On the molecular level, scyllo-inositol might be a more highly perturbed system than the other inositols, which have been discussed thus far. The average error for scyllo-inositol, 13.3 cm^{-1}, is higher and the quality of the fit of the calculated frequencies to the observed frequencies is poorer than for the other inositols. But overall, the degree to which the observed frequencies are perturbed did not significantly affect the interpretation of the vibrational spectra of the inositols.

The conclusion that the observed frequencies are, in general, perturbed by second-order potential effects to a relatively minor degree validates the assumptions which were made in defining the potential energy for the molecular model, which included the harmonic oscillator approximation and the negligibility of all intermolecular interactions. The molecular model and normal coordinate calculations very satisfactorily reproduced the observed vibrational frequencies of the inositols, with the exception of the hydroxyl torsional modes. The results of the normal coordinate analyses of the inositols discussed thus far demonstrates that the molecular model used is a valid model which can be used to semiquantitatively interpret the vibrational modes. All the assumptions made in defining the model have been shown to be valid assumptions. The validation of the molecular model for the inositols also lends further credence to the valid use of the

same molecular model in the studies of the 1,5-anhydropentitols (18), pentitols (21), pentoses (22), hexoses (23), and the cellodextrins (95).

CONCLUSIONS FROM PART I

The normal coordinate calculations satisfactorily reproduced the observed vibrational frequencies of scyllo-inositol, neo-inositol, myo-inositol, epi-inositol, deuterated scyllo-inositol, and deuterated neo-inositol. In the final refinement, involving these six molecules, two-hundred thirty-four assigned frequencies were reproduced with an average error of 10.4 cm^{-1}. The calculated potential energy distributions gave reasonable descriptions of the motions involved in the fundamental vibrations. The validity of the potential energy distributions was further substantiated by the inclusion of the deuterated analogues in the final refinement. The potential energy distributions demonstrated that below 1500 cm^{-1} a large majority of the vibrational modes were composed of complex motions and that substantial coupling was occurring between the methine hydrogen bending, in-plane hydroxyl bending, C-O and C-C stretching, heavy atom bending and the C-O and C-C torsional deformations. It was also concluded that the higher the symmetry of the inositol, the more delocalized the vibrations were around the ring.

The assumptions involved in defining the potential energy and the molecular geometries used in the molecular model were all found to be valid. The second-order potential effects, the intermolecular interactions and the anharmonic terms in the potential energy, were concluded to not be, in general, perturbing the observed frequencies to a large degree. But the second-order potential effects were concluded to be the major factor contributing to the average errors.

Several temperature sensitive, unassigned bands observed in the 750-450 cm^{-1} region in the Raman and infrared spectra of scyllo-inositol, neo-inositol, myo-inositol and epi-inositol were interpreted as modes involving deformations of the hydrogen bonded hydroxyl hydrogens. This interpretation was substantiated by frequency calculations using a simple hydrogen bonding model of neo-inositol, which predicted the O-H•••O out-of-plane and the O•••H stretching deformations to occur in the region of the observed temperature sensitive bands.

PART II

AN INVESTIGATION OF THE VIBRATIONAL SPECTRA OF CIS-INOSITOL, L-CHIRO-INOSITOL AND MUCO-INOSITOL

INTRODUCTION

An important quality in verifying the validity of a force field is its capability for predicting the vibrational frequencies for molecules not involved in the force constant refinements. The predictive capabilities provides a measure of the transferability of the force constants to molecules of similar structure. In Part II, the predictive capabilities of the inositol force field developed in Part I will be examined.

The final inositol force field was used to predict the vibrational spectra of three inositols: cis-inositol, L-chiro-inositol, and muco-inositol. cis-Inositol and muco-inositol were not included in any of the force constant refinements. L-chiro-Inositol was included in two refinements in the latter stages of development of the final force field but not in the final refinements. In Part II, the frequencies calculated from normal coordinate analyses of cis-inositol, L-chiro-inositol and muco-inositol using the final inositol force field will be compared to the experimentally observed Raman and infrared frequencies and the calculated potential energy distributions will be used as a basis for interpreting their vibrational spectra. In addition, the calculated frequencies for cis-inositol based on the assumed tetrahedral structure will be compared to the frequencies based on the x-ray crystal structure.

EXPERIMENTAL

SAMPLE PREPARATION

A sample of L-chiro-inositol was obtained from Dr. Laurens Anderson of the University of Wisconsin at Madison. He gave a melting point for the sample of

245-247°C. The reported melting point ranges from 236°C to 247°C (61). The L-chiro-Inositol was not purified further.

Purification of cis-Inositol

A sample, approximately 100 mg, of cis-inositol was obtained from Dr. Stephen Angyal of the University of New South Wales, Kensington, Australia. Initial attempts to record the Raman spectrum of the cis-inositol resulted in burning of the sample pellet in the laser beam. The cis-inositol was recrystallized from a 4:1 doubly distilled ethanol-triply distilled water solution. The recrystallization was done in an acid-washed polyethylene beaker to prevent cation contamination in the solution from a glass container, a suspected problem in earlier recrystallizations. A pellet made from the resulting slowly grown crystals withstood the full intensity of the laser beam without burning at room temperature but the pellet still burned at liquid nitrogen temperature. Thus the liquid nitrogen temperature Raman spectrum was not obtained.

Preparation of muco-Inositol

A sample of muco-inositol was obtained as the diisopropylidene derivative from Dr. Laurens Anderson of the University of Wisconsin at Madison. One-half of the diisopropylidene muco-inositol was dissolved in a solution of 70% methanol-30% water by volume. Amberlite IR-120 resin, which had been previously washed, was added to the solution to catalyze removal of the isopropylidene groups (62). The reaction solution was then refluxed for approximately eight hours. The progression of the reaction was monitored using thin-layer chromatography. The plate developing solvent used was $CHCl_3$-ethyl acetate (1:1). After refluxing, the reaction solution was poured off the resin. The resin was washed with methanol which was then added to the reaction solution. The reaction solution was evaporated in vacuo to dryness, leaving lightly yellow colored crystals.

The reaction procedure was repeated using the remaining half of the diisopropylidene muco-inositol. The crystals from the two reactions were combined and then recrystallized from an ethanol-water solution (~15:1). The crystals were then dried in a vacuum oven. The melting point of the crystals was 284°C with decomposition. The crystals turned light brown at approximately 275°C. The reported melting points are 284°C with decomposition (63) and 286°C (64).

MEASUREMENT OF THE RAMAN AND INFRARED SPECTRA OF cis-INOSITOL, L-chiro-INOSITOL AND muco-INOSITOL

The room temperature and liquid nitrogen temperature Raman and infrared spectra were recorded using the same instruments and sampling modes as detailed in Part I. The solution spectra and depolarization ratios were also recorded and determined as detailed in Part I.

EXPERIMENTAL RESULTS

ROOM TEMPERATURE AND LIQUID NITROGEN TEMPERATURE RAMAN AND INFRARED SPECTRA OF cis-INOSITOL, L-chiro-INOSITOL AND muco-INOSITOL IN THE CRYSTALLINE STATE

cis-Inositol

The Raman and infrared spectra are shown in Fig. 47 and 48, respectively. The frequencies of the bands are tabulated in Table XXVII.

L-chiro-Inositol

The Raman and infrared spectra are shown in Fig. 49 and 50, respectively. The frequencies of the bands are tabulated in Table XXVIII.

muco-Inositol

The Raman and infrared spectra are shown in Fig. 51 and 52, respectively. The frequencies of the bands are tabulated in Table XXIX.

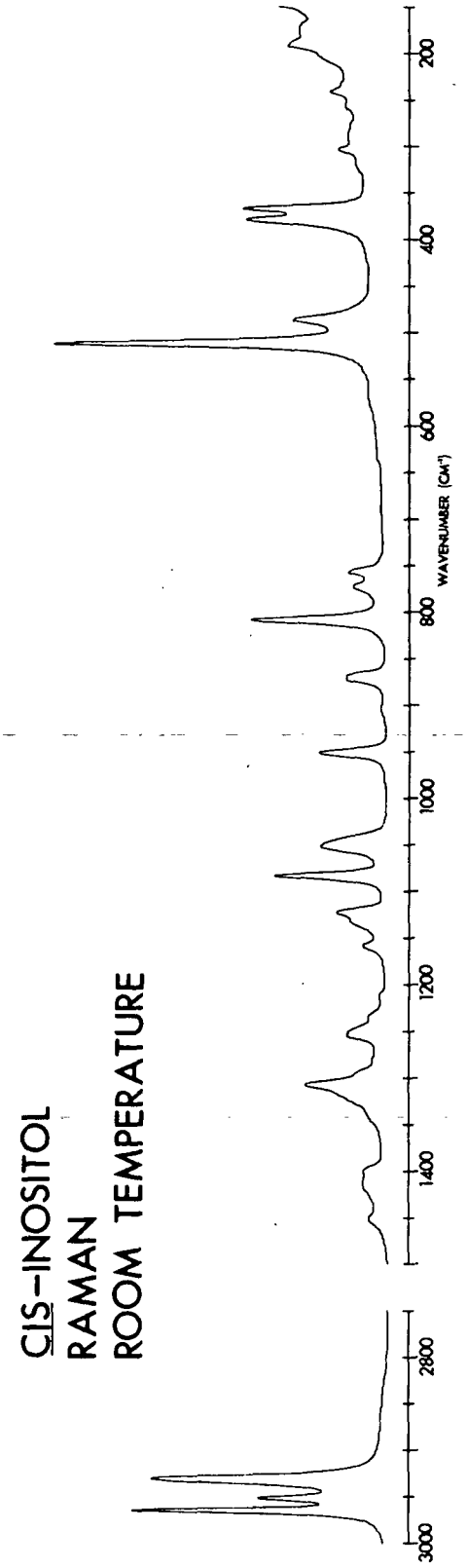

Figure 47. The Room Temperature Raman Spectrum of Crystalline cis-Inositol

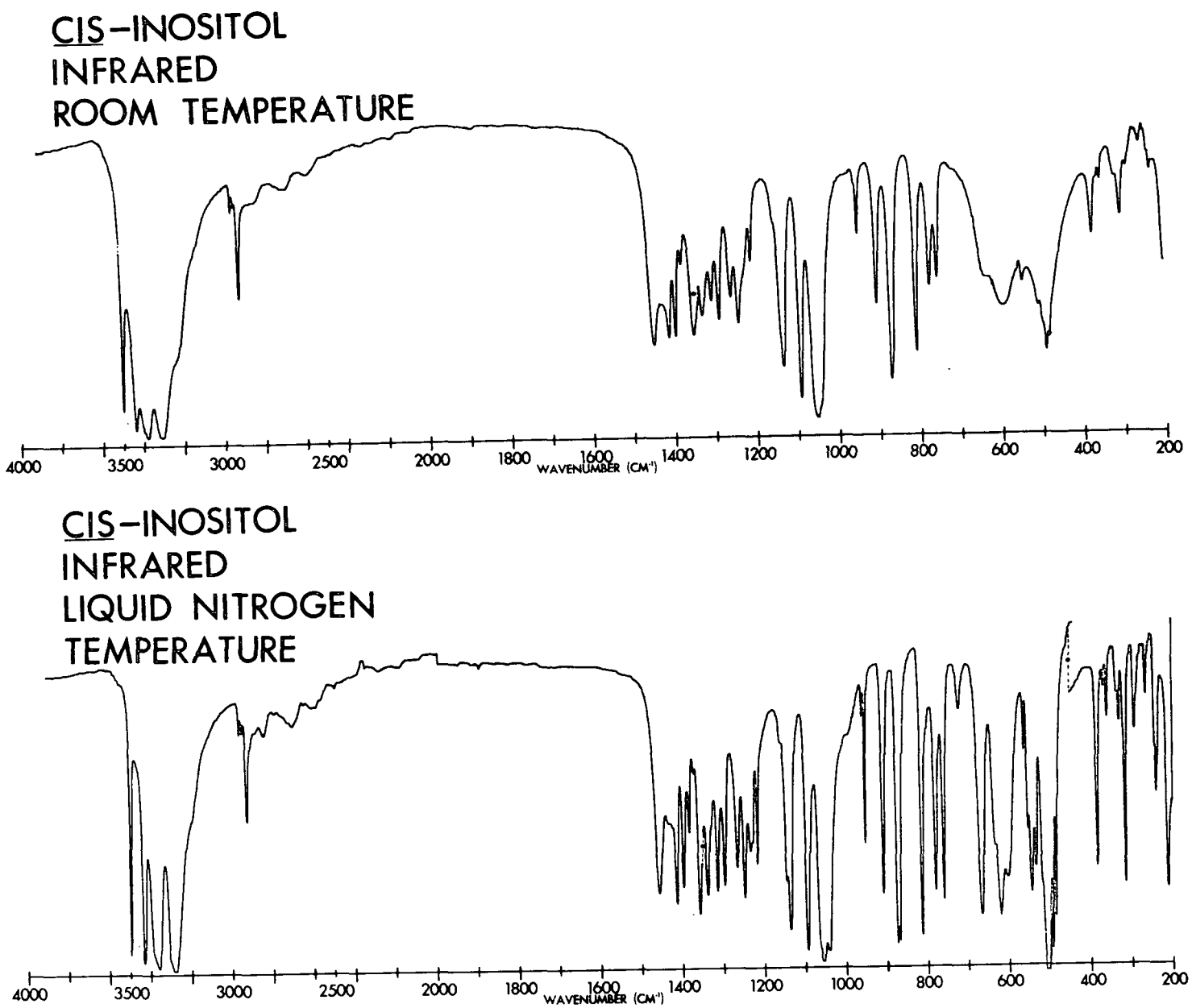

Figure 48. The Room Temperature and Liquid Nitrogen Temperature Infrared Spectra of Crystalline cis-Inositol

TABLE XXVII

TABULATED FREQUENCIES FOR THE ROOM TEMPERATURE RAMAN SPECTRUM AND ROOM TEMPERATURE AND LIQUID NITROGEN TEMPERATURE INFRARED SPECTRA OF cis-INOSITOL

RAMAN	INFRARED		RAMAN	INFRARED	
ROOM TEMPERATURE (cm^{-1})	ROOM TEMPERATURE (cm^{-1})	LIQUID NITROGEN TEMPERATURE (cm^{-1})	ROOM TEMPERATURE (cm^{-1})	ROOM TEMPERATURE (cm^{-1})	LIQUID NITROGEN TEMPERATURE (cm^{-1})
	3500 (s)	3500 (s)			~903 (sh)
	3442 (s)	3435 (vs)	871 (w)	871 (s)	874 (s)
	3385 (vs)	3390 (sh)	867 (w)	867 (sh)	869 (s)
	3320 (vs)	3360 (vs)			~861 (sh)
	3240 (sh)	3280 (vs)	811 (m)	811 (s)	814 (s)
2966 (s)	2965 (vw)	2962 (vw)			~802 (vw,sh)
2952 (m)	2952 (vw)	2955 (vw)	774 (w)	776 (m)	780 (m)
2932 (s)	2930 (w)	2930 (m)	758 (w)	758 (m)	760 (m)
1450 (w)	1452 (m)	1460 (m)			721 (w)
		~1437 (m)			667 (s)
	~1425 (vw,sh)	~1427 (vw)		~644 (m,sh)	635 (m)
1413 (w)	1415 (m)	1416 (m)			621 (s)
1400 (w)	1398 (m)	1399 (m)		598 (m,b)	603 (m)
	1382 (w)	1385 (w)			562 (w)
		1372 (vw)			554 (m)
	1354 (m)	1359 (m)		550 (m)	545 (m)
	~1347 (sh)	~1351 (sh)			534 (m)
~1335 (sh)	1333 (m)	1335 (m)			~519 (sh)
~1319 (sh)		~1325 (sh)	513 (vs)	512 (sh)	
1309 (m)	1310 (m)	1312 (m)		501 (sh)	506 (vs)
1294 (sh)	1291 (m)	1293 (m)		493 (s)	498 (s)
	1262 (m)	1263 (m)	485 (m)	485 (s,sh)	485 (s)
1253 (w)	1244 (m)	1245 (m)			~481 (sh)
~1236 (w,sh)	~1229 (sh)	1231 (w)	381 (m)	379 (w)	384 (m)
		1225 (w)	368 (m)	~366 (vw,sh)	368 (w)
1212 (vw)	1212 (w)	1214 (m)		357 (vw)	359 (w)
1159 (w)	~1157 (vw,sh)	~1159 (vw)			336 (vw)
	~1138 (sh)	1144 (m)			330 (w)
~1132 (sh)	1134 (s)	1136 (s)	~318 (vvw)	~323 (sh)	~320 (sh)
1123 (w)				310 (w)	315 (m)
1085 (m)	1092 (s)	1094 (s)	301 (vw)	292 (vw)	293 (w)
		~1087 (sh)	288 (vvw)		~289 (sh)
		~1062 (sh)	275 (vvw)		
1052 (m)	1054 (vs)	1055 (vs)	~253 (vvw)	262 (vw)	264 (w)
~1046 (sh)	~1043 (sh)	1042 (s)	239 (vw)	~242 (sh)	241 (sh)
		~1026 (w,sh)	~235 (vw,sh)	236 (w)	237 (m)
	~957 (vw,sh)	959 (w)	~202 (sh)	204 (m)	208 (m)
952 (m)	950 (w)	952 (m)	188 (w)		
906 (vvw)	906 (m)	909 (m)	~177 (vw)		

Conventional symbolism indicating relative intensity: s = strong, m = medium, w = weak, sh = shoulder, b = broad, v = very

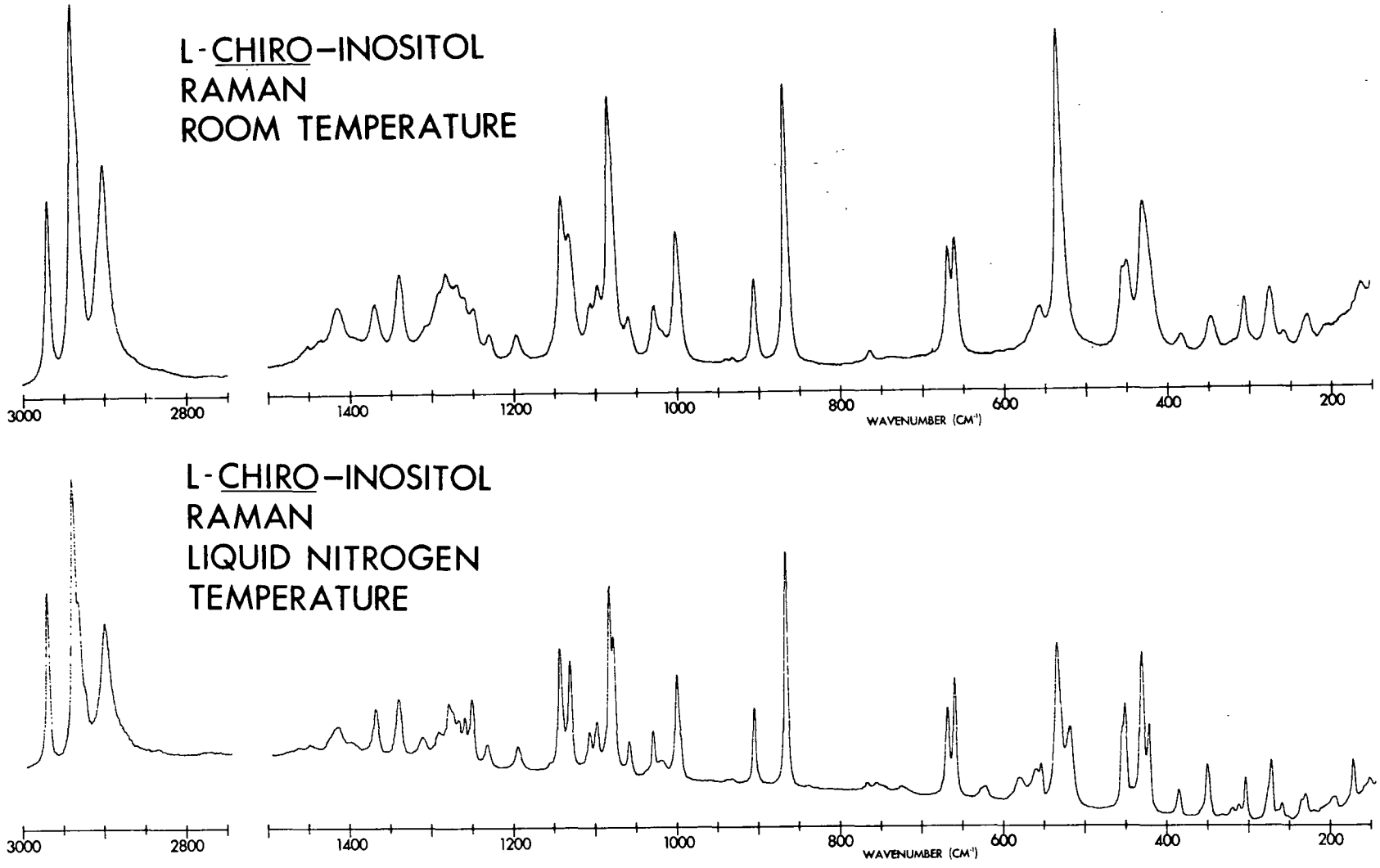

Figure 49. The Room Temperature and Liquid Nitrogen Temperature Raman Spectra of Crystalline L-chiro-Inositol

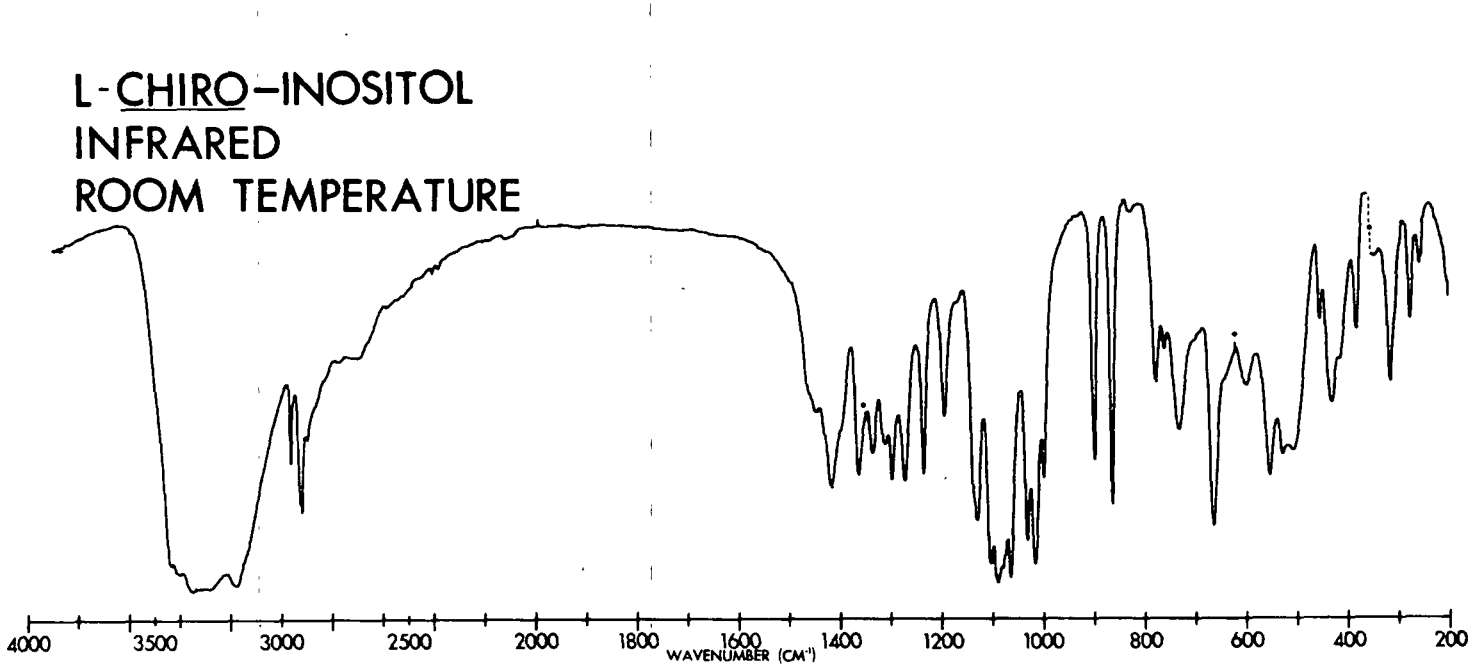

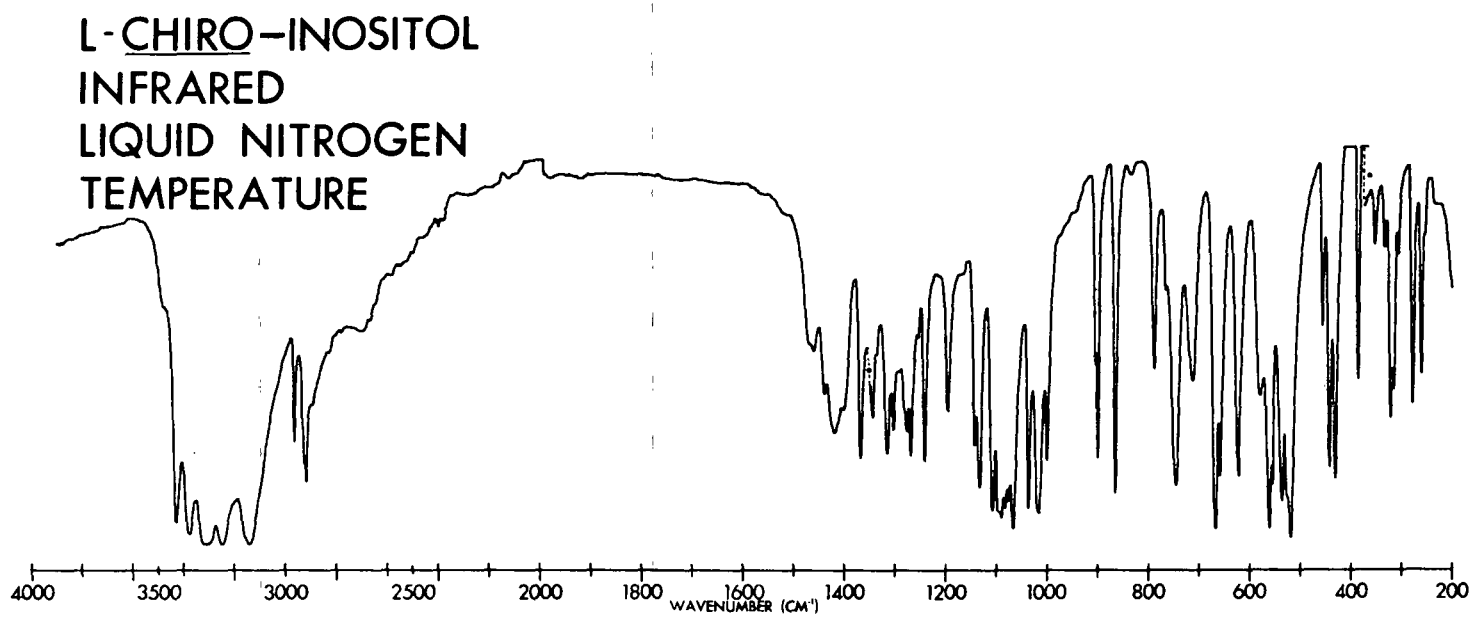

Figure 50. The Room Temperature and Liquid Nitrogen Temperature Infrared Spectra of Crystalline L-chiro-Inositol

TABLE XXVIII

TABULATED FREQUENCIES FOR THE ROOM TEMPERATURE AND LIQUID NITROGEN TEMPERATURE RAMAN AND INFRARED SPECTRA OF *L-chiro*-INOSITOL

RAMAN		INFRARED		RAMAN		INFRARED	
ROOM TEMPERATURE (cm^{-1})	LIQUID NITROGEN TEMPERATURE (cm^{-1})	ROOM TEMPERATURE (cm^{-1})	LIQUID NITROGEN TEMPERATURE (cm^{-1})	ROOM TEMPERATURE (cm^{-1})	LIQUID NITROGEN TEMPERATURE (cm^{-1})	ROOM TEMPERATURE (cm^{-1})	LIQUID NITROGEN TEMPERATURE (cm^{-1})
		3440 (s)	3430(vs)				∿955 (vw,sh)
		3400 (s)	3380 (vs)	∿937 (vvw)	∿934 (vvw)		
		3350 (vs)	3315 (vs)	∿928 (vvw)			
		3280 (vs)	3255 (vs)	903 (m)	905 (m)	898 (s)	905 (m)
		3180 (vs)	3140 (vs)				900 (m)
2967 (s)	2969 (s)	2967 (m)	2970 (m)	864 (s)	866 (vs)	864 (s)	866 (s)
2937 (vs)	2936 (vs)		∿2935 (sh)			∿829 (vw)	835 (vw)
∿2931 (sh)	2931 (sh)	2930 (m)	2930 (m)			777 (w)	790 (m)
	2923 (w,sh)	2922 (m)	2920 (m)	761 (vvw)	766 (vvw)	761 (w)	766 (w)
2900 (s)	2898 (s)	2895 (w)	2895 (w)		754 (vvw)	732 (m,b)	747 (s)
			1471 (sh)		723 (vvw)		713 (m)
	1458 (vvw)	∿1463 (sh)	1462 (w)			∿667 (sh,vw)	
∿1449 (vw)	1444 (vw)	1450 (w)	1441 (m)	665 (m)	669 (m)	665 (s)	668 (vs)
∿1429 (vw,sh)		∿1428 (sh)	1428 (sh)	656 (m)	659 (m)	∿657 (sh)	659 (s)
		1419 (m)	1421 (m)			∿640 (sh,vw)	
1410 (m)	1413 (w)				623 (vw)		622 (s)
	1398 (sh)	∿1397 (sh)	1400 (m)			600 (w,b)	
1366 (m)	1368 (m)	1364 (m)	1367 (m)		579 (w)		580 (m)
1336 (m)	1340 (m)	1336 (m)	1342 (m)		559 (w)		561 (vs)
			1334 (sh)	554 (w)	553 (w)	553 (m)	555 (s)
	1309 (w)	1313 (m)	1314 (m)				536 (s)
∿1302 (vw,sh)		1297 (m)	1301 (m)	528 (vs)	534 (s)	528 (m)	∿527 (sh)
∿1285 (sh)	1289 (w)		∿1282 (sh)		518 (m)		519 (vs)
1279 (m)	1278 (m)	1272 (m)	1275 (m)			509 (m)	
	1274 (sh)			451 (m)	455 (sh)	453 (w)	456 (m)
1266 (m)	1265 (m)		1267 (m)	446 (m)	452 (m)		443 (s)
1259 (sh)	1258 (m)			425 (s)	430 (s)	430 (m)	431 (s)
1245 (m)	1249 (m)		1251 (vw)		422 (m)	415 (w)	∿423 (sh)
		1235 (m)	1239 (s)	379 (w)	385 (w)	381 (w)	386 (m)
1225 (w)	1230 (w)			343 (w)	351 (m)	343 (vvw)	350 (w)
1192 (w)	1194 (w)	1194 (m)	1195 (m)				331 (w)
		∿1170 (vw,sh)	∿1168 (vw)		319 (vw)	315 (m)	319 (m)
1137 (s)	1143 (m)	∿1138 (sh)	1143 (m)		312 (vw)		313 (m)
1129 (m)	1131 (m)	1130 (s)	1133 (s)	303 (m)	304 (w)	∿305 (sh)	304 (w)
1102 (m)	1107 (w)	1104 (vs)	1107 (s)	272 (m)	272 (m)	277 (w)	275 (m)
			1096 (sh)	255 (w)	259 (vw)	257 (w)	259 (m)
1094 (m)	1098 (w)	1090 (vs)	1091 (s)				252 (vw)
1079 (s)	1082 (s)	∿1081 (sh)	1082 (s)		235 (w)		235 (vw)
	1078 (s)	∿1075 (sh)	1076 (s)	226 (w)	229 (w)		
1056 (w)	1058 (w)	1065 (vs)	1066 (vs)	∿184 (sh,vw)	194 (vw)		
1024 (w)	1029 (w)	1032 (s)	1036 (s)	160 (w)	173 (w)		
∿1016 (sh)	1018 (vw)	1017 (vs)	1023 (s)		151 (vw)		
997 (s)	1000 (m)	998 (m)	1000 (m)				

Conventional symbolism indicating relative intensity: s = strong, m = medium, w = weak, sh = shoulder, b = broad, v = very

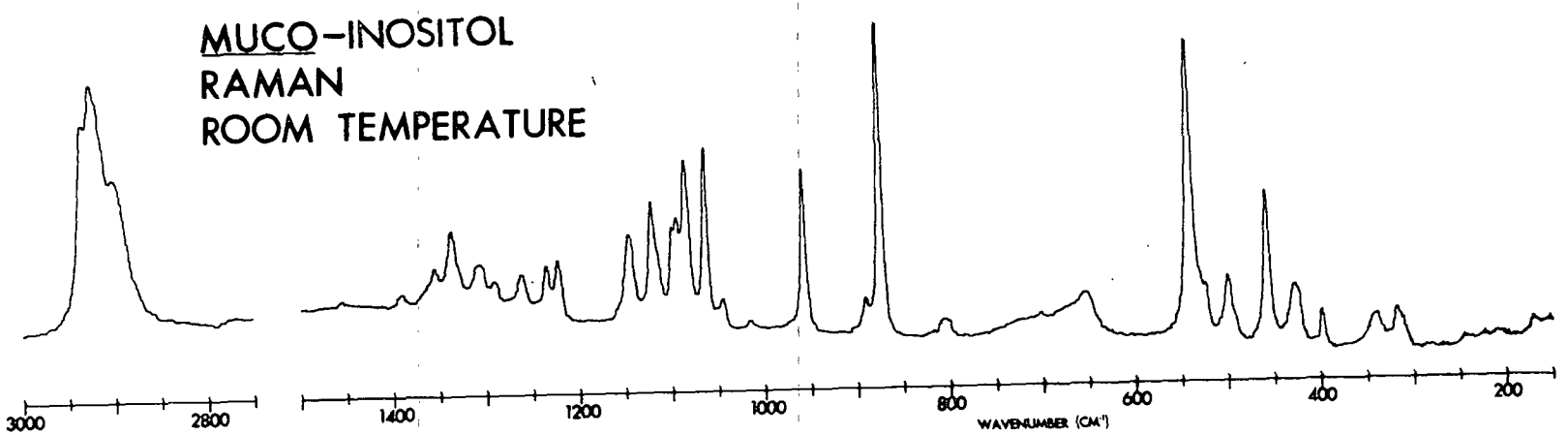

Figure 51. The Room Temperature Raman Spectrum of Crystalline muco-Inositol

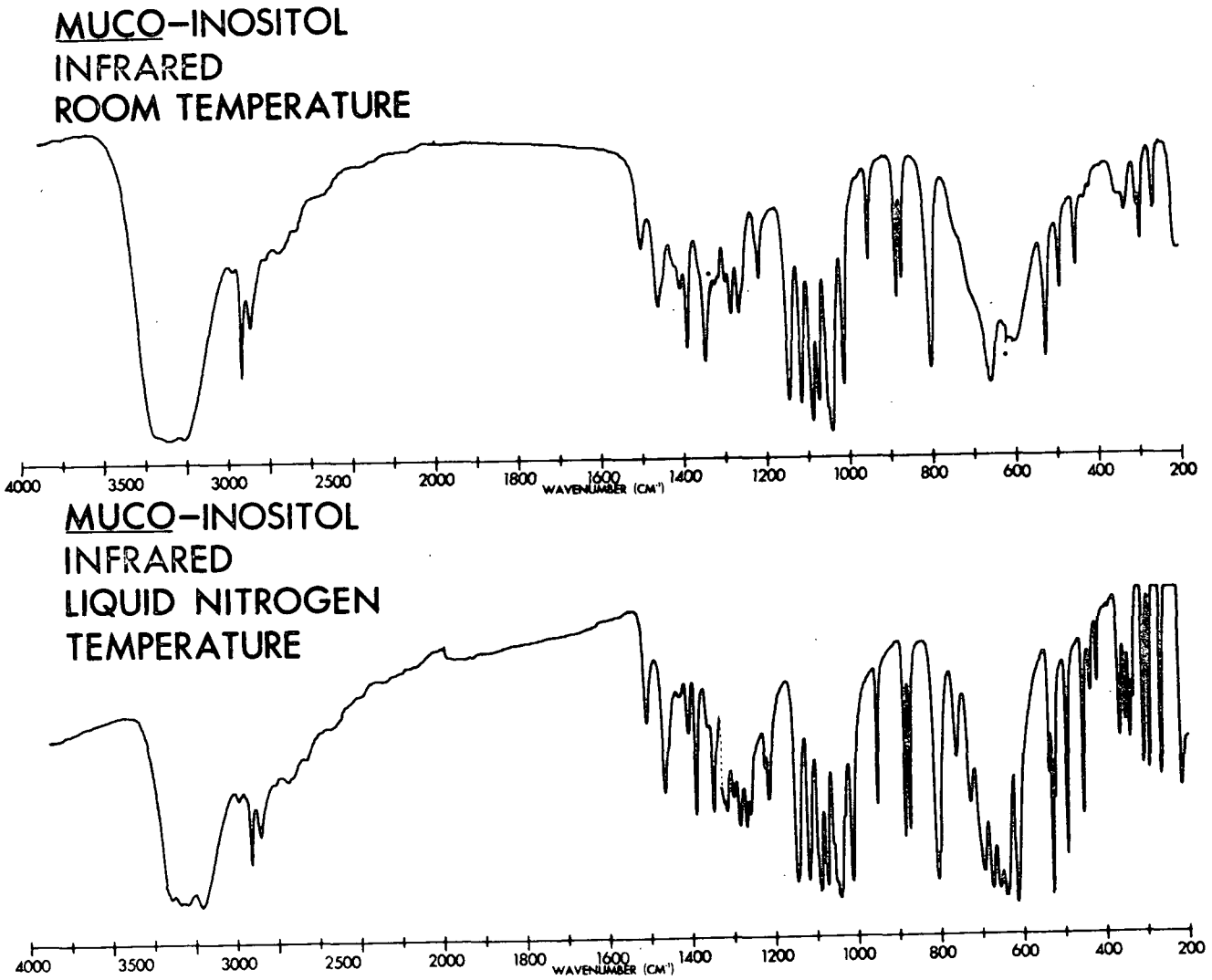

Figure 52. The Room Temperature and Liquid Nitrogen Temperature Infrared Spectra of Crystalline muco-Inositol

TABLE XXIX

TABULATED FREQUENCIES FOR THE ROOM TEMPERATURE RAMAN SPECTRUM AND ROOM TEMPERATURE AND LIQUID NITROGEN TEMPERATURE INFRARED SPECTRA OF muco-INOSITOL

RAMAN	INFRARED		RAMAN	INFRARED	
ROOM TEMPERATURE (cm^{-1})	ROOM TEMPERATURE (cm^{-1})	LIQUID NITROGEN TEMPERATURE (cm^{-1})	ROOM TEMPERATURE (cm^{-1})	ROOM TEMPERATURE (cm^{-1})	LIQUID NITROGEN TEMPERATURE (cm^{-1})
	3355 (vs)	3320 (vs)	949 (m)	950 (m)	952 (m)
	3300 (vs)	3280 (vs)	881 (vw)	885 (m)	885 (m)
	3270 (vs)	3240 (vs)	866 (vs)	872 (m)	873 (m)
	3220 (vs)	3170 (vs)			807 (s)
	2970 (w)	2990 (w)	794 (vw)	802 (s)	801 (sh)
	2938 (w)	2935 (m)		~735 (sh)	761 (m)
2928 (vs)			719 (vw,b)	~705 (sh)	727 (m)
2915 (vs)					~707 (sh)
2893 (s)	2893 (w)	2885 (w)	~692 (vw)	667 (sh)	695 (s)
	1500 (w)	1512 (w)			675 (s)
	1461 (m)	1467 (m)	~662 (w,b)	659 (s)	657 (s)
	1451 (sh)	1456 (sh)	~646 (w,b)	~622 (m)	640 (vs)
	~1423 (sh)	1430 (vw)		600 (m,b)	614 (vs)
	1406 (w)	1408 (w)			536 (m)
1380 (vw)	1389 (m)	1390 (m)	531 (s)	526 (m)	528 (vs)
	~1361 (sh)	1367 (w)	~515 (w,sh)		~521 (m)
1345 (vw)	1345 (m)	1348 (m)	490 (w)	490 (m)	492 (s)
1337 (sh)		1338 (sh)	449 (m)	450 (m)	452 (m)
1327 (w)	1322 (vw)	1323 (sh)		430 (vw)	435 (w)
1319 (sh)	1312 (sh)	1315 (w)	418 (w)	417 (vw)	418 (w)
1296 (w)	1297 (w)	1299 (w)	390 (w)	390 (vw)	391 (vvw)
1280 (w)	1284 (m)	1285 (m)			364 (m)
1264 (vw)	1265 (m)	1268 (m)		~352 (vw)	350 (m)
1252 (w)	~1258 (sh)	1259 (w)			339 (m)
1225 (w)	~1221 (sh)	1223 (w)	331 (w)	332 (w)	332 (m)
1214 (w)	1216 (w)	1216 (m)	308 (w)	303 (w)	307 (w)
		1212 (sh)		294 (w)	293 (w)
	1144 (s)	1148 (s)		283 (w,sh)	
1136 (m)		1143 (sh)		275 (vw)	
1112 (m)	1115 (s)	1119 (s)	~269 (vw)	263 (w)	265 (w)
		1114 (sh)		250 (vw)	
1089 (m)	1088 (vs)	1094 (sh)		241 (vw)	245 (vvw)
1085 (m)		1090 (s)	~230 (vw,b)	227 (vw,sh)	
	~1077 (sh)	1079 (sh)		210 (w)	
1075 (m)	1073 (s)	1074 (s)			
1054 (m)	1050 (sh)	1052 (s,sh)			
	1042 (vs)	1043 (vs)			
~1035 (vw)	~1029 (w,sh)	1031 (w,sh)			
	1013 (s)	1014 (s)			

Conventional symbolism indicating relative intensity: s = strong, m = medium, w = weak, sh = shoulder, b = broad, v = very

The liquid nitrogen temperature Raman spectra of cis-inositol and muco-inositol could not be recorded due to fluorescence of the samples.

The symbol '∿' which appears in the tables of tabulated bands means 'approximately' and indicates that the frequency could not be determined with the accuracy attained for the other bands.

RAMAN SPECTRA OF cis-INOSITOL, L-chiro-INOSITOL AND muco-INOSITOL IN WATER SOLUTION

cis-Inositol

The Raman spectrum of cis-inositol in water solution is shown in Fig. 53. The frequencies of the bands are tabulated in Table XXX.

TABLE XXX

TABULATED FREQUENCIES FOR THE RAMAN WATER SOLUTION SPECTRUM OF cis-INOSITOL

RAMAN FREQUENCIES (cm^{-1})	RAMAN FREQUENCIES (cm^{-1})
∿2945 (s,b)	953 (w)
∿1442 (sh,vw)	921 (vvw)
∿1412 (vw)	869 (w)
1289 (w,vb)	810 (m)
∿1160 (sh)	∿785 (sh)
1137 (w)	507 (s)
1100 (w)	374 (w)
1062 (w)	

Conventional symbolism indicating relative intensity: s = strong, m = medium, w = weak, b = broad, sh = shoulder, v = very.

L-chiro-Inositol

The Raman spectrum of L-chiro-inositol in water solution is shown in Fig. 53 also. The frequencies of the bands are tabulated in Table XXXI.

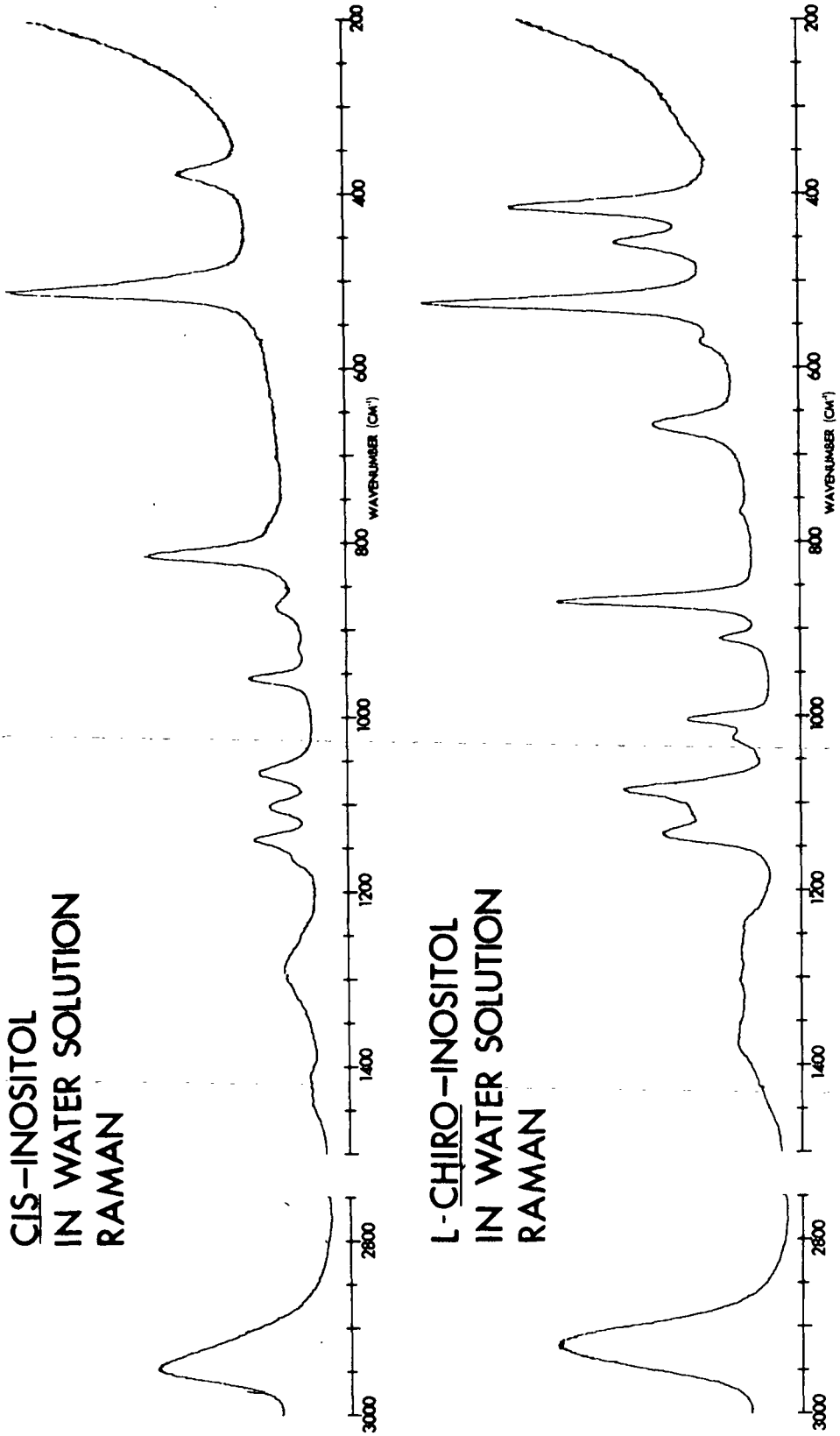

Figure 53. The Raman Spectra of the Water Solutions of cis-Inositol and L-chiro-Inositol

TABLE XXXI

TABULATED FREQUENCIES FOR THE RAMAN WATER SOLUTION SPECTRUM OF L-chiro-INOSITOL

RAMAN FREQUENCIES (cm^{-1})	RAMAN FREQUENCIES (cm^{-1})
2920 (s,b)	911 (w)
∿1375 (w,vb)	868 (s)
∿1300 (w,vb)	767 (vvw)
∿1230 (w,sh)	666 (m,b)
1134 (m)	569 (w)
∿1111 (sh)	526 (vs)
1086 (m)	457 (m)
1025 (w)	416 (s)
1004 (m)	

Conventional symbolism indicating relative intensity: s = strong, m = medium, w = weak, b = broad, sh = shoulder, v = very.

muco-Inositol

The Raman spectrum of muco-inositol in water solution is shown in Fig. 54. The frequencies of the bands are tabulated in Table XXXII.

TABLE XXXII

TABULATED FREQUENCIES FOR THE RAMAN WATER SOLUTION SPECTRUM OF muco-INOSITOL

RAMAN FREQUENCIES (cm^{-1})	RAMAN FREQUENCIES (cm^{-1})
1400-1200 (weak, broad envelope)	805 (w,b)
∿1121 (sh)	650 (m)
1095 (m)	543 (s)
1067 (m)	500 (w)
1025 (vw)	456 (m)
955 (m)	429 (w,sh)
879 (m)	414 (sh)

Conventional symbolism indicating relative intensity: s = strong, m = medium, w = weak, b = broad, v = very, sh = shoulder.

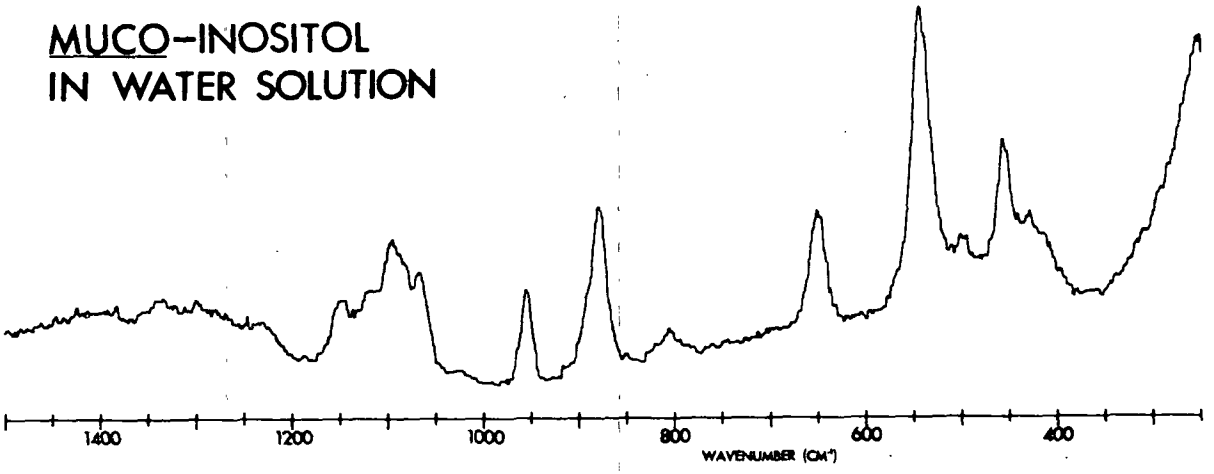

Figure 54. The Raman Spectrum of the Water Solution of muco-Inositol

MEASURED DEPOLARIZATION RATIOS FOR WATER SOLUTIONS OF cis-INOSITOL AND L-chiro-INOSITOL

Depolarization ratios were calculated for the vibrational bands observed in the water solution spectra of cis-inositol and L-chiro-inositol. The depolarization ratios are listed in Tables XXXIII and XXXIV, respectively. The depolarization ratios for some of the bands are questionable either because the bands are weak or because they overlap with adjacent bands. The bands in question are noted in the tables. Bands above 1150 cm^{-1} were not considered because their broadness and low intensity prohibited identification of individual bands.

TABLE XXXIII

MEASURED DEPOLARIZATION RATIOS FOR A WATER SOLUTION OF cis-INOSITOL

RAMAN FREQUENCIES (cm^{-1})	ρ^a, H_2O	RAMAN FREQUENCIES (cm^{-1})	ρ^a, H_2O
1137	0.08	869[b]	0.50
1100	0.68	810	0.001
1062	0.70	507	0.08
953	0.65	374	0.79

[a] ρ designates the depolarization ratio.
[b] Measured depolarization ratio is questionable because band is weak.

TABLE XXXIV

MEASURED DEPOLARIZATION RATIOS FOR A WATER SOLUTION OF L-chiro-INOSITOL

RAMAN FREQUENCIES (cm^{-1})	ρ^a, H_2O	RAMAN FREQUENCIES (cm^{-1})	ρ^a, H_2O
1134[b]	0.53	767[c]	--
1111[b]	--	666	0.25
1086[b]	0.52	569[b]	--
1025	0.44	526	0.06
1004	0.41	457	0.66
911	0.64	416	0.19
868	0.02		

[a] ρ designates the depolarization ratio.
[b] Measured depolarization ratio is questionable because band is overlapped with neighboring bands.
[c] Measured depolarization ratio is questionable because band is weak.

VIBRATIONAL ANALYSES

The molecular model used in the normal coordinate analyses of cis-inositol, L-chiro-inositol and muco-inositol is the same as described in Part I. Seventy-eight internal coordinates were defined for each of the three molecules. This includes twelve redundant internal coordinates. The torsion coordinates around the C-O and C-C bonds were defined after the procedure of Hilderbrandt (32). The internal coordinates defined for cis-inositol, L-chiro-inositol and muco-inositol are listed in Appendix II.

For construction of the $\underset{\sim}{G}$ matrices, tetrahedral model geometries were assumed. The same bond lengths listed in Table XVII in Part I were used. Ball-and-stick drawings for the tetrahedral models of cis-inositol, L-chiro-inositol and muco-inositol and the atom numbering sequencies for defining the relative atom positions and the internal coordinates are shown in Fig. 55.

The x-ray crystal structure for cis-inositol has been determined by Freeman, et al. (65). A $\underset{\sim}{G}$ matrix was also constructed based on the x-ray crystal structure.

The force field used in the normal coordinate calculations was the final inositol force field listed in Table XIX in Part I. There was no further refinement of the force constants involving these three inositols. The calculations for cis-inositol, L-chiro-inositol, and muco-inositol were run in both the unsymmetrized and symmetrized forms. The symmetry coordinates constructed for symmetrizing the $\underset{\sim}{G}$ and $\underset{\sim}{Z}$ matrices of cis-inositol, L-chiro-inositol and muco-inositol are presented in Appendix VI.

The room temperature Raman and infrared observed frequencies, the frequencies assigned in the refinements, the frequencies calculated using the force

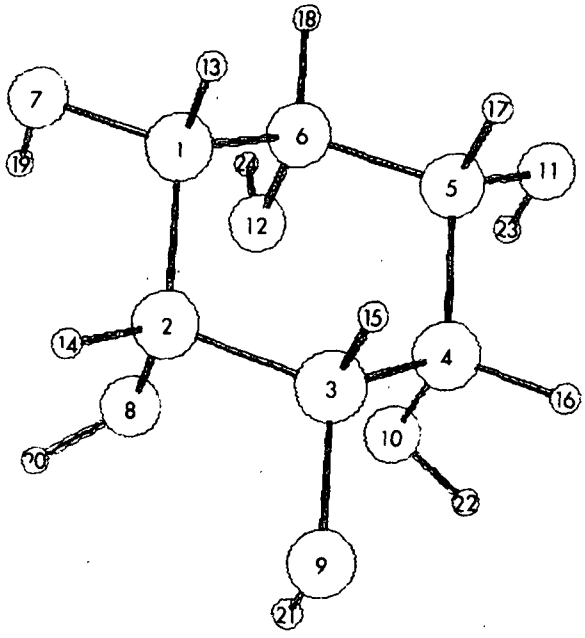

cis-Inositol

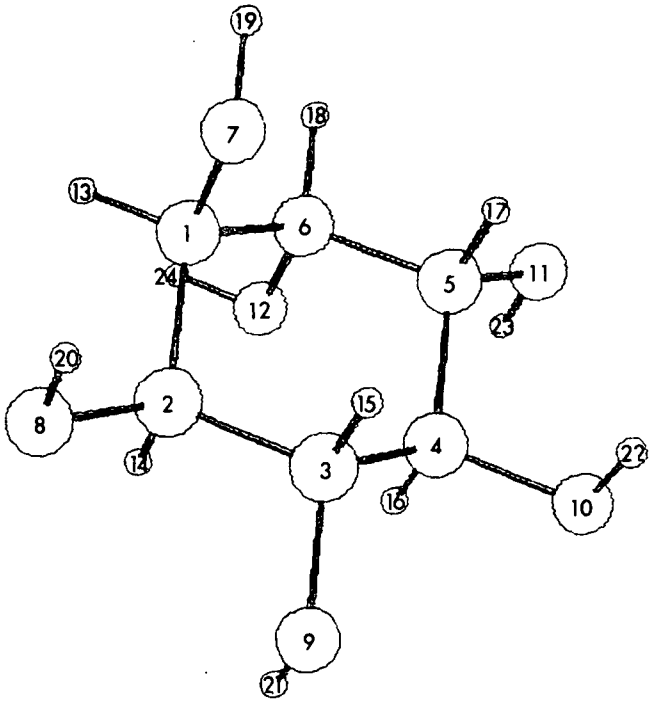

L-chiro-Inositol

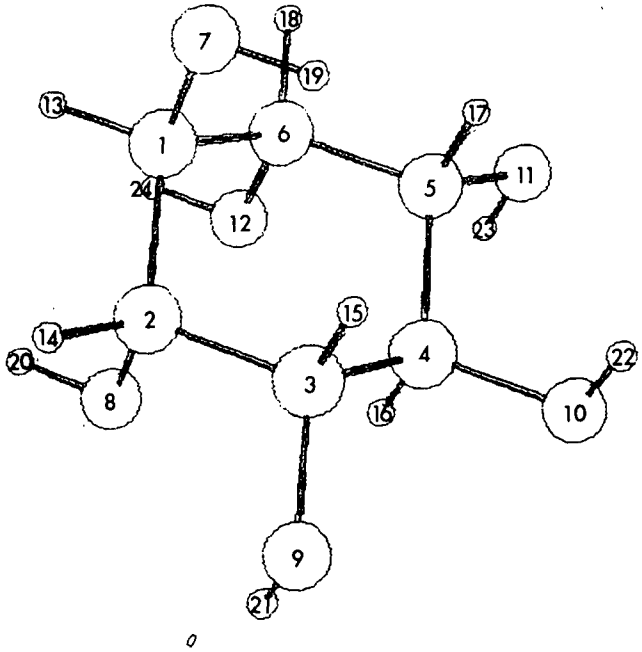

muco-Inositol

Figure 55. Representations of the Tetrahedral Models for cis-Inositol, L-chiro-Inositol and muco-Inositol

constants presented in Table XIX and the calculated symmetry class for each frequency for cis-inositol, L-chiro-inositol and muco-inositol are listed in Appendix V. Also given are the potential energy distributions in terms of internal coordinates and the force constants.

DISCUSSION OF RESULTS

First in this section, the ability of the final inositol force field to predict the vibrational spectra of cis-inositol, L-chiro-inositol and muco-inositol will be evaluated by comparing the assigned experimentally observed frequencies with the calculated frequencies. The calculated frequencies and assigned frequencies for cis-inositol will then be compared to the frequencies calculated based on the x-ray crystal structure.

The experimentally observed frequencies for cis-inositol, L-chiro-inositol and muco-inositol will be briefly interpreted based on the calculated potential energy distributions.

At this point, the observed spectra and calculated spectra of seven of the inositol isomers will have been discussed. The effect on the vibrational frequencies of the axial-equatorial orientations of the hydroxyl groups for the seven inositols will be examined.

COMPARISON OF THE ASSIGNED EXPERIMENTALLY OBSERVED FREQUENCIES AND THE CALCULATED FREQUENCIES FOR cis-INOSITOL, L-chiro-INOSITOL AND muco-INOSITOL

A bar graph representation of the assigned experimental frequencies and calculated frequencies for cis-inositol is shown in Fig. 56. For clarity, the frequencies have been divided into two groups; those frequencies belonging to the A_1 and A_2 symmetry species and the frequencies belonging to the E symmetry species. The calculated E symmetry species frequencies are doubly degenerate. In all but

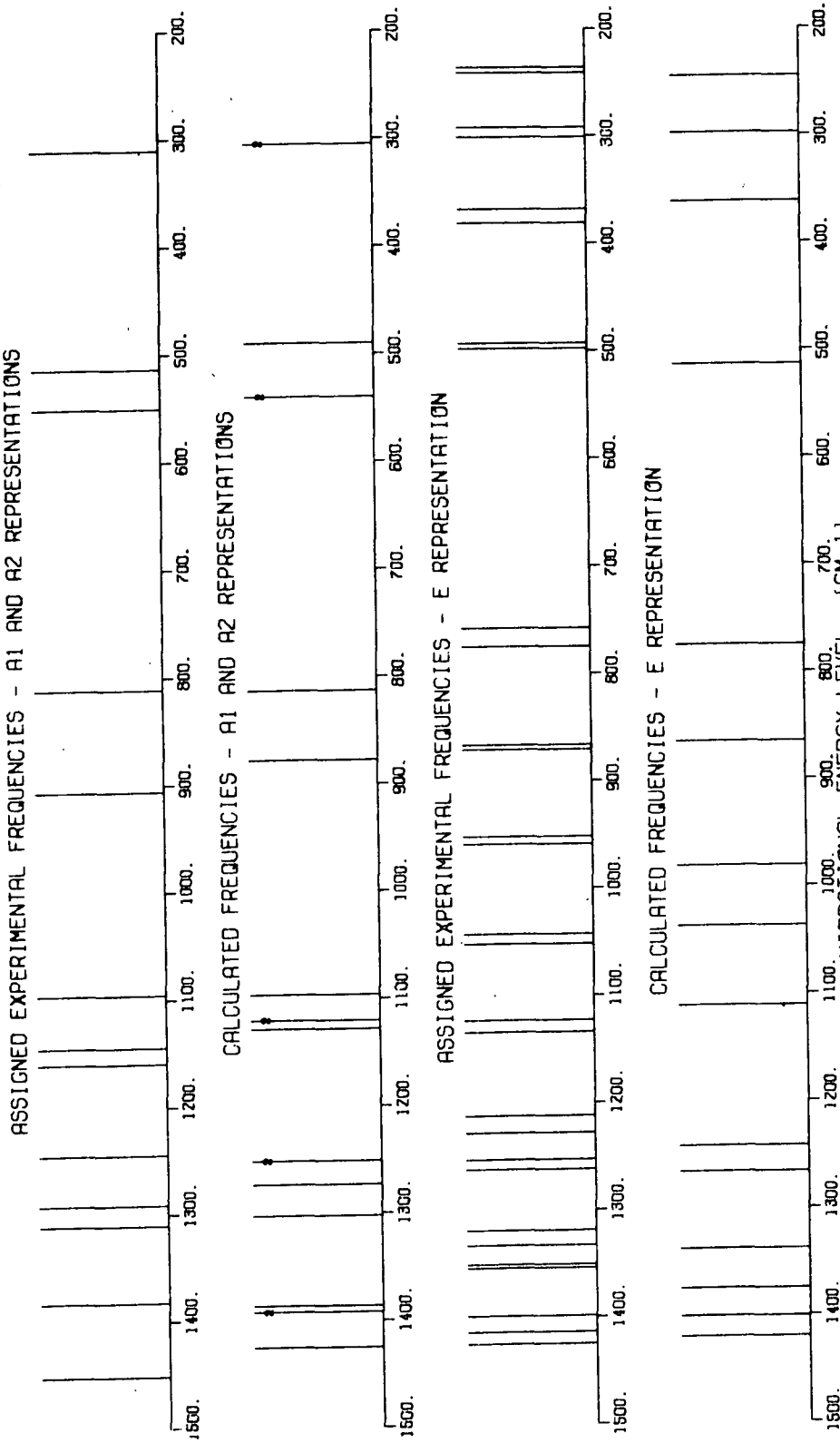

Figure 56. Bar Graph Representation of the Assigned Experimentally Observed Frequencies and Calculated Frequencies for cis-Inositol

one case, two experimental bands observed at different frequencies were assigned to the E symmetry species doubly degenerate modes. For cis-inositol, forty-two bands were assigned with an average error of 13.4 cm^{-1}. This average error is slightly higher than the average errors of the inositols previously discussed. Despite the higher average error, Fig. 56 clearly shows the distribution of assigned experimental frequencies is generally reproduced by the calculated frequencies. The reason for the higher average error is believed to be due in part to the distortion of the cis-inositol structure resulting from interactions between the three axial hydroxyl groups. This aspect and its effect on the symmetry of the molecule and the vibrational selection rules will be discussed later in this section.

The assigned experimental and calculated frequencies for L-chiro-inositol are shown in Fig. 57. The frequencies have been divided into the A and B symmetry species of the C_2 point group to which L-chiro-inositol belongs. Forty-three bands were assigned with an average error of 10.5 cm^{-1}. This average error is more comparable to the average errors of the inositols discussed in Part I.

For muco-inositol, forty-two frequencies were assigned with an average error of 10.4 cm^{-1}. The assigned frequencies for the A' and A'' symmetry species are shown in Fig. 58. The agreement between the assigned frequencies and the calculated frequencies is again seen to be quite good.

It should be noted that both L-chiro-inositol and muco-inositol have axial hydroxyl groups on adjacent carbons. This combination of axial hydroxyl groups does not exist in any of the inositols used in the force constant refinements and therefore the influence of this type of structure on the vibrational frequencies would not be present in the force constants. If the presence of two adjacent axial hydroxyl groups in an inositol structure results in unique coupling of

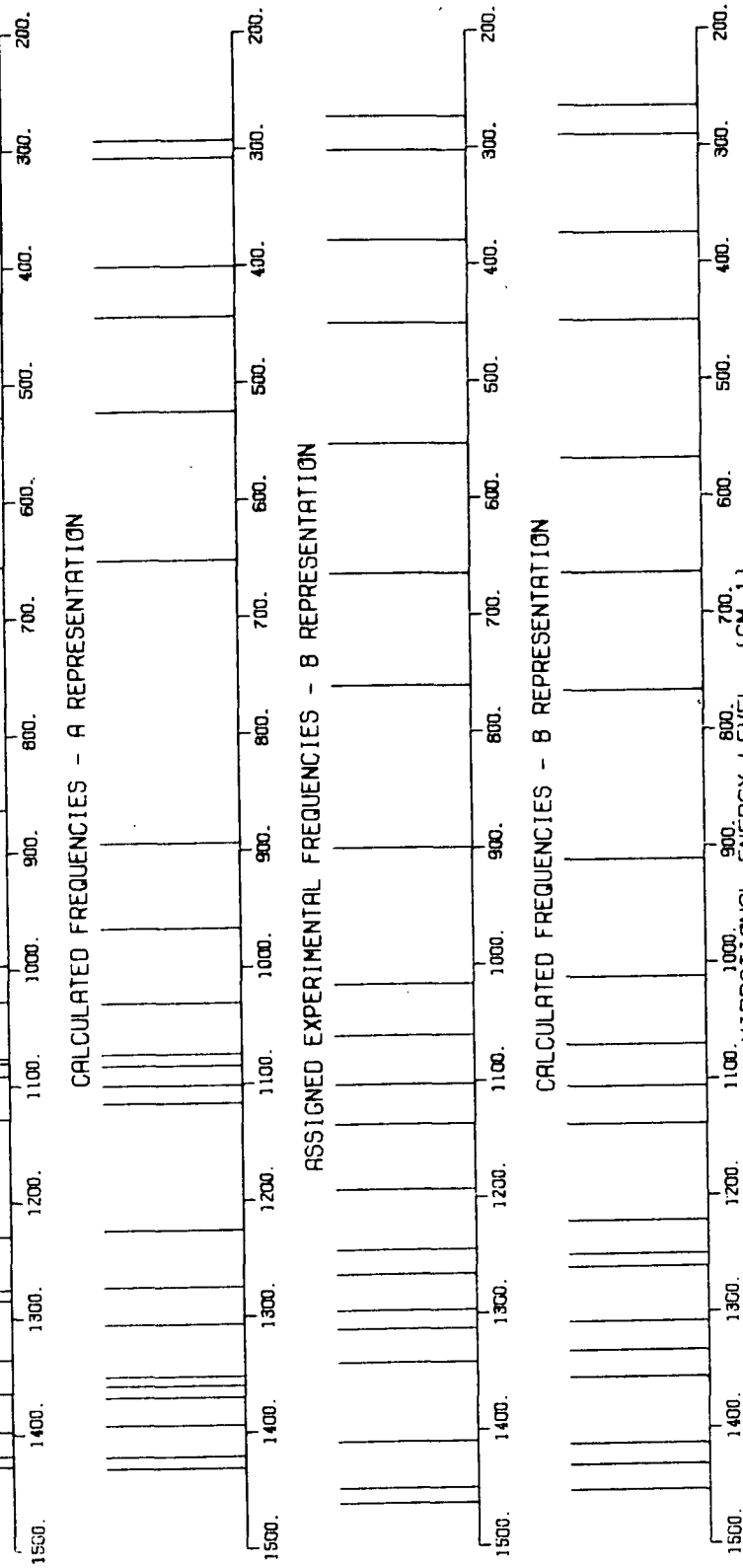

Figure 57. Bar Graph Representation of the Assigned Experimentally Observed Frequencies and Calculated Frequencies for L-chiro-Inositol

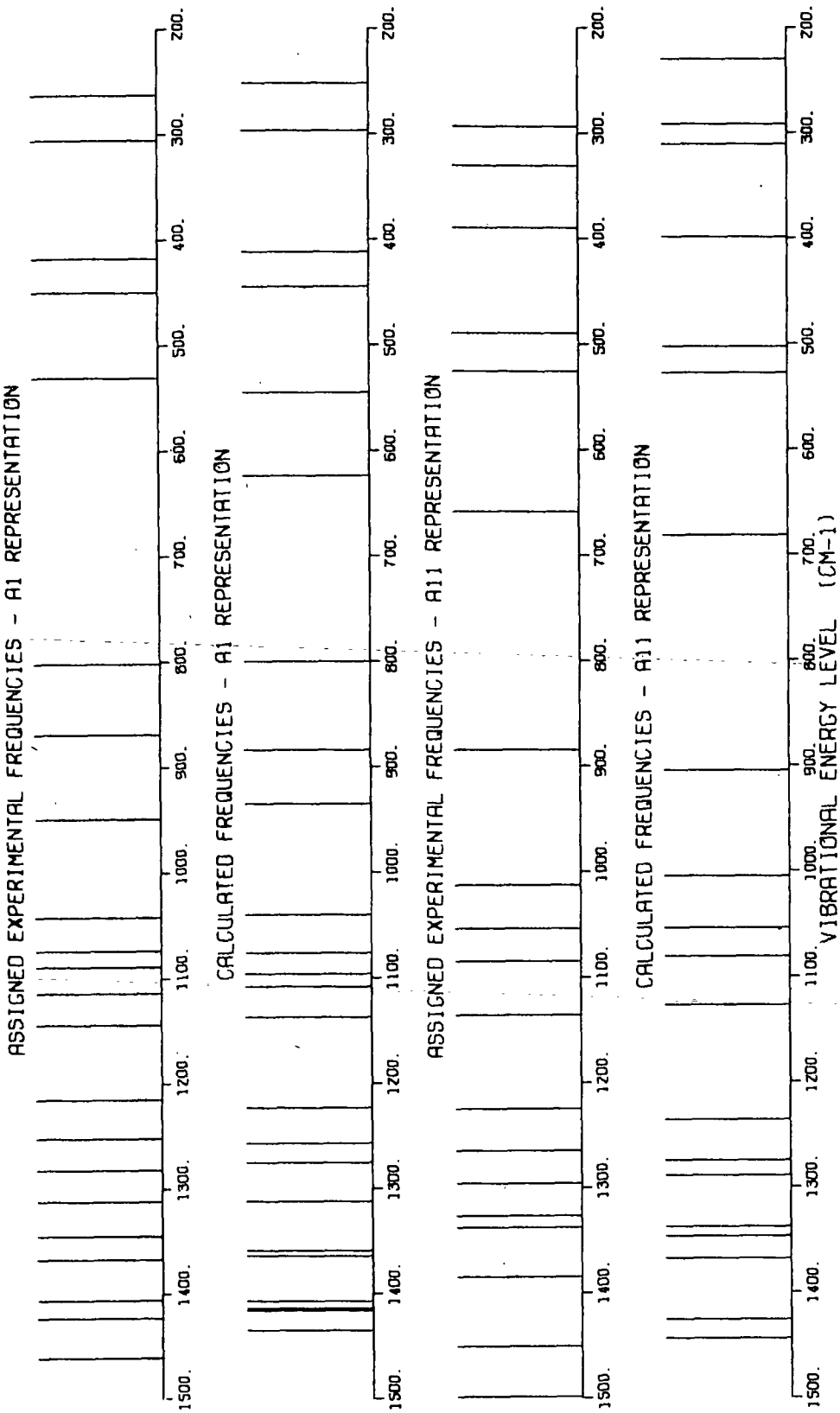

Figure 58. Bar Graph Representation of the Assigned Experimentally Observed Frequencies and Calculated Frequencies for muco-Inositol

deformations, the ability of the force field to predict the vibrational frequencies could potentially be adversely affected. Figures 57 and 58, which show reproduction of the assigned experimental frequencies by the calculated frequencies comparable to the other inositols, suggest that if such an effect is present it is resulting in only minor perturbations of the observed frequencies. Any effect seems to be adequately accounted for by the corresponding terms in the $\underset{\sim}{G}$ matrices.

The same types of information described in making the frequency assignments in Part I, including the molecular symmetry, depolarization ratios and the liquid nitrogen temperature spectra, were also utilized in making the frequency assignments of these inositols.

Figures 56 through 58 illustrate the satisfactory reproduction of the assigned experimental frequencies by the calculated frequencies for cis-inositol, L-chiro-inositol and muco-inositol. This demonstrates the adequate predictive capabilities of the inositol force field and further establishes its validity. For the nine inositols for which frequency assignments were made, including deuterated scyllo-inositol and deuterated neo-inositol, the inositol force field reproduced three-hundred sixty-one frequencies with an overall average error of 10.8 cm^{-1}.

Returning to the case of cis-inositol, the tetrahedral model in Fig. 55 shows the molecule to have axial hydroxyl groups on carbons C2, C4 and C6. Each of the axial hydroxyls is in a 1:3 position on the ring relative to the other two axial hydroxyl groups. In the case of epi-inositol, illustrated in Fig. 46 in Part I, where two axial hydroxyl groups are present in 1:3 relative positions, the resulting 1:3 diaxial interaction was seen to substantially distort the molecule from the tetrahedral structure. Based on this observation, one would expect distortion in the structure of cis-inositol. Examination of the crystal

structure data obtained from Freeman, et al. (65) bears out this expectation. Assuming the same numbering system as shown in Fig. 55, the distances between the axial hydroxyls are: 08-010, 3.1 A; 08-012, 2.9 A; and 010-012, 3.0 A. In the tetrahedral model these distances are all 2.5 A. The 1:3 diaxial interactions result in a substantial increase in the 1:3 diaxial O-O distances. Distortion is also present in the ring where the C-C-C angles centered at C1, C3 and C5 all increase to an average of 113.5° from the tetrahedral angle of 109.5°.

The frequencies calculated using the x-ray crystal structure are compared with those calculated for the tetrahedral model and the assigned experimental frequencies in Fig. 59. The tetrahedral model bands belonging to the doubly degenerate E symmetry species are labelled with an 'E' in Fig. 59. The average error for the x-ray structure frequencies was 13.4 cm^{-1}, the same average error reported for the tetrahedral model. Although the average errors are the same, there are noticeable differences between some of the frequencies calculated using the x-ray crystal structure and the tetrahedral structure. Apparently, the cis-inositol structure is distorted enough to destroy the C_{3v} symmetry. Table XVIII in Part I shows the frequencies belonging to the A_2 symmetry species are inactive in both the Raman and infrared. But several of the frequencies calculated in the A_2 species were assigned to observed frequencies, as shown in Fig. 56. The frequencies calculated in the A_2 species are labelled with a '2' in Fig. 56. The fact that these frequencies are observed would suggest that the C_{3v} symmetry does not occur in the actual structure. The frequencies calculated using the x-ray crystal structure also illustrate that the E mode degeneracies have broken down. The average difference calculated between the frequencies corresponding to the degenerate E modes of the tetrahedral model was 12 cm^{-1}. The average difference between the experimental frequencies assigned to the degenerate E modes was 10 cm^{-1}. In the case of cis-inositol, then, the degree

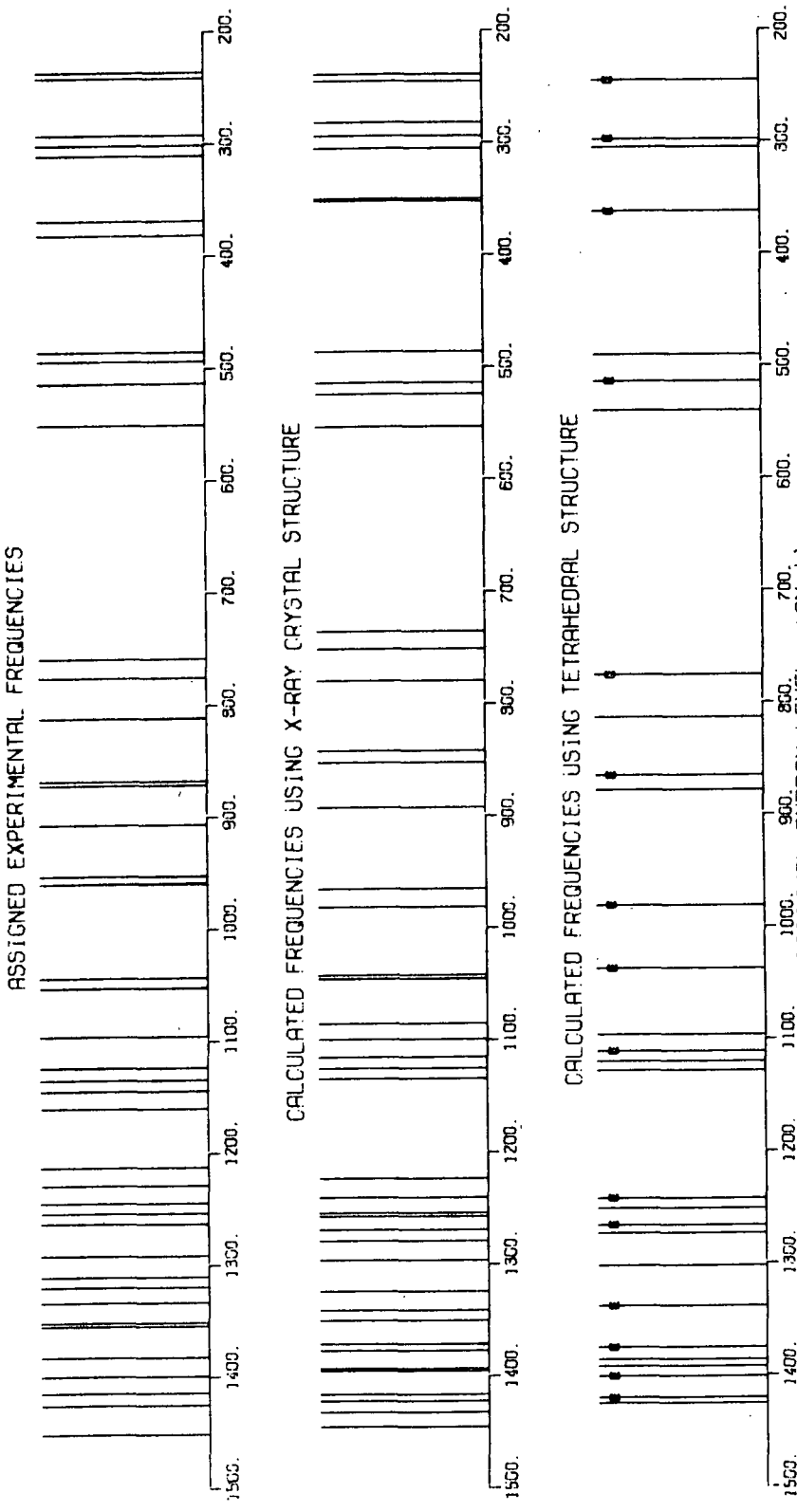

Figure 59. Bar Graph Representation of the Frequencies Calculated Using the X-ray Crystal Structure and the Tetrahedral Structure and the Assigned Experimental Frequencies for cis-Inositol

of distortion from the assumed tetrahedral structure is likely making a more substantial contribution to the average error than was observed in the case of epi-inositol.

INTERPRETATION OF THE EXPERIMENTALLY OBSERVED FREQUENCIES FOR CRYSTALLINE cis-INOSITOL, L-chiro-INOSITOL AND muco-INOSITOL

The interpretation of the experimentally observed frequencies for cis-inositol, L-chiro-inositol and muco-inositol is very similar to the interpretations presented in Part I. The observed frequencies can again be divided into two groups, those which were assigned to calculated frequencies and those which were left unassigned.

The assigned experimentally observed frequencies can be interpreted based on the calculated potential energy distributins. Again, space limitations prohibit an interpretation of each individual band. For a detailed interpretation of any individual frequency or compound, the interested reader is referred to the potential energy distributions for cis-inositol, L-chiro-inositol and muco-inositol which are presented in Tables XLIX through LI, respectively, in Appendix V. The calculated potential energy distributions for cis-inositol, L-chiro-inositol, and muco-inositol closely resemble those discussed in Part I. The same types of motions are predicted to occur in the same regions of the spectra. This is illustrated in Fig. 60, which is a bar graph representation of the potential energy distribution for L-chiro-inositol. Comparison of Fig. 60 with Fig. 29 in Part I for neo-inositol shows similar contributions in the region 1500-200 cm^{-1} of the different internal coordinate groups. The methine hydrogen bending deformations, both in-plane and out-of-plane, and the hydroxyl hydrogen in-plane bending deformations dominate in region II from 1460-1160 cm^{-1}. The C-O and C-C stretches are predominant in region III from 1160-850 cm^{-1} and

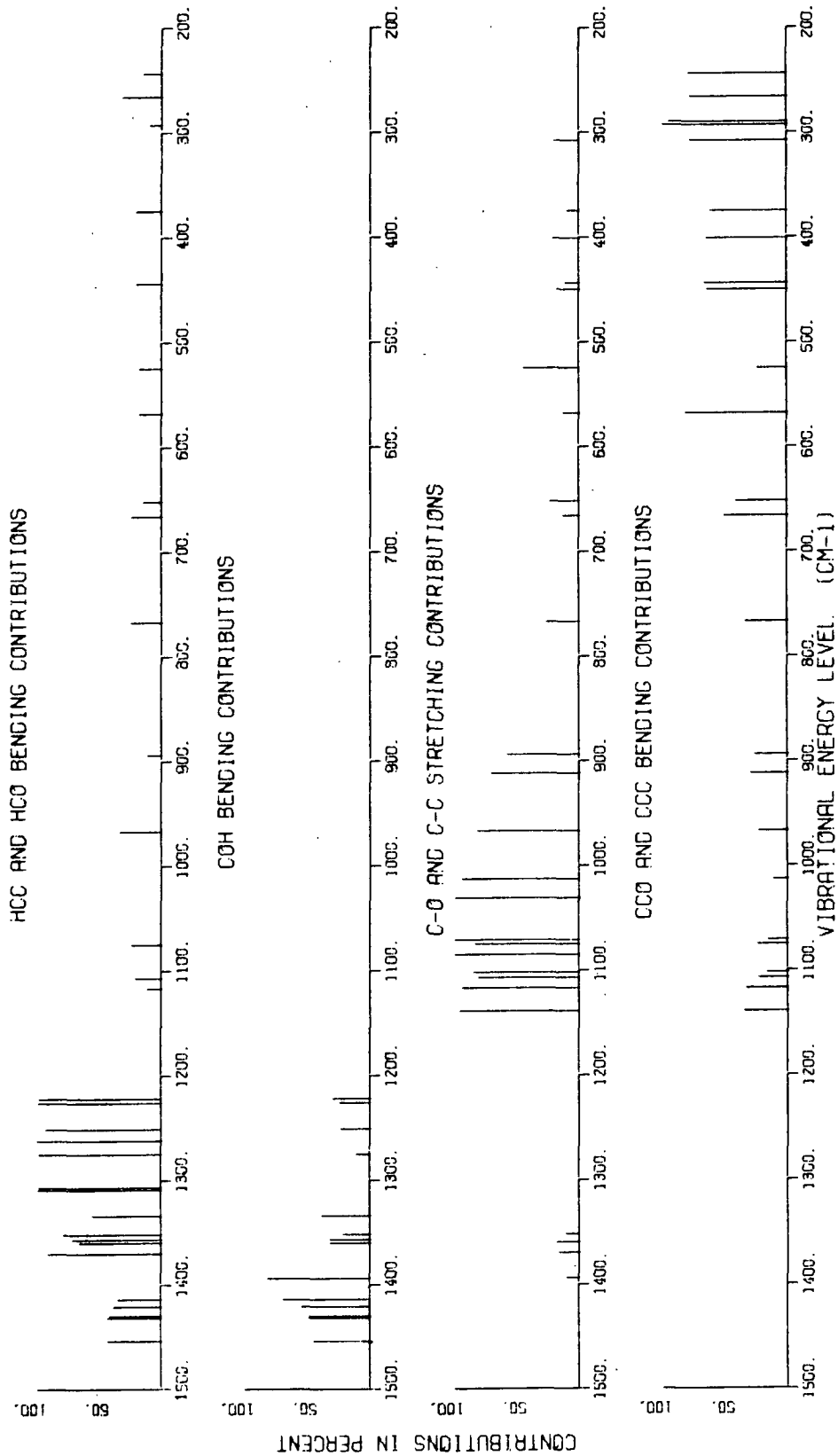

Figure 60. Bar Graph Representation of the Internal Coordinate Potential Energy Distribution for L-chiro-Inositol

the heavy atom bending deformations, the CCO and CCC deformations, dominate in region IV from 850-250 cm^{-1}.

Temperature sensitive bands, which remained unassigned, were identified in the spectra of cis-inositol, L-chiro-inositol and muco-inositol. For cis-inositol, temperature sensitive bands were observed at 644 and 598 cm^{-1}, for L-chiro-inositol at 777, 732, 697, and 600 cm^{-1}, and for muco-inositol at 735, 705, 667, and 600 cm^{-1}. These bands are all observed in the region where temperature sensitive bands were observed in the other inositols. As in the previous cases, these bands can be interpreted as modes involving the motions of the hydrogen bonded hydrogens.

EFFECT OF THE VIBRATIONAL FREQUENCIES OF THE AXIAL-EQUATORIAL ORIENTATIONS OF THE HYDROXYL GROUPS

The spectra of seven of the inositol isomers, including scyllo-inositol, neo-inositol, myo-inositol, epi-inositol, cis-inositol, L-chiro-inositol and muco-inositol, have now been presented and discussed. Among these inositols there is substantial variation in the relative orientations of the hydroxyl groups and in the observed and calculated frequencies of the vibrational modes. This is illustrated in Fig. 61 which shows the frequencies calculated in the region 1000-400 cm^{-1} for the seven inositols. Also shown are the hydroxyl group orientations, E for equatorial and A for axial, at each carbon position as numbered at the top of the figure. Figure 61 was constructed to see if there was any readily discernible pattern between the relative hydroxyl orientations and the frequency positions. The hydroxyl group orientations obviously have a pronounced effect on the vibrational mode frequencies. Since the same force field was used in calculating the frequencies for all the molecules, the differences in the frequency positions are primarily a reflection of the differences in the $\underset{\sim}{G}$ matrices. For example, the differences in the $\underset{\sim}{G}$ matrices between scyllo-inositol and myo-

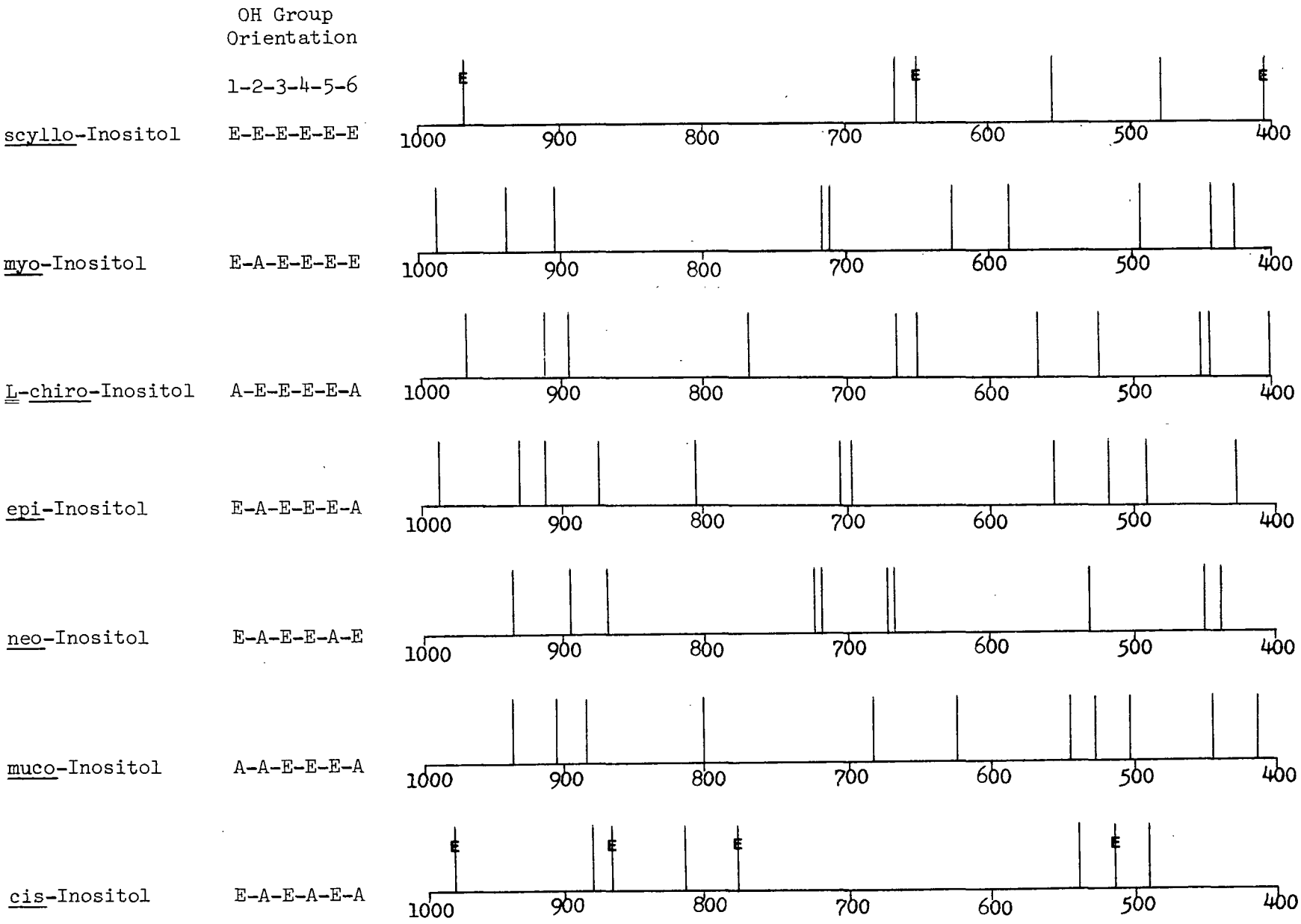

Figure 61. Comparison of the Calculated Frequencies in the 1000-400 cm^{-1} Region for Seven of the Inositol Isomers

inositol primarily involve the internal coordinates defined around carbon 2, where the hydroxyl group is changed from equatorial to axial in myo-inositol.

A close examination of Fig. 61 revealed no discernable pattern between the hydroxyl group orientations, such as number of axial hydroxyl groups and/or relative proximities on the ring, and the frequencies of the vibrational modes. That is, examination of the frequency patterns in Fig. 61 for L-chiro-inositol and epi-inositol, both of which have two axial hydroxyl groups, would not allow prediction of the frequency pattern for neo-inositol, which also has two axial hydroxyl groups but at different relative positions on the ring. The changes in the coupling patterns upon changes in hydroxyl group orientation are too complicated to be predicted without the aid of the normal coordinate calculations.

CONCLUSIONS FROM PART II

The final inositol force field was shown to satisfactorily predict the vibrational frequencies for cis-inositol, L-chiro-inositol and muco-inositol. The calculated potential energy distributions were very similar to the potential energy distributions calculated for the inositols discussed in Part I. Temperature sensitive bands involving the motions of the hydrogen bonded hydroxyl groups were identified in the spectra of all three inositols.

The calculated frequencies in the region 1000-400 cm^{-1} for seven of the inositol isomers were compared and no pattern could be discerned between the vibrational frequencies and the hydroxyl group orientations.

PART III

A RAMAN SPECTRAL INVESTIGATION OF SOME CARBOHYDRATE-GROUP II METAL CATION COMPLEXES IN AQUEOUS SOLUTION

INTRODUCTION

Interest has increased in recent years in the study of metal cation-carbohydrate complexes (66-77). Several of these studies have focused on the complexing abilities of the inositols. In 1961, Mills (66) reported electrophoretic mobilities for several carbohydrates, including cis-inositol and epi-inositol, when in the presence of such cations as Ca^{++}, Sr^{++}, Ba^{++} and Mg^{++}. The mobilities were interpreted as evidence of complexing between the carbohydrates and the cations. Angyal and Davies (69) and Angyal and Hickman (74) studied the ^1H NMR spectra of several inositols in the presence of cations. It was found that the addition of calcium chloride to a D_2O solution of epi-inositol resulted in downfield shifts of the proton signals. From the proton shifts, the largest shift being observed for the hydrogen attached to Cl, it was concluded that the calcium ion was coordinated with three hydroxyl groups, as envisioned in Fig. 62.

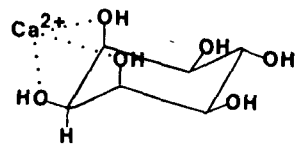

Figure 62. Representation of the epi-Inositol-Calcium Ion Complex

The methine hydrogen attached to Cl is shown in the figure. It was found that cis-inositol and allo-inositol also complexed strongly (69) but myo-inositol exhibited no pronounced proton signal shifts indicating no strong complexing was occurring. The strong complexers, epi-inositol, cis-inositol and allo-inositol, all have in common an axial-equatorial-axial (ax-eq-ax) sequence of hydroxyl groups. Interpretation of the NMR spectrum showed epi-inositol complexes at this

sequence of hydroxyl groups, as shown in Fig. 62. It was suggested (69) that the ax-eq-ax sequence is favorable for complex formation. myo-Inositol and neo-inositol do not possess this hydroxyl group sequence and do not complex strongly. Further investigation (69-72,74,75) substantiated the postulation that an ax-eq-ax sequence of hydroxyl groups is favorable for complex formation. For example, studies with D-allose (70,71) showed the equilibrium between the α-pyranose, α-furanose, β-pyranose and β-furanose forms in solution was altered by the presence of some cations. Complexes were preferentially formed with the α-pyranose and α-furanose forms which contain the ax-eq-ax sequence. This resulted in a shift of the equilibrium to these forms from the β- forms which do not contain this hydroxyl group sequence.

Although the metal ion complexes of several inositols and other carbohydrates have been investigated using primarily NMR and electrophoresis, little work has been reported on the effect of metal ion complex formation on the vibrational spectra of carbohydrates. The purpose of the present investigation was to examine the effect of metal ion complex formation on the Raman solution spectra of some carbohydrates, including some inositols. The impetus behind investigating the metal ion complexes was to further clarify the results of earlier work reported on the effect of metal ion complex formation on the Raman solution spectrum of ethylene glycol (78) and to extend this work to more complicated carbohydrate-metal ion complexes. The complexes investigated in this study were chosen so as to utilize and complement work previously reported in the literature. The desired advantage of studying the metal ion-inositol complexes is that they have been characterized using techniques other than Raman spectroscopy, whereas the ethylene glycol complexes had not been as extensively characterized. To assess the effect of complex stability on the ligand vibrational frequencies, the inositol complexes chosen for study ranged in strength from a relatively strong inositol complex

(epi-inositol-calcium ion complex) to relatively weak complexes (epi-inositol-magnesium ion and myo-inositol-calcium ion complexes). To observe the effect of complex formation which occurs with an attendant change in the geometry of the ligand molecule, the calcium ion complex of another carbohydrate, 1,5-anhydro-ribitol, was investigated. It was hypothesized that the 1,5-anhydroribitol would change conformation to the alternate conformation to form the calcium ion complex because the alternate conformation has the preferential ax-eq-ax sequence for complex formation.

The results of these investigations will be presented and discussed first. The results will then be compared to the results of the ethylene glycol study (78). The major results of the ethylene glycol study will be reproduced in some detail in order to present an overall perspective of the findings on metal ion complexes.

EXPERIMENTAL

The Raman instrument described in Part I was used to record all the solution spectra. The solution spectra were recorded with the solutions in capillary tubes. The capillary tubes were placed in a holder with the scattered radiation viewed at 90° to the incident beam.

RESULTS AND DISCUSSION

epi-Inositol has been shown to complex with calcium ions (66,69,71,74) in the preferred conformation as shown in Fig. 62. Angyal and Hickman (74) reported a stability constant of $K = 2.2 \pm 0.2$ mole^{-1}liter for the epi-inositol-calcium ion complex, which in comparison to the other inositol complexes is relatively strong. The effect of calcium ion complex formation on the Raman solution spectrum of epi-inositol is shown in Fig. 63. Figure 63(A) is the spectrum of a

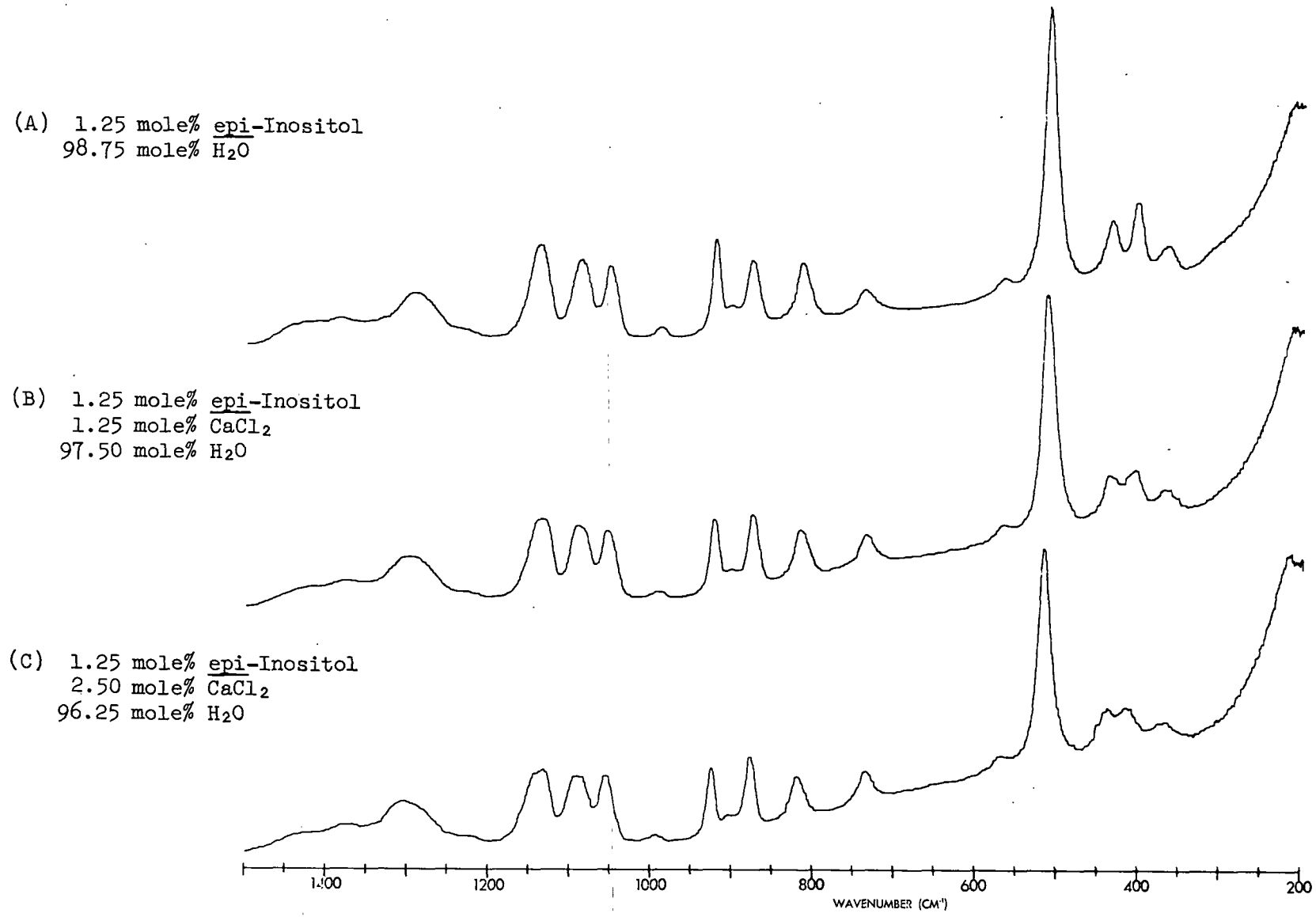

Figure 63. Raman Spectra of the 1500-200 cm^{-1} Region for Three epi-Inositol Solutions

1.25 mole% epi-inositol solution. Figures 63(B) and 63(C) show spectra of the same 1.25 mole% epi-inositol concentration but with 1.25 mole% $CaCl_2$ and 2.50 mole% $CaCl_2$ added, respectively. Figure 63 shows no major changes in the epi-inositol vibrational spectrum are observed upon addition of the calcium chloride and formation of the complex. A change in the relative intensities of the two bands between 850 and 950 cm^{-1} is the most observable change. The epi-inositol and calcium chloride concentrations used are in the same range as those used by Angyal and Hickman (74). They reported NMR signal shifts for 1M calcium chloride and 0.60M cyclitol solutions. This is the equivalent of 1.04 mole% epi-inositol and 1.74 mole% calcium chloride.

Although epi-inositol complexes relatively strongly with calcium ions, the presence of magnesium ions does not alter the NMR spectrum of epi-inositol. This indicates no complex or only a very weak complex is formed. In order to compare a strong epi-inositol complex, with calcium ions, to a very weak epi-inositol complex, with magnesium ions, the Raman solution spectrum of epi-inositol in the presence of magnesium ions was recorded. The spectrum of a 1.25 mole% epi-inositol-2.50 mole% $MgCl_2$ solution is compared to the solution spectrum of epi-inositol in Fig. 64. The figure shows no detectable changes in the spectra are observed, including no changes in the relative intensities of the bands in the region 950-850 cm^{-1} as observed for the calcium ion complex.

myo-Inositol, which does not contain the ax-eq-ax sequence of hydroxyl groups, complexes only weakly with calcium ions (74). The reported stability constant for the myo-inositol-calcium ion complex is $K = 0.2$ $mole^{-1}$ liter (74). Figure 65 compares the Raman solution spectrum of myo-inositol, at 1.30 mole% concentration, with the myo-inositol spectra in the presence of two concentrations of calcium chloride, 1.30 mole% and 2.6 mole%. Again no detectable changes are observed in the myo-inositol spectrum with increasing calcium ion concentration.

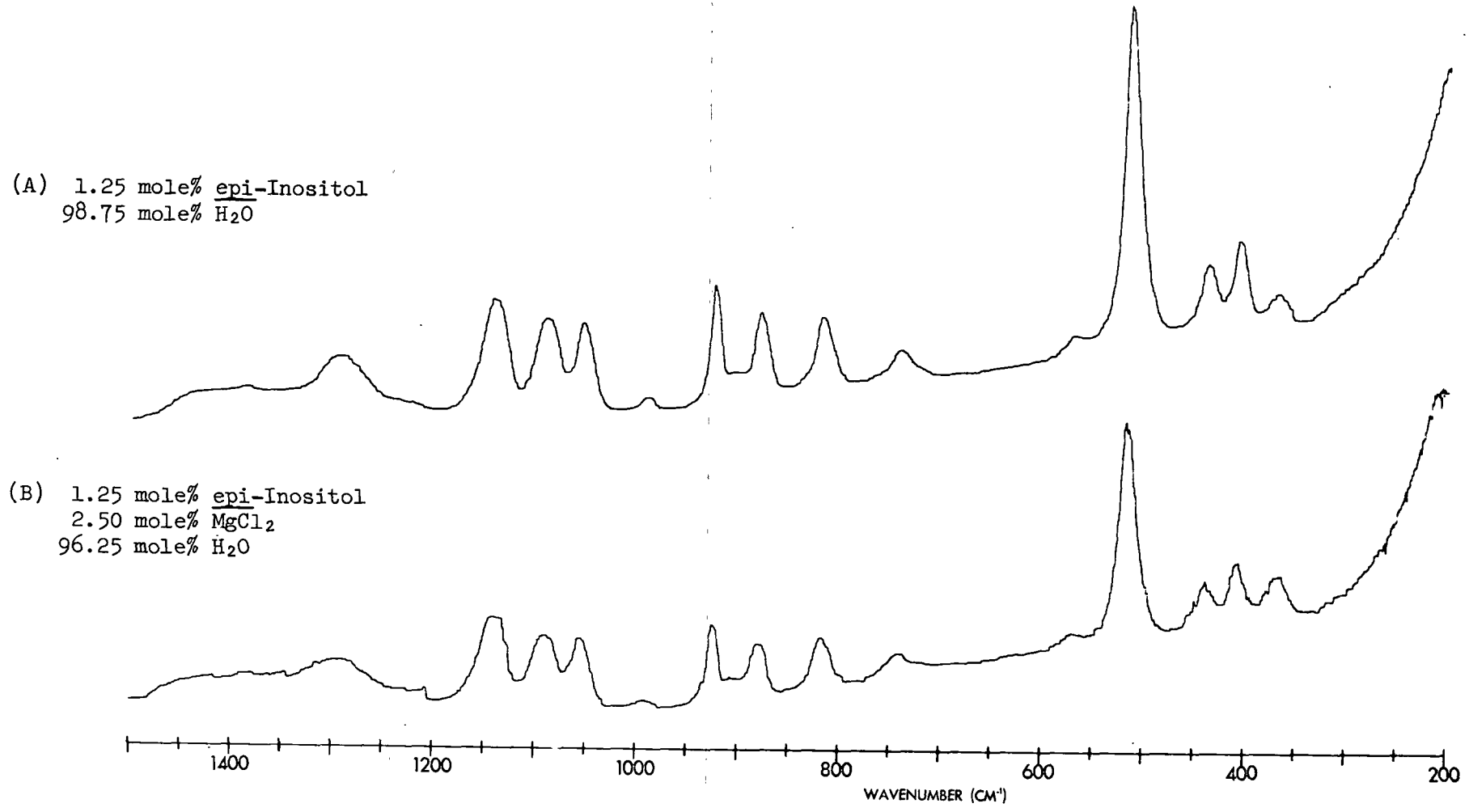

Figure 64. Raman Spectra of the 1500-200 cm^{-1} Region for Two epi-Inositol Solutions

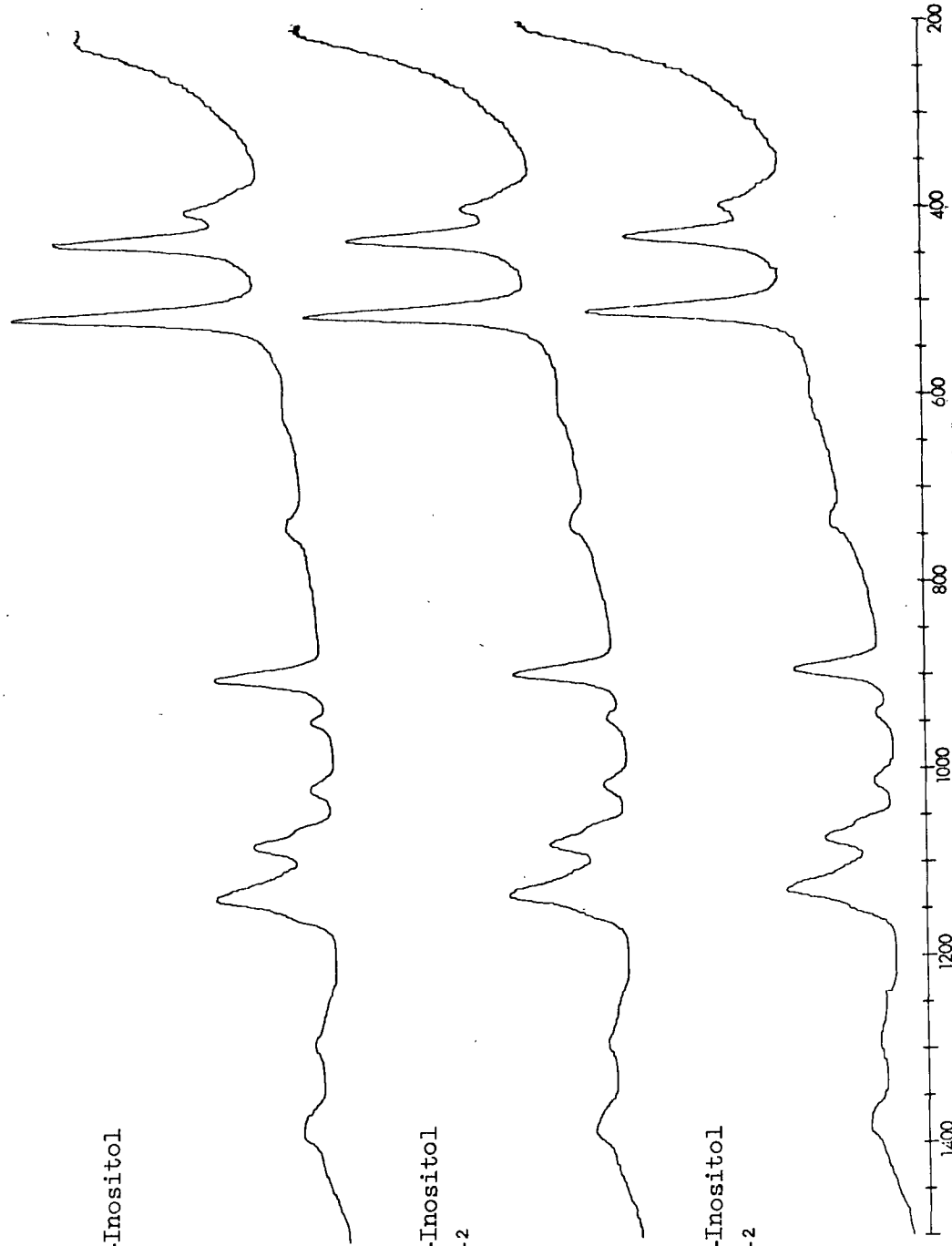

Figure 65. Raman Spectra of the 1500-200 cm^{-1} Region for Three myo-Inositol Solutions

The three complexes just discussed span the range from a relatively strong complex to very weak complexes. For the weak complexes, the epi-inositol-magnesium ion and myo-inositol-calcium ion complexes, the inositol vibrational spectra remained essentially unchanged upon complex formation. For the strong complex, the epi-inositol-calcium ion complex, changes in the inositol spectrum were observed upon complex formation, but they were of a minor nature involving changes in the relative intensities of two bands. The absence of major changes in the inositol spectra, such as sizable shifts of bands or the appearance of new bands, suggests no large change in the inositol structural geometries are occurring upon complex formation. A large change in the inositol geometries would be expected to result in more pronounced changes in the spectra than those observed.

Perturbations of the electronic structure of the inositols almost certainly occurs upon complex formation. The degree of the perturbation would be expected to be dependent on the strength of the complex. The relative band intensity changes observed in the epi-inositol spectrum upon complex formation are likely a manifestation of an electronic perturbation. If complex formation results in a change in the inositol's electron distribution, this will affect the polarizability of certain bonds which could in turn affect the intensity of the bands. A conceivable example would be a change in the electron distribution at the oxygens directly involved in the complex where the cation would tend to withdraw the oxygen electrons. This would result in a change in the polarizability of the C-O bond and could consequently alter the intensity of the C-O stretching band.

To further explore the expectation that a major change in the ligand geometry upon complex formation would result in substantial changes in the ligand vibrational spectrum, a molecule was sought which would change conformation to form a metal ion complex. Such a case was provided by 1,5-anhydroribitol, the structure of which is shown in Fig. 66. In the preferred conformation,

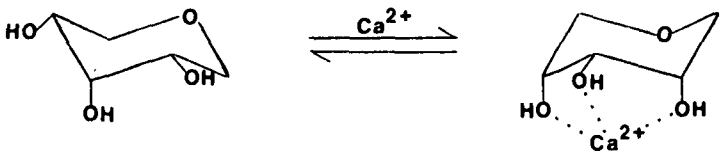

1,5-Anhydroribitol

1,5-Anhydroribitol-Calcium Ion Complex

Figure 66. Representation of the 1,5-Anhydroribitol Chair Inversion to Form the 1,5-Anhydroribitol-Calcium Ion Complex

1,5-anhydroribitol has an eq-ax-eq sequence of hydroxyl groups. But in the alternate conformation 1,5-anhydroribitol has an ax-eq-ax sequence of hydroxyl groups, the hydroxyl group sequence Angyal found to be preferential for complex formation. Pitzner (18) calculated that approximately 26% of the 1,5-anhydroribitol molecules would be in the alternate conformation at equilibrium in solution. If the alternate conformation ax-eq-ax sequence of hydroxyl groups is preferential for complex formation, then addition of calcium chloride to a 1,5-anhydroribitol solution should shift the equilibrium toward the alternate conformation as the complex is formed. The change in conformation of the 1,5-anhydroribitol with complex formation is envisioned in Fig. 66. Figure 67(A) shows the vibrational spectrum of crystalline 1,5-anhydroribitol, which is in the preferred conformation. Figure 67(B) shows the Raman spectrum of a 2.0 mole% 1,5-anhydroribitol solution. Comparison of Fig. 67(B) with Fig. 67(A) shows that several new bands appear in the solution spectrum. New bands are labelled at 695, 800, 840, and 1296 cm^{-1} in Fig. 67(B). These new bands can be associated with the presence of the 1,5-anhydroribitol alternate conformer in the solution. Frequency calculations performed by Pitzner (18) on the alternate conformation of 1,5-anhydroribitol support the contention that the new bands do arise from the alternate conformer. Figure 67(C) shows the Raman solution spectrum of a 2.0 mole% 1,5-anhydroribitol solution containing 4.0 mole% calcium chloride. Comparison of Fig. 67(C) with Fig. 67(B) clearly shows that the new bands associated with the

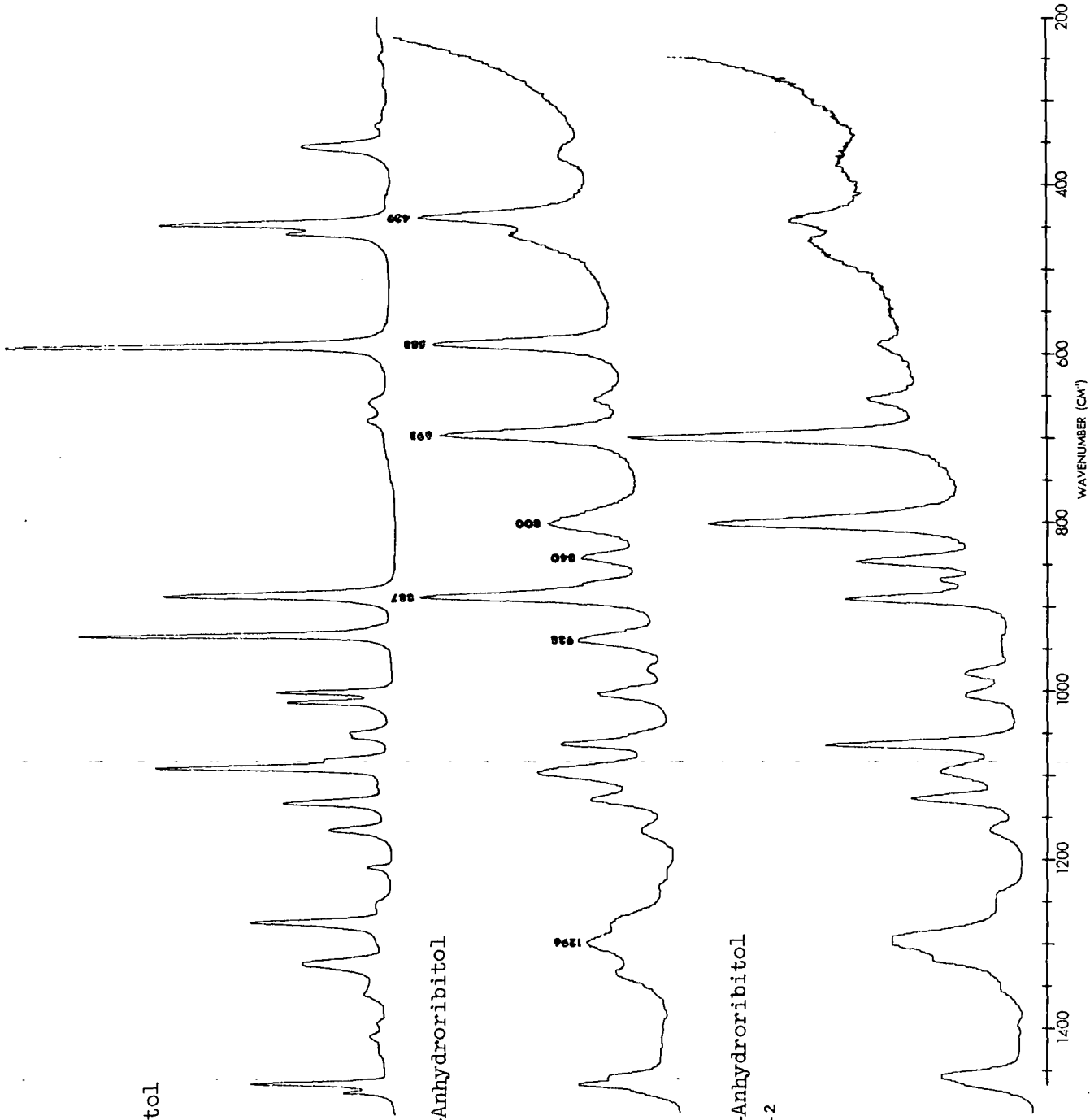

Figure 67. Raman Spectra of the 1500-200 cm^{-1} Region for (A) Crystalline 1,5-Anhydroribitol and Two (B) and (C) 1,5-Anhydroribitol Solutions

alternate conformer at 695, 800, 840, and 1296 cm^{-1} have all substantially increased in relative intensity. In comparison, the bands arising from the preferred conformer, such as the bands labelled at 439, 588, 887, and 938 cm^{-1}, all diminish in relative intensity in Fig. 67(C). The addition of calcium chloride has shifted the equilibrium toward formation of the alternate conformation.

Several pieces of information can be gained from this experiment. First, the shifting of the equilibrium to the alternate conformer in order to form the calcium ion complex provides Raman spectral evidence in support of the evidence put forth by Angyal that the ax-eq-ax hydroxyl sequence is a preferential sequence for complexing with metal ions. Second, a large change in the ligand molecular geometry, such as the change in the conformation of the 1,5-anhydroribitol, results in pronounced changes in the ligand vibrational frequencies. This is illustrated by the observance of several new bands in the solution spectrum arising from the vibrations of the alternate conformer. Third, the bands at 695, 800, 840, and 1296 cm^{-1} arising from the calcium ion complexed alternate conformer in Fig. 67(C) are not significantly perturbed from the frequencies of the uncomplexed alternate bands labelled in Fig. 67(B). The formation of the 1,5-anhydroribitol-calcium ion complex did not significantly perturb the vibrational frequencies of the 1,5-anhydroribitol alternate conformer, strongly suggesting that the observed changes are not the result of complex formation. The observed changes can be accounted for, to a good approximation, by the change in the 1,5-anhydroribitol structural geometry. This third result is essentially the same as observed for the epi-inositol and myo-inositol complexes. In these cases, where no major change in ligand geometry accompanied complex formation, complex formation also resulted in only minor perturbations in the vibrational frequencies.

The results found for the inositol and 1,5-anhydroribitol complexes closely parallel the results reported by Williams and Atalla (78) for several metal ion complexes of the carbohydrate model compound ethylene glycol. In that study, the Raman spectra of aqueous solutions of ethylene glycol in the presence of several Group II cations, including Ca^{++}, Ba^{++}, Cd^{++}, Zn^{++}, Mg^{++} and Sr^{++} ions, were examined. Inspection of the spectra showed that the cations could be classified into two groups according to the extent to which they altered the vibrational spectrum of ethylene glycol. The presence of magnesium, barium or cadmium ions, added as the chlorides, produced only minor changes in the 1000-1100 cm^{-1} region, but almost no change in other regions of the ethylene glycol Raman solution spectrum. An example of this group is illustrated in Fig. 68 which shows the Raman spectra of a 5.0 mole% ethylene glycol solution and a 5.0 mole% ethylene glycol-6.7 mole% $MgCl_2$ solution. Only minor changes are seen to occur. In contrast, the addition of calcium, zinc or strontium chloride was found to cause extensive changes throughout the 1300-800 cm^{-1} region. The characteristic changes observed are illustrated in Fig. 69. The addition of 5.0 mole% calcium chloride resulted in a substantial shift of the strong band at 866 cm^{-1} in the ethylene glycol spectrum, shown in Fig. 69(A), to 887 cm^{-1} as shown in Fig. 69(B). Normal coordinate calculations performed by Matsuura and Miyazawa (79) and Williams and Atalla (78) showed the intense highly polarized band at 866 cm^{-1} could be attributed to primarily the C-C stretching motion. After addition of 10.0 mole% calcium chloride, Fig. 69(C), the 887 cm^{-1} band is decidedly the dominant band. In the region 1200-1300 cm^{-1}, as the calcium chloride concentration was increased the band at 1274 cm^{-1} in the ethylene glycol solution spectrum decreased in relative intensity while a new band at 1241 cm^{-1} increased in relative intensity. These bands are labelled in Fig. 69. Band shifts were also noted in the 1000-1100 cm^{-1} region.

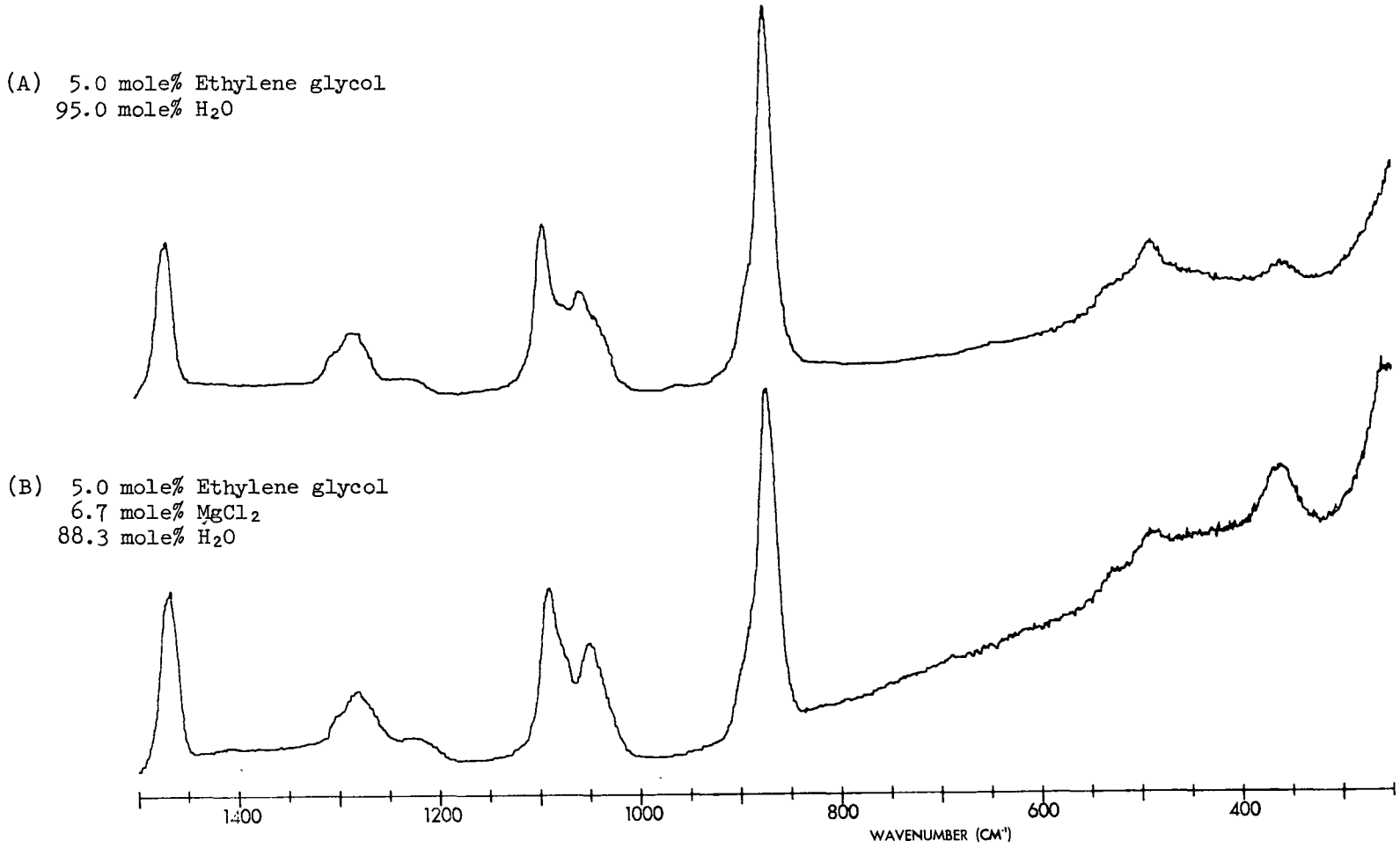

Figure 68. Raman Spectra of the 1500-250 cm^{-1} Region for Two Ethylene Glycol Solutions

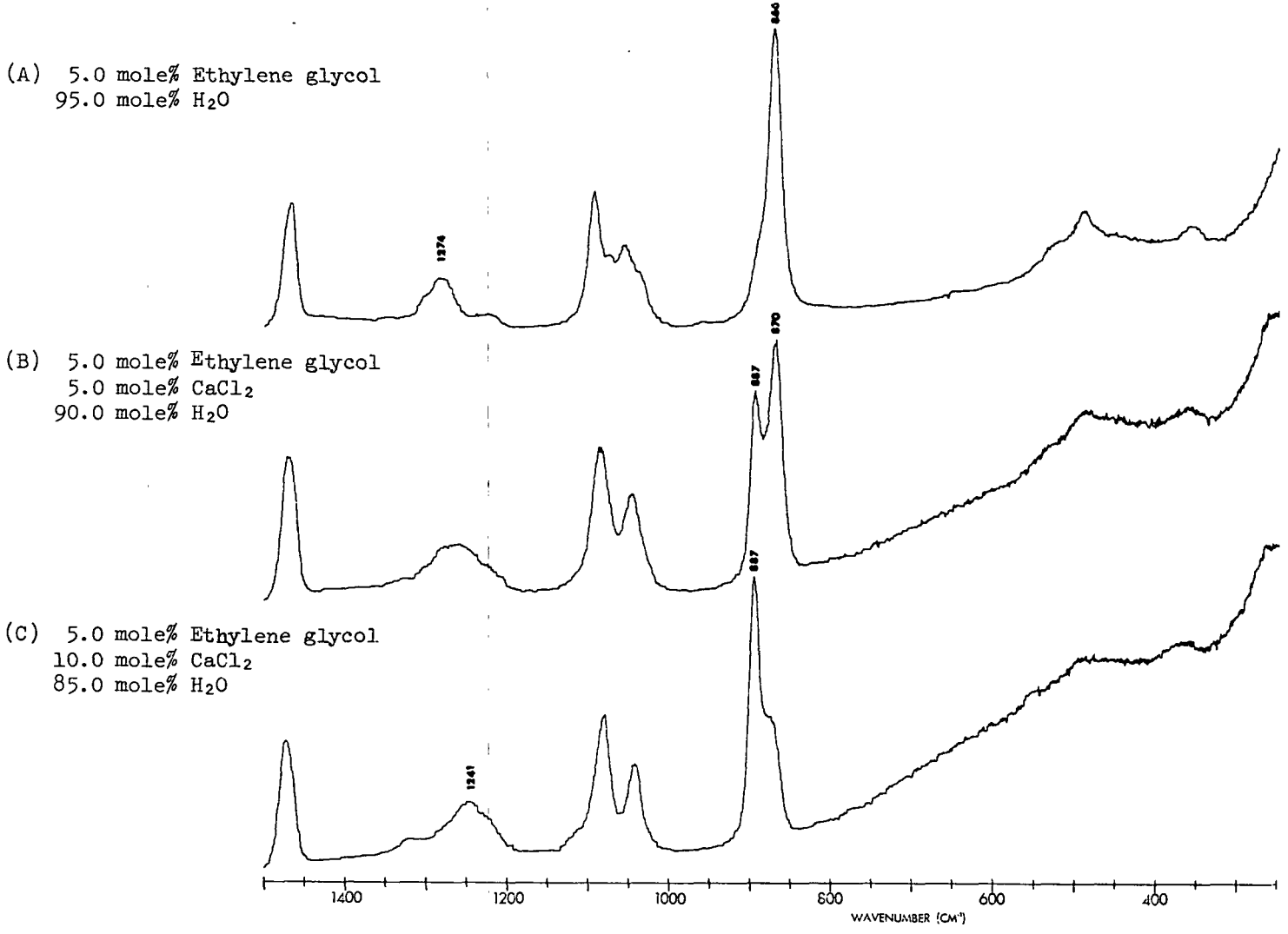

Figure 69. Raman Spectra of the 1500-250 cm^{-1} Region for Three Ethylene Glycol Solutions

The relative changes produced in the vibrational spectrum of ethylene glycol by the two groups of cations suggested two different types of interactions with the ethylene glycol were being observed. The relatively minor changes produced by the presence of magnesium, barium or cadmium ions were interpreted as corresponding to monodentate coordination of the metal ions with the ethylene glycol hydroxyl groups. This interpretation was supported by additional experiments with methanol and ethanol solutions, at 5.0 mole% concentration, containing varying amounts of calcium chloride. In these cases, where monodentate coordination is the only mode of interaction possible, only minor changes in the region 1000-1100 cm^{-1} were observed, which was the same type of change observed in the ethylene glycol spectrum.

The more pronounced changes in the ethylene glycol spectrum produced by the presence of calcium, zinc or strontium ions were interpreted as resulting from bidentate coordination of the metal ions accompanied by conversion of the ethylene glycol molecules from the trans-conformation (i.e., anti-conformation) to the gauche-conformation in order to form the complex. The validity of this interpretation was also subjected to further experimental exploration.

cis- and trans-Cyclohexane-1,2-diols have the same capacity to form bidentate complexes as ethylene glycol, but without the possibility of conformational change. It was postulated that any electronic effects resulting from complex formation which could significantly perturb the vibrational frequencies would occur in the cases of the cyclohexanediols. The Raman solution spectra of the two cyclohexanediols with and without added calcium chloride were recorded. For cis-cyclohexanediol virtually no change in the solution spectrum was observed after addition of calcium chloride. For trans-cyclohexanediol some changes in relative band intensities in the regions 1400-1325 and 1150-1100 cm^{-1} were observed after addition of calcium chloride. This suggests an electronic

perturbation is occurring and its effect observed in the spectrum as it was in the case of the epi-inositol-calcium ion complex and for methanol and ethanol in the presence of calcium ions. Based on these results, it was concluded that the electronic perturbation resulting from bidentate coordination of the calcium ions could not by itself account for the major changes observed in the ethylene glycol spectrum in the presence of calcium ions.

The solution spectrum and calcium ion complex spectrum of ethylenediamine were also examined. As with ethylene glycol, it was postulated that ethylenediamine also has the capability for bidentate coordination and a conformational change. Furthermore, ethylenediamine is known to complex in the gauche-conformation (80). "The similarities between the geometries of ethylene glycol and ethylenediamine suggest that if the major changes in the spectrum of ethylene glycol upon bidentate coordination are indeed due to conformational changes, then similar changes should be detectable in the Raman spectrum of ethylenediamine upon bidentate coordination of metal ions (78)." Figure 70, as taken from Williams and Atalla (78), shows the Raman spectra of a 5.0 mole% ethylenediamine solution and a 5.0 mole% ethylenediamine-5.0 mole% calcium chloride solution. Some of the calcium chloride complex precipitated out of the latter solution but enough remained in solution to obtain a spectrum. Figure 70 illustrates that significant changes occurred in the spectrum of ethylenediamine upon addition of calcium chloride. The strong C-C stretch band at 845 cm^{-1} in the ethylenediamine spectrum shifts up to 873 cm^{-1} upon complex formation. The degree of observed change in the ethylenediamine spectrum and the shifting pattern of the C-C stretch band at 845 cm^{-1} closely parallels the behavior exhibited by ethylene glycol in the presence of calcium ions. But in the case of ethylenediamine, the pronounced spectral changes can be more definitely associated with a conformation change from the trans to the gauche-conformation to form the calcium ion complex,

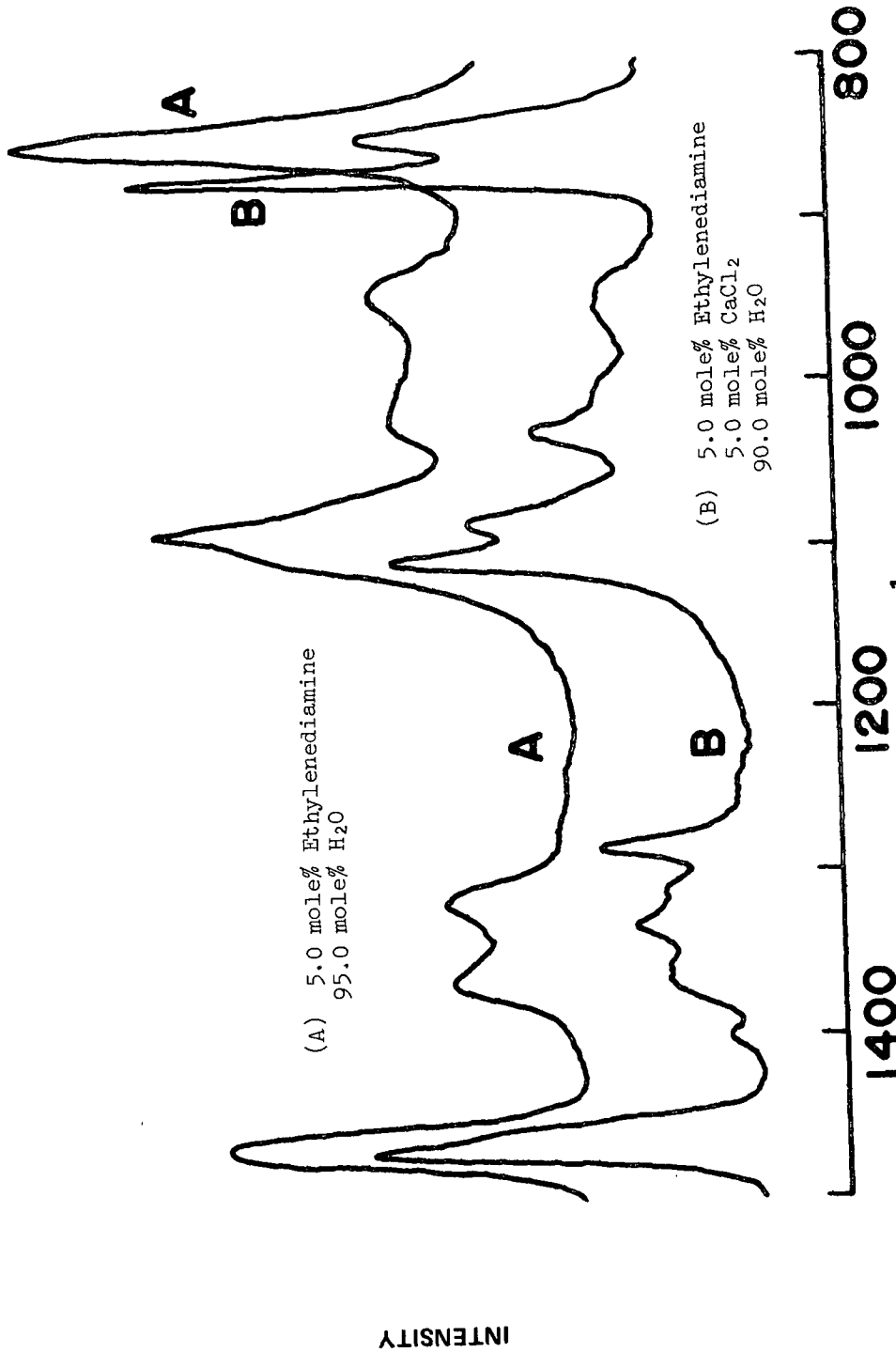

Figure 70. Raman Spectra of the 1500-800 cm^{-1} Region for Two Ethylenediamine Solutions (78)

same observed behavior by ethylene glycol supports the interpretation of a change in the ethylene glycol conformation from the trans to the gauche to form a complex with calcium, zinc or strontium ions.

In comparing the ethylene glycol study results with the inositol and 1,5-anhydroribitol results, two common trends stand out. First, in the cases where complex formation occurred without a corresponding change in the geometry of the ligand molecule, the observed changes in the ligand vibrational frequencies were of a relatively minor nature, being confined to changes in relative band intensities and some band shifts on the order of 10 cm^{-1} or less. This degree of spectral change was observed in the complexes between the metal ions and epi-inositol, myo-inositol, cis- and trans-cyclohexanediols, methanol, ethanol and for ethylene glycol in the presence of magnesium, barium and cadmium ions. The observation of spectral changes upon addition of the metal salts, such as the changes in relative band intensities in the spectra of the epi-inositol-calcium ion and trans-cyclohexanediol-calcium ion complexes, is evidence that a perturbation of the electron distribution around the ligand is occurring. The degree of electronic perturbation seems dependent on the strength of the complex. For example, changes in relative band intensities were observed in the epi-inositol-calcium ion complex spectrum, which is a relatively strong complex, but no detectable changes were observed in the spectra of the epi-inositol-magnesium ion or the myo-inositol-calcium ion complexes, which are weak complexes.

Second, in the cases where complex formation was accompanied by a considerable change in the geometry of the ligand molecule, such as a change in conformation, the resulting changes in the ligand vibrational spectrum were much more extensive than those just discussed. The characteristic changes, which affected a majority of the bands in the spectra, included band shifts up to 28 cm^{-1}, changes in relative band intensities and the appearance of new bands. Such

changes were observed in the cases of 1,5-anhydroribitol, ethylene glycol in the presence of calcium, zinc and strontium ions and ethylenediamine. Furthermore, the changes observed in the case of the 1,5-anhydroribitol-calcium ion complex were shown to result almost solely from the change in conformation and not from electronic perturbations induced by complex formation.

In summary, the observed spectral changes in the ligand vibrational frequencies upon metal ion complex formation can be attributed to two individual effects: 1) perturbation of the ligand electron distribution as a result of complex formation, which results in relatively minor spectral changes, and 2) changes in the ligand structural geometry which results in more pronounced spectral changes than the former. It is felt that, in general, these results are characteristic of carbohydrate-metal ion complexes which fall in the range of complex stability investigated in this study. But this is not to imply that this brief investigation is complete in its scope. On the contrary, there is ample opportunity for further work in the investigation of carbohydrate-metal ion complexes using vibrational spectroscopy.

PART IV

A RAMAN SPECTRAL INVESTIGATION OF SOME AQUEOUS INOSITOL SOLUTIONS CONTAINING BORATE ANIONS

INTRODUCTION

A second kind of carbohydrate complex which has received considerable attention are carbohydrate-borate complexes. In aqueous solution the reacting species is the borate anion which has the structure $B(OH)^-_4$. As with the metal ion complexes, the inositols have been the subjects of several studies on borate complexes (81-87).

In 1957, Angyal and McHugh (81) reported the paper ionophoretic mobilities for several cyclitols in sodium tetraborate solutions. Two inositols, cis-inositol and epi-inositol, showed substantially higher mobilities than the other inositols studied, which included: scyllo-inositol, D-chiro-inositol, neo-inositol, myo-inositol, muco-inositol and allo-inositol. cis-Inositol and the alternate chair form of epi-inositol both have three axial hydroxyl groups in 1:3:5 relative positions on the ring. Angyal and McHugh (81) postulated that the borate ions were forming a tridentate complex with the three syn-axial hydroxyl groups of cis-inositol and epi-inositol. For cis-inositol, the proposed complex is shown in Fig. 71(A) and for epi-inositol the chair inversion and subsequent complex formation is shown in Fig. 71(B). Garegg and Lindstrom (84) examined the NMR spectra of epi-inositol in D_2O and in D_2O containing borate ions and found the subsequent changes consistent with inversion to the alternate conformation to form the tridentate complex. This was confirmed by Angyal, et al. (72). To further study the relation between borate complex stability constants and substituent group interaction energies, Angyal, et al. (86) investigated the NMR spectra of several inositol derivatives in borate solutions. In 1958, Weissbach (82) isolated and characterized the scyllo-inositol-diborate complex. In the

alternate conformation, scyllo-inositol has six axial hydroxyl groups in 1:3:5 relative positions on each side of the ring and thus is capable of forming a diborate complex. Inversion of the scyllo-inositol ring to form the diborate complex was also confirmed by Posternak, et al. (83) using NMR analysis. Gorin and Mazurek (85) investigated the ^{13}C NMR spectra of several polyhydroxy compounds, including several inositols, in borate solutions. Their results for the inositols further confirmed what had been previously found.

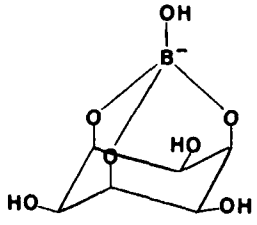

(A) cis-Inositol Borate

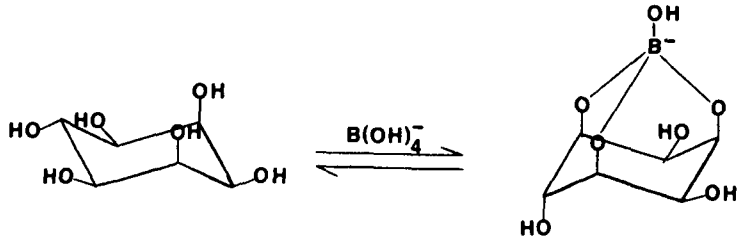

(B) epi-Inositol epi-Inositol Borate

Figure 71. Representations of (A) cis-Inositol Borate and (B) the epi-Inositol Chair Inversion to Form the epi-Inositol Borate

These investigations suggest that the term 'borate complex' is a misnomer in the case of the inositols. The inositol borates are not complexes in the usual sense of the term but are actually anionic esters formed from a condensation reaction between the borate ions and the inositols. For the purposes of this investigation, then, the term 'borate complex' will not be employed so as not to further perpetuate the use of this inaccurate term. The term 'inositol borate' will instead be used.

As was the situation with the metal ion complexes, although the borates of several inositols have been rather extensively investigated, no known work has been published on the effect of borate formation on the inositols vibrational spectra. The purpose of this exploratory investigation was to examine the effect of borate formation on the Raman solution spectra of several inositols. It was suspected that the inositol bands could be significantly perturbed as a result of borate formation. This is because reaction to form the borates results in the addition of the borate moiety to the inositols through the formation of new bonds.

The spectra of six inositols in the presence of borate ions were investigated. cis-Inositol was examined because it is unique in that the borate forms with no major change in the cis-inositol geometry. epi-Inositol, myo-inositol and scyllo-inositol were investigated because they can form the tridentate borate in their alternate conformations. Third, muco-inositol and L-chiro-inositol were investigated because they do not have the axial hydroxyl sequence necessary for tridentate borate formation. The results for these six inositols will be discussed in the order in which they were just described.

EXPERIMENTAL

The Raman instrument described in Part I was used to record all the solution spectra. The solution spectra were recorded with the solutions in capillary tubes. The capillary tubes were placed in a holder with the scattered radiation viewed at 90° to the incident beam.

The borate ions were generated in the solutions by addition of sodium tetraborate ($Na_2B_4O_7$). From a known concentration sodium tetraborate solution, the approximate 'available borate ion' concentration can be calculated from the equation (85):

$$Na_2B_4O_7\ 7\ H_2O \rightleftharpoons 2\ Na^+ + 2\ B(OH)^-_4 + 2\ H_3BO_3$$

Thus each mole of sodium tetraborate yields two moles of available borate ion $[B(OH)_4]$ for complexing.

RESULTS AND DISCUSSION

cis-Inositol, as shown in Fig. 71(A), readily forms a tridentate borate, $K = 1.1 \times 10^6$ mole^{-1}liter (87), because it has axial hydroxyl groups in 1:3:5 relative positions on the ring. Importantly, the borate is formed with no major change in the cis-inositol geometry (72) thus allowing the effect of just borate formation to be assessed. The effect of borate formation on the vibrational spectrum of cis-inositol is shown in Fig. 72. Figure 72(A) is a cis-inositol solution spectrum and Fig. 72(B) a cis-inositol solution containing added sodium tetraborate. The exact concentrations were not determined, however, the degree of borate formation is fairly complete as further addition of sodium tetraborate produced no additional changes in the spectrum. Comparison of the two spectra shows definite effects resulting from the addition of sodium tetraborate. The band at 817 cm^{-1} in the cis-inositol spectrum disappears and four new bands at 884, 718, 619 and 568 cm^{-1} in the borate spectrum are observed. Less pronounced shifts in many of the other bands are also noted. These observed changes could arise from several sources, including perturbed cis-inositol or borate ion bands resulting from formation of the borate or from the free borate ions in the solution.

To further characterize the changes observed in the borate spectrum, the Raman solution spectrum of sodium tetraborate was recorded at two concentrations as shown in Fig. 73. Figure 73(A) is the spectrum of a saturated sodium tetraborate solution and Fig. 73(B) the spectrum of a 0.7 mole% sodium tetraborate solution. The latter solution approximates the sodium tetraborate concentration used in several inositol solutions to be presented shortly. In addition, the

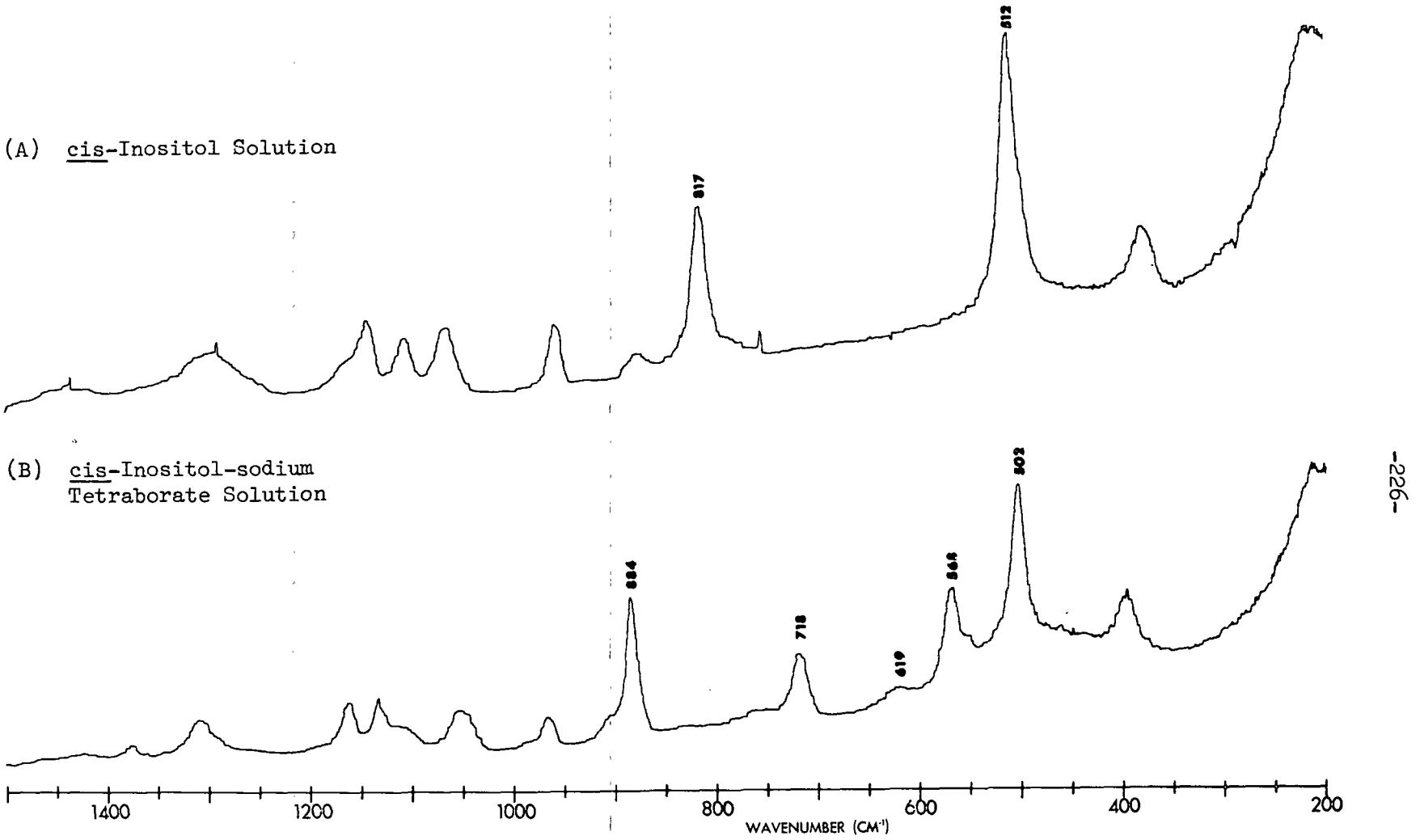

Figure 72. Raman Spectra of the 1500-200 cm^{-1} Region for the Two cis-Inositol Solutions

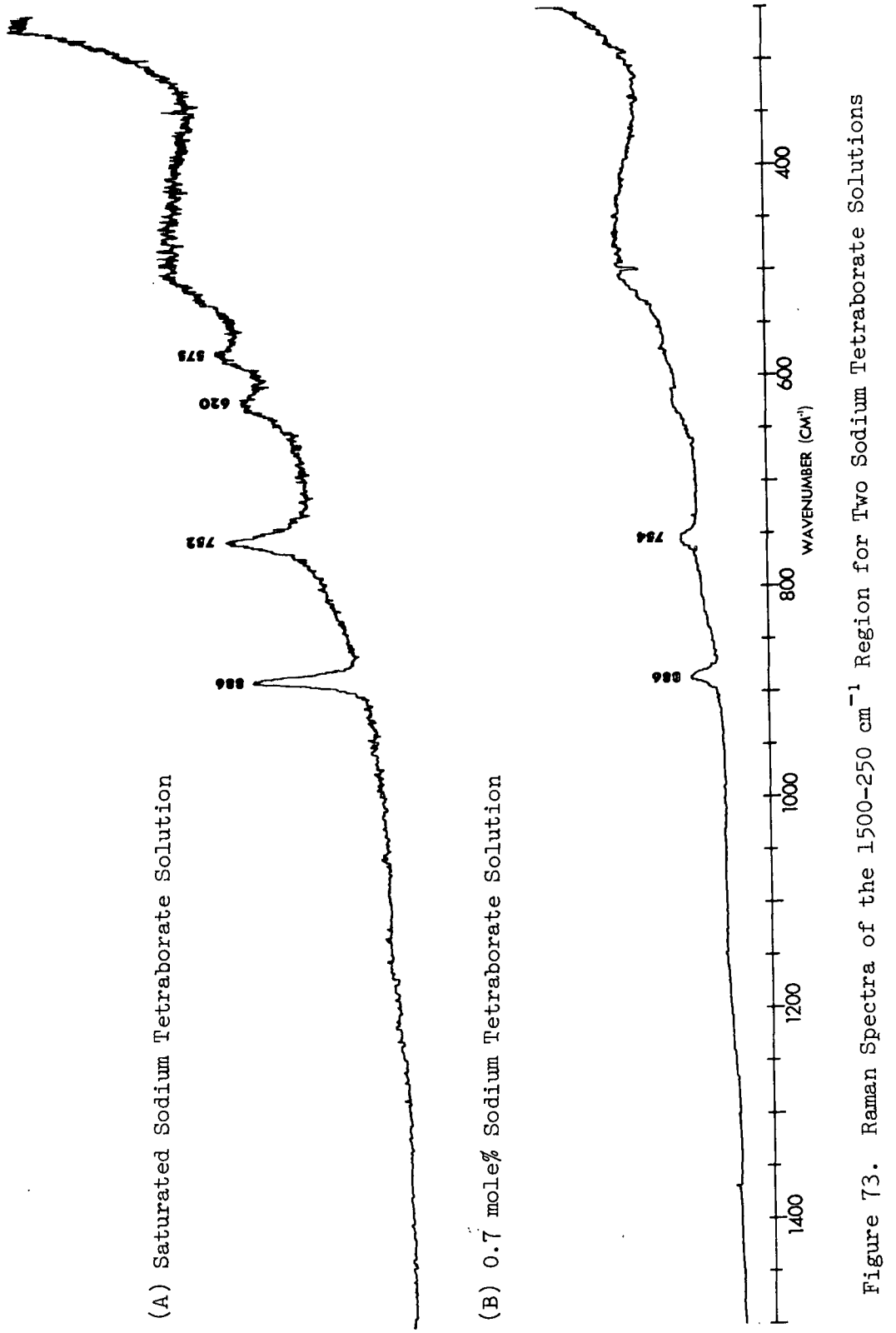

Figure 73. Raman Spectra of the 1500-250 cm^{-1} Region for Two Sodium Tetraborate Solutions

latter spectrum was recorded under similar instrumental conditions as the inositol solutions to illustrate the weak intensities of the borate solution bands relative to the intensities of the inositol bands. Figure 73(A) shows four distinct bands can be identified at 866, 752, 620 and 575 cm^{-1}. These bands, however, cannot be definitely associated with the borate ion but may arise from other species present in the solution, such as H_3BO_3.

It was noted that three of the bands in Fig. 73(A), at 886, 620 and 575 cm^{-1}, correspond closely in frequency with three of the new bands at 884, 619 and 568 cm^{-1} which appear in the cis-inositol borate spectrum shown in Fig. 72(B). A counterpart to the fourth band observed in the sodium tetraborate solution spectrum at 752 cm^{-1} appears in the cis-inositol borate spectrum, but only as a very weak shoulder on the new 718 cm^{-1} band. The similarity in the sodium tetraborate and cis-inositol borate spectra suggests an association of the new bands observed in the cis-inositol borate spectrum with the borate moiety. However, the weak intensities of the 0.7 mole% sodium tetraborate solution bands shown in Fig. 73(B) relative to the intensities of the new bands observed in the cis-inositol borate spectrum and the very weak intensity of the 718 cm^{-1} sodium tetraborate band in the cis-inositol borate spectrum suggests that the new bands observed in the cis-inositol borate spectrum do not arise from the presence of free borate ions in the solution. Beyond this no further conclusions can be drawn at this time.

Three inositols, epi-inositol, myo-inositol and scyllo-inositol, have the three syn-axial hydroxyl groups necessary to form the tridentate borates in the conformationally less stable chair form. epi-Inositol has been shown (81,84) to change conformation and form the tridentate borate as illustrated in Fig. 71(B). The reported equilibrium constant for the epi-inositol borate is K = 7000 $mole^{-1}liter$ (81,87). The effect on the epi-inositol vibrational spectrum

of reaction with borate ions is shown in Fig. 74. Figure 74 shows the 1.25 mole% epi-inositol solution spectrum, Fig. 74(A), and two spectra at the same epi-inositol concentration but at two different concentration levels of added sodium tetraborate. In Fig. 74(B) the inositol-borate ion ratio is 2:1 and in Fig. 74(C) the ratio is 1:1. Figure 74 shows that virtually the entire spectrum from 1400-350 cm^{-1} has been affected by the formation of the borate. In Fig. 74(B), the strong band at 503 cm^{-1}, the symmetric ring breathing mode, decreases in relative intensity and a new band at 475 cm^{-1} appears. In comparing the three spectra in Fig. 74, as the borate concentration increases several bands increase in relative intensity, including bands at 415, 475, 540, 684, 876, 933, 962, 1057, 1095, and 1142 cm^{-1}. Simultaneously, as the borate concentration increases several bands decrease in relative intensity, including bands at 360, 396, 428, 503, 806, 915, 1046 and 1080 cm^{-1}. These observed changes in relative intensities are consistent with a shift in the epi-inositol conformational equilibrium to the alternate chair form with borate formation and a corresponding decrease in the preferred form. The extent of the changes observed in the epi-inositol spectrum, where a conformation change is occurring with borate formation, are substantially greater than the changes observed in the cis-inositol spectrum, where no conformation change took place upon borate formation.

To determine if any correlation existed between the new bands observed in the epi-inositol spectrum upon borate formation and calculated changes in the frequencies in going from the preferred to the alternate conformation, frequencies for the alternate conformation of epi-inositol were calculated using the inositol force field developed in Part I. A bar graph representation of the observed Raman frequencies for the epi-inositol solution, the calculated frequencies for the preferred chair conformation, the new observed Raman bands resulting

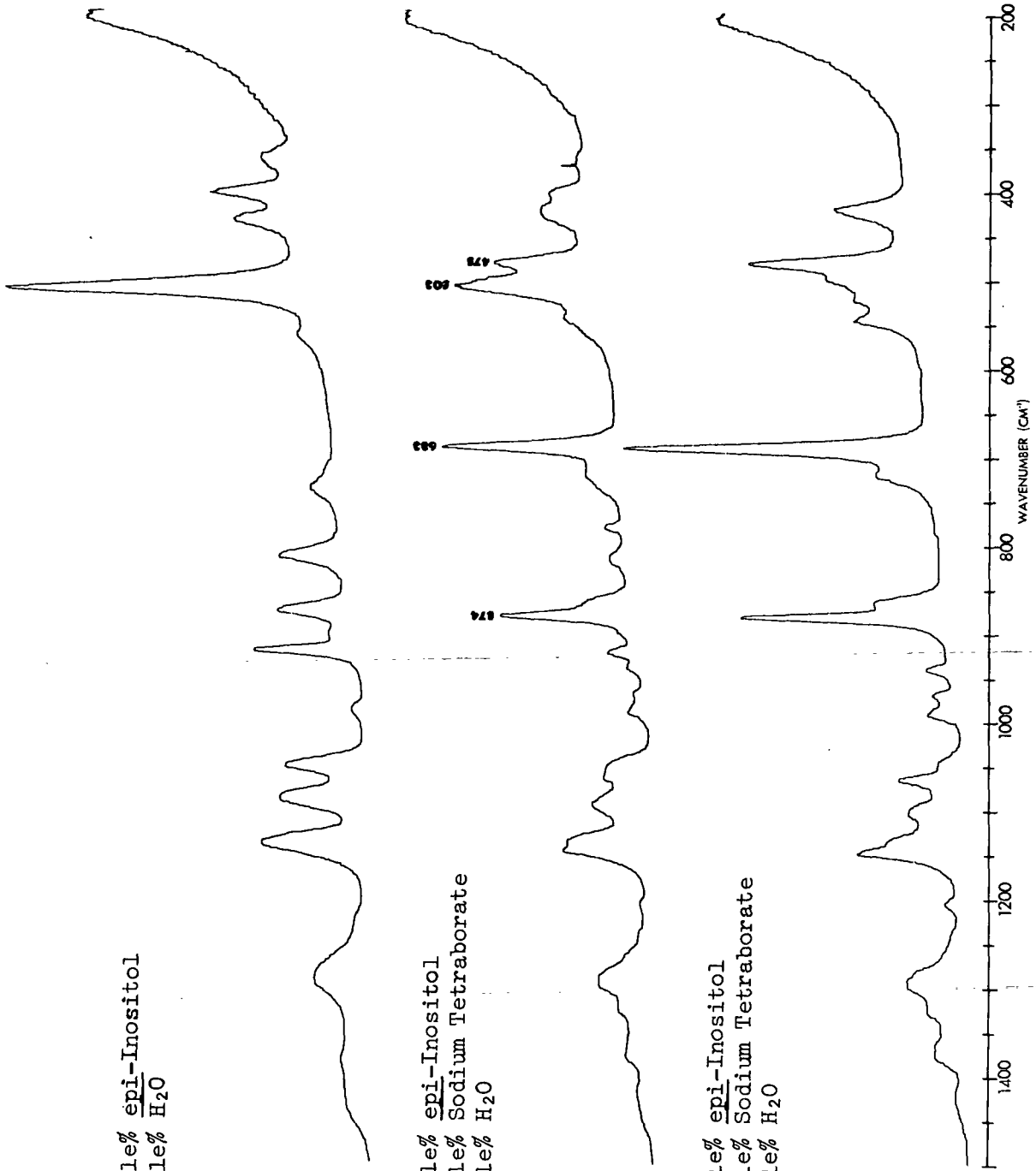

Figure 74. Raman Spectra of the 1500-200 cm^{-1} Region for Three epi-Inositol Solutions

from the epi-inositol borate and the calculated frequencies for the alternate chair conformation are shown in Fig. 75. The correspondence between the observed epi-inositol solution bands and the calculated frequencies for the preferred conformation is seen to be quite good. Definite changes in the frequencies are calculated in going to the alternate conformation. But Fig. 75 shows the calculated alternate conformation bands do not correlate well with the new observed bands resulting from the epi-inositol borate. The poor correlation suggests that formation of the epi-inositol borate significantly perturbs the frequencies of the epi-inositol alternate conformer. In addition, borate formation almost certainly perturbs the bands arising from the borate moiety and also, inositol borate formation would result in a lowering of the tetrahedral symmetry (97) of the borate ion skeleton. Also noted was that two of the more intense new bands, at 874 and 683 cm^{-1}, occur at frequencies similar to two of the new bands, at 884 and 718 cm^{-1}, observed in the cis-inositol borate spectrum.

In the alternate conformation, myo-inositol also has the three syn-axial hydroxyl groups necessary for tridentate borate formation and NMR evidence for the myo-inositol borate has been reported (85). The equilibrium constant for the borate, K = 25 $mole^{-1}$liter (81,87) is much lower than for epi-inositol, K = 7000 $mole^{-1}$liter (81,87). This is because the interaction energy for the alternate conformation of myo-inositol, where two axial hydroxyl groups are not involved in the tridentate borate, is higher than for epi-inositol, where there is only one uncomplexed axial hydroxyl group in the alternate conformation. The effect of added borate on the myo-inositol solution spectrum is shown in Fig. 76. Figure 76(A) is the Raman spectrum of a 1.30 mole% myo-inositol solution. Figures 76(B) and 76(C) are spectra recorded at two levels of added sodium tetraborate. In Fig. 76(B) the inositol:borate ratio is 2:1 and in Fig. 76(C) the ratio is 1:1. The observed changes are not nearly as dramatic as those observed

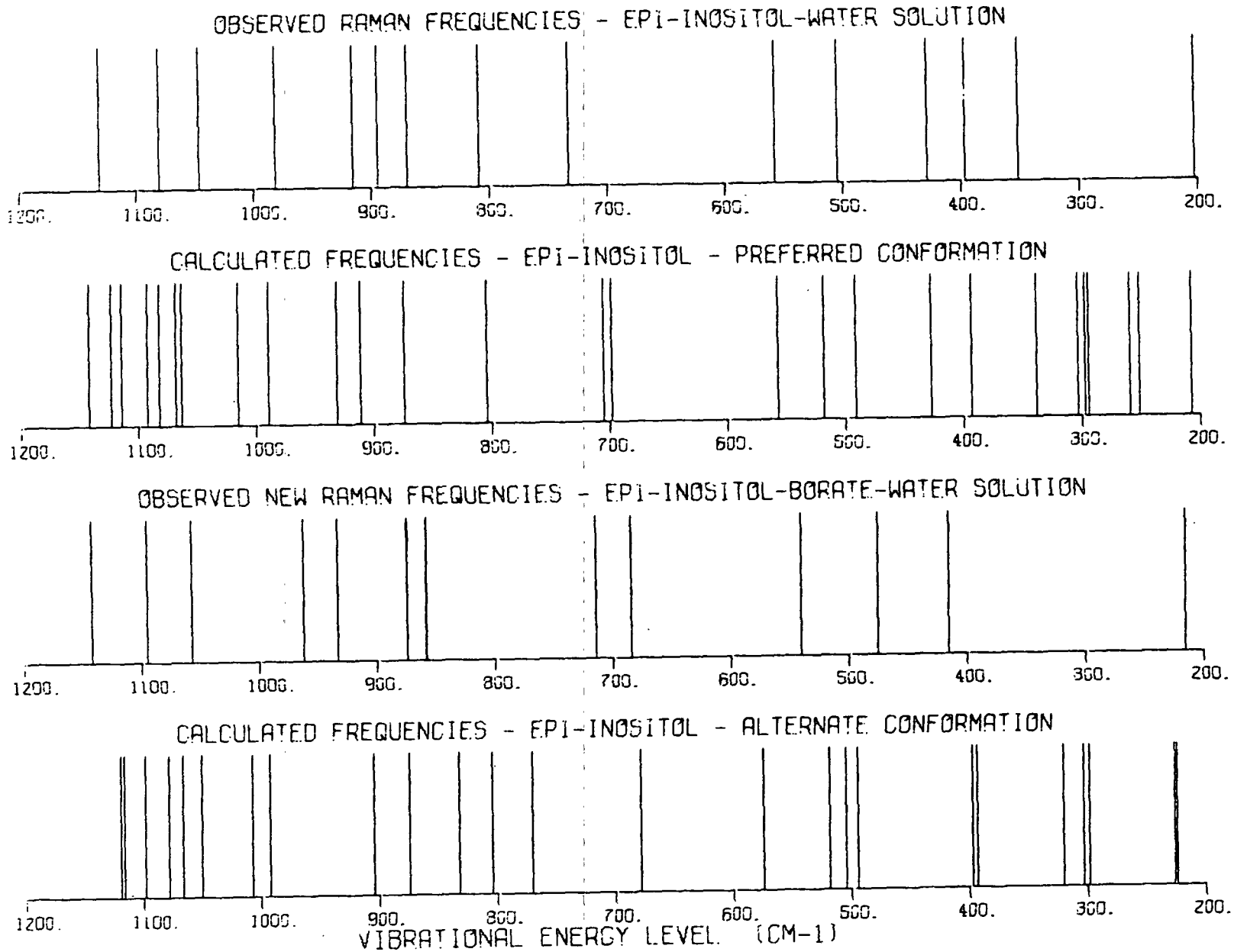

Figure 75. Bar Graph Representation of the Observed Raman Frequencies for epi-Inositol in Solution, the Calculated Frequencies for the epi-Inositol Preferred Chair Conformation, the New Observed Raman Frequencies for the epi-Inositol-Sodium Tetraborate Solution and the Calculated Frequencies for the epi-Inositol Alternate Chair Conformation

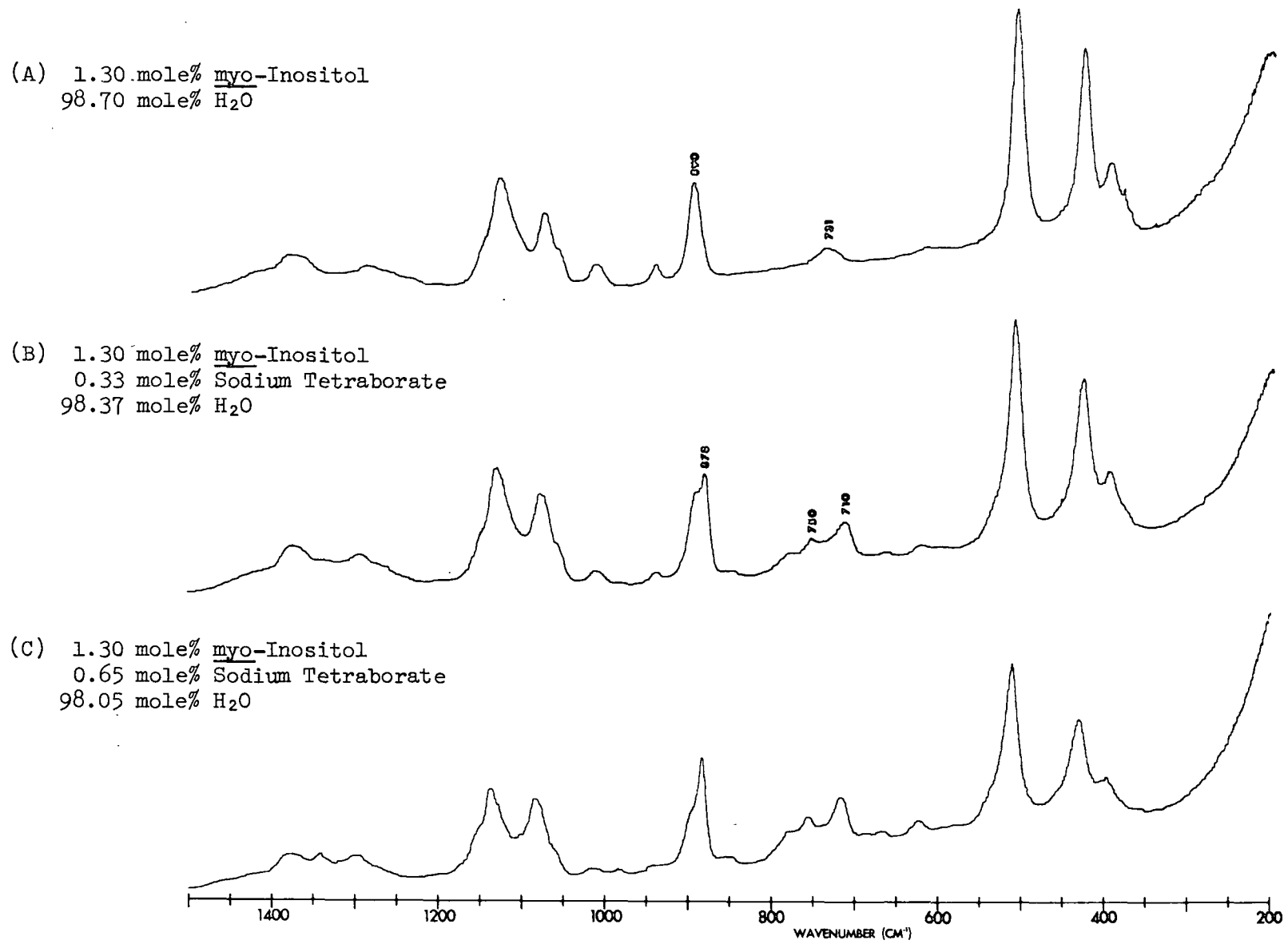

Figure 76. Raman Spectra of the 1500-200 cm^{-1} Region for Three myo-Inositol Solutions

in the epi-inositol spectrum. As the borate concentation increases, the minor changes observed include a decrease in the relative intensity of the bands at 890 and 731 cm^{-1} and a correponding increase in the relative intensities of the bands at 878, 750 and 710 cm^{-1}. The apparent reason for the observation of only minor changes, even though a conformation change occurs to form the borate, is that at the concentration levels employed only a small fraction of the myo-inositol molecules are reacted to form the borate. However, using the equilibrium constant, K = 25 $mole^{-1}$liter (81,87), a calculation of the percent myo-inositol borate formed, using the 1:1 myo-inositol-borate ion concentrations shown in the case of Fig. 76(C), shows that ~75% of the myo-inositol should be in the borate form. The Raman spectra presented in Fig. 76 suggest a much smaller percentage has been formed. This inconsistency raises a question as to the accuracy of the equilibrium constant, which was calculated from pH changes in several myo-inositol borate solutions. Additional work would be needed, though, to more completely resolve this inconsistency. It is difficult to assess whether the changes observed in the myo-inositol spectrum arise from the tridentate borate species or from a different borate involving the myo-inositol in the preferred conformation.

scyllo-Inositol is unique among the inositols in that in the alternate conformation two sets of triaxial hydroxyl groups are available for borate formation. The chair inversion of scyllo-inositol to form the diborate is envisioned in Fig. 77. The scyllo-inositol diborate has been previously identified and characterized (82,83). The diborate is very stable with a reported equilibrium constant of K = 7.8×10^5 (83). Weissbach (82) isolated and characterized the diborate as a solid. His analysis stemmed from a white compound which precipitated from a reaction mixture. For the formula $C_6H_8O_8B_2Na_2 \cdot 9H_2O$ the elemental percentages he calculated were C 16.45, H 5.99, B 4.94, and water 37.02. For the isolated compound he found C 16.52, H 6.07, B 4.87 and a weight loss of 37.27

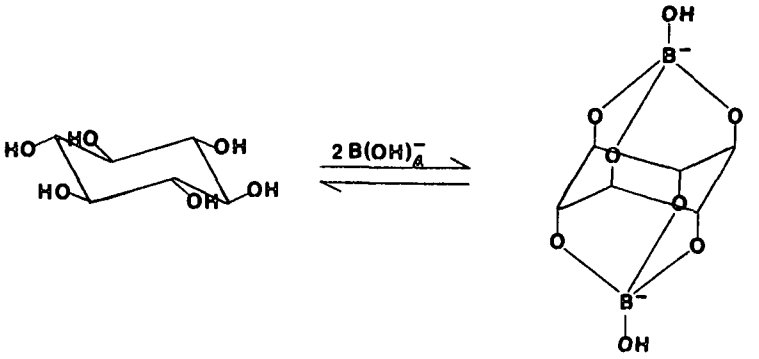

scyllo-Inositol scyllo-Inositol Diborate

Figure 77. Representation of the scyllo-Inositol Chair Inversion to Form the scyllo-Inositol Diborate

after drying at 100°C for eighteen hours. For this work, attempts were made to record the Raman spectrum of the scyllo-inositol diborate in solution but were unsuccessful. During the final attempt, the scyllo-inositol solution containing sodium tetraborate was allowed to stand for several hours, during which time a white precipitate formed. The precipitate was washed with distilled water and dried at ∿80°F. The Raman spectrum of the dried precipitate is shown in Fig. 78(A). The Raman spectrum of crystalline scyllo-inositol is shown in Fig. 78(B) for comparison. The spectrum in Fig. 78(A) is of neither scyllo-inositol nor sodium tetraborate, although some weak residual scyllo-inositol bands are observed. Comparison of the Raman spectra in Fig. 78 shows virtually every band in the scyllo-inositol spectrum has changed in frequency. Only a weak remnant of the strong 464 cm^{-1} scyllo-inositol band is observed in Fig. 78(A). Several new bands, at 552, 558, 706, and 884 cm^{-1}, are observed in Fig. 78(A). In the borate spectra of cis-inositol and epi-inositol new bands were also observed around 880 and 700 cm^{-1}. The two bands at 1336 and 1348 cm^{-1} in Fig. 78(A) increase substantially in relative intensity and the bands above 1400 cm^{-1} are no longer observed. Substantial band shifts are also observed in the C-H stretching region, 2850-3000 cm^{-1}. The three C-H stretching bands, observed at 2890, 2929 and 2942 cm^{-1} in the scyllo-inositol spectrum, are shifted up to 2925, 2956 and 2963 cm^{-1} in the precipitate spectrum.

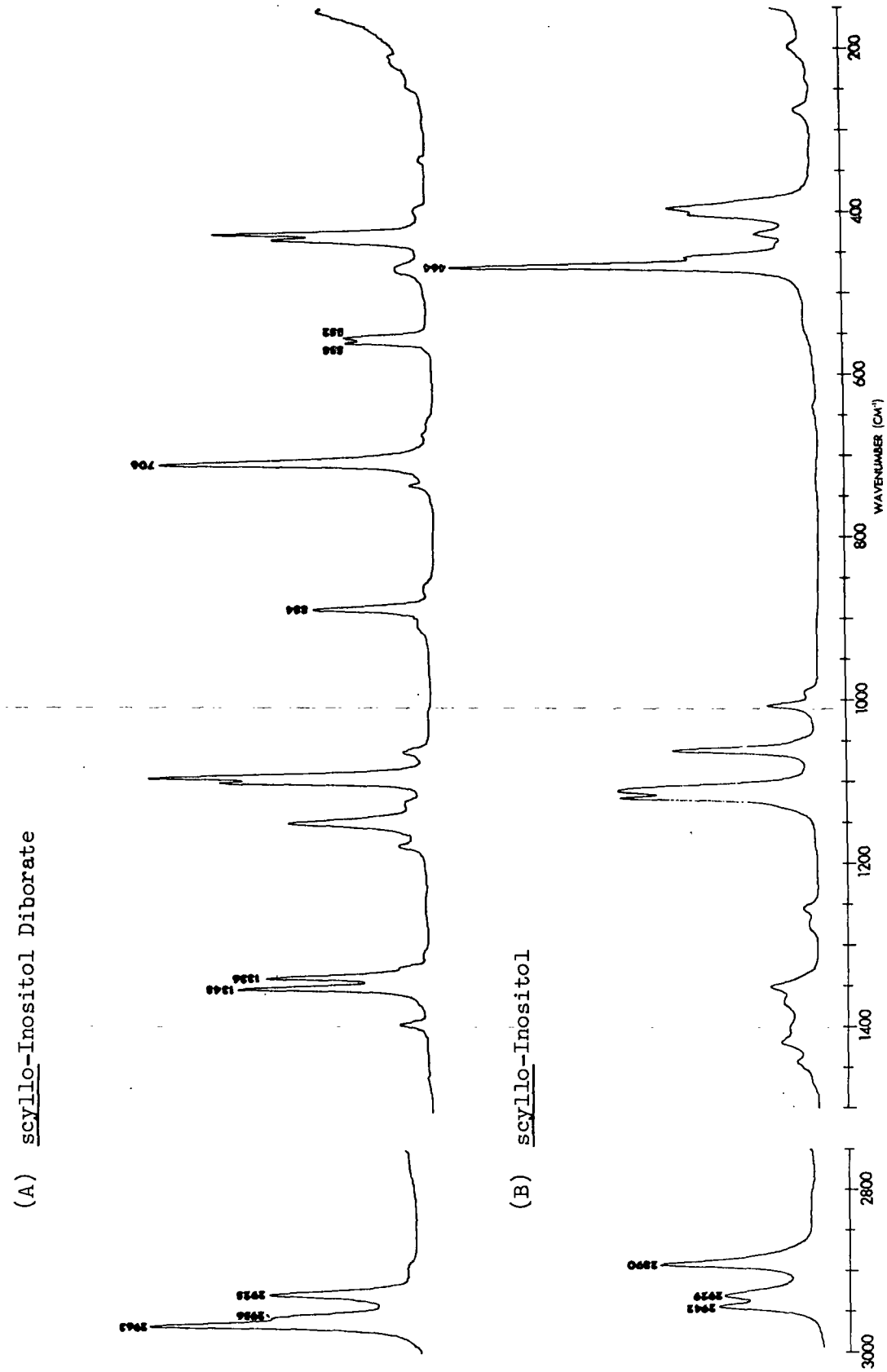

Figure 78. The Room Temperature Raman Spectra of (A) Crystalline scyllo-Inositol Diborate and (B) Crystalline scyllo-Inositol

To further characterize the precipitate, the room temperature infrared spectrum, as the Fluorolube and Nujol mulls, was also recorded. It was theorized that if the compound was indeed the scyllo-inositol diborate, as shown in Fig. 77, then the loss of the hydroxyl hydrogens in forming the diborate should result in the scyllo-inositol O-H stretching and COH bending modes not being observed. The room temperature infrared spectrum of the compound is shown in Fig. 79(A) along with the infrared spectrum of scyllo-inositol, Fig. 79(B). Extensive changes throughout the entire spectrum are again observed. The scyllo-inositol O-H stretching bands are indeed absent in Fig. 79(A) except for remnants which appear as shoulders. The new O-H stretching band results from the water present in the compound. The potential energy distribution for scyllo-inositol shows the COH bending modes primarily occur above 1400 cm^{-1}. The bands observed above 1400 cm^{-1} in Fig. 79(B) are not observed in Fig. 79(A). This is the same result observed in the Raman spectra in Fig. 78. In addition, the temperature sensitive scyllo-inositol infrared bands at 522 and 485 cm^{-1}, which were interpreted as arising from the motions of the hydrogen bonded hydrogens, are also not observed in Fig. 79(A). The infrared and Raman spectra both strongly support the identity of the compound precipitated from the scyllo-inositol-sodium tetraborate solution as the scyllo-inositol diborate. Two additional changes noted in the infrared spectrum of the diborate, Fig. 79(A), are the new sets of relatively intense bands observed between 850-950 cm^{-1} and around 1200 cm^{-1}.

The few number of bands observed in the Raman scyllo-inositol diborate spectrum and the observation that few of the Raman bands have counterparts in the infrared and vice versa suggests that the symmetry of the scyllo-inositol is preserved in the alternate conformation complex and mutual exclusion is being observed. Attempts to more conclusively prove this assertion by calculating the frequencies for the scyllo-inositol in the alternate conformation and comparing

(A) scyllo-Inositol Diborate

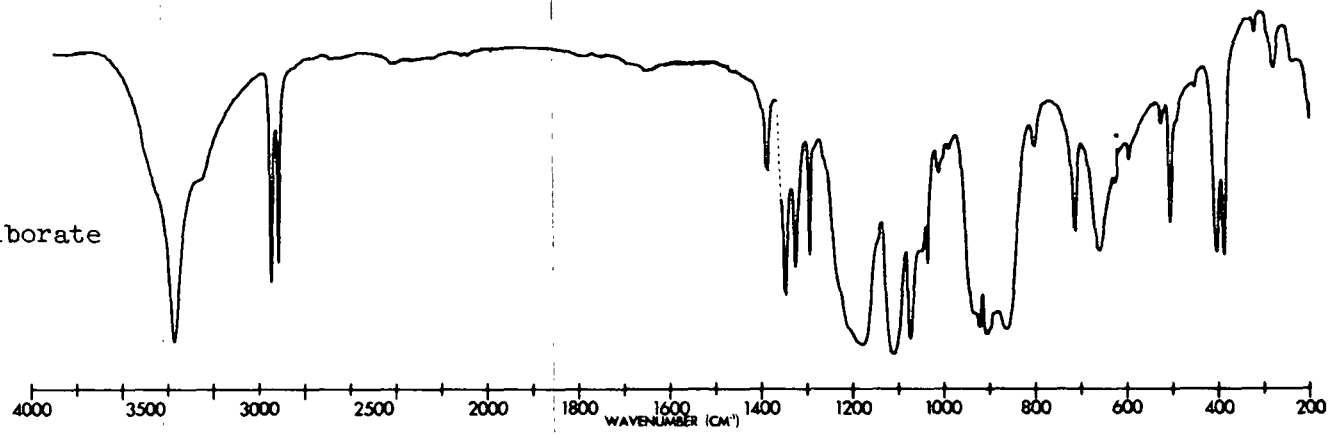

(B) scyllo-Inositol

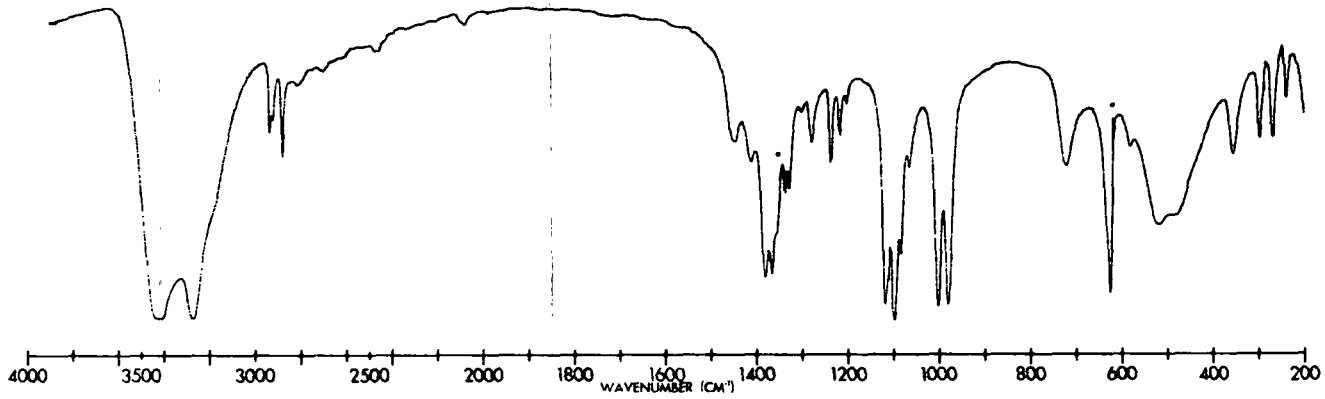

Figure 79. The Room Temperature Infrared Spectra of (A) Crystalline scyllo-Inositol Diborate and (B) Crystalline scyllo-Inositol

the calculated frequencies with the observed complex frequencies were unsuccessful. The calculated Raman active and infrared active frequencies did not correspond to any significant degree with the observed Raman and infrared complex frequencies. Even the observed changes in the Raman C-H stretching frequencies were not reproduced at all by the calculations, which suggests a significant electronic perturbation has occurred.

In order to compare the relative changes observed in the molecular systems which form tridentate borates with systems which do not have the sequence of axial hydroxyl groups needed to form the tridentate borates, the Raman solution spectra of muco-inositol and L-chiro-inositol with and without added sodium tetraborate were recorded. Although muco-inositol and L-chiro-inositol cannot form tridentate borates, this is not meant to imply that interactions between borate ions and these two inositols cannot take place. Interactions between two hydroxyl groups and borate ions are well known and characterized (81,84,85,88). However, electrophoretic mobilities (81) show that inositol borates of this type are not as stable as the tridentate borates.

muco-Inositol, as shown in Fig. 55 in Part II, has axial hydroxyl groups on C3, C4 and C5 and thus both conformations have the same structure. muco-Inositol does not have axial hydroxyl groups in 1:3:5 relative positions and thus cannot form a tridentate borate. The Raman spectra of a saturated muco-inositol solution, with and without added sodium tetraborate, are shown in Fig. 80. The observed changes after addition of sodium tetraborate are seen to be minor. The most distinct change is the more pronounced shoulder at 910 cm^{-1}. Better resolution spectra would be needed to further characterize the minor changes. It can be noted that bands resulting from the presence of borate ions are not observed with any appreciable intensity. For the case of muco-inositol, then, the addition of sodium tetraborate does not result in any significant perturbation of

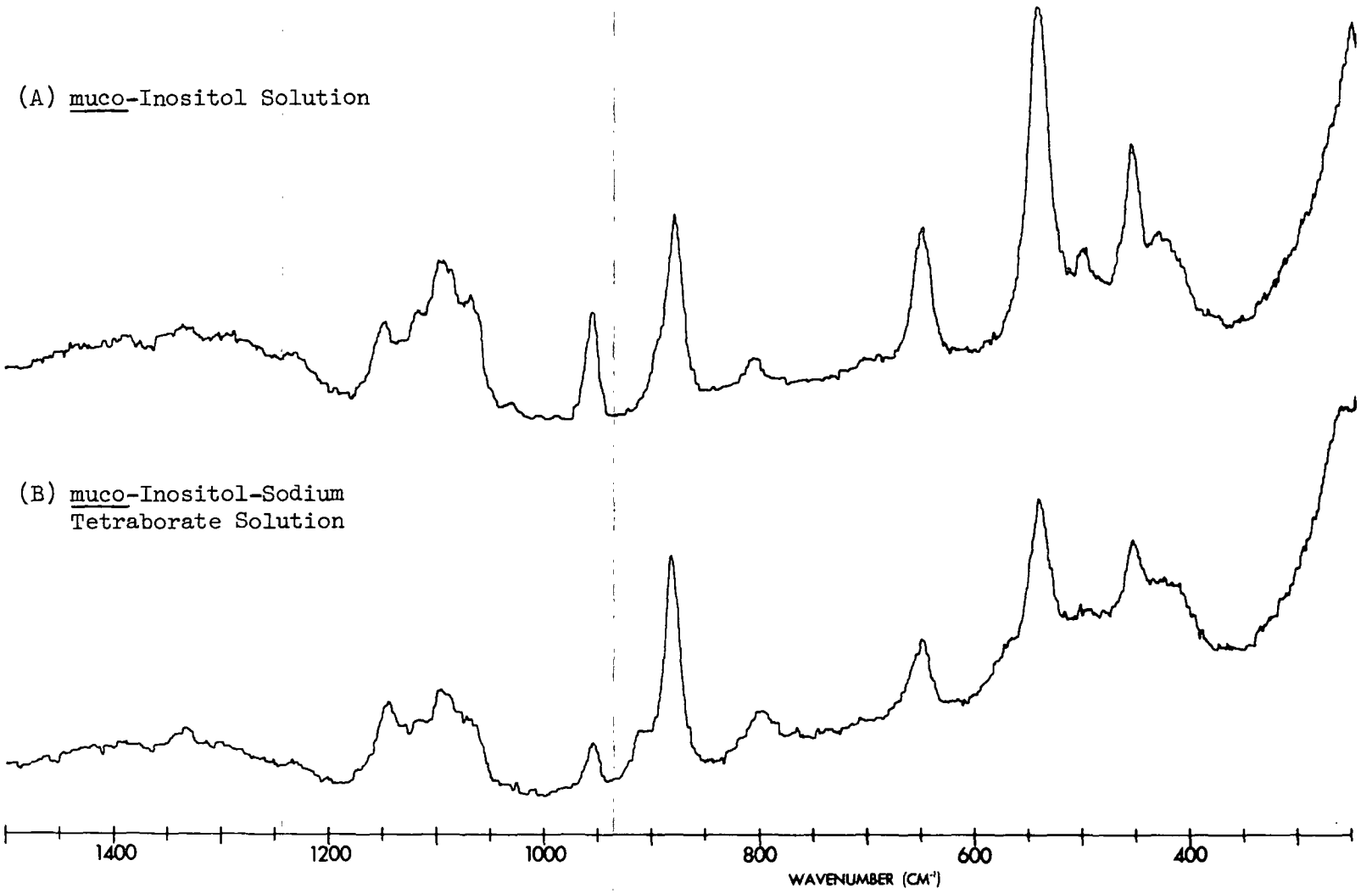

Figure 80. Raman Spectra of the 1500-250 cm^{-1} Region for Two muco-Inositol Solutions

the muco-inositol vibrational spectrum, although the electrophoretic mobility (81) strongly suggests an interaction or borate formation is occurring.

L-chiro-Inositol, as shown in Fig. 55, has axial hydroxyl groups on carbons C1 and C6. Therefore in neither the preferred nor the alternate conformation does the necessary sequence of axial hydroxyl groups for tridentate complexing occur. Figure 81(A) shows the Raman spectrum of a 1.30 mole% L-chiro-inositol solution and Fig. 81(B) the Raman spectrum of a 1.30 mole% L-chiro-inositol-0.65 mole% sodium tetraborate solution. In Fig. 81(B) the inositol-borate ion ratio is 1:1. Figure 81 shows that the changes observed in the L-chiro-inositol spectrum in the presence of borate ions are more pronounced than those observed in muco-inositol. At least three new bands are observed at 1110, 800 and 713 cm^{-1} in Fig. 81(B). Band shifts and changes in relative band intensities are also noted. The new bands do not correspond with the bands observed in the sodium tetraborate spectrum shown in Fig. 73. The observed changes illustrate that even though a tridentate borate cannot be formed, the interaction between L-chiro-inositol and borate ions is sufficiently strong to produce significant changes in the vibrational spectrum of L-chiro-inositol. Without further investigation, postulation as to the origin of the observed changes, whether they arise from major changes in the L-chiro-inositol geometry or from vibrations involving bonds formed in the borate, is difficult to make. Two possibilities are that a compact L-chiro-inositol dimer, linked by a borate ion is occurring in this case but not in the case of muco-inositol, or that the L-chiro-inositol-borate interaction involves a conformation other than a chair conformation, such as a boat or skew conformation.

The observed effects of borate formation on the vibrational spectra of several inositols have been seen to range from no detectable effect to pronounced changes affecting virtually every band in the spectrum. Significant changes were observed

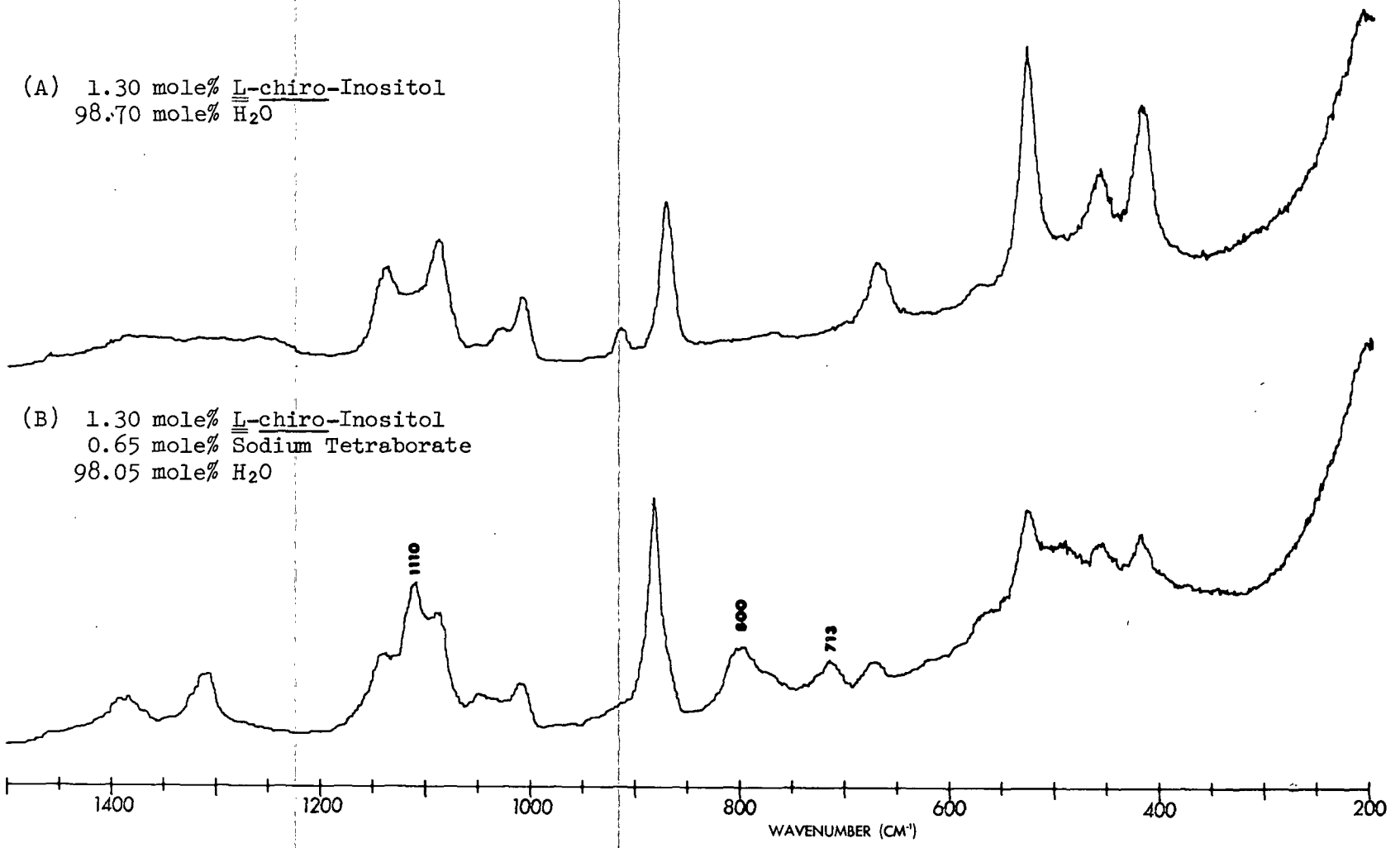

Figure 81. Raman Spectra of the 1500-200 cm^{-1} Region for Two L-chiro-Inositol Solutions

in the spectrum of cis-inositol, where borate formation occurred with little change in the cis-inositol geometry. The observed changes were more extensive when borate formation was accompanied by a change in the inositol conformation, as in the cases of epi-inositol and scyllo-inositol. The changes observed in the spectrum of L-chiro-inositol after addition of sodium tetraborate illustrated that a significant L-chiro-inositol-borate interaction was occurring even though a tridentate borate could not be formed.

The observed epi-inositol borate and scyllo-inositol borate spectra could not be reproduced to any significant degree using frequencies calculated for the alternate chair forms. The reaction to form the borates rendered the simple, unperturbed inositol model used to calculate the frequency changes ineffective in predicting the observed changes. The borates are of such a strength that they result in a major perturbation of the inositol vibrational frequencies and the borate vibrational frequencies. This further supports the contention that the complexes are actually anionic esters. In the borate spectra one is then observing the vibrational frequencies of what is essentially a new compound. Interpretation of the inositol borate spectra based on normal coordinate calculations would require incorporation of the borate moiety into the molecular model, which would necessitate determination of force constants for the B-O bonds, etc. Without a normal coordinate analysis, interpretation of the observed changes or individual bands in the borate spectra are difficult. In the borate spectra of cis-inositol, epi-inositol and scyllo-inositol new bands were observed in the vicinity of 884 and 700 cm^{-1}. A possible correspondence between these bands and bands observed in the sodium tetraborate solution spectrum at 886 and 752 cm^{-1} was postulated. A relationship may exist but further investigation would be needed to supply additional evidence.

PART V

THE CONTRIBUTION OF VIBRATIONAL ENERGY TO THE CONFORMATIONAL ENERGY OF THE INOSITOLS

INTRODUCTION

Several semiquantitative approaches have been employed in attempts to predict the favored conformations of carbohydrates in the pyranoid ring form (89). The most widely used approach, developed by Angyal and McHugh (87) and Angyal (90), involves the summation of nonbonded interaction energies for various substituent groups to determine the relative conformational free energies of the different conformations. Predictions of predominant conformations for the D-aldopyranoses in solution based on this method have resulted in excellent agreement with experimentally determined conformation populations in solution (89,90). "The calculations are based on two assumptions: (1) that the pyranose ring has the same geometry as cyclohexane, and (2) that the free energies of conformational isomers are additive functions of energy terms associated with the presence of nonbonded interactions; that is, that the occurrence of one interaction in a molecule does not affect the magnitude of another one. Both of these assumptions are only approximations (90)." For calculating the conformational free energies, two types of nonbonded interactions are taken into account: (1) Nonbonded 1,3-diaxial interactions between syn-axial ligands other than those between two hydrogen atoms. This interaction is designated as (X_a:Y_a). (2) Nonbonded 1,2-interactions between ligands gauche to each other on adjacent carbon atoms apart from those involving hydrogen atoms. Axial-equatorial and equatorial-equatorial interactions are assumed to be equivalent. This interaction is designated as (X_1:Y_2) (91). Interaction energies for several different types of possible interactions have been determined from studies on the equilibria of inositol borates (87) and from studies on the anomeric equilibria of pyranoses (90).

Implicit in this method of calculating conformational free energies is an additional assumption. It is assumed that the vibrational energies for different conformations are essentially the same and thus do not contribute substantially to the differences in conformational energies. The validity of this assumption, however, has not been rigorously demonstrated. The purpose of this investigation was to test the validity of this assumption by calculating the vibrational energies for the preferred and alternate conformations of the inositols.

From the vibrational partition function, the following equation for the vibrational energy, assuming harmonic vibrations, of a diatomic molecule can be derived (92):

$$E_{vib} = \frac{Nhv}{2} + \frac{Nhv}{\exp(hv/kT) - 1} , \qquad (12)$$

where N = Avagadro's number

h = Planck's constant

v = frequency of the harmonic oscillator

k = Boltzmann's constant

T = temperature, °K

This treatment can be extended to polyatomic molecules by summing Equation (12) for each of the normal vibrational frequencies (92). For a polyatomic molecule, then, Equation (12) can be written as

$$E_{vib} = \sum_{i=1}^{3n-6} \frac{Nhv_i}{2} + \sum_{i=1}^{3n-6} \frac{Nhv_i}{\exp(hv_i/kT) - 1} , \qquad (13)$$

where 3n-6 represents the number of vibrational degrees of freedom. Equation (13) was used to calculate the vibrational energies for the preferred and alternate conformations of the inositols.

EXPERIMENTAL

VIBRATIONAL ANALYSES

Normal coordinate analyses of eight of the inositol isomers in the preferred and alternate (nonpreferred) conformations were done. This included: scyllo-inositol, neo-inositol, myo-inositol, epi-inositol, L-chiro-inositol, cis-inositol, muco-inositol and allo-inositol. D-chiro-Inositol was not included because the results would be the same as obtained for L-chiro-inositol.

To more closely approximate the conditions as they would be in aqueous solution, the molecular models were defined excluding the hydroxyl hydrogens. In solution, the hydroxyl hydrogens are rapidly exchanging and thus need not be considered part of the basic molecular structure. Exclusion of the hydroxyl hydrogens also avoids the problem of frequency dependence on hydroxyl group orientation in the calculations.

Sixty internal coordinates were defined for the 18-atom models. The internal coordinates defined were the same as defined for the 24-atom models in Part I, except the O-H stretching, COH bending, and O-H torsion coordinates were not included.

The molecular geometries of the models were assumed to be tetrahedral. The same bond lengths defined in Table XVII in Part I were again employed. The $\underset{\sim}{G}$ matrices for the 18-atom models were calculated based on these parameters. Representations of the preferred and alternate conformations of the 18-atom inositol models used in the calculations are shown in Fig. 82. The atom numbering sequence employed for all the models are labelled in Fig. 82(A) and 82(B) for scyllo-inositol. It should be noted that the preferred and alternate conformations for

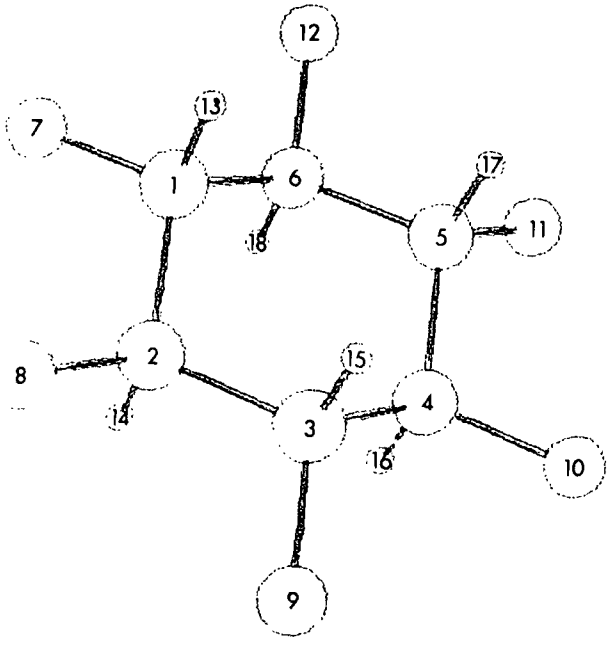

(A) scyllo-Inositol
Preferred Conformation

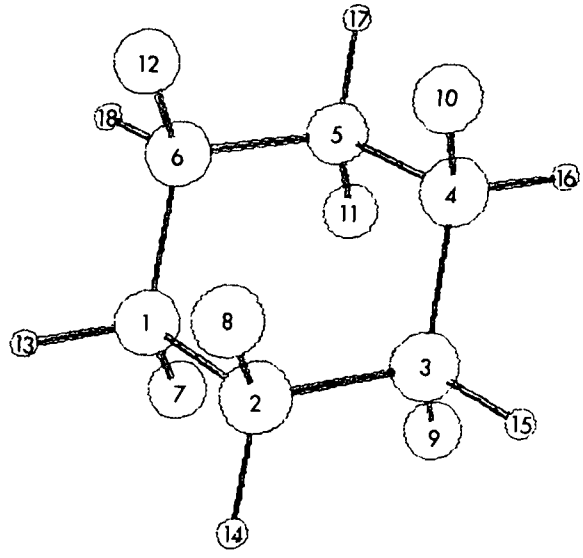

(B) scyllo-Inositol
Alternate Conformation

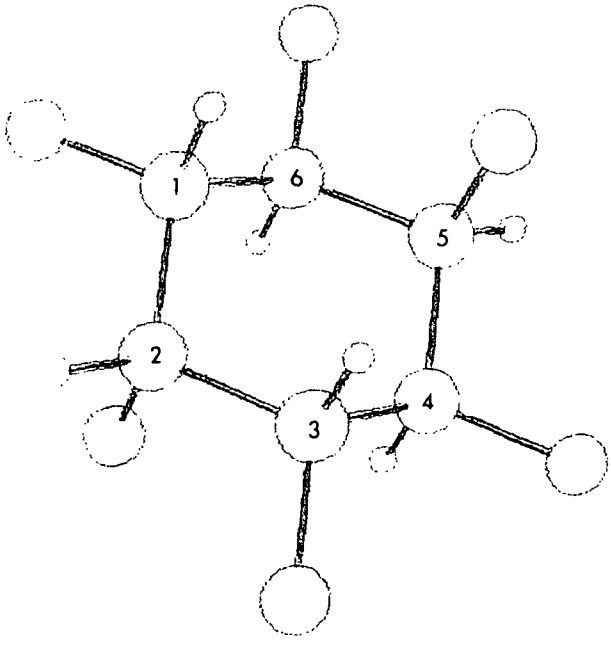

(C) neo-Inositol
Preferred Conformation

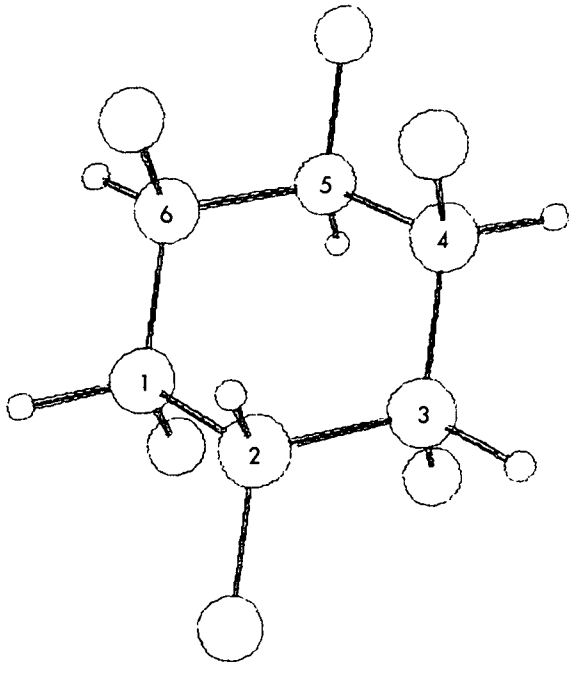

(D) neo-Inositol
Alternate Conformation

Figure 82. Representations of the Tetrahedral 18-Atom Models for scyllo-Inositol, neo-Inositol, myo-Inositol, epi-Inositol, L-chiro-Inositol, cis-Inositol, muco-Inositol and allo-Inositol

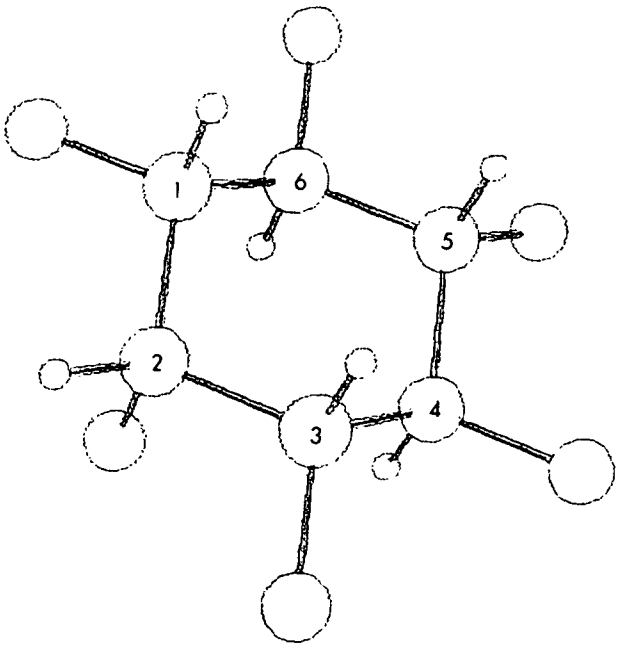

(E) myo-Inositol
Preferred Conformation

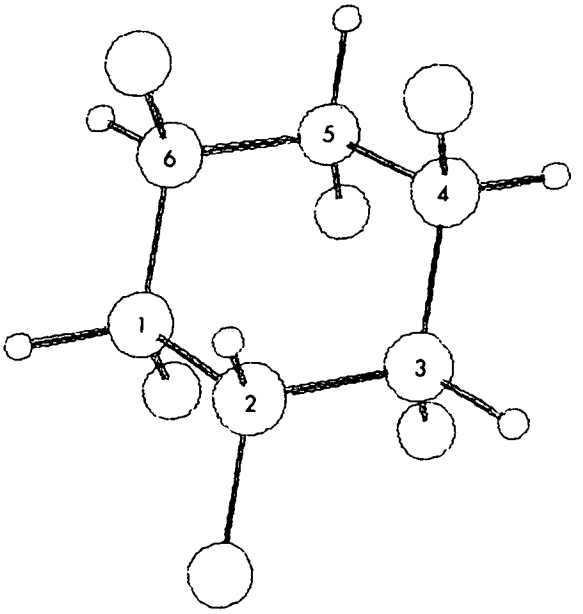

(F) myo-Inositol
Alternate Conformation

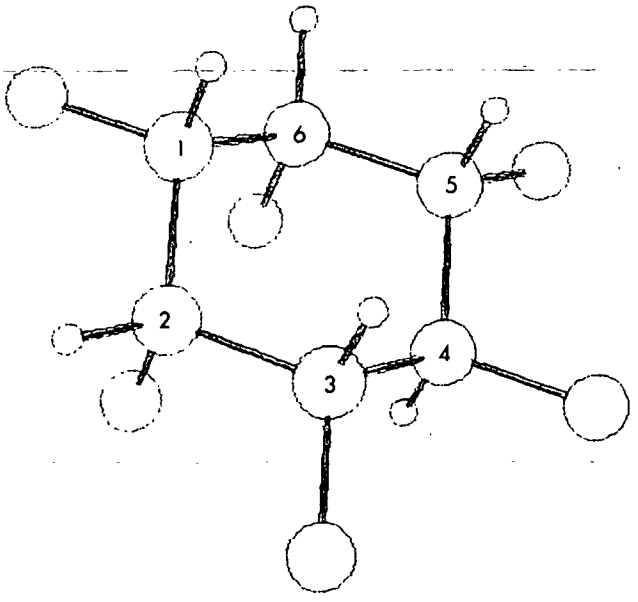

(G) epi-Inositol
Preferred Conformation

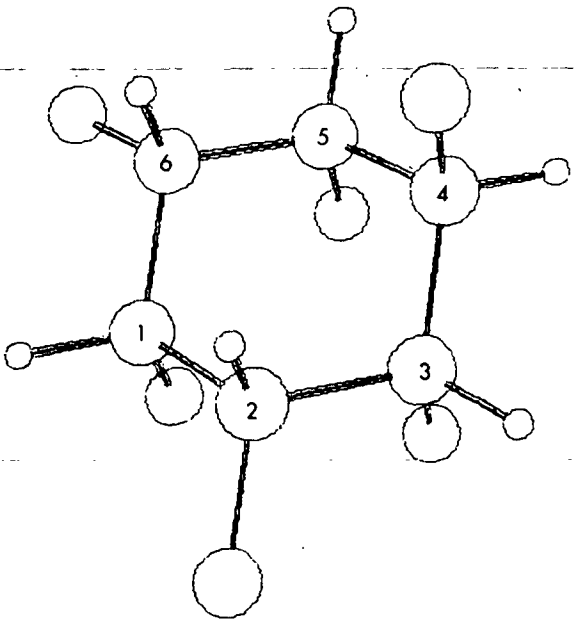

(H) epi-Inositol
Alternate Conformation

Figure 82 (cont'd). Representations of the Tetrahedral 18-Atom Models for scyllo-Inositol, neo-Inositol, myo-Inositol, epi-Inositol, L-chiro-Inositol, cis-Inositol, muco-Inositol and allo-Inositol

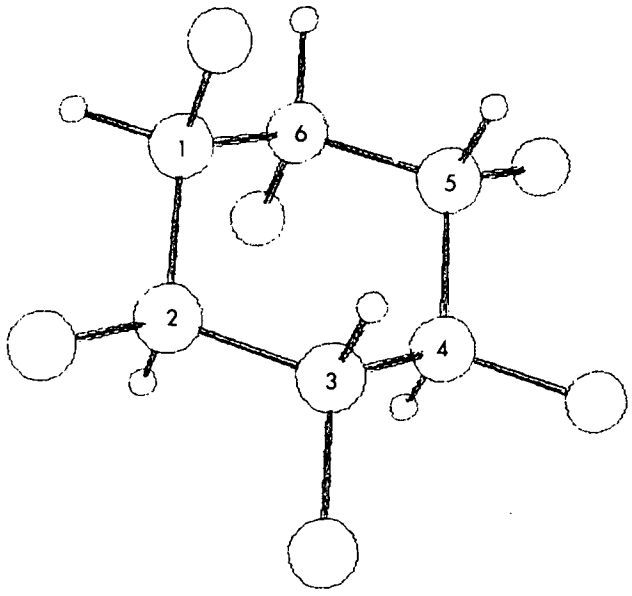

(I) L-chiro-Inositol
Preferred Conformation

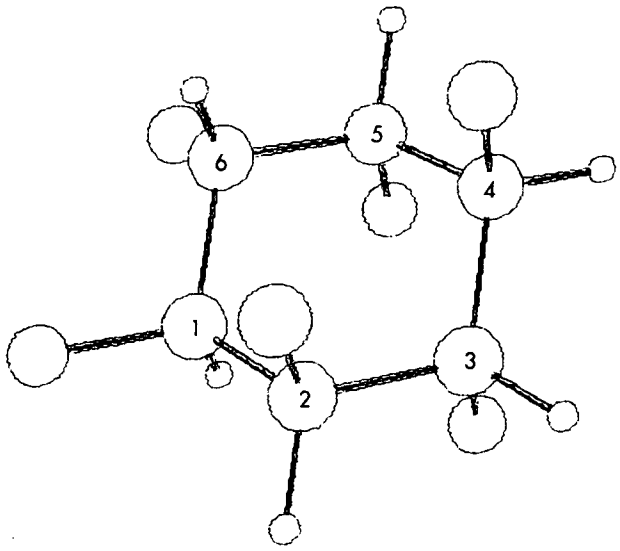

(J) L-chiro-Inositol
Alternate Conformation

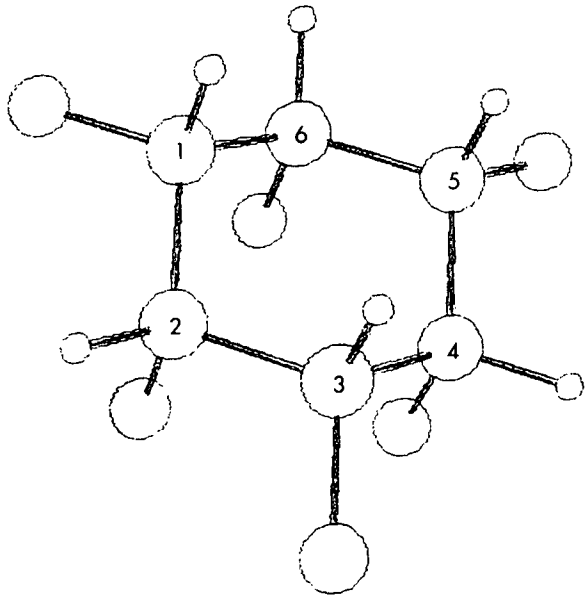

(K) cis-Inositol
Preferred Conformation

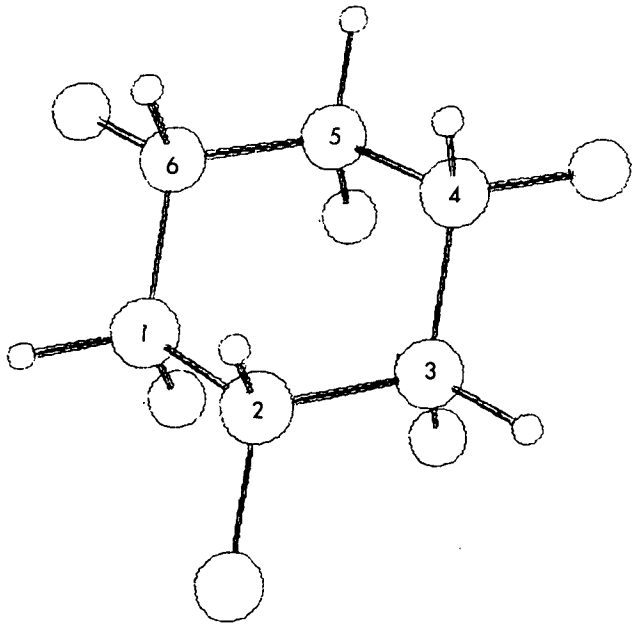

(L) cis-Inositol
Alternate Conformation

Figure 82 (cont'd). Represenations of the Tetrahedral 18-Atom Models for scyllo-Inositol, neo-Inositol, myo-Inositol, epi-Inositol, L-chiro-Inositol, cis-Inositol, muco-Inositol and allo-Inositol

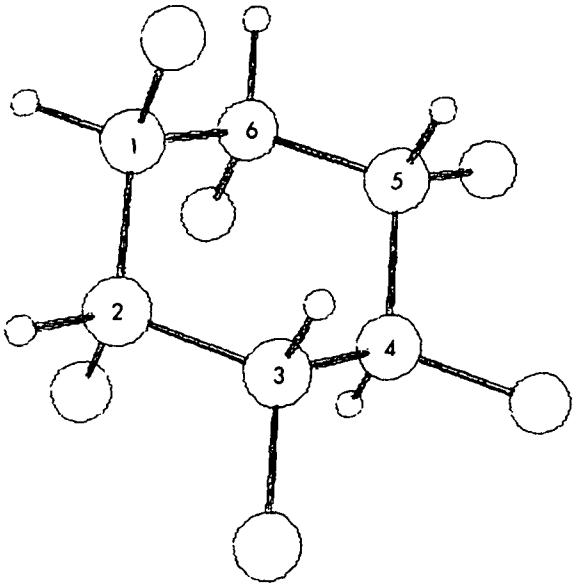

(M) muco-Inositol
Preferred Conformation

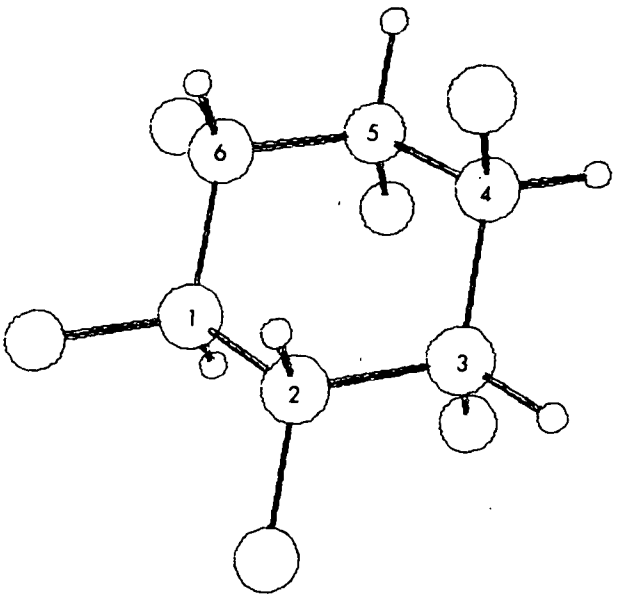

(N) muco-Inositol
Alternate Conformation

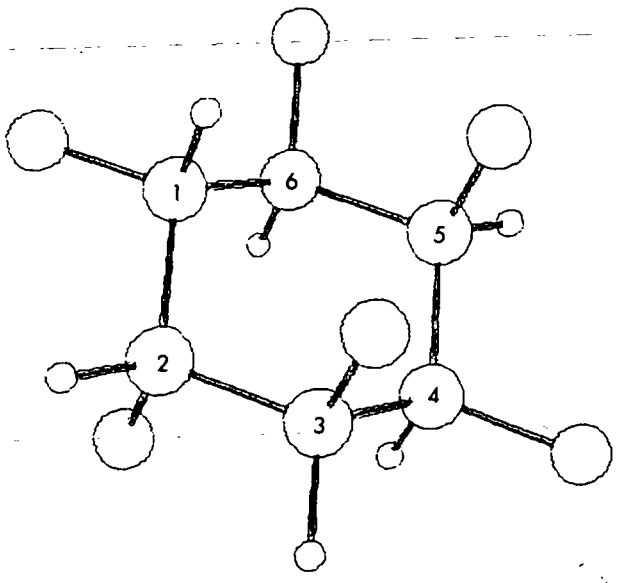

(O) allo-Inositol
Preferred Conformation

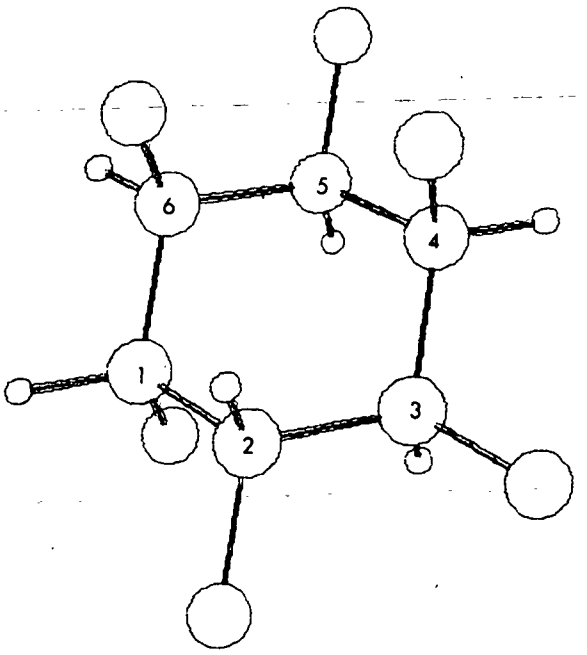

(P) allo-Inositol
Alternate Conformation

Figure 82 (cont'd). Representations of the Tetrahedral 18-Atom Models for scyllo-Inositol, neo-Inositol, myo-Inositol, epi-Inositol, L-chiro-Inositol, cis-Inositol, muco-Inositol and allo-Inositol

cis-inositol, muco-inositol and allo-inositol are identical. Both conformations were used as a check on the calculations.

The 18-atom models also necessitated construction of new Z matrices. The Z matrices were still based on the force constant numberings defined in Table XIX in Part I.

The calculations were run using the final inositol force field, shown in Table XIX. The calculations were done for the 18-atom models in unsymmetrized form using the computer program EIGV.

CALCULATION OF THE VIBRATIONAL ENERGIES

Equation (13) was programmed in FORTRAN for use on the IBM 360 computer. A temperature of 300°K was used in the computations. The computer program yielded the following information: (1) the sum of all the vibrational frequencies in wavenumbers, (2) the total sum of the first term in Equation (13), (3) the total sum of the second term in Equation (13), and (4) the total vibrational energy, E_{vib}. The input for the program was the vibrational frequencies calculated for the 18-atom inositol models.

RESULTS AND DISCUSSION

The conformational free energies for the preferred and alternate conformations for scyllo-inositol, myo-inositol, L-chiro-inositol, epi-inositol, neo-inositol, muco-inositol, allo-inositol, and cis-inositol were calculated using the method of Angyal with the interaction energies defined below in Fig. 83 as taken from Angyal (90). In addition to the summed nonbonded interaction energies, factors of 1.1 kcal/mole for scyllo-inositol, 0.65 kcal/mole for cis-inositol, 0.4 kcal/mole for neo-inositol, and 0.4 kcal/mole for L-chiro-inositol were added to the conformational free energies as a result of the entropy contributions due to

the symmetry of these molecules (91,93). The calculated conformational free energies and the calculated vibrational energies for the above listed inositols are tabulated in Table XXXV.

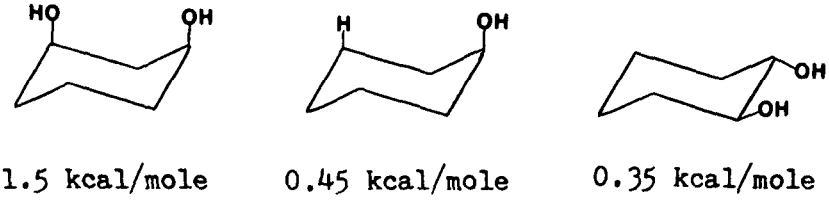

1.5 kcal/mole 0.45 kcal/mole 0.35 kcal/mole

Figure 83. Nonbonded Interactions and Interaction Energies Used to Calculate Conformational Free Energies for the Inositols

Table XXXV shows that the differences in the vibrational energies between the preferred and alternate conformations are very small compared to the differences in the conformational free energies. The largest contribution a difference in the vibrational energies could make to the differences in the conformational free energies is 0.6% in the case of myo-inositol. For the inositols then, these calculations demonstrate that the differences in the vibrational energy between the preferred and alternate conformations are negligible compared to the differences in conformational free energies. In the case of the inositols, this validates the assumption that the vibrational energies of different conformations are essentially equal. The validation of this assumption for the inositols, however, should not be blindly extended to other molecular systems. In fact, in calculations with other carbohydrate systems, such as the 1,5-anhydropentitols, the differences in zero point vibrational energy, as represented by the sum of the vibrational frequencies, between the preferred and alternate conformations were substantially greater than those found here, on thy order of 1 kcal/mole.

Additional information can be noted from Table XXXV. The differences in the conformational free energies between the preferred and alternate conformations

TABLE XXXV

THE CONFORMATIONAL FREE ENERGIES AND VIBRATIONAL ENERGIES FOR THE PREFERRED AND ALTERNATE CONFORMATIONS OF THE INOSITOLS

	CONFORMATIONAL FREE ENERGIES			VIBRATIONAL ENERGIES		
	PREFERRED CONFORMATION (kcal/mole)	ALTERNATE CONFORMATION (kcal/mole)	DIFFERENCE[a] (kcal/mole)	PREFERRED CONFORMATION (kcal/mole)	ALTERNATE CONFORMATION (kcal/mole)	DIFFERENCE[a] (kcal/mole)
scyllo-Inositol	3.2	10.1	-6.9	80.523	80.505	0.018
myo-Inositol	3.0	7.6	-4.6	80.441	80.415	0.026
L-chiro-Inositol	3.95	6.25	-2.3	80.440	80.435	0.005
epi-Inositol	4.5	6.8	-2.3	80.358	80.353	0.005
neo-Inositol	4.3	6.6	-2.3	80.359	80.347	0.012
muco-Inositol	4.7	4.7	0.0	80.437	80.437	0.0
allo-Inositol	4.65	4.65	0.0	80.357	80.357	0.0
cis-Inositol	7.25	7.25	0.0	80.274	80.274	0.0

[a]Difference = preferred - alternate.

for scyllo-inositol, myo-inositol, L-chiro-inositol, epi-inositol and neo-inositol are all relatively large. Only when the calculated conformational energy difference is less than 0.7 kcal/mole is a substantial percentage (20%) of the alternate conformation expected in solution (90). According to the calculated conformational energy differences, where the smallest difference is 2.3 kcal/mole, for none of the inositols should a substantial percentage of the alternate conformation be present in solution. Examination of the water solution spectra of scyllo-inositol (Fig. 15), myo-inositol (Fig. 15), epi-inositol (Fig. 16), and L-chiro-inositol (Fig. 53) show no new bands are observed illustrating no detectable amounts of the alternate conformers are present. All the solution spectra recorded closely resemble the major features of the solid state spectra. Some band broadening and loss of resolution and detail was observed in the solution spectra, which is likely due to interactions with the water.

Table XXXV also shows that for all the inositols having an alternate conformation of different energy, the vibrational energy of the alternate conformation is slightly lower than for the preferred conformation. The preferred conformation of scyllo-inositol has the highest vibrational energy but the second lowest conformational free energy, while cis-inositol has the lowest vibrational energy and the highest conformational free energy. A close examination of the calculations showed that the second term in Equation (13) contributed only about 6% to the total vibrational energy in all cases. It was also noted that this second term was always slightly higher, an average of 0.012 kcal/mole, for the alternate conformation compared to the preferred conformation.

ACKNOWLEDGMENTS

I wish to sincerely thank Dr. Rajai Atalla, the Chairman of the Thesis Advisory Committee, for his guidance and inspiration throughout the course of this thesis and for allowing me an opportunity to work with him. He has been not only an advisor, but a good friend.

I also wish to gratefully acknowlege Drs. G. A. Baum and R. D. McKelvey, who served on the Thesis Advisory Committee, for their contributions through many discussions during the course of this thesis.

I would like to especially thank H. Wells, who was always willing to give unselfishly of his broad knowledge in spectroscopy. Without his help on many of the experimental and theoretical facets of this work, the quality of this thesis would have suffered greatly.

Of upmost importance to this work, were the inositol samples given to me by Dr. Laurens Anderson and Dr. Stephen Angyal. To both of them I am deeply indebted.

There are a multitude of others to whom I am indebted for their help. S. Edwards for his many discussions and help with the computer software. K. P. Carlson for many discussions in the area of spectroscopy and concerning this work. Messrs. J. J. Bachhuber and J. O. Church for their ready willingness to help me diagnose computer and software problems and from whom I have learned a great deal. D. Beyer, F. Sweeney and the people in the Duplicating Department for their considerable effort in preparing a large majority of the many figures and tables which appear in this thesis.

I am deeply indebted to The Institute of Paper Chemistry for their financial support and for the opportunity to further my education under their fine program.

And there are others, whose sacrifice so this thesis could become a reality will always be remembered.

I especially wish to thank my parents for their invaluable guidance and endless support. I know there were many times when they wondered if I would ever get the hell out of school. Well, tis done.

LITERATURE CITED

1. Beckett, C. W., Pitzer, K. S., and Spitzer, R., J.A.C.S. 69:2488-95(1947).

2. Burkett, S. C. and Badger, R. M., J.A.C.S. 72:4397-4405(1950).

3. Kuhn, L. D., Analytical Chemistry 22(2):277-83(1950).

4. Barker, S. A., Bourne, E. J., Stacey, M., and Whiffen, D. H., J.C.S. 1954: 171-6.

5. Barker, S. A., Bourne, E. J., Stacey, M., and Whiffen, D. H., J.C.S. 1954: 3468-73.

6. Barker, S. A., Bourne, E. J., Stacey, M., and Whiffen, D. H., J.C.S. 1954: 4211-15.

7. Neely, W. B., Adv. Carbohyd. Chem. 12:13-33(1957).

8. Spedding, H., Adv. Carbohyd. Chem. 19:23-49(1964).

9. Tipson, R. S., NBS Monograph 110, June 1968. 21 p.

10. Snyder, R. G. and Schachtschneider, J. H., Spectrochim. Acta 19:85-116(1963).

11. Schachtschneider, J. H. and Snyder, R. G., Spectrochim. Acta 19:117-68(1963).

12. Snyder, R. G. and Schachtschneider, J. H., Spectrochim. Acta 21:169-95(1965).

13. Snyder, R. G. and Zerbi, G., Spectrochim. Acta 23A:391-437(1967).

14. Pickett, H. and Strauss, H., J. Chem. Phys. 53:376-88(1970).

15. Vasko, P. D., Blackwell, J., and Koenig, J. L., Carbohyd. Res. 23:407-16 (1972).

16. Cael, J. J., Koenig, J. L., and Blackwell, J., Carbohyd. Res. 32:79-91(1974).

17. Cael, J. J., Gardner, K. H., Koenig, J. L., and Blackwell, J., J. Chem. Phys. 62:1145-53(1975).

18. Pitzner, L. J. An Investigation of the Vibrational Spectra of the 1,5-Anhydro-pentitols. Doctoral Dissertation. Appleton, Wisconsin, The Institute of Paper Chemistry, 1973. 402 p.

19. Pitzner, L. J. and Atalla, R. H., Spectrochim. Acta 31A:911-29(1975).

20. Fletcher, R. and Powell, M. J. D., Computer J. 6:163-8(1963).

21. Watson, G. M. An Investigation of the Vibrational Spectra of the Pentitols and Erythritol. Doctoral Dissertation. Appleton, Wisconsin, The Institute of Paper Chemistry, 1974. 202 p.

22. Edwards, S. L. An Investigation of the Vibrational Spectra of the Pentose Sugars. Doctoral Dissertation. Appleton, Wisconsin, The Institute of Paper Chemistry, 1976. 272 p.

23. Wells, H. A. An Investigation of the Vibrational Spectra of Glucose, Galactose, and Mannose. Doctoral Dissertation. Appleton, Wisconsin, The Institute of Paper Chemistry, 1976. 482 p.

24. Pigman, W. and Horton, D. The Carbohydrates. p. 521. New York, Academic Press, Inc., 1972.

25. Shay, J. F., Skilling, S., and Stafford, R. W., Anal. Chem. 26(4):652-6 (1954).

26. Posternak, T., Biochem. Preparations 2:57(1952).

27. Stanacev, N. Z. and Kates, M., J. Org. Chem. 26:912-18(1960).

28. Angyal, S. J. and Matheson, N. K., J.A.C.S. 77:4344-6(1955).

29. Allemand, C. D., Appl. Spectroscopy 24(3):348-53(1970).

30. Rahn, L. A., Temple, P. A., and Hathaway, C. E., Appl. Spectroscopy 25(6): 675-7(1971).

31. Wilson, E. B., Decius, J. C., and Cross, P. C. Molecular Vibrations. New York, McGraw-Hill Book Co., 1955. 388 p.

32. Hilderbrandt, R., J. Mol. Spec. 44:599-601(1972).

33. Shields, P. C. Elementary Linear Algebra. New York, Worth Publishers, Inc., 1968. 349 p.

34. Rabinowitz, I. N. and Kraut, J., Acta Cryst. 17:159-68(1964).

35. Jeffrey, G. A. and Kim, H. S., Acta Cryst. B27:1812-17(1971).

36. Jeffrey, G. A. and Kim, H. S., Carbohyd. Res. 15:310-14(1970).

37. Gans, P., J.C.S.(A) 1971:2017-20.

38. Christopher, R. E. and Gans, P., J.C.S. Dalton 1975:153-8.

39. Gans, P., J. Mol. Struct. 12:411(1972).

40. Schonland, D. S. Molecular Symmetry. London, Van Nostrand Reinhold Co., 1965. 298 p.

41. Cotton, F. A. Chemical Applications of Group Theory. New York, Wiley-Interscience, 1971. 386 p.

42. Ferraro, J. R. and Ziomek, J. S. Introductory Group Theory and Its Application to Molecular Structure. New York, Plenum Press, 1976. 292 p.

43. Stoddard, J. F. Stereochemistry of Carbohydrates. New York, Wiley-Interscience, 1971. 249 p.

44. Reference 31, page 115.

45. Reference 40, page 109.

46. Reference 41, page 313.

47. Schachtschneider, J. H., Technical Report No. 231-64. Emeryville, California, Shell Development Co., 1964.

48. Schachtschneider, J. H., Technical Report No. 57-65. Emeryville, California, Shell Development Co., 1965.

49. IBM System/360 Scientific Subroutine Package Version III, 5th ed., p. 221. International Business Machine Corporation, Aug. 1970.

50. Cole, A. J. and Adamson, P. G., Acta Cryst. 25:535-9(1969).

51. Steele, D. Theory of Vibrational Spectroscopy, Philadelphia, W. B. Saunders Co., 1971. 226 p.

52. Gans, P. Vibrating Molecules, London, Chapman and Hall Ltd., 1971. 236 p.

53. Reference 31, page 93.

54. Katon, J. E., Miller, J. T., and Bently, F. F., Arch. Biochem. Biophys. 121:798-9(1967).

55. Katon, J. E., Miller, J. T., and Bently, F. F., Carbohyd. Res. 10:505-16(1969).

56. Michell, A. J., Aust. J. Chem. 21:1257-66(1968).

57. Michell, A. J., Aust. J. Chem. 23:833-8(1970).

58. Dempster, A. B. and Zerbi, G., J. Chem. Phys. 54:3600-9(1971).

59. Kogan, G. A., Tul'Chinskiĭ, V. M., Schulman, M. L., Zurabyan, S. E., and Khorlin, A. Ya., Carbohyd. Res. 26:191-200(1973).

60. Michell, A. J., Aust. J. Chem. 28:335-41(1975).

61. Posternak, T. The Cyclitols. San Francisco, California, Holden-Day Inc., 1965. 431 p.

62. Schroeder, L. R. and Baker, T., Personal communication, The Institute of Paper Chemistry.

63. Suami, T., Frieder, W. L., and Oqawa, S., Bull. Chem. Soc. Jap. 40(6):1488-95(1967).

64. Angyal, S. J., Bender, V., and Curtin, J. H., J.C.S.(C) 1966:798-800.

65. Freeman, H. C., Langs, D. A., Nockolds, C. E., and Oh, Y. L., Unpublished data.

66. Mills, J. A., Biochem. Biophys. Res. Comm. 6(6):418-21(1961/62).

67. McGavin, D. G., Natusch, D. F. S., and Young, J. F. Proceedings of the 12th International Conference on Coordination Chemistry, 1969:134-5.

68. Richards, N. J. and Williams, D. G., Carbohyd. Res. 12:409-20(1970).

69. Angyal, S. J. and Davies, K. P., Chem. Commun. 1971:500-1.

70. Angyal, S. J., Aust. J. Chem. 25:1957-66(1972).

71. Angyal, S. J., Pure Appl. Chem. 35:131-46(1973).

72. Angyal, S. J., Greeves, D., and Pickles, V. A., Carbohyd. Res. 35:165-73 (1974).

73. Angyal, S. J., Greeves, D., and Mills, J. A., Aust. J. Chem. 27:1447-56 (1974).

74. Angyal, S. J. and Hickman, R. J., Aust. J. Chem. 28:1279-87(1975).

75. Lenkinski, R. E. and Reuben, J., J.A.C.S. 98(11):3089-94(1976).

76. Angyal, S. J. and Greeves, D., Aust. J. Chem. 29:1223-30(1976).

77. Angyal, S. J., Greeves, D., Littlemore, L., and Pickles, V. A., Aust. J. Chem. 29:1231-7(1976).

78. Williams, R. M. and Atalla, R. H., J.C.S. 1975:1155-61.

79. Matsuura, H. and Miyazawa, T., Bull. Chem. Soc. Jap. 40:85-94(1967).

80. Hawkins, C. J. Absolute Configuration of Metal Complexes. p. 64. New York, Wiley-Interscience, 1971.

81. Angyal, S. J. and McHugh, D. J., J.C.S. 1957:1423-31.

82. Weissbach, A., J. Org. Chem. 23:329-30(1958).

83. Posternak, T., Lucken, E. A. C., and Szente, A., Helv. Chim. Acta 50:326-30 (1967).

84. Garegg, P. J. and Lindstrom, K., Acta Chem. Scand. 25:1559-66(1971).

85. Gorin, P. A. J. and Mazurek, M., Carbohyd. Res. 27:325-39(1973).

86. Angyal, S. J., Klavins, J. E., and Mills, J. A., Aust. J. Chem. 27:1075-86 (1974).

87. Angyal, S. J. and McHugh, D. J., Chem. Ind. 1956:1147-8.

88. Dale, J., J.C.S. 1961:922-30.

89. Durette, P. L. and Horton, D. Advances in Carbohydrate Chemistry and Biochemistry 26:49-125(1971).

90. Angyal, S. J., Aust. J. Chem. 21:2737-46(1968).

91. Reference 43, page 60.

92. Rice, O. K. Statistical Mechanics, Thermodynamics and Kinetics. p. 45. San Francisco, California, W. H. Freeman and Company, 1967.

93. Eliel, E. L., Allinger, N. L., Angyal, S. J., and Morrison, G. A. Conformational Analysis. New York, Interscience Publishers, 1965. 524 p.

94. Atalla, R. H., Personal communication, The Institute of Paper Chemistry.

95. Carlson, K. P. An Investigation of the Vibrational Spectra of the Cellodextrins. Doctoral Dissertation in progresss. Appleton, Wisconsin, The Institute of Paper Chemistry.

96. Woodward, L. A. Introduction to the theory of Molecular Vibrations and Vibrational Spectroscopy. p. 345. London, Oxford University Press, 1972.

97. Edwards, J. O., Morrison, G. C., Ross, V. F., and Schultz, J. W., J.A.C.S. 77:266-8(1955).

APPENDIX I

INSTRUMENTAL PARAMETERS

RAMAN

Instrument: SPEX Model 1401 Grating Spectrometer

Control Settings:

Slits — within the range 120-150 μm (~3 cm^{-1} resolution)

Gain — 20,000 cps or 50,000 cps scale

Scan Speed — 25 cm^{-1}/min

Time Constant — 0.25 sec

Laser Wavelength — 5145 A

Laser Power — 0.7-1.1 w

Photomultipler Tube Voltage — 1900 v

Photomultiplier Tube Temperature — -20°C

INFRARED

Instrument: Perkin-Elmer Model 621 Grating Spectrophotometer

Control Settings:	Regular Spectra	Expanded Spectra
Slit Program —	1000	1000
Gain —	5.0	5.0
Attenuator Speed —	1300	1300
Scan Time —	10 x 4	10 x 16
Scale Expansion —	1 x	1 x 4
Suppression —	6.0	6.0
Source Current —	0.8	0.8

Optics — 3900-1350 cm^{-1} - CaF_2

1350-200 cm^{-1} - CsI

APPENDIX II

INTERNAL COORDINATE DEFINITIONS AND INPUT FOR THE COMPUTER PROGRAMS CART, PAMOLE AND GMAT

Contents Page

The GMAT input as shown for the different molecules, will result in generation of both the unsymmetrized $\underset{\sim}{G}$ matrix and the $\underset{\sim}{G}$ matrix in symmetry block form.

TABLE XXXVI

INTERNAL COORDINATE DEFINITIONS FOR NEO-INOSITOL

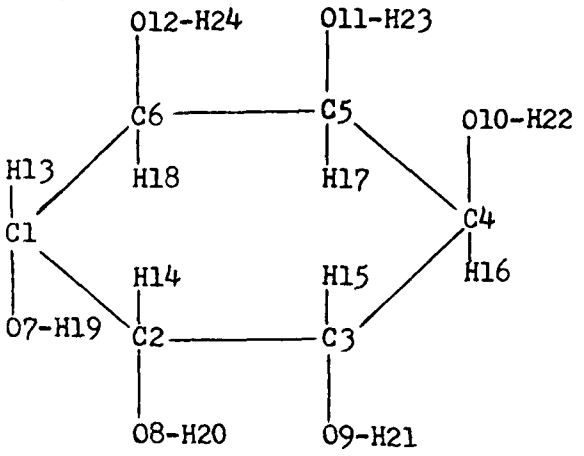

Valence Bond Coordinates

1. C1-C2	7. C1-O7	13. C1-H13	19. O7-H19
2. C2-C3	8. C2-O8	14. C2-H14	20. O8-H20
3. C3-C4	9. C3-O9	15. C3-H15	21. O9-H21
4. C4-C5	10. C4-O10	16. C4-H16	22. O10-H22
5. C5-C6	11. C5-O11	17. C5-H17	23. O11-H23
6. C6-C1	12. C6-O12	18. C6-H18	24. O12-H24

Valence Bond Angle Coordinates

25. C1-C2-C3	36. O9-C3-C4	47. H15-C3-C2	57. H15-C3-O9
26. C2-C3-C4	37. O10-C4-C3	48. H15-C3-C4	58. H16-C4-O10
27. C3-C4-C5	38. O10-C4-C5	49. H16-C4-C3	59. H17-C5-O11
28. C4-C5-C6	39. O11-C5-C4	50. H16-C4-C5	60. H18-C6-O12
29. C5-C6-C1	40. O11-C5-C6	51. H17-C5-C4	61. C1-O7-H19
30. C6-C1-C2	41. O12-C6-C5	52. H17-C5-C6	62. C2-O8-H20
31. O7-C1-C6	42. O12-C6-C1	53. H18-C6-C5	63. C3-O9-H21
32. O7-C1-C2	43. H13-C1-C6	54. H18-C6-C1	64. C4-O10-H22
33. O8-C2-C1	44. H13-C1-C2	55. H13-C1-O7	65. C5-O11-H23
34. O8-C2-C3	45. H14-C2-C1	56. H14-C2-O8	66. C6-O12-H24
35. O9-C2-C3	46. H14-C2-C3		

Valence Bond Angle Torsion Coordinates

67. C6-C1-C2-H14 O7-C1-C2-C3 H13-C1-C2-O8	70. C3-C4-C5-H17 O10-C4-C5-C6 H16-C4-C5-O11	73. H19-O7-C1-H13 H19-O7-C1-C6 H19-O7-C1-C2	76. H22-O10-C4-H16 H22-O10-C4-C3 H22-O10-C4-C5
68. C1-C2-C3-O9 O8-C2-C3-H15 H14-C2-C3-C4	71. C4-C5-C6-O12 O11-C5-C6-H18 H17-C5-C6-C1	74. H20-O8-C2-H14 H20-O8-C2-C1 H20-O8-C2-C3	77. H23-O11-C5-H17 H23-O11-C5-C4 H23-O11-C5-C6
69. C2-C3-C4-O10 O9-C3-C4-C5 H15-C3-C4-H16	72. C5-C6-C1-O7 O12-C6-C1-C2 H18-C6-C1-H13	75. H21-O9-C3-H15 H21-O9-C3-C2 H21-O9-C3-C4	78. H24-O12-C6-H18 H24-O12-C6-C5 H24-O12-C6-C1

TABLE XXXVI (Continued)

INTERNAL COORDINATE DEFINITIONS FOR MYO-INOSITOL

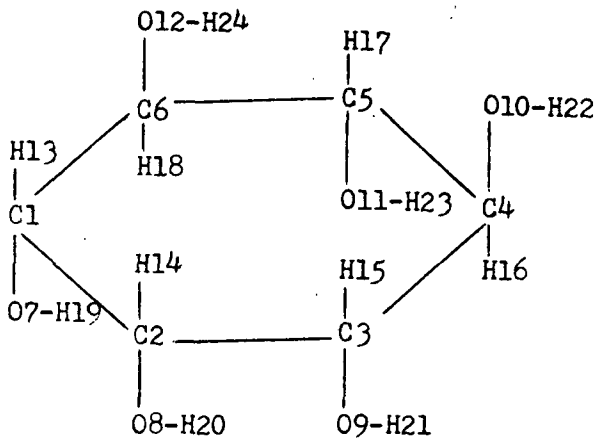

Valence Bond Coordinates

1. C1-C2	7. C1-O7	13. C1-H13	19. O7-H19
2. C2-C3	8. C2-O8	14. C2-H14	20. O8-H20
3. C3-C4	9. C3-O9	15. C3-H15	21. O9-H21
4. C4-C5	10. C4-O10	16. C4-H16	22. O10-H22
5. C5-C6	11. C5-O11	17. C5-H17	23. O11-H23
6. C6-C1	12. C6-O12	18. C6-H18	24. O12-H24

Valence Bond Angle Coordinates

25. C1-C2-C3	36. O9-C3-C4	47. H15-C3-C2	57. H15-C3-O9
26. C2-C3-C4	37. O10-C4-C3	48. H15-C3-C4	58. H16-C4-O10
27. C3-C4-C5	38. O10-C4-C5	49. H16-C4-C3	59. H17-C5-O11
28. C4-C5-C6	39. O11-C5-C4	50. H16-C4-C5	60. H18-C6-O12
29. C5-C6-C1	40. O11-C5-C6	51. H17-C5-C4	61. C1-O7-H19
30. C6-C1-C2	41. O12-C6-C5	52. H17-C5-C6	62. C2-O8-H20
31. O7-C1-C6	42. O12-C6-C1	53. H18-C6-C5	63. C3-O9-H21
32. O7-C1-C2	43. H13-C1-C6	54. H18-C6-C1	64. C4-O10-H22
33. O8-C2-C1	44. H13-C1-C2	55. H13-C1-O7	65. C5-O11-H23
34. O8-C2-C3	45. H14-C2-C1	56. H14-C2-O8	66. C6-O12-H24
35. O9-C2-C3	46. H14-C2-C3		

Valence Bond Angle Torsion Coordinates

67. C6-C1-C2-H14 H13-C1-C2-O8 O7-C1-C2-C3	70. C3-C4-C5-O11 O10-C4-C5-C6 H16-C4-C5-H17	73. H19-O7-C1-H13 H19-O7-C1-C6 H19-O7-C1-C2	76. H22-O10-C4-H16 H22-O10-C4-C3 H22-O10-C4-C5
68. C1-C2-C3-O9 H14-C2-C3-C4 O8-C2-C3-H15	71. C4-C5-C6-O12 O11-C5-C6-C1 H17-C5-C6-H18	74. H20-O8-C2-H14 H20-O8-C2-C1 H20-O8-C2-C3	77. H23-O11-C5-H17 H23-O11-C5-C4 H23-O11-C5-C6
69. C2-C3-C4-O10 H15-C3-C4-H16 O9-C3-C4-C5	72. C5-C6-C1-O7 O12-C6-C1-C2 H18-C6-C1-H13	75. H21-O9-C3-H15 H21-O9-C3-C2 H21-O9-C3-C4	78. H24-O12-C6-H18 H24-O12-C6-C5 H24-O12-C6-C1

TABLE XXXVI (Continued)

INTERNAL COORDINATE DEFINITIONS FOR EPI-INOSITOL

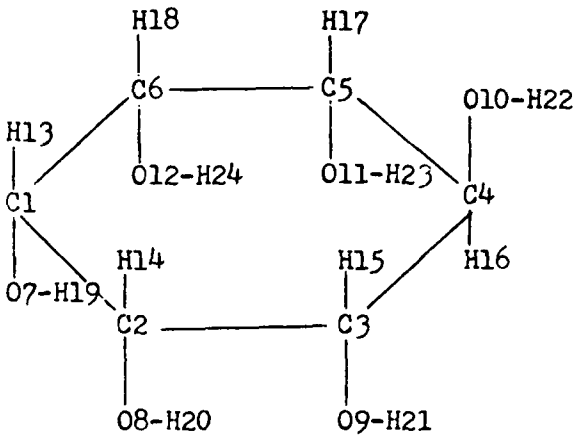

Valence Bond Coordinates

1. C1-C2	7. C1-O7	13. C1-H13	19. O7-H19
2. C2-C3	8. C2-O8	14. C2-H14	20. O8-H20
3. C3-C4	9. C3-O9	15. C3-H15	21. O9-H21
4. C4-C5	10. C4-O10	16. C4-H16	22. O10-H22
5. C5-C6	11. C5-O11	17. C5-H17	23. O11-H23
6. C6-C1	12. C6-O12	18. C6-H18	24. O12-H24

Valence Bond Angle Coordinates

25. C1-C2-C3	36. O9-C3-C4	47. H15-C3-C2	57. H15-C3-O9
26. C2-C3-C4	37. O10-C4-C3	48. H15-C3-C4	58. H16-C4-O10
27. C3-C4-C5	38. O10-C4-C5	49. H16-C4-C3	59. H17-C5-O11
28. C4-C5-C6	39. O11-C5-C4	50. H16-C4-C5	60. H18-C6-O12
29. C5-C6-C1	40. O11-C5-C6	51. H17-C5-C4	61. C1-O7-H19
30. C6-C1-C2	41. O12-C6-C5	52. H17-C5-C6	62. C2-O8-H20
31. O7-C1-C6	42. O12-C6-C1	53. H18-C6-C5	63. C3-O9-H21
32. O7-C1-C2	43. H13-C1-C6	54. H18-C6-C1	64. C4-O10-H22
33. O8-C2-C1	44. H13-C1-C2	55. H13-C1-O7	65. C5-O11-H23
34. O8-C2-C3	45. H14-C2-C1	56. H14-C2-O8	66. C6-O12-H24
35. O9-C2-C3	46. H14-C2-C3		

Valence Bond Angle Torsion Coordinates

67. C6-C1-C2-H14 O7-C1-C2-C3 H13-C1-C2-O9	70. C3-C4-C5-O11 O10-C4-C5-C6 H16-C4-C5-H17	73. H19-O7-C1-H13 H19-O7-C1-C6 H19-O7-C1-C2	76. H22-O10-C4-H16 H22-O10-C4-C5 H22-O10-C4-C3
68. C1-C2-C3-O9 O8-C2-C3-H15 H14-C2-C3-C4	71. C4-C5-C6-H18 O11-C5-C6-C1 H17-C5-C6-O12	74. H20-O8-C2-H14 H20-O8-C2-C1 H20-O8-C2-C3	77. H23-O11-C5-H17 H23-O11-C5-C4 H23-O11-C5-C6
69. C2-C3-C4-O10 O9-C3-C4-C5 H15-C3-C4-H16	72. C5-C6-C1-O7 O12-C6-C1-H13 H18-C6-C1-C2	75. H21-O9-C3-H15 H21-O9-C3-C2 H21-O9-C3-C4	78. H24-O12-C6-H18 H24-O12-C6-C5 H24-O12-C6-C1

TABLE XXXVI (Continued)

INTERNAL COORDINATE DEFINITIONS FOR CIS-INOSITOL

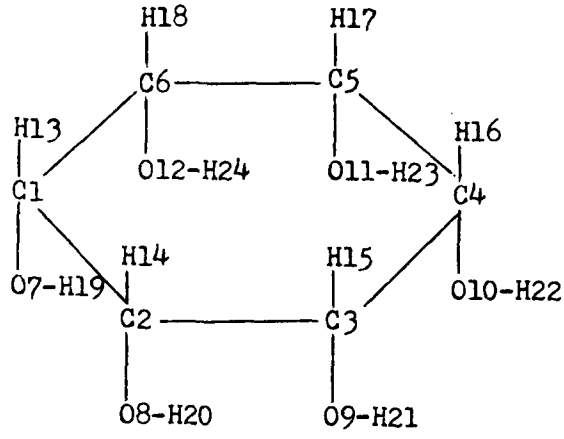

Valence Bond Coordinates

1. C1-C2	7. C1-O7	13. C1-H13	19. O7-H19
2. C2-C3	8. C2-O8	14. C2-H14	20. O8-H20
3. C3-C4	9. C3-O9	15. C3-H15	21. O9-H21
4. C4-C5	10. C4-O10	16. C4-H16	22. O10-H22
5. C5-C6	11. C5-O11	17. C5-H17	23. O11-H23
6. C6-C1	12. C6-O12	18. C6-H18	24. O12-H24

Valence Bond Angle Coordinates

25. C1-C2-C3	36. O9-C3-C4	47. H15-C3-C2	57. H15-C3-O9
26. C2-C3-C4	37. O10-C4-C3	48. H15-C3-C4	58. H16-C4-O10
27. C3-C4-C5	38. O10-C4-C5	49. H16-C4-C3	59. H17-C5-O11
28. C4-C5-C6	39. O11-C5-C4	50. H16-C4-C5	60. H18-C6-O12
29. C5-C6-C1	40. O11-C5-C6	51. H17-C5-C4	61. C1-O7-H19
30. C6-C1-C2	41. O12-C6-C5	52. H17-C5-C6	62. C2-O8-H20
31. O7-C1-C6	42. O12-C6-C1	53. H18-C6-C5	63. C3-O9-H21
32. O7-C1-C2	43. H13-C1-C6	54. H18-C6-C1	64. C4-O10-H22
33. O8-C2-C1	44. H13-C1-C2	55. H13-C1-O7	65. C5-O11-H23
34. O8-C2-C3	45. H14-C2-C1	56. H14-C2-O8	66. C6-O12-H24
35. O9-C2-C3	46. H14-C2-C3		

Valence Bond Angle Torsion Coordinates

67. C6-C1-C2-H14 O7-C1-C2-C3 H13-C1-C2-O8	70. C3-C4-C5-O11 O10-C4-C5-H17 H16-C4-C5-C6	73. H19-O7-C1-H13 H19-O7-C1-C6 H19-O7-C1-C2	76. H22-O10-C4-H16 H22-O10-C4-C3 H22-O10-C4-C5
68. C1-C2-C3-O9 O8-C2-C3-H15 H14-C2-C3-C4	71. C4-C5-C6-H18 O11-C5-C6-C1 H17-C5-C6-O12	74. H20-O8-C2-H14 H20-O8-C2-C1 H20-O8-C2-C3	77. H23-O11-C5-H17 H23-O11-C5-C4 H23-O11-C5-C6
69. C2-C3-C4-H16 O9-C3-C4-C5 H15-C3-C4-O10	72. C5-C6-C1-O7 O12-C6-C1-H13 H18-C6-C1-C2	75. H21-O9-C3-H15 H21-O9-C3-C2 H21-O9-C3-C4	78. H24-O12-C6-H18 H24-O12-C6-C5 H24-O12-C6-C1

TABLE XXXVI (Continued)

INTERNAL COORDINATE DEFINITIONS FOR L-CHIRO-INOSITOL

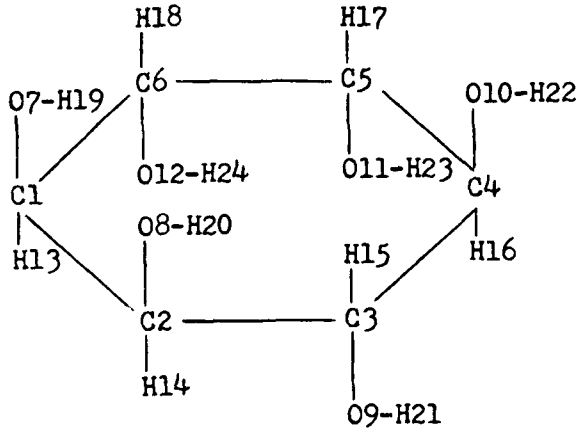

Valence Bond Coordinates

1. C1-C2	7. C1-O7	13. C1-H13	19. O7-H19
2. C2-C3	8. C2-O8	14. C2-H14	20. O8-H20
3. C3-C4	9. C3-O9	15. C3-H15	21. O9-H21
4. C4-C5	10. C4-O10	16. C4-H16	22. O10-H22
5. C5-C6	11. C5-O11	17. C5-H17	23. O11-H23
6. C6-C1	12. C6-O12	18. C6-H18	24. O12-H24

Valence Bond Angle Coordinates

25. C1-C2-C3	36. O9-C3-C4	47. H15-C3-C2	57. H15-C3-O9
26. C2-C3-C4	37. O10-C4-C3	48. H15-C3-C4	58. H16-C4-O10
27. C3-C4-C5	38. O10-C4-C5	49. H16-C4-C3	59. H17-C5-O11
28. C4-C5-C6	39. O11-C5-C4	50. H16-C4-C5	60. H18-C6-O12
29. C5-C6-C1	40. O11-C5-C6	51. H17-C5-C4	61. C1-O7-H19
30. C6-C1-C2	41. O12-C6-C5	52. H17-C5-C6	62. C2-O8-H20
31. O7-C1-C6	42. O12-C6-C1	53. H18-C6-C5	63. C3-O9-H21
32. O7-C1-C2	43. H13-C1-C6	54. H18-C6-C1	64. C4-O10-H22
33. O8-C2-C1	44. H13-C1-C2	55. H13-C1-O7	65. C5-O11-H23
34. O8-C2-C3	45. H14-C2-C1	56. H14-C2-O8	66. C6-O12-H24
35. O9-C2-C3	46. H14-C2-C3		

Valence Bond Angle Torsion Coordinates

67. C6-C1-C2-O8 O7-C1-C2-H14 H13-C1-C2-C3	70. C3-C4-C5-O11 O10-C4-C5-C6 H16-C4-C5-H17	73. H19-O7-C1-H13 H19-O7-C1-C6 H19-O7-C1-C2	76. H22-O10-C4-H16 H22-O10-C4-C3 H22-O10-C4-C5
68. C1-C2-C3-O9 O8-C2-C3-C4 H14-C2-C3-H15	71. C4-C5-C6-H18 O11-C5-C6-C1 H17-C5-C6-O12	74. H20-O8-C2-H14 H20-O8-C2-C1 H20-O8-C2-C3	77. H23-O11-C5-H17 H23-O11-C5-C4 H23-O11-C5-C6
69. C2-C3-C4-O10 O9-C3-C4-C5 H15-C3-C4-H16	72. C5-C6-C1-H13 O12-C6-C1-O7 H18-C6-C1-C2	75. H21-O9-C3-H15 H21-O9-C3-C2 H21-O9-C3-C4	78. H24-O12-C6-H18 H24-O12-C6-C5 H24-O12-C6-C1

TABLE XXXVI (Continued)

INTERNAL COORDINATE DEFINITIONS FOR MUCO-INOSITOL

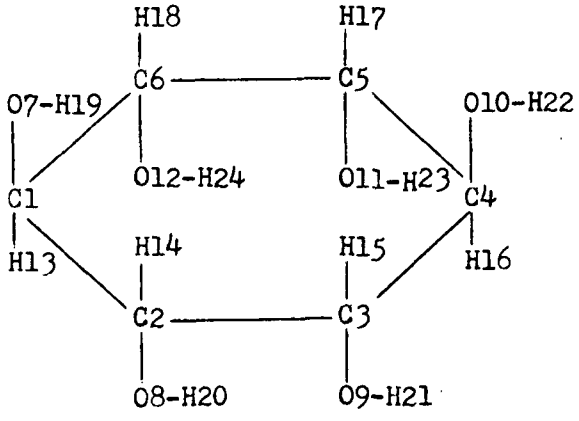

Valence Bond Coordinates

1. C1-C2	7. C1-O7	13. C1-H13	19. O7-H19
2. C2-C3	8. C2-O8	14. C2-H14	20. O8-H20
3. C3-C4	9. C3-O9	15. C3-H15	21. O9-H21
4. C4-C5	10. C4-O10	16. C4-H16	22. O10-H22
5. C5-C6	11. C5-O11	17. C5-H17	23. O11-H23
6. C6-C1	12. C6-O12	18. C6-H18	24. O12-H24

Valence Bond Angle Coordinates

25. C1-C2-C3	36. O9-C3-C4	47. H15-C3-C2	57. H15-C3-O9
26. C2-C3-C4	37. O10-C4-C3	48. H15-C3-C4	58. H16-C4-O10
27. C3-C4-C5	38. O10-C4-C5	49. H16-C4-C3	59. H17-C5-O11
28. C4-C5-C6	39. O11-C5-C4	50. H16-C4-C5	60. H18-C6-O12
29. C5-C6-C1	40. O11-C5-C6	51. H17-C5-C4	61. C1-O7-H19
30. C6-C1-C2	41. O12-C6-C5	52. H17-C5-C6	62. C2-O8-H20
31. O7-C1-C6	42. O12-C6-C1	53. H18-C6-C5	63. C3-O9-H21
32. O7-C1-C2	43. H13-C1-C6	54. H18-C6-C1	64. C4-O10-H22
33. O8-C2-C1	44. H13-C1-C2	55. H13-C1-O7	65. C5-O11-H23
34. O8-C2-C3	45. H14-C2-C1	56. H14-C2-O8	66. C6-O12-H24
35. O9-C2-C3	46. H14-C2-C3		

Valence Bond Angle Torsion Coordinates

67. C6-C1-C2-H14 O7-C1-C2-O8 H13-C1-C2-C3	70. C3-C4-C5-O11 O10-C4-C5-C6 H16-C4-C5-H17	73. H19-O7-C1-H13 H19-O7-C1-C6 H19-O7-C1-C2	76. H22-O10-C4-H16 H22-O10-C4-C5 H22-O10-C4-C3
68. C1-C2-C3-O9 O8-C2-C3-H15 H14-C2-C3-C4	71. C4-C5-C6-H18 O11-C5-C6-C1 H17-C5-C6-O12	74. H20-O8-C2-H14 H20-O8-C2-C1 H20-O8-C2-C3	77. H23-O11-C5-H17 H23-O11-C5-C6 H23-O11-C5-C4
69. C2-C3-C4-O10 O9-C3-C4-C5 H15-C3-C4-H16	72. C5-C6-C1-H13 O12-C6-C1-O7 H18-C6-C1-C2	75. H21-O9-C3-H15 H21-O9-C3-C4 H21-O9-C3-C2	78. H24-O12-C6-H18 H24-O12-C6-C5 H24-O12-C6-C1

TABLE XXXVII

CART INPUT FOR THE INOSITOLS

```
-09
-09  24   0   1
  SCYLLO-INOSITOL    C-C 1.525   C-O 1.425   C-H 1.10    O-H 0.97
     ALL ANGLES ASSUMED TETRAHEDRAL      DIHEDRAL ANGLES 60
  1
  2  1        1.525
  3  2  1     1.525        0.0
  4  3  2  1  1.525          0.0          60.
  5  4  3  2  1.525          0.0         -60.
  6  5  4  3  1.525            0.0        60.
  7  1  2  6  1.425          0.0         -120.
  8  2  3  1  1.425            0.0        120.
  9  3  4  2  1.425          0.0         -120.
 10  4  5  3 1.425            0.0         120.
 11  5  6  4 1.425           0.0         -120.
 12  6  1  5  1.425             0.0        120.
 13  1  2  6  1.10           0.0          120.
 14  2  3  1  1.10             0.0        -120.
 15  3  4  2  1.10           0.0          120.
 16  4  5  3  1.10           0.0         -120.
 17  5  6  4  1.10           0.0          120.
 18  6  1  5  1.10            0.0        -120.
 19  7  1 13  0.97            0.0         180.
 20  8  2 14  0.97            0.0         180.
 21  9  3 15  0.97            0.0         180.
 22 10  4 16  0.97            0.0         180.
 23 11  5 17  0.97            0.0         180.
 24 12  6 18   0.97           0.0         180.
```

```
-09
-09  24   0   1
     NEO-INOSITOL    C-C 1.525   C-O 1.425   C-H 1.10    O-H 0.97
     ALL ANGLES ASSUMED TETRAHEDRAL      DIHEDRAL ANGLES 60
  1
  2  1        1.525
  3  2  1     1.525        0.0
  4  3  2  1  1.525          0.0          60.
  5  4  3  2  1.525          0.0         -60.
  6  5  4  3  1.525            0.0        60.
  7  1  2  6  1.425          0.0         -120.
  8  2  3  1  1.425            0.0        -120.
  9  3  4  2  1.425          0.0         -120.
 10  4  5  3 1.425            0.0         120.
 11  5  6  4 1.425           0.0          120.
 12  6  1  5  1.425             0.0        120.
 13  1  2  6  1.10           0.0          120.
 14  2  3  1  1.10             0.0        120.
 15  3  4  2  1.10           0.0          120.
 16  4  5  3  1.10           0.0         -120.
 17  5  6  4  1.10           0.0         -120.
 18  6  1  5  1.10            0.0        -120.
 19  7  1 13  0.97            0.0         180.
 20  8  2 14  0.97            0.0         180.
 21  9  3 15  0.97            0.0         180.
 22 10  4 16  0.97            0.0         180.
 23 11  5 17  0.97            0.0         180.
 24 12  6 18   0.97           0.0         180.
999
```

```
-09
-09  24   0   1
     MYO-INOSITOL    C-C 1.525   C-O 1.425   C-H 1.10    O-H 0.97
     ALL ANGLES ASSUMED TETRAHEDRAL      DIHEDRAL ANGLES 60
  1
  2  1        1.525
  3  2  1     1.525        0.0
  4  3  2  1  1.525          0.0          60.
  5  4  3  2  1.525          0.0         -60.
  6  5  4  3  1.525            0.0        60.
  7  1  2  6  1.425          0.0         -120.
  8  2  3  1  1.425            0.0        -120.
  9  3  4  2  1.425          0.0         -120.
 10  4  5  3 1.425            0.0         120.
 11  5  6  4 1.425           0.0          -120.
 12  6  1  5  1.425             0.0        120.
 13  1  2  6  1.10           0.0          120.
 14  2  3  1  1.10             0.0        120.
 15  3  4  2  1.10           0.0          120.
 16  4  5  3  1.10           0.0         -120.
 17  5  6  4  1.10           0.0          120.
 18  6  1  5  1.10            0.0        -120.
 19  7  1 13  0.97            0.0         180.
 20  8  2 14  0.97            0.0         180.
 21  9  3 15  0.97            0.0         180.
 22 10  4 16  0.97            0.0         180.
 23 11  5 17  0.97            0.0         180.
 24 12  6 18   0.97           0.0         180.
```

```
-09
-09  24   0   1
     EPI-INOSITOL    C-C 1.525   C-O 1.425   C-H 1.10    O-H 0.97
     ALL ANGLES ASSUMED TETRAHEMAL       DIHEDRAL ANGLES 60
  1
  2  1        1.525
  3  2  1     1.525        0.0
  4  3  2  1  1.525          0.0          60.
  5  4  3  2  1.525          0.0         -60.
  6  5  4  3  1.525            0.0        60.
  7  1  2  6  1.425          0.0         -120.
  8  2  3  1  1.425            0.0        -120.
  9  3  4  2  1.425          0.0         -120.
 10  4  5  3  1.425          0.0          120.
 11  5  6  4  1.425          0.0         -120.
 12  6  1  5  1.425             0.0        -120.
 13  1  2  6  1.10           0.0          120.
 14  2  3  1  1.10             0.0        120.
 15  3  4  2  1.10           0.0          120.
 16  4  5  3  1.10           0.0         -120.
 17  5  6  4  1.10           0.0          120.
 18  6  1  5  1.10            0.0        120.
 19  7  1 13  0.97            0.0         180.
 20  8  2 14  0.97            0.0         -60.
 21  9  3 15  0.97            0.0         180.
 22 10  4 16  0.97            0.0         180.
 23 11  5 17  0.97            0.0         180.
 24 12  6 18   0.97           0.0          60.
999
```

TABLE XXXVII (Continued)

CART INPUT FOR THE INOSITOLS

```
-09
-09  24   0   1
     CIS-INOSITOL   C-C 1.525   C-O 1.425   C-H 1.10    O-H 0.97
     ALL ANGLES ASSUMED TETRAHEDRAL      DIHEDRAL ANGLES 60
   1
   2  1          1.525
   3  2  1       1.525       0.0
   4  3  2  1    1.525         0.0          60.
   5  4  3  2    1.525         0.0         -60.
   6  5  4  3    1.525         0.0          60.
   7  1  2  6    1.425         0.0        -120.
   8  2  3  1    1.425         0.0        -120.
   9  3  4  2    1.425         0.0        -120.
  10  4  5  3    1.425         0.0        -120.
  11  5  6  4    1.425         0.0        -120.
  12  6  1  5    1.425         0.0        -120.
  13  1  2  6    1.10          0.0         120.
  14  2  3  1    1.10          0.0         120.
  15  3  4  2    1.10          0.0         120.
  16  4  5  3    1.10          0.0         120.
  17  5  6  4    1.10          0.0         120.
  18  6  1  5    1.10          0.0         120.
  19  7  1 13    0.97          0.0        180.
  20  8  2 14    0.97          0.0         0.0
  21  9  3 15    0.97          0.0        180.
  22 10  4 16    0.97          0.0         0.0
  23 11  5 17    0.97          0.0        180.
  24 12  6 18     0.97         0.0         0.0
```

```
-09
-09  24   0   1
     L-CHIRO-INOSITOL   C-C 1.525   C-O 1.425   C-H 1.10   O-H 0.97
     ALL ANGLES ASSUMED TETRAHEDRAL      DIHEDRAL ANGLES 60
   1
   2  1          1.525
   3  2  1       1.525       0.0
   4  3  2  1    1.525         0.0          60.
   5  4  3  2    1.525         0.0         -60.
   6  5  4  3    1.525         0.0          60.
   7  1  2  6    1.425         0.0         120.
   8  2  3  1    1.425         0.0         120.
   9  3  4  2    1.425         0.0        -120.
  10  4  5  3 1.425            0.0         120.
  11  5  6  4 1.425            0.0        -120.
  12  6  1  5    1.425         0.0        -120.
  13  1  2  6    1.10          0.0        -120.
  14  2  3  1    1.10          0.0        -120.
  15  3  4  2    1.10          0.0         120.
  16  4  5  3    1.10          0.0        -120.
  17  5  6  4    1.10          0.0         120.
  18  6  1  5    1.10          0.0         120.
  19  7  1 13    0.97          0.0          60.
  20  8  2 14    0.97          0.0         180.
  21  9  3 15    0.97          0.0         180.
  22 10  4 16    0.97          0.0         180.
  23 11  5 17    0.97          0.0         180.
  24 12  6 18     0.97         0.0          60.
999
```

```
-09
-09  24   0   1
     MUCO-INOSITOL   C-C 1.525   C-O 1.425   C-H 1.10   O-H 0.97
     ALL ANGLES ASSUMED TETRAHEDRAL      DIHEDRAL ANGLES 60
   1
   2  1          1.525
   3  2  1       1.525       0.0
   4  3  2  1    1.525         0.0          60.
   5  4  3  2    1.525         0.0         -60.0
   6  5  4  3    1.525         0.0          60.
   7  1  2  6    1.425         0.0         120.
   8  2  3  1    1.425         0.0        -120.
   9  3  4  2    1.425         0.0        -120.
  10  4  5  3 1.425            0.0         120.
  11  5  6  4 1.425            0.0        -120.
  12  6  1  5    1.425         0.0        -120.
  13  1  2  6    1.10          0.0        -120.
  14  2  3  1    1.10          0.0         120.
  15  3  4  2    1.10          0.0         120.
  16  4  5  3    1.10          0.0        -120.
  17  5  6  4    1.10          0.0         120.
  18  6  1  5    1.10          0.0         120.
  19  7  1 13    0.97          0.0         180.
  20  8  2 14    0.97          0.0         -60.
  21  9  3 15    0.97          0.0         180.
  22 10  4 16    0.97          0.0         180.
  23 11  5 17    0.97          0.0         180.
  24 12  6 18     0.97         0.0          60.
999
```

TABLE XXXVIII

PAMOLE INPUT FOR THE INOSITOLS

```
-09  24   5   1   1.0   0.0  0.21
                SCYLLO-INOSITOL
SCALE  1.2
SIZES C   .29O   .27H   .12
C1    0.000  0.000  0.000 C2   O7   H13  C6
C2    1.525  0.000  0.000 C1   O8   H14  C3
C3    2.033  1.438  0.000 C2   O9   H15  C4
C4    1.525  2.157 -1.245 C3   O10  H16  C5
C5    0.000  2.157 -1.245 C4   O11  H17  C6
C6   -0.508  0.719 -1.245 C5   O12  H18  C1
O7   -0.475 -1.344  0.000 C1   H19
O8    2.000 -0.672  1.164 C2   H20
O9    3.458  1.437  0.000 C3   H21
O10   2.000  3.500 -1.245 C4   H22
O11  -0.475  2.828 -2.409 C5   H23
O12  -1.933  0.719 -1.245 C6   H24
H13  -0.367  0.519  0.898 C1
H14   1.892 -0.519 -0.898 C2
H15   1.667  1.956  0.898 C3
H16   1.892  1.638 -2.143 C4
H17  -0.367  2.675 -0.347 C5
H18  -0.142  0.200 -2.143 C6
H19  -0.152 -1.801 -0.792 O7
H20   1.667 -0.214  1.956 O8
H21   3.782  0.981 -0.792 O9
H22   1.667  3.957 -0.453 O10
H23  -0.152  2.371 -3.201 O11
H24  -2.257  1.176 -0.453 O12
VIEW     5.  5. 15.
VIEW     1.  1. 20.
VIEW    15.-20. 15.
VIEW    -5. -2.  5.
VIEW     5.  5.  0.
999
```

```
-09  24   5   1   1.0   0.0  0.21
                NEO-INOSITOL
SCALE  1.2
SIZES C   .29O   .27H   .12
C1    0.000  0.000  0.000 C2   O7   H13  C6
C2    1.525  0.000  0.000 C1   O8   H14  C3
C3    2.033  1.438  0.000 C2   O9   H15  C4
C4    1.525  2.157 -1.245 C3   O10  H16  C5
C5    0.000  2.157 -1.245 C4   O11  H17  C6
C6   -0.508  0.719 -1.245 C5   O12  H18  C1
O7   -0.475 -1.344  0.000 C1   H19
O8    2.000 -0.672 -1.164 C2   H20
O9    3.458  1.437  0.000 C3   H21
C10   2.000  3.500 -1.245 C4   H22
O11  -0.475  2.828 -0.082 C5   H23
O12  -1.933  0.719 -1.245 C6   H24
H13  -0.367  0.519  0.898 C1
H14   1.892 -0.519  0.898 C2
H15   1.667  1.956  0.898 C3
H16   1.892  1.638 -2.143 C4
H17  -0.367  2.675 -2.143 C5
H18  -0.142  0.200 -2.143 C6
H19  -0.152 -1.801 -0.792 O7
H20   1.676 -0.214 -1.956 O8
H21   3.782  0.981 -0.792 O9
H22   1.667  3.957 -0.453 O10
H23  -0.152  2.371  0.710 O11
H24  -2.257  1.176 -0.453 O12
VIEW     5.  5. 15.
VIEW     1.  1. 20.
VIEW    15.-20. 15.
VIEW    -5. -2.  5.
VIEW     5.  5.  0.
999
```

```
-09  24   6   1   1.0   0.0  0.21
                MYO-INOSITOL
SCALE  1.2
SIZES C   .29O   .27H   .12
C1    0.000  0.000  0.000 C2   O7   H13  C6
C2    1.525  0.000  0.000 C1   O8   H14  C3
C3    2.033  1.438  0.000 C2   O9   H15  C4
C4    1.525  2.157 -1.245 C3   O10  H16  C5
C5    0.000  2.157 -1.245 C4   O11  H17  C6
C6   -0.508  0.719 -1.245 C5   O12  H18  C1
O7   -0.475 -1.344  0.000 C1   H19
O8    2.000 -0.672 -1.164 C2   H20
O9    3.458  1.437  0.000 C3   H21
O10   2.000  3.500 -1.245 C4   H22
O11  -0.475  2.828 -2.409 C5   H23
O12  -1.933  0.719 -1.245 C6   H24
H13  -0.367  0.519  0.898 C1
H14   1.892 -0.519  0.898 C2
H15   1.667  1.956  0.898 C3
H16   1.892  1.638 -2.143 C4
H17  -0.367  2.675 -0.347 C5
H18  -0.142  0.200 -2.143 C6
H19  -0.152 -1.801 -0.792 O7
H20   1.667 -0.214 -1.956 O8
H21   3.782  0.981 -0.792 O9
H22   1.667  3.957 -0.453 O10
H23  -0.152  2.371 -3.201 O11
H24  -2.257  1.176 -0.453 O12
VIEW     5.  5. 15.
VIEW     5.  5.  5.
VIEW    15.-20. 15.
VIEW    -5. -2.  5.
VIEW    -5. -2. 20.
VIEW     5.  5.  0.
999
```

```
-09  24   5   1   1.0   0.0  0.21
                EPI-INOSITOL
SCALE  1.2
SIZES C   .29O   .27H   .12
C1    0.000  0.000  0.000 C2   O7   H13  C6
C2    1.525  0.000  0.000 C1   O8   H14  C3
C3    2.033  1.438  0.000 C2   O9   H15  C4
C4    1.525  2.157 -1.245 C3   O10  H16  C5
C5    0.000  2.157 -1.245 C4   O11  H17  C6
C6   -0.508  0.719 -1.245 C5   O12  H18  C1
O7   -0.475 -1.344  0.000 C1   H19
O8    2.000 -0.672 -1.164 C2   H20
O9    3.458  1.437  0.000 C3   H21
O10   2.000  3.500 -1.245 C4   H22
O11  -0.475  2.828 -2.409 C5   H23
O12  -0.033  0.047 -2.409 C6   H24
H13  -0.367  0.519  0.898 C1
H14   1.892 -0.519  0.898 C2
H15   1.667  1.956  0.898 C3
H16   1.892  1.638 -2.143 C4
H17  -0.367  2.675 -0.347 C5
H18  -1.608  0.719 -1.245 C6
H19  -0.152 -1.801 -0.792 O7
H20   1.667 -1.586 -1.164 O8
H21   3.782  0.981 -0.792 O9
H22   1.667  3.957 -0.453 O10
H23  -0.152  2.371 -3.201 O11
H24  -0.357 -0.867 -2.409 O12
VIEW     5.  2.  5.
VIEW     0. -5. -5.
VIEW     0. 10.  3.
VIEW     0.  0.-10.
VIEW     1. 10.  2.
999
```

TABLE XXXVIII (Continued)

PAMOLE INPUT FOR THE INOSITOLS

```
-09  24   5   1   1.0   0.0  0.21
                CIS-INOSITOL
SCALE  1.2
SIZES C   .290    .27H    .12
C1    0.000   0.000   0.000 C2    O7    H13   C6
C2    1.525   0.000   0.000 C1    O8    H14   C3
C3    2.033   1.438   0.000 C2    O9    H15   C4
C4    1.525   2.157  -1.245 C3    O10   H16   C5
C5    0.000   2.157  -1.245 C4    O11   H17   C6
C6   -0.508   0.719  -1.245 C5    O12   H18   C1
O7   -0.475  -1.344   0.000 C1    H19
O8    2.000  -0.672  -1.164 C2    H20
O9    3.458   1.437   0.000 C3    H21
O10   2.000   1.485  -2.409 C4    H22
O11  -0.475   2.828  -2.409 C5    H23
O12  -0.033   0.047  -2.409 C6    H24
H13  -0.367   0.519   0.898 C1
H14   1.892  -0.519   0.898 C2
H15   1.667   1.956   0.898 C3
H16   1.892   3.194  -1.245 C4
H17  -0.367   2.675  -0.347 C5
H18  -1.608   0.719  -1.245 C6
H19  -0.152  -1.801  -0.792 O7
H20   2.539  -1.434  -0.900 O8
H21   3.782   0.981  -0.792 O9
H22   2.539   2.095  -2.937
H23  -0.152   2.371  -3.201 O11
H24  -0.788  -0.258  -2.937 O12
VIEW    5.   5.  15.
VIEW    1.   1.  20.
VIEW   15.-20.  15.
VIEW   -5.  -2.   5.
VIEW    5.   5.   0.
999
```

```
-09  24   6   1   1.0   0.0  0.21
              L-CHIRO-INOSITOL
SCALE  1.2
SIZES C   .290    .27H    .12
C1    0.000   0.000   0.000 C2    O7    H13   C6
C2    1.525   0.000   0.000 C1    O8    H14   C3
C3    2.033   1.438   0.000 C2    O9    H15   C4
C4    1.525   2.157  -1.245 C3    O10   H16   C5
C5    0.000   2.157  -1.245 C4    O11   H17   C6
C6   -0.508   0.719  -1.245 C5    O12   H18   C1
O7   -0.475   0.672   1.164 C1    H19
O8    2.000  -0.672   1.164 C2    H20
O9    3.458   1.437   0.000 C3    H21
O10   2.000   3.500  -1.245 C4    H22
O11  -0.475   2.828  -2.409 C5    H23
O12  -0.033   0.047  -2.409 C6    H24
H13  -0.367  -1.037   0.000 C1
H14   1.892  -0.519  -0.898 C2
H15   1.667   1.956   0.898 C3
H16   1.892   1.638  -2.143 C4
H17  -0.367   2.675  -0.347 C5
H18  -1.608   0.719  -1.245 C6
H19  -1.445   0.672   1.164 O7
H20   1.667  -0.214   1.956 O8
H21   3.782   0.981  -0.792 O9
H22   1.677   3.957  -0.453 O10
H23  -0.152   2.371  -3.201 O11
H24  -0.357  -0.867  -2.409 O12
VIEW    5.   5.  15.
VIEW    5.   5.   5.
VIEW   15.-20.  15.
VIEW   -5.  -2.   5.
VIEW   -5.  -2.  20.
VIEW    5.   5.   0.
999
```

```
-09  24   6   1   1.0   0.0  0.21
                MUCO-INOSITOL
SCALE  1.2
SIZES C   .290    .27H    .12
C1    0.000   0.000   0.000 C2    O7    H13   C6
C2    1.525   0.000   0.000 C1    O8    H14   C3
C3    2.033   1.438   0.000 C2    O9    H15   C4
C4    1.525   2.157  -1.245 C3    O10   H16   C5
C5    0.000   2.157  -1.245 C4    O11   H17   C6
C6   -0.508   0.719  -1.245 C5    O12   H18   C1
O7   -0.475   0.672   1.164 C1    H19
O8    2.000  -0.672  -1.164 C2    H20
O9    3.458   1.437   0.000 C3    H21
O10   2.000   3.500  -1.245 C4    H22
O11  -0.475   2.828  -2.409 C5    H23
O12  -0.033   0.047  -2.409 C6    H24
H13  -0.367  -1.037   0.000 C1
H14   1.892  -0.519   0.898 C2
H15   1.667   1.956   0.898 C3
H16   1.892   1.638  -2.143 C4
H17  -0.367   2.675  -0.347 C5
H18  -1.608   0.719  -1.245 C6
H19  -0.152   1.586   1.164 O7
H20   1.667  -1.586  -1.164 O8
H21   3.782   0.981  -0.792 O9
H22   1.677   3.957  -0.453 O10
H23  -0.152   2.371  -3.201 O11
H24  -0.357  -0.867  -2.409 O12
VIEW    5.   5.  15.
VIEW    5.   5.   5.
VIEW   15.-20.  15.
VIEW   -5.  -2.   5.
VIEW   -5.  -2.  20.
VIEW    5.   5.   0.
999
```

TABLE XXXIX. GMAT INPUT FOR SCYLLO-INOSITOL

```
-09
-09     1  24   78  1   6    0   0
   SCYLLO-INOSITOL - SYMMETRIZED AND UNSYMMETRIZED G MATRIX
   TETRAHEDRAL STRUCTURE - C-C 1.525  C-O 1.425  C-H 1.10  O-H 0.97
 1  2    1.525000   1  3   -2.033332   2  3    1.437781   1  4    1.524998
 2  4    2.156676   3  4   -1.245157   2  4   -2.156675   3  5   -1.245154
 1  6   -0.508336   2  6    0.718892   3  6   -1.245153   1  7   -0.475000
 2  7   -1.343501   1  8    1.999998   2  8   -0.671751   3  8    1.163507
 1  9    3.458330   2  9    1.437781   1 10    1.999995   2 10    3.500177
 3 10   -1.245154   1 11   -0.475006   2 11    2.828425   3 11   -2.408660
 1 12   -1.933335   2 12    0.718892   3 12   -1.245149   1 13   -0.366666
 2 13   -0.518544   3 13    0.898147   1 14    1.891665   2 14   -0.518545
 3 14   -0.858147   1 15    1.666663   2 15    1.956326   3 15    0.898147
 1 16    1.891661   2 16    1.638130   3 16   -2.143302   1 17   -0.366669
 2 17    2.675220   3 17   -0.347007   1 18   -0.141670   2 18    0.200348
 3 18   -2.143300   1 19   -0.151666   2 19   -1.800761   3 19   -0.192004
 1 20    1.676662   2 20   -0.214488   3 20    1.955508   1 21    3.781663
 2 21    0.980521   3 21   -0.792005   1 22    1.676661   2 22    3.957436
 3 22   -0.453150   1 23   -0.151674   2 23    2.371161   3 23   -3.200661
 1 24   -2.256665   2 24    1.176154   3 24   -0.453144  -1  0    0.0
 1  1  1  2  0  0  0  0  C  2  1  2  3  0  0  0  3  1  3  4  0  0  0  0  0
 4  1  4  5  0  0  0  0  C  5  1  5  6  0  0  0  6  1  6  1  0  0  0  0  0
 7  1  1  7  0  0  0  0  C  8  1  2  8  0  0  0  9  1  3  9  0  0  0  0  0
10  1  4 10  0  0  0  0  C 11  1  5 11  0  0  0 12  1  6 12  0  0  0  0  0
13  1  1 13  0  0  0  0  C 14  1  2 14  0  0  0 15  1  3 15  0  0  0  0  0
16  1  4 16  0  0  0  0  C 17  1  5 17  0  0  0 18  1  6 18  0  0  0  0  0
19  1  7 19  0  0  0  0  O 20  1  8 20  0  0  0 21  1  9 21  0  0  0  0  0
22  1 10 22  0  0  0  0  C 23  1 11 23  0  0  0 24  1 12 24  0  0  0  0  0
25  2  1  2  3  0  0  0  C 26  2  2  3  4  0  0 27  2  4  5  0  0  0  0  0
28  2  4  5  6  0  0  0  C 29  2  5  6  1  0  0 30  2  6  1  2  0  0  0  0
31  2  7  1  6  0  0  0  C 32  2  7  1  2  0  0 33  2  8  2  1  0  0  0  0
34  2  8  2  3  0  0  0  C 35  2  9  3  2  0  0 36  2  9  3  4  0  0  0  0
37  2 10  4  3  0  0  0  C 38  2 10  4  5  0  0 39  2 11  5  4  0  0  0  0
40  2 11  5  6  0  0  0  C 41  2 12  6  5  0  0 42  2 12  6  1  0  0  0  0
43  2 13  1  6  0  0  0  C 44  2 13  1  2  0  0 45  2 14  2  1  0  0  0  0
46  2 14  2  3  0  0  0  C 47  2 15  3  2  0  0 48  2 15  3  4  0  0  0  0
49  2 16  4  3  0  0  0  O 50  2 16  4  5  0  0 51  2 17  5  4  0  0  0  0
52  2 17  5  6  0  0  0  C 53  2 18  6  5  0  0 54  2 18  6  1  0  0  0  0
55  2 13  1  7  0  0  0  C 56  2 14  2  8  0  0 57  2 15  3  9  0  0  0  0
58  2 16  4 10  0  0  0  C 59  2 17  5 11  0  0 60  2 18  6 12  0  0  0  0
61  2  1  7 19  0  0  0  O 62  2  2  8 20  0  0 63  2  6 12 24  0  0  0  0
64  2  4 10 22  0  0  0  C 65  2  6 11 23  0  0 66  2  6 12 24  0  0  0  0
67  4  6  1  2  8  3  0  C  0  4 13  1  2 14  3  0  0  4  7  1  2  3  3  0
68  4  1  2  3  9  3  0  C  0  4  8  2  3 15  3  0  0  4 14  2  3 15  3  0
69  4  2  3  4 10  3  0  C  0  4  9  3  4  5  3  0  0  4 15  3  4 16  3  0
70  4  3  4  5 11  3  0  C  0  4 10  4  5  6  3  0  0  4 16  4  5 17  3  0
71  4  4  5  6 12  3  0  C  0  4 11  5  6  1  3  0  0  4 17  5  6 18  3  0
72  4  5  6  1  7  3  0  C  0  4 12  6  1  2  3  0  0  4 18  6  1 13  3  0
73  4 19  7  1 13  3  0  O  0  4 19  7  1  6  3  0  0  4 19  7  1  2  3  0
74  4 20  8  2 14  3  0  C  0  4 20  8  2  1  3  0  0  4 20  8  2  3  3  0
75  4 21  9  3 15  3  0  C  0  4 21  9  3  2  3  0  0  4 21  9  3  4  3  0
76  4 22 10  4 16  3  0  C  0  4 22 10  4  3  3  0  0  4 22 10  4  5  3  0
77  4 23 11  5 17  3  0  C  0  4 23 11  5  4  3  0  0  4 23 11  5  6  3  0
78  4 24 12  6 18  3  0  O  0  4 24 12  6  5  3  0  0  4 24 12  6  1  3  0
-02
-06  1  7 52
  12.00000    12.00000    12.00000    12.00000    12.00000    12.00000
  15.994915   15.994915   15.994915   15.994915   15.994915   15.994915
   1.007825    1.007825    1.007825    1.007825    1.007825    1.007825
   1.007825    1.007825    1.007825    1.007825    1.007825    1.007825
   1  1   2     1  2   2     1  3   2     1  4   2     1  5   2     1  6   2
   1  5   2     1  6   2     2  7   2     2  8   2     2  9   2     2 10   2
   2  9   2     2 10   2     2 11   2     2 12   2     3 13   2     3 14   2
   3 13   2     3 14   2     3 15   2     4 16   2     4 17   2     4 18   2
   3 17   2     3 18   2     4 19   2     4 20   2     4 21   2     4 22   2
   4 21   2     4 22   2     4 23   2     4 24   2     5 25   2     5 26   2
   5 25   2     5 26   2     5 27   2     5 28   2     5 29   2     5 30   2
   5 29   2     5 30   2     6 31   1     6 32   1     6 33   1     6 34   1
   6 33   1     6 34   1     6 35   1     6 36   1     6 37   1     6 38   1
   6 37   1     6 38   1     6 39   1     6 40   1     6 41   1     6 42   1
   6 41   1     6 42   1     7 43   1     7 44   1     7 45   1     7 46   1
   7 45   1     7 46   1     7 47   1     7 48   1     7 49   1     7 50   1
   7 49   1     7 50   1     7 51   1     7 52   1     7 53   1     7 54   1
   7 53   1     7 54   1     8 55   2     8 56   2     8 57   2     8 58   2
   8 57   2     8 58   2     8 59   2     8 60   2     9 61   2     9 62   2
   9 61   2     9 62   2     9 63   2     9 64   2     9 65   2     9 66   2
   9 65   2     9 66   2    10 67   2    10 68   2    10 69   2    10 70  -2
  10 69   2    10 70  -2    10 71   2    10 72  -2    11 31   1    11 32  -1
  11 31   1    11 32  -1    11 33   1    11 34  -1    11 35   1    11 36  -1
  11 35   1    11 36  -1    11 37   1    11 38  -1    11 39   1    11 40  -1
  11 39   1    11 40  -1    11 41   1    11 42  -1    12 43   1    12 44  -1
  12 43   1    12 44  -1    12 45   1    12 46  -1    12 47   1    12 48  -1
  12 47   1    12 48  -1    12 49   1    12 50  -1    12 51   1    12 52  -1
  12 51   1    12 52  -1    12 53   1    12 54  -1    13 73   2    13 74  -2
  13 73   2    13 74  -2    13 75   2    13 76  -2    13 77   2    13 78  -2
  14  1   1    14  2  -2    14  3   1    14  4   1    14  5   1    14  6   1
  14  5  -1    14  6   1    15  7   2    15  8  -1    15  9  -1    15 10   2
  15  9  -1    15 10   2    15 11  -1    15 12  -1    16 13   2    16 14  -1
  16 13   2    16 14  -1    16 15  -1    16 16   2    16 17  -1    16 18  -1
  16 17  -1    16 18  -1    17 19   2    17 20  -1    17 21  -1    17 22   2
  17 21  -1    17 22   2    17 23  -1    17 24  -1    18 25  -1    18 26  -1
  18 25  -1    18 26  -1    18 27   2    18 28  -1    18 29  -1    18 30   2
  18 29  -1    18 30   2    19 33   3    19 34  -3    19 39  -3    19 36   3
  19 39  -3    19 36   3    19 39   3    19 40  -3    19 41  -3    19 42   3
  19 41  -3    19 42   3    20 31  -2    20 32  -2    20 33   1    20 34   1
  20 33   1    20 34   1    20 35   1    20 36   1    20 37  -2    20 38  -2
  20 37  -2    20 38  -2    20 39   1    20 40   1    20 41   1    20 42   1
  20 41   1    20 42   1    21 45   3    21 46  -3    21 47  -3    21 48   3
  21 47  -3    21 48   3    21 51   3    21 52  -3    21 53  -3    21 54   3
  21 53  -3    21 54   3    22 43  -2    22 44  -2    22 45   1    22 46   1
  22 45   1    22 46   1    22 47   1    22 48   1    22 49  -2    22 50  -2
  22 49  -2    22 50  -2    22 51   1    22 52   1    22 53   1    22 54   1
  22 53   1    22 54   1    23 55   2    23 56  -1    23 57  -1    23 58   2
  23 57  -1    23 58   2    23 59  -1    23 60  -1    24 61  -1    24 62  -1
  24 61  -1    24 62  -1    24 63  -1    24 64   2    24 65  -1    24 66  -1
  24 65  -1    24 66  -1    25 67  -1    25 68  -2    25 69  -1    25 70   1
  25 69  -1    25 70   1    25 71   2    25 72   1    26 74  -3    26 75  -3
  26 74  -3    26 75  -3    26 77   3    26 78   3    27  1   2    27  2  -2
  27  1   2    27  2  -2    27  3   2    27  4  -2    27  5   2    27  6  -2
  27  5   2    27  6  -2    28 31   1    28 32  -1    28 33  -1    28 34   1
  28 33  -1    28 34   1    28 35   1    28 36  -1    28 37  -1    28 38   1
  28 37  -1    28 38   1    28 39   1    28 40  -1    28 41  -1    28 42   1
  28 41  -1    28 42   1    29 43   1    29 44  -1    29 45  -1    29 46   1
  29 45  -1    29 46   1    29 47   1    29 48  -1    29 49  -1    29 50   1
  29 49  -1    29 50   1    29 51   1    29 52  -1    29 53  -1    29 54   1
  29 53  -1    29 54   1    30 67   2    30 68   2    30 69   2    30 70   2
  30 69   2    30 70   2    30 71   2    30 72   2    31 73   2    31 74   2
  31 73   2    31 74   2    31 75   2    31 76   2    31 77   2    31 78   2
  32  7   2    32  8  -2    32  9   2    32 10  -2    32 11   2    32 12  -2
  32 11   2    32 12  -2    33 13   2    33 14  -2    33 15   2    33 16  -2
  33 15   2    33 16  -2    33 17   2    33 18  -2    34 19   2    34 20  -2
  34 19   2    34 20  -2    34 21   2    34 22  -2    34 23   2    34 24  -2
  34 23   2    34 24  -2    35 25   2    35 26  -2    35 27   2    35 28  -2
  35 27   2    35 28  -2    35 29   2    35 30  -2    36 31   1    36 32   1
  36 31   1    36 32   1    36 33  -1    36 34  -1    36 35   1    36 36   1
  36 35   1    36 36   1    36 37  -1    36 38  -1    36 39   1    36 40   1
  36 39   1    36 40   1    36 41  -1    36 42  -1    37 43   1    37 44   1
  37 43   1    37 44   1    37 45  -1    37 46  -1    37 47   1    37 48   1
  37 47   1    37 48   1    37 49  -1    37 50  -1    37 51   1    37 52   1
  37 51   1    37 52   1    37 53  -1    37 54  -1    38 55   2    38 56  -2
  38 55   2    38 56  -2    38 57   2    38 58  -2    38 59   2    38 60  -2
  38 59   2    38 60  -2    39 61   2    39 62  -2    39 63   2    39 64  -2
  39 63   2    39 64  -2    39 65   2    39 66  -2    40  1   3    40  3  -3
  40  1   3    40  3  -3    40  4  -3    40  6   3    41  7   2    41  8   1
  41  7   2    41  8   1    41  9  -1    41 10  -2    41 11  -1    41 12   1
  41 11  -1    41 12   1    42 13   2    42 14   1    42 15  -1    42 16  -2
  42 15  -1    42 16  -2    42 17  -1    42 18   1    43 19   2    43 20  -2
  43 19   2    43 20  -2    43 21  -1    43 22   2    43 23  -1    43 24   1
  43 23  -1    43 24   1    44 25   1    44 26  -1    44 27  -2    44 28  -1
  44 27  -2    44 28  -1    44 29   1    44 30   2    45 33  -3    45 34  -3
  45 33  -3    45 34  -3    45 35  -3    45 36  -3    45 39  -3    45 40   3
  45 39  -3    45 40   3    45 41  -3    45 42   3    46 31  -2    46 32  -2
  46 31  -2    46 32  -2    46 33  -1    46 34  -1    46 35   1    46 36   1
  46 35   1    46 36   1    46 37  -1    46 38   1    46 39   1    46 40  -1
  46 39   1    46 40  -1    46 41  -1    46 42  -1    47 45  -3    47 46  -3
  47 45  -3    47 46  -3    47 47  -3    47 48  -3    47 51  -3    47 52   3
  47 51  -3    47 52   3    47 53  -3    47 54   3    48 43  -2    48 44  -2
  48 43  -2    48 44  -2    48 45  -1    48 46  -1    48 47   1    48 48   1
  48 47   1    48 48   1    48 49  -1    48 50   1    48 51   1    48 52  -1
  48 51   1    48 52  -1    48 53  -1    48 54  -1    49 55   2    49 56  -2
  49 55   2    49 56  -2    49 57  -1    49 58   2    49 59  -1    49 60   1
  49 59  -1    49 60   1    49 61  -1    49 62   1    50 63  -1    50 64  -2
  50 63  -1    50 64  -2    50 65  -1    50 66   1    51 67  -3    51 69   3
  51 67  -3    51 69   3    51 70  -3    51 72   3    52 74  -3    52 75   3
  52 74  -3    52 75   3    52 77  -3    52 78   3
  -3
   1  11  14  27  32  40  53
999
```

TABLE XXXIX (Continued)

GMAT INPUT FOR NEO-INOSITOL

```
-09
-09
    1  24  78   1   0   0   0
    NEO-INOSITOL - SYMMETRIZED AND UNSYMMETRIZED G MATRIX
    TETRAHEDRAL STRUCTURE - C-C 1.525  C-O 1.425  C-H 1.10   O-H 0.97
  1  2     1.525000   1  4     2.033332   2  3     1.437783   1  4     1.524998
  2  4     2.156676   3  4    -1.245157   2  5     2.156675   3  5    -1.245154
  1  6    -0.508336   2  6     0.718892   3  6    -1.245153   1  7    -0.475000
  2  7    -1.343501   1  8     1.999998   2  8    -0.671751   3  8    -1.163507
  1  9     3.458330   2  9     1.437781   1 10     1.999995   2 10     3.500177
  3 10    -1.245154   1 11    -0.475001   2 11     2.828425   3 11    -0.081645
  1 12    -1.933335   2 12     0.718892   3 12    -1.245149   1 13    -0.366666
  2 13     0.518544   3 13     0.898147   1 14     1.891665   2 14    -0.518545
  3 14     0.898147   1 15     1.666663   2 15     1.996326   3 15     0.898147
  1 16     1.891661   2 16     1.638130   3 16    -2.143302   1 17    -0.366672
  2 17     2.675220   3 17    -2.143300   1 18    -0.141670   2 18     0.200348
  3 18    -2.143300   1 19    -0.151666   2 19    -1.800761   3 19    -0.792004
  1 20     1.676663   2 20    -0.214487   3 20    -1.955508   1 21     3.781663
  2 21     0.980521   3 21    -0.792005   1 22     1.676661   2 22     3.957436
  3 22    -0.453150   1 23    -0.151665   2 23     2.371161   3 23     0.710356
  1 24    -2.256665   2 24     1.176154   3 24    -0.453144  -1  0     0.0
  1  1  1  2  0  0  0  0  0  2  1  2  3  0  0  0  0  0  3  1  3  4  0  0  0  0
  4  1  4  5  0  0  0  0  0  5  1  5  6  0  0  0  0  0  6  1  6  1  0  0  0  0
  7  1  1  7  0  0  0  0  0  8  1  2  8  0  0  0  0  0  9  1  3  9  0  0  0  0
 10  1  4 10  0  0  0  0  0 11  1  5 11  0  0  0  0  0 12  1  6 12  0  0  0  0
 13  1  1 13  0  0  0  0  0 14  1  2 14  0  0  0  0  0 15  1  3 15  0  0  0  0
 16  1  4 16  0  0  0  0  0 17  1  5 17  0  0  0  0  0 18  1  6 18  0  0  0  0
 19  1  7 19  0  0  0  0  0 20  1  8 20  0  0  0  0  0 21  1  9 21  0  0  0  0
 22  1 10 22  0  0  0  0  0 23  1 11 23  0  0  0  0  0 24  1 12 24  0  0  0  0
 25  2  1  2  3  0  0  0  0 26  2  2  3  4  0  0  0  0 27  2  3  4  5  0  0  0
 28  2  4  5  6  0  0  0  0 29  2  5  6  1  0  0  0  0 30  2  6  1  2  0  0  0
 31  2  7  1  6  0  0  0  0 32  2  7  1  2  0  0  0  0 33  2  8  2  1  0  0  0
 34  2  8  2  3  0  0  0  0 35  2  9  3  2  0  0  0  0 36  2  9  3  4  0  0  0
 37  2 10  4  3  0  0  0  0 38  2 10  4  5  0  0  0  0 39  2 11  5  4  0  0  0
 40  2 11  5  6  0  0  0  0 41  2 12  6  5  0  0  0  0 42  2 12  6  1  0  0  0
 43  2 13  1  6  0  0  0  0 44  2 13  1  2  0  0  0  0 45  2 14  2  1  0  0  0
 46  2 14  2  3  0  0  0  0 47  2 15  3  2  0  0  0  0 48  2 15  3  4  0  0  0
 49  2 16  4  3  0  0  0  0 50  2 16  4  5  0  0  0  0 51  2 17  5  4  0  0  0
 52  2 17  5  6  0  0  0  0 53  2 18  6  5  0  0  0  0 54  2 18  6  1  0  0  0
 55  2 13  1  7  0  0  0  0 56  2 14  2  8  0  0  0  0 57  2 15  3  9  0  0  0
 58  2 16  4 10  0  0  0  0 59  2 17  5 11  0  0  0  0 60  2 18  6 12  0  0  0
 61  2  1  7 19  0  0  0  0 62  2  5 11 20  0  0  0  0 63  2  3  9 21  0  0  0
 64  2  4 10 22  0  0  0  0 65  2  5 11 23  0  0  0  0 66  2  6 12 24  0  0  0
 67  4  6  1  2 14  3  0  0  0  4  7  1  2  3  3  0  0  0  4 13  1  2  8  3  0
 68  4  1  2  3  9  3  0  0  4  8  2  3 15  3  0  0  4 14  2  3  4  3  0
 69  4  2  3  4 10  3  0  0  4  9  3  4  5  3  0  0  4 15  3  4 16  3  0
 70  4  3  4  5 17  3  0  0  4 10  4  5  6  3  0  0  4 16  4  5 11  3  0
 71  4  4  5  6 12  3  0  0  4 11  5  6 18  3  0  0  4 17  5  6  1  3  0
 72  4  5  6  1  7  3  0  0  4 12  6  1  2  3  0  0  4 18  6  1 13  3  0
 73  4 19  7  1 13  3  0  0  4 19  7  1  6  3  0  0  4 19  7  1  2  3  0
 74  4 20  8  2 14  3  0  0  4 20  8  2  1  3  0  0  4 20  8  2  3  3  0
 75  4 21  9  3 15  3  0  0  4 21  9  3  2  3  0  0  4 21  9  3  4  3  0
 76  4 22 10  4 16  3  0  0  4 22 10  4  3  3  0  0  4 22 10  4  5  3  0
 77  4 23 11  5 17  3  0  0  4 23 11  5  4  3  0  0  4 23 11  5  6  3  0
 78  4 24 12  6 18  3  0  0  4 24 12  6  5  3  0  0  4 24 12  6  1  3  0
-02
-06  1  3 78
 12.00000    12.00000    12.00000    12.00000    12.00000    12.00000
 15.994915   15.994915   15.994915   15.994915   15.994915   15.994915
  1.007825    1.007825    1.007825    1.007825    1.007825    1.007825
  1.007825    1.007825    1.007825    1.007825    1.007825    1.007825
  1  1  1        1  2  2        1        1  4  1        1  5  1        1
  2  3  2        2  6  2        2        3  7  1        3  9  1        2
  3 10  1        5 12  1        1        4  8  2        4 11  2        2
  5 13  1        5 15  1        1        5 16  1        5 18  1        1
  6 14  2        6 17  2        2        7 19  1        7 21  1        1
  7 22  1        7 24  1        1        8 20  2        8 23  2        2
  9 25  2        9 28  2        2       10 26  1       10 27  1        1
 10 29  1       10 30  1        1       11 31  1       11 36  1        1
 11 37  1       11 42  1        1       12 32  1       12 35  1        1
 12 38  1       12 41  1        1       13 33  1       13 34  1        1
 13 39  1       13 40  1        1       14 43  1       14 48  1        1
 14 49  1       14 54  1        1       15 44  1       15 47  1        1
 15 50  1       15 53  1        1       16 45  1       16 46  1        1
 16 51  1       16 52  1        1       17 55  1       17 57  1        1
 17 58  1       17 60  1        1       18 56  2       18 59  2        2
 19 61  1       19 63  1        1       19 64  1       19 66  1        1
 20 62  2       20 65  2        2       21 67  1       21 68  -1       1
 21 70  -1      21 71  1        1       22 69  2       22 72  -2       2
 23 73  1       23 75  -1       1       23 76  -1      23 78  1        1
 24  4  1       24  2  -1       1       24  4  1       24  5  -1       1
 25  7  1       25  9  -1       1       25 10  1       25 12  -1       1
 26 14  1       26 15  -1       1       26 16  1       26 18  -1       1
 27 19  1       27 21  -1       1       27 22  1       27 24  -1       1
 28 26  1       28 27  -1       1       28 29  1       28 30  -1       1
 29 31  1       29 36  -1       1       29 37  1       29 42  -1       1
 30 32  1       30 35  -1       1       30 38  1       30 41  -1       1
 31 33  1       31 34  -1       1       31 39  1       31 40  -1       1
 32 43  1       32 48  -1       1       32 49  1       32 54  -1       1
 33 44  1       33 47  -1       1       33 50  1       33 53  -1       1
 34 45  1       34 44  -1       1       34 51  1       34 52  -1       1
 35 55  1       35 57  -1       1       35 58  1       35 60  -1       1
 36 61  1       36 63  -1       1       36 64  1       36 66  -1       1
 37 67  1       37 69  1        1       37 70  -1      37 71  1        1
 38 73  1       38 75  1        1       38 76  -1      38 78  -1       1
 39 74  2       39 77  -2       2
 40  1  1       40  2  -1       1       40  4  -1       40  5  1        1
 41  3  2       41  6  -2       2       42  7  1       42  9  -1       1
 42 10  -1      42 12  1        1       43 13  1       43 15  -1       1
 43 16  -1      43 18  1        1       44 19  1       44 21  -1       1
 44 22  -1      44 24  1        1       45 26  1       45 27  1        1
 45 29  -1      45 30  -1       1       46 31  1       46 36  -1       1
 46 37  -1      46 42  1        1       47 32  1       47 35  -1       1
 47 38  -1      47 41  1        1       48 33  1       48 34  -1       1
 48 39  -1      48 40  1        1       49 43  1       49 48  -1       1
 49 49  -1      49 54  1        1       50 44  1       50 47  -1       1
 50 50  -1      50 53  1        1       51 45  1       51 46  -1       1
 51 51  -1      51 52  1        1       52 55  1       52 57  -1       1
 52 58  -1      52 60  1        1       53 61  1       53 63  -1       1
 53 66  -1      53 66  1        1       54 67  1       54 68  1        1
 54 70  1       54 71  1        1       55 69  2       55 72  -2       2
 56 73  1       56 75  1        1       56 76  1       56 78  1        1
 57 74  2       57 77  2        2
 58  1  1       58  2  1        1       58  4  -1      58  5  -1       1
 59  7  1       59  9  1        1       59 10  -1      59 12  -1       1
 60  8  2       60 11  -2       2       61 13  1       61 15  -1       1
 61 16  -1      61 18  -1       1       62 14  2       62 17  -2       2
 63 19  1       63 21  1        1       63 22  -1      63 24  -1       1
 64 20  2       64 23  -2       2       65 25  2       65 28  -2       2
 66 26  1       66 27  -1       1       66 29  -1      66 30  1        1
 67 31  1       67 36  1        1       67 37  -1      67 42  -1       1
 68 32  1       68 35  1        1       68 38  -1      68 41  -1       1
 69 33  1       69 34  1        1       69 39  -1      69 40  -1       1
 70 43  1       70 48  1        1       70 49  -1      70 54  -1       1
 71 44  1       71 47  1        1       71 50  -1      71 53  -1       1
 72 45  1       72 46  1        1       72 51  -1      72 52  -1       1
 73 55  1       73 57  1        1       73 58  -1      73 60  -1       1
 74 56  2       74 59  -2       2       75 61  1       75 63  1        1
 75 64  -1      75 66  -1       1       76 62  2       76 65  -2       2
 77 67  1       77 68  -1       1       77 70  1       77 71  -1       1
 78 73  1       78 75  -1       1       78 76  1       78 78  -1       1
-3
  1 24 40 58 79
999
```

TABLE XXXIX (Continued)

GMAT INPUT FOR MYO-INOSITOL

```
-09
-09      1  24  78   1   0   0   0
     MYO-INOSITOL - SYMMETRIZED AND UNSYMMETRIZED G MATRIX
     TETRAHEDRAL STRUCTURE - C-C 1.525  C-O 1.425  C-H 1.10  O-H 0.97
  1  2     1.525000   1  3     2.033332   2  3     1.437783   1  4     1.524998
  2  4     2.156676   3  4    -1.245157   2  5     2.156675   3  5    -1.245154
  1  6    -0.508336   2  6     0.718892   3  6    -1.245153   1  7    -0.475000
  2  7    -1.343501   1  8     1.999998   2  8    -0.671751   3  8    -1.163507
  1  9     3.458330   2  9     1.437781   1 10     1.999995   2 10     3.500177
  3 10    -1.245154   1 11    -0.475006   2 11     2.828425   3 11    -2.408660
  1 12    -1.933335   2 12     0.718892   3 12    -1.245149   1 13    -0.366666
  2 13     0.518544   3 13     0.898147   1 14     1.891665   2 14    -0.518545
  3 14     0.898147   1 15     1.666663   2 15     1.956326   3 15     0.898147
  1 16     1.891661   2 16     1.638130   3 16    -2.143302   1 17    -0.366669
  2 17     2.675220   3 17    -0.347007   1 18    -0.141670   2 18     0.200348
  3 18    -2.143300   1 19    -0.151666   2 19    -1.800761   3 19    -0.792004
  1 20     1.676663   2 20    -0.214487   3 20    -1.955508   1 21     3.781663
  2 21     0.980521   3 21    -0.792005   1 22     1.676661   2 22     3.957436
  3 22    -0.453150   1 23    -0.151674   2 23     2.371161   3 23    -3.200661
  1 24    -2.256665   2 24     1.176154   3 24    -0.453144  -1  0     0.0
  1  1  1  2  0  0  0  C  2  1  2  3  0  0  0  0  3  1  3  4  0  0  0  0
  4  1  4  5  0  0  0  C  5  1  5  6  0  0  0  0  6  1  6  1  0  0  0  0
  7  1  1  7  0  0  0  C  8  1  2  8  0  0  0  0  9  1  3  9  0  0  0  0
 10  1  4 10  0  0  0  C 11  1  5 11  0  0  0  0 12  1  6 12  0  0  0  0
 13  1  1 13  0  0  0  C 14  1  2 14  0  0  0  0 15  1  3 15  0  0  0  0
 16  1  4 16  0  0  0  C 17  1  5 17  0  0  0  0 18  1  6 18  0  0  0  0
 19  1  7 19  0  0  0  C 20  1  8 20  0  0  0  0 21  1  9 21  0  0  0  0
 22  1 10 22  0  0  0  C 23  1 11 23  0  0  0  0 24  1 12 24  0  0  0  0
 25  2  1  2  3  0  0  C 26  2  2  3  4  0  0  0 27  2  3  4  5  0  0  0
 28  2  4  5  6  0  0  C 29  2  5  6  1  0  0  0 30  2  6  1  2  0  0  0
 31  2  7  1  6  0  0  C 32  2  7  1  2  0  0  0 33  2  8  2  1  0  0  0
 34  2  8  2  3  0  0  C 35  2  9  3  2  0  0  0 36  2  9  3  4  0  0  0
 37  2 10  4  3  0  0  C 38  2 10  4  5  0  0  0 39  2 11  5  4  0  0  0
 40  2 11  5  6  0  0  C 41  2 12  6  5  0  0  0 42  2 12  6  1  0  0  0
 43  2 13  1  6  0  0  C 44  2 13  1  2  0  0  0 45  2 14  2  1  0  0  0
 46  2 14  2  3  0  0  C 47  2 15  3  2  0  0  0 48  2 15  3  4  0  0  0
 49  2 16  4  3  0  0  C 50  2 16  4  5  0  0  0 51  2 17  5  4  0  0  0
 52  2 17  5  6  0  0  C 53  2 18  6  5  0  0  0 54  2 18  6  1  0  0  0
 55  2 13  1  7  0  0  C 56  2 14  2  8  0  0  0 57  2 15  3  9  0  0  0
 58  2 16  4 10  0  0  C 59  2 17  5 11  0  0  0 60  2 18  6 12  0  0  0
 61  2  1  7 19  0  0  C 62  2  2  8 20  0  0  0 63  2  3  9 21  0  0  0
 64  2  4 10 22  0  0  C 65  2  5 11 23  0  0  0 66  2  6 12 24  0  0  0
 67  4  6  1  2 14  3  C  0  4 13  1  2  8  3  0  0  4  7  1  2  3  3  0
 68  4  1  2  3  9  3  C  0  4 14  2  3  4  3  0  0  4  8  2  3 15  3  0
 69  4  2  3  4 10  3  C  0  4 15  3  4 16  3  0  0  4  9  3  4  5  3  0
 70  4  3  4  5 11  3  C  0  4 10  4  5  6  3  0  0  4 16  4  5 17  3  0
 71  4  4  5  6 12  3  C  0  4 11  5  6  1  3  0  0  4 17  5  6 18  3  0
 72  4  5  6  1  7  3  C  0  4 12  6  1  2  3  0  0  4 18  6  1 13  3  0
 73  4 19  7  1 13  3  C  0  4 19  7  1  6  3  0  0  4 19  7  1  2  3  0
 74  4 20  8  2 14  3  C  0  4 20  8  2  1  3  0  0  4 20  8  2  3  3  0
 75  4 21  9  3 15  3  C  0  4 21  9  3  2  3  0  0  4 21  9  3  4  3  0
 76  4 22 10  4 16  3  C  0  4 22 10  4  3  3  0  0  4 22 10  4  5  3  0
 77  4 23 11  5 17  3  C  0  4 23 11  5  4  3  0  0  4 23 11  5  6  3  0
 78  4 24 12  6 18  3  C  0  4 24 12  6  5  3  0  0  4 24 12  6  1  3  0
-02
-06  1  3 78
 12.00000    12.00000    12.00000    12.00000    12.00000    12.00000
 15.994915   15.994915   15.994915   15.994915   15.994915   15.994915
  1.007825    1.007825    1.007825    1.007825    1.007825    1.007825
  1.007825    1.007825    1.007825    1.007825    1.007825    1.007825
  1  1     1      1  2     1      2  3     1      2  6     1
  3  4     1      3  5     1      4  7     1      4  9     1
  5  8     2      6 10     1      6 12     1      7 11     2
  8 13     1      8 15     1      9 14     2     10 16     1
 10 18     1     11 17     2     12 19     1     12 21     1
 13 20     2     14 22     1     14 24     1     15 23     2
 16 25     2     17 26     1     17 30     1     18 27     1
 18 29     1     19 28     2     20 31     1     20 36     1
 21 32     1     21 35     1     22 33     1     22 34     1
 23 37     1     23 42     1     24 38     1     24 41     1
 25 39     1     25 40     1     26 43     1     26 48     1
 27 44     1     27 47     1     28 45     1     28 46     1
 29 49     1     29 54     1     30 50     1     30 53     1
 31 51     1     31 52     1     32 55     1     32 57     1
 33 56     2     34 58     1     34 60     1     35 59     2
 36 61     1     36 63     1     37 62     2     38 64     1
 38 66     1     39 65     2     40 67     1     40 68    -1
 41 69     1     41 72    -1     42 70     1     42 71    -1
 43 73     1     43 75    -1     44 76     1     44 78    -1
 45  1     1     45  2    -1     46  3     1     46  6    -1
 47  4     1     47  5    -1     48  7     1     48  9    -1
 49 10     1     49 12    -1     50 13     1     50 15    -1
 51 16     1     51 18    -1     52 19     1     52 21    -1
 53 22     1     53 24    -1     54 26     1     54 30    -1
 55 27     1     55 29    -1     56 31     1     56 36    -1
 57 32     1     57 35    -1     58 33     1     58 34    -1
 59 37     1     59 42    -1     60 38     1     60 41    -1
 61 39     1     61 40    -1     62 43     1     62 48    -1
 63 44     1     63 47    -1     64 45     1     64 46    -1
 65 49     1     65 54    -1     66 50     1     66 53    -1
 67 51     1     67 52    -1     68 55     1     68 57    -1
 69 58     1     69 60    -1     70 61     1     70 63    -1
 71 64     1     71 66    -1     72 67     1     72 68     1
 73 69     1     73 72     1     74 70     1     74 71     1
 75 73     1     75 75     1     76 74     2     77 76     1
 77 78     1     78 77     2     -3
  1 45 79
999
```

TABLE XXXIX (Continued)

GMAT INPUT FOR EPI-INOSITOL

```
-09
-09      1  24  78   1   0   0   0
     EPI-INOSITOL - SYMMETRIZED AND UNSYMMETRIZED G MATRIX
     TETRAHEDRAL STRUCTURE - C-C 1.525  C-O 1.425  C-H 1.10  O-H 0.97
  1  2     1.525000  1  3     2.033332  2  3     1.437783  1  4     1.524998
  2  4     2.156676  3  4    -1.245157  2  5     2.156675  3  5    -1.245154
  1  6    -0.508336  2  6     0.718892  3  6    -1.245153  1  7    -0.475000
  2  7    -1.343501  1  8     1.999998  2  8    -0.671751  3  8    -1.163507
  1  9     3.458330  2  9     1.437781  1 10     1.999995  2 10     3.500177
  3 10    -1.245154  1 11    -0.475006  2 11     2.828425  3 11    -2.408660
  1 12    -0.033337  2 12     0.047142  3 12    -2.408661  1 13    -0.366666
  2 13     0.518544  3 13     0.898147  1 14     1.891665  2 14    -0.518545
  3 14     0.898147  1 15     1.666663  2 15     1.956326  3 15     0.898147
  1 16     1.891661  2 16     1.638130  3 16    -2.143302  1 17    -0.366669
  2 17     2.675220  3 17    -0.347007  1 18    -1.608335  2 18     0.718893
  3 18    -1.245150  1 19    -0.151666  2 19    -1.800761  3 19    -0.792004
  1 20     1.676661  2 20    -1.586275  3 20    -1.163507  1 21     3.781663
  2 21     0.980521  3 21    -0.792005  1 22     1.676661  2 22     3.957436
  3 22    -0.453150  1 23    -0.151674  2 23     2.371161  3 23    -3.200661
  1 24    -0.356670  2 24    -0.867384  3 24    -2.408661 -1  0     0.0
  1  1  1  2  0  0  0  C  2  1  2  3  0  0  0  0  3  1  3  4  0  0  0  0
  4  1  4  5  0  0  0  C  5  1  5  6  0  0  0  0  6  1  6  1  0  0  0  0
  7  1  1  7  0  0  0  C  8  1  2  8  0  0  0  0  9  1  3  9  0  0  0  0
 10  1  4 10  0  0  0  C 11  1  5 11  0  0  0  0 12  1  6 12  0  0  0  0
 13  1  1 13  0  0  0  C 14  1  2 14  0  0  0  0 15  1  3 15  0  0  0  0
 16  1  4 16  0  0  0  C 17  1  5 17  0  0  0  0 18  1  6 18  0  0  0  0
 19  1  7 19  0  0  0  C 20  1  8 20  0  0  0  0 21  1  9 21  0  0  0  0
 22  1 10 22  0  0  0  C 23  1 11 23  0  0  0  0 24  1 12 24  0  0  0  0
 25  2  1  2  3  0  0  C 26  2  2  3  4  0  0  0 27  2  3  4  5  0  0  0
 28  2  4  5  6  0  0  C 29  2  5  6  1  0  0  0 30  2  6  1  2  0  0  0
 31  2  7  1  6  0  0  C 32  2  7  1  2  0  0  0 33  2  8  2  1  0  0  0
 34  2  8  2  3  0  0  C 35  2  9  3  2  0  0  0 36  2  9  3  4  0  0  0
 37  2 10  4  3  0  0  C 38  2 10  4  5  0  0  0 39  2 11  5  4  0  0  0
 40  2 11  5  6  0  0  C 41  2 12  6  5  0  0  0 42  2 12  6  1  0  0  0
 43  2 13  1  6  0  0  C 44  2 13  1  2  0  0  0 45  2 14  2  1  0  0  0
 46  2 14  2  3  0  0  C 47  2 15  3  2  0  0  0 48  2 15  3  4  0  0  0
 49  2 16  4  3  0  0  C 50  2 16  4  5  0  0  0 51  2 17  5  4  0  0  0
 52  2 17  5  6  0  0  C 53  2 18  6  5  0  0  0 54  2 18  6  1  0  0  0
 55  2 13  1  7  0  0  C 56  2 14  2  8  0  0  0 57  2 15  3  9  0  0  0
 58  2 16  4 10  0  0  C 59  2 17  5 11  0  0  0 60  2 18  6 12  0  0  0
 61  2  1  7 19  0  0  C 62  2  2  8 20  0  0  0 63  2  3  9 21  0  0  0
 64  2  4 10 22  0  0  C 65  2  5 11 23  0  0  0 66  2  6 12 24  0  0  0
 67  4  6  1  2 14  3  C  0  4  7  1  2  3  3  0  0  4 13  1  2  8  3  0
 68  4  1  2  3  9  3  C  0  4  8  2  3 15  3  0  0  4 14  2  3  4  3  0
 69  4  2  3  4 10  3  C  0  4  9  3  4  5  3  0  0  4 15  3  4 16  3  0
 70  4  3  4  5 11  3  C  0  4 10  4  5  6  3  0  0  4 16  4  5 17  3  0
 71  4  4  5  6 18  3  C  0  4 11  5  6  1  3  0  0  4 17  5  6 12  3  0
 72  4  5  6  1  7  3  C  0  4 12  6  1 13  3  0  0  4 18  6  1  2  3  0
 73  4 19  7  1 13  3  C  0  4 19  7  1  6  3  0  0  4 19  7  1  2  3  0
 74  4 20  8  2 14  3  C  0  4 20  8  2  1  3  0  0  4 20  8  2  3  3  0
 75  4 21  9  3 15  3  C  0  4 21  9  3  2  3  0  0  4 21  9  3  4  3  0
 76  4 22 10  4 16  3  C  0  4 22 10  4  3  3  0  0  4 22 10  4  5  3  0
 77  4 23 11  5 17  3  C  0  4 23 11  5  4  3  0  0  4 23 11  5  6  3  0
 78  4 24 12  6 18  3  C  0  4 24 12  6  5  3  0  0  4 24 12  6  1  3  0
-02
-06  1  3 78
 12.00000    12.00000    12.00000    12.00000    12.00000    12.00000
 15.994915   15.994915   15.994915   15.994915   15.994915   15.994915
  1.007825    1.007825    1.007825    1.007825    1.007825    1.007825
  1.007825    1.007825    1.007825    1.007825    1.007825    1.007825
  1  1     1        1  6     1        2  2     1        2  5     1
  3  3     1        3  4     1        4  7     2        5  8     1
  5 12     1        6  9     1        6 11     1        7 10     2
  8 13     2        9 14     1        9 18     1       10 15     1
 10 17     1       11 16     2       12 19     2       13 20     1
 13 24     1       14 21     1       14 23     1       15 22     2
 16 25     1       16 29     1       17 26     1       17 28     1
 18 27     2       19 30     2       20 31     1       20 32     1
 21 33     1       21 42     1       22 34     1       22 41     1
 23 35     1       23 40     1       24 36     1       24 39     1
 25 37     1       25 38     1       26 43     1       26 44     1
 27 45     1       27 54     1       28 46     1       28 53     1
 29 47     1       29 52     1       30 48     1       30 51     1
 31 49     1       31 50     1       32 55     2       33 56     1
 33 60     1       34 57     1       34 59     1       35 58     2
 36 61     2       37 62     1       37 66     1       38 63     1
 38 65     1       39 64     2       40 67     1       40 72    -1
 41 68     1       41 71    -1       42 69     1       42 70    -1
 43 74     1       43 78    -1       44 75     1       44 77    -1
 45  1     1       45  6    -1       46  2     1       46  5    -1
 47  3     1       47  4    -1       48  8     1       48 12    -1
 49  9     1       49 11    -1       50 14     1       50 18    -1
 51 15     1       51 17    -1       52 20     1       52 24    -1
 53 21     1       53 23    -1       54 25     1       54 29    -1
 55 26     1       55 28    -1       56 31     1       56 32    -1
 57 33     1       57 42    -1       58 34     1       58 41    -1
 59 35     1       59 40    -1       60 36     1       60 39    -1
 61 37     1       61 36    -1       62 43     1       62 44    -1
 63 45     1       63 54    -1       64 46     1       64 53    -1
 65 47     1       65 52    -1       66 48     1       66 51    -1
 67 49     1       67 50    -1       68 56     1       68 60    -1
 69 57     1       69 58    -1       70 62     1       70 66    -1
 71 63     1       71 65    -1       72 67     1       72 72     1
 73 68     1       73 71     1       74 69     1       74 70     1
 75 73     2       76 74     1       76 78     1       77 75     1
 77 77     1       78 76     1
 -3
  1 45 79
999
```

TABLE XXXIX (Continued)

GMAT INPUT FOR CIS-INOSITOL

```
-09
-09      1  24  78   0   0   0   0
     CIS-INOSITOL --- G MATRIX - SYMMETRIZED AND UNSYMMETRIZED
     A1 AND A2 REPRESENTATIONS ONLY
  1  2     1.525000   1  3     2.033332   2  3     1.437783   1  4     1.524998
  2  4     2.156676   3  4    -1.245157   2  5     2.156675   3  5    -1.245154
  1  6    -0.508336   2  6     0.718892   3  6    -1.245153   1  7    -0.475000
  2  7    -1.343501   1  8     1.999998   2  8    -0.671751   3  8    -1.163507
  1  9     3.458330   2  9     1.437781   1 10     1.999994   2 10     1.484926
  3 10    -2.408663   1 11    -0.475006   2 11     2.828425   3 11    -2.408660
  1 12    -0.033337   2 12     0.047142   3 12    -2.408661   1 13    -0.366666
  2 13     0.518544   3 13     0.898147   1 14     1.891665   2 14    -0.518545
  3 14     0.898147   1 15     1.666663   2 15     1.956326   3 15     0.898147
  1 16     1.891662   2 16     3.193765   3 16    -1.245155   1 17    -0.366669
  2 17     2.675220   3 17    -0.347007   1 18    -1.608335   2 18     0.718893
  3 18    -1.245150   1 19    -0.151666   2 19    -1.800761   3 19    -0.792004
  1 20     2.538885   2 20    -1.433856   3 20    -0.899506   1 21     3.781663
  2 21     0.980521   3 21    -0.792005   1 22     2.538881   2 22     2.094609
  3 22    -2.936665   1 23    -0.151674   2 23     2.371161   3 23    -3.200661
  1 24    -0.787782   2 24    -0.257700   3 24    -2.936662  -1  0     0.0
  1  1  1  2  0  0  0  0  2  1  2  3  0  0  0  0  3  1  3  4  0  0  0  0
  4  1  4  5  0  0  0  0  5  1  5  6  0  0  0  0  6  1  6  1  0  0  0  0
  7  1  1  7  0  0  0  0  8  1  2  8  0  0  0  0  9  1  3  9  0  0  0  0
 10  1  4 10  0  0  0  0 11  1  5 11  0  0  0  0 12  1  6 12  0  0  0  0
 13  1  1 13  0  0  0  0 14  1  2 14  0  0  0  0 15  1  3 15  0  0  0  0
 16  1  4 16  0  0  0  0 17  1  5 17  0  0  0  0 18  1  6 18  0  0  0  0
 19  1  7 19  0  0  0  0 20  1  8 20  0  0  0  0 21  1  9 21  0  0  0  0
 22  1 10 22  0  0  0  0 23  1 11 23  0  0  0  0 24  1 12 24  0  0  0  0
 25  2  1  2  3  0  0  0 26  2  2  3  4  0  0  0 27  2  3  4  5  0  0  0
 28  2  4  5  6  0  0  0 29  2  5  6  1  0  0  0 30  2  6  1  2  0  0  0
 31  2  7  1  6  0  0  0 32  2  7  1  2  0  0  0 33  2  8  2  1  0  0  0
 34  2  8  2  3  0  0  0 35  2  9  3  2  0  0  0 36  2  9  3  4  0  0  0
 37  2 10  4  3  0  0  0 38  2 10  4  5  0  0  0 39  2 11  5  4  0  0  0
 40  2 11  5  6  0  0  0 41  2 12  6  5  0  0  0 42  2 12  6  1  0  0  0
 43  2 13  1  6  0  0  0 44  2 13  1  2  0  0  0 45  2 14  2  1  0  0  0
 46  2 14  2  3  0  0  0 47  2 15  3  2  0  0  0 48  2 15  3  4  0  0  0
 49  2 16  4  3  0  0  0 50  2 16  4  5  0  0  0 51  2 17  5  4  0  0  0
 52  2 17  5  6  0  0  0 53  2 18  6  5  0  0  0 54  2 18  6  1  0  0  0
 55  2 13  1  7  0  0  0 56  2 14  2  8  0  0  0 57  2 15  3  9  0  0  0
 58  2 16  4 10  0  0  0 59  2 17  5 11  0  0  0 60  2 18  6 12  0  0  0
 61  2  1  7 19  0  0  0 62  2  2  8 20  0  0  0 63  2  3  9 21  0  0  0
 64  2  4 10 22  0  0  0 65  2  5 11 23  0  0  0 66  2  6 12 24  0  0  0
 67  4  6  1  2 14  3  0  0  4 13  1  2  8  3  0  0  4  7  1  2  3  3  0
 68  4  1  2  3  9  3  0  0  4 14  2  3  4  3  0  0  4  8  2  3 15  3  0
 69  4  2  3  4 16  3  0  0  4 15  3  4 10  3  0  0  4  9  3  4  5  3  0
 70  4  3  4  5 11  3  0  0  4 10  4  5 17  3  0  0  4 16  4  5  6  3  0
 71  4  4  5  6 18  3  0  0  4 11  5  6  1  3  0  0  4 17  5  6 12  3  0
 72  4  5  6  1  7  3  0  0  4 12  6  1 13  3  0  0  4 18  6  1  2  3  0
 73  4 19  7  1 13  3  0  0  4 19  7  1  6  3  0  0  4 19  7  1  2  3  0
 74  4 20  8  2 14  3  0  0  4 20  8  2  1  3  0  0  4 20  8  2  3  3  0
 75  4 21  9  3 15  3  0  0  4 21  9  3  2  3  0  0  4 21  9  3  4  3  0
 76  4 22 10  4 16  3  0  0  4 22 10  4  3  3  0  0  4 22 10  4  5  3  0
 77  4 23 11  5 17  3  0  0  4 23 11  5  4  3  0  0  4 23 11  5  6  3  0
 78  4 24 12  6 18  3  0  0  4 24 12  6  5  3  0  0  4 24 12  6  1  3  0
-02
-06  1  3 27
  12.00000     12.00000     12.00000     12.00000     12.00000     12.00000
  15.994915    15.994915    15.994915    15.994915    15.994915    15.994915
   1.007825     1.007825     1.007825     1.007825     1.007825     1.007825
   1.007825     1.007825     1.007825     1.007825     1.007825     1.007825
   1  1     1      1  2     1      1  3     1      1  4     1
   1  5     1      1  6     1      2  7     2      2  9     2
   2 11     2      3  8     2      3 10     2      3 12     2
   4 13     2      4 15     2      4 17     2      5 14     2
   5 16     2      5 18     2      6 19     2      6 21     2
   6 23     2      7 20     2      7 22     2      7 24     2
   8 25     2      8 27     2      8 29     2      9 26     2
   9 28     2      9 30     2     10 31     1     10 32     1
  10 35     1     10 36     1     10 39     1     10 40     1
  11 33     1     11 34     1     11 37     1     11 38     1
  11 41     1     11 42     1     12 43     1     12 44     1
  12 47     1     12 48     1     12 51     1     12 52     1
  13 45     1     13 46     1     13 49     1     13 50     1
  13 53     1     13 54     1     14 55     2     14 57     2
  14 59     2     15 56     2     15 58     2     15 60     2
  16 61     2     16 63     2     16 65     2     17 62     2
  17 64     2     17 66     2     18 67     1     18 68    -1
  18 69     1     18 70    -1     18 71     1     18 72    -1
  19  1     1     19  2    -1     19  3     1     19  4    -1
  19  5     1     19  6    -1     20 31     1     20 32    -1
  20 35     1     20 36    -1     20 39     1     20 40    -1
  21 33     1     21 34    -1     21 37     1     21 38    -1
  21 41     1     21 42    -1     22 43     1     22 44    -1
  22 47     1     22 48    -1     22 51     1     22 52    -1
  23 45     1     23 46    -1     23 49     1     23 50    -1
  23 53     1     23 54    -1     24 67     1     24 68     1
  24 69     1     24 70     1     24 71     1     24 72     1
  25 73     2     25 75     2     25 77     2     26 74     2
  26 76     2     26 78     2     -3
   1 19 28
999
```

TABLE XXXIX (Continued)

GMAT INPUT FOR L-CHIRO-INOSITOL

```
-09
-09     1  24  78   1   0   0   0
     L-CHIRO-INOSITOL - SYMMETRIZED AND UNSYMMETRIZED G MATRIX
     TETRAHEDRAL STRUCTURE - C-C 1.525  C-O 1.425  C-H 1.10  O-H 0.97
  1  2     1.525000  1  3     2.033332  2  3     1.437783  1  4     1.524998
  2  4     2.156676  3  4    -1.245157  2  5     2.156675  3  5    -1.245154
  1  6    -0.508336  2  6     0.718892  3  6    -1.245153  1  7    -0.475000
  2  7     0.671749  3  7     1.163507  1  8     1.999998  2  8    -0.671751
  3  8     1.163507  1  9     3.458330  2  9     1.437781  1 10     1.999995
  2 10     3.500177  3 10    -1.245154  1 11    -0.475006  2 11     2.828425
  3 11    -2.408660  1 12    -0.033337  2 12     0.047142  3 12    -2.408661
  1 13    -0.366666  2 13    -1.037089  1 14     1.891665  2 14    -0.518545
  3 14    -0.898147  1 15     1.666663  2 15     1.956326  3 15     0.898147
  1 16     1.891661  2 16     1.638130  3 16    -2.143302  1 17    -0.366669
  2 17     2.675220  3 17    -0.347007  1 18    -1.608335  2 18     0.718893
  3 18    -1.245150  1 19    -1.445000  2 19     0.671749  3 19     1.163506
  1 20     1.676662  2 20    -0.214488  3 20     1.955508  1 21     3.781663
  2 21     0.980521  3 21    -0.792005  1 22     1.676661  2 22     3.957436
  3 22    -0.453150  1 23    -0.151674  2 23     2.371161  3 23    -3.200661
  1 24    -0.356670  2 24    -0.867384  3 24    -2.408661 -1  0     0.0
  1  1  1  2  0  0  0  C  2  1  2  3  0  0  0  0  3  1  3  4  0  0  0  0
  4  1  4  5  0  0  0  C  5  1  5  6  0  0  0  0  6  1  6  1  0  0  0  0
  7  1  1  7  0  0  0  C  8  1  2  8  0  0  0  0  9  1  3  9  0  0  0  0
 10  1  4 10  0  0  0  C 11  1  5 11  0  0  0  0 12  1  6 12  0  0  0  0
 13  1  1 13  0  0  0  C 14  1  2 14  0  0  0  0 15  1  3 15  0  0  0  0
 16  1  4 16  0  0  0  C 17  1  5 17  0  0  0  0 18  1  6 18  0  0  0  0
 19  1  7 19  0  0  0  C 20  1  8 20  0  0  0  0 21  1  9 21  0  0  0  0
 22  1 10 22  0  0  0  C 23  1 11 23  0  0  0  0 24  1 12 24  0  0  0  0
 25  2  1  2  3  0  0  C 26  2  2  3  4  0  0  0 27  2  3  4  5  0  0  0
 28  2  4  5  6  0  0  C 29  2  5  6  1  0  0  0 30  2  6  1  2  0  0  0
 31  2  7  1  6  0  0  C 32  2  7  1  2  0  0  0 33  2  8  2  1  0  0  0
 34  2  8  2  3  0  0  C 35  2  9  3  2  0  0  0 36  2  9  3  4  0  0  0
 37  2 10  4  3  0  0  C 38  2 10  4  5  0  0  0 39  2 11  5  4  0  0  0
 40  2 11  5  6  0  0  C 41  2 12  6  5  0  0  0 42  2 12  6  1  0  0  0
 43  2 13  1  6  0  0  C 44  2 13  1  2  0  0  0 45  2 14  2  1  0  0  0
 46  2 14  2  3  0  0  C 47  2 15  3  2  0  0  0 48  2 15  3  4  0  0  0
 49  2 16  4  3  0  0  C 50  2 16  4  5  0  0  0 51  2 17  5  4  0  0  0
 52  2 17  5  6  0  0  C 53  2 18  6  5  0  0  0 54  2 18  6  1  0  0  0
 55  2 13  1  7  0  0  C 56  2 14  2  8  0  0  0 57  2 15  3  9  0  0  0
 58  2 16  4 10  0  0  C 59  2 17  5 11  0  0  0 60  2 18  6 12  0  0  0
 61  2  1  7 19  0  0  C 62  2  2  8 20  0  0  0 63  2  3  9 21  0  0  0
 64  2  4 10 22  0  0  C 65  2  5 11 23  0  0  0 66  2  6 12 24  0  0  0
 67  4  6  1  2  8  3  C  0  4 13  1  2  3  3  0  0  4  7  1  2 14  3  0
 68  4  1  2  3  9  3  C  0  4 14  2  3 15  3  0  0  4  8  2  3  4  3  0
 69  4  2  3  4 10  3  C  0  4 15  3  4 16  3  0  0  4  9  3  4  5  3  0
 70  4  3  4  5 11  3  C  0  4 10  4  5  6  3  0  0  4 16  4  5 17  3  0
 71  4  4  5  6 18  3  C  0  4 11  5  6  1  3  0  0  4 17  5  6 12  3  0
 72  4  5  6  1 13  3  C  0  4 12  6  1  7  3  0  0  4 18  6  1  2  3  0
 73  4 19  7  1 13  3  C  0  4 19  7  1  6  3  0  0  4 19  7  1  2  3  0
 74  4 20  8  2 14  3  C  0  4 20  8  2  1  3  0  0  4 20  8  2  3  3  0
 75  4 21  9  3 15  3  C  0  4 21  9  3  2  3  0  0  4 21  9  3  4  3  0
 76  4 22 10  4 16  3  C  0  4 22 10  4  3  3  0  0  4 22 10  4  5  3  0
 77  4 23 11  5 17  3  C  0  4 23 11  5  4  3  0  0  4 23 11  5  6  3  0
 78  4 24 12  6 18  3  C  0  4 24 12  6  5  3  0  0  4 24 12  6  1  3  0
-02
-06  1  3 78
 12.00000    12.00000    12.00000    12.00000    12.00000    12.00000
 15.994915   15.994915   15.994915   15.994915   15.994915   15.994915
  1.007825    1.007825    1.007825    1.007825    1.007825    1.007825
  1.007825    1.007825    1.007825    1.007825    1.007825    1.007825
  1  1     1        1  5     1        2  2     1        2  4     1
  3  3     2        4  6     2        5  7     1        5 12     1
  6  8     1        6 11     1        7  9     1        7 10     1
  8 13     1        8 12     1        9 14     1        9 17     1
 10 15     1       10 16     1       11 19     1       11 24     1
 12 20     1       12 23     1       13 21     1       13 22     1
 14 25     1       14 28     1       15 26     1       15 27     1
 16 29     1       16 30     1       17 31     1       17 42     1
 18 32     1       18 41     1       19 33     1       19 40     1
 20 34     1       20 39     1       21 35     1       21 38     1
 22 36     1       22 37     1       23 43     1       23 54     1
 24 44     1       24 53     1       25 45     1       25 52     1
 26 46     1       26 51     1       27 47     1       27 50     1
 28 48     1       28 49     1       29 55     1       29 60     1
 30 56     1       30 59     1       31 57     1       31 58     1
 32 61     1       32 66     1       33 62     1       33 65     1
 34 63     1       34 64     1       35 67     1       35 71     1
 36 68     1       36 70     1       37 69     2       38 72     2
 39 73     1       39 78     1       40 74     1       40 77     1
 41 75     1       41 76     1
 42  1     1       42  5    -1       43  2     1       43  4    -1
 44  7     1       44 12    -1       45  8     1       45 11    -1
 46  9     1       46 10    -1       47 13     1       47 18    -1
 48 14     1       48 17    -1       49 15     1       49 16    -1
 50 19     1       50 24    -1       51 20     1       51 23    -1
 52 21     1       52 22    -1       53 25     1       53 28    -1
 54 26     1       54 27    -1       55 29     1       55 30    -1
 56 31     1       56 42    -1       57 32     1       57 41    -1
 58 33     1       58 40    -1       59 34     1       59 39    -1
 60 35     1       60 38    -1       61 36     1       61 37    -1
 62 43     1       62 54    -1       63 44     1       63 53    -1
 64 45     1       64 52    -1       65 46     1       65 51    -1
 66 47     1       66 50    -1       67 48     1       67 49    -1
 68 55     1       68 60    -1       69 56     1       69 59    -1
 70 57     1       70 58    -1       71 61     1       71 66    -1
 72 62     1       72 65    -1       73 63     1       73 64    -1
 74 67     1       74 71    -1       75 68     1       75 70    -1
 76 73     1       76 78    -1       77 74     1       77 77    -1
 78 75     1       78 76    -1       -3
  1 42 79
999
```

TABLE XXXIX (Continued)

GMAT INPUT FOR MUCO-INOSITOL

```
-09
-09      1  24  78   1   0   0   0
     MUCO-INOSITOL - SYMMETRIZED AND UNSYMMETRIZED G MATRIX
     TETRAHEDRAL STRUCTURE - C-C 1.525  C-O 1.425  C-H 1.10  O-H 0.97
  1  2     1.525000   1  3     2.033332   2  3     1.437783   1  4     1.524998
  2  4     2.156676   3  4    -1.245157   2  5     2.156675   3  5    -1.245154
  1  6    -0.508336   2  6     0.718892   3  6    -1.245153   1  7    -0.475000
  2  7     0.671749   3  7     1.163507   1  8     1.999998   2  8    -0.671751
  3  8    -1.163507   1  9     3.458330   2  9     1.437781   1 10     1.999995
  2 10     3.500177   3 10    -1.245154   1 11    -0.475006   2 11     2.828425
  3 11    -2.408660   1 12    -0.033337   2 12     0.047142   3 12    -2.408661
  1 13    -0.366666   2 13    -1.037089   1 14     1.891665   2 14    -0.518545
  3 14     0.898147   1 15     1.666663   2 15     1.956326   3 15     0.898147
  1 16     1.891661   2 16     1.638130   3 16    -2.143302   1 17    -0.366669
  2 17     2.675220   3 17    -0.347007   1 18    -1.608335   2 18     0.718893
  3 18    -1.245150   1 19    -0.151666   2 19     1.586274   3 19     1.163507
  1 20     1.676661   2 20    -1.586275   3 20    -1.163507   1 21     3.781663
  2 21     0.980521   3 21    -0.792005   1 22     1.676661   2 22     3.957436
  3 22    -0.453150   1 23    -0.151674   2 23     2.371161   3 23    -3.200661
  1 24    -0.356670   2 24    -0.867384   3 24    -2.408661  -1  0     0.0
  1  1  1  2  0  0  0  C  2  1  2  3  0  0  0  0  3  1  3  4  0  0  0  0
  4  1  4  5  0  0  0  C  5  1  5  6  0  0  0  0  6  1  6  1  0  0  0  0
  7  1  1  7  0  0  0  C  8  1  2  8  0  0  0  0  9  1  3  9  0  0  0  0
 10  1  4 10  0  0  0  C 11  1  5 11  0  0  0  0 12  1  6 12  0  0  0  0
 13  1  1 13  0  0  0  C 14  1  2 14  0  0  0  0 15  1  3 15  0  0  0  0
 16  1  4 16  0  0  0  C 17  1  5 17  0  0  0  0 18  1  6 18  0  0  0  0
 19  1  7 19  0  0  0  C 20  1  8 20  0  0  0  0 21  1  9 21  0  0  0  0
 22  1 10 22  0  0  0  C 23  1 11 23  0  0  0  0 24  1 12 24  0  0  0  0
 25  2  1  2  3  0  0  C 26  2  2  3  4  0  0  0 27  2  3  4  5  0  0  0
 28  2  4  5  6  0  0  0 29  2  5  6  1  0  0  0 30  2  6  1  2  0  0  0
 31  2  7  1  6  0  0  C 32  2  7  1  2  0  0  0 33  2  8  2  1  0  0  0
 34  2  8  2  3  0  0  C 35  2  9  3  2  0  0  0 36  2  9  3  4  0  0  0
 37  2 10  4  3  0  0  C 38  2 10  4  5  0  0  0 39  2 11  5  4  0  0  0
 40  2 11  5  6  0  0  C 41  2 12  6  5  0  0  0 42  2 12  6  1  0  0  0
 43  2 13  1  6  0  0  C 44  2 13  1  2  0  0  0 45  2 14  2  1  0  0  0
 46  2 14  2  3  0  0  C 47  2 15  3  2  0  0  0 48  2 15  3  4  0  0  0
 49  2 16  4  3  0  0  C 50  2 16  4  5  0  0  0 51  2 17  5  4  0  0  0
 52  2 17  5  6  0  0  C 53  2 18  6  5  0  0  0 54  2 18  6  1  0  0  0
 55  2 13  1  7  0  0  C 56  2 14  2  8  0  0  0 57  2 15  3  9  0  0  0
 58  2 16  4 10  0  0  C 59  2 17  5 11  0  0  0 60  2 18  6 12  0  0  0
 61  2  1  7 19  0  0  C 62  2  2  8 20  0  0  0 63  2  3  9 21  0  0  0
 64  2  4 10 22  0  0  C 65  2  5 11 23  0  0  0 66  2  6 12 24  0  0  0
 67  4  6  1  2 14  3  C  0  4 13  1  2  3  3  0  0  4  7  1  2  8  3  0
 68  4  1  2  3  9  3  C  0  4 14  2  3  4  3  0  0  4  8  2  3 15  3  0
 69  4  2  3  4 10  3  C  0  4 15  3  4 16  3  0  0  4  9  3  4  5  3  0
 70  4  3  4  5 11  3  C  0  4 10  4  5  6  3  0  0  4 16  4  5 17  3  0
 71  4  4  5  6 18  3  C  0  4 11  5  6  1  3  0  0  4 17  5  6 12  3  0
 72  4  5  6  1 13  3  C  0  4 12  6  1  7  3  0  0  4 18  6  1  2  3  0
 73  4 19  7  1 13  3  C  0  4 19  7  1  6  3  0  0  4 19  7  1  2  3  0
 74  4 20  8  2 14  3  C  0  4 20  8  2  1  3  0  0  4 20  8  2  3  3  0
 75  4 21  9  3 15  3  C  0  4 21  9  3  2  3  0  0  4 21  9  3  4  3  0
 76  4 22 10  4 16  3  C  0  4 22 10  4  3  3  0  0  4 22 10  4  5  3  0
 77  4 23 11  5 17  3  C  0  4 23 11  5  4  3  0  0  4 23 11  5  6  3  0
 78  4 24 12  6 18  3  C  0  4 24 12  6  5  3  0  0  4 24 12  6  1  3  0
-02
-06  1  3 78
 12.00000    12.00000    12.00000    12.00000    12.00000    12.00000
 15.994915   15.994915   15.994915   15.994915   15.994915   15.994915
  1.007825    1.007825    1.007825    1.007825    1.007825    1.007825
  1.007825    1.007825    1.007825    1.007825    1.007825    1.007825
  1  1     1        1  6     1        2  2     1        2  5     1
  3  3     1        3  4     1        4  7     2        5  8     1
  5 12     1        6  9     1        6 11     1        7 10     2
  8 13     2        9 14     1        9 18     1       10 15     1
 10 17     1       11 16     2       12 19     2       13 20     1
 13 24     1       14 21     1       14 23     1       15 22     2
 16 25     1       16 29     1       17 26     1       17 28     1
 18 27     2       19 30     2       20 31     1       20 32     1
 21 33     1       21 42     1       22 34     1       22 41     1
 23 35     1       23 40     1       24 36     1       24 39     1
 25 37     1       25 38     1       26 43     1       26 44     1
 27 45     1       27 54     1       28 46     1       28 53     1
 29 47     1       29 52     1       30 48     1       30 51     1
 31 49     1       31 50     1       32 55     2       33 56     1
 33 60     1       34 57     1       34 59     1       35 58     2
 36 61     2       37 62     1       37 66     1       38 63     1
 38 65     1       39 64     2       40 67     1       40 72    -1
 41 68     1       41 71    -1       42 69     1       42 70    -1
 43 74     1       43 78    -1       44 75     1       44 77    -1
 45  1     1       45  6    -1       46  2     1       46  5    -1
 47  3     1       47  4    -1       48  8     1       48 12    -1
 49  9     1       49 11    -1       50 14     1       50 18    -1
 51 15     1       51 17    -1       52 20     1       52 24    -1
 53 21     1       53 23    -1       54 25     1       54 29    -1
 55 26     1       55 28    -1       56 31     1       56 32    -1
 57 33     1       57 42    -1       58 34     1       58 41    -1
 59 35     1       59 40    -1       60 36     1       60 39    -1
 61 37     1       61 38    -1       62 43     1       62 44    -1
 63 45     1       63 54    -1       64 46     1       64 53    -1
 65 47     1       65 52    -1       66 48     1       66 51    -1
 67 49     1       67 50    -1       68 56     1       68 60    -1
 69 57     1       69 59    -1       70 62     1       70 66    -1
 71 63     1       71 65    -1       72 67     1       72 72     1
 73 68     1       73 71     1       74 69     1       74 70     1
 75 73     2       76 74     1       76 78     1       77 75     1
 77 77     1       78 76     1
 -3
  1 45 79
999
```

TABLE XXXIX (Cont'd). GMAT INPUT FOR DEUTERATED SCYLLO-INOSITOL

```
-09
-09
    1  24  78   1   0   0   0
   DEUTERATED SCYLLO-INOSITOL - SYMMETRIZED AND UNSYMMETRIZED G MATRIX
   TETRAHEDRAL STRUCTURE - C-C 1.525  C-O 1.425  C-H 1.10   O-H 0.97
  1  2    1.529000   1  3    2.033332   2  3    1.537783   1  4   -1.524998
  2  4    2.156676   3  4   -1.245157   2  5    2.156675   3  5   -1.245154
  1  6   -0.508336   2  6    0.718892   3  6   -1.245153   1  7   -0.475000
  2  7   -1.343501   1  8    1.999998   2  8   -0.671751   3  8    1.163507
  1  9    3.458330   2  9    1.437781   1 10    1.999995   2 10    3.500177
  3 10   -1.245154   1 11   -0.475006   2 11    2.828425   3 11   -2.408660
  1 12   -1.933335   2 12    0.718892   3 12   -1.245149   1 13   -0.366666
  2 13    0.518544   3 13    0.898147   1 14    1.691665   2 14   -0.518545
  3 14   -0.898147   1 15    1.666663   2 15    1.956376   3 15    0.898147
  1 16    1.891661   2 16    1.638130   3 16   -2.143302   1 17   -0.366669
  2 17    2.675220   3 17   -0.347007   1 18   -0.141670   2 18    0.200348
  3 18   -2.143300   1 19   -0.151666   2 19   -1.800761   3 19   -0.792004
  1 20    1.676662   2 20   -0.214488   3 20    1.955508   1 21    3.781663
  2 21    0.980521   3 21   -0.792005   1 22    1.676661   2 22    3.957436
  3 22   -0.453150   1 23   -0.151674   2 23    2.371161   3 23   -3.200661
  1 24   -2.256665   2 24    1.176154   3 24   -0.453144  -1   0    0.0
  1  1    2  0  0  0  0  C    2  3    0  0  0    3  1    4  0  0  0  0
  4  1    4  5  0  0  0  C    5  1    5  6    0  0  0    6  1    1  0  0  0  0
  7  1    1  7  0  0  0  C    8  1    2  8    0  0  0    9  1    3  9    0  0  0  0
 10  1    4 10  0  0  0  C   11  1    5 11    0  0  0   12  1    6 12    0  0  0  0
 13  1    1 13  0  0  0  C   14  1    2 14    0  0  0   15  1    3 15    0  0  0  0
 16  1    4 16  0  0  0  C   17  1    5 17    0  0  0   18  1    6 18    0  0  0  0
 19  1    7 19  0  0  0  C   20  1    8 20    0  0  0   21  1    6 21    0  0  0  0
 22  1   10 22  0  0  0  C   23  1   11 23    0  0  0   24  1   12 24    0  0  0  0
 25  2    1  2  3  0  0  0  C   26  2    2  3    4  0  0  0   27  2    3  4    5  0  0  0
 28  2    4  5  6  0  0  0  C   29  2    5  6    1  0  0  0   30  2    6  1    2  0  0  0
 31  2    7  1  6  0  0  0  C   32  2    7  1    2  0  0  0   33  2    8  2    1  0  0  0
 34  2    8  2  3  0  0  0  C   35  2    9  3    3  0  0  0   36  2    3  3    4  0  0  0
 37  2   10  4  3  0  0  0  C   38  2   10  4    5  0  0  0   39  2   11  5    4  0  0  0
 40  2   11  5  6  0  0  0  C   41  2   12  6    5  0  0  0   42  2   12  6    1  0  0  0
 43  2   13  1  6  0  0  0  C   44  2   13  1    2  0  0  0   45  2   14  2    1  0  0  0
 46  2   14  2  3  0  0  0  C   47  2   15  3    2  0  0  0   48  2   15  3    4  0  0  0
 49  2   16  4  3  0  0  0  C   50  2   16  4    5  0  0  0   51  2   17  5    4  0  0  0
 52  2   17  5  6  0  0  0  C   53  2   18  6    5  0  0  0   54  2   18  6    1  0  0  0
 55  2   13  1  7  0  0  0  C   56  2   14  2    8  0  0  0   57  2   15  3    9  0  0  0
 58  2   16  4 10  0  0  0  C   59  2   17  5   11  0  0  0   60  2   18  6   12  0  0  0
 61  2    1  7 19  0  0  0  C   62  2    2  8   20  0  0  0   63  2    3  9   21  0  0  0
 64  2    4 10 22  0  0  0  C   65  2    5 11   23  0  0  0   66  2    6 12   24  0  0  0
 67  4    6  1  2  8  3  0  C    0  4   13  1    2 14  3  0  0  0  4   14  2    3 15  3  0
 68  4    1  2  3  9  3  0  C    0  4    8  2    3  4  3  0  0  0  4   14  2    3 15  3  0
 69  4    2  3  4 10  3  0  C    0  4    9  3    4  5  3  0  0  0  4   15  3    4 16  3  0
 70  4    3  4  5 11  3  0  C    0  4   10  4    5  6  3  0  0  0  4   16  4    5 17  3  0
 71  4    4  5  6 12  3  0  C    0  4   11  5    6  1  3  0  0  0  4   17  5    6 18  3  0
 72  4    5  6  1  7  3  0  C    0  4   12  6    1  2  3  0  0  0  4   18  6    1 13  3  0
 73  4   19  7  1 13  3  0  C    0  4   19  7    1  6  3  0  0  0  4   19  7    1  2  3  0
 74  4   20  8  2 14  3  0  C    0  4   20  8    2  1  3  0  0  0  4   20  8    2  3  3  0
 75  4   21  9  3 15  3  0  C    0  4   21  9    3  2  3  0  0  0  4   21  9    3  4  3  0
 76  4   22 10  4 16  3  0  C    0  4   22 10    4  3  3  0  0  0  4   22 10    4  5  3  0
 77  4   23 11  5 17  3  0  C    0  4   23 11    5  4  3  0  0  0  4   23 11    5  6  3  0
 78  4   24 12  6 18  3  0  C    0  4   24 12    6  5  3  0  0  0  4   24 12    6  1  3  0
-02
-06   1   7  52
 12.00000   12.00000   12.00000   12.00000   12.00000   12.00000
 15.994915  15.994915  15.994915  15.994915  15.994915  15.994915
  1.007825   1.007825   1.007825   1.007825   1.007825   1.007825
  2.014099   2.014099   2.014099   2.014099   2.014099   2.014099
  1  1    2          1  2    2          1  3    2          1  4    2
  1  5    2          1  6    2          2  7    2          2  8    2
  2  9    2          2 10    2          2 11    2          2 12    2
  3 13    2          3 14    2          3 15    2          3 16    2
  3 17    2          3 18    2          4 19    2          4 20    2
  4 21    2          4 22    2          4 23    2          4 24    2
  5 25    2          5 26    2          5 27    2          5 28    2
  5 29    2          5 30    2          6 31    1          6 32    1
  6 33    1          6 34    1          6 35    1          6 36    1
  6 37    1          6 38    1          6 39    1          6 40    1
  6 41    1          6 42    1          7 43    1          7 44    1
  7 45    1          7 46    1          7 47    1          7 48    1
  7 49    1          7 50    1          7 51    1          7 52    1
  7 53    1          7 54    1          8 55    2          8 56    2
  8 57    2          8 58    2          8 59    2          8 60    2
  9 61    2          9 62    2          9 63    2          9 64    2
  9 65    2          9 66    2         10 67    2         10 68   -2
 10 69    2         10 70   -2         10 71    2         10 72   -2
 11 31    1         11 32   -1         11 33    1         11 34   -1
 11 35    1         11 36   -1         11 37    1         11 38   -1
 11 39    1         11 40   -1         11 41    1         11 42   -1
 12 43    1         12 44   -1         12 45    1         12 46   -1
 12 47    1         12 48   -1         12 49    1         12 50   -1
 12 51    1         12 52   -1         12 53    1         12 54   -1
 13 73    2         13 74   -2         13 75    2         13 76   -2
 13 77    2         13 78   -2
 14  1    1         14  2   -2         14  3    1         14  4    1
 14  5   -2         14  6    1         15  7    2         15  8   -1
 15  9   -1         15 10    2         15 11   -1         15 12   -1
 16 13    2         16 14   -1         16 15   -1         16 16    2
 16 17   -1         16 18   -1         17 19   -2         17 20   -1
 17 21   -1         17 22    2         17 23   -1         17 24   -1
 18 25   -1         18 26   -1         18 27    2         18 28   -1
 18 29   -1         18 30    2         19 33    3         19 34   -3
 19 35   -3         19 36    3         19 39    3         19 40   -3
 19 41   -3         19 42    3         20 31   -2         20 32   -2
 20 33    1         20 34    1         20 35    1         20 36    1
 20 37   -2         20 38   -2         20 39    1         20 40    1
 20 41    1         20 42    1         21 45    3         21 46   -3
 21 47   -3         21 48    3         21 51    3         21 52   -3
 21 53   -3         21 54    3         22 43   -2         22 44   -2
 22 45    1         22 46    1         22 47    1         22 48    1
 22 49   -2         22 50   -2         22 51    1         22 52    1
 22 53    1         22 54    1         23 55    2         23 56   -1
 23 57   -1         23 58    2         23 59   -1         23 60   -1
 24 61    2         24 62   -1         24 63   -1         24 64    2
 24 65   -1         24 66   -1         25 67   -1         25 68   -2
 25 69   -1         25 70    1         25 71    2         25 72    1
 26 74   -3         26 75   -3         26 77    3         26 78    3
 27  1    2         27  2   -2         27  3    2         27  4   -2
 27  5    2         27  6   -2         28 31    1         28 32   -1
 28 33   -1         28 34    1         28 35    1         28 36   -1
 28 37   -1         28 38    1         28 39    1         28 40   -1
 28 41   -1         28 42    1         29 43    1         29 44   -1
 29 45   -1         29 46    1         29 47    1         29 48   -1
 29 49   -1         29 50    1         29 51    1         29 52   -1
 29 53   -1         29 54    1         30 67    2         30 68    2
 30 69    2         30 70    2         30 71    2         30 72    2
 31 73    2         31 74    2         31 75    2         31 76    2
 31 77    2         31 78    2
 32  7    2         32  8   -2         32  9    2         32 10   -2
 32 11    2         32 12   -2         33 13    2         33 14   -2
 33 15    2         33 16   -2         33 17    2         33 18   -2
 34 19    2         34 20   -2         34 21    2         34 22   -2
 34 23    2         34 24   -2         35 25    2         35 26   -2
 35 27    2         35 28   -2         35 29    2         35 30   -2
 36 31    1         36 32    (         36 33   -1         36 34   -1
 36 35    1         36 36    1         36 37   -1         36 38   -1
 36 39    1         36 40    1         36 41   -1         36 42   -1
 37 43    1         37 44    1         37 45   -1         37 46   -1
 37 47    1         37 48    1         37 49   -1         37 50   -1
 37 51    1         37 52    1         37 53   -1         37 54   -1
 38 55    2         38 56   -2         38 57    2         38 58   -2
 38 59    2         38 60   -2         39 61    2         39 62   -2
 39 63    2         39 64   -2         39 65    2         39 66   -2
 40  1    3         40  3   -3         40  4   -3         40  6    3
 41  7    1         41  8    1         41  9   -1         41 10   -2
 41 11   -1         41 12    1         42 13    2         42 14    1
 42 15   -1         42 16   -2         42 17   -1         42 18    1
 43 19    2         43 20    1         43 21   -1         43 22   -2
 43 23   -1         43 24    1         44 25    1         44 26   -1
 44 27   -2         44 28   -1         44 29    1         44 30    2
 45 33    3         45 34   -3         45 35    3         45 36   -3
 45 39   -3         45 40    3         45 41   -3         45 42    3
 46 31   -2         46 32   -2         46 33   -1         46 34   -1
 46 35    1         46 36    1         46 37    2         46 38    2
 46 39    1         46 40    1         46 41   -1         46 42   -1
 47 45    3         47 46   -3         47 47    3         47 48   -3
 47 51   -3         47 52    3         47 53   -3         47 54    3
 48 43   -2         48 44   -2         48 45   -1         48 46   -1
 48 47    1         48 48    1         48 49    2         48 50    2
 48 51    2         48 52   -1         48 53   -1         48 54   -1
 49 55    2         49 56    1         49 57   -1         49 58   -2
 49 59   -1         49 60    1         50 61    2         50 62    1
 50 63   -1         50 64   -2         50 65   -1         50 66    1
 51 67   -3         51 68    3         51 70   -3         51 72    3
 52 74   -3         52 75    3         52 77   -3         52 78    3
-3
 1 11 14 27 32 40 53
999
```

TABLE XXXIX (Continued)

GMAT INPUT FOR DEUTERATED NEO-INOSITOL

```
-09
-09      1  24  78   1   0   0   0
    DEUTERATED NEO-INOSITOL - SYMMETRIZED AND UNSYMMETRIZED G MATRIX
    TETRAHEDRAL STRUCTURE - C-C 1.525  C-O 1.425  C-H 1.10  O-H 0.97
  1   2     1.525000    1   3    2.033332    2   3     1.437783    1   4     1.524998
  2   4     2.156678    3   4   -1.245157    2   5     2.156675    3   5    -1.245154
  1   6    -0.508336    2   6    0.718892    3   6    -1.245153    1   7    -0.475000
  2   7    -1.343501    1   8    1.999998    2   8    -0.671761    3   8    -1.163507
  1   9     3.458330    2   9    1.437781    1  10     1.999995    2  10     3.500177
  3  10    -1.245154    1  11   -0.475001    2  11     2.828425    3  11    -0.081645
  1  12    -1.933335    2  12    0.718892    3  12    -1.245149    1  13    -0.366666
  2  13     0.518544    3  13    0.898147    1  14     1.891665    2  14    -0.518545
  3  14     0.898147    1  15    1.666663    2  15     1.956326    3  15     0.898147
  1  16     1.891661    2  16    1.638130    3  16    -2.143302    1  17    -0.366672
  2  17     2.675220    3  17   -2.143300    1  18    -0.141670    2  18     0.200348
  3  18    -2.143300    1  19   -0.151666    2  19    -1.880761    3  19    -0.792004
  1  20     1.676663    2  20   -0.214487    3  20    -1.955508    1  21     1.781663
  2  21     0.980521    3  21   -0.792005    1  22     1.676661    2  22     3.957436
  3  22    -0.453150    1  23   -0.151665    2  23     2.371161    3  23     0.710356
  1  24    -2.256665    2  24    1.176154    3  24    -0.453144   -1   0      0.0
  1   1   1   2   0   0   0   0   C   2   1   2   3   0   0   0   0   0   3   1   3   4   0   0   0   0
  1   1   4   5   0   0   0   0   C   5   1   5   6   0   0   0   0   0   6   1   6   1   0   0   0   0
  1   1   7   0   0   0   0   0   C   8   1   2   8   0   0   0   0   0   9   1   3   9   0   0   0   0
 10   1   4  10   0   0   0   0   C  11   1   5  11   0   0   0   0   0  12   1   6  12   0   0   0   0
 13   1   1  13   0   0   0   0   C  14   1   2  14   0   0   0   0   0  15   1   3  15   0   0   0   0
 16   1   4  16   0   0   0   0   C  17   1   5  17   0   0   0   0   0  18   1   6  18   0   0   0   0
 19   1   7  19   0   0   0   0   C  20   1   8  20   0   0   0   0   0  21   1   9  21   0   0   0   0
 22   1  10  22   0   0   0   0   C  23   1  11  23   0   0   0   0   0  24   1  12  24   0   0   0   0
 25   2   1   2   3   0   0   0   C  26   2   2   3   4   0   0   0   0  27   2   3   4   5   0   0   0
 28   2   4   5   6   0   0   0   C  29   2   5   6   1   0   0   0   0  30   2   6   1   2   0   0   0
 31   2   7   1   6   0   0   0   C  32   2   7   1   2   0   0   0   0  33   2   8   2   1   0   0   0
 34   2   8   2   3   0   0   0   C  35   2   9   3   2   0   0   0   0  36   2   9   3   4   0   0   0
 37   2  10   4   3   0   0   0   C  38   2  10   4   5   0   0   0   0  39   2  11   5   4   0   0   0
 40   2  11   5   6   0   0   0   C  41   2  12   6   5   0   0   0   0  42   2  12   6   1   0   0   0
 43   2  13   1   6   0   0   0   C  44   2  13   1   2   0   0   0   0  45   2  14   2   1   0   0   0
 46   2  14   2   3   0   0   0   C  47   2  15   3   2   0   0   0   0  48   2  15   3   4   0   0   0
 49   2  16   4   3   0   0   0   C  50   2  16   4   5   0   0   0   0  51   2  17   5   4   0   0   0
 52   2  17   5   6   0   0   0   C  53   2  18   6   5   0   0   0   0  54   2  18   6   1   0   0   0
 55   2  13   1   7   0   0   0   C  56   2  14   2   8   0   0   0   0  57   2  15   3   9   0   0   0
 58   2  16   4  10   0   0   0   C  59   2  17   5  11   0   0   0   0  60   2  18   6  12   0   0   0
 61   2   1   7  19   0   0   0   C  62   2   2   8  20   0   0   0   0  63   2   3   9  21   0   0   0
 64   2   4  10  22   0   0   0   C  65   2   5  11  23   0   0   0   0  66   2   6  12  24   0   0   0
 67   4   6   1   2  14   3   0   0   4   7   1   2   3   3   0   0   4  13   1   2   8   3   0
 68   4   1   2   3   9   3   0   0   4   8   2   3  15   3   0   0   4  14   2   3   4   3   0
 69   4   2   3   4  10   3   0   0   4   9   3   4   5   3   0   0   4  15   3   4  16   3   0
 70   4   3   4   5  17   3   0   0   4  10   4   5   6   3   0   0   4  16   4   5  11   3   0
 71   4   4   5   6  12   3   0   0   4  11   5   6  18   3   0   0   4  17   5   6   1   3   0
 72   4   5   6   1   7   3   0   0   4  12   6   1   2   3   0   0   4  18   6   1  13   3   0
 73   4  19   7   1  13   3   0   0   4  19   7   1   6   3   0   0   4  19   7   1   2   3   0
 74   4  20   8   2  14   3   0   0   4  20   8   2   1   3   0   0   4  20   8   2   3   3   0
 75   4  21   9   3  15   3   0   0   4  21   9   3   2   3   0   0   4  21   9   3   4   3   0
 76   4  22  10   4  16   3   0   0   4  22  10   4   3   3   0   0   4  22  10   4   5   3   0
 77   4  23  11   5  17   3   0   0   4  23  11   5   4   3   0   0   4  23  11   5   6   3   0
 78   4  24  12   6  18   3   0   0   4  24  12   6   5   3   0   0   4  24  12   6   1   3   0
-02
-06   1   3  78
 12.00000    12.00000    12.00000    12.00000    12.00000    12.00000
 15.994915   15.994915   15.994915   15.994915   15.994915   15.994915
  1.007825    1.007825    1.007825    1.007825    1.007825    1.007825
  2.014099    2.014099    2.014099    2.014099    2.014099    2.014099
  1   1   1   2   1   1   4   1   1   5   1
  2   3   2   6   2   3   7   1   3   9   1
  3  10   1   3  12   4   8   2   4  11   2
  5  13   1   5  15   5  16   1   5  18   1
  6  14   2   6  17   7  19   1   7  21   1
  7  22   1   7  24   8  20   2   8  23   2
  9  25   2   9  28   9  26   1  10  27   1
 10  27   1  10  30  11  31   1  11  36   1
 11  37   1  11  42  12  32   1  12  35   1
 12  38   1  12  41  13  33   1  13  34   1
 13  39   1  13  40  14  43   1  14  48   1
 14  49   1  14  54  15  44   1  15  47   1
 15  50   1  15  53  16  45   1  16  46   1
 16  51   1  16  52  17  55   1  17  57   1
 17  58   1  17  60  18  56   2  18  59   2
 19  61   1  19  63  19  64   1  19  66   1
 20  62   2  20  65   2  21  67   1  21  68  -1
 21  70  -1  21  71   1  22  69   2  22  72  -2
 23  73   1  23  75  -1  23  76  -1  23  78   1
 24   1   1  24   2  -1  24   4   1  24   5  -1
 25   7   1  25   9  -1  25  10   1  25  12  -1
 26  13   1  26  15  -1  26  16   1  26  18  -1
 27  19   1  27  21  -1  27  22   1  27  24  -1
 28  26   1  28  27  -1  28  29   1  28  30  -1
 29  31   1  29  36  -1  29  37   1  29  42  -1
 30  32   1  30  35  -1  30  38   1  30  41  -1
 31  33   1  31  34  -1  31  39   1  31  40  -1
 32  43   1  32  48  -1  32  49   1  32  54  -1
 33  44   1  33  47  -1  33  50   1  33  53  -1
 34  45   1  34  46  -1  34  51   1  34  52  -1
 35  55   1  35  57  -1  35  58   1  35  60  -1
 36  61   1  36  63  -1  36  64   1  36  66  -1
 37  67   1  37  68   1  37  70  -1  37  71  -1
 38  73   1  38  75   1  38  76  -1  38  78  -1
 39  74   2  39  77  -2
 40   1   1  40   2  -1  40   4  -1  40   5   1
 41   3   2  41   6  -2  42   7   1  42   9  -1
 42  10  -1  42  12   1  43  13   1  43  15  -1
 43  16  -1  43  18   1  44  19   1  44  21  -1
 44  22  -1  44  24   1  45  26   1  45  27   1
 45  29  -1  45  30  -1  46  31   1  46  36  -1
 46  37  -1  46  42   1  47  32   1  47  35  -1
 47  38  -1  47  41   1  48  33   1  48  34  -1
 48  39  -1  48  40   1  49  43   1  49  48  -1
 49  49  -1  49  54   1  50  44   1  50  47  -1
 50  50  -1  50  53   1  51  45   1  51  46  -1
 51  51  -1  51  52   1  52  55   1  52  57  -1
 52  58  -1  52  60   1  53  61   1  53  63  -1
 53  64  -1  53  66   1  54  67   1  54  68
 54  70   1  54  71   1  55  69   2  55  72   2
 56  73   1  56  75   1  56  76   1  56  78   1
 57  74   2  57  77   2
 58   1   1  58   2   1  58   4  -1  58   5  -1
 59   7   1  59   9   1  59  10  -1  59  12  -1
 60   8   2  60  11  -2  61  13   1  61  15   1
 61  16  -1  61  18  -1  62  14   2  62  17  -2
 63  19   1  63  21   1  63  22  -1  63  24  -1
 64  20   2  64  23  -2  65  25   2  65  28  -2
 66  26   1  66  27  -1  66  29  -1  66  30   1
 67  31   1  67  36   1  67  37  -1  67  42  -1
 68  32   1  68  35   1  68  38  -1  68  41  -1
 69  33   1  69  34   1  69  39  -1  69  40  -1
 70  43   1  70  48   1  70  49  -1  70  54  -1
 71  44   1  71  47   1  71  50  -1  71  53  -1
 72  45   1  72  46   1  72  51  -1  72  52  -1
 73  55   1  73  57   1  73  58  -1  73  60  -1
 74  56   2  74  59  -2  75  61   1  75  63   1
 75  64  -1  75  66  -1  76  62   2  76  65  -2
 77  67   1  77  68  -1  77  70   1  77  71  -1
 78  73   1  78  75  -1  78  76   1  78  78  -1
-3
  1  24  40  58  79
999
```

TABLE XXXIX (Continued)

GMAT INPUT FOR DEUTERATED MYO-INOSITOL

```
-09
-09      1  24  78   1   0   0   0
     DEUTERATED MYO-INOSITOL - SYMMETRIZED AND UNSYMMETRIZED G MATRIX
     TETRAHEDRAL STRUCTURE - C-C 1.525  C-O 1.425  C-H 1.10  O-H 0.97
  1  2     1.525000  1  3     2.033332  2  3     1.437783  1  4     1.524998
  2  4     2.156676  3  4    -1.245157  2  5     2.156675  3  5    -1.245154
  1  6    -0.508336  2  6     0.718892  3  6    -1.245153  1  7    -0.475000
  2  7    -1.343501  1  8     1.999998  2  8    -0.671751  3  8    -1.163507
  1  9     3.458330  2  9     1.437781  1 10     1.999995  2 10     3.500177
  3 10    -1.245154  1 11    -0.475006  2 11     2.828425  3 11    -2.408660
  1 12    -1.933335  2 12     0.718892  3 12    -1.245149  1 13    -0.366666
  2 13     0.518544  3 13     0.898147  1 14     1.891665  2 14    -0.518545
  3 14     0.898147  1 15     1.666663  2 15     1.956326  3 15     0.898147
  1 16     1.891661  2 16     1.638130  3 16    -2.143302  1 17    -0.366669
  2 17     2.675220  3 17    -0.347007  1 18    -0.141670  2 18     0.700348
  3 18    -2.143300  1 19    -0.151666  2 19    -1.800761  3 19    -0.792004
  1 20     1.676663  2 20    -0.214487  3 20    -1.955508  1 21     3.781663
  2 21     0.980521  3 21    -0.792005  1 22     1.676661  2 22     3.957436
  3 22    -0.453150  1 23    -0.151674  2 23     2.371161  3 23    -3.200661
  1 24    -2.256665  2 24     1.176154  3 24    -0.453144 -1  0      0.0
  1  1  1  2  0  0  0  0  2  1  2  3  0  0  0  0  3  1  3  4  0  0  0  0
  4  1  4  5  0  0  0  C  5  1  5  6  0  0  0  0  0  6  1  6  1  0  0  0  0
  7  1  1  7  0  0  0  C  8  1  2  8  0  0  0  0  0  9  1  3  9  0  0  0  0
 10  1  4 10  0  0  0  C 11  1  5 11  0  0  0  0  0 12  1  6 12  0  0  0  0
 13  1  1 13  0  0  0  C 14  1  2 14  0  0  0  0  0 15  1  3 15  0  0  0  0
 16  1  4 16  0  0  0  C 17  1  5 17  0  0  0  0  0 18  1  6 18  0  0  0  0
 19  1  7 19  0  0  0  C 20  1  8 20  0  0  0  0  0 21  1  9 21  0  0  0  0
 22  1 10 22  0  0  0  C 23  1 11 23  0  0  0  0  0 24  1 12 24  0  0  0  0
 25  2  1  2  3  0  0  C 26  2  2  3  4  0  0  0  0 27  2  3  4  5  0  0  0
 28  2  4  5  6  0  0  C 29  2  5  6  1  0  0  0  0 30  2  6  1  2  0  0  0
 31  2  7  1  6  0  0  C 32  2  7  1  2  0  0  0  0 33  2  8  2  1  0  0  0
 34  2  8  2  3  0  0  C 35  2  9  3  2  0  0  0  0 36  2  9  3  4  0  0  0
 37  2 10  4  3  0  0  C 38  2 10  4  5  0  0  0  0 39  2 11  5  4  0  0  0
 40  2 11  5  6  0  0  C 41  2 12  6  5  0  0  0  0 42  2 12  6  1  0  0  0
 43  2 13  1  6  0  0  C 44  2 13  1  2  0  0  0  0 45  2 14  2  1  0  0  0
 46  2 14  2  3  0  0  C 47  2 15  3  2  0  0  0  0 48  2 15  3  4  0  0  0
 49  2 16  4  3  0  0  C 50  2 16  4  5  0  0  0  0 51  2 17  5  4  0  0  0
 52  2 17  5  6  0  0  C 53  2 18  6  5  0  0  0  0 54  2 18  6  1  0  0  0
 55  2 13  1  7  0  0  C 56  2 14  2  8  0  0  0  0 57  2 15  3  9  0  0  0
 58  2 16  4 10  0  0  C 59  2 17  5 11  0  0  0  0 60  2 18  6 12  0  0  0
 61  2  1  7 19  0  0  C 62  2  2  8 20  0  0  0  0 63  2  3  9 21  0  0  0
 64  2  4 10 22  0  0  C 65  2  5 11 23  0  0  0  0 66  2  6 12 24  0  0  0
 67  4  6  1  2 14  3  C  0  4 13  1  2  8  3  0  0  4  7  1  2  3  3  0
 68  4  1  2  3  9  3  C  0  4 14  2  3  4  3  0  0  4  8  2  3 15  3  0
 69  4  2  3  4 10  3  C  0  4 15  3  4 16  3  0  0  4  9  3  4  5  3  0
 70  4  3  4  5 11  3  C  0  4 10  4  5  6  3  0  0  4 16  4  5 17  3  0
 71  4  4  5  6 12  3  C  0  4 11  5  6  1  3  0  0  4 17  5  6 18  3  0
 72  4  5  6  1  7  3  C  0  4 12  6  1  2  3  0  0  4 18  6  1 13  3  0
 73  4 19  7  1 13  3  C  0  4 19  7  1  6  3  0  0  4 19  7  1  2  3  0
 74  4 20  8  2 14  3  C  0  4 20  8  2  1  3  0  0  4 20  8  2  3  3  0
 75  4 21  9  3 15  3  C  0  4 21  9  3  2  3  0  0  4 21  9  3  4  3  0
 76  4 22 10  4 16  3  C  0  4 22 10  4  3  3  0  0  4 22 10  4  5  3  0
 77  4 23 11  5 17  3  C  0  4 23 11  5  4  3  0  0  4 23 11  5  6  3  0
 78  4 24 12  6 18  3  C  0  4 24 12  6  5  3  0  0  4 24 12  6  1  3  0
-02
-06  1  3 78
 12.00000   12.00000   12.00000   12.00000   12.00000   12.00000
 15.994915  15.994915  15.994915  15.994915  15.994915  15.994915
  1.007825   1.007825   1.007825   1.007825   1.007825   1.007825
  2.014099   2.014099   2.014099   2.014099   2.014099   2.014099
  1  1    1     1  2    1     2  3    1     2  6    1
  3  4    1     3  5    1     4  7    1     4  9    1
  5  8    2     6 10    1     6 12    1     7 11    2
  8 13    1     8 15    1     9 14    2    10 16    1
 10 18    1    11 17    2    12 19    1    12 21    1
 13 20    2    14 22    1    14 24    1    15 23    2
 16 25    2    17 26    1    17 30    1    18 27    1
 18 29    1    19 28    2    20 31    1    20 36    1
 21 32    1    21 35    1    22 33    1    22 34    1
 23 37    1    23 42    1    24 38    1    24 41    1
 25 39    1    25 40    1    26 43    1    26 48    1
 27 44    1    27 47    1    28 45    1    28 46    1
 29 49    1    29 54    1    30 50    1    30 53    1
 31 51    1    31 52    1    32 55    1    32 57    1
 33 56    2    34 58    1    34 60    1    35 59    2
 36 61    1    36 63    1    37 62    2    38 64    1
 38 66    1    39 65    2    40 67    1    40 68   -1
 41 69    1    41 72   -1    42 70    1    42 71   -1
 43 73    1    43 75   -1    44 76    1    44 78   -1
 45  1    1    45  2   -1    46  3    1    46  6   -1
 47  4    1    47  5   -1    48  7    1    48  9   -1
 49 10    1    49 12   -1    50 13    1    50 15   -1
 51 16    1    51 18   -1    52 19    1    52 21   -1
 53 22    1    53 24   -1    54 26    1    54 30   -1
 55 27    1    55 29   -1    56 31    1    56 36   -1
 57 32    1    57 35   -1    58 33    1    58 34   -1
 59 37    1    59 42   -1    60 38    1    60 41   -1
 61 39    1    61 40   -1    62 43    1    62 48   -1
 63 44    1    63 47   -1    64 45    1    64 46   -1
 65 49    1    65 54   -1    66 50    1    66 53   -1
 67 51    1    67 52   -1    68 55    1    68 57   -1
 69 58    1    69 60   -1    70 61    1    70 63   -1
 71 64    1    71 66   -1    72 67    1    72 68    1
 73 69    1    73 72    1    74 70    1    74 71    1
 75 73    1    75 75    1    76 74    2    77 76    1
 77 78    1    78 77    2   -3
  1 45 79
999
```

TABLE XXXIX (Continued)

GMAT INPUT FOR DEUTERATED EPI-INOSITOL

```
-09
-09      1  24  78   1   0   0   0
      DEUTERATED EPI-INOSITOL - SYMMETRIZED AND UNSYMMETRIZED G MATRIX
      TETRAHEDRAL STRUCTURE - C-C 1.525  C-O 1.425  C-H 1.10  O-H 0.97
  1  2     1.525000   1  3     2.033332   2  3     1.437783   1  4     1.524998
  2  4     2.156676   3  4    -1.245157   2  5     2.156675   3  5    -1.245154
  1  6    -0.508336   2  6     0.718892   3  6    -1.245153   1  7    -0.475000
  2  7    -1.343501   1  8     1.999998   2  8    -0.671751   3  8    -1.163507
  1  9     3.458330   2  9     1.437781   1 10     1.999995   2 10     3.500177
  3 10    -1.245154   1 11    -0.475006   2 11     2.828425   3 11    -2.408660
  1 12    -0.033337   2 12     0.047142   3 12    -2.408661   1 13    -0.366666
  2 13     0.518544   3 13     0.898147   1 14     1.891665   2 14    -0.518545
  3 14     0.898147   1 15     1.666663   2 15     1.956326   3 15     0.898147
  1 16     1.891661   2 16     1.638130   3 16    -2.143302   1 17    -0.366669
  2 17     2.675220   3 17    -0.347007   1 18    -1.608335   2 18     0.718893
  3 18    -1.245150   1 19    -0.151666   2 19    -1.800761   3 19    -0.792004
  1 20     1.676661   2 20    -1.586275   3 20    -1.163507   1 21     3.781663
  2 21     0.980521   3 21    -0.792005   1 22     1.676661   2 22     3.957436
  3 22    -0.453150   1 23    -0.151674   2 23     2.371161   3 23    -3.200661
  1 24    -0.356670   2 24    -0.867384   3 24    -2.408661  -1  0     0.0
  1  1  1  2  0  0  0  0  2  1  2  3  0  0  0  0  3  1  3  4  0  0  0  0
  4  1  4  5  0  0  0  0  5  1  5  6  0  0  0  0  6  1  6  1  0  0  0  0
  7  1  1  7  0  0  0  0  8  1  2  8  0  0  0  0  9  1  3  9  0  0  0  0
 10  1  4 10  0  0  0  0 11  1  5 11  0  0  0  0 12  1  6 12  0  0  0  0
 13  1  1 13  0  0  0  0 14  1  2 14  0  0  0  0 15  1  3 15  0  0  0  0
 16  1  4 16  0  0  0  0 17  1  5 17  0  0  0  0 18  1  6 18  0  0  0  0
 19  1  7 19  0  0  0  0 20  1  8 20  0  0  0  0 21  1  9 21  0  0  0  0
 22  1 10 22  0  0  0  0 23  1 11 23  0  0  0  0 24  1 12 24  0  0  0  0
 25  2  1  2  3  0  0  0 26  2  2  3  4  0  0  0 27  2  3  4  5  0  0  0
 28  2  4  5  6  0  0  0 29  2  5  6  1  0  0  0 30  2  6  1  2  0  0  0
 31  2  7  1  6  0  0  0 32  2  7  1  2  0  0  0 33  2  8  2  1  0  0  0
 34  2  8  2  3  0  0  0 35  2  9  3  2  0  0  0 36  2  9  3  4  0  0  0
 37  2 10  4  3  0  0  0 38  2 10  4  5  0  0  0 39  2 11  5  4  0  0  0
 40  2 11  5  6  0  0  0 41  2 12  6  5  0  0  0 42  2 12  6  1  0  0  0
 43  2 13  1  6  0  0  0 44  2 13  1  2  0  0  0 45  2 14  2  1  0  0  0
 46  2 14  2  3  0  0  0 47  2 15  3  2  0  0  0 48  2 15  3  4  0  0  0
 49  2 16  4  3  0  0  0 50  2 16  4  5  0  0  0 51  2 17  5  4  0  0  0
 52  2 17  5  6  0  0  0 53  2 18  6  5  0  0  0 54  2 18  6  1  0  0  0
 55  2 13  1  7  0  0  0 56  2 14  2  8  0  0  0 57  2 15  3  9  0  0  0
 58  2 16  4 10  0  0  0 59  2 17  5 11  0  0  0 60  2 18  6 12  0  0  0
 61  2  1  7 19  0  0  0 62  2  2  8 20  0  0  0 63  2  3  9 21  0  0  0
 64  2  4 10 22  0  0  0 65  2  5 11 23  0  0  0 66  2  6 12 24  0  0  0
 67  4  6  1  2 14  3  C  0  4  7  1  2  3  3  0  0  4 13  1  2  8  3  0
 68  4  1  2  3  9  3  C  0  4  8  2  3 15  3  0  0  4 14  2  3  4  3  0
 69  4  2  3  4 10  3  C  0  4  9  3  4  5  3  0  0  4 15  3  4 16  3  0
 70  4  3  4  5 11  3  C  0  4 10  4  5  6  3  0  0  4 16  4  5 17  3  0
 71  4  4  5  6 18  3  C  0  4 11  5  6  1  3  0  0  4 17  5  6 12  3  0
 72  4  5  6  1  7  3  C  0  4 12  6  1 13  3  0  0  4 18  6  1  2  3  0
 73  4 19  7  1 13  3  C  0  4 19  7  1  6  3  0  0  4 19  7  1  2  3  0
 74  4 20  8  2 14  3  C  0  4 20  8  2  1  3  0  0  4 20  8  2  3  3  0
 75  4 21  9  3 15  3  C  0  4 21  9  3  2  3  0  0  4 21  9  3  4  3  0
 76  4 22 10  4 16  3  C  0  4 22 10  4  3  3  0  0  4 22 10  4  5  3  0
 77  4 23 11  5 17  3  C  0  4 23 11  5  4  3  0  0  4 23 11  5  6  3  0
 78  4 24 12  6 18  3  C  0  4 24 12  6  5  3  0  0  4 24 12  6  1  3  0
-02
-06  1  3 78
 12.00000    12.00000    12.00000    12.00000    12.00000    12.00000
 15.994915   15.994915   15.994915   15.994915   15.994915   15.994915
  1.007825    1.007825    1.007825    1.007825    1.007825    1.007825
  2.014099    2.014099    2.014099    2.014099    2.014099    2.014099
  1  1     1        1  6     1        2  2     1        2  5     1
  3  3     1        3  4     1        4  7     2        5  8     1
  5 12     1        6  5     1        6 11     1        7 10     2
  8 13     2        9 14     1        9 18     1       10 15     1
 10 17     1       11 16     2       12 19     2       13 20     1
 13 24     1       14 21     1       14 23     1       15 22     2
 16 25     1       16 25     1       17 26     1       17 28     1
 18 27     2       19 30     2       20 31     1       20 32     1
 21 33     1       21 42     1       22 34     1       22 41     1
 23 35     1       23 40     1       24 36     1       24 39     1
 25 37     1       25 38     1       26 43     1       26 44     1
 27 45     1       27 54     1       28 46     1       28 53     1
 29 47     1       29 52     1       30 48     1       30 51     1
 31 49     1       31 50     1       32 55     2       33 56     1
 33 60     1       34 57     1       34 59     1       35 58     2
 36 61     2       37 62     1       37 66     1       38 63     1
 38 65     1       39 64     2       40 67     1       40 72    -1
 41 68     1       41 71    -1       42 69     1       42 70    -1
 43 74     1       43 78    -1       44 75     1       44 77    -1
 45  1     1       45  6    -1       46  2     1       46  5    -1
 47  3     1       47  4    -1       48  8     1       48 12    -1
 49  9     1       49 11    -1       50 14     1       50 18    -1
 51 15     1       51 17    -1       52 20     1       52 24    -1
 53 21     1       53 23    -1       54 25     1       54 29    -1
 55 26     1       55 28    -1       56 31     1       56 32    -1
 57 33     1       57 42    -1       58 34     1       58 41    -1
 59 35     1       59 40    -1       60 36     1       60 39    -1
 61 37     1       61 38    -1       62 43     1       62 44    -1
 63 45     1       63 54    -1       64 46     1       64 53    -1
 65 47     1       65 52    -1       66 48     1       66 51    -1
 67 49     1       67 50    -1       68 56     1       68 60    -1
 69 57     1       69 59    -1       70 62     1       70 66    -1
 71 63     1       71 65    -1       72 67     1       72 72     1
 73 68     1       73 71     1       74 69     1       74 70     1
 75 73     2       76 74     1       76 78     1       77 75     1
 77 77     1       78 76     1
-3
  1 45 79
999
```

APPENDIX III

UNSYMMETRIZED AND SYMMETRIZED Z MATRICES FOR THE INOSITOLS

Contents Page

The same Z matrices were used for the deuterated analogues of scyllo-inositol, neo-inositol, myo-inositol and epi-inositol as those listed in Table XL.

TABLE XL. UNSYMMETRIZED AND SYMMETRIZED $\underset{\sim}{Z}$ MATRICES FOR THE INOSITOLS

SCYLLO-INOSITOL - Z MATRIX - UNSYMMETRIZED

1	1	2	1.000000	1	2	11	1.000000	1	6	11	1.000000	1	7	10	1.000000
1	8	10	1.000000	1	13	33	1.000000	1	14	33	1.000000	1	25	17	1.000000
1	30	17	1.000000	1	32	16	1.000000	1	33	16	1.000000	1	44	15	1.000000
1	45	15	1.000000	2	2	2	1.000000	2	3	11	1.000000	2	8	10	1.000000
2	9	10	1.000000	2	14	33	1.000000	2	15	33	1.000000	2	25	17	1.000000
2	26	17	1.000000	2	34	16	1.000000	2	35	16	1.000000	2	46	15	1.000000
2	47	15	1.000000	3	3	2	1.000000	3	4	11	1.000000	3	9	10	1.000000
3	10	10	1.000000	3	15	33	1.000000	3	16	33	1.000000	3	26	17	1.000000
3	27	17	1.000000	3	36	16	1.000000	3	37	16	1.000000	3	48	15	1.000000
3	49	15	1.000000	4	4	2	1.000000	4	5	11	1.000000	4	10	10	1.000000
4	11	10	1.000000	4	16	33	1.000000	4	17	33	1.000000	4	27	17	1.000000
4	28	17	1.000000	4	38	16	1.000000	4	39	16	1.000000	4	50	15	1.000000
4	51	15	1.000000	5	5	2	1.000000	5	6	11	1.000000	5	11	10	1.000000
5	12	10	1.000000	5	17	33	1.000000	5	18	33	1.000000	5	28	17	1.000000
5	29	17	1.000000	5	40	16	1.000000	5	41	16	1.000000	5	52	15	1.000000
5	53	15	1.000000	6	6	2	1.000000	6	7	10	1.000000	6	12	10	1.000000
6	13	33	1.000000	6	18	33	1.000000	6	29	17	1.000000	6	30	17	1.000000
6	31	16	1.000000	6	42	16	1.000000	6	43	15	1.000000	6	54	15	1.000000
7	7	1	1.000000	7	13	33	1.000000	7	19	33	1.000000	7	31	14	1.000000
7	32	14	1.000000	7	55	12	1.000000	7	61	13	1.000000	8	8	1	1.000000
8	14	33	1.000000	8	20	33	1.000000	8	33	14	1.000000	8	34	14	1.000000
8	56	12	1.000000	8	62	13	1.000000	9	9	1	1.000000	9	15	33	1.000000
9	21	33	1.000000	9	35	14	1.000000	9	36	14	1.000000	9	57	12	1.000000
9	63	13	1.000000	10	10	1	1.000000	10	16	33	1.000000	10	22	33	1.000000
10	37	14	1.000000	10	38	14	1.000000	10	58	12	1.000000	10	64	13	1.000000
11	11	1	1.000000	11	17	33	1.000000	11	23	33	1.000000	11	39	14	1.000000
11	40	14	1.000000	11	59	12	1.000000	11	65	13	1.000000	12	12	1	1.000000
12	18	33	1.000000	12	24	33	1.000000	12	41	14	1.000000	12	42	14	1.000000
12	60	12	1.000000	12	66	13	1.000000	13	13	3	1.000000	13	43	33	1.000000
13	44	33	1.000000	13	55	33	1.000000	14	14	3	1.000000	14	45	33	1.000000
14	46	33	1.000000	14	56	33	1.000000	15	15	3	1.000000	15	47	33	1.000000
15	48	33	1.000000	15	57	33	1.000000	16	16	3	1.000000	16	49	33	1.000000
16	50	33	1.000000	16	58	33	1.000000	17	17	3	1.000000	17	51	33	1.000000
17	52	33	1.000000	17	59	33	1.000000	18	18	3	1.000000	18	53	33	1.000000
18	54	33	1.000000	18	60	33	1.000000	19	19	4	1.000000	19	61	33	1.000000
20	20	4	1.000000	20	62	33	1.000000	21	21	4	1.000000	21	63	33	1.000000
22	22	4	1.000000	22	64	33	1.000000	23	23	4	1.000000	23	65	33	1.000000
24	24	4	1.000000	24	66	33	1.000000	25	25	9	1.000000	25	26	21	1.000000
25	30	21	1.000000	25	32	22	1.000000	25	33	20	1.000000	25	34	20	1.000000
25	35	22	1.000000	25	44	25	1.000000	25	45	19	1.000000	25	46	19	1.000000
25	47	25	1.000000	26	26	9	1.000000	26	27	21	1.000000	26	34	22	1.000000
26	35	20	1.000000	26	36	20	1.000000	26	37	22	1.000000	26	46	25	1.000000
26	47	19	1.000000	26	48	19	1.000000	26	49	25	1.000000	27	27	9	1.000000
27	28	21	1.000000	27	36	22	1.000000	27	37	20	1.000000	27	38	20	1.000000
27	39	22	1.000000	27	48	25	1.000000	27	49	19	1.000000	27	50	19	1.000000
27	51	25	1.000000	28	28	9	1.000000	28	29	21	1.000000	28	38	22	1.000000
28	39	20	1.000000	28	40	20	1.000000	28	41	22	1.000000	28	50	25	1.000000
28	51	19	1.000000	28	52	19	1.000000	28	53	25	1.000000	29	29	9	1.000000
29	30	21	1.000000	29	31	22	1.000000	29	40	22	1.000000	29	41	20	1.000000
29	42	20	1.000000	29	43	25	1.000000	29	52	25	1.000000	29	53	19	1.000000
29	54	19	1.000000	30	30	9	1.000000	30	31	20	1.000000	30	32	20	1.000000
30	33	22	1.000000	30	42	22	1.000000	30	43	19	1.000000	30	44	19	1.000000
30	45	25	1.000000	30	54	25	1.000000	31	31	8	1.000000	31	32	20	1.000000
31	42	21	1.000000	31	43	19	1.000000	31	54	23	1.000000	31	55	19	1.000000
31	61	30	1.000000	32	32	8	1.000000	32	33	21	1.000000	32	44	19	1.000000
32	45	23	1.000000	32	55	19	1.000000	32	61	30	1.000000	33	33	8	1.000000
33	34	20	1.000000	33	44	23	1.000000	33	45	19	1.000000	33	56	19	1.000000
33	62	30	1.000000	34	34	8	1.000000	34	35	21	1.000000	34	46	19	1.000000

TABLE XL (Continued)

```
34 47 23 1.000000 34 56 19 1.000000 34 62 30 1.000000 35 35  8 1.000000
35 36 20 1.000000 35 46 23 1.000000 35 47 19 1.000000 35 57 19 1.000000
35 63 30 1.000000 36 36  8 1.000000 36 37 21 1.000000 36 48 19 1.000000
36 49 23 1.000000 36 57 19 1.000000 36 63 30 1.000000 37 37  8 1.000000
37 38 20 1.000000 37 48 23 1.000000 37 49 19 1.000000 37 58 19 1.000000
37 64 30 1.000000 38 38  8 1.000000 38 39 21 1.000000 38 50 19 1.000000
38 51 23 1.000000 38 58 19 1.000000 38 64 30 1.000000 39 39  8 1.000000
39 40 20 1.000000 39 50 23 1.000000 39 51 19 1.000000 39 59 19 1.000000
39 65 30 1.000000 40 40  8 1.000000 40 41 21 1.000000 40 52 19 1.000000
40 53 23 1.000000 40 59 19 1.000000 40 65 30 1.000000 41 41  8 1.000000
41 42 20 1.000000 41 52 23 1.000000 41 53 19 1.000000 41 60 19 1.000000
41 66 30 1.000000 42 42  8 1.000000 42 43 23 1.000000 42 54 19 1.000000
42 60 19 1.000000 42 66 30 1.000000 43 43  5 1.000000 43 44 33 1.000000
43 54 28 1.000000 43 55 18 1.000000 44 44  5 1.000000 44 45 28 1.000000
44 55 18 1.000000 45 45  5 1.000000 45 46 33 1.000000 45 56 18 1.000000
46 46  5 1.000000 46 47 28 1.000000 46 56 18 1.000000 47 47  5 1.000000
47 48 33 1.000000 47 57 18 1.000000 48 48  5 1.000000 48 49 28 1.000000
48 57 18 1.000000 49 49  5 1.000000 49 50 33 1.000000 49 58 18 1.000000
50 50  5 1.000000 50 51 28 1.000000 50 58 18 1.000000 51 51  5 1.000000
51 52 33 1.000000 51 59 18 1.000000 52 52  5 1.000000 52 53 28 1.000000
52 59 18 1.000000 53 53  5 1.000000 53 54 33 1.000000 53 60 18 1.000000
54 54  5 1.000000 54 60 18 1.000000 55 55  6 1.000000 55 61 29 1.000000
56 56  6 1.000000 56 62 29 1.000000 57 57  6 1.000000 57 63 29 1.000000
58 58  6 1.000000 58 64 29 1.000000 59 59  6 1.000000 59 65 29 1.000000
60 60  6 1.000000 60 66 29 1.000000 61 61  7 1.000000 62 62  7 1.000000
63 63  7 1.000000 64 64  7 1.000000 65 65  7 1.000000 66 66  7 1.000000
67 67 31 1.000000 68 68 31 1.000000 69 69 31 1.000000 70 70 31 1.000000
71 71 31 1.000000 72 72 31 1.000000 73 73 32 1.000000 74 74 32 1.000000
75 75 32 1.000000 76 76 32 1.000000 77 77 32 1.000000 78 78 32 1.000000
-2  0  0 0.0
```

SCYLLO-INOSITOL - Z MATRIX - A1G SYMMETRY SPECIES

```
 2  2  1 1.000000  3  3  3 1.000000  1  1  2 1.000000  4  4  4 1.000000
 7  7  5 1.000000  6  6  8 1.000000  9  9  7 1.000000  5  5  9 1.000000
 8  8  6 1.000000  1  2 10 1.999998  1  1 11 1.999998  2  3 33 1.000000
 1  3 33 1.999998  2  4 33 1.000000  2  8 12 1.000000  2  6 14 1.414209
 1  6 16 1.414209  1  7 15 1.414209  1  5 17 1.999998  3  7 33 1.414209
 3  8 33 1.000000  2  9 13 1.000000  4  9 33 1.000000  7  8 18 1.414211
 6  7 19 1.000000  5  7 19 1.414209  6  8 19 1.414211  7  7 33 1.000000
 6  6 20 1.000000  5  6 20 1.414209  6  6 21 1.000000  5  5 21 1.999998
 5  6 22 1.414209  6  7 23 1.000000  8  9 29 1.000000  7  7 28 1.000000
 5  7 25 1.414209  6  9 30 1.414211 10 10 31 1.000000 -2  0  0 0.0
```

SCYLLO-INOSITOL - Z MATRIX - A2G SYMMETRY SPECIES

```
 2  2  5 1.000000  1  1  8 1.000000  1  2 19 1.000000  2  2 33-1.000000
 1  1 20-1.000000  1  1 21-1.000000  1  2 23-1.000000  2  2 28-1.000000
 3  3 32 1.000000 -2  0  0 0.0
```

TABLE XL (Continued)

SCYLLO-INOSITOL - Z MATRIX - EG SYMMETRY SPECIES

```
 2  2  1 1.000000  3  3  3 1.000000  1  1  2 1.000000  4  4  4 1.000000
 8  8  5 0.999999  9  9  5 1.000000  6  6  8 0.999999  7  7  8 1.000000
11 11  7 0.999999  5  5  9 0.999999 10 10  6 0.999999  1  2 10 0.999999
 1  1 11-0.999999  2  3 33 0.999999  1  3 33 0.999999  2  4 33 0.999999
 2 10 12 0.999999  2  7 14-1.414208  1  6 16 1.224743  1  7 16-0.707106
 1  8 15 1.224743  1  9 15-0.707106  1  5 17 0.999999  3  9 33-1.414208
 3 10 33 0.999999  2 11 13 0.999999  4 11 33 0.999999  9 10 18-1.414210
 6  8 19 0.999999  7  9 19 1.000000  5  9 19-1.414208  7 10 19-1.414210
 8  8 33-0.999999  9  9 33 1.000000  6  6 20-0.999999  7  7 20 1.000000
 5  7 20-1.414208  6  6 21 0.500000  6  7 21-0.866025  7  7 21-0.500000
 5  5 21-0.999999  5  6 22 1.224743  5  7 22 0.707106  6  8 23 0.500000
 6  9 23-0.866025  7  8 23-0.866025  7  9 23-0.500000 10 11 29 0.999999
 8  8 28 0.500000  8  9 28-0.866025  9  9 28-0.500000  5  8 25 1.224743
 5  9 25 0.707106  7 11 30-1.414210 12 12 31 0.999999 13 13 32 1.000000
-2  0  0 0.0
```

SCYLLO-INOSITOL - Z MATRIX - A1U SYMMETRY SPECIES

```
 1  1  2 1.000000  3  3  5 1.000000  2  2  8 1.000000  1  1 11-1.999998
 1  2 16-1.414209  1  3 15-1.414209  2  3 19 1.000000  3  3 33-1.000000
 2  2 20-1.000000  2  2 21 1.000000  2  3 23 1.000000  3  3 28 1.000000
 4  4 31 1.000000  5  5 32 1.000000 -2  0  0 0.0
```

SCYLLO-INOSITOL - Z MATRIX - A2U SYMMETRY SPECIES

```
 1  1  1 1.000000  2  2  3 1.000000  3  3  4 1.000000  6  6  5 1.000000
 5  5  8 1.000000  8  8  7 1.000000  4  4  9 1.000000  7  7  6 1.000000
 1  2 33 1.000000  1  3 33 1.000000  1  7 12 1.000000  1  5 14 1.414209
 2  6 33 1.414209  2  7 33 1.000000  1  8 13 1.000000  3  8 33 1.000000
 6  7 18 1.414211  5  6 19 1.000000  4  6 19-1.414209  5  7 19 1.414211
 6  6 33 1.000000  5  5 20 1.000000  4  5 20-1.414209  5  5 21-1.000000
 4  4 21-1.999998  4  5 22 1.414209  5  6 23-1.000000  7  8 29 1.000000
 6  6 28-1.000000  4  6 25 1.414209  5  8 30 1.414211 -2  0  0 0.0
```

SCYLLO-INOSITOL - Z MATRIX - EU SYMMETRY SPECIES

```
 2  2  1 1.000000  3  3  3 1.000000  1  1  2 1.000000  4  4  4 1.000000
 8  8  5 0.999999  9  9  5 1.000000  6  6  8 0.999999  7  7  8 1.000000
11 11  7 0.999999  5  5  9 0.999999 10 10  6 0.999999  1  2 10 1.732047
 1  1 11 1.000000  2  3 33 0.999999  1  3 33 1.732047  2  4 33 0.999999
 2 10 12 0.999999  2  7 14-1.414208  1  6 16 0.707106  1  7 16-1.224743
 1  8 15 0.707106  1  9 15-1.224743  1  5 17 1.732047  3  9 33-1.414208
 3 10 33 0.999999  2 11 13 0.999999  4 11 33 0.999999  9 10 18-1.414210
 6  8 19 0.999999  7  9 19 1.000000  5  9 19-1.414208  7 10 19-1.414210
 8  8 33-0.999999  9  9 33 1.000000  6  6 20-0.999999  7  7 20 1.000000
 5  7 20-1.414208  6  6 21-0.500000  6  7 21-0.866025  7  7 21 0.500000
 5  5 21 0.999999  5  6 22 1.224743  5  7 22-0.707106  6  8 23-0.500000
 6  9 23-0.866025  7  8 23-0.866025  7  9 23 0.500000 10 11 29 0.999999
 8  8 28-0.500000  8  9 28-0.866025  9  9 28 0.500000  5  8 25 1.224743
 5  9 25-0.707106  7 11 30-1.414210 12 12 31 1.000000 13 13 32 1.000000
-2  0  0 0.0
```

TABLE XL (Continued)

NEO-INOSITOL - $\underset{\sim}{Z}$ MATRIX - UNSYMMETRIZED

1	1	2	1.000000	1	2	11	1.000000	1	6	11	1.000000	1	7	10	1.000000
1	8	10	1.000000	1	13	33	1.000000	1	14	33	1.000000	1	25	17	1.000000
1	30	17	1.000000	1	32	16	1.000000	1	33	16	1.000000	1	44	15	1.000000
1	45	15	1.000000	2	2	2	1.000000	2	3	11	1.000000	2	8	10	1.000000
2	9	10	1.000000	2	14	33	1.000000	2	15	33	1.000000	2	25	17	1.000000
2	26	17	1.000000	2	34	16	1.000000	2	35	16	1.000000	2	46	15	1.000000
2	47	15	1.000000	3	3	2	1.000000	3	4	11	1.000000	3	9	10	1.000000
3	10	10	1.000000	3	15	33	1.000000	3	16	33	1.000000	3	26	17	1.000000
3	27	17	1.000000	3	36	16	1.000000	3	37	16	1.000000	3	48	15	1.000000
3	49	15	1.000000	4	4	2	1.000000	4	5	11	1.000000	4	10	10	1.000000
4	11	10	1.000000	4	16	33	1.000000	4	17	33	1.000000	4	27	17	1.000000
4	28	17	1.000000	4	38	16	1.000000	4	39	16	1.000000	4	50	15	1.000000
4	51	15	1.000000	5	5	2	1.000000	5	6	11	1.000000	5	11	10	1.000000
5	12	10	1.000000	5	17	33	1.000000	5	18	33	1.000000	5	28	17	1.000000
5	29	17	1.000000	5	40	16	1.000000	5	41	16	1.000000	5	52	15	1.000000
5	53	15	1.000000	6	6	2	1.000000	6	7	10	1.000000	6	12	10	1.000000
6	13	33	1.000000	6	18	33	1.000000	6	29	17	1.000000	6	30	17	1.000000
6	31	16	1.000000	6	42	16	1.000000	6	43	15	1.000000	6	54	15	1.000000
7	7	1	1.000000	7	13	33	1.000000	7	19	33	1.000000	7	31	14	1.000000
7	32	14	1.000000	7	55	12	1.000000	7	61	13	1.000000	8	8	1	1.000000
8	14	33	1.000000	8	20	33	1.000000	8	33	14	1.000000	8	34	14	1.000000
8	56	12	1.000000	8	62	13	1.000000	9	9	1	1.000000	9	15	33	1.000000
9	21	33	1.000000	9	35	14	1.000000	9	36	14	1.000000	9	57	12	1.000000
9	63	13	1.000000	10	10	1	1.000000	10	16	33	1.000000	10	22	33	1.000000
10	37	14	1.000000	10	38	14	1.000000	10	58	12	1.000000	10	64	13	1.000000
11	11	1	1.000000	11	17	33	1.000000	11	23	33	1.000000	11	39	14	1.000000
11	40	14	1.000000	11	59	12	1.000000	11	65	13	1.000000	12	12	1	1.000000
12	18	33	1.000000	12	24	33	1.000000	12	41	14	1.000000	12	42	14	1.000000
12	60	12	1.000000	12	66	13	1.000000	13	13	3	1.000000	13	43	33	1.000000
13	44	33	1.000000	13	55	33	1.000000	14	14	3	1.000000	14	45	33	1.000000
14	46	33	1.000000	14	56	33	1.000000	15	15	3	1.000000	15	47	33	1.000000
15	48	33	1.000000	15	57	33	1.000000	16	16	3	1.000000	16	49	33	1.000000
16	50	33	1.000000	16	58	33	1.000000	17	17	3	1.000000	17	51	33	1.000000
17	52	33	1.000000	17	59	33	1.000000	18	18	3	1.000000	18	53	33	1.000000
18	54	33	1.000000	18	60	33	1.000000	19	19	4	1.000000	19	61	33	1.000000
20	20	4	1.000000	20	62	33	1.000000	21	21	4	1.000000	21	63	33	1.000000
22	22	4	1.000000	22	64	33	1.000000	23	23	4	1.000000	23	65	33	1.000000
24	24	4	1.000000	24	66	33	1.000000	25	25	9	1.000000	25	26	21	1.000000
25	30	21	1.000000	25	32	22	1.000000	25	33	20	1.000000	25	34	20	1.000000
25	35	22	1.000000	25	44	25	1.000000	25	45	19	1.000000	25	46	19	1.000000
25	47	25	1.000000	26	26	9	1.000000	26	27	21	1.000000	26	34	21	1.000000
26	35	20	1.000000	26	36	20	1.000000	26	37	22	1.000000	26	46	26	1.000000
26	47	19	1.000000	26	48	19	1.000000	26	49	25	1.000000	27	27	9	1.000000
27	28	21	1.000000	27	36	22	1.000000	27	37	20	1.000000	27	38	20	1.000000
27	39	21	1.000000	27	48	25	1.000000	27	49	19	1.000000	27	50	19	1.000000
27	51	26	1.000000	28	28	9	1.000000	28	29	21	1.000000	28	38	22	1.000000
28	39	20	1.000000	28	40	20	1.000000	28	41	22	1.000000	28	50	25	1.000000
28	51	19	1.000000	28	52	19	1.000000	28	53	25	1.000000	29	29	9	1.000000
29	30	21	1.000000	29	31	22	1.000000	29	40	21	1.000000	29	41	20	1.000000
29	42	20	1.000000	29	43	25	1.000000	29	52	26	1.000000	29	53	19	1.000000
29	54	19	1.000000	30	30	9	1.000000	30	31	20	1.000000	30	32	20	1.000000
30	33	21	1.000000	30	42	22	1.000000	30	43	19	1.000000	30	44	19	1.000000
30	45	26	1.000000	30	54	25	1.000000	31	31	8	1.000000	31	32	20	1.000000
31	42	21	1.000000	31	43	19	1.000000	31	54	23	1.000000	31	55	19	1.000000
31	61	30	1.000000	32	32	8	1.000000	32	33	21	1.000000	32	44	19	1.000000
32	45	23	1.000000	32	55	19	1.000000	32	61	30	1.000000	33	33	8	1.000000
33	34	20	1.000000	33	44	24	1.000000	33	45	19	1.000000	33	56	19	1.000000

TABLE XL (Continued)

```
33 62 30 1.000000 34 34  8 1.000000 34 35 21 1.000000 34 46 19 1.000000
34 47 24 1.000000 34 56 19 1.000000 34 62 30 1.000000 35 35  8 1.000000
35 36 20 1.000000 35 46 23 1.000000 35 47 19 1.000000 35 57 19 1.000000
35 63 30 1.000000 36 36  8 1.000000 36 37 21 1.000000 36 48 19 1.000000
36 49 23 1.000000 36 57 19 1.000000 36 63 30 1.000000 37 37  8 1.000000
37 38 20 1.000000 37 48 23 1.000000 37 49 19 1.000000 37 58 19 1.000000
37 64 30 1.000000 38 38  8 1.000000 38 39 21 1.000000 38 50 19 1.000000
38 51 23 1.000000 38 58 19 1.000000 38 64 30 1.000000 39 39  8 1.000000
39 40 20 1.000000 39 50 24 1.000000 39 51 19 1.000000 39 59 19 1.000000
39 65 30 1.000000 40 40  8 1.000000 40 41 21 1.000000 40 52 19 1.000000
40 53 24 1.000000 40 59 19 1.000000 40 65 30 1.000000 41 41  8 1.000000
41 42 20 1.000000 41 52 23 1.000000 41 53 19 1.000000 41 60 19 1.000000
41 66 30 1.000000 42 42  8 1.000000 42 43 23 1.000000 42 54 19 1.000000
42 60 19 1.000000 42 66 30 1.000000 43 43  5 1.000000 43 44 33 1.000000
43 54 28 1.000000 43 55 18 1.000000 44 44  5 1.000000 44 45 27 1.000000
44 55 18 1.000000 45 45  5 1.000000 45 46 33 1.000000 45 56 18 1.000000
46 46  5 1.000000 46 47 27 1.000000 46 56 18 1.000000 47 47  5 1.000000
47 48 33 1.000000 47 57 18 1.000000 48 48  5 1.000000 48 49 28 1.000000
48 57 18 1.000000 49 49  5 1.000000 49 50 33 1.000000 49 58 18 1.000000
50 50  5 1.000000 50 51 27 1.000000 50 58 18 1.000000 51 51  5 1.000000
51 52 33 1.000000 51 59 18 1.000000 52 52  5 1.000000 52 53 27 1.000000
52 59 18 1.000000 53 53  5 1.000000 53 54 33 1.000000 53 60 18 1.000000
54 54  5 1.000000 54 60 18 1.000000 55 55  6 1.000000 55 61 29 1.000000
56 56  6 1.000000 56 62 29 1.000000 57 57  6 1.000000 57 63 29 1.000000
58 58  6 1.000000 58 64 29 1.000000 59 59  6 1.000000 59 65 29 1.000000
60 60  6 1.000000 60 66 29 1.000000 61 61  7 1.000000 62 62  7 1.000000
63 63  7 1.000000 64 64  7 1.000000 65 65  7 1.000000 66 66  7 1.000000
67 67 31 1.000000 68 68 31 1.000000 69 69 31 1.000000 70 70 31 1.000000
71 71 31 1.000000 72 72 31 1.000000 73 73 32 1.000000 74 74 32 1.000000
75 75 32 1.000000 76 76 32 1.000000 77 77 32 1.000000 78 78 32 1.000000
-2
```

NEO-INOSITOL - $\underset{\sim}{Z}$ MATRIX - AG SYMMETRY SPECIES

```
 3  3  1 1.000000  4  4  1 1.000000  5  5  3 1.000000  6  6  3 1.000000
 1  1  2 1.000000  2  2  2 1.000000  7  7  4 1.000000  8  8  4 1.000000
14 14  5 1.000000 15 15  5 1.000000 16 16  5 1.000000 13 13  8 1.000000
11 11  8 1.000000 12 12  8 1.000000 19 19  7 1.000000 20 20  7 1.000000
 9  9  9 1.000000 10 10  9 1.000000 17 17  6 1.000000 18 18  6 1.000000
 1  4 10 1.414210  1  3 10 1.000000  2  3 10 1.414210  1  1 11 1.000000
 1  2 11 1.414210  3  5 33 1.000000  4  6 33 1.000000  1  5 33 1.000000
 1  6 33 1.414210  2  5 33 1.414210  3  7 33 1.000000  4  8 33 1.000000
 3 17 12 1.000000  4 18 12 1.000000  4 13 14 1.414210  3 11 14 1.000000
 3 12 14 1.000000  1 13 16 1.000000  1 12 16 1.000000  2 11 16 1.414210
 1 15 15 1.000000  1 16 15 1.000000  2 14 15 1.414210  1  9 17 1.414210
 1 10 17 1.000000  2 10 17 1.414210  5 14 33 1.000000  5 15 33 1.000000
 6 16 33 1.414210  5 17 33 1.000000  6 18 33 1.000000  3 19 13 1.000000
 4 20 13 1.000000  7 19 33 1.000000  8 20 33 1.000000 14 17 18 1.000000
15 17 18 1.000000 16 18 18 1.414210 11 14 19 1.000000 12 15 19 1.000000
13 16 19 1.000000  9 16 19 1.414210 10 14 19 1.000000 10 15 19 1.000000
11 17 19 1.000000 12 17 19 1.000000 13 18 19 1.414210 14 15 33 1.000000
16 16 33 1.000000 11 12 20 1.000000 13 13 20 1.000000  9 13 20 1.414210
10 11 20 1.000000 10 12 20 1.000000 10 13 21 1.000000 11 11 21 1.000000
12 13 21 1.000000  9 10 21 1.414210 10 10 21 1.000000  9 12 22 1.414210
```

TABLE XL (Continued)

```
10 11 22 1.000000 11 14 23 1.000000 12 16 23 1.000000 13 15 24 1.000000
17 19 29 1.000000 18 20 29 1.000000 15 16 27 1.000000 14 14 28 1.000000
 9 15 25 1.414210 10 14 25 1.000000 10 16 26 1.000000 11 19 30 1.000000
12 19 30 1.000000 13 20 30 1.414210 21 21 31 1.000000 22 22 31 1.000000
23 23 32 1.000000 -2  0  0 0.0
```

NEO-INOSITOL - $\underset{\sim}{Z}$ MATRIX - BG SYMMETRY SPECIES

```
 2  2  1 1.000000  3  3  3 1.000000  1  1  2 1.000000  4  4  4 1.000000
 9  9  5 1.000000 10 10  5 1.000000 11 11  5 1.000000  8  8  8 1.000000
 6  6  8 1.000000  7  7  8 1.000000 13 13  7 1.000000  5  5  9 1.000000
12 12  6 1.000000  1  2 10 1.000000  1  1 11-1.000000  2  3 33 1.000000
 1  3 33 1.000000  2  4 33 1.000000  2 12 12 1.000000  2  6 14 1.000000
 2  7 14 1.000000  1  8 16 1.000000  1  7 16 1.000000  1 10 15 1.000000
 1 11 15 1.000000  1  5 17-1.000000  3  9 33 1.000000  3 10 33 1.000000
 3 12 33 1.000000  2 13 13 1.000000  4 13 33 1.000000  9 12 18 1.000000
10 12 18 1.000000  6  9 19 1.000000  7 10 19 1.000000  8 11 19 1.000000
 5  9 19-1.000000  5 10 19-1.000000  6 12 19 1.000000  7 12 19 1.000000
 9 10 33 1.000000 11 11 33-1.000000  6  7 20 1.000000  8  8 20-1.000000
 7  8 21 1.000000  5  5 21-1.000000  5  6 22 1.000000  6  9 23-1.000000
 7 11 23 1.000000  8 10 24 1.000000 12 13 29 1.000000 10 11 27 1.000000
 9  9 28-1.000000  5  9 25 1.000000  5 11 26-1.000000  6 13 30 1.000000
 7 13 30 1.000000 14 14 31 1.000000 15 15 32 1.000000 16 16 32 1.000000
 5  6 20-1.000000  5  7 20-1.000000  5  8 21-1.000000  6  6 21-1.000000
-2  0  0 0.0
```

NEO-INOSITOL - $\underset{\sim}{Z}$ MATRIX - AU SYMMETRY SPECIES

```
 3  3  1 1.000000  4  4  3 1.000000  1  1  2 1.000000  2  2  2 1.000000
 5  5  4 1.000000 10 10  5 1.000000 11 11  5 1.000000 12 12  5 1.000000
 9  9  8 1.000000  7  7  8 1.000000  8  8  8 1.000000 14 14  7 1.000000
 6  6  9 1.000000 13 13  6 1.000000  1  3 10 1.000000  2  3 10-1.414210
 1  1 11-1.000000  1  2 11-1.414210  3  4 33 1.000000  1  4 33 1.000000
 2  4 33-1.414210  3  5 33 1.000000  3 13 12 1.000000  3  7 14 1.000000
 3  8 14 1.000000  1  9 16 1.000000  1  8 16 1.000000  2  7 16-1.414210
 1 11 15 1.000000  1 12 15 1.000000  2 10 15-1.414210  1  6 17-1.000000
 2  6 17 1.414210  4 10 33 1.000000  4 11 33 1.000000  4 13 33 1.000000
 3 14 13 1.000000  5 14 33 1.000000 10 13 18 1.000000 11 13 18 1.000000
 7 10 19 1.000000  8 11 19 1.000000  9 12 19 1.000000  6 10 19-1.000000
 6 11 19-1.000000  7 13 19 1.000000  8 13 19 1.000000 10 11 33 1.000000
12 12 33-1.000000  7  8 20 1.000000  9  9 20-1.000000  6  7 20-1.000000
 6  8 20-1.000000  6  9 21-1.000000  7  7 21 1.000000  8  9 21 1.000000
 6  6 21 1.000000  6  7 22-1.000000  7 10 23 1.000000  8 12 23 1.000000
 9 11 24 1.000000 13 14 29 1.000000 11 12 27 1.000000 10 10 28 1.000000
 6 10 25-1.000000  6 12 26-1.000000  7 14 30 1.000000  8 14 30 1.000000
15 15 31 1.000000 16 16 31 1.000000 17 17 32 1.000000 18 18 32 1.000000
-2  0  0 0.0
```

TABLE XL (Continued)

NEO-INOSITOL - Z MATRIX - BU SYMMETRY SPECIES

2	2	1	1.000000	3	3	1	1.000000	4	4	3	1.000000	5	5	3	1.000000
1	1	2	1.000000	6	6	4	1.000000	7	7	4	1.000000	13	13	5	1.000000
14	14	5	1.000000	15	15	5	1.000000	12	12	8	1.000000	10	10	8	1.000000
11	11	8	1.000000	18	18	7	1.000000	19	19	7	1.000000	8	8	9	1.000000
9	9	9	1.000000	16	16	6	1.000000	17	17	6	1.000000	1	3	10	1.414210
1	2	10	1.000000	1	1	11	1.000000	2	4	33	1.000000	3	5	33	1.000000
1	4	33	1.000000	1	5	33	1.414210	2	6	33	1.000000	3	7	33	1.000000
2	16	12	1.000000	3	17	12	1.000000	3	12	14	1.414210	2	10	14	1.000000
2	11	14	1.000000	1	12	16	1.000000	1	11	16	1.000000	1	14	15	1.000000
1	15	15	1.000000	1	8	17	1.414210	1	9	17	1.000000	4	13	33	1.000000
4	14	33	1.000000	5	15	33	1.414210	4	16	33	1.000000	5	17	33	1.000000
2	18	13	1.000000	3	19	13	1.000000	6	18	33	1.000000	7	19	33	1.000000
13	16	18	1.000000	14	16	18	1.000000	15	17	18	1.414210	10	13	19	1.000000
11	14	19	1.000000	12	15	19	1.000000	8	15	19	1.414210	9	13	19	1.000000
9	14	19	1.000000	10	16	19	1.000000	11	16	19	1.000000	12	17	19	1.414210
13	14	33	1.000000	15	15	33	1.000000	10	11	20	1.000000	12	12	20	1.000000
8	12	20	1.414210	9	10	20	1.000000	9	11	20	1.000000	9	12	21	1.000000
10	10	21	-1.000000	11	12	21	1.000000	8	9	21	1.414210	9	9	21	-1.000000
8	11	22	1.414210	9	10	22	-1.000000	10	13	23	-1.000000	11	15	23	1.000000
12	14	24	1.000000	16	18	29	1.000000	17	19	29	1.000000	14	15	27	1.000000
13	13	28	-1.000000	8	14	25	1.414210	9	13	25	-1.000000	9	15	26	1.000000
10	18	30	1.000000	11	18	30	1.000000	12	19	30	1.414210	20	20	31	1.000000
21	21	32	1.000000	-2	0	0	0.0								

MYO-INOSITOL - Z MATRIX - UNSYMMETRIZED

1	1	2	1.000000	1	2	11	1.000000	1	6	11	1.000000	1	7	10	1.000000
1	8	10	1.000000	1	13	33	1.000000	1	14	33	1.000000	1	25	17	1.000000
1	30	17	1.000000	1	32	16	1.000000	1	33	16	1.000000	1	44	15	1.000000
1	45	15	1.000000	2	2	2	1.000000	2	3	11	1.000000	2	8	10	1.000000
2	9	10	1.000000	2	14	33	1.000000	2	15	33	1.000000	2	25	17	1.000000
2	26	17	1.000000	2	34	16	1.000000	2	35	16	1.000000	2	46	15	1.000000
2	47	15	1.000000	3	3	2	1.000000	3	4	11	1.000000	3	9	10	1.000000
3	10	10	1.000000	3	15	33	1.000000	3	16	33	1.000000	3	26	17	1.000000
3	27	17	1.000000	3	36	16	1.000000	3	37	16	1.000000	3	48	15	1.000000
3	49	15	1.000000	4	4	2	1.000000	4	5	11	1.000000	4	10	10	1.000000
4	11	10	1.000000	4	16	33	1.000000	4	17	33	1.000000	4	27	17	1.000000
4	28	17	1.000000	4	38	16	1.000000	4	39	16	1.000000	4	50	15	1.000000
4	51	15	1.000000	5	5	2	1.000000	5	6	11	1.000000	5	11	10	1.000000
5	12	10	1.000000	5	17	33	1.000000	5	18	33	1.000000	5	28	17	1.000000
5	29	17	1.000000	5	40	16	1.000000	5	41	16	1.000000	5	52	15	1.000000
5	53	15	1.000000	6	6	2	1.000000	6	7	10	1.000000	6	12	10	1.000000
6	13	33	1.000000	6	18	33	1.000000	6	29	17	1.000000	6	30	17	1.000000
6	31	16	1.000000	6	42	16	1.000000	6	43	15	1.000000	6	54	15	1.000000
7	7	1	1.000000	7	13	33	1.000000	7	19	33	1.000000	7	31	14	1.000000
7	32	14	1.000000	7	55	12	1.000000	7	61	13	1.000000	8	8	1	1.000000
8	14	33	1.000000	8	20	33	1.000000	8	33	14	1.000000	8	34	14	1.000000
8	56	12	1.000000	8	62	13	1.000000	9	9	1	1.000000	9	15	33	1.000000

TABLE XL (Continued)

9	21	33	1.000000	9	35	14	1.000000	9	36	14	1.000000	9	57	12	1.000000
9	63	13	1.000000	10	10	1	1.000000	10	16	33	1.000000	10	22	33	1.000000
10	37	14	1.000000	10	38	14	1.000000	10	58	12	1.000000	10	64	13	1.000000
11	11	1	1.000000	11	17	33	1.000000	11	23	33	1.000000	11	39	14	1.000000
11	40	14	1.000000	11	59	12	1.000000	11	65	13	1.000000	12	12	1	1.000000
12	18	33	1.000000	12	24	33	1.000000	12	41	14	1.000000	12	42	14	1.000000
12	60	12	1.000000	12	66	13	1.000000	13	13	3	1.000000	13	43	33	1.000000
13	44	33	1.000000	13	55	33	1.000000	14	14	3	1.000000	14	45	33	1.000000
14	46	33	1.000000	14	56	33	1.000000	15	15	3	1.000000	15	47	33	1.000000
15	48	33	1.000000	15	57	33	1.000000	16	16	3	1.000000	16	49	33	1.000000
16	50	33	1.000000	16	58	33	1.000000	17	17	3	1.000000	17	51	33	1.000000
17	52	33	1.000000	17	59	33	1.000000	18	18	3	1.000000	18	53	33	1.000000
18	54	33	1.000000	18	60	33	1.000000	19	19	4	1.000000	19	61	33	1.000000
20	20	4	1.000000	20	62	33	1.000000	21	21	4	1.000000	21	63	33	1.000000
22	22	4	1.000000	22	64	33	1.000000	23	23	4	1.000000	23	65	33	1.000000
24	24	4	1.000000	24	66	33	1.000000	25	25	9	1.000000	25	26	21	1.000000
25	30	21	1.000000	25	32	22	1.000000	25	33	20	1.000000	25	34	20	1.000000
25	35	22	1.000000	25	44	25	1.000000	25	45	19	1.000000	25	46	19	1.000000
25	47	25	1.000000	26	26	9	1.000000	26	27	21	1.000000	26	34	21	1.000000
26	35	20	1.000000	26	36	20	1.000000	26	37	22	1.000000	26	46	26	1.000000
26	47	19	1.000000	26	48	19	1.000000	26	49	25	1.000000	27	27	9	1.000000
27	28	21	1.000000	27	36	22	1.000000	27	37	20	1.000000	27	38	20	1.000000
27	39	22	1.000000	27	48	25	1.000000	27	49	19	1.000000	27	50	19	1.000000
27	51	25	1.000000	28	28	9	1.000000	28	29	21	1.000000	28	38	22	1.000000
28	39	20	1.000000	28	40	20	1.000000	28	41	22	1.000000	28	50	25	1.000000
28	51	19	1.000000	28	52	19	1.000000	28	53	25	1.000000	29	29	9	1.000000
29	30	21	1.000000	29	31	22	1.000000	29	40	22	1.000000	29	41	20	1.000000
29	42	20	1.000000	29	43	25	1.000000	29	52	25	1.000000	29	53	19	1.000000
29	54	19	1.000000	30	30	9	1.000000	30	31	20	1.000000	30	32	20	1.000000
30	33	21	1.000000	30	42	22	1.000000	30	43	19	1.000000	30	44	19	1.000000
30	45	26	1.000000	30	54	25	1.000000	31	31	8	1.000000	31	32	20	1.000000
31	42	21	1.000000	31	43	19	1.000000	31	54	23	1.000000	31	55	19	1.000000
31	61	30	1.000000	32	32	8	1.000000	32	33	21	1.000000	32	44	19	1.000000
32	45	23	1.000000	32	55	19	1.000000	32	61	30	1.000000	33	33	8	1.000000
33	34	20	1.000000	33	44	24	1.000000	33	45	19	1.000000	33	56	19	1.000000
33	62	30	1.000000	34	34	8	1.000000	34	35	21	1.000000	34	46	19	1.000000
34	47	24	1.000000	34	56	19	1.000000	34	62	30	1.000000	35	35	8	1.000000
35	36	20	1.000000	35	46	23	1.000000	35	47	19	1.000000	35	57	19	1.000000
35	63	30	1.000000	36	36	8	1.000000	36	37	21	1.000000	36	48	19	1.000000
36	49	23	1.000000	36	57	19	1.000000	36	63	30	1.000000	37	37	8	1.000000
37	38	20	1.000000	37	48	23	1.000000	37	49	19	1.000000	37	58	19	1.000000
37	64	30	1.000000	38	38	8	1.000000	38	39	21	1.000000	38	50	19	1.000000
38	51	23	1.000000	38	58	19	1.000000	38	64	30	1.000000	39	39	8	1.000000
39	40	20	1.000000	39	50	23	1.000000	39	51	19	1.000000	39	59	19	1.000000
39	65	30	1.000000	40	40	8	1.000000	40	41	21	1.000000	40	52	19	1.000000
40	53	23	1.000000	40	59	19	1.000000	40	65	30	1.000000	41	41	8	1.000000
41	42	20	1.000000	41	52	23	1.000000	41	53	19	1.000000	41	60	19	1.000000
41	66	30	1.000000	42	42	8	1.000000	42	43	23	1.000000	42	54	19	1.000000
42	60	19	1.000000	42	66	30	1.000000	43	43	5	1.000000	43	44	33	1.000000
43	54	28	1.000000	43	55	18	1.000000	44	44	5	1.000000	44	45	27	1.000000
44	55	18	1.000000	45	45	5	1.000000	45	46	33	1.000000	45	56	18	1.000000
46	46	5	1.000000	46	47	27	1.000000	46	56	18	1.000000	47	47	5	1.000000
47	48	33	1.000000	47	57	18	1.000000	48	48	5	1.000000	48	49	28	1.000000
48	57	18	1.000000	49	49	5	1.000000	49	50	33	1.000000	49	58	18	1.000000
50	50	5	1.000000	50	51	28	1.000000	50	58	18	1.000000	51	51	5	1.000000
51	52	33	1.000000	51	59	18	1.000000	52	52	5	1.000000	52	53	28	1.000000
52	59	18	1.000000	53	53	5	1.000000	53	54	33	1.000000	53	60	18	1.000000

TABLE XL (Continued)

```
54 54  5 1.0CCCCO 54 60 18 1.000000 55 55  6 1.000000 55 61 29 1.000000
56 56  6 1.000000 56 62 29 1.000000 57 57  6 1.000000 57 63 29 1.000000
58 58  6 1.000000 58 64 29 1.000000 59 59  6 1.000000 59 65 29 1.000000
60 60  6 1.0CC000 60 66 29 1.000000 61 61  7 1.000000 62 62  7 1.000000
63 63  7 1.000000 64 64  7 1.000000 65 65  7 1.000000 66 66  7 1.000000
67 67 31 1.000000 68 68 31 1.000000 69 69 31 1.000000 70 70 31 1.000000
71 71 31 1.0CC000 72 72 31 1.000000 73 73 32 1.000000 74 74 32 1.000000
75 75 32 1.0CC0C0 76 76 32 1.000000 77 77 32 1.000000 78 78 32 1.000000
-2  0  0 0.0
```

MYO-INOSITOL - Z MATRIX - A1 SYMMETRY SPECIES

```
 4  4  1 1.0CC000  5  5  1 1.000000  6  6  1 1.000000  7  7  1 1.000000
 8  8  3 1.0CC000  9  9  3 1.000000 10 10  3 1.000000 11 11  3 1.000000
 1  1  2 1.0CC000  2  2  2 1.000000  3  3  2 1.000000 12 12  4 1.000000
13 13  4 1.000000 14 14  4 1.000000 15 15  4 1.000000 26 26  5 1.000000
27 27  5 1.0CC000 28 28  5 1.000000 29 29  5 1.000000 30 30  5 1.000000
31 31  5 1.000000 22 22  8 1.000000 20 20  8 1.000000 21 21  8 1.000000
23 23  8 1.000000 24 24  8 1.000000 25 25  8 1.000000 36 36  7 1.000000
37 37  7 1.0CC000 38 38  7 1.000000 39 39  7 1.000000 16 16  9 1.000000
17 17  9 1.0CC000 18 18  9 1.000000 19 19  9 1.000000 32 32  6 1.000000
33 33  6 1.000000 34 34  6 1.000000 35 35  6 1.000000  1  5 10 1.414210
 1  4 10 1.0CC000  2  4 10 1.000000  2  6 10 1.000000  3  6 10 1.000000
 3  7 10 1.414210  1  1 11 1.000000  1  2 11 1.000000  2  3 11 1.000000
 3  3 11 1.0CC000  4  8 33 1.000000  5  9 33 1.000000  6 10 33 1.000000
 7 11 33 1.000000  1  8 33 1.000000  1  9 33 1.414210  2  8 33 1.000000
 2 10 33 1.000000  3 10 33 1.000000  3 11 33 1.414210  4 12 33 1.000000
 5 13 33 1.0C0000  6 14 33 1.000000  7 15 33 1.000000  4 32 12 1.000000
 5 33 12 1.0CC0C0  6 34 12 1.000000  7 35 12 1.000000  5 22 14 1.414210
 4 20 14 1.0CC000  4 21 14 1.000000  6 23 14 1.000000  6 24 14 1.000000
 7 25 14 1.414210  1 22 16 1.000000  1 21 16 1.000000  2 20 16 1.000000
 2 23 16 1.000000  3 24 16 1.000000  3 25 16 1.000000  1 27 15 1.000000
 1 28 15 1.000000  2 26 15 1.000000  2 29 15 1.000000  3 30 15 1.000000
 3 31 15 1.000000  1 16 17 1.414210  1 17 17 1.000000  2 17 17 1.000000
 2 18 17 1.000000  3 18 17 1.000000  3 19 17 1.414210  8 26 33 1.000000
 8 27 33 1.000000  9 28 33 1.414210 10 29 33 1.000000 10 30 33 1.000000
11 31 33 1.414210  8 32 33 1.000000  9 33 33 1.000000 10 34 33 1.000000
11 35 33 1.000000  4 36 13 1.000000  5 37 13 1.000000  6 38 13 1.000000
 7 39 13 1.000000 12 36 33 1.000000 13 37 33 1.000000 14 38 33 1.000000
15 39 33 1.0CC000 26 32 18 1.000000 27 32 18 1.000000 28 33 18 1.414210
29 34 18 1.0CC000 30 34 18 1.000000 31 35 18 1.414210 20 26 19 1.000000
21 27 19 1.000000 22 28 19 1.000000 23 29 19 1.000000 24 30 19 1.000000
25 31 19 1.0CC000 16 28 19 1.414210 17 26 19 1.000000 17 27 19 1.000000
18 29 19 1.0CC000 18 30 19 1.000000 19 31 19 1.414210 20 32 19 1.000000
21 32 19 1.000000 22 33 19 1.414210 23 34 19 1.000000 24 34 19 1.000000
25 35 19 1.414210 26 27 33 1.000000 28 28 33 1.000000 29 30 33 1.000000
31 31 33 1.000000 20 21 20 1.000000 22 22 20 1.000000 23 24 20 1.000000
25 25 20 1.000000 16 22 20 1.414210 17 20 20 1.000000 17 21 20 1.000000
18 23 20 1.0CC000 18 24 20 1.000000 19 25 20 1.414210 17 22 21 1.000000
20 23 21 1.000000 21 22 21 1.000000 24 25 21 1.000000 16 17 21 1.414210
17 18 21 1.0CC000 18 19 21 1.414210 16 21 22 1.414210 17 23 22 1.000000
18 20 22 1.000000 18 25 22 1.000000 19 24 22 1.414210 20 29 23 1.000000
21 28 23 1.000000 23 26 23 1.000000 24 31 23 1.000000 25 30 23 1.000000
22 27 24 1.000000 32 36 29 1.000000 33 37 29 1.000000 34 38 29 1.000000
35 39 29 1.0CC000 27 28 27 1.000000 26 29 28 1.000000 30 31 28 1.000000
```

TABLE XL (Continued)

```
16 27 25 1.414210 17 29 25 1.000000 18 26 25 1.000000 18 31 25 1.000000
19 30 25 1.414210 17 28 26 1.000000 20 36 30 1.000000 21 36 30 1.000000
22 37 30 1.414210 23 38 30 1.000000 24 38 30 1.000000 25 39 30 1.414210
40 40 31 1.000000 41 41 31 1.000000 42 42 31 1.000000 43 43 32 1.000000
44 44 32 1.000000 -2  0  0 0.0
```

MYO-INOSITOL - Z MATRIX - All SYMMETRY SPECIES

```
 4  4  1 1.000000  5  5  1 1.000000  6  6  3 1.000000  7  7  3 1.000000
 1  1  2 1.000000  2  2  2 1.000000  3  3  2 1.000000  8  8  4 1.000000
 9  9  4 1.000000 18 18  5 1.000000 19 19  5 1.000000 20 20  5 1.000000
21 21  5 1.000000 22 22  5 1.000000 23 23  5 1.000000 14 14  8 1.000000
12 12  8 1.000000 13 13  8 1.000000 15 15  8 1.000000 16 16  8 1.000000
17 17  8 1.000000 26 26  7 1.000000 27 27  7 1.000000 10 10  9 1.000000
11 11  9 1.000000 24 24  6 1.000000 25 25  6 1.000000  1  4 10 1.000000
 2  4 10-1.000000  2  5 10 1.000000  3  5 10 1.000000  1  1 11-1.000000
 1  2 11-1.000000  2  3 11 1.000000  3  3 11-1.000000  4  6 33 1.000000
 5  7 33 1.000000  1  6 33 1.000000  2  6 33-1.000000  2  7 33 1.000000
 3  7 33 1.000000  4  8 33 1.000000  5  9 33 1.000000  4 24 12 1.000000
 5 25 12 1.000000  4 12 14 1.000000  4 13 14 1.000000  5 15 14 1.000000
 5 16 14 1.000000  1 14 16 1.000000  1 13 16 1.000000  2 12 16-1.000000
 2 15 16 1.000000  3 16 16 1.000000  3 17 16 1.000000  1 19 15 1.000000
 1 20 15 1.000000  2 18 15-1.000000  2 21 15 1.000000  3 22 15 1.000000
 3 23 15 1.000000  1 10 17-1.000000  2 10 17 1.000000  2 11 17 1.000000
 3 11 17 1.000000  6 18 33 1.000000  6 19 33 1.000000  7 21 33 1.000000
 7 22 33 1.000000  6 24 33 1.000000  7 25 33 1.000000  4 26 13 1.000000
 5 27 13 1.000000  8 26 33 1.000000  9 27 33 1.000000 18 24 18 1.000000
19 24 18 1.000000 21 25 18 1.000000 22 25 18 1.000000 12 18 19 1.000000
13 19 19 1.000000 14 20 19 1.000000 15 21 19 1.000000 16 22 19 1.000000
17 23 19 1.000000 10 18 19-1.000000 10 19 19-1.000000 11 21 19 1.000000
11 22 19 1.000000 12 24 19 1.000000 13 24 19 1.000000 15 25 19 1.000000
16 25 19 1.000000 18 19 33 1.000000 20 20 33-1.000000 21 22 33 1.000000
23 23 33-1.000000 12 13 20 1.000000 14 14 20-1.000000 15 16 20 1.000000
17 17 20-1.000000 10 12 20-1.000000 10 13 20-1.000000 11 15 20 1.000000
11 16 20 1.000000 10 14 21-1.000000 12 15 21-1.000000 13 14 21 1.000000
16 17 21 1.000000 10 11 21 1.000000 10 15 22 1.000000 11 12 22-1.000000
11 17 22 1.000000 12 21 23-1.000000 13 20 23 1.000000 15 18 23-1.000000
16 23 23 1.000000 17 22 23 1.000000 14 19 24 1.000000 24 26 29 1.000000
25 27 29 1.000000 19 20 27 1.000000 18 21 28-1.000000 22 23 28 1.000000
10 21 25 1.000000 11 18 25-1.000000 11 23 25 1.000000 10 20 26-1.000000
12 26 30 1.000000 13 26 30 1.000000 15 27 30 1.000000 16 27 30 1.000000
28 28 31 1.000000 29 29 31 1.000000 30 30 31 1.000000 31 31 32 1.000000
32 32 32 1.000000 33 33 32 1.000000 34 34 32 1.000000 -2  0  0 0.0
```

TABLE XL (Continued)

EPI-INOSITOL - $\underset{\sim}{Z}$ MATRIX - UNSYMMETRIZED

1	1	2	1.000000	1	2	11	1.000000	1	6	11	1.000000	1	7	10	1.000000
1	8	10	1.000000	1	13	33	1.000000	1	14	33	1.000000	1	25	17	1.000000
1	30	17	1.000000	1	32	16	1.000000	1	33	16	1.000000	1	44	15	1.000000
1	45	15	1.000000	2	2	2	1.000000	2	3	11	1.000000	2	8	10	1.000000
2	9	10	1.000000	2	14	33	1.000000	2	15	33	1.000000	2	25	17	1.000000
2	26	17	1.000000	2	34	16	1.000000	2	35	16	1.000000	2	46	15	1.000000
2	47	15	1.000000	3	3	2	1.000000	3	4	11	1.000000	3	9	10	1.000000
3	10	10	1.000000	3	15	33	1.000000	3	16	33	1.000000	3	26	17	1.000000
3	27	17	1.000000	3	36	16	1.000000	3	37	16	1.000000	3	48	15	1.000000
3	49	15	1.000000	4	4	2	1.000000	4	5	11	1.000000	4	10	10	1.000000
4	11	10	1.000000	4	16	33	1.000000	4	17	33	1.000000	4	27	17	1.000000
4	28	17	1.000000	4	38	16	1.000000	4	39	16	1.000000	4	50	15	1.000000
4	51	15	1.000000	5	5	2	1.000000	5	6	11	1.000000	5	11	10	1.000000
5	12	10	1.000000	5	17	33	1.000000	5	18	33	1.000000	5	28	17	1.000000
5	29	17	1.000000	5	40	16	1.000000	5	41	16	1.000000	5	52	15	1.000000
5	53	15	1.000000	6	6	2	1.000000	6	7	10	1.000000	6	12	10	1.000000
6	13	33	1.000000	6	18	33	1.000000	6	29	17	1.000000	6	30	17	1.000000
6	31	16	1.000000	6	42	16	1.000000	6	43	15	1.000000	6	54	15	1.000000
7	7	1	1.000000	7	13	33	1.000000	7	19	33	1.000000	7	31	14	1.000000
7	32	14	1.000000	7	55	12	1.000000	7	61	13	1.000000	8	8	1	1.000000
8	14	33	1.000000	8	20	33	1.000000	8	33	14	1.000000	8	34	14	1.000000
8	56	12	1.000000	8	62	13	1.000000	9	9	1	1.000000	9	15	33	1.000000
9	21	33	1.000000	9	35	14	1.000000	9	36	14	1.000000	9	57	12	1.000000
9	63	13	1.000000	10	10	1	1.000000	10	16	33	1.000000	10	22	33	1.000000
10	37	14	1.000000	10	38	14	1.000000	10	58	12	1.000000	10	64	13	1.000000
11	11	1	1.000000	11	17	33	1.000000	11	23	33	1.000000	11	39	14	1.000000
11	40	14	1.000000	11	59	12	1.000000	11	65	13	1.000000	12	12	1	1.000000
12	18	33	1.000000	12	24	33	1.000000	12	41	14	1.000000	12	42	14	1.000000
12	60	12	1.000000	12	66	13	1.000000	13	13	3	1.000000	13	43	33	1.000000
13	44	33	1.000000	13	55	33	1.000000	14	14	3	1.000000	14	45	33	1.000000
14	46	33	1.000000	14	56	33	1.000000	15	15	3	1.000000	15	47	33	1.000000
15	48	33	1.000000	15	57	33	1.000000	16	16	3	1.000000	16	49	33	1.000000
16	50	33	1.000000	16	58	33	1.000000	17	17	3	1.000000	17	51	33	1.000000
17	52	33	1.000000	17	59	33	1.000000	18	18	3	1.000000	18	53	33	1.000000
18	54	33	1.000000	18	60	33	1.000000	19	19	4	1.000000	19	61	33	1.000000
20	20	4	1.000000	20	62	33	1.000000	21	21	4	1.000000	21	63	33	1.000000
22	22	4	1.000000	22	64	33	1.000000	23	23	4	1.000000	23	65	33	1.000000
24	24	4	1.000000	24	66	33	1.000000	25	25	9	1.000000	25	26	21	1.000000
25	30	21	1.000000	25	32	22	1.000000	25	33	20	1.000000	25	34	20	1.000000
25	35	22	1.000000	25	44	25	1.000000	25	45	19	1.000000	25	46	19	1.000000
25	47	25	1.000000	26	26	9	1.000000	26	27	21	1.000000	26	34	21	1.000000
26	35	20	1.000000	26	36	20	1.000000	26	37	22	1.000000	26	46	26	1.000000
26	47	19	1.000000	26	48	19	1.000000	26	49	25	1.000000	27	27	9	1.000000
27	28	21	1.000000	27	36	22	1.000000	27	37	20	1.000000	27	38	20	1.000000
27	39	22	1.000000	27	48	25	1.000000	27	49	19	1.000000	27	50	19	1.000000
27	51	25	1.000000	28	28	9	1.000000	28	29	21	1.000000	28	38	22	1.000000
28	39	20	1.000000	28	40	20	1.000000	28	41	21	1.000000	28	50	25	1.000000
28	51	19	1.000000	28	52	19	1.000000	28	53	26	1.000000	29	29	9	1.000000
29	30	21	1.000000	29	31	22	1.000000	29	40	22	1.000000	29	41	20	1.000000
29	42	20	1.000000	29	43	25	1.000000	29	52	25	1.000000	29	53	19	1.000000
29	54	19	1.000000	30	30	9	1.000000	30	31	20	1.000000	30	32	20	1.000000
30	33	21	1.000000	30	42	21	1.000000	30	43	19	1.000000	30	44	19	1.000000
30	45	26	1.000000	30	54	26	1.000000	31	31	8	1.000000	31	32	20	1.000000
31	42	21	1.000000	31	43	19	1.000000	31	54	23	1.000000	31	55	19	1.000000
31	61	30	1.000000	32	32	8	1.000000	32	33	21	1.000000	32	44	19	1.000000
32	45	23	1.000000	32	55	19	1.000000	32	61	30	1.000000	33	33	8	1.000000
33	34	20	1.000000	33	44	24	1.000000	33	45	19	1.000000	33	56	19	1.000000

TABLE XL (Continued)

```
33 62 30 1.000000 34 34  8 1.000000 34 35 21 1.000000 34 46 19 1.000000
34 47 24 1.000000 34 56 19 1.000000 34 62 30 1.000000 35 35  8 1.000000
35 36 20 1.000000 35 46 23 1.000000 35 47 19 1.000000 35 57 19 1.000000
35 63 30 1.000000 36 36  8 1.000000 36 37 21 1.000000 36 48 19 1.000000
36 49 23 1.000000 36 57 19 1.000000 36 63 30 1.000000 37 37  8 1.000000
37 38 20 1.000000 37 48 23 1.000000 37 49 19 1.000000 37 58 19 1.000000
37 64 30 1.000000 38 38  8 1.000000 38 39 21 1.000000 38 50 19 1.000000
38 51 23 1.000000 38 58 19 1.000000 38 64 30 1.000000 39 39  8 1.000000
39 40 20 1.000000 39 50 23 1.000000 39 51 19 1.000000 39 59 19 1.000000
39 65 30 1.000000 40 40  8 1.000000 40 41 21 1.000000 40 52 19 1.000000
40 53 23 1.000000 40 59 19 1.000000 40 65 30 1.000000 41 41  8 1.000000
41 42 20 1.000000 41 52 24 1.000000 41 53 19 1.000000 41 60 19 1.000000
41 66 30 1.000000 42 42  8 1.000000 42 43 24 1.000000 42 54 19 1.000000
42 60 19 1.000000 42 66 30 1.000000 43 43  5 1.000000 43 44 33 1.000000
43 54 27 1.000000 43 55 18 1.000000 44 44  5 1.000000 44 45 27 1.000000
44 55 18 1.000000 45 45  5 1.000000 45 46 33 1.000000 45 56 18 1.000000
46 46  5 1.000000 46 47 27 1.000000 46 56 18 1.000000 47 47  5 1.000000
47 48 33 1.000000 47 57 18 1.000000 48 48  5 1.000000 48 49 28 1.000000
48 57 18 1.000000 49 49  5 1.000000 49 50 33 1.000000 49 58 18 1.000000
50 50  5 1.000000 50 51 28 1.000000 50 58 18 1.000000 51 51  5 1.000000
51 52 33 1.000000 51 59 18 1.000000 52 52  5 1.000000 52 53 27 1.000000
52 59 18 1.000000 53 53  5 1.000000 53 54 33 1.000000 53 60 18 1.000000
54 54  5 1.000000 54 60 18 1.000000 55 55  6 1.000000 55 61 29 1.000000
56 56  6 1.000000 56 62 29 1.000000 57 57  6 1.000000 57 63 29 1.000000
58 58  6 1.000000 58 64 29 1.000000 59 59  6 1.000000 59 65 29 1.000000
60 60  6 1.000000 60 66 29 1.000000 61 61  7 1.000000 62 62  7 1.000000
63 63  7 1.000000 64 64  7 1.000000 65 65  7 1.000000 66 66  7 1.000000
67 67 31 1.000000 68 68 31 1.000000 69 69 31 1.000000 70 70 31 1.000000
71 71 31 1.000000 72 72 31 1.000000 73 73 32 1.000000 74 74 32 1.000000
75 75 32 1.000000 76 76 32 1.000000 77 77 32 1.000000 78 78 32 1.000000
-2  0  0 0.0
```

EPI-INOSITOL - Z MATRIX - A1 SYMMETRY SPECIES

```
 4  4  1 1.000000  5  5  1 1.000000  6  6  1 1.000000  7  7  1 1.000000
 8  8  3 1.000000  9  9  3 1.000000 10 10  3 1.000000 11 11  3 1.000000
 1  1  2 1.000000  2  2  2 1.000000  3  3  2 1.000000 12 12  4 1.000000
13 13  4 1.000000 14 14  4 1.000000 15 15  4 1.000000 26 26  5 1.000000
27 27  5 1.000000 28 28  5 1.000000 29 29  5 1.000000 30 30  5 1.000000
31 31  5 1.000000 20 20  8 1.000000 21 21  8 1.000000 22 22  8 1.000000
23 23  8 1.000000 24 24  8 1.000000 25 25  8 1.000000 36 36  7 1.000000
37 37  7 1.000000 38 38  7 1.000000 39 39  7 1.000000 16 16  9 1.000000
17 17  9 1.000000 18 18  9 1.000000 19 19  9 1.000000 32 32  6 1.000000
33 33  6 1.000000 34 34  6 1.000000 35 35  6 1.000000  1  4 10 1.414211
 1  5 10 1.000000  2  5 10 1.000000  2  6 10 1.000000  3  6 10 1.000000
 3  7 10 1.414211  1  1 11 1.000000  1  2 11 1.000000  2  3 11 1.000000
 3  3 11 1.000000  4  8 33 1.000000  5  9 33 1.000000  6 10 33 1.000000
 7 11 33 1.000000  1  8 33 1.414211  1  9 33 1.000000  2  9 33 1.000000
 2 10 33 1.000000  3 10 33 1.000000  3 11 33 1.414211  4 12 33 1.000000
 5 13 33 1.000000  6 14 33 1.000000  7 15 33 1.000000  4 32 12 1.000000
 5 33 12 1.000000  6 34 12 1.000000  7 35 12 1.000000  4 20 14 1.414211
 5 21 14 1.000000  5 22 14 1.000000  6 23 14 1.000000  6 24 14 1.000000
 7 25 14 1.414211  1 21 16 1.000000  2 22 16 1.000000  1 20 16 1.000000
 2 23 16 1.000000  3 24 16 1.000000  3 25 16 1.000000  1 26 15 1.000000
 1 27 15 1.000000  2 28 15 1.000000  2 29 15 1.000000  3 30 15 1.000000
 3 31 15 1.000000  1 16 17 1.000000  1 19 17 1.414211  2 16 17 1.000000
 2 17 17 1.000000  3 17 17 1.000000  3 18 17 1.414211  8 26 33 1.414211
 9 27 33 1.000000  9 28 33 1.000000 10 29 33 1.000000 10 30 33 1.000000
```

TABLE XL (Continued)

```
11 31 33 1.414211  8 32 33 1.000000  9 33 33 1.000000 10 34 33 1.000000
11 35 33 1.000000  4 36 13 1.000000  5 37 13 1.000000  6 38 13 1.000000
 7 39 13 1.000000 12 36 33 1.000000 13 37 33 1.000000 14 38 33 1.000000
15 39 33 1.000000 26 32 18 1.414211 27 33 18 1.000000 28 33 18 1.000000
29 34 18 1.000000 30 34 18 1.000000 31 35 18 1.414211 20 26 19 1.000000
21 27 19 1.000000 22 28 19 1.000000 23 29 19 1.000000 24 30 19 1.000000
25 31 19 1.000000 16 27 19 1.000000 16 28 19 1.000000 17 29 19 1.000000
17 30 19 1.000000 18 31 19 1.414211 19 26 19 1.414211 20 32 19 1.414211
21 33 19 1.000000 22 33 19 1.000000 23 34 19 1.000000 24 34 19 1.000000
25 35 19 1.414211 26 26 33 1.000000 27 28 33 1.000000 29 30 33 1.000000
31 31 33 1.000000 20 20 20 1.000000 21 22 20 1.000000 23 24 20 1.000000
25 25 20 1.000000 16 21 20 1.000000 16 22 20 1.000000 17 23 20 1.000000
17 24 20 1.000000 18 25 20 1.414211 19 20 20 1.414211 17 22 21 1.000000
19 21 21 1.414211 20 21 21 1.000000 22 23 21 1.000000 24 25 21 1.000000
16 17 21 1.000000 16 19 21 1.414211 17 18 21 1.414211 16 20 22 1.000000
16 23 22 1.000000 17 25 22 1.000000 18 24 22 1.414211 20 27 23 1.000000
23 28 23 1.000000 24 31 23 1.000000 25 30 23 1.000000 21 26 24 1.000000
22 29 24 1.000000 33 37 29 1.000000 32 36 29 1.000000 34 38 29 1.000000
35 39 29 1.000000 26 27 27 1.000000 28 29 27 1.000000 30 31 28 1.000000
16 26 25 1.000000 16 29 25 1.000000 17 31 25 1.000000 18 30 25 1.414211
17 28 26 1.000000 19 27 26 1.414211 20 36 30 1.414211 21 37 30 1.000000
23 38 30 1.000000 24 38 30 1.000000 25 39 30 1.414211 22 37 30 1.000000
40 40 31 1.000000 41 41 31 1.000000 42 42 31 1.000000 43 43 32 1.000000
44 44 32 1.000000 -2  0  0 0.0
```

EPI-INOSITOL - Z MATRIX - All SYMMETRY SPECIES

```
 4  4  1 1.000000  5  5  1 1.000000  6  6  3 1.000000  7  7  3 1.000000
 1  1  2 1.000000  2  2  2 1.000000  3  3  2 1.000000  8  8  4 1.000000
 9  9  4 1.000000 18 18  5 1.000000 19 19  5 1.000000 20 20  5 1.000000
21 21  5 1.000000 22 22  5 1.000000 23 23  5 1.000000 12 12  8 1.000000
13 13  8 1.000000 14 14  8 1.000000 15 15  8 1.000000 16 16  8 1.000000
17 17  8 1.000000 26 26  7 1.000000 27 27  7 1.000000 10 10  9 1.000000
11 11  9 1.000000 24 24  6 1.000000 25 25  6 1.000000  1  4 10 1.000000
 2  4 10 1.000000  2  5 10 1.000000  3  5 10 1.000000  1  1 11-1.000000
 1  2 11 1.000000  2  3 11 1.000000  3  3 11-1.000000  4  6 33 1.000000
 5  7 33 1.000000  1  6 33 1.000000  2  6 33 1.000000  2  7 33 1.000000
 3  7 33 1.000000  4  8 33 1.000000  5  9 33 1.000000  4 24 12 1.000000
 5 25 12 1.000000  4 13 14 1.000000  4 14 14 1.000000  5 15 14 1.000000
 5 16 14 1.000000  1 13 16 1.000000  2 14 16 1.000000  1 12 16-1.000000
 2 15 16 1.000000  3 16 16 1.000000  3 17 16 1.000000  1 18 15-1.000000
 1 19 15 1.000000  2 20 15 1.000000  2 21 15 1.000000  3 22 15 1.000000
 3 23 15 1.000000  1 10 17 1.000000  2 10 17 1.000000  2 11 17 1.000000
 3 11 17 1.000000  6 19 33 1.000000  6 20 33 1.000000  7 21 33 1.000000
 7 22 33 1.000000  6 24 33 1.000000  7 25 33 1.000000  4 26 13 1.000000
 5 27 13 1.000000  8 26 33 1.000000  9 27 33 1.000000 19 24 18 1.000000
20 24 18 1.000000 21 25 18 1.000000 22 25 18 1.000000 12 18 19 1.000000
13 19 19 1.000000 14 20 19 1.000000 15 21 19 1.000000 16 22 19 1.000000
17 23 19 1.000000 10 19 19 1.000000 10 20 19 1.000000 11 21 19 1.000000
11 22 19 1.000000 13 24 19 1.000000 14 24 19 1.000000 15 25 19 1.000000
16 25 19 1.000000 18 18 33-1.000000 19 20 33 1.000000 21 22 33 1.000000
23 23 33-1.000000 12 12 20-1.000000 13 14 20 1.000000 15 16 20 1.000000
17 17 20-1.000000 10 13 20 1.000000 10 14 20 1.000000 11 15 20 1.000000
11 16 20 1.000000 11 14 21 1.000000 12 13 21-1.000000 14 15 21 1.000000
16 17 21 1.000000 10 11 21 1.000000 10 12 22-1.000000 10 15 22 1.000000
11 17 22 1.000000 12 19 23-1.000000 15 20 23 1.000000 16 23 23 1.000000
17 22 23 1.000000 13 18 24-1.000000 14 21 24 1.000000 24 26 29 1.000000
25 27 29 1.000000 18 19 27-1.000000 20 21 27 1.000000 22 23 28 1.000000
```

TABLE XL (Continued)

```
10 18 25-1.000000 10 21 25 1.000000 11 23 25 1.000000 11 20 26 1.000000
13 26 30 1.000000 15 27 30 1.000000 16 27 30 1.000000 14 26 30 1.000000
28 28 31 1.000000 29 29 31 1.000000 30 30 31 1.000000 31 31 32 1.000000
32 32 32 1.000000 33 33 32 1.000000 34 34 32 1.000000 -2  0  0 0.0
```

CIS-INOSITOL - Z MATRIX - UNSYMMETRIZED

```
 1  1  2 1.000000  1  2 11 1.000000  1  6 11 1.000000  1  7 10 1.000000
 1  8 10 1.000000  1 13 33 1.000000  1 14 33 1.000000  1 25 17 1.000000
 1 30 17 1.000000  1 32 16 1.000000  1 33 16 1.000000  1 44 15 1.000000
 1 45 15 1.000000  2  2  2 1.000000  2  3 11 1.000000  2  8 10 1.000000
 2  9 10 1.000000  2 14 33 1.000000  2 15 33 1.000000  2 25 17 1.000000
 2 26 17 1.000000  2 34 16 1.000000  2 35 16 1.000000  2 46 15 1.000000
 2 47 15 1.000000  3  3  2 1.000000  3  4 11 1.000000  3  9 10 1.000000
 3 10 10 1.000000  3 15 33 1.000000  3 16 33 1.000000  3 26 17 1.000000
 3 27 17 1.000000  3 36 16 1.000000  3 37 16 1.000000  3 48 15 1.000000
 3 49 15 1.000000  4  4  2 1.000000  4  5 11 1.000000  4 10 10 1.000000
 4 11 10 1.000000  4 16 33 1.000000  4 17 33 1.000000  4 27 17 1.000000
 4 28 17 1.000000  4 38 16 1.000000  4 39 16 1.000000  4 50 15 1.000000
 4 51 15 1.000000  5  5  2 1.000000  5  6 11 1.000000  5 11 10 1.000000
 5 12 10 1.000000  5 17 33 1.000000  5 18 33 1.000000  5 28 17 1.000000
 5 29 17 1.000000  5 40 16 1.000000  5 41 16 1.000000  5 52 15 1.000000
 5 53 15 1.000000  6  6  2 1.000000  6  7 10 1.000000  6 12 10 1.000000
 6 13 33 1.000000  6 18 33 1.000000  6 29 17 1.000000  6 30 17 1.000000
 6 31 16 1.000000  6 42 16 1.000000  6 43 15 1.000000  6 54 15 1.000000
 7  7  1 1.000000  7 13 33 1.000000  7 19 33 1.000000  7 31 14 1.000000
 7 32 14 1.000000  7 55 12 1.000000  7 61 13 1.000000  8  8  1 1.000000
 8 14 33 1.000000  8 20 33 1.000000  8 33 14 1.000000  8 34 14 1.000000
 8 56 12 1.000000  8 62 13 1.000000  9  9  1 1.000000  9 15 33 1.000000
 9 21 33 1.000000  9 35 14 1.000000  9 36 14 1.000000  9 57 12 1.000000
 9 63 13 1.000000 10 10  1 1.000000 10 16 33 1.000000 10 22 33 1.000000
10 37 14 1.000000 10 38 14 1.000000 10 58 12 1.000000 10 64 13 1.000000
11 11  1 1.000000 11 17 33 1.000000 11 23 33 1.000000 11 39 14 1.000000
11 40 14 1.000000 11 59 12 1.000000 11 65 13 1.000000 12 12  1 1.000000
12 18 33 1.000000 12 24 33 1.000000 12 41 14 1.000000 12 42 14 1.000000
12 60 12 1.000000 12 66 13 1.000000 13 13  3 1.000000 13 43 33 1.000000
13 44 33 1.000000 13 55 33 1.000000 14 14  3 1.000000 14 45 33 1.000000
14 46 33 1.000000 14 56 33 1.000000 15 15  3 1.000000 15 47 33 1.000000
15 48 33 1.000000 15 57 33 1.000000 16 16  3 1.000000 16 49 33 1.000000
16 50 33 1.000000 16 58 33 1.000000 17 17  3 1.000000 17 51 33 1.000000
17 52 33 1.000000 17 59 33 1.000000 18 18  3 1.000000 18 53 33 1.000000
18 54 33 1.000000 18 60 33 1.000000 19 19  4 1.000000 19 61 33 1.000000
20 20  4 1.000000 20 62 33 1.000000 21 21  4 1.000000 21 63 33 1.000000
22 22  4 1.000000 22 64 33 1.000000 23 23  4 1.000000 23 65 33 1.000000
24 24  4 1.000000 24 66 33 1.000000 25 25  9 1.000000 25 26 21 1.000000
25 30 21 1.000000 25 32 22 1.000000 25 33 20 1.000000 25 34 20 1.000000
25 35 22 1.000000 25 44 25 1.000000 25 45 19 1.000000 25 46 19 1.000000
25 47 25 1.000000 26 26  9 1.000000 26 27 21 1.000000 26 34 21 1.000000
26 35 20 1.000000 26 36 20 1.000000 26 37 21 1.000000 26 46 26 1.000000
26 47 19 1.000000 26 48 19 1.000000 26 49 26 1.000000 27 27  9 1.000000
27 28 21 1.000000 27 36 22 1.000000 27 37 20 1.000000 27 38 20 1.000000
27 39 22 1.000000 27 48 25 1.000000 27 49 19 1.000000 27 50 19 1.000000
27 51 25 1.000000 28 28  9 1.000000 28 29 21 1.000000 28 38 21 1.000000
28 39 20 1.000000 28 40 20 1.000000 28 41 21 1.000000 28 50 26 1.000000
28 51 19 1.000000 28 52 19 1.000000 28 53 26 1.000000 29 29  9 1.000000
29 30 21 1.000000 29 31 22 1.000000 29 40 22 1.000000 29 41 20 1.000000
29 42 20 1.000000 29 43 25 1.000000 29 52 25 1.000000 29 53 19 1.000000
29 54 19 1.000000 30 30  9 1.000000 30 31 20 1.000000 30 32 20 1.000000
```

TABLE XL (Continued)

```
30 33 21 1.0CCCOO 30 42 21 1.OOOOCC 30 43 19 1.000000 30 44 19 1.000000
30 45 26 1.0CCCOO 30 54 26 1.COOOCO 31 31  8 1.000000 31 32 20 1.000000
31 42 21 1.0CCCOO 31 43 19 1.CCOOCO 31 54 23 1.000000 31 55 19 1.000000
31 61 30 1.0CCCOO 32 32  8 1.COOOOO 32 33 21 1.000000 32 44 19 1.000000
32 45 23 1.0CCCOO 32 55 19 1.COOOCO 32 61 30 1.000000 33 33  8 1.000000
33 34 20 1.0CCOOO 33 44 24 1.OOOOOO 33 45 19 1.000000 33 56 19 1.000000
33 62 30 1.0CCCOO 34 34  8 1.COOOOO 34 35 21 1.000000 34 46 19 1.000000
34 47 24 1.0CCOOO 34 56 19 1.OOOOCO 34 62 30 1.000000 35 35  8 1.000000
35 36 20 1.0CCCOO 35 46 23 1.COOOOO 35 47 19 1.000000 35 57 19 1.000000
35 63 30 1.0CCCOO 36 36  8 1.000000 36 37 21 1.000000 36 48 19 1.000000
36 49 23 1.0CCOOO 36 57 19 1.COOOCO 36 63 30 1.000000 37 37  8 1.000000
37 38 20 1.0CCOOO 37 48 24 1.COOOCO 37 49 19 1.000000 37 58 19 1.000000
37 64 30 1.0CCOOO 38 38  8 1.COOOCO 38 39 21 1.000000 38 50 19 1.000000
38 51 24 1.0CCCOO 38 58 19 1.CCCCOO 38 64 30 1.000000 39 39  8 1.000000
39 40 20 1.0CCOOO 39 50 23 1.OOOOCO 39 51 19 1.000000 39 59 19 1.000000
39 65 30 1.0CCOOO 40 40  8 1.COOOCO 40 41 21 1.000000 40 52 19 1.000000
40 53 23 1.0CCCOO 40 59 19 1.COOOOO 40 65 30 1.000000 41 41  8 1.000000
41 42 20 1.0CCCOO 41 52 24 1.COOOCO 41 53 19 1.000000 41 60 19 1.000000
41 66 30 1.0CCCOO 42 42  8 1.000000 42 43 24 1.000000 42 54 19 1.000000
42 60 19 1.0CCCOO 42 66 30 1.COOOCO 43 43  5 1.000000 43 44 33 1.000000
43 54 27 1.0CCCOO 43 55 18 1.COOCCO 44 44  5 1.000000 44 45 27 1.000000
44 55 18 1.0CCCOO 45 45  5 1.000000 45 46 33 1.000000 45 56 18 1.000000
46 46  5 1.0CCOOO 46 47 27 1.COOOCO 46 56 18 1.000000 47 47  5 1.000000
47 48 33 1.0CCCOO 47 57 18 1.000000 48 48  5 1.000000 48 49 27 1.000000
48 57 18 1.0CCOOO 49 49  5 1.000000 49 50 33 1.000000 49 58 18 1.000000
50 50  5 1.0CCCOO 50 51 27 1.OOOOCO 50 58 18 1.000000 51 51  5 1.000000
51 52 33 1.0CCOOO 51 59 18 1.COOOCO 52 52  5 1.000000 52 53 27 1.000000
52 59 18 1.0CCOOO 53 53  5 1.CCOCCO 53 54 33 1.000000 53 60 18 1.000000
54 54  5 1.0CCOOO 54 60 18 1.CCOOOO 55 55  6 1.000000 55 61 29 1.000000
56 56  6 1.0CCCOO 56 62 29 1.COOOCO 57 57  6 1.000000 57 63 29 1.000000
58 58  6 1.0CCOOO 58 64 29 1.000000 59 59  6 1.000000 59 65 29 1.000000
60 60  6 1.0CCCOC 60 66 29 1.000000 61 61  7 1.000000 62 62  7 1.000000
63 63  7 1.0CCCOO 64 64  7 1.COOOCO 65 65  7 1.000000 66 66  7 1.000000
67 67 31 1.0CCCOO 68 68 31 1.OOOOCO 69 69 31 1.000000 70 70 31 1.000000
71 71 31 1.0CCOOO 72 72 31 1.OCOOCC 73 73 32 1.000000 74 74 32 1.000000
75 75 32 1.0CCOOO 76 76 32 1.000000 77 77 32 1.000000 78 78 32 1.000000
-2  0  0 0.0
```

CIS-INOSITOL - Z MATRIX - A1 SYMMETRY SPECIES

```
 2  2  1 1.0CCCOO  3  3  1 1.CCOOCO  4  4  3 1.000000  5  5  3 1.000000
 1  1  2 1.0CCCOO  6  6  4 1.COOOCO  7  7  4 1.000000 12 12  5 1.000000
13 13  5 1.CCCCOO 10 10  8 1.CCOOCO 11 11  8 1.000000 16 16  7 1.000000
17 17  7 1.0CCOOO  8  8  9 1.OOOOCO  9  9  9 1.000000 14 14  6 1.000000
15 15  6 1.0CCCOO  1  2 10 1.414212  1  3 10 1.414212  1  1 11 1.999998
 2  4 33 1.0CCCOO  3  5 33 1.000000  1  4 33 1.414212  1  5 33 1.414212
 2  6 33 1.0CCCOO  3  7 33 1.000000  2 14 12 1.000000  3 15 12 1.000000
 2 10 14 1.414211  3 11 14 1.414211  1 10 16 1.000000  1 11 16 1.000000
 1 12 15 1.0CCCOO  1 13 15 1.COOOOO  1  8 17 1.414212  1  9 17 1.414212
 4 12 33 1.414211  5 13 33 1.414211  4 14 33 1.000000  5 15 33 1.000000
 2 16 13 1.0000000 3 17 13 1.000000  6 16 33 1.000000  7 17 33 1.000000
12 14 18 1.414212 13 15 18 1.414212 10 12 19 1.000000 11 13 19 1.000000
 8 13 19 1.414211  9 12 19 1.414211 10 14 19 1.414212 11 15 19 1.414212
12 12 33 1.0CCOOO 13 13 33 1.COOOOO 10 10 20 1.000000 11 11 20 1.000000
 8 11 20 1.414211  9 10 20 1.414211  9 11 21 1.414211 10 11 21 1.000000
 8  9 21 1.999998  8 10 22 1.414211 10 13 23 1.000000 11 12 24 1.000000
15 17 29 1.0CCCOO 14 16 29 1.OOOOCO 12 13 27 1.000000  8 12 25 1.414211
 9 13 26 1.414211 10 16 30 1.414212 11 17 30 1.414212 18 18 31 1.000000
-2  0  0 0.0
```

TABLE XL (Continued)

CIS-INOSITOL - $\underset{\sim}{Z}$ MATRIX - A2 SYMMETRY SPECIES

1	1	2	1.000000	4	4	5	1.000000	5	5	5	1.000000	2	2	8	1.000000
3	3	8	1.000000	1	1	11	-1.999998	1	2	16	-1.000000	1	3	16	1.000000
1	4	15	-1.000000	1	5	15	1.000000	2	4	19	1.000000	3	5	19	1.000000
4	4	33	-1.000000	5	5	33	-1.000000	2	2	20	-1.000000	3	3	20	-1.000000
2	3	21	-1.000000	2	5	23	-1.000000	3	4	24	-1.000000	4	5	27	-1.000000
6	6	31	1.000000	7	7	32	1.000000	8	8	32	1.000000	-2	0	0	0.0

L-CHIRO-INOSITOL - $\underset{\sim}{Z}$ MATRIX - UNSYMMETRIZED

1	1	2	1.000000	1	2	11	1.000000	1	6	11	1.000000	1	7	10	1.000000
1	8	10	1.000000	1	13	33	1.000000	1	14	33	1.000000	1	25	17	1.000000
1	30	17	1.000000	1	32	16	1.000000	1	33	16	1.000000	1	44	15	1.000000
1	45	15	1.000000	2	2	2	1.000000	2	3	11	1.000000	2	8	10	1.000000
2	9	10	1.000000	2	14	33	1.000000	2	15	33	1.000000	2	25	17	1.000000
2	26	17	1.000000	2	34	16	1.000000	2	35	16	1.000000	2	46	15	1.000000
2	47	15	1.000000	3	3	2	1.000000	3	4	11	1.000000	3	9	10	1.000000
3	10	10	1.000000	3	15	33	1.000000	3	16	33	1.000000	3	26	17	1.000000
3	27	17	1.000000	3	36	16	1.000000	3	37	16	1.000000	3	48	15	1.000000
3	49	15	1.000000	4	4	2	1.000000	4	5	11	1.000000	4	10	10	1.000000
4	11	10	1.000000	4	16	33	1.000000	4	17	33	1.000000	4	27	17	1.000000
4	28	17	1.000000	4	38	16	1.000000	4	39	16	1.000000	4	50	15	1.000000
4	51	15	1.000000	5	5	2	1.000000	5	6	11	1.000000	5	11	10	1.000000
5	12	10	1.000000	5	17	33	1.000000	5	18	33	1.000000	5	28	17	1.000000
5	29	17	1.000000	5	40	16	1.000000	5	41	16	1.000000	5	52	15	1.000000
5	53	15	1.000000	6	6	2	1.000000	6	7	10	1.000000	6	12	10	1.000000
6	13	33	1.000000	6	18	33	1.000000	6	29	17	1.000000	6	30	17	1.000000
6	31	16	1.000000	6	42	16	1.000000	6	43	15	1.000000	6	54	15	1.000000
7	7	1	1.000000	7	13	33	1.000000	7	19	33	1.000000	7	31	14	1.000000
7	32	14	1.000000	7	55	12	1.000000	7	61	13	1.000000	8	8	1	1.000000
8	14	33	1.000000	8	20	33	1.000000	8	33	14	1.000000	8	34	14	1.000000
8	56	12	1.000000	8	62	13	1.000000	9	9	1	1.000000	9	15	33	1.000000
9	21	33	1.000000	9	35	14	1.000000	9	36	14	1.000000	9	57	12	1.000000
9	63	13	1.000000	10	10	1	1.000000	10	16	33	1.000000	10	22	33	1.000000
10	37	14	1.000000	10	38	14	1.000000	10	58	12	1.000000	10	64	13	1.000000
11	11	1	1.000000	11	17	33	1.000000	11	23	33	1.000000	11	39	14	1.000000
11	40	14	1.000000	11	59	12	1.000000	11	65	13	1.000000	12	12	1	1.000000
12	18	33	1.000000	12	24	33	1.000000	12	41	14	1.000000	12	42	14	1.000000
12	60	12	1.000000	12	66	13	1.000000	13	13	3	1.000000	13	43	33	1.000000
13	44	33	1.000000	13	55	33	1.000000	14	14	3	1.000000	14	45	33	1.000000
14	46	33	1.000000	14	56	33	1.000000	15	15	3	1.000000	15	47	33	1.000000
15	48	33	1.000000	15	57	33	1.000000	16	16	3	1.000000	16	49	33	1.000000
16	50	33	1.000000	16	58	33	1.000000	17	17	3	1.000000	17	51	33	1.000000
17	52	33	1.000000	17	59	33	1.000000	18	18	3	1.000000	18	53	33	1.000000
18	54	33	1.000000	18	60	33	1.000000	19	19	4	1.000000	19	61	33	1.000000
20	20	4	1.000000	20	62	33	1.000000	21	21	4	1.000000	21	63	33	1.000000
22	22	4	1.000000	22	64	33	1.000000	23	23	4	1.000000	23	65	33	1.000000
24	24	4	1.000000	24	66	33	1.000000	25	25	9	1.000000	25	26	21	1.000000
25	30	21	1.000000	25	32	21	1.000000	25	33	20	1.000000	25	34	20	1.000000
25	35	22	1.000000	25	44	26	1.000000	25	45	19	1.000000	25	46	19	1.000000
25	47	25	1.000000	26	26	9	1.000000	26	27	21	1.000000	26	34	22	1.000000
26	35	20	1.000000	26	36	20	1.000000	26	37	22	1.000000	26	46	25	1.000000
26	47	19	1.000000	26	48	19	1.000000	26	49	25	1.000000	27	27	9	1.000000
27	28	21	1.000000	27	36	22	1.000000	27	37	20	1.000000	27	38	20	1.000000
27	39	22	1.000000	27	48	25	1.000000	27	49	19	1.000000	27	50	19	1.000000
27	51	25	1.000000	28	28	9	1.000000	28	29	21	1.000000	28	38	22	1.000000

TABLE XL (Continued)

```
28 39 20 1.000000 28 40 20 1.000000 28 41 21 1.000000 28 50 25 1.000000
28 51 19 1.000000 28 52 19 1.000000 28 53 26 1.000000 29 29  9 1.000000
29 30 21 1.000000 29 31 21 1.000000 29 40 22 1.000000 29 41 20 1.000000
29 42 20 1.000000 29 43 26 1.000000 29 52 25 1.000000 29 53 19 1.000000
29 54 19 1.000000 30 30  9 1.000000 30 31 20 1.000000 30 32 20 1.000000
30 33 22 1.000000 30 42 21 1.000000 30 43 19 1.000000 30 44 19 1.000000
30 45 25 1.000000 30 54 26 1.000000 31 31  8 1.000000 31 32 20 1.000000
31 42 22 1.000000 31 43 19 1.000000 31 54 23 1.000000 31 55 19 1.000000
31 61 30 1.000000 32 32  8 1.000000 32 33 21 1.000000 32 44 19 1.000000
32 45 24 1.000000 32 55 19 1.000000 32 61 30 1.000000 33 33  8 1.000000
33 34 20 1.000000 33 44 23 1.000000 33 45 19 1.000000 33 56 19 1.000000
33 62 30 1.000000 34 34  8 1.000000 34 35 21 1.000000 34 46 19 1.000000
34 47 23 1.000000 34 56 19 1.000000 34 62 30 1.000000 35 35  8 1.000000
35 36 20 1.000000 35 46 23 1.000000 35 47 19 1.000000 35 57 19 1.000000
35 63 30 1.000000 36 36  8 1.000000 36 37 21 1.000000 36 48 19 1.000000
36 49 23 1.000000 36 57 19 1.000000 36 63 30 1.000000 37 37  8 1.000000
37 38 20 1.000000 37 48 23 1.000000 37 49 19 1.000000 37 58 19 1.000000
37 64 30 1.000000 38 38  8 1.000000 38 39 21 1.000000 38 50 19 1.000000
38 51 23 1.000000 38 58 19 1.000000 38 64 30 1.000000 39 39  8 1.000000
39 40 20 1.000000 39 50 23 1.000000 39 51 19 1.000000 39 59 19 1.000000
39 65 30 1.000000 40 40  8 1.000000 40 41 21 1.000000 40 52 19 1.000000
40 53 23 1.000000 40 59 19 1.000000 40 65 30 1.000000 41 41  8 1.000000
41 42 20 1.000000 41 52 24 1.000000 41 53 19 1.000000 41 60 19 1.000000
41 66 30 1.000000 42 42  8 1.000000 42 43 23 1.000000 42 54 19 1.000000
42 60 19 1.000000 42 66 30 1.000000 43 43  5 1.000000 43 44 33 1.000000
43 54 27 1.000000 43 55 18 1.000000 44 44  5 1.000000 44 45 27 1.000000
44 55 18 1.000000 45 45  5 1.000000 45 46 33 1.000000 45 56 18 1.000000
46 46  5 1.000000 46 47 28 1.000000 46 56 18 1.000000 47 47  5 1.000000
47 48 33 1.000000 47 57 18 1.000000 48 48  5 1.000000 48 49 28 1.000000
48 57 18 1.000000 49 49  5 1.000000 49 50 33 1.000000 49 58 18 1.000000
50 50  5 1.000000 50 51 28 1.000000 50 58 18 1.000000 51 51  5 1.000000
51 52 33 1.000000 51 59 18 1.000000 52 52  5 1.000000 52 53 27 1.000000
52 59 18 1.000000 53 53  5 1.000000 53 54 33 1.000000 53 60 18 1.000000
54 54  5 1.000000 54 60 18 1.000000 55 55  6 1.000000 55 61 29 1.000000
56 56  6 1.000000 56 62 29 1.000000 57 57  6 1.000000 57 63 29 1.000000
58 58  6 1.000000 58 64 29 1.000000 59 59  6 1.000000 59 65 29 1.000000
60 60  6 1.000000 60 66 29 1.000000 61 61  7 1.000000 62 62  7 1.000000
63 63  7 1.000000 64 64  7 1.000000 65 65  7 1.000000 66 66  7 1.000000
67 67 31 1.000000 68 68 31 1.000000 69 69 31 1.000000 70 70 31 1.000000
71 71 31 1.000000 72 72 31 1.000000 73 73 32 1.000000 74 74 32 1.000000
75 75 32 1.000000 76 76 32 1.000000 77 77 32 1.000000 78 78 32 1.000000
-2  0  0 0.0
```

L-CHIRO-INOSITOL - $\underset{\sim}{Z}$ MATRIX - A SYMMETRY SPECIES

```
 5  5  1 1.000000  6  6  1 1.000000  7  7  1 1.000000  8  8  3 1.000000
 9  9  3 1.000000 10 10  3 1.000000  1  1  2 1.000000  2  2  2 1.000000
 3  3  2 1.000000  4  4  2 1.000000 11 11  4 1.000000 12 12  4 1.000000
13 13  4 1.000000 23 23  5 1.000000 24 24  5 1.000000 25 25  5 1.000000
26 26  5 1.000000 27 27  5 1.000000 28 28  5 1.000000 17 17  8 1.000000
18 18  8 1.000000 19 19  8 1.000000 20 20  8 1.000000 21 21  8 1.000000
22 22  8 1.000000 32 32  7 1.000000 33 33  7 1.000000 34 34  7 1.000000
14 14  9 1.000000 15 15  9 1.000000 16 16  9 1.000000 29 29  6 1.000000
30 30  6 1.000000 31 31  6 1.000000  1  5 10 1.000000  1  6 10 1.000000
 2  6 10 1.000000  2  7 10 1.000000  3  7 10 1.414212  4  5 10 1.414212
 1  2 11 1.000000  1  4 11 1.414212  2  3 11 1.414212  5  8 33 1.000000
```

TABLE XL (Continued)

6	9	33	1.000000	7	10	33	1.000000	1	8	33	1.000000	1	9	33	1.000000
2	9	33	1.000000	2	10	33	1.000000	3	10	33	1.414212	4	8	33	1.414212
5	11	33	1.000000	6	12	33	1.000000	7	13	33	1.000000	5	29	12	1.000000
6	30	12	1.000000	7	31	12	1.000000	5	17	14	1.000000	5	18	14	1.000000
6	19	14	1.000000	6	20	14	1.000000	7	21	14	1.000000	7	22	14	1.000000
1	18	16	1.000000	1	19	16	1.000000	2	20	16	1.000000	2	21	16	1.000000
3	22	16	1.414212	4	17	16	1.414212	1	24	15	1.000000	1	25	15	1.000000
2	26	15	1.000000	2	27	15	1.000000	3	28	15	1.414212	4	23	15	1.414212
1	14	17	1.000000	1	16	17	1.000000	2	14	17	1.000000	2	15	17	1.000000
3	15	17	1.414212	4	16	17	1.414212	8	23	33	1.000000	8	24	33	1.000000
9	25	33	1.000000	9	26	33	1.000000	10	27	33	1.000000	10	28	33	1.000000
8	29	33	1.000000	9	30	33	1.000000	10	31	33	1.000000	5	32	13	1.000000
6	33	13	1.000000	7	34	13	1.000000	11	32	33	1.000000	12	33	33	1.000000
13	34	33	1.000000	23	29	18	1.000000	24	29	18	1.000000	25	30	18	1.000000
26	30	18	1.000000	27	31	18	1.000000	28	31	18	1.000000	17	23	19	1.000000
18	24	19	1.000000	19	25	19	1.000000	20	26	19	1.000000	21	27	19	1.000000
22	28	19	1.000000	14	25	19	1.000000	14	26	19	1.000000	15	27	19	1.000000
15	28	19	1.000000	16	23	19	1.000000	16	24	19	1.000000	17	29	19	1.000000
18	29	19	1.000000	19	30	19	1.000000	20	30	19	1.000000	21	31	19	1.000000
22	31	19	1.000000	23	24	33	1.000000	25	26	33	1.000000	27	28	33	1.000000
17	18	20	1.000000	19	20	20	1.000000	21	22	20	1.000000	14	19	20	1.000000
14	20	20	1.000000	15	21	20	1.000000	15	22	20	1.000000	16	17	20	1.000000
16	18	20	1.000000	14	18	21	1.000000	16	17	21	1.000000	18	19	21	1.000000
20	21	21	1.000000	22	22	21	1.000000	14	15	21	1.000000	14	16	21	1.000000
15	15	21	1.000000	16	16	21	1.000000	14	21	22	1.000000	15	20	22	1.000000
15	22	22	1.000000	16	19	22	1.000000	17	17	22	1.000000	17	23	23	1.000000
19	24	23	1.000000	20	27	23	1.000000	21	26	23	1.000000	22	28	23	1.000000
18	25	24	1.000000	29	32	29	1.000000	30	33	29	1.000000	31	34	29	1.000000
23	23	27	1.000000	24	25	27	1.000000	26	27	28	1.000000	28	28	28	1.000000
14	27	25	1.000000	15	26	25	1.000000	15	28	25	1.000000	16	25	25	1.000000
14	24	26	1.000000	16	23	26	1.000000	17	32	30	1.000000	18	32	30	1.000000
19	33	30	1.000000	20	33	30	1.000000	21	34	30	1.000000	22	34	30	1.000000
35	35	31	1.000000	36	36	31	1.000000	37	37	31	1.000000	38	38	31	1.000000
39	39	32	1.000000	40	40	32	1.000000	41	41	32	1.000000	-2	0	0	0.0

L-CHIRO-INOSITOL - Z_{mn} MATRIX - B SYMMETRY SPECIES

3	3	1	1.000000	4	4	1	1.000000	5	5	1	1.000000	6	6	3	1.000000
7	7	3	1.000000	8	8	3	1.000000	1	1	2	1.000000	2	2	2	1.000000
9	9	4	1.000000	10	10	4	1.000000	11	11	4	1.000000	21	21	5	1.000000
22	22	5	1.000000	23	23	5	1.000000	24	24	5	1.000000	25	25	5	1.000000
26	26	5	1.000000	15	15	8	1.000000	16	16	8	1.000000	17	17	8	1.000000
18	18	8	1.000000	19	19	8	1.000000	20	20	8	1.000000	30	30	7	1.000000
31	31	7	1.000000	32	32	7	1.000000	12	12	9	1.000000	13	13	9	1.000000
14	14	9	1.000000	27	27	6	1.000000	28	28	6	1.000000	29	29	6	1.000000
1	3	10	1.000000	1	4	10	1.000000	2	4	10	1.000000	2	5	10	1.000000
1	2	11	1.000000	3	6	33	1.000000	4	7	33	1.000000	5	8	33	1.000000
1	6	33	1.000000	1	7	33	1.000000	2	7	33	1.000000	2	8	33	1.000000
3	9	33	1.000000	4	10	33	1.000000	5	11	33	1.000000	3	27	12	1.000000
4	28	12	1.000000	5	29	12	1.000000	3	15	14	1.000000	3	16	14	1.000000
4	17	14	1.000000	4	18	14	1.000000	5	19	14	1.000000	5	20	14	1.000000
1	16	16	1.000000	1	17	16	1.000000	2	18	16	1.000000	2	19	16	1.000000
1	22	15	1.000000	1	23	15	1.000000	2	24	15	1.000000	2	25	15	1.000000
1	12	17	1.000000	1	14	17	-1.000000	2	12	17	1.000000	2	13	17	1.000000
6	21	33	1.000000	6	22	33	1.000000	7	23	33	1.000000	7	24	33	1.000000

TABLE XL (Continued)

```
 8 25 33 1.000000  8 26 33 1.000000  6 27 33 1.000000  7 28 33 1.000000
 8 29 33 1.000000  3 30 13 1.000000  4 31 13 1.000000  5 32 13 1.000000
 9 30 33 1.000000 10 31 33 1.000000 11 32 33 1.000000 21 27 18 1.000000
22 27 18 1.000000 23 28 18 1.000000 24 28 18 1.000000 25 29 18 1.000000
26 29 18 1.000000 15 21 19 1.000000 16 22 19 1.000000 17 23 19 1.000000
18 24 19 1.000000 19 25 19 1.000000 20 26 19 1.000000 12 23 19 1.000000
12 24 19 1.000000 13 25 19 1.000000 13 26 19 1.000000 14 21 19-1.000000
14 22 19-1.000000 15 27 19 1.000000 16 27 19 1.000000 17 28 19 1.000000
18 28 19 1.000000 19 29 19 1.000000 20 29 19 1.000000 21 22 33 1.000000
23 24 33 1.000000 25 26 33 1.000000 15 16 20 1.000000 17 18 20 1.000000
19 20 20 1.000000 12 17 20 1.000000 12 18 20 1.000000 13 19 20 1.000000
13 20 20 1.000000 14 15 20-1.000000 14 16 20-1.000000 12 16 21 1.000000
14 15 21 1.000000 16 17 21 1.000000 18 19 21 1.000000 20 20 21-1.000000
12 13 21 1.000000 12 14 21-1.000000 13 13 21-1.000000 14 14 21-1.000000
12 19 22 1.000000 13 18 22 1.000000 13 20 22-1.000000 14 17 22-1.000000
15 15 22-1.000000 15 21 23-1.000000 17 22 23 1.000000 18 25 23 1.000000
19 24 23 1.000000 20 26 23-1.000000 16 23 24 1.000000 27 30 29 1.000000
28 31 29 1.000000 29 32 29 1.000000 21 21 27-1.000000 22 23 27 1.000000
24 25 28 1.000000 26 26 28-1.000000 12 25 25 1.000000 13 24 25 1.000000
13 26 25-1.000000 14 23 25-1.000000 12 22 26 1.000000 14 21 26 1.000000
15 30 30 1.000000 16 30 30 1.000000 17 31 30 1.000000 18 31 30 1.000000
19 32 30 1.000000 20 32 30 1.000000 33 33 31 1.000000 34 34 31 1.000000
35 35 32 1.000000 36 36 32 1.000000 37 37 32 1.000000 -2  0  0 0.0
```

MUCO-INOSITOL - $\underset{\sim}{Z}$ MATRIX - UNSYMMETRIZED

```
 1  1  2 1.000000  1  2 11 1.000000  1  6 11 1.000000  1  7 10 1.000000
 1  8 10 1.000000  1 13 33 1.000000  1 14 33 1.000000  1 25 17 1.000000
 1 30 17 1.000000  1 32 16 1.000000  1 33 16 1.000000  1 44 15 1.000000
 1 45 15 1.000000  2  2  2 1.000000  2  3 11 1.000000  2  8 10 1.000000
 2  9 10 1.000000  2 14 33 1.000000  2 15 33 1.000000  2 25 17 1.000000
 2 26 17 1.000000  2 34 16 1.000000  2 35 16 1.000000  2 46 15 1.000000
 2 47 15 1.000000  3  3  2 1.000000  3  4 11 1.000000  3  9 10 1.000000
 3 10 10 1.000000  3 15 33 1.000000  3 16 33 1.000000  3 26 17 1.000000
 3 27 17 1.000000  3 36 16 1.000000  3 37 16 1.000000  3 48 15 1.000000
 3 49 15 1.000000  4  4  2 1.000000  4  5 11 1.000000  4 10 10 1.000000
 4 11 10 1.000000  4 16 33 1.000000  4 17 33 1.000000  4 27 17 1.000000
 4 28 17 1.000000  4 38 16 1.000000  4 39 16 1.000000  4 50 15 1.000000
 4 51 15 1.000000  5  5  2 1.000000  5  6 11 1.000000  5 11 10 1.000000
 5 12 10 1.000000  5 17 33 1.000000  5 18 33 1.000000  5 28 17 1.000000
 5 29 17 1.000000  5 40 16 1.000000  5 41 16 1.000000  5 52 15 1.000000
 5 53 15 1.000000  6  6  2 1.000000  6  7 10 1.000000  6 12 10 1.000000
 6 13 33 1.000000  6 18 33 1.000000  6 29 17 1.000000  6 30 17 1.000000
 6 31 16 1.000000  6 42 16 1.000000  6 43 15 1.000000  6 54 15 1.000000
 7  7  1 1.000000  7 13 33 1.000000  7 19 33 1.000000  7 31 14 1.000000
 7 32 14 1.000000  7 55 12 1.000000  7 61 13 1.000000  8  8  1 1.000000
 8 14 33 1.000000  8 20 33 1.000000  8 33 14 1.000000  8 34 14 1.000000
 8 56 12 1.000000  8 62 13 1.000000  9  9  1 1.000000  9 15 33 1.000000
 9 21 33 1.000000  9 35 14 1.000000  9 36 14 1.000000  9 57 12 1.000000
 9 63 13 1.000000 10 10  1 1.000000 10 16 33 1.000000 10 22 33 1.000000
10 37 14 1.000000 10 38 14 1.000000 10 58 12 1.000000 10 64 13 1.000000
11 11  1 1.000000 11 17 33 1.000000 11 23 33 1.000000 11 39 14 1.000000
11 40 14 1.000000 11 59 12 1.000000 11 65 13 1.000000 12 12  1 1.000000
12 18 33 1.000000 12 24 33 1.000000 12 41 14 1.000000 12 42 14 1.000000
12 60 12 1.000000 12 66 13 1.000000 13 13  3 1.000000 13 43 33 1.000000
13 44 33 1.000000 13 55 33 1.000000 14 14  3 1.000000 14 45 33 1.000000
```

TABLE XL (Continued)

```
14 46 33 1.000000 14 56 33 1.000000 15 15  3 1.000000 15 47 33 1.000000
15 48 33 1.000000 15 57 33 1.000000 16 16  3 1.000000 16 49 33 1.000000
16 50 33 1.000000 16 58 33 1.000000 17 17  3 1.000000 17 51 33 1.000000
17 52 33 1.000000 17 59 33 1.000000 18 18  3 1.000000 18 53 33 1.000000
18 54 33 1.000000 18 60 33 1.000000 19 19  4 1.000000 19 61 33 1.000000
20 20  4 1.000000 20 62 33 1.000000 21 21  4 1.000000 21 63 33 1.000000
22 22  4 1.000000 22 64 33 1.000000 23 23  4 1.000000 23 65 33 1.000000
24 24  4 1.000000 24 66 33 1.000000 25 25  9 1.000000 25 26 21 1.000000
25 30 21 1.000000 25 32 21 1.000000 25 33 20 1.000000 25 34 20 1.000000
25 35 22 1.000000 25 44 26 1.000000 25 45 19 1.000000 25 46 19 1.000000
25 47 25 1.000000 26 26  9 1.000000 26 27 21 1.000000 26 34 21 1.000000
26 35 20 1.000000 26 36 20 1.000000 26 37 22 1.000000 26 46 26 1.000000
26 47 19 1.000000 26 48 19 1.000000 26 49 25 1.000000 27 27  9 1.000000
27 28 21 1.000000 27 36 22 1.000000 27 37 20 1.000000 27 38 20 1.000000
27 39 22 1.000000 27 48 25 1.000000 27 49 19 1.000000 27 50 19 1.000000
27 51 25 1.000000 28 28  9 1.000000 28 29 21 1.000000 28 38 22 1.000000
28 39 20 1.000000 28 40 20 1.000000 28 41 21 1.000000 28 50 25 1.000000
28 51 19 1.000000 28 52 19 1.000000 28 53 26 1.000000 29 29  9 1.000000
29 30 21 1.000000 29 31 21 1.000000 29 40 22 1.000000 29 41 20 1.000000
29 42 20 1.000000 29 43 26 1.000000 29 52 25 1.000000 29 53 19 1.000000
29 54 19 1.000000 30 30  9 1.000000 30 31 20 1.000000 30 32 20 1.000000
30 33 21 1.000000 30 42 21 1.000000 30 43 19 1.000000 30 44 19 1.000000
30 45 26 1.000000 30 54 26 1.000000 31 31  8 1.000000 31 32 20 1.000000
31 42 22 1.000000 31 43 19 1.000000 31 54 23 1.000000 31 55 19 1.000000
31 61 30 1.000000 32 32  8 1.000000 32 33 22 1.000000 32 44 19 1.000000
32 45 23 1.000000 32 55 19 1.000000 32 61 30 1.000000 33 33  8 1.000000
33 34 20 1.000000 33 44 23 1.000000 33 45 19 1.000000 33 56 19 1.000000
33 62 30 1.000000 34 34  8 1.000000 34 35 21 1.000000 34 46 19 1.000000
34 47 24 1.000000 34 56 19 1.000000 34 62 30 1.000000 35 35  8 1.000000
35 36 20 1.000000 35 46 23 1.000000 35 47 19 1.000000 35 57 19 1.000000
35 63 30 1.000000 36 36  8 1.000000 36 37 21 1.000000 36 48 19 1.000000
36 49 23 1.000000 36 57 19 1.000000 36 63 30 1.000000 37 37  8 1.000000
37 38 20 1.000000 37 48 23 1.000000 37 49 19 1.000000 37 58 19 1.000000
37 64 30 1.000000 38 38  8 1.000000 38 39 21 1.000000 38 50 19 1.000000
38 51 23 1.000000 38 58 19 1.000000 38 64 30 1.000000 39 39  8 1.000000
39 40 20 1.000000 39 50 23 1.000000 39 51 19 1.000000 39 59 19 1.000000
39 65 30 1.000000 40 40  8 1.000000 40 41 21 1.000000 40 52 19 1.000000
40 53 23 1.000000 40 59 19 1.000000 40 65 30 1.000000 41 41  8 1.000000
41 42 20 1.000000 41 52 24 1.000000 41 53 19 1.000000 41 60 19 1.000000
41 66 30 1.000000 42 42  8 1.000000 42 43 23 1.000000 42 54 19 1.000000
42 60 19 1.000000 42 66 30 1.000000 43 43  5 1.000000 43 44 33 1.000000
43 54 27 1.000000 43 55 18 1.000000 44 44  5 1.000000 44 45 27 1.000000
44 55 18 1.000000 45 45  5 1.000000 45 46 33 1.000000 45 56 18 1.000000
46 46  5 1.000000 46 47 27 1.000000 46 56 18 1.000000 47 47  5 1.000000
47 48 33 1.000000 47 57 18 1.000000 48 48  5 1.000000 48 49 28 1.000000
48 57 18 1.000000 49 49  5 1.000000 49 50 33 1.000000 49 58 18 1.000000
50 50  5 1.000000 50 51 28 1.000000 50 58 18 1.000000 51 51  5 1.000000
51 52 33 1.000000 51 59 18 1.000000 52 52  5 1.000000 52 53 27 1.000000
52 59 18 1.000000 53 53  5 1.000000 53 54 33 1.000000 53 60 18 1.000000
54 54  5 1.000000 54 60 18 1.000000 55 55  6 1.000000 55 61 29 1.000000
56 56  6 1.000000 56 62 29 1.000000 57 57  6 1.000000 57 63 29 1.000000
58 58  6 1.000000 58 64 29 1.000000 59 59  6 1.000000 59 65 29 1.000000
60 60  6 1.000000 60 66 29 1.000000 61 61  7 1.000000 62 62  7 1.000000
63 63  7 1.000000 64 64  7 1.000000 65 65  7 1.000000 66 66  7 1.000000
67 67 31 1.000000 68 68 31 1.000000 69 69 31 1.000000 70 70 31 1.000000
71 71 31 1.000000 72 72 31 1.000000 73 73 32 1.000000 74 74 32 1.000000
75 75 32 1.000000 76 76 32 1.000000 77 77 32 1.000000 78 78 32 1.000000
-2  0  0 0.0
```

TABLE XL (Continued)

MUCO-INOSITOL - Z_{sa} MATRIX - A1 SYMMETRY SPECIES

4	4	1	1.000000	5	5	1	1.000000	6	6	1	1.000000	7	7	1	1.000000
8	8	3	1.000000	9	9	3	1.000000	10	10	3	1.000000	11	11	3	1.000000
1	1	2	1.000000	2	2	2	1.000000	3	3	2	1.000000	12	12	4	1.000000
13	13	4	1.000000	14	14	4	1.000000	15	15	4	1.000000	26	26	5	1.000000
27	27	5	1.000000	28	28	5	1.000000	29	29	5	1.000000	30	30	5	1.000000
31	31	5	1.000000	20	20	8	1.000000	21	21	8	1.000000	22	22	8	1.000000
23	23	8	1.000000	24	24	8	1.000000	25	25	8	1.000000	36	36	7	1.000000
37	37	7	1.000000	38	38	7	1.000000	39	39	7	1.000000	16	16	9	1.000000
17	17	9	1.000000	18	18	9	1.000000	19	19	9	1.000000	32	32	6	1.000000
33	33	6	1.000000	34	34	6	1.000000	35	35	6	1.000000	1	4	10	1.414212
1	5	10	1.000000	2	5	10	1.000000	2	6	10	1.000000	3	6	10	1.000000
3	7	10	1.414212	1	1	11	1.000000	1	2	11	1.000000	2	3	11	1.000000
3	3	11	1.000000	4	8	33	1.000000	5	9	33	1.000000	6	10	33	1.000000
7	11	33	1.000000	1	8	33	1.414212	1	9	33	1.000000	2	9	33	1.000000
2	10	33	1.000000	3	10	33	1.000000	3	11	33	1.414212	4	12	33	1.000000
5	13	33	1.000000	6	14	33	1.000000	7	15	33	1.000000	4	32	12	1.000000
5	33	12	1.000000	6	34	12	1.000000	7	35	12	1.000000	4	20	14	1.414212
5	21	14	1.000000	5	22	14	1.000000	6	23	14	1.000000	6	24	14	1.000000
7	25	14	1.414212	1	20	16	1.000000	1	21	16	1.000000	2	22	16	1.000000
2	23	16	1.000000	3	24	16	1.000000	3	25	16	1.000000	1	26	15	1.000000
1	27	15	1.000000	2	28	15	1.000000	2	29	15	1.000000	3	30	15	1.000000
3	31	15	1.000000	1	16	17	1.000000	1	19	17	1.414212	2	16	17	1.000000
2	17	17	1.000000	3	17	17	1.000000	3	18	17	1.414212	8	26	33	1.414212
9	27	33	1.000000	9	28	33	1.000000	10	29	33	1.000000	10	30	33	1.000000
11	31	33	1.414212	8	32	33	1.000000	9	33	33	1.000000	10	34	33	1.000000
11	35	33	1.000000	4	36	13	1.000000	5	37	13	1.000000	6	38	13	1.000000
7	39	13	1.000000	12	36	33	1.000000	13	37	33	1.000000	14	38	33	1.000000
15	39	33	1.000000	26	32	18	1.414212	27	33	18	1.000000	28	33	18	1.000000
29	34	18	1.000000	30	34	18	1.000000	31	35	18	1.414212	20	26	19	1.000000
21	27	19	1.000000	22	28	19	1.000000	23	29	19	1.000000	24	30	19	1.000000
25	31	19	1.000000	16	27	19	1.000000	16	28	19	1.000000	17	29	19	1.000000
17	30	19	1.000000	18	31	19	1.414212	19	26	19	1.414212	20	32	19	1.414212
21	33	19	1.000000	22	33	19	1.000000	23	34	19	1.000000	24	34	19	1.000000
25	35	19	1.414212	26	26	33	1.000000	27	28	33	1.000000	29	30	33	1.000000
31	31	33	1.000000	20	20	20	1.000000	21	22	20	1.000000	23	24	20	1.000000
25	25	20	1.000000	16	21	20	1.000000	16	22	20	1.000000	17	23	20	1.000000
17	24	20	1.000000	18	25	20	1.414212	19	20	20	1.414212	16	20	21	1.000000
17	22	21	1.000000	19	21	21	1.414212	22	23	21	1.000000	24	25	21	1.000000
16	17	21	1.000000	16	19	21	1.414212	17	18	21	1.414212	16	23	22	1.000000
17	25	22	1.000000	18	24	22	1.414212	20	21	22	1.000000	20	27	23	1.000000
21	26	23	1.000000	23	28	23	1.000000	24	31	23	1.000000	25	30	23	1.000000
22	29	24	1.000000	33	37	29	1.000000	32	36	29	1.000000	34	38	29	1.000000
35	39	29	1.000000	26	27	27	1.000000	28	29	27	1.000000	30	31	28	1.000000
16	29	25	1.000000	17	31	25	1.000000	18	30	25	1.414212	16	26	26	1.000000
17	28	26	1.000000	19	27	26	1.414212	20	36	30	1.414212	21	37	30	1.000000
22	37	30	1.000000	23	38	30	1.000000	24	38	30	1.000000	25	39	30	1.414212
40	40	31	1.000000	41	41	31	1.000000	42	42	31	1.000000	43	43	32	1.000000
44	44	32	1.000000	-2	0	0	0.0								

TABLE XL (Continued)

MUCO-INOSITOL - Z MATRIX - All SYMMETRY SPECIES

```
 4  4  1 1.000000  5  5  1 1.000000  6  6  3 1.000000  7  7  3 1.000000
 1  1  2 1.000000  2  2  2 1.000000  3  3  2 1.000000  8  8  4 1.000000
 9  9  4 1.000000 18 18  5 1.000000 19 19  5 1.000000 20 20  5 1.000000
21 21  5 1.000000 22 22  5 1.000000 23 23  5 1.000000 12 12  8 1.000000
13 13  8 1.000000 14 14  8 1.000000 15 15  8 1.000000 16 16  8 1.000000
17 17  8 1.000000 26 26  7 1.000000 27 27  7 1.000000 10 10  9 1.000000
11 11  9 1.000000 24 24  6 1.000000 25 25  6 1.000000  1  4 10 1.000000
 2  4 10 1.000000  2  5 10 1.000000  3  5 10 1.000000  1  1 11-1.000000
 1  2 11 1.000000  2  3 11 1.000000  3  3 11-1.000000  4  6 33 1.000000
 5  7 33 1.000000  1  6 33 1.000000  2  6 33 1.000000  2  7 33 1.000000
 3  7 33 1.000000  4  8 33 1.000000  5  9 33 1.000000  4 24 12 1.000000
 5 25 12 1.000000  4 13 14 1.000000  4 14 14 1.000000  5 15 14 1.000000
 5 16 14 1.000000  1 12 16-1.000000  1 13 16 1.000000  2 14 16 1.000000
 2 15 16 1.000000  3 16 16 1.000000  3 17 16 1.000000  1 18 15-1.000000
 1 19 15 1.000000  2 20 15 1.000000  2 21 15 1.000000  3 22 15 1.000000
 3 23 15 1.000000  1 10 17 1.000000  2 10 17 1.000000  2 11 17 1.000000
 3 11 17 1.000000  6 19 33 1.000000  6 20 33 1.000000  7 21 33 1.000000
 7 22 33 1.000000  6 24 33 1.000000  7 25 33 1.000000  4 26 13 1.000000
 5 27 13 1.000000  8 26 33 1.000000  9 27 33 1.000000 19 24 18 1.000000
20 24 18 1.000000 21 25 18 1.000000 22 25 18 1.000000 12 18 19 1.000000
13 19 19 1.000000 14 20 19 1.000000 15 21 19 1.000000 16 22 19 1.000000
17 23 19 1.000000 10 19 19 1.000000 10 20 19 1.000000 11 21 19 1.000000
11 22 19 1.000000 13 24 19 1.000000 14 24 19 1.000000 15 25 19 1.000000
16 25 19 1.000000 18 18 33-1.000000 19 20 33 1.000000 21 22 33 1.000000
23 23 33-1.000000 12 12 20-1.000000 13 14 20 1.000000 15 16 20 1.000000
17 17 20-1.000000 10 13 20 1.000000 10 14 20 1.000000 11 15 20 1.000000
11 16 20 1.000000 10 12 21-1.000000 11 14 21 1.000000 14 15 21 1.000000
16 17 21 1.000000 10 11 21 1.000000 10 15 22 1.000000 11 17 22 1.000000
12 13 22-1.000000 12 19 23-1.000000 13 18 23-1.000000 15 20 23 1.000000
16 23 23 1.000000 17 22 23 1.000000 14 21 24 1.000000 24 26 29 1.000000
25 27 29 1.000000 18 19 27-1.000000 20 21 27 1.000000 22 23 28 1.000000
10 21 25 1.000000 11 23 25 1.000000 10 18 26-1.000000 11 20 26 1.000000
13 26 30 1.000000 14 26 30 1.000000 15 27 30 1.000000 16 27 30 1.000000
28 28 31 1.000000 29 29 31 1.000000 30 30 31 1.000000 31 31 32 1.000000
32 32 32 1.000000 33 33 32 1.000000 34 34 32 1.000000 -2  0  0 0.0
```

APPENDIX IV

COMPUTER PROGRAM INPUT FOR THE X-RAY CRYSTAL STRUCTURES

Contents Page

TABLE XLI

X-RAY DATA INPUT FOR THE COMPUTER PROGRAM CARTSET FOR MYO-INOSITOL, EPI-INOSITOL AND CIS-INOSITOL

MYO-INOSITOL X-RAY CRYSTAL STRUCTURE

CELL 6.64 12.084 19.681 90.0 105.83 90.0

24

C	1	.3948	.4077	.2435	
C	2	.2320	.4768	.2663	
C	3	.0796	.4009	.2902	
C	4	-.0316	.3251	.2297	
C	5	.1297	.2569	.2059	
C	6	.2879	.3301	.1844	
O	7	.5479	.4762	.2267	
O	8	.1204	.5451	.2093	
O	9	-.0656	.4653	.3159	
O	10	-.1713	.2552	.2529	
O	11	.0272	.1895	.1470	
O	12	.4444	.2631	.1673	
H	13	.473	.360	.289	
H	14	.305	.522	.307	
H	15	.168	.346	.338	
H	16	-.115	.374	.187	
H	17	.214	.199	.246	
H	18	.215	.370	.145	
H	19	.508	.508	.189	
H	20	.138	.613	.223	
H	21	-.189	.465	.279	
H	22	-.310	.258	.228	
H	23	.350	.114	.161	
H	24	.370	.223	.113	

1				
2	1			
3	2	1		
4	3	2	1	
5	4	3	2	
6	5	4	3	
7	1	2	6	
8	2	3	1	
9	3	4	2	
10	4	5	3	
11	5	6	4	
12	6	1	5	
13	1	2	6	
14	2	3	1	
15	3	4	2	
16	4	5	3	
17	5	6	4	
18	6	1	5	
19	7	1	13	
20	8	2	14	
21	9	3	15	
22	10	4	16	
23	11	5	17	
24	12	6	18	

EPI-INOSITOL X-RAY CRYSTAL STRUCTURE

CELL 4.841 14.727 11.236 90.0 115.85 90.0

24

C	1	0.1075	0.3706	0.3896
C	2	0.1343	0.4609	0.3280
C	3	-0.1102	0.4636	0.1846
C	4	-0.0753	0.3833	0.1068
C	5	-0.1218	0.2950	0.1670
C	6	0.1139	0.2864	0.3113
O	7	0.3330	0.3641	0.5248
O	8	0.4328	0.4724	0.3335
O	9	-0.0907	0.5476	0.1249
O	10	-0.3023	0.3871	-0.0287
O	11	-0.1123	0.2179	0.0930
O	12	0.4047	0.2723	0.3107
H	13	-0.088	0.370	0.392
H	14	0.092	0.512	0.381
H	15	-0.306	0.457	0.182
H	16	0.138	0.386	0.108
H	17	-0.319	0.302	0.160
H	18	0.067	0.232	0.355
H	19	0.476	0.344	0.526
H	20	0.501	0.521	0.372
H	21	-0.235	0.566	0.095
H	22	-0.241	0.410	-.066
H	23	0.040	0.210	0.103
H	24	0.502	0.232	0.367

1				
2	1			
3	2	1		
4	3	2	1	
5	4	3	2	
6	5	4	3	
7	1	2	6	
8	2	3	1	
9	3	4	2	
10	4	5	3	
11	5	6	4	
12	6	1	5	
13	1	2	6	
14	2	3	1	
15	3	4	2	
16	4	5	3	
17	5	6	4	
18	6	1	5	
19	7	1	13	
20	8	2	14	
21	9	3	15	
22	10	4	16	
23	11	5	17	
24	12	6	18	

CIS-INOSITOL X-RAY CRYSTAL STRUCTURE

CELL 9.900 9.926 17.795 90.0 90.5 90.0

24

C	1	0.2889	0.2246	-0.1695
C	2	0.1358	0.2260	-0.1625
C	3	0.0795	0.0816	-0.1909
C	4	0.1409	-0.0463	-0.1497
C	5	0.2949	-0.0390	-0.1542
C	6	0.3560	0.1013	-0.1277
O	7	0.3491	0.3582	-0.1480
O	8	0.0930	0.2567	-0.0873
O	9	-0.0635	0.0781	-0.1887
O	10	0.0972	-0.0495	-0.0728
O	11	0.3481	-0.1564	-0.1123
O	12	0.3433	0.1196	-0.0482
H	13	0.3134	0.2159	-0.2271
H	14	0.0961	0.3113	-0.1958
H	15	0.0994	0.0714	-0.2485
H	16	0.1068	-0.1439	-0.1738
H	17	0.3208	-0.0536	-0.2116
H	18	0.4597	0.1013	-0.1387
H	19	0.3068	0.3929	-0.1052
H	20	0.0535	0.1759	-0.0664
H	21	-0.0941	0.1051	-0.1417
H	22	0.0215	-0.1091	-0.0677
H	23	0.4400	-0.1395	-0.1030
H	24	0.3999	0.1955	-0.0330

1				
2	1			
3	2	1		
4	3	2	1	
5	4	3	2	
6	5	4	3	
7	1	2	6	
8	2	3	1	
9	3	4	2	
10	4	5	3	
11	5	6	4	
12	6	1	5	
13	1	2	6	
14	2	3	1	
15	3	4	2	
16	4	5	3	
17	5	6	4	
18	6	1	5	
19	7	1	13	
20	8	2	14	
21	9	3	15	
22	10	4	16	
23	11	5	17	
24	12	6	18	

TABLE XLII. X-RAY DATA INPUT FOR THE COMPUTER PROGRAM CARTSET FOR MYO-INOSITOL, EPI-INOSITOL AND CIS-INOSITOL

```
-09
-09   24    0    1
      MYO-INOSITOL      CART COORD CALCULATED FRCM X-RAY STRUCTURE
      C-H BOND LENGTHS 1.10    O-H    0.97
   1
   2   1          1.527013
   3   2    1     1.531718     110.0936
   4   3    2    1 1.523911    109.9164      59.8462
   5   4    3    2 1.522957    109.5651     -58.5201
   6   5    4    3 1.519016    111.6613      56.7938
   7   1    2    6 1.418210    111.1034    -126.5709
   8   2    3    1 1.426620    110.1044    -121.4416
   9   3    4    2 1.434237    111.9263    -122.8971
  10   4    5    3 1.418970    110.7287     120.2541
  11   5    6    4 1.428251    108.6292    -121.1747
  12   6    1    5 1.428078    108.3409     120.7185
  13   1    2    6 1.10        105.6482     117.6878
  14   2    3    1 1.10        107.7005     117.7264
  15   3    4    2 1.10        108.5539     121.4853
  16   4    5    3 1.10        108.6622    -118.7932
  17   5    6    4 1.10        108.6142     125.1846
  18   6    1    5 1.10        110.4505    -118.6180
  19   7    1   13 0.97        114.4221    -170.1214
  20   8    2   14 0.97        107.9786       1.4011
  21   9    3   15 0.97        104.8237     138.3075
  22  10    4   16 0.97        117.0985      -2.77117
  23  11    5   17 0.97          0.0        128.7675
  24  12    6   18 0.97        107.5656      43.2265

-09
-09   24    0    1
      EPI-INOSITOL     CART COORD CALCULATED FROM X-RAY STRUCTURE
      C-H BOND LENGTHS 1.10      O-H   0.97
   1
   2   1          1.530583
   3   2    1     1.528265     108.7113
   4   3    2    1 1.523149    110.9124      57.43434
   5   4    3    2 1.527089    109.4563     -62.16591
   6   5    4    3 1.527582    110.8164      59.75851
   7   1    2    6 1.436115    111.2121    -126.8950
   8   2    3    1 1.429253    110.3024    -122.5033
   9   3    4    2 1.429832    110.9001    -122.1509
  10   4    5    3 1.438645    108.0959     120.5183
  11   5    6    4 1.419873    110.8611    -124.8084
  12   6    1    5 1.425915    112.9192    -119.5317
  13   1    2    6 1.10        107.5168     117.6407
  14   2    3    1 1.10        109.4043     116.6422
  15   3    4    2 1.10        105.3840     118.5719
  16   4    5    3 1.10        111.6712    -120.6633
  17   5    6    4 1.10        111.3677     113.0802
  18   6    1    5 1.1         107.3124     121.0642
  19   7    1   13 0.97        108.4889    -155.0275
  20   8    2   14 0.97        106.9510       5.7094
  21   9    3   15 0.97        108.1336       9.2656
  22  10    4   16 0.97        109.0820      26.8480
  23  11    5   17 0.97        109.7503     174.6841
  24  12    6   18 0.97        109.1895      18.3870
```

TABLE XLII (Cont'd). X-RAY DATA INPUT FOR THE COMPUTER PROGRAM CARTSET FOR MYO-INOSITOL, EPI-INOSITOL AND CIS-INOSITOL

```
-09
-09   24    0    1
      CIS-INOSITOL          CART COORD CALCULATED FROM X-RAY STRUCTURE
      C-H BOND LENGTHS 1.10   O-H   0.97
  1
  2   1          1.521947
  3   2    1     1.617262     107.9339
  4   3    2    1 1.584596     115.8746     -55.7966
  5   4    3    2 1.529117     108.4970      53.7773
  6   5    4    3 1.5883       113.8315     -50.7551
  7   1    2    6 1.502053     111.4128     128.9769
  8   2    3    1 1.439800     112.0466     124.0762
  9   3    4    2 1.4170       110.3456     126.8179
 10   4    5    3 1.439137     111.0856     120.8433
 11   5    6    4 1.477979     114.1516     122.7626
 12   6    1    5 1.432927     109.1527     124.3958
 13   1    2    6 1.10         108.5114    -118.3720
 14   2    3    1 1.10         113.1209    -119.6856
 15   3    4    2 1.10         107.4977    -121.9145
 16   4    5    3 1.10         108.7676    -124.3994
 18   6    1    5 1.10         108.8198    -120.1471
 19   7    1   13 C.97         110.6635    -157.8219
 20   8    2   14 C.97         107.8018    -132.6931
 21   9    3   15 C.97         110.5732     167.5404
 22  10    4   16 C.97         110.2305      24.7793
 23  11    5   17 C.97         106.8309     -81.7796
 24  12    6   18 C.97         108.4973     -48.9408
```

TABLE XLIII. INPUT FOR THE COMPUTER PROGRAM GMAT FOR THE X-RAY CRYSTAL STRUCTURES FOR MYO-INOSITOL, EPI-INOSITOL AND CIS-INOSITOL

```
-09
-09      1  24  78   1   0   0   0
     MYO-INOSITOL - G MATRIX CALCULATED USING X-RAY CRYSTAL STRUCTURE
     C-H 1.10 AND O-H 0.97
  1   2     1.527013   1   3     2.053241   2   3     1.438485   1   4     1.555680
  2   4     2.173265   3   4    -1.238884   1   5     0.032884   2   5     2.165112
  3   5    -1.259468   1   6    -0.520967   2   6     0.751521   3   6    -1.210274
  1   7    -0.510628   2   7    -1.318583   3   7     0.109162   1   8     2.014829
  2   8    -0.700609   3   8    -1.142990   1   9     3.484820   2   9     1.443966
  3   9     0.087077   1  10     2.050552   2  10     3.502964   3  10    -1.217104
  1  11    -0.437172   2  11     2.798104   3  11    -2.450377   1  12    -1.946375
  2  12     0.793601   3  12    -1.133788   1  13    -0.296702   2  13     0.537185
  3  13     0.912907   1  14     1.869982   2  14    -0.481586   3  14     0.927602
  1  15     1.708817   2  15     1.982781   3  15     0.891691   1  16     1.922604
  2  16     1.649334   3  16    -2.133792   1  17    -0.410051   2  17     2.744609
  3  17    -0.436065   1  18    -0.206819   2  18     0.250952   3  18    -2.138034
  1  19    -0.441777   2  19    -1.843866   3  19    -0.703388   1  20     2.562530
  2  20    -1.437895   3  20    -0.831007   1  21     3.787786   2  21     1.620353
  3  21    -0.817356   1  22     2.586978   2  22     3.787232   3  22    -1.973633
  1  23    -0.823621   2  23     2.131690   3  23    -3.039826   1  24    -2.279435
  2  24     1.040420   3  24    -2.010742  -1   0     0.0
  1   1   1   2   0   0   0   0   2   1   2   3   0   0   0   0   3   1   3   4   0   0   0   0
  4   1   4   5   0   0   0   0   5   1   5   6   0   0   0   0   6   1   6   1   0   0   0   0
  7   1   1   7   0   0   0   0   8   1   2   8   0   0   0   0   9   1   3   9   0   0   0   0
 10   1   4  10   0   0   0   0  11   1   5  11   0   0   0   0  12   1   6  12   0   0   0   0
 13   1   1  13   0   0   0   0  14   1   2  14   0   0   0   0  15   1   3  15   0   0   0   0
 16   1   4  16   0   0   0   0  17   1   5  17   0   0   0   0  18   1   6  18   0   0   0   0
 19   1   7  19   0   0   0   0  20   1   8  20   0   0   0   0  21   1   9  21   0   0   0   0
 22   1  10  22   0   0   0   0  23   1  11  23   0   0   0   0  24   1  12  24   0   0   0   0
 25   2   1   2   3   0   0   0  26   2   2   3   4   0   0   0  27   2   3   4   5   0   0   0
 28   2   4   5   6   0   0   0  29   2   5   6   1   0   0   0  30   2   6   1   2   0   0   0
 31   2   7   1   6   0   0   0  32   2   7   1   2   0   0   0  33   2   8   2   1   0   0   0
 34   2   8   2   3   0   0   0  35   2   9   3   2   0   0   0  36   2   9   3   4   0   0   0
 37   2  10   4   3   0   0   0  38   2  10   4   5   0   0   0  39   2  11   5   4   0   0   0
 40   2  11   5   6   0   0   0  41   2  12   6   5   0   0   0  42   2  12   6   1   0   0   0
 43   2  13   1   6   0   0   0  44   2  13   1   2   0   0   0  45   2  14   2   1   0   0   0
 46   2  14   2   3   0   0   0  47   2  15   3   2   0   0   0  48   2  15   3   4   0   0   0
 49   2  16   4   3   0   0   0  50   2  16   4   5   0   0   0  51   2  17   5   4   0   0   0
 52   2  17   5   6   0   0   0  53   2  18   6   5   0   0   0  54   2  18   6   1   0   0   0
 55   2  13   1   7   0   0   0  56   2  14   2   8   0   0   0  57   2  15   3   9   0   0   0
 58   2  16   4  10   0   0   0  59   2  17   5  11   0   0   0  60   2  18   6  12   0   0   0
 61   2   1   7  19   0   0   0  62   2   2   8  20   0   0   0  63   2   3   9  21   0   0   0
 64   2   4  10  22   0   0   0  65   2   5  11  23   0   0   0  66   2   6  12  24   0   0   0
 67   4   6   1   2  14   3   0   0   4  13   1   2   8   3   0   0   4   7   1   2   3   3   0
 68   4   1   2   3   9   3   0   0   4  14   2   3   4   3   0   0   4   8   2   3  15   3   0
 69   4   2   3   4  10   3   0   0   4  15   3   4  16   3   0   0   4   9   3   4   5   3   0
 70   4   3   4   5  11   3   0   0   4  10   4   5   6   3   0   0   4  16   4   5  17   3   0
 71   4   4   5   6  12   3   0   0   4  11   5   6   1   3   0   0   4  17   5   6  18   3   0
 72   4   5   6   1   7   3   0   0   4  12   6   1   2   3   0   0   4  18   6   1  13   3   0
 73   4  19   7   1  13   3   0   0   4  19   7   1   6   3   0   0   4  19   7   1   2   3   0
 74   4  20   8   2  14   3   0   0   4  20   8   2   1   3   0   0   4  20   8   2   3   3   0
 75   4  21   9   3  15   3   0   0   4  21   9   3   2   3   0   0   4  21   9   3   4   3   0
 76   4  22  10   4  16   3   0   0   4  22  10   4   3   3   0   0   4  22  10   4   5   3   0
 77   4  23  11   5  17   3   0   0   4  23  11   5   4   3   0   0   4  23  11   5   6   3   0
 78   4  24  12   6  18   3   0   0   4  24  12   6   5   3   0   0   4  24  12   6   1   3   0
-02
-06  0
  12.00000      12.00000      12.00000      12.00000      12.00000      12.00000
  15.994915     15.994915     15.994915     15.994915     15.994915     15.994915
   1.007825      1.007825      1.007825      1.007825      1.007825      1.007825
   1.007825      1.007825      1.007825      1.007825      1.007825      1.007825
```

TABLE XLIII

```
-09
-09      1  24  78    1    0    0    0
      EPI-INOSITOL - G MATRIX CALCULATED USING X-RAY CRYSTAL STRUCTURE
      C-H 1.10 AND O-H 0.97
   1   2     1.530582   1   3     2.020848   2   3     1.447492   1   4     1.469881
   2   4     2.208114   3   4    -1.199112   1   5    -0.054307   2   5     2.252984
   3   5    -1.116421   1   6    -0.639448   2   6     0.841925   3   6    -1.110995
   1   7    -0.519615   2   7    -1.338799   3   7    -0.006082   1   8     2.053717
   2   8    -0.700773   3   8    -1.130491   1   9     3.450451   2   9     1.472108
   3   9     0.006656   1  10     1.957008   2  10     3.561753   3  10    -1.206944
   1  11    -0.617477   2  11     3.029871   3  11    -2.162997   1  12    -0.422618
   2  12     0.300887   3  12    -2.412338   1  13    -0.331083   2  13     0.446707
   3  13     0.949124   1  14     1.853994   2  14    -0.495388   3  14     0.927358
   1  15     1.627217   2  15     1.971105   3  15     0.883676   1  16     1.812338
   2  16     1.715828   3  16    -2.121271   1  17    -0.220573   2  17     2.759513
   3  17    -0.154244   1  18    -1.722630   2  18     0.866311   3  18    -0.920938
   1  19    -0.608317   2  19    -1.630154   3  19    -0.927029   1  20     2.642710
   2  20    -1.391006   3  20    -0.787615   1  21     3.738778   2  21     2.071956
   3  21     0.712310   1  22     2.767642   2  22     3.603986   3  22    -1.737967
   1  23    -0.547896   2  23     2.548664   3  23    -3.002341   1  24    -1.218552
   2  24    -0.175279   3  24    -2.696343  -1   0     0.0
   1   1   1   2   0   0   0   0   2   1   2   3   0   0   0   0   3   1   3   4   0   0   0   0
   4   1   4   5   0   0   0   0   5   1   5   6   0   0   0   0   6   1   6   1   0   0   0   0
   7   1   1   7   0   0   0   0   8   1   2   8   0   0   0   0   9   1   3   9   0   0   0   0
  10   1   4  10   0   0   0   0  11   1   5  11   0   0   0   0  12   1   6  12   0   0   0   0
  13   1   1  13   0   0   0   0  14   1   2  14   0   0   0   0  15   1   3  15   0   0   0   0
  16   1   4  16   0   0   0   0  17   1   5  17   0   0   0   0  18   1   6  18   0   0   0   0
  19   1   7  19   0   0   0   0  20   1   8  20   0   0   0   0  21   1   9  21   0   0   0   0
  22   1  10  22   0   0   0   0  23   1  11  23   0   0   0   0  24   1  12  24   0   0   0   0
  25   2   1   2   3   0   0   0  26   2   2   3   4   0   0   0  27   2   3   4   5   0   0   0
  28   2   4   5   6   0   0   0  29   2   5   6   1   0   0   0  30   2   6   1   2   0   0   0
  31   2   7   1   6   0   0   0  32   2   7   1   2   0   0   0  33   2   8   2   1   0   0   0
  34   2   8   2   3   0   0   0  35   2   9   3   2   0   0   0  36   2   9   3   4   0   0   0
  37   2  10   4   3   0   0   0  38   2  10   4   5   0   0   0  39   2  11   5   4   0   0   0
  40   2  11   5   6   0   0   0  41   2  12   6   5   0   0   0  42   2  12   6   1   0   0   0
  43   2  13   1   6   0   0   0  44   2  13   1   2   0   0   0  45   2  14   2   1   0   0   0
  46   2  14   2   3   0   0   0  47   2  15   3   2   0   0   0  48   2  15   3   4   0   0   0
  49   2  16   4   3   0   0   0  50   2  16   4   5   0   0   0  51   2  17   5   4   0   0   0
  52   2  17   5   6   0   0   0  53   2  18   6   5   0   0   0  54   2  18   6   1   0   0   0
  55   2  13   1   7   0   0   0  56   2  14   2   8   0   0   0  57   2  15   3   9   0   0   0
  58   2  16   4  10   0   0   0  59   2  17   5  11   0   0   0  60   2  18   6  12   0   0   0
  61   2   1   7  19   0   0   0  62   2   2   8  20   0   0   0  63   2   3   9  21   0   0   0
  64   2   4  10  22   0   0   0  65   2   5  11  23   0   0   0  66   2   6  12  24   0   0   0
  67   4   6   1   2  14   3   0   0   4   7   1   2   3   3   0   0   4  13   1   2   8   3   0
  68   4   1   2   3   9   3   0   0   4   8   2   3  15   3   0   0   4  14   2   3   4   3   0
  69   4   2   3   4  10   3   0   0   4   9   3   4   5   3   0   0   4  15   3   4  16   3   0
  70   4   3   4   5  11   3   0   0   4  10   4   5   6   3   0   0   4  16   4   5  17   3   0
  71   4   4   5   6  18   3   0   0   4  11   5   6   1   3   0   0   4  17   5   6  12   3   0
  72   4   5   6   1   7   3   0   0   4  12   6   1  13   3   0   0   4  18   6   1   2   3   0
  73   4  19   7   1  13   3   0   0   4  19   7   1   6   3   0   0   4  19   7   1   2   3   0
  74   4  20   8   2  14   3   0   0   4  20   8   2   1   3   0   0   4  20   8   2   3   3   0
  75   4  21   9   3  15   3   0   0   4  21   9   3   2   3   0   0   4  21   9   3   4   3   0
  76   4  22  10   4  16   3   0   0   4  22  10   4   3   3   0   0   4  22  10   4   5   3   0
  77   4  23  11   5  17   3   0   0   4  23  11   5   4   3   0   0   4  23  11   5   6   3   0
  78   4  24  12   6  18   3   0   0   4  24  12   6   5   3   0   0   4  24  12   6   1   3   0
-02
-06  0
 12.00000     12.00000     12.00000     12.00000     12.00000     12.00000
 15.994915    15.994915    15.994915    15.994915    15.994915    15.994915
  1.007825     1.007825     1.007825     1.007825     1.007825     1.007825
  1.007825     1.007825     1.007825     1.007825     1.007825     1.007825
```

TABLE XLIII

```
-09
-09      1  24  78    0    0    0    0
      CIS-INOSITOL - G MATRIX CALCULATED USING X-RAY CRYSTAL STRUCTURE
      C-H 1.10 AND O-H 0.97
  1   2     1.521947   1   3     2.019932   2   3     1.538683   1   4     1.470346
  2   4     2.443387   3   4     1.179155   1   5    -0.055830   2   5     2.349455
  3   5     1.191817   1   6    -0.607239   2   6     0.860001   3   6     1.179827
  1   7    -0.548375   2   7    -1.396598   3   7    -0.070449   1   8     2.066929
  2   8    -0.744422   3   8     1.105375   1   9     3.434130   2   9     1.607969
  3   9    -0.056089   1  10     2.026500   2  10     2.004401   3  10     2.431793
  1  11    -0.520073   2  11     3.156928   3  11     2.339374   1  12    -0.355754
  2  12     0.195107   3  12     2.423993   1  13    -0.349242   2  13     0.449700
  3  13    -0.941169   1  14     1.865609   2  14    -0.565221   3  14    -0.878873
  1  15     1.717024   2  15     2.009508   3  15    -0.946873   1  16     1.759130
  2  16     3.501892   3  16     1.100616   1  17    -0.415588   2  17     2.854274
  3  17     0.283118   1  18    -1.700858   2  18     0.895214   3  18     1.066872
  1  19    -0.042583   2  19    -1.992320   3  19     0.504172   1  20     2.485505
  2  20    -0.112610   3  20     1.710773   1  21     3.830253   2  21     1.051064
  3  21     0.632276   1  22     2.786152   2  22     2.557015   3  22     2.673543
  1  23    -1.441149   2  23     2.903148   3  23     2.507052   1  24    -0.882116
  2  24    -0.619257   3  24     2.449614  -1   0     0.0
  1   1   1   2   0   0   0   0   2   1   2   3   0   0   0   0   3   1   3   4   0   0   0   0
  4   1   4   5   0   0   0   0   5   1   5   6   0   0   0   0   6   1   6   1   0   0   0   0
  7   1   1   7   0   0   0   0   8   1   2   8   0   0   0   0   9   1   3   9   0   0   0   0
 10   1   4  10   0   0   0   0  11   1   5  11   0   0   0   0  12   1   6  12   0   0   0   0
 13   1   1  13   0   0   0   0  14   1   2  14   0   0   0   0  15   1   3  15   0   0   0   0
 16   1   4  16   0   0   0   0  17   1   5  17   0   0   0   0  18   1   6  18   0   0   0   0
 19   1   7  19   0   0   0   0  20   1   8  20   0   0   0   0  21   1   9  21   0   0   0   0
 22   1  10  22   0   0   0   0  23   1  11  23   0   0   0   0  24   1  12  24   0   0   0   0
 25   2   1   2   3   0   0   0  26   2   2   3   4   0   0   0  27   2   3   4   5   0   0   0
 28   2   4   5   6   0   0   0  29   2   5   6   1   0   0   0  30   2   6   1   2   0   0   0
 31   2   7   1   6   0   0   0  32   2   7   1   2   0   0   0  33   2   8   2   1   0   0   0
 34   2   8   2   3   0   0   0  35   2   9   3   2   0   0   0  36   2   9   3   4   0   0   0
 37   2  10   4   3   0   0   0  38   2  10   4   5   0   0   0  39   2  11   5   4   0   0   0
 40   2  11   5   6   0   0   0  41   2  12   6   5   0   0   0  42   2  12   6   1   0   0   0
 43   2  13   1   6   0   0   0  44   2  13   1   2   0   0   0  45   2  14   2   1   0   0   0
 46   2  14   2   3   0   0   0  47   2  15   3   2   0   0   0  48   2  15   3   4   0   0   0
 49   2  16   4   3   0   0   0  50   2  16   4   5   0   0   0  51   2  17   5   4   0   0   0
 52   2  17   5   6   0   0   0  53   2  18   6   5   0   0   0  54   2  18   6   1   0   0   0
 55   2  13   1   7   0   0   0  56   2  14   2   8   0   0   0  57   2  15   3   9   0   0   0
 58   2  16   4  10   0   0   0  59   2  17   5  11   0   0   0  60   2  18   6  12   0   0   0
 61   2   1   7  19   0   0   0  62   2   2   8  20   0   0   0  63   2   3   9  21   0   0   0
 64   2   4  10  22   0   0   0  65   2   5  11  23   0   0   0  66   2   6  12  24   0   0   0
 67   4   6   1   2  14   3   0   0   4  13   1   2   8   3   0   0   4   7   1   2   3   3   0
 68   4   1   2   3   9   3   0   0   4  14   2   3   4   3   0   0   4   8   2   3  15   3   0
 69   4   2   3   4  16   3   0   0   4  15   3   4  10   3   0   0   4   9   3   4   5   3   0
 70   4   3   4   5  11   3   0   0   4  10   4   5  17   3   0   0   4  16   4   5   6   3   0
 71   4   4   5   6  18   3   0   0   4  11   5   6   1   3   0   0   4  17   5   6  12   3   0
 72   4   5   6   1   7   3   0   0   4  12   6   1  13   3   0   0   4  18   6   1   2   3   0
 73   4  19   7   1  13   3   0   0   4  19   7   1   6   3   0   0   4  19   7   1   2   3   0
 74   4  20   8   2  14   3   0   0   4  20   8   2   1   3   0   0   4  20   8   2   3   3   0
 75   4  21   9   3  15   3   0   0   4  21   9   3   2   3   0   0   4  21   9   3   4   3   0
 76   4  22  10   4  16   3   0   0   4  22  10   4   3   3   0   0   4  22  10   4   5   3   0
 77   4  23  11   5  17   3   0   0   4  23  11   5   4   3   0   0   4  23  11   5   6   3   0
 78   4  24  12   6  18   3   0   0   4  24  12   6   5   3   0   0   4  24  12   6   1   3   0
-02
-06  0
  12.00000      12.00000      12.00000      12.00000      12.00000      12.00000
  15.994915     15.994915     15.994915     15.994915     15.994915     15.994915
   1.007825      1.007825      1.007825      1.007825      1.007825      1.007825
   1.007825      1.007825      1.007825      1.007825      1.007825      1.007825
```

APPENDIX V

SPECTRAL DATA, CALCULATED FREQUENCIES, CALCULATED SYMMETRY SPECIES AND CALCULATED POTENTIAL ENERGY DISTRIBUTIONS FOR THE INOSITOLS

Contents Page

In the following tables are tabulated the observed Raman and infrared frequencies, the frequencies assigned for the refinements, the corresponding calculated frequencies, the calculated symmetry species and the potential energy distributions in terms of both the internal coordinates and the force constants. The potential energy distributions may be interpreted by associating the description codes in the tables with the internal coordinates, key on page 316, or the force constants, key on page 317.

The numbers in parentheses in the potential energy distributions are percentages. Contributions of less than 2% do not appear in the tables.

Key for the Internal Coordinate Description Codes Used in the Potential Energy Distributions

	Internal Coordinate	Description Code		Internal Coordinate	Description Code
1.	C1-C2	C1C2	40.	O11-C5-C6	1156
2.	C2-C3	C2C3	41.	O12-C6-C5	1265
3.	C3-C4	C3C4	42.	O12-C6-C1	1261
4.	C4-C5	C4C5	43.	H13-C1-C6	1316
5.	C5-C6	C5C6	44.	H13-C1-C2	1312
6.	C6-C1	C6C1	45.	H14-C2-C1	1421
7.	C1-O7	C1O7	46.	H14-C2-C3	1423
8.	C2-O8	C2O8	47.	H15-C3-C2	1532
9.	C3-O9	C3O9	48.	H15-C3-C4	1534
10.	C4-O10	C4O0	49.	H16-C4-C3	1643
11.	C5-O11	C5O1	50.	H16-C4-C5	1645
12.	C6-O12	C6O2	51.	H17-C5-C4	1754
13.	C1-H13	C1H3	52.	H17-C5-C6	1756
14.	C2-H14	C2H4	53.	H18-C6-C5	1865
15.	C3-H15	C3H5	54.	H18-C6-C1	1861
16.	C4-H16	C4H6	55.	H13-C1-O7	HC1O
17.	C5-H17	C5H7	56.	H14-C2-O8	HC2O
18.	C6-H18	C6H8	57.	H15-C3-O9	HC3O
19.	O7-H19	O7H9	58.	H16-C4-O10	HC4O
20.	O8-H20	O8H0	59.	H17-C5-O11	HC5O
21.	O9-H21	O9H1	60.	H18-C6-O12	HC6O
22.	O10-H22	O1OH	61.	C1-O7-H19	C1OH
23.	O11-H23	O11H	62.	C2-O8-H20	C2OH
24.	O12-H24	O12H	63.	C3-O9-H21	C3OH
25.	C1-C2-C3	CC2C	64.	C4-O10-H22	C4OH
26.	C2-C3-C4	CC3C	65.	C5-O11-H23	C5OH
27.	C3-C4-C5	CC4C	66.	C6-O12-H24	C6OH
28.	C4-C5-C6	CC5C	67.	X-C1-C2-Y	TC12
29.	C5-C6-C1	CC6C	68.	X-C2-C3-Y	TC23
30.	C6-C1-C2	CC1C	69.	X-C3-C4-Y	TC34
31.	O7-C1-C6	O716	70.	X-C4-C5-Y	TC45
32.	O7-C1-C2	O712	71.	X-C5-C6-Y	TC56
33.	O8-C2-C1	O821	72.	X-C6-C1-Y	TC61
34.	O8-C2-C3	O823	73.	X-O7-C1-Y	TC1O
35.	O9-C2-C3	O923	74.	X-O8-C2-Y	TC2O
36.	O9-C3-C4	O934	75.	X-O9-C3-Y	TC3O
37.	O10-C4-C3	1043	76.	X-O10-C4-Y	TC4O
38.	O10-C4-C5	1045	77.	X-O11-C5-Y	TC5O
39.	O11-C5-C4	1154	78.	X-O12-C6-Y	TC6O

Key for the Force Constant Description Codes Used in the Potential Energy Distributions

FORCE CONSTANT NUMBER	GROUP	COORDINATES INVOLVED	COMMON ATOMS	DESCRIPTION CODE
		Stretching Constants		
1	C-OH	C-O	--	CO
2	C-C	C-C	--	CC
3	H-C-OH	C-H	--	CH
4	O-H	O-H	--	OH
		Bending Constants		
5	C-C(H)-OH	HCC	--	HCC
6	H-C-OH	HCO	--	HCO
7	C-O-H	COH	--	COH
8	C-C-OH	CCO	--	CCO
9	C-C-C	CCC	--	CCC
		Stretch-Stretch Interaction Constants		
10	C-C-OH	C-C,C-O	C	CCCO
11	C-C-C	C-C,C-C	C	CCCC
		Stretch-Bend Interaction Constants		
12	H-C-OH	C-O,HCO	CO	SB12
13	C-O-H	C-O,COH	CO	SB13
14	C-C-OH	C-O,CCO	CO	SB14
15	C-C(H)-OH	C-C,HCC	CC	SB15
16	C-C-OH	C-C,CCO	CC	SB16
17	C-C-C	C-C,CCC	CC	SB17
		Bend-Bend Interaction Constants		
18	C-C(H)-OH	HCO,HCC	CH	BB18
19	C-C(H)-OH	HCC,CCO	CC	BB19
	C-C(H)-C	HCC,CCC	CC	
	C-C(H)-OH	HCO,CCO	CO	
20	C-C(OH)-C	CCO,CCO	CO	BB20
	C-C(OH)-C	CCO,CCC	CC	
21	C-C-C-OH	CCC,CCO	(C)C-C(O) gauche	BB21
	HO-C-C-OH	CCO,CCO	(O)C-C(O) gauche	
	C-C-C-C	CCC,CCC	(C)C-C(C) gauche	
22	C-C-C-OH	CCC,CCO	(C)C-C(O) trans	BB22
	HO-C-C-OH	CCO,CCO	(O)C-C(O) trans	
23	H-C-C-OH	CCO,HCC	(H)C-C(O) gauche	BB23
24	H-C-C-OH	CCO,HCC	(H)C-C(O) trans	BB24
25	H-C-C-C	CCC,HCC	(C)C-C(H) gauche	BB25
26	H-C-C-C	CCC,HCC	(C)C-C(H) trans	BB26
27	H-C-C-H	HCC,HCC	$(H_a)C-C(H_b)$ gauche	BB27
28	H-C-C-H	HCC,HCC	$(H_a)C-C(H_b)$ trans	BB28
29	H-C-OH	COH,HCO	(H)O-C(H) gauche	BB29
	H-C-OH	COH,HCO	(H)O-C(H) trans	
30	C-C-OH	CCO,COH	(C)C-O(H) gauche	BB30
	C-C-OH	CCO,COH	(C)C-O(H) trans	
		TORSION CONSTANTS		
31	C-C	C-C	--	TOCC
32	C-OH	C-O	--	TOCO

TABLE XLIV. SCYLLO-INOSITOL

EXPERIMENTAL FREQUENCY (CM-1) RAMAN	INFRARED	ASSIGNED FREQUENCY (CM-1)	CALCULATED FREQUENCY (CM-1)	CALCULATED SYMMETRY SPECIE	SPECTRAL INTERPRETATION --- POTENTIAL ENERGY DISTRIBUTIONS INTERNAL COORDINATES	FORCE CONSTANTS
	3430 (VS)		3357.		07H9(31) 012H(22) 09H1(20) 08H0(13) 011H(8) 010H(6)	DIAGONAL- OH (100)
	3275 (VS)		3357.		09H1(54) 012H(20) 07H9(14) 010H(7) 08H0(3)	DIAGONAL- OH (100)
			3357.		011H(39) 07H9(22) 08H0(15) 010H(15) 012H(8)	DIAGONAL- OH (100)
			3357.		012H(40) 010H(19) 011H(14) 09H1(13) 07H9(10) 08H0(4)	DIAGONAL- OH (100)
			3357.		08H0(55) 07H9(17) 010H(13) 011H(12) 09H1(3)	DIAGONAL- OH (100)
			3357.		010H(40) 011H(26) 08H0(10) 09H1(10) 012H(9) 07H9(5)	DIAGONAL- OH (100)
2942 (M)			2952.	A1G	C2H4(16) C3H5(16) C4H6(16) C1H3(16) C5H7(16) C6H8(16)	DIAGONAL- CH (98)
	2940 (M)		2946.	EU	C6H8(25) C3H5(25) C1H3(24) C4H6(24)	DIAGONAL- CH (98)
	2930 (M)		2946.	EU	C2H4(33) C5H7(33) C4H6(9) C1H3(8) C6H8(8) C3H5(8)	DIAGONAL- CH (98)
2929 (M)			2935.	EG	C4H6(31) C1H3(31) C3H5(15) C6H8(15) C5H7(3) C2H4(3)	DIAGONAL- CH (99)
2890 (M)			2935.	EG	C2H4(30) C5H7(30) C3H5(18) C6H8(18) C1H3(2) C4H6(2)	DIAGONAL- CH (99)
	2885 (M)		2931.	A2U	C6H8(17) C5H7(17) C1H3(17) C4H6(17) C3H5(17) C2H4(17)	DIAGONAL- CH (100)
	1454 (M)	1454.	1441.	EU	C2OH(14) C5OH(14) 1312(6) 1645(6) C3OH(5) C6OH(5) 1532(5) 1865(5) 1316(5) 1643(5) 1534(3) 1861(3) C4OH(2) C1OH(2)	DIAGONAL- COH (42) HCC (40) CCO (4) HCO (2) CCC (1) OFF-DIAG- BB23(6) BB25(2) SB13(2) SB15(1) BB29(1) BB19(1) SB14(-1) BB30(-4)
			1441.	EU	C1OH(12) C4OH(12) C3OH(8) C6OH(8) 1421(7) 1754(7) 1423(6) 1756(6) 1861(4) 1534(4) 1643(2) 1316(2)	DIAGONAL- COH (42) HCC (40) CCO (4) HCO (2) CCC (1) OFF-DIAG- BB23(6) BB25(2) SB13(2) SB15(1) BB29(1) BB19(1) SB14(-1) BB30(-4)
1442 (W)		1442.	1432.	EG	C4OH(15) C1OH(15) C6OH(8) C3OH(8) 1754(5) 1421(5) HC4O(4) HC1O(4) 1756(4) 1423(4) 1534(4) 1861(4) HC3O(2) HC6O(2)	DIAGONAL- COH (50) HCC (32) HCO (14) OFF-DIAG- BB29(3) BB23(2) BB25(1) SB13(-1) BB30(-2) BB18(-2)
1416 (W)		1416.	1432.	EG	C2OH(15) C5OH(15) C3OH(8) C6OH(8) 1312(5) 1645(5) HC2O(4) HC5O(4) 1643(4) 1316(4) 1532(4) 1865(4) HC3O(2) HC6O(2) 1534(2) 1861(2)	DIAGONAL- COH (50) HCC (32) HCO (14) OFF-DIAG- BB29(3) BB23(2) BB25(1) SB13(-1) BB30(-2) BB18(-2)
	1416 (M)	1416.	1413.	A2U	C1OH(12) C3OH(12) C5OH(12) C6OH(12) C2OH(12) C4OH(12) HC1O(4) HC2O(4) HC3O(4) HC4O(4) HC5O(4) HC6O(4)	DIAGONAL- COH (71) HCO (27) HCC (7) CO (2) CCC (1) OFF-DIAG- BB29(6) BB25(1) SB12(-3) SB13(-5) BB18(-6)
1398 (W)		1398.	1402.	A1G	C1OH(13) C2OH(13) C3OH(13) C4OH(13) C6OH(13) C5OH(13)	DIAGONAL- COH (79) HCC (6) CCO (5) CCC (3) CC (2) CO (1) OFF-DIAG- SB13(4) BB23(3) BB19(2) SB15(2) BB25(2) SB16(-2) SB14(-2) SB17(-2) BB30(-6)
1367 (W)		1367.	1371.	A1G	HC1O(10) HC2O(10) HC3O(10) HC4O(10) HC5O(10) HC6O(10) 1312(3) 1421(3) 1423(3) 1532(3) 1756(3) 1865(3) 1643(3) 1645(3) 1754(3) 1316(3) 1534(3) 1861(3) C1O7(2) C2O8(2) C3O9(2) C4OO(2) C5O1(2) C6O2(2)	DIAGONAL- HCO (62) HCC (38) CO (15) COH (8) CC (2) TOCC (2) CCC (1) OFF-DIAG- BB28(5) BB29(3) BB23(3) BB25(3) SB17(1) BB19(1) CCCO(-1) SB14(-3) SB13(-4) SB15(-4) SB12(-10) BB18(-23)
			1358.	A1U	1423(8) 1532(8) 1756(8) 1865(8) 1421(8) 1534(8) 1754(8) 1861(8) 1316(8) 1312(8) 1643(8) 1645(8) C2C3(2) C5C6(2) C3C4(2) C4C5(2) C1C2(2) C6C1(2)	DIAGONAL- HCC (97) CC (13) OFF-DIAG- BB28(13) SB16(-1) BB23(-2) SB15(-19)
	1383 (S)	1383.	1357.	EU	C2OH(10) C5OH(10) HC2O(9) HC5O(9) 1312(7) 1645(7) C4OH(6) C1OH(6) HC4O(6) HC1O(6) 1532(6) 1865(6) 1421(-5) 1754(-5) 1534(-3) 1861(3) C2O8(2) C5O1(2)	DIAGONAL- HCC (43) COH (14) HCO (30) CO (6) CC (2) CCO (1) OFF-DIAG- BB29(4) BB28(4) BB23(2) BB30(1) BB19(-1) SB14(-1) SB12(-4) SB15(-5) SB13(-6) BB18(-10)
	1369 (S)	1369.	1357.	EU	C3OH(11) C6OH(11) HC3O(10) HC6O(10) 1316(7) 1643(7) 1423(6) 1756(6) C4OH(5) C1OH(5) HC1O(4) HC4O(4) 1534(4) 1861(4) 1421(2) 1754(2) C3O9(2) C6O2(2)	DIAGONAL- HCC (43) COH (34) HCO (30) CO (6) CC (2) CCO (1) OFF-DIAG- BB29(4) BB28(4) BB23(2) BB30(1) BB19(-1) SB14(-1) SB12(-4) SB15(-5) SB13(-6) BB18(-10)
1350 (LT,M)		1350.	1348.	EG	1861(11) 1534(11) 1865(10) 1532(10) C5OH(7) C2OH(7) 1316(7) 1643(7) C4OH(6) C1OH(6) 1756(4) 1423(4) HC5O(3) HC2O(3) HC4O(2) HC1O(2)	DIAGONAL- HCC (66) COH (26) HCO (10) CC (5) CO (2) CCO (1) OFF-DIAG- BB28(7) BB29(2) BB30(1) BB25(-1) BB19(-1) SB12(-2) SB13(-3) BB18(-3) SB15(-10)
1340 (LT,W)		1340.	1348.	EG	1421(11) 1754(11) 1645(10) 1312(10) C3OH(9) C6OH(9) 1423(7) 1756(7) 1643(4) 1316(4) HC3O(3) HC6O(3) C4OH(3) C1OH(3) C1C2(2) C4C5(2)	DIAGONAL- HCC (66) COH (26) HCO (10) CC (5) CO (2) CCO (1) OFF-DIAG- BB28(7) BB29(2) BB30(1) BB25(-1) BB19(-1) SB12(-2) SB11(-3) BB18(-3) SB15(-10)
	1341 (M)					
	1331 (M)					
	1305 (W)					

Conventional symbolism indicating relative intensity: s = strong, m = medium, w = weak, sh = shoulder, b = broad, v = very, lt = low temperature band

TABLE XLIV (Continued)

EXPERIMENTAL FREQUENCY (CM-1) RAMAN	INFRARED	ASSIGNED FREQUENCY (CM-1)	CALCULATED FREQUENCY (CM-1)	CALCULATED SYMMETRY SPECIE	SPECTRAL INTERPRETATION --- POTENTIAL ENERGY DISTRIBUTIONS INTERNAL COORDINATES	FORCE CONSTANTS
	1282 (M)					
			1276.	A2G	1312(8) 1532(8) 1421(8) 1423(8) 1316(8) 1534(8) 1643(8) 1645(8) 1754(8) 1756(8) 1865(8) 1861(8)	DIAGONAL- HCC (95) CCO (8) OFF-DIAG- BB23(14) BB19(-5) BB28(-12)
			1252.	EU	HC10(16) HC40(16) HC20(12) HC50(12) C10H(7) C40H(7) 1423(6) 1756(6) 1643(5) 1316(5) C20H(5) C50H(5) 1532(3) 1865(3) 1534(2) 1861(2)	DIAGONAL- HCO (57) HCC (36) COH (23) TOCC(2) CCO (1) OFF-DIAG- BB23(4) BB28(-4) BB29(-5) BB18(-16)
			1252.	EU	HC30(19) HC60(19) C30H(8) C60H(8) HC50(7) HC20(7) 1754(6) 1421(6) 1645(5) 1312(5) 1534(4) 1861(4) HC10(3) HC40(3) C50H(3) C20H(3) 1865(3) 1532(3)	DIAGONAL- HCO (57) HCC (36) COH (23) TOCC(2) CCO (1) OFF-DIAG- BB23(4) BB28(-4) BB29(-5) BB18(-16)
	1240 (M)					
	1220 (M)	1220.	1226.	A2U	HC30(11) HC40(11) HC20(11) HC50(11) HC10(11) HC60(11) C30H(5) C40H(5) C20H(5) C50H(5) C10H(5) C60H(5) 1643(2) 1645(2) 1754(2) 1756(2) 1421(2) 1423(2) 1532(2) 1534(2) 1316(2) 1312(2) 1865(2) 1861(2) C107(2) C208(2) C309(2) C400(2) C501(2) C602(2)	DIAGONAL- HCO (68) COH (29) HCC (23) CO (9) CCC (9) CCO (4) OFF-DIAG- SB13(6) BB25(5) BB28(-3) BB30(-3) BB23(-5) SB14(-5) BB19(-5) BB29(-6) SB12(-8) BB18(-19)
1253 (VW)		1253.	1224.	EG	HC10(19) HC40(19) HC20(18) HC50(18) C10H(6) C40H(6) C20H(6) C50H(6) 1312(4) 1645(4) 1421(4) 1754(4) 1316(3) 1643(3) 1423(3) 1756(3)	DIAGONAL- HCO (75) HCC (26) COH (25) OFF-DIAG- SB15(1) BB28(-2) BB24(-5) BB18(-21)
			1224.	EG	HC60(25) HC30(25) C60H(8) C30H(8) HC50(7) HC20(6) HC10(6) HC40(6) 1865(4) 1532(4) 1861(4) 1534(4) C50H(2) C20H(2) C10H(2) C40H(2) 1756(2) 1423(2)	DIAGONAL- HCO (75) HCC (26) COH (25) OFF-DIAG- SB15(1) BB28(-2) BB29(-5) BB18(-21)
	1206 (W)					
	1119 (S)	1119.	1149.	A2U	C107(13) C208(13) C309(13) C400(13) C501(13) C602(13) CC2C(4) CC3C(4) CC4C(4) CC5C(4) CC6C(4) CC1C(4)	DIAGONAL- CO (75) CCC (22) CCO (13) HCO (5) COH (3) HCC (2) OFF-DIAG- SB12(7) BB19(2) BB23(2) BB30(2) BB22(2) BB18(-2) BB25(-2) SB13(-6) SB14(-25)
1116 (M)		1116.	1110.	A1G	C107(12) C309(12) C400(12) C602(12) C501(12) C208(12) HC10(2) HC20(2) HC30(2) HC40(2) HC50(2) HC60(2)	DIAGONAL- CO (72) HCO (14) CC (9) COH (8) CCC (2) CCO (1) OFF-DIAG- SB12(10) SB17(4) SB16(2) SB15(1) BB18(-1) BB29(-1) CCCO(-7) SB14(-7) SB13(-9)
1107 (M)		1107.	1107.	EG	C1C2(20) C4C5(20) C3C4(14) C6C2(14) C3C4(13) C6C1(13) C501(9) C208(9) CC3C(5) CC6C(5) 0823(4) 1156(4) CC5C(3) CC2C(3) 0932(3) 1265(3) 0716(3) 1043(3)	DIAGONAL- CC (68) CO (46) CCO (23) CCC (17) HCO (4) HCC (2) OFF-DIAG- BB22(2) SB13(2) BB18(-1) BB19(-2) BB23(-3) SB12(-4) SB15(-5) SB16(-6) CCCO(-7) SB17(-16) SB14(-19)
			1107.	EG	C2C3(22) C5C6(22) C107(15) C400(15) C3C4(10) C6C1(10) C208(7) C501(7) CC4C(6) CC1C(6) 0821(4) 1154(4) 0934(3) 1261(3) 0712(3) 1045(3) CC5C(3) CC2C(3) C1C2(2) C4C5(2) C309(2) C602(2)	DIAGONAL- CC (68) CO (46) CCO (23) CCC (17) HCO (4) HCC (2) OFF-DIAG- BB22(2) SB13(2) BB18(-1) BB19(-2) BB23(-3) SB12(-4) SB15(-5) SB16(-6) CCCO(-7) SB17(-16) SB14(-19)
			1097.	A1U	C5C6(19) C2C3(19) C3C4(19) C4C5(19) C1C2(19) C6C1(19)	DIAGONAL- CC (111) CCO (4) OFF-DIAG- CCCC(-2) SB16(-13)
	1099 (VS)	1099.	1076.	EU	C602(20) C309(20) C6C1(16) C3C4(16) C107(12) C400(12) C5C6(8) C2C3(8) 0821(3) 1154(3) 1156(2) 0823(2) 1045(2) 0712(2) C1C2(2) C4C5(2)	DIAGONAL- CO (67) CC (51) CCO (15) CCC (3) HCO (3) OFF-DIAG- BB23(-2) SB12(-5) SB16(-5) SB14(-6) SB17(-10) CCCO(-13)
	1085 (M)	1085.	1076.	EU	C501(21) C208(21) C4C5(15) C1C2(15) C400(10) C107(10) C5C6(9) C2C3(9) 0934(3) 1261(3) C309(2) C602(2) 1043(2) 0716(2) 1265(2) 0932(2)	DIAGONAL- CO (67) CC (51) CCO (15) CCC (3) HCO (3) OFF-DIAG- BB23(-2) SB12(-5) SB16(-5) SB14(-6) SB17(-10) CCCO(-13)
	1067 (W)					
1058 (M)		1058.	1074.	A1G	C2C3(7) C1C2(7) C3C4(7) C6C1(7) C4C5(7) C5C6(7) HC10(4) HC20(4) HC30(4) HC40(4) HC50(4) HC60(4) C10H(2) C20H(2) C30H(2) C40H(2) C50H(2) C60H(2)	DIAGONAL- CC (41) HCO (25) CCO (14) COH (10) CCC (8) CO (3) HCC (2) OFF-DIAG- BB19(6) SB14(6) SB15(5) BB30(4) BB18(4) BB23(3) SB13(2) BB25(2) BB22(1) BB29(-2) SB12(-3) CCCO(-3) SB16(-15) SB17(-17)
1004 (W)		1004.	1008.	EG	C107(19) C400(19) C2C3(12) C5C6(12) C309(12) C602(12) C4C5(8) C1C2(8)	DIAGONAL- CO (63) CC (42) CCO (5) COH (2) HCC (1) OFF-DIAG- CCCO(7) SB17(2) BB23(-1) SB15(-3) SB13(-5) SB14(-6) SB16(-9)
987 (VW)		987.	1008.	EG	C208(20) C501(20) C3C4(13) C6C1(13) C309(9) C602(9) C4C5(6) C1C2(6) C107(2) C400(2)	DIAGONAL- CO (63) CC (42) CCO (5) COH (2) HCC (1) OFF-DIAG- CCCO(7) SB17(2) BB23(-1) SB15(-3) SB13(-5) SB14(-6) SB16(-9)

TABLE XLIV (Continued)

EXPERIMENTAL FREQUENCY (CM-1) RAMAN	INFRARED	ASSIGNED FREQUENCY (CM-1)	CALCULATED FREQUENCY (CM-1)	CALCULATED SYMMETRY SPECIE	SPECTRAL INTERPRETATION --- POTENTIAL ENERGY DISTRIBUTIONS INTERNAL COORDINATES	FORCE CONSTANTS
	1002 (S)	1002.	969.	EU	C3C4(10) C6C1(10) C3O9(10) C6O2(10) C4OO(9) C1O7(9) O823(3) 1156(3) 1154(3) O821(3) C5C6(3) C2C3(3) C1C2(2) C4C5(2) O716(2) 1043(2) O934(2) 1261(2) HC3O(2) HC6O(2) HC4O(2) HC1O(2) CC3C(2) CC6C(2) CC4C(2) CC1C(2)	DIAGONAL- CO (38) CC (31) CCO (22) HCC (10) HCO (8) CCC (7) COH (5) OFF-DIAG- CCCO(8) SB12(6) BB23(4) BB18(2) BB22(1) BB30(1) BB28(-1) SB15(-1) BB25(-2) SB13(-5) SB14(-8) SB17(-12) SB16(-13)
	981 (S)	981.	969.	EU	C2O8(13) C5O1(13) C1C2(8) C4C5(8) C2C3(8) C5C6(8) O932(4) 1265(4) 1045(4) O712(4) C4OO(3) C1O7(3) C3O9(3) C6O2(3) HC2O(3) HC5O(3) CC2C(2) CC5C(2) C2OH(2) C5OH(2) 1534(2) 1861(2) 1643(2) 1316(2) O934(2) 1261(2)	DIAGONAL- CO (38) CC (31) CCO (22) HCC (10) HCO (8) CCC (7) COH (5) OFF-DIAG- CCCO(8) SB12(6) BB23(4) BB18(2) BB22(1) BB30(1) BB28(-1) SB15(-1) BB25(-2) SB13(-5) SB14(-8) SB17(-12) SB16(-13)
	724 (M,B)					
			667.	A2G	O716(8) O712(8) O821(8) O823(8) O932(8) O934(8) 1043(8) 1045(8) 1154(8) 1156(8) 1265(8) 1261(8) 1316(2) 1312(2) 1421(2) 1423(2) 1532(2) 1643(2) 1754(2) 1865(2) 1861(2) 1756(2) 1645(2) 1534(2)	DIAGONAL- CCO (97) HCC (23) OFF-DIAG- BB19(8) BB20(-1) BB28(-3) BB23(-23)
	635 (SH)	635.	651.	EU	1423(7) 1756(7) 1532(7) 1865(7) O823(6) 1156(6) 1043(6) O716(6) 1265(5) O932(5) O712(5) 1045(5) 1316(4) 1643(4) 1312(3) 1645(3)	DIAGONAL- HCC (46) CCO (44) CCC (3) HCO (2) CC (2) CO (1) OFF-DIAG- BB19(11) SB14(5) BB18(3) SB16(2) SB17(2) BB25(-1) BB20(-5) BB23(-17)
	627 (S)	627.	651.	EU	O821(7) 1154(7) O934(7) 1261(7) 1421(7) 1754(7) 1534(7) 1861(7) 1312(4) 1645(4) 1643(4) 1316(4) O712(2) 1045(2) 1265(2) O932(2) O716(2) 1043(2)	DIAGONAL- HCC (46) CCO (44) CCC (3) HCO (2) CC (2) CO (1) OFF-DIAG- BB19(11) SB14(5) BB18(3) SB16(2) SB17(2) BB25(-1) BB28(-5) BB23(-17)
	585 (W)	585.	555.	A2U	CC2C(6) CC3C(6) CC4C(6) CC5C(6) CC6C(6) CC1C(6) C1O7(4) C2O8(4) C3O9(4) C4OO(4) C5O1(4) C6O2(4) O716(2) O712(2) O821(2) O823(2) O932(2) O934(2) 1043(2) 1045(2) 1154(2) 1156(2) 1265(2) 1261(2)	DIAGONAL- CCC (37) CO (26) CCO (19) OFF-DIAG- SB14(18) BB22(3) BB23(2) BB19(1) BB30(-1) SB12(-2) BB25(-2) SB13(-2)
	522 (M,B)					
	485 (M,B)					
464 (VS)		464.	458.	A1G	C1C2(8) C2C3(8) C3C4(8) C4C5(8) C5C6(8) C6C1(8) C1O7(3) C2O8(3) C3O9(3) C4OO(3) C5O1(3) C6O2(3)	DIAGONAL- CC (51) CO (16) CCO (2) CCC (2) HCO (1) HCC (1) OFF-DIAG- SB17(9) CCCO(7) SB16(6) SB14(5) CCCC(1) BB19(1) SB12(-2) SB15(-5)
420 (LT,M)		420.	406.	EG	CC2C(8) CC5C(8) 1532(6) 1865(6) O934(6) 1261(6) 1043(6) O716(6) 1645(5) 1312(5) 1756(5) 1423(5) 1421(4) 1754(4) CC3C(3) CC6C(3) 1154(3) O821(3) C2O8(2) C5O1(2) TC34(2) TC61(2) 1156(2) O823(2) 1045(2) O712(2)	DIAGONAL- HCC (41) CCO (37) CCC (25) CO (5) TOCC(5) OFF-DIAG- BB19(7) BB18(2) BB22(1) BB23(-4) BB28(-5) SB14(-7) BB25(-11)
400 (LT,M)		400.	406.	EG	CC4C(7) CC1C(7) 1534(7) 1861(7) 1643(7) 1316(7) O932(6) 1265(6) CC6C(6) CC3C(6) 1045(5) O712(5) 1156(5) O823(5) O821(3) 1154(3) 1754(3) 1421(3) 1756(2) 1423(2) 1645(2) 1312(2) C1O7(2) C4OO(2)	DIAGONAL- HCC (41) CCO (37) CCC (25) CO (5) TOCC(5) OFF-DIAG- BB19(7) BB18(2) BB22(1) BB23(-4) BB28(-5) SB14(-7) BB25(-11)
391 (M)		391.	387.	EG	O823(9) 1156(9) 1154(9) O821(9) CC2C(7) CC5C(7) O932(5) 1265(5) O934(4) 1261(4) C3C4(3) C6C1(3) CC3C(3) CC6C(3) 1532(2) 1865(2) 1756(2) 1423(2)	DIAGONAL- CCO (56) CCC (21) HCC (12) CC (10) CO (1) OFF-DIAG- SB14(7) SB17(7) BB25(5) BB22(2) BB30(-1) BB28(-1) SB16(-7) BB23(-11)
382 (LT,M)		382.	387.	EG	O716(9) 1043(9) O712(8) 1045(8) CC4C(6) CC1C(6) O934(6) 1261(6) 1265(5) O932(5) CC6C(4) CC3C(4) C2C3(3) C5C6(3) 1534(2) 1861(2) C4C5(2) C1C2(2) 1643(2) 1316(2)	DIAGONAL- CCO (56) CCC (21) HCC (12) CC (10) CO (1) OFF-DIAG- SB14(7) SB17(7) BB25(5) BB22(2) BB30(-1) BB28(-1) SB16(-7) BB23(-11)
	360 (M)					
	302 (M)	302.	309.	EU	O823(9) 1156(9) C3C4(9) C6C1(9) 1154(9) O821(9) O716(5) 1043(5) C5C6(4) C2C3(4) O712(3) 1045(3) O934(2) 1261(2)	DIAGONAL- CCO (57) CC (28) TOCO(5) CCC (2) HCC (1) OFF-DIAG- SB16(15) BB19(2) BB22(-1) BB23(-3) SB17(-6)
	273 (M)	273.	309.	EU	O932(9) 1265(9) C1C2(8) C4C5(8) O934(8) 1261(8) O712(7) 1045(7) C2C3(5) C5C6(5) 1043(4) O716(4)	DIAGONAL- CCO (57) CC (28) TOCO(5) CCC (2) HCC (1) OFF-DIAG- SB16(15) BB19(2) BB22(-1) BB23(-3) SB17(-6)
			288.	A1U	O716(10) O712(10) O821(10) O823(10) O934(10) 1043(10) 1045(10) 1154(10) 1156(10) 1265(10) 1261(10) O932(10)	DIAGONAL- CCO (122) HCC (17) CC (8) TOCO(7) OFF-DIAG- BB28(2) BB20(-2) SB15(-6) BB19(-7) SB16(-20) BB23(-23)

TABLE XLIV (Continued)

EXPERIMENTAL FREQUENCY (CM-1) RAMAN	INFRARED	ASSIGNED FREQUENCY (CM-1)	CALCULATED FREQUENCY (CM-1)	CALCULATED SYMMETRY SPECIE	SPECTRAL INTERPRETATION --- POTENTIAL ENERGY DISTRIBUTIONS INTERNAL COORDINATES	FORCE CONSTANTS
271 (M)		271.	278.	EG	0932(12) 1265(12) 0934(11) 1261(11) 0712(6) 1045(6) CC2C(5) CC5C(5) CC1C(4) CC4C(4) 1043(3) 0716(3) TC30(3) TC60(3) 0821(3) 1154(3) 1423(2) 1756(2) 1643(2) 1316(2)	DIAGONAL- CCO (73) CCC (18) HCC (12) TOCO(10) TOCC(4) CO (1) OFF-DIAG- BB19(3) BB25(-2) BB22(-4) BB23(-14)
			278.	EG	1156(11) 0823(11) 1154(9) 0821(9) 0716(9) 1043(9) 0712(6) 1045(6) CC3C(6) CC6C(6) TC20(3) TC50(3) CC4C(2) CC1C(2) TC40(2) TC10(2) 1532(2) 1865(2) 1534(2) 1861(2)	DIAGONAL- CCO (73) CCC (18) HCC (12) TOCO(10) TOCC(4) CO (1) OFF-DIAG- BB19(3) BB25(-2) BB22(-4) BB23(-14)
	244 (M)	244.	220.	A2U	1316(6) 1312(6) 1421(6) 1423(6) 1532(6) 1534(6) 1643(6) 1645(6) 1754(6) 1756(6) 1865(6) 1861(6) 0716(5) 0712(5) 0821(5) 0823(5) 0932(5) 0934(5) 1043(5) 1045(5) 1154(5) 1156(5) 1265(5) 1261(5) CC2C(3) CC3C(3) CC4C(3) CC5C(3) CC6C(3) CC1C(3)	DIAGONAL- HCC (72) CCO (58) CCC (18) CO (8) OFF-DIAG- BB19(19) BB20(2) BB22(-4) BB28(-9) BB25(-13) SB14(-17) BB23(-32)
			178.	A2G	TC40(17) TC10(17) TC30(17) TC60(17) TC20(16) TC50(16)	DIAGONAL- TOCO(99)
			172.	EU	TC60(30) TC30(30) TC10(14) TC40(14) TC50(3) TC20(3)	DIAGONAL- TOCO(95) CCO (4) CC (1)
			172.	EU	TC20(29) TC50(29) TC40(17) TC10(17)	DIAGONAL- TOCO(95) CCO (4) CC (1)
			170.	A1U	TC10(16) TC20(16) TC60(15) TC30(15) TC40(15) TC50(15)	DIAGONAL- TOCO(93) CCO (10) OFF-DIAG- BB23(-1) SB16(-2)
			169.	EG	TC30(30) TC60(30) TC40(8) TC10(8) TC20(7) TC50(7)	DIAGONAL- TOCO(90) CCO (9) HCC (2) CCC (1) OFF-DIAG- BB23(-2)
			169.	EG	TC50(23) TC40(22) TC20(22) TC10(22)	DIAGONAL- TOCO(90) CCO (9) HCC (2) CCC (1) OFF-DIAG- BB23(-2)
			130.	A1G	CC2C(7) CC3C(7) CC4C(7) CC5C(7) CC6C(7) CC1C(7) TC12(7) TC23(7) TC34(7) TC45(7) TC56(7) TC61(7) 0712(2) 0821(2) 1261(2) 1156(2) 1265(2) 0716(2) 0823(2) 0932(2) 0934(2) 1043(2) 1045(2) 1154(2)	DIAGONAL- CCC (42) TOCC(41) CCO (29) CO (8) CC (5) OFF-DIAG- SB16(7) BB23(1) BB20(-1) BB25(-1) CCCO(-2) BB22(-4) SB14(-12) SB17(-13)
			90.	EU	TC23(15) TC56(15) CC3C(12) CC6C(12) TC61(8) TC34(8) CC5C(7) CC2C(7) 0932(3) 1265(3) 0934(2) 1261(2) 0823(2) 1156(2)	DIAGONAL- TOCC(47) CCC (40) CCO (16) CO (3) OFF-DIAG- SB17(1) BB22(-2) SB14(-6)
			90.	EU	TC45(15) TC12(15) CC4C(13) CC1C(13) TC34(8) TC61(8) CC5C(6) CC2C(6) 0712(3) 1045(3) 1043(2) 0716(2) 0821(2) 1154(2)	DIAGONAL- TOCC(47) CCC (40) CCO (16) CO (3) OFF-DIAG- SB17(1) BB22(-2) SB14(-6)

TABLE XLV. NEO-INOSITOL

EXPERIMENTAL FREQUENCY (CM-1) RAMAN	INFRARED	ASSIGNED FREQUENCY (CM-1)	CALCULATED FREQUENCY (CM-1)	CALCULATED SYMMETRY SPECIE	SPECTRAL INTERPRETATION --- POTENTIAL ENERGY DISTRIBUTIONS INTERNAL COORDINATES	FORCE CONSTANTS
	3410 (VS)		3357.	AU	O9H1(51) O10H(17) O8H0(11) O11H(10) O12H(6) O7H9(4)	DIAGONAL- OH (100)
	3330 (VS)		3357.	BU	O12H(51) O9H1(22) O11H(13) O7H9(13)	DIAGONAL- OH (100)
	3190 (VS)		3357.	BU	O11H(51) O10H(27) O12H(15) O8H0(7)	DIAGONAL- OH (100)
			3357.	AG	O10H(38) O11H(24) O7H9(18) O8H0(11) O9H1(6) O12H(2)	DIAGONAL- OH (100)
			3357.	AG	O7H9(40) O12H(22) O10H(16) O9H1(13) O8H0(9)	DIAGONAL- OH (100)
			3357.	BG	O8H0(62) O7H9(25) O9H1(8) O12H(3) O11H(2)	DIAGONAL- OH (100)
2968 (VS)			2945.	AG	C3H5(23) C4H6(23) C1H3(22) C6H8(22) C2H4(4) C5H7(4)	DIAGONAL- CH (98)
	2965 (W)		2944.	AU	C1H3(25) C6H8(25) C3H5(24) C4H6(24)	DIAGONAL- CH (99)
	2942 (W)		2939.	BU	C2H4(50) C5H7(48)	DIAGONAL- CH (99)
2923 (VS)			2938.	AG	C5H7(46) C2H4(44) C1H3(2) C3H5(2) C6H8(2) C4H6(2)	DIAGONAL- CH (99)
	2920 (M)		2935.	BU	C4H6(26) C3H5(26) C6H8(23) C1H3(23)	DIAGONAL- CH (99)
			2934.	BU	C6H8(26) C1H3(26) C4H6(23) C3H5(23)	DIAGONAL- CH (99)
1443 (VW)		1443.	1433.	AG	C1OH(9) C6OH(9) C3OH(9) C4OH(9) C5OH(6) C2OH(6) 1312(4) 1865(4) 1645(4) 1532(4) HC2O(4) HC5O(4) 1643(3) 1316(3) 1534(3) 1861(3) HC1O(2) HC6O(2) HC3O(2) HC4O(2)	DIAGONAL- COH (46) HCC (31) HCO (15) CO (2) CCO (1) CCC (1) OFF-DIAG- BB29(3) BB23(2) BB28(2) BB25(1) SB12(-1) BB18(-2) SB13(-2) BB30(-2)
	1425 (M)	1425.	1425.	AU	C3OH(12) C1OH(12) C4OH(12) C6OH(12) 1316(5) 1534(5) 1643(5) 1861(5) 1532(4) BB23(3) BB28(2) BB29(2) 1645(4) 1865(4) 1312(4) BB25(1) SB15(-2) BB30(-4)	DIAGONAL- COH (49) HCC (34) HCO (6) CCO (3) CC (2) OFF-DIAG-
1425 (VVW)		1425.	1418.	BG	C1OH(14) C6OH(14) C4OH(14) C3OH(14) HC6O(6) HC1O(6) HC4O(6) HC3O(6) 1421(4) 1423(4) 1754(4) 1756(4) 1316(2) 1861(2) 1534(2) 1643(2)	DIAGONAL- COH (56) HCO (24) HCC (24) CO (2) CC (2) CCC (1) OFF-DIAG- BB29(5) BB28(-1) SB15(-2) SB12(-2) SB13(-4) BB18(-5)
	1425 (M)	1425.	1417.	BU	C3OH(13) C4OH(13) C1OH(13) C6OH(13) C5OH(8) C2OH(8) HC3O(6) HC4O(6) HC1O(6) HC6O(6) HC5O(2) HC2O(2)	DIAGONAL- COH (69) HCO (28) HCC (6) CO (2) CCC (2) OFF-DIAG- BB29(5) BB25(1) SB12(-3) SB13(-5) BB18(-6)
	1401 (W)	1401.	1402.	BU	C2OH(28) C5OH(27) HC2O(9) HC5O(9) C1OH(4) C3OH(4) C4OH(4) C6OH(4)	DIAGONAL- COH (71) HCO (21) HCC (12) CO (3) CC (1) OFF-DIAG- BB29(5) BB30(-1) SB12(-2) BB18(-4) SB13(-5)
1397 (M)		1397.	1396.	AG	C5OH(30) C2OH(30) HC5O(7) HC2O(7) C4OH(5) C3OH(5) C6OH(5) C1OH(5)	DIAGONAL- COH (80) HCO (19) HCC (4) CC (3) CO (1) OFF-DIAG- BB29(5) SB15(-1) SB12(-1) BB30(-2) SB13(-4) BB18(-4)
	1386 (M)	1386.	1395.	AU	1756(14) 1421(14) 1754(14) 1423(14) C6C1(6) C3C4(6) 1643(4) 1316(4) 1534(4) 1861(4) C1OH(3) C6OH(3) C3OH(3) C4OH(3) HC1O(3) HC3O(3) HC6O(3) HC4O(3)	DIAGONAL- HCC (72) CC (13) COH (12) HCO (11) CO (5) CCO (3) OFF-DIAG- BB23(4) BB28(2) BB29(1) BB26(1) SB14(-1) SB16(-1) CCCO(-2) SB17(-2) SB19(-2) SB12(-2) SB13(-3) BB18(-3) SB15(-9)
1363 (M)		1363.	1370.	BG	1421(16) 1423(16) 1754(16) 1756(16) C3OH(5) C4OH(5) C6OH(5) C1OH(5)	DIAGONAL- HCC (69) COH (19) CCO (5) CC (1) OFF-DIAG- BB23(7) SB13(2) BB30(-1) BB19(-2) SB15(-2)
1348 (M)		1348.	1356.	AG	1316(13) 1534(13) 1643(13) 1861(13) HC1O(5) HC3O(5) HC4O(5) HC6O(5) C2OH(5) C4OH(5) C5OH(5) C3OH(4) C4OH(4) C1OH(4) C6OH(4) C3C4(2) C6C1(2) 1865(2) 1312(2) 1532(2) 1645(2)	DIAGONAL- HCC (57) COH (26) HCO (22) CO (5) CC (3) OFF-DIAG- BB28(7) BB29(2) SB14(-1) SB13(-3) SB12(-3) SB15(-7) BB18(-7)
	1335 (M)	1335.	1339.	BU	1312(14) 1645(14) 1532(14) 1865(14) C2OH(6) C5OH(6) 1534(5) 1861(5) 1643(5) 1316(5) C2O8(4) C5O1(4)	DIAGONAL- HCC (77) COH (13) CO (9) HCO (6) CCO (5) OFF-DIAG- SB11(3) BB23(3) BB25(2) BB30(-1) BB19(-2) SB12(-2) BB24(-2) BB28(-3) BB18(-3) SB14(-5)
	1323 (SH)	1323.	1335.	AU	1861(9) 1534(9) 1643(9) 1316(9) 1423(7) 1754(7) 1756(7) 1421(7) C1OH(4) C3OH(4) C4OH(4) C6OH(4) HC1O(3) HC3O(3) HC4O(3) HC6O(3)	DIAGONAL- HCC (66) COH (15) HCO (13) CC (4) OFF-DIAG- BB28(5) BB23(2) BB29(2) SB15(-3) BB18(-5)
	----		1303.	AG	HC4O(11) HC3O(11) HC1O(11) HC6O(11) 1312(9) 1645(9) 1532(9) 1865(9) C4OH(5) C3OH(5) C6OH(5) C1OH(5) C2O8(3) C5O1(3) C3O9(2) C6O2(2) C4O0(2) C1O7(2)	DIAGONAL- HCO (43) HCC (38) COH (22) CO (14) CCO (4) CCC (3) TOCC (1) OFF-DIAG- SB13(6) BB25(4) BB24(-1) BB30(-2) BB29(-4) SB14(-6) SB12(-7) BB18(-17)
	1281 (M)	1281.	1270.	BU	HC2O(17) HC5O(17) HC3O(6) HC4O(6) HC1O(6) HC6O(6) 1754(5) 1756(5) 1421(5) 1423(5) C4O0(3) C6O2(3) C1O7(3) C3O9(3) C1OH(3) C3OH(3) C4OH(3) C5OH(2) C2OH(2)	DIAGONAL- HCO (57) HCC (29) COH (15) CO (13) CCC (7) CCO (3) OFF-DIAG- SB13(5) BB23(2) BB25(2) BB26(2) BB10(-2) BB29(-4) SB14(-5) SB12(-6) BB18(-19)

Conventional symbolism indicating relative intensity: s = strong, m = medium, w = weak, sh = shoulder, b = broad, v = very, lt = low temperature band

TABLE XLV (Continued)

EXPERIMENTAL FREQUENCY (CM-1) RAMAN	INFRARED	ASSIGNED FREQUENCY (CM-1)	CALCULATED FREQUENCY (CM-1)	CALCULATED SYMMETRY SPECIE	SPECTRAL INTERPRETATION --- POTENTIAL ENERGY DISTRIBUTIONS INTERNAL COORDINATES	FORCE CONSTANTS
1271 (S)		1271.	1269.	BG	1532(15) 1645(15) 1865(15) 1312(15) 1643(7) 1316(7) 1534(7) 1861(7) C1C2(3) C2C3(3) C4C5(3) C5C6(3) 1754(2) 1756(2) 1421(2) 1423(2)	DIAGONAL- HCC (98) CC (13) CCO (6) CO (5) HCO (4) CCC (2) OFF-DIAG- BB23 (6) BB27 (1) CCCO(-1) SB12(-2) BB24(-2) BB18(-2) SB16(-2) BB25(-2) SB17(-2) SB14(-3) BB19(-4) BB28(-4) SB15(-14)
	1267 (M)	1267.	1258.	AU	HC10(16) HC30(16) HC40(16) HC60(16) 1532(9) 1865(9) 1312(9) 1645(9) C1OH(6) C3OH(6) C4OH(6) C6OH(6)	DIAGONAL- HCO (63) HCC (37) COH (23) CO (2) TOCC (2) CC (1) OFF-DIAG- SB13 (3) SB15(-3) SB12(-4) BB29(-5) BB18(-19)
1265 (S)		1265.	1257.	AG	HC20(28) HC50(28) 1754(8) 1756(8) 1421(8) 1423(8) C2OH(8) C5OH(8) C3C4(4) C6C1(4)	DIAGONAL- HCO (56) HCC (32) COH (15) CC (9) CO (2) CCO (2) TOCC(1) CCC (1) OFF-DIAG- SB15(3) BB23(3) SB16(-2) SB17(-2) BB29(-4) BB18(-20)
	1232 (W)	1232.	1226.	BU	HC20(13) HC50(13) HC40(9) HC30(9) HC10(9) HC60(9) 1534(5) 1643(5) 1316(5) 1861(5) C3OH(5) C4OH(5) C1OH(5) C6OH(5) C5OH(4) C2OH(4) 1754(2) 1423(2) 1756(2) 1421(2)	DIAGONAL- HCO (63) HCC (30) COH (29) TOCC(2) CO (1) OFF-DIAG- SB12(2) SB13(-2) BB28(-3) BB29(-5) BB18(-17)
1241 (M)		1241.	1224.	BG	HC10(17) HC60(17) HC30(17) HC40(17) C1OH(6) C6OH(6) C4OH(6) C3OH(6) 1316(4) 1861(4) 1643(4) 1534(4) 1532(2) 1645(2) 1865(2) 1312(2)	DIAGONAL- HCO (67) COH (26) HCC (26) CC (3) CCO (1) OFF-DIAG- SB12(1) BB28(-2) BB29(-5) BB18(-18)
	1130 (VS)	1130.	1136.	BU	C1O7(13) C3O9(13) C4OO(13) C6O2(13) C5O1(9) C2O8(9) C5C6(4) C2C3(4) C4C5(4) C1C2(4) CC3C(4) CC4C(4) CC6C(4) CC1C(4) HC2O(3) HC5O(3) 1043(3) 1261(3) O716(3) O934(3) C2OH(2) C5OH(2)	DIAGONAL- CO (69) CC (17) CCC (15) CCO (11) HCO (7) COH (5) OFF-DIAG- SB12(4) SB15(2) SB16(1) BB22(1) SB17(-5) SB13(-5) CCCO(-7) SB14(-15)
1132 (S)		1132.	1125.	AG	C2O8(15) C5O1(15) C2C3(10) C5C6(10) C1C2(10) C4C5(10) C3C4(8) C6C1(8) HC5O(7) HC2O(7) CC2C(5) C5C(5) 1045(4) 1265(4) O712(4) O932(4) HC3O(3) HC4O(3) HC1O(3) HC6O(3)	DIAGONAL- CC (56) CO (34) HCO (27) CCO (17) CCC (10) HCC (7) COH (5) OFF-DIAG- BB22(1) BB3O(1) SB13(1) BB25(-1) BB29(-1) BB18(-2) BB23(-3) SB12(-4) CCCO(-6) SB16(-7) SB15(-10) SB14(-10) SB17(-13)
	1091 (S)	1091.	1123.	AU	C1C2(22) C2C3(22) C4C5(22) C5C6(22) C3C4(10) C6C1(10) O821(3) O823(3) 1154(3) 1156(3) C1O7(2) C3O9(2) C4OO(2) C6O2(2)	DIAGONAL- CC (109) CCO (15) CO (7) HCC (3) OFF-DIAG- SB14(-2) CCCC(-2) SB15(-9) SB16(-18)
1098 (S)		1098.	1092.	AG	C3O9(17) C6O2(17) C4OO(17) C1O7(17) C5O1(7) C2O8(7) C2C3(4) C5C6(4) C4C5(4) C1C2(4) C3C4(3) C6C1(3) HC2O(2) HC5O(2)	DIAGONAL- CO (83) CC (21) HCO (4) COH (2) CCC (2) OFF-DIAG- SB12(4) SB15(2) SB16(2) SB14(-4) SB13(-5) CCCO(-10)
1098 (S)		1098.	1090.	BG	C1C2(15) C4C5(15) C2C3(15) C5C6(15) C1O7(7) C4OO(7) C3O9(7) C6O2(7) O716(3) O934(3) 1043(3) 1261(3) CC3C(3) CC4C(3) CC6C(3) CC1C(3) 1316(2) 1534(2) 1643(2) 1861(2)	DIAGONAL- CC (62) CO (29) CCO (19) CCC (13) HCC (11) HCO (4) OFF-DIAG- SB15(8) BB25(2) SB13(2) BB22(1) BB18(-1) BB26(-1) SB12(-4) BB23(-5) CCCO(-5) SB16(-6) SB14(-13) SB17(-13)
1074 (S)		1074.	1063.	AG	C3C4(19) C6C1(19) C2O8(9) C5O1(9) O821(3) O823(3) 1154(3) 1156(3) HC5O(3) HC2O(3) CC6C(3) CC1C(3) CC3C(3) CC4C(3) HC3O(2) HC4O(2) HC1O(2) HC6O(2) C1C2(2) C4C5(2) C5C6(2) C2C3(2) C1O7(2) C6O2(2) C3O9(2) C4OO(2) C2OH(2) C5OH(2) 1043(2) O716(2) O934(2) 1261(2) 1312(2) 1532(2) 1645(2) 1865(2)	DIAGONAL- CC (46) CO (26) CCO (19) HCO (13) CCC (11) HCC (9) COH (9) OFF-DIAG- SB12(6) CCCO(4) BB19(3) BB18(3) BB3O(3) BB25(-1) BB29(-1) BB24(-2) SB15(-5) SB13(-5) SB17(-10) SB14(-14) SB16(-15)
	1037 (VS)	1037.	1059.	BU	C5O1(15) C2O8(15) C4C5(10) C5C6(10) C1C2(10) C2C3(10) CC2C(6) CC5C(6) HC2O(6) HC5O(6) 1045(5) 1265(5) O712(5) O932(5) C3O9(3) C4OO(3) C1O7(3) C6O2(3) HC3O(2) HC4O(2) HC1O(2) HC6O(2) 1645(2) 1865(2) 1312(2) 1532(2)	DIAGONAL- CC (42) CO (41) CCO (22) HCO (20) CCC (13) HCC (10) COH (3) OFF-DIAG- BB22(2) BB18(-2) BB19(-2) SB12(-3) BB25(-3) CCCO(-4) SB15(-8) SB14(-9) SB16(-10) SB17(-13)
	1037 (VS)	1037.	1041.	AU	C6O2(23) C3O9(23) C4OO(23) C1O7(23) C6C1(9) C3C4(8) 1421(2) 1423(2) 1754(2) 1756(2)	DIAGONAL- CO (93) CC (18) HCC (7) CCO (3) COH (2) OFF-DIAG- SB12(2) SB15(-1) BB23(-2) SB13(-6) CCCO(-6) SB14(-12)
1023 (VS)		1023.	1007.	BG	C3O9(18) C1O7(18) C4OO(18) C6O2(18) C1C2(8) C2C3(8) C4C5(8) C5C6(8)	DIAGONAL- CO (74) CC (31) CCO (5) HCC (3) COH (2) CCC (2) OFF-DIAG- CCCO(6) SB17(3) BB23(-1) SB15(-4) SB13(-4) SB16(-7) SB14(-8)
974 (VW)						
	922 (W)	922.	935.	BU	C2O8(28) C5O1(28) C4C5(5) C5C6(5) C1C2(5) C2C3(5) O716(2) O934(2) 1043(2) 1261(2) O823(2) 1154(2) 1156(2) O821(2) 1316(2) 1534(2) 1643(2) 1861(2) C3O9(2) C4OO(2) C1O7(2) C6O2(2)	DIAGONAL- CO (62) CC (22) CCO (20) HCC (12) COH (3) HCO (1) OFF-DIAG- SB15(5) CCCO(5) BB19(3) BB3O(1) BB23(-2) SB13(-5) SB16(-10) SB14(-18)
	901 (W)	901.	894.	AU	C3C4(21) C6C1(21) 1312(6) 1532(6) 1645(6) 1865(6) O716(4) O934(4) 1043(4) 1261(4) CC1C(3) CC4C(3) CC6C(3) CC1C(3) C1C2(3) C4C5(3) C5C6(3) C2C3(3) HC1O(2) HC3O(2) HC4O(2) HC6O(2)	DIAGONAL- CC (53) HCC (27) CCO (17) CCC (13) HCO (8) COH (3) OFF-DIAG- SB15(5) BB19(4) BB18(4) BB3O(2) CCCO(1) BB22(1) BB26(-1) BB23(-1) BB24(-1) SB14(-2) SB16(-14) SB17(-21)

TABLE XLV (Continued)

EXPERIMENTAL FREQUENCY (CM-1) RAMAN	INFRARED	ASSIGNED FREQUENCY (CM-1)	CALCULATED FREQUENCY (CM-1)	CALCULATED SYMMETRY SPECIE	SPECTRAL INTERPRETATION --- POTENTIAL ENERGY DISTRIBUTIONS INTERNAL COORDINATES	FORCE CONSTANTS
872 (VS)		872.	869.	AG	C2O8 (22) C5O1 (22) C3C4 (5) C6C1 (5) 1312 (3) 1532 (3) 1645 (3) 1865 (3) C5C6 (3) C2C3 (3) C1C2 (3) C4C5 (3) 0716 (2) 0934 (2) 1043 (2) 1261 (2)	DIAGONAL- CO (45) CC (22) HCC (13) CCO (11) CCC (3) HCO (3) COH (2) OFF-DIAG- SB15 (5) CCCO (4) BB19 (3) BB18 (2) BB25 (1) SB14 (1) SB13 (-3) SB17 (-7) SB16 (-8)
758 (VW,B)	758 (M)					
	738 (S)	738.	723.	AU	C3C4 (14) C6C1 (14) 0712 (7) 1045 (7) 0932 (7) 1265 (7) 1154 (5) 0821 (5) 1156 (5) 0823 (5) 1421 (2) 1754 (2) 1423 (2) 1756 (2) 1312 (2) 1645 (2) 1532 (2) 1865 (2)	DIAGONAL- CCO (46) CC (30) HCC (18) CO (5) OFF-DIAG- SB14 (7) BB19 (4) CCCO (2) SB16 (1) BB24 (-2) SB15 (-4) BB23 (-8)
	726 (S)	726.	721.	BU	C107 (6) C400 (6) C602 (6) C309 (6) CC3C (5) CC4C (5) CC6C (5) CC1C (5) 0823 (3) 1156 (3) 1154 (3) 0821 (3) 1423 (2) 1756 (2) 1754 (2) 1421 (2) C501 (2) C208 (2)	DIAGONAL- CO (26) CCC (22) CCO (19) HCC (15) CC (3) HCO (2) COH (1) OFF-DIAG- SB14 (9) BB19 (6) BB26 (3) SB16 (2) CCCO (2) BB24 (-1) SB13 (-2) SB12 (-2) SB17 (-2) BB25 (-3)
688 (M)		688.	673.	AG	C3C4 (17) C6C1 (17) CC2C (3) CC5C (3) 1421 (3) 1423 (3) 1754 (3) 1756 (3) 0821 (3) 1154 (3) 0823 (3) 1156 (3) CC4C (2) CC3C (2) CC6C (2) CC1C (2)	DIAGONAL- CC (35) CCC (16) HCC (13) CCO (11) CO (3) HCO (1) OFF-DIAG- SB17 (11) BB19 (5) BB26 (2) SB14 (2) BB18 (2) CCCO (2) BB25 (-1) SB16 (-4)
665 (S)		665.	668.	BG	0712 (10) 0932 (10) 1045 (10) 1265 (10) 1156 (8) 0823 (8) 0821 (8) 1154 (8) 0934 (4) 1043 (4) 0716 (4) 1261 (4) 1421 (2) 1423 (2) 1754 (2) 1756 (2)	DIAGONAL- CCO (88) HCC (13) CCC (3) CO (2) OFF-DIAG- BB19 (5) BB20 (-1) SB14 (-2) BB24 (-2) BB23 (-6)
	604 (M,B)					
584 (VW,B)						
	538 (M)	538.	531.	BU	0716 (7) 0934 (7) 1043 (7) 1261 (7) CC2C (6) CC5C (6) 0823 (6) 1154 (6) 1156 (6) 0821 (6) 1316 (5) 1534 (5) 1643 (5) 1861 (5) 0712 (2) 0932 (2) 1265 (2) 1045 (2)	DIAGONAL- CCO (60) HCC (24) CCC (13) CO (3) OFF-DIAG- SB14 (11) BB19 (4) BB25 (2) BB22 (1) BB18 (1) BB30 (-1) SB17 (-2) BB28 (-3) BB23 (-14)
451 (M)		451.	452.	BG	0716 (14) 0934 (14) 1043 (14) 1261 (14) 1316 (6) 1534 (6) 1643 (6) 1861 (6) 0823 (6) 1154 (6) 1156 (6) 0821 (6)	DIAGONAL- CCO (78) HCC (27) CCC (4) TOCC (3) CC (3) TOCO (1) OFF-DIAG- BB19 (7) SB16 (5) SB15 (2) BB22 (-1) BB24 (-1) SB17 (-2) SB14 (-2) BB25 (-2) BB28 (-3) BB23 (-18)
435 (VS)		435.	438.	AG	C1C2 (8) C2C3 (8) C4C5 (8) C5C6 (8) CC2C (6) CC5C (6) C400 (3) C602 (3) C107 (3) C309 (3) 0712 (2) 0932 (2) 1045 (2) 1265 (2)	DIAGONAL- CC (35) CCC (12) CO (11) CCO (9) HCC (3) HCO (2) OFF-DIAG- SB17 (10) SB14 (8) SB16 (7) CCCO (3) BB23 (2) BB19 (2) BB18 (1) SB12 (-1) SB15 (-5)
362 (W)						
345 (M)		345.	367.	BG	CC3C (12) CC4C (12) CC6C (12) CC1C (12) 0712 (9) 0932 (9) 1045 (9) 1265 (9) 1421 (2) 1423 (2) 1754 (2) 1756 (2) C1C2 (2) C2C3 (2) C4C5 (2) C5C6 (2)	DIAGONAL- CCC (47) CCO (45) HCC (10) CC (9) CO (3) OFF-DIAG- SB17 (9) SB14 (8) BB22 (1) BB30 (-1) BB20 (-1) SB15 (-4) BB26 (-4) BB23 (-10) SB16 (-10)
	349 (M)	349.	324.	BU	0712 (9) 0932 (9) 1045 (9) 1265 (9) 0934 (6) 1261 (6) 1043 (6) C1C2 (6) C4C5 (6) 0716 (6) C2C3 (6) C5C6 (6)	DIAGONAL- CCO (65) CC (25) HCC (7) CCC (4) TOCO (4) CO (1) OFF-DIAG- SB16 (9) BB19 (3) SB15 (2) BB22 (-1) SB17 (-6) BB23 (-10)
	329 (M)	329.	324.	AU	0821 (12) 1154 (12) 1156 (12) 0823 (12) 0716 (6) 1043 (6) 1261 (6) 0934 (6) C2C3 (2) C5C6 (2) C4C5 (2) C1C2 (2)	DIAGONAL- CCO (70) CC (7) HCC (3) TOCO (3) HCO (2) OFF-DIAG- SB16 (10) BB24 (2) SB15 (-2)
307 (M)		307.	309.	AG	1043 (14) 0934 (14) 1261 (14) 0716 (14) 0932 (8) 1045 (8) 1265 (8) 0712 (8) 0823 (3) 1154 (3) 0821 (3) 1156 (3)	DIAGONAL- CCO (101) HCC (10) TOCO (3) CCC (2) CC (2) OFF-DIAG- BB24 (1) SB14 (-1) BB20 (-1) SB17 (-1) SB15 (-2) BB19 (-3) BB23 (-11)
	310 (M)	310.	289.	AU	1045 (12) 0932 (12) 0712 (12) 1265 (12) 0934 (9) 1043 (9) 0716 (9) 1261 (9) 1154 (6) 1156 (6) 0821 (6) 0823 (6) C1C2 (2) C2C3 (2) C4C5 (2) C5C6 (2) 1421 (2) 1423 (2) 1754 (2) 1756 (2)	DIAGONAL- CCO (107) HCC (13) CC (8) TOCO (7) OFF-DIAG- SB17 (-1) BB20 (-1) SB15 (-3) BB19 (-5) SB16 (-12) BB23 (-15)
265 (W)		265.	263.	BG	0821 (9) 0823 (9) 1154 (9) 1156 (9) 1316 (5) 1534 (5) 1643 (5) 1861 (5) TC20 (4) TC50 (4) 0932 (4) 1265 (4) 1045 (4) 0712 (4) CC6C (3) CC1C (3) CC3C (3) CC4C (3)	DIAGONAL- CCO (52) HCC (24) CCC (12) TOCO (9) TOCC (5) CO (3) HCO (1) OFF-DIAG- BB19 (6) BB18 (2) BB24 (2) BB28 (-2) BB25 (-4) SB14 (-6) BB23 (-6)
251 (W)		251.	253.	AG	CC2C (17) CC5C (17) 0821 (7) 0823 (7) 1154 (7) 1156 (7) TC34 (3) TC61 (3) 0932 (3) 1265 (3) 1045 (3) 0712 (3) TC10 (2) TC30 (2) TC40 (2) TC60 (2)	DIAGONAL- CCO (43) CCC (40) TOCO (8) TOCC (7) HCC (5) CC (2) CO (2) OFF-DIAG- SB16 (5) BB24 (2) BB19 (2) SB15 (-1) BB22 (-3) BB25 (-3) SB17 (-4) SB14 (-4)
	245 (W)					
			207.	BU	0821 (6) 0823 (6) 1154 (6) 1156 (6) CC2C (6) CC5C (6) 1534 (6) 1316 (6) 1643 (6) 1861 (6) CC4C (4) CC3C (4) CC6C (4) CC1C (4) 1043 (3) 0716 (3) 0934 (3) 1261 (3) 0712 (2) 0932 (2) 1265 (2) 1045 (2) 1532 (2) 1645 (2) 1865 (2) 1312 (2)	DIAGONAL- CCO (46) HCC (35) CCC (26) CO (7) CC (2) TOCO (2) OFF-DIAG- BB19 (9) SB16 (5) BB24 (3) BB18 (1) BB26 (-1) BB22 (-2) SB15 (-3) BB28 (-3) BB23 (-5) BB25 (-8) SB14 (-14)
198 (M)						
			177.	BG	TC60 (24) TC40 (24) TC30 (24) TC10 (24)	DIAGONAL- TOCO (98) CCO (1)

TABLE XLV (Continued)

EXPERIMENTAL FREQUENCY (CM-1) RAMAN	INFRARED	ASSIGNED FREQUENCY (CM-1)	CALCULATED FREQUENCY (CM-1)	CALCULATED SYMMETRY SPECIE	SPECTRAL INTERPRETATION --- POTENTIAL ENERGY DISTRIBUTIONS
					INTERNAL COORDINATES / FORCE CONSTANTS
			173.	AU	TC50(38) TC20(38) TC30(5) TC60(5) TC10(5) TC40(5) DIAGONAL- TOCO(96) CCO (3)
			172.	BU	TC40(24) TC10(24) TC60(23) TC30(23) DIAGONAL- TOCO(94) CCO (4) CC (1) OFF-DIAG- SB16(1)
			170.	AU	TC60(18) TC10(18) TC40(18) TC30(18) TC50(10) TC20(10) DIAGONAL- TOCO(91) CCO (6) CCC (2) HCC (1)
			170.	BG	TC20(44) TC50(44) DIAGONAL- TOCO(92) CCO (8) OFF-DIAG- SB16(-1)
			169.	AG	TC30(22) TC40(22) TC60(22) TC10(22) DIAGONAL- TOCO(89) CCO (8) CCC (2)
			126.	AG	CC3C(9) CC4C(9) CC6C(9) CC1C(9) TC12(8) TC23(8) TC45(8) TC56(8) TC34(6) TC61(6) 0712(3) 0932(3) 1045(3) 1265(3) CC5C(3) CC2C(3) 1043(2) 0716(2) 0934(2) 1261(2) DIAGONAL- TOCC(42) CCC (40) CCO (26) HCC (6) CO (6) CC (2) HCO (1) OFF-DIAG- SB16(2) BB19(2) BB22(-2) BB26(-3) BB23(-4) SB17(-8) SB14(-10)
			98.	BU	TC12(12) TC45(12) TC23(12) TC56(12) CC2C(11) CC5C(11) CC4C(4) CC1C(4) CC6C(4) CC3C(4) DIAGONAL- TOCC(48) CCC (38) CCO (7) HCC (5) HCO (2) CO (1) OFF-DIAG- SB17(4) BB19(2) BB18(1) BB23(-1) BB26(-1) SB14(-2) BB25(-2)
			87.	AU	TC34(16) TC61(16) CC3C(10) CC6C(10) CC4C(10) CC1C(10) TC56(4) TC45(4) TC23(4) TC12(4) 0934(2) 0716(2) 1043(2) 1261(2) 1265(2) 0712(2) 0932(2) 1045(2) DIAGONAL- TOCC(48) CCC (40) CCO (16) CO (4) HCC (3) OFF-DIAG- SB17(2) BB22(-2) BB26(-2) BB23(-2) SB14(-6)

TABLE XLVI. MYO-INOSITOL

EXPERIMENTAL FREQUENCY (CM-1) RAMAN	INFRARED	ASSIGNED FREQUENCY (CM-1)	CALCULATED FREQUENCY (CM-1)	CALCULATED SYMMETRY SPECIE	SPECTRAL INTERPRETATION --- POTENTIAL ENERGY DISTRIBUTIONS INTERNAL COORDINATES	FORCE CONSTANTS
	3380 (VS)		3357.		O12H(44) O11H(17) O10H(17) O7H9(13) O9H1(5) O8H0(3)	DIAGONAL- OH (100)
	3220 (VS)		3357.		O10H(51) O12H(23) O9H1(15) O7H9(9)	DIAGONAL- OH (100)
	3170 (VS)		3357.		O7H9(44) O11H(19) O9H1(16) O8H0(13) O12H(7)	DIAGONAL- OH (100)
			3357.		O9H1(41) O7H9(26) O12H(16) O11H(9) O10H(7)	DIAGONAL- OH (100)
			3357.		O11H(53) O10H(24) O9H1(10) O12H(10) O8H0(4)	DIAGONAL- OH (100)
			3357.		O8H0(79) O9H1(13) O7H9(7)	DIAGONAL- OH (100)
2964 (M)			2950.	A'	C5H7(33) C4H6(25) C6H8(25) C3H5(7) C1H3(7)	DIAGONAL- CH (98)
	2955 (W)		2945.	A''	C4H6(28) C6H8(28) C1H3(22) C3H5(22)	DIAGONAL- CH (98)
2940 (M)	2935 (W)		2940.	A'	C5H7(28) C2H4(25) C1H3(23) C3H5(23)	DIAGONAL- CH (99)
2925 (VS)	2920 (M)		2938.	A'	C2H4(73) C1H3(10) C3H5(10) C5H7(6)	DIAGONAL- CH (99)
	2900 (W)		2935.	A''	C1H3(28) C3H5(28) C6H8(22) C4H6(22)	DIAGONAL- CH (99)
2887 (M)	2880 (VW)		2932.	A'	C5H7(31) C4H6(25) C6H8(24) C3H5(10) C1H3(10)	DIAGONAL- CH (100)
	1445 (M)	1445.	1438.	A''	C6OH(20) C4OH(20) 1754(11) 1756(11) 1316(6) 1534(6) HC4O(3) HC6O(3) 1312(2) 1532(2)	DIAGONAL- COH (42) HCC (40) HCO (6) CCO (3) OFF-DIAG- BB23(5) BB29(2) BB25(2) BB30(-3)
			1436.	A'	C5OH(27) 1865(10) 1645(10) C3OH(9) C1OH(9) 1861(6) 1643(6) HC5O(4) HC1O(3) HC3O(3) C2OH(2)	DIAGONAL- COH (46) HCC (34) HCO (11) CCO (2) OFF-DIAG- BB23(3) BB29(3) BB25(1) BB18(-1) BB30(-3)
1427 (VW)		1427.	1423.	A'	C4OH(16) C6OH(16) C2OH(10) 1534(7) 1316(7) HC2O(6) C5OH(6) 1312(5) 1532(5) C2O8(2)	DIAGONAL- COH (51) HCC (29) HCO (8) CCO (3) CO (2) CCC (2) OFF-DIAG- BB23(4) BB25(2) BB29(2) SB15(2) BB19(1) SB14(-1) BB18(-1) BB30(-4)
			1418.	A''	C3OH(29) C1OH(29) HC3O(9) HC1O(8) 1643(5) 1861(5) 1421(2) 1423(2)	DIAGONAL- COH (60) HCC (21) HCO (19) CC (2) CCC (1) CO (1) OFF-DIAG- BB29(4) SB12(-1) BB30(-2) SB15(-2) SB13(-3) BB18(-3)
1418 (W)	1416 (M)	1417.	1415.	A'	C5OH(16) C4OH(11) C6OH(11) C1OH(11) C3OH(11) C2OH(9) HC5O(6) HC1O(5) HC3O(5) HC4O(5) HC6O(5) HC2O(2)	DIAGONAL- COH (70) HCO (28) HCC (6) CO (3) CCC (2) OFF-DIAG- BB29(5) BB25(1) SB12(-3) SB13(-5) BB18(-6)
1406 (SH)		1406.	1395.	A'	C2OH(51) HC2O(12) C1OH(11) C3OH(11) C5OH(5) C4OH(3) C6OH(3) HC3O(2) HC1O(2)	DIAGONAL- COH (82) HCO (17) HCC (3) CC (3) CCO (1) OFF-DIAG- BB29(5) SB15(-1) SB16(-1) SB12(-1) BB30(-2) BB18(-3) SB13(-3)
	1379 (W,SH)	1379.	1386.	A''	1421(26) 1423(26) 1316(6) 1534(6) C4OH(4) C6OH(4) C3C4(4) C6C1(4) 1643(4) 1861(4) 1756(2) 1754(2)	DIAGONAL- HCC (79) CC (9) COH (9) HCO (5) CCO (4) CO (3) OFF-DIAG- BB23(5) BB28(3) SB17(-1) SB12(-1) SB14(-1) BB18(-2) BB19(-2) SB15(-9)
1373 (SH)	1371 (M)	1371.	1365.	A'	HC5O(16) HC4O(13) HC6O(13) 1534(7) 1316(7) 1865(6) 1645(6) C4OH(6) C6OH(6) C5OH(6) C2OH(5) 1754(4) 1756(4) C5O1(3) C6O2(3) C4O0(3) HC3O(2) HC1O(2) 1861(2) 1643(2)	DIAGONAL- HCO (45) HCC (40) COH (22) CO (10) CC (2) TOCC (1) OFF-DIAG- BB28(4) BB29(3) BB23(2) BB25(1) SB14(-2) SB13(-4) SB15(-4) SB12(-7) BB18(-16)
1360 (M)	1355 (W)	1357.	1353.	A''	1754(23) 1756(23) C6OH(11) C4OH(11) 1645(9) 1865(9) HC4O(7) HC6O(7) C4C5(3) C5C6(3)	DIAGONAL- HCC (66) COH (23) HCO (14) CC (6) CO (3) CCO (1) OFF-DIAG- BB28(8) BB29(2) BB30(1) BB19(-1) SB12(-2) SB13(-3) BB18(-5) SB15(-10)
1344 (W)	1343 (W)	1343.	1351.	A'	C5OH(16) 1861(12) 1643(12) 1865(9) 1645(9) HC5O(7) 1534(7) 1316(7) C3OH(5) C1OH(5) HC3O(3) HC1O(3) C2OH(2) 1756(2) 1754(2) C6C1(2) C3C4(2)	DIAGONAL- HCC (61) COH (28) HCO (14) CC (4) CO (3) CCO (1) OFF-DIAG- BB28(7) BB29(2) BB30(1) SB14(-1) BB25(-1) BB19(-1) SB12(-2) SB13(-3) BB18(-5) SB15(-8)
1328 (M)	1323 (W)	1323.	1348.	A''	1861(14) 1643(14) 1421(11) 1423(11) C1OH(8) C3OH(8) 1316(5) 1534(5) 1865(4) 1645(4) HC1O(4) HC3O(4) HC4O(1) HC6O(3)	DIAGONAL- HCC (66) COH (17) HCO (13) CC (3) CCO (1) CO (1) OFF-DIAG- BB28(4) BB23(3) BB29(2) SB12(-1) SB13(-1) BB18(-4) SB15(-5)
1305 (W)	1312 (SH)	1305.	1322.	A'	1312(21) 1532(21) HC1O(7) HC3O(7) C2O8(7) 1643(4) 1861(4) C2OH(4) HC6O(3) HC4O(3) C4OH(3) C6OH(3) C5OH(3) HC5O(3) C3OH(3) C1OH(3) C3O9(2) C1O7(2) CC2C(2) HC2O(2)	DIAGONAL- HCC (56) HCO (24) COH (18) CO (12) CCO (5) CCC (3) OFF-DIAG- SB13(5) BB25(3) BB23(2) BB28(-1) BB24(-2) BB30(-2) BB29(-2) SB12(-5) SB14(-6) BB18(-10)
1282 (M)	1281 (VW,SH)	1282.	1274.	A''	1312(19) 1532(19) 1316(10) 1534(10) 1865(6) 1645(6) 1643(5) 1861(5) 1754(5) 1756(5) C1C2(3) C2C3(3) 1421(2) 1423(2)	DIAGONAL- HCC (95) CC (8) CCO (7) CO (3) HCO (3) OFF-DIAG- BB23(9) SB17(-1) SB14(-1) BB19(-4) BB28(-7) SB15(-8)
1268 (VW)	1271 (W)	1271.	1266.	A'	HC2O(38) 1423(11) 1421(11) C2OH(7) HC3O(5) HC1O(5) C1O7(4) C3O9(4) HC6O(3) HC4O(3) C1OH(3) C3OH(3) 1643(2) 1861(2) C3C4(2) C6C1(2)	DIAGONAL- HCO (55) HCC (30) COH (16) CO (9) CCC (5) CC (3) CCO (2) OFF-DIAG- SB13(3) BB23(3) HB25(2) BB26(2) SB15(1) BB30(-1) SB14(-3) BB29(-4) SB12(-4) BB18(-19)

Conventional symbolism indicating relative intensity: s = strong, m = medium, w = weak, sh = shoulder, b = broad, v = very, lt = low temperature band

TABLE XLVI (Continued)

EXPERIMENTAL FREQUENCY (CM-1) RAMAN	INFRARED	ASSIGNED FREQUENCY (CM-1)	CALCULATED FREQUENCY (CM-1)	CALCULATED SYMMETRY SPECIE	SPECTRAL INTERPRETATION --- POTENTIAL ENERGY DISTRIBUTIONS INTERNAL COORDINATES	FORCE CONSTANTS
	1258 (LT,W)	1258.	1254.	A'	HC10 (16) HC30 (16) HC40 (13) HC60 (13) 1645 (7) 1865 (7) 1312 (6) 1532 (6) C10H (6) C30H (6) C40H (6) C60H (6) 1756 (4) 1754 (4)	DIAGONAL- HCO (59) HCC (37) COH (23) TOCC (2) CCO (1) OFF-DIAG- BB23 (2) SB13 (1) SB12 (-2) BB28 (-2) BB29 (-5) BB18 (-17)
1248 (W)	1245 (M)	1247.	1239.	A'	HC50 (29) HC30 (12) HC10 (12) HC20 (11) C50H (10) 1534 (6) 1316 (6) C30H (5) C10H (5) 1756 (5) 1754 (5) C20H (3) 1423 (2) 1421 (2)	DIAGONAL- HCO (64) HCC (30) COH (24) TOCC (2) CC (2) OFF-DIAG- BB23 (2) SB15 (1) BB28 (-2) BB29 (-5) BB18 (-18)
1220 (W)	1217 (W)	1218.	1224.	A''	HC40 (19) HC60 (19) HC30 (17) HC10 (17) C40H (7) C60H (7) C30H (6) C10H (6) 1316 (4) 1534 (4) 1643 (4) 1861 (4) 1645 (3) 1865 (3) 1532 (2) 1312 (2)	DIAGONAL- HCO (71) HCC (26) COH (25) CC (2) OFF-DIAG- BB28 (-2) BB29 (-5) BB18 (-19)
1198 (VW)	1194 (M)	1196.	1220.	A'	HC50 (24) HC60 (17) HC40 (17) HC20 (10) C50H (9) C60H (7) C40H (7) 1756 (4) 1754 (4) C20H (3) 1865 (3) 1645 (3) 1643 (3) 1861 (3) HC10 (2) HC30 (2)	DIAGONAL- HCO (72) COH (30) HCC (26) CCC (3) CO (2) CCO (1) OFF-DIAG- BB25 (3) SB13 (2) BB30 (-2) BB23 (-2) BB19 (-3) BB28 (-3) SB12 (-3) BB29 (-6) BB18 (-20)
1143 (M)	1145 (S)	1144.	1147.	A'	C40O (15) C602 (15) C501 (14) C208 (11) C309 (8) C107 (8) C1C2 (7) C2C3 (7) CC5C (6) CC4C (4) CC6C (4) C6C1 (3) C3C4 (3) CC3C (2) CC1C (2) 1045 (2) 1265 (2) 0716 (2) 0934 (2)	DIAGONAL- CO (71) CC (21) CCC (20) CCO (15) COH (2) HCO (1) OFF-DIAG- SB12 (3) BB22 (2) BB23 (1) BB30 (1) BB25 (-1) SB16 (-1) SB13 (-4) CCCO (-5) SB17 (-5) SB14 (-21)
1131 (M)		1131.	1119.	A''	C2C3 (33) C1C2 (33) C3C4 (13) C6C1 (13) 0821 (5) 0823 (5) C107 (4) C309 (4) C400 (4) C602 (4) 0716 (3) 0934 (3) CC4C (2) CC6C (2)	DIAGONAL- CC (92) CCO (19) CO (17) CCC (7) HCO (3) HCC (2) OFF-DIAG- BB23 (-1) BB19 (-1) CCCC (-2) SB12 (-2) SB15 (-3) CCCO (-3) SB17 (-7) SB14 (-8) SB16 (-14)
1122 (M)		1122.	1111.	A'	C309 (12) C107 (12) HC20 (10) C501 (10) C208 (8) CC2C (7) C6C1 (6) C3C4 (6) HC30 (6) HC30 (6) C1C2 (4) C2C3 (4) 0932 (4) 0712 (4) HC50 (4) C602 (4) C400 (4) C50H (2) C30H (2) C10H (2)	DIAGONAL- CO (50) HCO (28) CC (21) CCO (11) COH (9) CCC (9) HCC (3) OFF-DIAG- SB12 (6) BB30 (2) BB22 (1) BB25 (-1) BB23 (-2) BB29 (-2) SB16 (-2) BB18 (-3) CCCO (-3) SB17 (-4) SB15 (-4) SB13 (-6) SB14 (-14)
1112 (SH)	1111 (S)	1111.	1098.	A''	C5C6 (40) C4C5 (40) C400 (13) C602 (13) 1154 (4) 1156 (4) CC4C (3) CC6C (3) 1261 (2) 1043 (2)	DIAGONAL- CC (85) CO (28) CCO (15) CCC (8) HCO (2) HCC (2) OFF-DIAG- SB13 (1) BB22 (1) BB19 (-1) CCCC (-1) BB23 (-2) SB12 (-2) SB15 (-3) CCCO (-5) SB17 (-9) SB14 (-9) SB16 (-9)
1107 (LT,M)	1107 (LT,SH)	1107.	1093.	A'	C501 (35) C4C5 (17) C5C6 (17) C6C1 (10) C3C4 (10) HC20 (5) C400 (3) C602 (3) C208 (3) C107 (3) C309 (3) CC5C (3) 1265 (3) 1045 (3) CC1C (3) CC3C (3) 1261 (2) 1043 (2) C20H (2)	DIAGONAL- CC (53) CO (51) CCO (15) CCC (10) HCO (7) HCC (3) COH (3) OFF-DIAG- BB22 (1) BB23 (-2) SB15 (-3) SB16 (-5) CCCO (-8) SB17 (-11) SB14 (-11)
1097 (M)	1096 (SH)	1097.	1088.	A'	C208 (26) C602 (19) C400 (19) C2C3 (12) C1C2 (12) C107 (4) C309 (4) C5C6 (2) C4C5 (2) C6C1 (2) C3C4 (2)	DIAGONAL- CO (73) CC (33) CCO (7) CCC (5) HCO (2) HCC (2) OFF-DIAG- SB12 (2) SB16 (-3) SB14 (-4) SB17 (-7) CCCO (-10)
1066 (S)	1063 (SH)	1066.	1057.	A'	C3C4 (12) C6C1 (12) C501 (8) C4C5 (7) C5C6 (7) C2C3 (7) C1C2 (7) HC40 (5) HC60 (5) 0716 (5) 0934 (5) HC50 (5) HC20 (4) CC5C (3) 1312 (3) 1532 (3) C107 (2) C309 (2) 1045 (2) 1265 (2) C40H (2) C60H (2) 0823 (2) 0821 (2)	DIAGONAL- CC (52) CCO (20) HCO (19) CO (14) CCC (8) COH (8) HCC (7) OFF-DIAG- BB19 (3) BB30 (2) BB18 (2) BB22 (1) BB23 (1) BB29 (-1) SB15 (-2) SB14 (-2) SB17 (-13) SB16 (-18)
1053 (M)	1047 (VS)	1050.	1046.	A''	C107 (25) C309 (25) C400 (17) C602 (17) C3C4 (11) C6C1 (11) 1421 (2) 1423 (2)	DIAGONAL- CO (84) CC (27) HCC (9) CCO (5) OFF-DIAG- SB17 (-3) BB23 (-3) SB13 (-3) CCCO (-9) SB14 (-10)
1012 (M)	1012 (M)	1012.	1008.	A'	C107 (20) C309 (20) C400 (15) C602 (15) C4C5 (10) C5C6 (10) C1C2 (8) C2C3 (8)	DIAGONAL- CO (69) CC (35) CCO (5) HCC (2) COH (2) CCC (1) OFF-DIAG- CCCO (6) SB17 (3) BB23 (-1) SB15 (-4) SB13 (-4) SB14 (-7) SB16 (-8)
1003 (SH)	999 (S)	999.	987.	A'	C501 (29) C208 (11) C4C5 (11) C5C6 (11) C309 (9) C107 (9) C3C4 (4) C6C1 (4) 1045 (3) 1265 (3) C50H (3) HC50 (2) CC2C (2) 1643 (2) 1861 (2)	DIAGONAL- CO (58) CC (29) CCO (14) HCC (8) HCO (5) CCC (4) COH (4) OFF-DIAG- CCCO (6) SB12 (3) BB23 (1) BB25 (-1) SB15 (-2) SB13 (-5) SB17 (-5) SB16 (-9) SB14 (-10)
936 (M)	927 (M)	932.	938.	A''	C3C4 (18) C6C1 (18) 1043 (6) 1261 (6) C1C2 (5) C2C3 (5) 1312 (5) 1532 (5) 1156 (5) 1154 (5) C400 (4) C602 (4) CC3C (3) CC1C (3) HC10 (2) HC30 (2) HC40 (2) HC60 (2) CC6C (2) CC4C (2) C5C6 (2) C4C5 (2) C107 (2) C309 (2)	DIAGONAL- CC (49) CCO (24) HCC (16) CCC (11) CO (10) HCO (8) COH (4) OFF-DIAG- CCCO (5) SB15 (3) SB12 (3) BB18 (2) BB19 (2) BB22 (1) BB30 (1) BB25 (-1) SB13 (-2) SB14 (-5) SB16 (-14) SB17 (-18)
902 (S)	896 (M)	899.	904.	A'	C208 (44) C2C3 (9) C1C2 (9) 1043 (5) 1261 (5) C6C1 (5) C3C4 (5) 0712 (2) 0932 (2) C20H (2) 1532 (2) 1312 (2) C501 (2)	DIAGONAL- CO (46) CC (28) CCO (17) HCC (10) COH (3) HCO (2) CCC (1) OFF-DIAG- CCCO (5) SB15 (5) BB19 (3) BB30 (1) SB11 (-4) SB17 (-4) SB14 (-7) SB16 (-10)
	750 (W,B)					
738 (W)	730 (M)	730.	717.	A''	0712 (11) 0932 (11) 0823 (10) 0821 (10) 1312 (4) 1532 (4) C6C1 (4) C3C4 (4) 1645 (3) 1865 (3) 1045 (3) 1265 (3) 1423 (2) 1421 (2) 1156 (2) 1154 (2)	DIAGONAL- CCO (55) HCC (25) CC (9) CO (3) CCC (1) OFF-DIAG- BB19 (7) SB14 (6) SB16 (2) SB17 (2) BB18 (1) CCCO (1) BB28 (-1) SB15 (-2) BB24 (-2) BB23 (-8)
	711 (LT,M)	711.	713.	A'	CC3C (8) CC1C (8) 0821 (7) 0823 (7) 1421 (5) 1423 (5) C400 (4) C602 (4) C3C4 (4) C6C1 (4) C208 (3) CC2C (2) C309 (2) C107 (2) 1312 (2) 1532 (2)	DIAGONAL- CCC (20) HCC (20) CO (17) CC (8) HCO (2) OFF-DIAG- BB19 (7) BB26 (3) SB14 (7) SB16 (1) BB24 (-1) SB17 (2) BB18 (1) SB12 (-1) BB25 (-3)

TABLE XLVI (Continued)

EXPERIMENTAL FREQUENCY (CM-1) RAMAN	INFRARED	ASSIGNED FREQUENCY (CM-1)	CALCULATED FREQUENCY (CM-1)	CALCULATED SYMMETRY SPECIE	SPECTRAL INTERPRETATION --- POTENTIAL ENERGY DISTRIBUTIONS INTERNAL COORDINATES	FORCE CONSTANTS
	665 (W,B)					
617 (W)	608 (W,SH)	608.	626.	A''	1045(13) 1265(13) 0716(12) 0934(12) 1156(7) 1154(7) 0932(6) 0712(6) 1645(6) 1865(6) 1756(5) 1754(5) 1043(4) 1261(4) 1021(2) 1423(2) C3C4(2) C6C1(2) 0821(2) 0823(2)	DIAGONAL- CCO (88) HCC (26) CC (3) CCC (2) OFF-DIAG- BB19(7) SB17(-2) SB16(-2) BB28(-3) BB23(-20)
593 (VW)	584 (M)	584.	586.	A'	0716(11) 0934(11) 1643(5) 1861(5) CC2C(5) CC5C(5) 1756(5) 1754(5) 1316(4) 1534(4) 1154(4) 1156(4) 1043(4) 1261(4) 0823(2) 0821(2) C400(2) C602(2) 1865(2) 1645(2)	DIAGONAL- CCO (45) HCC (33) CCC (11) CO (6) CC (4) HCO (1) OFF-DIAG- SB14(8) BB19(7) BB18(2) BB28(-4) BB23(-13)
509 (VS)		509.	494.	A'	C3C4(9) C6C1(9) C501(8) CC4C(6) CC6C(6) C309(4) C107(4) 1154(4) 1156(4) CC5C(4) C1C2(3) C2C3(3) C5C6(3) C4C5(3)	DIAGONAL- CC (30) CCC (17) CO (16) CCO (14) HCC (3) OFF-DIAG- SB14(8) SB17(6) CCCO(4) BB22(1) BB19(1) SB16(1) SB12(-1) SB15(-1)
467 (M)	450 (W)	458.	442.	A''	0821(10) 0823(10) 1643(10) 1861(10) 1043(7) 1261(7) 1265(4) 1045(4) 1316(4) 1534(4) 1154(4) 1156(4) 0716(3) 0934(3) CC4C(2) CC6C(2) CC3C(2) CC1C(2) 1756(2) 1754(2) C3C4(2) C6C1(2) 1865(2) 1645(2)	DIAGONAL- CCO (55) HCC (35) CCC (9) CC (6) TOCC(4) CO (2) OFF-DIAG- BB19(8) SB16(4) BB18(1) SB17(-2) SB14(-4) BB28(-4) BB25(-5) BB23(-11)
435 (VS)	432 (M)	434.	426.	A'	CC5C(10) C5C6(6) C4C5(6) CC2C(6) C1C2(5) C2C3(5) 1154(5) 1156(5) 1045(4) 1265(4) C400(3) C602(3) CC4C(2) CC6C(2)	DIAGONAL- CCO (23) CC (22) CCC (21) CO (8) HCC (4) HCO (1) OFF-DIAG- SB17(8) SB14(8) SB16(2) BB22(2) BB19(2) BB25(1) CCCO(1) BB23(-1) SB15(-3)
393 (M)	387 (W)	390.	380.	A''	CC3C(10) CC1C(10) CC6C(8) CC4C(8) 0712(6) 0932(6) 0716(5) 0934(5) 1043(4) 1261(4) 1265(4) 1045(4) C4C5(3) C5C6(3) C1C2(2) C2C3(2) 1421(2) 1423(2)	DIAGONAL- CCO (41) CCC (36) CC (11) HCC (5) CO (3) OFF-DIAG- SB14(8) SB17(8) BB22(3) BB25(2) BB20(-1) BB30(-1) SB15(-1) BB26(-2) SB16(-5) BB23(-7)
378 (M)	367 (VW)	373.	347.	A'	1043(15) 1261(15) 0821(8) 0823(8) 1645(7) 1865(7) CC2C(7) 0712(5) 0932(5) 0716(5) 0934(5) 1754(4) 1756(4) 1156(4) 1154(4) CC5C(3) 1421(2) 1423(2)	DIAGONAL- CCO (74) HCC (30) CCC (11) TOCC(3) CO (2) CC (2) OFF-DIAG- BB19(2) BB22(1) SB16(-1) SB15(-2) SB17(-2) BB28(-3) BB25(-5) SB14(-5) BB23(-10)
352 (VW)	344 (SH)					
327 (W)		327.	313.	A'	0712(10) 0932(10) C4C5(7) C5C6(7) C2C3(6) C1C2(6) 1045(6) 1265(6) 1043(6) 1261(6) 0716(6) 0934(6)	DIAGONAL- CCO (59) CC (27) TOCO(4) CCC (3) HCC (3) OFF-DIAG- SB16(14) BB19(2) BB22(-1) BB23(-4) SB17(-6)
312 (W)		312.	299.	A''	1265(13) 1045(13) 0716(13) 0934(13) 1043(11) 1261(11) C4C5(3) C5C6(3) 0932(3) 0712(3) C1C2(3) C2C3(3) 1043(3) 1861(3) 0821(2) 0823(2) 1154(2) 1156(2) 1756(2) 1754(2) 1312(2) 1532(2)	DIAGONAL- CCO (90) HCC (14) CC (12) TOCO(5) CCC (2) TOCC(1) OFF-DIAG- BB20(-1) SB17(-1) BB25(-1) BB19(-2) SB15(-4) SB16(-5) BB23(-12)
296 (W)	294 (SH)	295.	297.	A''	1154(19) 1156(19) 0712(10) 0932(10) 0821(10) 0823(10) 0716(3) 0934(3) TC50(3) C6C1(3) C3C4(3) 1423(2) 1421(2) CC6C(2) CC4C(2)	DIAGONAL- CCO (88) CC (8) TOCO(6) HCC (5) CCC (3) OFF-DIAG- BB20(-1) BB22(-1) BB19(-2) SB17(-2) BB23(-7)
289 (SH)		289.	274.	A'	1045(12) 1265(12) CC5C(9) CC2C(8) 0716(7) 0934(7) 0932(6) 0712(6) 1754(4) 1756(4) 1043(4) 1261(4) CC6C(2) TC40(2) CC4C(2) TC60(2) TC10(2) TC30(2) TC34(2) TC61(2) 1643(2) 1861(2) 0823(2) 0821(2)	DIAGONAL- CCO (64) CCC (23) HCC (15) TOCO(10) TOCC(5) CO (2) OFF-DIAG- BB19(5) SB16(1) BB28(-1) SB14(-2) BB25(-3) BB22(-4) BB23(-13)
	280 (M)	280.	272.	A''	0821(12) 0823(12) 1154(9) 1156(9) 1316(6) 1534(6) 1261(6) 1043(6) 0712(6) 0932(6) TC20(4) CC6C(4) CC4C(4) CC1C(3) CC3C(3) TC50(3) 1645(2) 1865(2) 1265(2) 1045(2)	DIAGONAL- CCO (68) HCC (21) CCC (14) TOCO(9) TOCC(4) CO (2) CC (2) OFF-DIAG- BB19(4) BB18(1) SB15(-1) BB22(-2) BB25(-3) SB14(-3) SB16(-4) BB23(-13)
		204.		A'	CC2C(14) 0821(10) 0823(10) 1316(6) 1534(6) 1643(5) 1861(5) 1154(4) 1156(4) 0716(4) 0934(4) 1865(4) 1645(4) CC3C(4) CC1C(4) 1754(4) 1756(4) 1045(4) 1265(4) 1043(3) 1261(3) 1532(3) 1312(3) 0932(2) 0712(2) CC6C(2) CC4C(2)	DIAGONAL- CCO (54) HCC (43) CCC (26) CO (7) CC (1) OFF-DIAG- BB19(11) SB16(3) BB24(2) SB17(-1) SB15(-2) BB22(-3) BB28(-5) BB25(-9) BB23(-14) SB14(-15)
			177.	A''	TC50(22) TC40(20) TC60(20) TC30(18) TC10(18)	DIAGONAL- TOCO(99)
			172.	A''	TC20(51) TC30(12) TC10(11) TC50(9) TC60(5) TC40(5)	DIAGONAL- TOCO(94) CCO (4) CC (1)
			172.	A'	TC40(28) TC60(27) TC10(21) TC30(19)	DIAGONAL- TOCO(94) CCO (4) HCC (1)
			170.	A''	TC20(40) TC50(18) TC30(17) TC10(16)	DIAGONAL- TOCO(93) CCO (6)
			169.	A''	TC50(43) TC40(22) TC60(21) 1156(2) 1154(2) TC30(2) TC10(2) 1043(2) 1261(2)	DIAGONAL- TOCO(91) CCO (10) HCC (1) OFF-DIAG- SB16(-1) BB23(-1)
			169.	A'	TC10(26) TC30(26) TC60(19) TC40(19)	DIAGONAL- TOCO(90) CCO (8) CCC (2) HCC (1) OFF-DIAG- BB23(-1)

TABLE XLVI (Continued)

EXPERIMENTAL FREQUENCY (CM-1) RAMAN	INFRARED	ASSIGNED FREQUENCY (CM-1)	CALCULATED FREQUENCY (CM-1)	CALCULATED SYMMETRY SPECIE	SPECTRAL INTERPRETATION --- POTENTIAL ENERGY DISTRIBUTIONS
					INTERNAL COORDINATES / FORCE CONSTANTS
			130.	A'	CC1C(9) CC3C(9) TC12(8) DIAGONAL- TOCC(42) CCC (41) CCO (27) TC23(8) CC6C(7) CC4C(7) CO (7) CC (3) HCC (3) TC61(7) TC34(7) TC56(6) OFF-DIAG- SB16(5) CCCO(-1) BB23(-1) TC45(6) CC5C(6) CC2C(4) BB26(-1) BB22(-3) SB17(-11) SB14(-11) 1045(3) 1265(3) 0712(3) 0932(3) 0716(3) 0934(3) 1261(2) 1043(2) 1154(2) 1156(2) 1421(2)
			92.	A'	CC5C(15) TC56(12) TC45(12) DIAGONAL- TOCC(48) CCC (39) CCO (12) TC23(12) TC12(12) CC2C(9) HCC (3) CO (2) CC3C(4) CC1C(4) CC6C(4) OFF-DIAG- SB17(2) BB19(1) BB25(-1) CC4C(3) 1156(3) 1154(3) BB22(-1) SB14(-4)
			89.	A''	TC34(16) TC61(16) CC1C(11) DIAGONAL- TOCC(48) CCC (40) CCO (16) CC3C(10) CC4C(9) CC6C(9) CO (3) HCC (2) TC45(4) TC56(4) TC12(4) OFF-DIAG- SB17(1) BB26(-1) BB23(-1) TC23(4) 1043(2) 1261(2) BB22(-2) SB14(-6) 0716(2) 0934(2) 0712(2) 0932(2)

TABLE XLVII. EPI-INOSITOL

EXPERIMENTAL FREQUENCY (CM-1) RAMAN	INFRARED	ASSIGNED FREQUENCY (CM-1)	CALCULATED FREQUENCY (CM-1)	CALCULATED SYMMETRY SPECIE	SPECTRAL INTERPRETATION --- POTENTIAL ENERGY DISTRIBUTIONS INTERNAL COORDINATES	FORCE CONSTANTS
	3450 (VS)		3357.		O8H0(98) O9H1(2)	DIAGONAL- OH (100)
	3435 (SH)		3357.		O12H(98) O11H(2)	DIAGONAL- OH (100)
	3390 (VS)		3357.		O12H(58)	DIAGONAL- OH (100)
	3370 (VS)		3357.		O9H1(62) O10H(30) O11H(6)	DIAGONAL- OH (100)
	3285 (VS)		3357.		O11H(55) O9H1(26) O10H(17)	DIAGONAL- OH (100)
	3235 (VS)		3357.		O10H(52) O11H(38) O9H1(10)	DIAGONAL- OH (100)
2964 (S)	2960 (SH)		2948.	A'	C4H6(51) C5H7(22) C3H5(22)	DIAGONAL- CH (98)
2951 (M)			2940.	A'	C1H3(35) C2H4(31) C6H8(30) C4H6(2)	DIAGONAL- CH (99)
	2942 (W)		2940.	A''	C3H5(45) C5H7(45) C6H8(4) C2H4(4)	DIAGONAL- CH (99)
2928 (VS)	2930 (VW)		2936.	A''	C6H8(46) C2H4(45) C5H7(4) C3H5(4)	DIAGONAL- CH (99)
	2918 (M)		2937.	A'	C1H3(64) C2H4(18) C6H8(17)	DIAGONAL- CH (99)
2913 (M)	2905 (M)		2933.	A'	C4H6(46) C3H5(27) C5H7(27)	DIAGONAL- CH (99)
	1433 (SH)	1433.	1442.	A'	C4OH(13) C6OH(13) C2OH(13) 1754(6) 1534(6) C1OH(5) 1423(5) 1865(5) 1421(5) 1861(5) HC1O(4) 1756(3) 1532(3) C6C1(2) C1C2(2)	DIAGONAL- COH (45) HCC (18) HCO (6) CC (5) CCO (4) CO (2) CCC (2) OFF-DIAG- BB23(4) BB25(1) BB19(-1) BB18(-1) SB14(-1) SB15(-3)
1428 (W,SH)		1428.	1430.	A''	C5OH(19) C3OH(19) 1643(9) 1645(9) C2OH(8) C6OH(8) HC3O(5) HC5O(5) 1532(2) 1756(2)	DIAGONAL- COH (53) HCC (28) HCO (10) CCO (3) OFF-DIAG- BB23(3) BB29(2) BB28(1) BB18(-1) BB30(-1)
	1418 (M)	1418.	1423.	A'	C4OH(35) C1OH(12) C2OH(7) C6OH(7) HC1O(6) 1754(6) 1534(6) HC4O(5) 1421(3) 1861(3) C1C2(2) C6C1(2)	DIAGONAL- COH (60) HCC (23) HCO (13) CC (6) CCO (2) CCC (2) CO (2) OFF-DIAG- BB29(3) BB23(2) SB12(-1) BB30(-1) SB17(-2) BB18(-2) SB13(-2) SB15(-3)
1410 (SH)	1407 (SH)	1410.	1421.	A''	C6OH(19) C2OH(19) 1861(9) 1421(9) 1865(8) 1423(8) C3OH(7) C5OH(7) C5C6(3) C2C3(3) HC3O(2) HC5O(2) 1643(2) 1645(2)	DIAGONAL- COH (51) HCC (39) CC (6) HCO (5) CCO (3) CO (1) OFF-DIAG- BB23(3) BB29(1) SB17(-1) BB19(-1) SB13(-2) SB15(-4)
1403 (M)		1403.	1411.	A'	C3OH(33) C5OH(33) HC3O(10) HC5O(10) HC4O(2) 1756(2) 1532(2)	DIAGONAL- COH (68) HCO (24) HCC (10) CC (3) CO (2) CCC (2) OFF-DIAG- BB29(5) SB17(-1) SB15(-2) SB12(-2) SB13(-4) BB18(-5)
1395 (M)	1386 (M)	1391.	1403.	A'	C1OH(51) HC1O(16) C2OH(10) C6OH(10) C4OH(3)	DIAGONAL- COH (74) HCO (19) HCC (6) CCO (3) CC (2) CO (1) OFF-DIAG- BB29(4) SB12(-1) BB30(-2) SB13(-3) BB18(-4)
	1379 (LT,W)	1379.	1374.	A''	1316(13) 1312(13) C6OH(12) C2OH(12) 1421(7) 1861(7) 1645(5) 1643(5) 1865(3) 1423(3) C4C5(2) C3C4(2) HC2O(2) HC6O(2) 1754(2) 1534(2) C2C3(2) C5C6(2)	DIAGONAL- HCC (60) COH (24) CC (9) HCO (6) CO (3) CCO (2) CCC (1) OFF-DIAG- SB13(3) BB23(2) BB28(2) BB25(1) BB29(-1) SB14(-1) SB12(-1) SB16(-2) BB18(-2) SB15(-3)
1366 (M)		1366.	1363.	A'	C4OH(22) HC4O(19) 1754(13) 1534(13) 1645(5) 1643(5) C2OH(5) C6OH(5) HC5O(4) HC3O(4) C4OO(4) 1423(3) 1865(3) 1756(2) 1532(2) C4C5(2) C3C4(2)	DIAGONAL- HCC (44) COH (31) HCO (30) CO (7) CC (4) CCO (3) OFF-DIAG- BB28(4) BB29(3) BB23(2) BB30(1) SB14(-1) SB12(-4) SB13(-5) SB15(-6) BB18(-10)
	1352 (M)	1352.	1358.	A''	1534(11) 1754(11) 1316(9) 1312(9) 1532(7) 1756(7) HC2O(6) HC6O(6) C3OH(6) C5OH(6) 1643(5) 1645(5) C2OH(3) C6O2(3) 1423(2) 1865(2) C3C4(2) C4C5(2) HC5O(2) HC3O(2) C2OH(2) C6OH(2)	DIAGONAL- HCC (72) HCO (16) COH (15) CO (7) CC (4) OFF-DIAG- BB28(4) BB29(2) SB14(-1) SB13(-3) SB12(-3) BB18(-5) SB15(-6)
1344 (W)	1341 (M)	1342.	1339.	A'	1861(12) 1421(12) 1865(11) 1423(11) C6OH(11) C2OH(11) HC4O(6) C1OH(3) C1O7(3) C5OH(2) C3OH(2) C1C2(2) C6C1(2) 1645(2) 1643(2)	DIAGONAL- HCC (52) COH (29) HCO (9) CC (5) CO (3) CCO (2) OFF-DIAG- BB23(4) BB26(1) SB13(1) SB12(-1) SB15(-2) BB18(-3)
1322 (M)		1322.	1337.	A''	1643(18) 1645(18) 1423(7) 1865(7) C3OH(6) C5OH(6) C2OH(5) C6OH(5) 1756(4) 1532(4) HC3O(3) HC5O(3) 1421(2) C6O2(2) C2OH(2) HC2O(2) HC6O(2) 1861(2)	DIAGONAL- HCC (65) COH (21) HCO (9) CO (4) CCO (3) OFF-DIAG- BB23(4) BB29(2) BB30(1) BB19(-1) SB14(-2) SB12(-2) SB13(-3) BB18(-4)
1306 (M)	1310 (M)	1308.	1306.	A'	1756(15) 1532(15) HC3O(11) HC5O(11) HC1O(7) C3OH(6) C5OH(6) C1OH(6) HC4O(5) C4OH(4) C2O8(3) C6O2(3) C5O1(3) C3O9(3) 1316(3) 1312(3) HC2O(3) HC6O(3) CC2C(2) CC6C(2) 1645(2) 1643(2)	DIAGONAL- HCC (42) HCO (39) COH (22) CO (14) CCO (5) CCC (5) CC (1) TOCC(1) OFF-DIAG- SB13(5) BB25(4) BB19(-1) BB24(-1) BB30(-2) BB29(-3) SB14(-6) SB12(-7) BB18(-15)
1276 (M)	1280 (W)	1280.	1284.	A'	HC2O(32) HC6O(32) 1423(8) 1865(8) 1421(6) 1861(6) HC1O(6) C1O7(6) HC4O(5)	DIAGONAL- HCO (75) HCC (34) CO (10) CC (4) COH (3) CCC (2) OFF-DIAG- SB13(2) BB23(2) BB26(2) CCCO(-1) BB29(-2) SB14(-2) SB15(-3) SB12(-5) BB18(-23)
	1271 (W)	1271.	1273.	A''	HC6O(19) HC2O(19) 1532(13) 1756(13) 1423(8) 1865(8) 1534(3) 1754(3) HC5O(3) HC3O(3) C3O9(2) C5O1(2) 1316(2) 1312(2) C1C2(2) C6C1(2)	DIAGONAL- HCC (58) HCO (43) CC (8) CO (5) CCO (3) COH (2) CCC (1) OFF-DIAG- BB23(4) SB13(1) BB28(-1) SB17(-1) SB14(-2) SB15(-5) BB18(-13)
1258 (W)		1258.	1258.	A''	1316(18) 1312(18) HC2O(12) HC6O(12) 1421(8) 1861(8) 1756(4) 1532(4) 1534(3) 1754(3) 1645(2) 1643(2)	DIAGONAL- HCC (71) HCO (25) COH (3) CC (2) CO (2) CCO (2) OFF-DIAG- BB23(3) SB12(2) BB27(1) BB29(-1) BB28(-1) BB18(-7)

Conventional symbolism indicating relative intensity: s = strong, m = medium, w = weak, sh = shoulder, b = broad, v = very, lt = low temperature band

TABLE XLVII (Continued)

EXPERIMENTAL FREQUENCY (CM-1) RAMAN	INFRARED	ASSIGNED FREQUENCY (CM-1)	CALCULATED FREQUENCY (CM-1)	CALCULATED SYMMETRY SPECIE	SPECTRAL INTERPRETATION --- POTENTIAL ENERGY DISTRIBUTIONS INTERNAL COORDINATES	FORCE CONSTANTS
1252 (W)	1251 (M)	1251.	1249.	A'	HC10(39) C10H(18) HC40(10) 1312(8) 1316(8) C40H(6) HC20(6) HC60(6) 1532(5) 1756(5) HC50(2) HC30(2) 1645(2) 1643(2)	DIAGONAL- HCO (65) HCC (33) COH (25) TOCC(-2) CCC (1) CC (1) OFF-DIAG- SB13 (2) SB15 (-3) BB19(-1) SB12(-2) BB29(-5) BB18(-18)
1243 (W,SH)	1233 (W)	1239.	1239.	A''	HC50(31) HC30(31) C30H(12) C50H(12) 1534(11) 1754(11) 1756(2) 1532(2) 1643(2) 1645(2)	DIAGONAL- HCO (64) HCC (32) COH (24) TOCC(1) OFF-DIAG- BB23(2) BB28(-2) BB29(-5) BB18(-18)
1204 (W)	1202 (M)	1203.	1221.	A'	HC40(35) C40H(14) HC50(13) HC30(13) HC10(7) 1645(6) 1643(6) C30H(6) C50H(6) 1754(4) 1534(4) C10H(2)	DIAGONAL- HCO (71) COH (28) HCC (27) CCC (1) OFF-DIAG- BB25(1) SB13(1) BB23(-1) SB12(-1) BB19(-2) BB28(-3) BB29(-5) BB18(-19)
1147 (W)	1149 (M,SH)	1148.	1142.	A'	C400(19) C309(14) C501(14) C208(8) C602(8) C5C6(7) C2C3(7) CC4C(6) C107(6) CC3C(5) CC5C(5) 0934(3) 1154(3) 1045(2) 1043(2) HC60(2) HC20(2) CC1C(2)	DIAGONAL- CO (69) CCC (18) CC (17) CCO (12) HCO (5) COH (2) HCC (2) OFF-DIAG- SB12(4) BB19(1) BB22(1) SB13(-4) SB17(-4) CCCO(-6) SB14(-19)
1130 (S)	1136 (S)	1133.	1123.	A''	C1C2(41) C6C1(41) HC20(8) HC60(8) 1316(4) 1312(4) CC2C(4) CC6C(4) 0716(4) 0712(4) 0932(3) 1156(3) C4C5(3) C3C4(3) C309(3) C501(3) 0821(2) 1261(2) C208(2) C602(2)	DIAGONAL- CC (88) CCO (21) HCO (17) HCC (15) CCC (10) CO (9) OFF-DIAG- BB22(1) BB19(-1) SB14(-2) SB12(-2) BB25(-3) CCCO(-3) SB17(-13) SB15(-14) SB16(-20)
1125 (SH)	1131 (S,SH)	1128.	1114.	A'	C107(19) C400(10) C2C3(8) C5C6(8) C208(6) C602(6) C501(6) C309(6) HC10(5) C3C4(5) C4C5(5) HC30(5) HC50(5) CC2C(5) CC6C(5) HC20(4) HC60(4) 0712(3) 0716(3) 1156(2) 0932(2) C10H(2) C30H(2) C50H(2)	DIAGONAL- CO (51) CC (28) HCO (24) CCO (15) CCC (11) COH (8) HCC (2) OFF-DIAG- SB12(4) BB30(2) BB22(1) BB23(-2) BB18(-2) SB16(-3) SB15(-3) CCCO(-4) SB17(-6) SB13(-7) SB14(-17)
1085 (SH)	1086 (S)	1086.	1092.	A''	C2C3(27) C5C6(27) C3C4(20) C4C5(20) C208(5) C602(5) C20H(4) C60H(4) C1C2(2) C6C1(2) C501(2) C309(2)	DIAGONAL- CC (97) CO (12) CCO (10) COH (8) HCC (5) HCO (2) CCC (1) OFF-DIAG- BB19(-1) CCCC(-2) SB12(-2) CCCO(-2) SB17(-3) SB13(-4) SB15(-7) SB16(-15)
1079 (S)	1076 (SH)	1079.	1082.	A'	C400(20) C208(18) C602(18) C4C5(10) C3C4(10) CC4C(7) C1C2(5) C6C1(5) HC40(4) 1154(4) 0934(4) C107(4) CC1C(3) 1265(3) 0823(3) HC10(2)	DIAGONAL- CO (62) CC (30) CCO (16) CCC (11) HCO (9) HCC (3) COH (3) OFF-DIAG- BB19(2) BB18(1) SB15(1) BB30(1) SB12(-2) SB16(-3) CCCO(-6) SB17(-13) SB14(-16)
1066 (VW)	1062 (VS)	1062.	1068.	A'	C400(37) C5C6(12) C2C3(12) C501(11) C309(11) C107(9) HC40(3) C40H(3) CC1C(2)	DIAGONAL- CO (68) CC (27) CCO (7) COH (6) HCC (5) HCO (4) CCC (4) OFF-DIAG- SB12(4) SB15(-1) SB17(-1) SB16(-3) CCCO(-4) SB13(-6) SB14(-9)
1050 (M)	1047 (VS)	1048.	1063.	A''	C309(25) C501(25) C3C4(13) C4C5(13) C602(9) C208(9) C1C2(5) C6C1(5) 1043(3) 1045(3) CC3C(3) CC5C(3) 1421(2) 1861(2) C5C6(2) C2C3(2) 1316(2) 1312(2)	DIAGONAL- CO (69) CC (40) HCC (12) CCO (11) CCC (6) HCO (2) OFF-DIAG- SB16(-2) SB12(-2) BB23(-3) SB15(-5) SB17(-8) CCCO(-9) SB14(-10)
1023 (M)	1033 (S)	1028.	1015.	A'	C107(50) C4C5(9) C3C4(9) C309(8) C501(8) C5C6(7) C2C3(7) 1421(3) 1861(3) C400(3)	DIAGONAL- CO (69) CC (31) HCC (11) CCO (8) COH (5) CCC (3) HCO (2) OFF-DIAG- BB23(-3) SB13(-4) SB15(-4) SB14(-8) SB16(-8)
988 (W)	984 (M)	986.	989.	A''	C309(21) C501(21) C208(17) C602(17) C3C4(7) C4C5(7) 0821(2) 1261(2) 1045(2) 1043(2) C2C3(2) C5C6(2) C1C2(2) C6C1(2)	DIAGONAL- CO (76) CC (21) CCO (12) HCC (8) CCC (3) COH (3) HCO (2) OFF-DIAG- CCCO(5) SB12(2) BB30(1) SB17(-3) SB16(-5) SB13(-5) SB14(-18)
919 (S)	919 (M)	919.	931.	A'	C1C2(9) C6C1(9) C208(9) C602(9) C4C5(8) C3C4(8) 1532(6) 1756(6) C5C6(6) C2C3(6) HC40(4) CC5C(3) CC3C(3) CC4C(2) 1045(2) 1043(2) 1154(2) 0934(2) C107(2)	DIAGONAL- CC (45) CO (19) HCC (18) CCC (9) CCO (9) HCO (8) COH (3) OFF-DIAG- SB15(7) BB19(3) BB18(2) CCCO(1) BB30(1) SB14(-2) SB16(-9) SB17(-15)
910 (W)	902 (S)	902.	911.	A''	C208(18) C602(18) C2C3(12) C5C6(12) C3C4(8) C4C5(8) 1043(6) 1045(6)	DIAGONAL- CC (39) CO (38) CCO (23) HCC (7) HCO (2) CCC (2) OFF-DIAG- CCCO(6) SB15(4) BB19(2) SB12(2) SB17(-5) SB14(-9) SB16(-11)
874 (M)	872 (M)	873.	874.	A'	C1C2(20) C6C1(20) 0821(6) 1261(6) 1156(4) 0932(4) C208(4) C602(4) 1421(3) 1861(3) C400(3) C501(2) C309(2) CC1C(2) CC6C(2) CC2C(2)	DIAGONAL- CC (40) CCO (23) CO (17) HCC (12) CCC (7) HCO (2) OFF-DIAG- BB19(5) SB15(4) BB23(2) CCCO(2) BB26(1) SB14(-3) SB16(-12)
791 (M)	793 (S)	792.	805.	A'	CC1C(12) C602(9) C208(9) 0821(7) 1261(7) 1316(6) 1312(6) C6C1(6) C1C2(6) C400(2) 0716(2) 0712(2) C4C5(2) C3C4(2) 1423(2) 1865(2)	DIAGONAL- CO (21) CCO (21) HCC (16) CC (16) CCC (13) COH (2) OFF-DIAG- SB14(9) BB19(5) CCCO(3) SB15(2) SB16(2) BB26(1) BB23(-1) SB13(-2) BB24(-2) SB17(-8)
750 (W,B)						
718 (M)	716 (S)	717.	705.	A'	C400(9) 0712(6) 0716(6) C4C5(6) C3C4(6) 0823(6) 1265(6) 1156(4) 0932(4) 1261(4) 0821(4) 1423(3) 1865(3) C107(2) 1316(2) 1312(2) CC3C(2) CC5C(2) 1154(2) 0934(2) 1756(2) 1532(2)	DIAGONAL- CCO (46) HCC (13) CC (13) CO (12) CCC (8) COH (1) OFF-DIAG- SB14(8) BB19(5) CCCO(2) SB15(-1) BB24(-2) BB23(-4)
695 (VVW)	689 (W)	689.	698.	A''	1265(13) 0823(13) 1156(5) 0932(5) 1532(5) 1756(5) 1423(4) 1865(4) CC3C(4) CC5C(4) 1534(3) 1754(3) 0716(3) 0712(3) 1645(2) 1641(2) C4C5(2) C3C4(2)	DIAGONAL- CCO (44) HCC (29) CCC (9) CC (4) CO (3) COH (3) OFF-DIAG- BB19(8) SB14(3) SB16(3) BB26(2) BB18(2) SB13(-1) BB30(-1) BB28(-1) BB25(-2) BB24(-3) BB23(-4)

TABLE XLVII (Continued)

EXPERIMENTAL FREQUENCY (CM-1) RAMAN	INFRARED	ASSIGNED FREQUENCY (CM-1)	CALCULATED FREQUENCY (CM-1)	CALCULATED SYMMETRY SPECIE	SPECTRAL INTERPRETATION --- POTENTIAL ENERGY DISTRIBUTIONS INTERNAL COORDINATES	FORCE CONSTANTS
625 (VW,B)						
	569 (M)					
556 (M)	552 (M)	554.	557.	A''	0934(18) 1154(18) 0716(12) 0712(12) 1045(7) 1043(7) 1643(5) 1645(5) 0932(4) 1156(4) 1534(3) 1754(3) 1421(3) 1861(3) 0821(3) 1261(3) C3C4(2) C4C5(2) C1C2(2) C6C1(2)	DIAGONAL- CCO (87) HCC (26) CC (9) CCC (3) TOCC (1) OFF-DIAG- BB19(5) BB25(-1) SB15(-2) BB28(-2) SB16(-3) SB17(-4) BB23(-22)
501 (M,SH)	501 (S)	501.	518.	A''	0934(7) 1154(7) 1421(6) 1861(6) C1C2(6) C6C1(6) 0821(5) 1261(5) 0716(5) 0712(5) 1156(5) 0932(5) CC2C(4) CC6C(4) CC5C(2) CC3C(2) 1754(2) 1534(2)	DIAGONAL- CCO (45) HCC (20) CC (15) CCC (13) CO (2) OFF-DIAG- SB17(6) BB19(6) SB14(5) BB18(1) BB25(1) SB16(-2) SB15(-4) BB23(-9)
518 (VS)		518.	491.	A'	C3C4(7) C4C5(7) C309(6) C501(6) CC4C(6) C6C1(5) C1C2(5) C107(5) C5C6(4) C2C3(4) CC2C(2) CC6C(2) 0932(2) 1156(2)	DIAGONAL- CC (34) CO (17) CCC (13) CCO (12) HCC (1) HCO (1) OFF-DIAG- SB14(9) SB17(7) CCCO(5) SB16(1) BB22(1) SB12(-1) SB15(-2)
	452 (M,B)					
431 (M)		431.	427.	A'	CC4C(14) CC1C(7) 0716(7) 0712(7) CC5C(6) CC3C(6) C2C3(6) C5C6(6) 1043(4) 1045(4) C400(3) 0934(3) 1154(3) 1423(2) 1865(2) CC6C(2) CC2C(2) C107(2)	DIAGONAL- CCO (61) HCC (27) CC (7) CCC (6) TOCC (2) OFF-DIAG- SB16(6) BB19(5) SB15(-1) SB17(-2) BB25(-2) BB28(-3) BB23(-9)
	417 (W)					
385 (M)	386 (M)	385.	393.	A'	0823(16) 1265(16) 1045(12) 1043(12) 1643(8) 1645(8) 1534(4) 1754(4) C2C3(2) C5C6(2) 1156(2) 0932(2) CC2C(2) CC6C(2)	DIAGONAL- CCC (37) CCO (29) CC (14) HCC (6) CO (5) OFF-DIAG- SB17(9) SB14(9) BB22(2) BB26(-2) SB16(-2) BB23(-3) SB15(-3)
367 (M)	350 (M)	358.	338.	A''	0821(21) 1261(21) 1156(11) 0932(11) CC2C(4) CC6C(4) 0716(3) 0712(3) CC5C(3) CC3C(3) 1423(2) 1865(2) C2C3(2) C5C6(2) 0934(2) 1154(2)	DIAGONAL- CCO (75) CCC (15) HCC (6) CC (5) TOCO (2) CO (1) OFF-DIAG- BB22(2) SB15(1) SB16(1) SB17(1) BB20(-1) BB19(-1) BB23(-6)
321 (W)	313 (W)	317.	303.	A''	1043(27) 1045(27) C2C3(8) C5C6(8) 1154(7) 0934(7) 0716(7) 0712(7) TC40(3) 1756(2) 1532(2) 1261(2) 0821(2) TC10(2) CC2C(2) CC6C(2) 1156(2) 0932(2)	DIAGONAL- CCO (89) CC (16) HCC (10) TOCO(5) CCC (3) OFF-DIAG- BB20(-1) BB19(-3) SB17(-4) SB15(-5) BB23(-10)
306 (W)	295 (SH)	306.	297.	A'	0932(18) 1156(18) 0934(18) 1154(18) CC4C(4) C4C5(3) C3C4(3) TC30(3) TC50(3) C6C1(2) C1C2(2) 0821(2) 1261(2) 1423(2) 1865(2) 1265(2) 0823(2)	DIAGONAL- CCO (80) CC (12) TOCO(7) CCC (6) HCC (6) OFF-DIAG- SB16(4) BB20(-1) BB22(-2) SB17(-3) BB23(-9)
285 (M)	285 (M)	285.	294.	A''	0716(19) 0712(19) 0821(8) 1261(8) 1265(7) 0823(7) 0934(5) 1154(5) 1045(5) 1043(5) TC10(3) 1156(2) 0932(2)	DIAGONAL- CCO (92) TOCO(6) HCC (5) CC (4) CCC (3) OFF-DIAG- SB16(1) SB17(-1) BB20(-1) BB22(-1) BB19(-2) BB23(-7)
252 (M)	243 (SH)	252.	259.	A'	0821(12) 1261(12) 1265(6) 0823(6) CC4C(6) 1534(5) 1754(5) 1645(4) 1643(4) CC1C(3) 0716(3) 0712(3) 1316(3) 1312(3) 0934(2) 1154(2) CC5C(2) CC3C(2) 0932(2) 1156(2)	DIAGONAL- CCO (53) HCC (24) CCC (15) TOCC(5) CO (3) TOCO(3) HCO (2) OFF-DIAG- BB19(7) BB24(3) BB18(2) BB28(-2) BB25(-4) SB14(-5) BB23(-7)
234 (VW,SH)	236 (M)	236.	251.	A''	0823(19) 1265(19) CC6C(10) CC2C(10) 1156(6) 0932(6) CC3C(5) CC5C(6) 1534(3) 1754(3) 1043(2) 1045(2) TC45(2) TC34(2) TC30(2) TC50(2)	DIAGONAL- CCO (56) CCC (28) HCC (12) TOCC(6) TOCO(5) CO (2) CC (1) OFF-DIAG- BB19(2) BB24(2) SB16(1) BB18(1) SB15(-1) BB22(-2) SB17(-2) BB25(-3) BB23(-3) SB14(-4)
		207.	A'	TC20(9) TC60(9) CC2C(7) CC6C(7) 1265(7) 0823(7) CC1C(6) 0821(5) 1261(5) 1534(4) 1754(4) 1645(3) 1643(3) 1043(3) 1045(3) 0934(3) 1154(3) 0932(2) 1156(2) 1316(2) 1312(2) 1532(2) 1756(2)	DIAGONAL- CCO (42) HCC (26) CCC (24) TOCO(18) CO (5) CC (1) OFF-DIAG- BB19(6) SB16(3) BB24(2) BB26(-1) BB22(-2) BB28(-2) SB15(-2) BB23(-5) BB25(-6) SB14(-11)
		180.	A'	TC60(31) TC20(31) TC10(21) TC40(8) TC50(4) TC30(4)	DIAGONAL- TOCO(98)
		175.	A''	TC50(25) TC30(25) TC40(24) TC60(11) TC20(11)	DIAGONAL- TOCO(97) CCO (2)
		174.	A'	TC20(36) TC60(36) CC2C(3) CC6C(3) 0821(3) 1261(3) 0716(2) 0712(2) TC12(2) TC61(2)	DIAGONAL- TOCO(74) CCO (14) CCC (8) HCC (5) TOCC(4) CO (2) OFF-DIAG- SB16(2) BB23(-1) SB17(-2) BB25(-2) SB14(-3)
		171.	A''	TC10(45) TC40(39) TC20(3) TC60(2) TC50(2) TC30(2)	DIAGONAL- TOCO(94) CCO (6)
		170.	A'	TC30(45) TC50(45) 0932(2) 1156(2)	DIAGONAL- TOCO(92) CCO (6) CCC (1)
		169.	A''	TC10(28) TC40(22) TC30(17) TC50(17) TC20(4) TC60(4)	DIAGONAL- TOCO(90) CCO (8) CCC (2)
		128.	A'	CC1C(10) CC5C(7) CC3C(7) CC4C(7) TC23(7) TC56(7) TC45(7) TC34(7) TC12(6) TC61(6) CC2C(3) CC6C(3) TC60(3) TC20(3) 1043(3) 1045(3) 0716(2) 0712(2) 0932(2) 1156(2) 1154(2) 0934(2) C400(2) 1423(2) 1865(2)	DIAGONAL- TOCC(40) CCC (38) CCO (23) HCC (6) CO (6) TOCO(6) CC (2) OFF-DIAG- SB16(3) BB19(2) BB22(-2) BB26(-3) BB23(-3) SB17(-8) SB14(-9)

TABLE XLVII (Continued)

EXPERIMENTAL FREQUENCY (CM-1) RAMAN	INFRARED	ASSIGNED FREQUENCY (CM-1)	CALCULATED FREQUENCY (CM-1)	CALCULATED SYMMETRY SPECIE	SPECTRAL INTERPRETATION --- POTENTIAL ENERGY DISTRIBUTIONS INTERNAL COORDINATES	FORCE CONSTANTS
			92.	A''	TC23(15) TC56(15) CC5C(13) CC3C(13) CC2C(6) CC6C(6) TC12(4) TC61(4) TC34(4) TC45(4) 0932(3) 1156(3) 1423(2) 1865(2) 1154(2) 0934(2)	DIAGONAL- TOCC(47) CCC (38) CCO (10) HCC (5) CO (2) HCO (1) TOCO(1) OFF-DIAG- SB17(3) BB19(2) BB25(-1) BB26(-2) BB23(-2) SB14(-3)
			88.	A'	CC1C(16) TC34(12) TC45(12) CC4C(12) TC12(12) TC61(12) CC5C(3) CC3C(3) 0716(3) 0712(3) 1043(2) 1045(2) CC6C(2) CC2C(2)	DIAGONAL- TOCC(48) CCC (39) CCO (14) HCC (4) CO (3) OFF-DIAG- SB17(2) BB22(-1) BB26(-2) BB23(-2) SB14(-5)

TABLE XLVIII. CIS-INOSITOL

EXPERIMENTAL FREQUENCY (CM-1) RAMAN	INFRARED	ASSIGNED FREQUENCY (CM-1)	CALCULATED FREQUENCY (CM-1)	CALCULATED SYMMETRY SPECIES	SPECTRAL INTERPRETATION --- POTENTIAL ENERGY DISTRIBUTIONS INTERNAL COORDINATES	FORCE CONSTANTS
	3500 (S)		3357.		O10H(48) O8HO(32) O12H(19)	DIAGONAL- OH (100)
	3442 (S)		3357.		O8HO(49) O10H(47) O12H(4)	DIAGONAL- OH (100)
	3385 (VS)		3357.		O12H(77) O8HO(19) O10H(4)	DIAGONAL- OH (100)
	3320 (VS)		3357.		O9H1(66) O11H(25) O7H9(8)	DIAGONAL- OH (100)
	3240 (SH)		3357.		O7H9(76) O11H(24)	DIAGONAL- OH (100)
			3357.		O11H(50) O9H1(33) O7H9(16)	DIAGONAL- OH (100)
2966 (S)	2965 (VW)		2942.	A1	C6H8(26) C2H4(26) C4H6(26) C1H3(7) C5H7(7) C3H5(7)	DIAGONAL- CH (99)
2952 (M)	2952 (VW)		2939.	E	C5H7(48) C2H4(18) C1H3(13) C3H5(10) C4H6(5) C6H8(4)	DIAGONAL- CH (99)
			2939.	E	C3H5(37) C1H3(34) C6H8(14) C4H6(13)	DIAGONAL- CH (99)
2932 (S)	2930 (W)		2938.	A1	C1H3(27) C3H5(26) C5H7(26) C6H8(7) C4H6(7) C2H4(7)	DIAGONAL- CH (99)
			2936.	E	C2H4(38) C6H8(34) C5H7(14) C3H5(13)	DIAGONAL- CH (99)
			2936.	E	C4H6(48) C1H3(18) C6H8(14) C2H4(10) C3H5(5) C5H7(4)	DIAGONAL- CH (99)
1450 (W)	1452 (M)	1451.	1425.	A1	C1OH(13) C3OH(13) C5OH(13) C2OH(9) C6OH(9) C4OH(9) HC1C(8) HC3O(8) HC5O(8)	DIAGONAL- COH (68) HCO (25) HCC (5) CCC (3) CO (2) OFF-DIAG- BB29(3) BB30(2) SB12(-3) SB13(-3) EB18(-5)
	1425 (VW,SH)	1425.	1420.	E	C5OH(24) C2OH(13) HC5O(13) C3OH(10) C6OH(6) HC3O(5) 1643(3) 1532(3) C1OH(3) 1645(3) 1312(3) 1861(2) 1756(2) HC2O(2) 1865(2) C5C1(2) C4OH(2) HC1O(2)	DIAGONAL- COH (57) HCC (23) HCC (19) CC (4) CO (3) CCC (2) OFF-DIAG- BB29(3) SB17(-1) SB13(-2) SB15(-3) SB12(-3) BB18(-5)
			1420.	E	C1OH(22) C3OH(15) C4OH(12) HC1C(12) C6OH(8) HC3O(8) 1423(3) 1421(3) 1534(3) 1316(3) 1754(2) HC4O(2) 1865(2)	DIAGONAL- COH (57) HCO (23) HCC (19) CC (4) CO (3) CCC (2) OFF-DIAG- EB29(2) SB17(-1) SB13(-2) SB15(-3) SB12(-3) BB18(-5)
1413 (W)	1415 (M)	1414.	1401.	E	C2OH(36) C4OH(12) C5OH(12) C6OH(6) HC5O(4) C1OH(4) HC2O(3) 1865(3) C1C2(2) 1645(2) C3OH(2) C2C3(2) 1861(2) C4C5(2)	DIAGONAL- COH (72) HCC (12) HCO (10) CC (7) CO (2) CCC (1) CCC (1) OFF-DIAG- SB15(-1) SB12(-1) SB16(-1) BB18(-2) SB17(-2)
1400 (W)	1398 (M)	1399.	1401.	E	C6OH(30) C4OH(24) C3OH(10) C1OH(8) HC3O(3) HC1O(3) 1423(3) 1421(2) C6C1(2) C3C4(2) HC6O(2) HC4O(2)	DIAGONAL- COH (72) HCC (12) HCO (10) CC (7) CO (2) CCC (1) CCC (1) OFF-DIAG- SB15(-1) SB12(-1) SB16(-1) BB18(-2) SB17(-2)
			1392.	A2	1421(12) 1423(12) 1643(12) 1645(12) 1865(12) 1861(12) 1316(3) 1312(3) 1754(3) 1756(3) 1532(3) 1534(3)	DIAGONAL- HCC (86) CCO (4) CC (3) OFF-DIAG- BB23(8) SB15(3) SB16(-1) BB27(-2) BB19(-2)
	1382 (W)	1382.	1386.	A1	C4OH(21) C6OH(21) C2OH(21) C5OH(9) C1OH(9) C3OH(9) HC1C(3) HC3O(3) HC5O(3)	DIAGONAL- COH (90) HCC (11) CC (3) HCC (2) CO (1) OFF-DIAG- SB15(-1) BB18(-2) SB13(-3)
	1354 (M)	1354.	1376.	B	1861(16) 1643(13) C5OH(13) 1865(12) 1645(8) 1532(5) C1OH(4) 1534(4) 1312(4) 1316(3) C3OH(2)	DIAGONAL- HCC (67) COH (20) CCC (5) CC (4) CO (3) HCC (2) OFF-DIAG- EB23(6) SB13(2) BB30(-2) BB19(-2) SB14(-2) SB15(-4)
	1351 (LT,SH)	1351.	1376.	E	1421(17) 1423(15) C3OH(11) 1645(8) C1OH(8) 1756(6) 1754(6) 1865(5) 1643(3) 1316(3)	DIAGONAL- HCC (67) COH (20) CCO (5) CC (4) CO (3) HCO (2) OFF-DIAG- BB23(6) SB13(2) EB3C(-2) BB19(-2) SB14(-2) SB15(-4)
1335 (SH)	1333 (M)	1333.	1338.	E	1316(15) 1312(15) C6OH(8) HC6O(8) 1423(8) 1756(7) 1643(7) 1865(6) C2OH(6) HC2O(6) C6O2(5) 1754(5) 1645(4) C2O8(4) 1532(3) C3C4(2) C4C5(2)	DIAGONAL- HCC (72) COH (16) HCC (10) CC (10) CC (7) CCO (2) OFF-DIAG- BB29(2) BB26(1) BB30(1) SB17(-2) EB24(-2) SB14(-3) SB12(-4) SB13(-4) BB18(-6) SB15(-7)
1319 (SH)		1319.	1338.	E	1534(14) 1532(12) 1754(10) C4OH(10) HC4O(9) 1421(9) 1756(8) 1861(8) C4O2(6) HC2O(4) 1645(4) C2OH(4) HC2O(4) C2O8(2) 1865(2) C6C1(2) 1643(2) C5C6(2) C1C2(2)	DIAGONAL- HCC (72) COH (16) HCO (14) CO (10) CC (7) CCC (2) OFF-DIAG- EB29(2) BB26(1) BB30(1) SB17(-2) EB24(-2) SB14(-3) SB12(-4) SB13(-4) BB18(-6) SB15(-7)
1309 (M)	1310 (M)	1310.	1302.	A1	HC1O(10) HC3O(10) HC5O(10) HC4O(7) HC2O(7) HC6O(7) C1O7(6) C3O9(6) C5O1(6) C1OH(6) C3OH(6) C5OH(6) 1534(2) 1754(2) 1756(2) 1316(2) 1312(2) 1532(2) 1423(2) 1861(2) 1645(2) 1421(2) 1643(2) 1865(2) CC2C(2) CC4C(2) CC6C(2)	DIAGONAL- HCO (49) HCC (27) CO (19) CCH (18) CCC (6) CCO (3) CC (3) OFF-DIAG- SB13(7) BB25(3) EB23(3) BB26(-1) CCCO(-1) BB30(-2) BB29(-3) SB14(-6) SB12(-7) BB18(-17)
1294 (SH)	1291 (M)	1291.	1273.	A1	HC6O(20) HC4O(20) HC2O(20) HC1O(5) HC3O(5) HC5O(5) 1865(4) 1861(4) 1421(4) 1423(4) 1643(4) 1645(4) C1OH(4) C3OH(4) C5OH(4) C2O8(3) C4O6(3) C6O2(3) 1756(2) 1532(2) 1534(2) 1316(2) 1312(2) 1754(2)	DIAGONAL- HCO (77) HCC (36) COH (14) CC (8) CC (2) TOCC (2) CCO (2) CCC (1) OFF-DIAG- BB25(1) SB17(-1) BB19(-2) SB14(-2) SB13(-2) BB23(-2) SB12(-7) BB18(-25)
	1262 (M)	1262.	1266.	E	HC4O(29) HC2O(28) 1643(7) 1423(7) 1645(4) 1421(4) 1534(3) 1532(3) 1754(3) 1312(3) HC1O(2) HC5O(2)	DIAGONAL- HCO (61) HCC (36) CC (4) CC (3) COH (2) CCO (2) TOCC (1) OFF-DIAG- SB15(4) SB12(3) BB23(3) BB19(1) SB14(-1) BB29(-1) BB18(-18)
1253 (W)		1253.	1266.	E	HC6O(38) HC2O(10) HC4O(9) 1865(7) 1316(4) 1861(7) 1645(4) 1756(4) 1421(4) HC3C(3) C6O2(2)	DIAGONAL- HCO (61) HCC (36) CO (4) CC (3) COH (2) CCO (2) TOCC (1) OFF-DIAG- SB15(4) SB12(3) BB23(3) BB19(1) SB14(-1) BB29(-1) BB18(-18)

TABLE XLVIII (Continued)

EXPERIMENTAL FREQUENCY (CM-1) RAMAN	INFRARED	ASSIGNED FREQUENCY (CM-1)	CALCULATED FREQUENCY (CM-1)	CALCULATED SYMMETRY SPECIES	SPECTRAL INTERPRETATION --- POTENTIAL ENERGY DISTRIBUTIONS INTERNAL COORDINATES	FORCE CONSTANTS
	1244 (M)	1244.	1251.	A2	1312(15) 1532(15) 1534(15) 1754(15) 1316(15) 1756(15) 1643(3) 1645(3) 1421(3) 1423(3) 1865(3) 1861(3)	DIAGONAL- HCC (105) CC (3) OFF-DIAG- BB27 (2) SB15 (-9)
1236 (W,SH)	1229 (SH)	1229.	1242.	E	HC30(40) HC50(21) C30H(15) 1534(9) 1754(8) C5CH(8) 1532(6) 1312(4) HC10(3) HC60(2)	DIAGONAL- HCO (68) HCC (30) COH (24) TCCC (1) OFF-DIAG- SB13 (1) SB12 (-2) BB29 (-5) BB18 (-19)
1212 (VW)	1212 (W)	1212.	1242.	E	HC10(40) HC50(22) C10H(15) 1316(9) C50H(8) 1756(8) 1312(6) 1532(3) HC30(3) HC40(2)	DIAGONAL- HCO (68) HCC (30) CCH (24) TCCC (1) OFF-DIAG- SB13 (1) SB12 (-2) BB29 (-5) BB18 (-19)
1159 (W)	1157 (VW,SH)	1159.	1128.	A1	C3C9 (16) C1C7 (16) C5C1 (16) HC20 (5) HC40 (5) HC60 (5) C4C0 (4) C2C8 (4) C6C2 (4) CC3C (3) CC5C (3) CC1C (3) CC2C (2) CC6C (2) CC4C (2) HC10 (2) HC50 (2) HC30 (2)	DIAGONAL- CO (62) HCO (19) CCC (13) CC (7) HCC (3) CCC (3) CCH (2) OFF-DIAG- SB12 (9) SB16 (3) SB15 (2) BB19 (2) SB17 (-1) BB25 (-1) BB18 (-3) SB13 (-3) CCCO (-5) SB14 (-11)
	1144 (M,LT)	1144.	1120.	A2	C1C2 (19) C2C3 (19) C3C4 (19) C4C5 (19) C6C1 (19) C5C6 (19) 0823 (3) 0821 (3) 1043 (3) 1045 (3) 1265 (3) 1261 (3)	DIAGONAL- CC (116) CCO (16) HCC (7) OFF-DIAG- BB19 (-2) CCCC (-2) SB15 (-13) SB16 (-21)
1132 (SH)	1134 (S)	1134.	1111.	E	C6C1 (25) C1C2 (22) C3C4 (17) C4C5 (11) HC20 (10) HC60 (8) C2C8 (6) 1316 (5) C602 (5) CC2C (5) 1312 (4) 0932 (4) C5C1 (4) 0712 (4) C20H (4) 1156 (4) CC6C (3) C3C9 (3) C2C3 (3) 0716 (3) C60H (3) 1534 (2) 1043 (2) 1045 (2)	DIAGONAL- CC (79) CCC (21) HCO (19) CO (18) HCC (15) CCC (10) COH (7) OFF-DIAG- BB29 (1) BB22 (1) BB24 (-1) BB18 (-1) BB23 (-1) BB19 (-2) BB25 (-3) SB13 (-4) SB12 (-4) SB14 (-4) CCCO (-5) SB17 (-14) SB15 (-14) SB16 (-17)
1123 (W)		1123.	1111.	E	C5C6 (26) C2C3 (23) C4C5 (15) HC40 (12) C3C4 (10) C4C0 (7) CC4C (5) 0934 (5) C1C7 (5) 1154 (5) 1756 (4) C4CH (4) HC6C (4) C1C2 (4) 1532 (4) 1754 (4) C602 (3) 1534 (2) 0716 (2) HC20 (2) CC6C (2) C3C9 (2) 0823 (2) C60H (2)	DIAGONAL- CC (79) CCC (21) HCC (19) CC (18) HCC (15) CCC (10) CCH (7) OFF-DIAG- BB29 (1) BB22 (1) BB24 (-1) BB18 (-1) BB23 (-1) BB19 (-2) BB25 (-3) SB13 (-4) SB12 (-4) SB14 (-4) CCCC (-5) SB17 (-14) SB15 (-14) SB16 (-17)
1085 (M)	1092 (S)	1089.	1097.	A1	C2C8 (21) C4C0 (21) C602 (21) HC1C (5) HC3C (5) HC5C (5) C1C7 (4) C5C1 (4) C3C9 (4) CC2C (3) CC4C (3) CC6C (3) 1045 (2) 1265 (2) 1261 (2) 0821 (2) 0823 (2) 1043 (2) C4C5 (2) C6C1 (2) C1C2 (2) C3C4 (2) C5C6 (2) C2C3 (2) C1OH (2) C3OH (2) C5OH (2)	DIAGONAL- CC (74) CCO (20) HCO (15) CCC (11) CC (11) CCH (6) HCC (3) OFF-DIAG- BB30 (3) BB19 (2) SB12 (2) BB22 (1) BB23 (-2) CCCO (-3) SB13 (-5) SB17 (-10) SB14 (-29)
1052 (M)	1054 (VS)	1053.	1038.	E	C1C7 (47) C3C9 (24) C4C0 (13) C602 (7) C3C4 (5) C5C1 (4) C4C5 (4) C6C1 (3) 1423 (3) 1421 (3) 1865 (2) CC1C (2)	DIAGONAL- CO (96) CC (14) HCC (13) CCO (4) CCC (3) COH (2) OFF-DIAG- BB26 (-1) SB12 (-2) SB17 (-2) SB15 (-2) EB23 (-3) SB13 (-5) CCCO (-7) SB14 (-12)
1046 (SH)	1043 (SH)	1043.	1038.	E	C5C1 (46) C3C9 (26) C2C8 (13) C602 (7) C2C3 (5) C1C2 (4) C5C6 (3) 1643 (3) C1C7 (3) 1645 (3) 1861 (2) CC5C (2) C6C1 (2)	DIAGONAL- CO (96) CC (14) HCC (13) CCO (4) CCC (3) COH (2) OFF-DIAG- BB26 (-1) SB12 (-2) SB17 (-2) SB15 (-2) EB23 (-3) SB13 (-5) CCCC (-7) SB14 (-12)
959 (W,LT)		959.	981.	E	C602 (29) C400 (26) C3C9 (11) C1C7 (9) C1C2 (6) C2C3 (6) 1265 (3) 1045 (3) C4C5 (2) 1754 (2) 1261 (2) 1756 (2) C3C4 (2) 1312 (2) C5C6 (2)	DIAGONAL- CO (76) CC (19) CCO (10) HCC (9) CCC (4) COH (1) HCC (1) OFF-DIAG- SB15 (4) CCCO (3) SB12 (1) BB19 (1) BB24 (1) SB13 (-2) SB16 (-3) SB17 (-3) SB14 (-21)
952 (M)	950 (W)	952.	981.	E	C2C8 (37) C5C1 (13) C4C0 (11) C602 (8) C6C1 (5) C5C6 (5) C3C4 (5) C4C5 (4) C1C7 (4) 0823 (3) C3C9 (3) 0821 (3) 1534 (2) 1316 (2) 1043 (2) CC5C (2)	DIAGONAL- CO (76) CC (19) CCC (10) HCC (9) CCC (4) COH (1) HCC (1) OFF-DIAG- SB15 (4) CCCO (3) SB12 (1) BB19 (1) BB24 (1) SB13 (-2) SB16 (-3) SB17 (-3) SB14 (-21)
906 (VVW)	906 (M)	906.	878.	A1	CC3C (6) CC5C (6) CC1C (6) C1C7 (3) C3C9 (3) C5C1 (3) C2CH (3) C4OH (3) C6OH (3) C4C5 (2) C5C6 (2) C6C1 (2) C1C2 (2) C2C3 (2) C3C4 (2) 1045 (2) 1265 (2) 1261 (2) 0821 (2) 0823 (2) 1043 (2) 1645 (2) 1865 (2) 1861 (2) 1421 (2) 1423 (2) 1643 (2) CC2C (2) CC6C (2) CC4C (2)	DIAGONAL- CCC (24) HCC (15) CC (15) CCC (15) CO (12) COH (9) HCO (3) OFF-DIAG- SB14 (8) BB19 (7) SB17 (5) BB26 (4) EB23 (2) SB15 (2) BB16 (1) BB24 (-1) SB12 (-2) BB25 (-2) SB13 (-3) CCCO (-3) BB30 (-4) SB16 (-8)
871 (W)	871 (S)	871.	865.	E	C6C1 (20) C3C4 (16) C1C2 (15) C2C3 (7) C400 (6) 1156 (4) C602 (4) 1154 (4) C4C5 (3) 1261 (3) 1861 (2) 0821 (2) 1043 (2) 0932 (2) 1643 (2) CC4C (2) 1421 (2)	DIAGONAL- CC (62) CCC (21) CO (11) HCC (8) CCC (4) HCO (3) COH (1) OFF-DIAG- SB15 (6) CCCO (4) BB19 (2) SB12 (1) SB13 (1) SB14 (-5) SB17 (-9) SB16 (-12)
867 (W)	867 (SH)	867.	865.	E	C5C6 (21) C4C5 (18) C2C3 (13) C2C8 (7) C1C2 (6) C3C4 (5) 0716 (4) 0712 (3) 1265 (3) C602 (3) 1045 (3) 0934 (3) 1865 (2) CC2C (2) 0932 (2) 1645 (2) 0823 (2) 1423 (2)	DIAGONAL- CC (62) CCO (21) CO (11) HCC (8) CCC (4) HCC (3) CCH (1) OFF-DIAG- SB15 (6) CCCO (4) BB19 (2) SB12 (1) SB13 (1) SB14 (-5) SB17 (-9) SB16 (-12)
811 (M)	811 (S)	811.	813.	A1	C2C8 (10) C4C0 (10) C602 (10) C4C5 (5) C5C6 (5) C6C1 (5) C1C2 (5) C2C3 (5) C3C4 (5) 0716 (2) 0712 (2) 0932 (2) 0934 (2) 1154 (2) 1156 (2)	DIAGONAL- CC (33) CO (29) CCC (13) HCC (8) CCC (5) OFF-DIAG- SB14 (10) CCCO (5) SB15 (5) BB19 (3) EB25 (2) BB18 (1) SB13 (-1) SB16 (-3) SB17 (-11)
774 (W)	776 (M)	775.	775.	E	0821 (11) 1261 (11) 1312 (6) CC1C (6) 1316 (6) 0712 (4) 0823 (4) C400 (4) 0716 (4) 1043 (3) 1265 (3) 1532 (3) 0932 (2) CC3C (2) 1756 (2) 1045 (2) 1156 (2) 1534 (2)	DIAGONAL- CCO (47) HCC (22) CCC (10) CO (6) CC (4) COH (2) OFF-DIAG- BB19 (7) SB14 (5) SB16 (2) SB15 (1) EB26 (1) BB18 (1) SB13 (-1) BB23 (-2) SB17 (-4) BB24 (-5)

TABLE XLVIII (Continued)

EXPERIMENTAL FREQUENCY (CM-1) RAMAN	INFRARED	ASSIGNED FREQUENCY (CM-1)	CALCULATED FREQUENCY (CM-1)	CALCULATED SYMMETRY SPECIES	SPECTRAL INTERPRETATION --- POTENTIAL ENERGY DISTRIBUTIONS INTERNAL COORDINATES	FORCE CONSTANTS
758 (W)	758 (M)	758.	775.	E	1045(10) 1265(9) 1043(8) 0823(7) 1754(6) CC5C(5) 1534(5) 1756(5) CC3C(4) 1154(4) 1532(4) 0934(4) C208(3) C602(3) 1156(3) C932(2)	DIAGONAL- CCO (47) HCC (22) CCC (10) CC (6) CC (4) COH (2) OFF-DIAG- BB19(7) SB14(5) SB16(2) SB15(1) BB26(1) BB18(1) SB13(-1) BB23(-2) SB17(-4) BB24(-5)
	644 (M,SH)					
	598 (M,B)					
	550 (M)	550.	540.	A2	C716(14) 0712(14) 0932(14) 0934(14) 1154(14) 1156(14) 1421(3) 1423(3) 1643(3) 1645(3) 1865(3) 1861(3) 1043(3) 1045(3) 0821(3) C823(3) 1265(3) 1261(3) C1C2(2) C2C3(2) C3C4(2) C4C5(2) C5C6(2) C6C1(2)	DIAGONAL- CCO (102) HCC (19) CC (10) TOCC (1) OFF-DIAG- BB19(2) BB20(-1) SB15(-5) SB16(-7) BB23(-20)
	493 (S)	493.	514.	E	C712(7) CC3C(6) 1154(6) 1645(5) C4C5(5) 0932(5) 1421(5) C1C2(5) 1045(5) 1865(5) 0934(4) 0821(4) C5C6(4) 1861(4) CC6C(4) 1265(4) C6C1(3) 1261(3) CC1C(2)	DIAGONAL- CCO (39) HCC (20) CC (18) CCC (15) CO (2) COH (1) OFF-DIAG- SB17(6) BB19(6) SB14(5) BB18(1) SB16(1) BB30(-1) SB15(-6) BB23(-7)
	485 (S,SH)	485.	514.	E	C716(7) 1156(7) 1643(6) 1423(6) C3C4(6) C2C3(6) 1043(5) 0823(5) CC5C(5) CC1C(4) 0934(3) CC2C(3) CC4C(3) C6C1(2) 0932(2) 1861(2) 1261(2) C5C6(2) 1865(2) 1265(2)	DIAGONAL- CCO (39) HCC (20) CC (18) CCC (15) CO (2) COH (1) OFF-DIAG- SB17(6) BB19(6) SB14(5) BB18(1) SB16(1) BB30(-1) SB15(-6) BB23(-7)
513 (VS)		513.	490.	A1	C107(6) C309(6) C501(6) C6C1(5) C3C4(5) C2C3(5) C1C2(5) C4C5(5) C5C6(5) CC2C(3) CC4C(3) CC6C(3)	DIAGONAL- CC (33) CO (18) CCC (14) CCC (12) HCO (2) OFF-DIAG- SB14(9) SB17(8) CCCO(4) BB22(1) BB25(1) SB15(-1) SB12(-2)
381 (M)	379 (M)	381.	362.	E	1045(17) 0821(16) CC6C(8) 1265(8) 1261(6) 0716(6) 1156(5) 0934(5) 0932(4) 0823(3) CC4C(3) CC3C(2) CC2C(2)	DIAGONAL- CCO (70) CCC (16) HCC (5) CC (3) TOCO(2) OFF-DIAG- SB14(3) SB17(2) BB22(2) BB20(-1) BB30(-1) BB23(-4)
368 (M)	366 (VW,SH)	368.	362.	E	1043(16) 0823(14) 1261(11) 1265(9) CC2C(7) 0712(6) 1154(6) CC4C(6) 0932(3) CC5C(2) 0934(2) CC1C(2)	DIAGONAL- CCO (70) CCC (16) HCC (5) CC (3) TOCO(2) OFF-DIAG- SB14(3) SB17(2) BB22(2) BB20(-1) BB30(-1) BB23(-4)
	310 (W)	310.	305.	A2	0821(13) 0823(13) 1043(13) 1045(13) 1265(13) 1261(13) 1154(4) 1156(4) 0932(4) 0934(4) 0716(4) 0712(4) TC20(2) TC40(2) TC60(2)	DIAGONAL- CCO (101) TOCC(7) HCC (6) OFF-DIAG- BB20(-1) BB24(-2) SB16(-2) BB19(-4) BB23(-5)
301 (VW)		301.	298.	E	1154(22) 1156(22) 0712(9) 0716(6) 0821(5) 0823(5) 0932(5) TC50(4) C6C1(4) C3C4(4) 0934(3) CC6C(2) 1045(2) C5C6(2) 1043(2)	DIAGONAL- CCO (82) CC (11) TOCO(7) HCC (5) CCC (3) OFF-DIAG- SB16(4) BB20(-1) BB22(-1) SB17(-3) BB23(-8)
	292 (VW)	292.	298.	E	0934(20) 0932(18) 0716(16) 0712(14) 1261(4) 1265(4) C1C2(3) 1043(3) TC30(3) 1045(3) C2C3(3) C4C5(3) TC1C(3) CC2C(2) C5C6(2) 1643(2)	DIAGONAL- CCO (82) CC (11) TOCO(7) HCC (5) CCC (3) OFF-DIAG- SB16(4) BB20(-1) BB22(-1) SB17(-3) BB23(-8)
239 (VW)	242 (SH)	241.	245.	E	CC4C(14) 0821(11) 1261(9) 1045(9) CC1C(6) CC2C(6) 1043(5) 1312(3) 1316(3) TC6C(3) 0712(2) 0716(2) CC5C(2) 1754(2) TC56(2) CC6C(2) TC20(2) TC61(2) TC23(2)	DIAGONAL- CCO (42) CCC (31) HCC (12) TOCC (6) TOCO(6) CO (2) CC (2) HCO (2) OFF-DIAG- SB16(4) BB24(3) BB19(3) BB18(2) SB15(-2) SB17(-2) BB25(-4) SB14(-6)
235 (VW,SH)	236 (W)	236.	245.	E	CC6C(13) 0823(12) 1265(10) CC2C(9) 1043(6) CC3C(5) CC5C(4) 1532(3) 1045(3) TC4C(3) 1756(3) 1261(3) 1534(2) 0932(2) TC45(2) 0934(2) TC34(2) 1156(2)	DIAGONAL- CCO (42) CCC (31) HCC (12) TOCC (6) TOCO(6) CO (2) CC (2) HCC (2) OFF-DIAG- SB16(4) BB19(3) BB24(3) BB18(2) SB15(-2) SB17(-2) BB25(-4) SB14(-6)
			197.	A1	CC2C(8) CC4C(8) CC6C(8) 0821(6) 0823(6) 1043(6) 1045(6) 1265(6) 1261(6) 1316(3) 1312(3) 1532(3) 1534(3) 1754(3) 1756(3) 0716(2) 0712(2) 1154(2) 1156(2) 0932(2) 0934(2) CC5C(2) CC3C(2) CC1C(2)	DIAGONAL- CCO (48) CCC (30) HCC (15) CO (6) CC (3) TOCC (2) OFF-DIAG- SB16(7) BB19(5) BB24(4) BB23(4) BB18(1) CCCO(-1) BB3C(-1) BB26(-1) BB22(-2) SB17(-3) SB15(-4) BB25(-7) SB14(-13)
			179.	A2	TC50(22) TC10(22) TC30(22) TC6C(11) TC40(11) TC20(11)	DIAGONAL- TOCO(99)
			172.	E	TC40(47) TC20(16) TC10(14) TC6C(8) TC50(5) TC30(2)	DIAGONAL- TOCO(92) CCO (5) HCC (1)
			172.	E	TC60(39) TC20(31) TC30(12) TC5C(9)	DIAGONAL- TOCO(92) CCO (5) HCC (1)
			170.	E	TC50(47) TC30(17) TC20(14) TC1C(8) TC60(5) TC40(2) 1156(2) 1154(2)	DIAGONAL- TOCO(92) CCO (7)
			170.	E	TC1C(40) TC30(31) TC40(12) TC60(9) 0716(2)	DIAGONAL- TOCO(92) CCO (7)
			169.	A2	TC60(21) TC40(21) TC20(21) TC50(10) TC10(10) TC30(10)	DIAGONAL- TOCO(93) CCO (9) HCC (1)
			128.	A1	CC5C(9) CC1C(9) CC3C(9) TC12(7) TC23(7) TC34(7) TC45(7) TC56(7) TC61(7) CC2C(4) CC6C(4) CC4C(4) C716(3) C712(3) 0932(3) 0934(3) 1154(3) 1156(3) 1421(2) 1423(2) 1643(2) 1645(2) 1865(2) 1861(2)	DIAGONAL- TOCC(43) CCC (39) CCO (22) HCC (10) CO (5) HCO (2) CC (1) OFF-DIAG- BB19(3) BB18(1) SB15(1) BB22(-2) BB26(-5) BB23(-6) SB17(-7) SB14(-8)

TABLE XLVIII (Continued)

EXPERIMENTAL FREQUENCY (CM-1) RAMAN	INFRARED	ASSIGNED FREQUENCY (CM-1)	CALCULATED FREQUENCY (CM-1)	CALCULATED SYMMETRY SPECIES	SPECTRAL INTERPRETATION --- POTENTIAL ENERGY DISTRIBUTIONS INTERNAL COORDINATES	FORCE CONSTANTS
			90.	E	CC3C (16) TC56 (16) TC23 (15) CC5C (11) TC61 (7) CC6C (7) TC34 (6) CC2C (5) 0932 (3) 0934 (3) TC12 (2) 1156 (2) 1154 (2) 1423 (2)	DIAGONAL- TOCC (48) CCC (39) CCO (10) HCC (6) CO (2) HCO (1) OFF-DIAG- SB17 (3) BB19 (2) BB26 (-3) SB14 (-3) BB23 (-3)
			90.	E	CC1C (17) TC45 (14) TC12 (14) TC34 (10) TC61 (9) CC4C (8) CC5C (7) CC2C (3) 0712 (3) 0716 (3) CC3C (2) 1421 (2) 1154 (2)	DIAGONAL- TOCC (48) CCC (39) CCC (10) HCC (6) CO (2) HCO (1) OFF-DIAG- SB17 (3) BB19 (2) BB26 (-3) SB14 (-3) BB23 (-3)

TABLE XLIX. L-CHIRO-INOSITOL

EXPERIMENTAL FREQUENCY (CM-1) RAMAN	INFRARED	ASSIGNED FREQUENCY (CM-1)	CALCULATED FREQUENCY (CM-1)	CALCULATED SYMMETRY SPECIE	SPECTRAL INTERPRETATION --- POTENTIAL ENERGY DISTRIBUTIONS INTERNAL COORDINATES	FORCE CONSTANTS
	3440 (S)		3357.		O12H(64) O7H9(34)	DIAGONAL- OH (100)
	3400 (S)		3357.		O7H9(64) O12H(34)	DIAGONAL- OH (100)
	3350 (VS)		3357.		O10H(51) O9H1(36) O11H(10) O8HO(3)	DIAGONAL- OH (100)
	3280 (VS)		3357.		O11H(55) O10H(27) O8HO(17)	DIAGONAL- OH (100)
	3180 (VS)		3357.		O9H1(45) O11H(29) O10H(15) O8HO(10)	DIAGONAL- OH (100)
			3357.		O8HO(69) O9H1(19) O10H(7) O11H(5)	DIAGONAL- OH (100)
2967 (S)	2967 (M)		2949.	A	C3H5(36) C4H6(36) C2H4(12) C5H7(12)	DIAGONAL- CH (98)
2937 (VS)			2943.	B	C5H7(33) C2H4(33) C4H6(15) C3H5(15)	DIAGONAL- CH (99)
2931 (SH)	2930 (M)		2938.	B	C1H3(48) C6H8(48)	DIAGONAL- CH (99)
	2922 (M)		2938.	A	C6H8(30) C1H3(30) C2H4(12) C5H7(12) C4H6(7) C3H5(7)	DIAGONAL- CH (99)
2900 (S)	2895 (W)		2936.	A	C5H7(25) C2H4(25) C6H8(19) C1H3(19) C3H5(5) C4H6(5)	DIAGONAL- CH (99)
			2932.	B	C4H6(34) C3H5(34) C5H7(16) C2H4(16)	DIAGONAL- CH (100)
	1463 (SH)	1463.	1454.	B	C1OH(20) C6OH(20) 1316(9) 1861(9) 1865(7) 1312(7) C1C2(2) C5C6(2) 1423(2) 1754(2) C4OH(2) C3OH(2)	DIAGONAL- COH (45) HCC (43) CC (5) CCO (3) HCO (1) OFF-DIAG- BB23(3) SB13(2) BB19(-1) SB15(-2)
1449 (VW)	1450 (W)	1450.	1432.	B	C3OH(13) C4OH(13) C2OH(8) C5OH(8) 1534(5) 1643(5) 1532(4) 1645(4) C1OH(4) C6OH(4) 1316(3) 1861(3) HC3O(2) HC4O(2) 1754(2) 1423(2) 1865(2) 1312(2) 1421(2) 1756(2) C1C2(2) C5C6(2)	DIAGONAL- COH (49) HCC (36) HCO (7) CC (3) CCO (2) OFF-DIAG- BB23(3) BB29(2) BB25(1) SB17(-1) SB15(-1) BB30(-3)
1429 (W,SH)	1428 (SH)	1428.	1431.	A	C3OH(21) C4OH(21) 1534(7) 1643(7) 1423(6) 1754(6) 1645(3) 1532(3) C2OH(3) HC5O(3) C5OH(3) HC2O(3) HC5O(3)	DIAGONAL- COH (48) HCC (34) HCO (8) CCO (3) CCC (1) CO (1) OFF-DIAG- BB23(4) BB29(2) BB25(2) BB18(-1) BB30(-3)
	1419 (M)	1419.	1421.	A	C5OH(20) C2OH(20) HC5O(6) HC2O(6) C1OH(5) C6OH(5) 1421(5) 1756(5) HC1O(2) HC6O(2) 1645(2) 1532(2) 1861(2) 1316(2) C3OH(2) C4OH(2) 1423(2) 1754(2)	DIAGONAL- COH (54) HCC (22) HCO (16) CCO (3) CO (2) CCC (1) OFF-DIAG- BB23(2) BB29(2) SB12(-1) BB30(-2) BB18(-3)
1410 (M)		1410.	1414.	B	C2OH(21) C5OH(21) C4OH(13) C3OH(13) HC2O(8) HC5O(8) HC4O(5) HC3O(5)	DIAGONAL- COH (69) HCO (27) HCC (8) CO (2) CCC (2) OFF-DIAG- BB29(5) SB12(-2) SB13(-5) BB18(-6)
1398 (LT,SH)	1397 (SH)	1397.	1394.	A	C1OH(33) C6OH(33) C2OH(6) C5OH(6) C1C2(5) C5C6(5) C3OH(2) C4OH(2) HC1O(2) HC6O(2)	DIAGONAL- COH (82) CC (11) HCC (5) HCO (4) CCO (3) OFF-DIAG- BB23(1) BB29(-1) BB30(-2) SB16(-3)
1366 (M)	1364 (M)	1365.	1370.	A	1423(12) 1754(12) 1645(9) 1532(9) HC4O(9) HC3O(9) HC2O(6) HC5O(6) 1312(5) 1865(5) 1316(4) 1861(4) C4OH(4) C3OH(4) C2C3(3) C4C5(3) C2O8(2) C5O1(2) C4OO(2) C3O9(2)	DIAGONAL- HCC (61) HCO (30) COH (9) CO (9) CC (8) CCO (2) CCC (1) OFF-DIAG- BB28(5) BB23(3) BB29(2) CCCO(-1) SB14(-2) SB13(-3) SB12(-5) SB15(-9) BB18(-11)
			1360.	A	1316(11) 1861(11) C3OH(8) C4OH(8) C1OH(7) C6OH(7) 1643(6) 1534(6) HC1O(5) HC6O(5) C1O7(5) C6O2(5) C6C1(4) HC3O(4) HC4O(4) 1421(4) 1756(4)	DIAGONAL- HCC (47) COH (31) HCO (19) CO (11) CC (6) CCO (4) CCC (2) OFF-DIAG- BB23(3) BB29(3) BB30(-1) BB26(1) BB28(1) SB16(1) CCCO(-1) BB19(-2) SB17(-2) SB14(-4) SB12(-4) SB13(-6) BB18(-6) SB15(-7)
	1342 (LT,M)	1342.	1357.	B	1754(11) 1423(11) 1645(10) 1532(10) C3OH(9) C4OH(9) C6OH(5) C1OH(5) HC3O(4) HC4O(4) HC2O(4) HC5O(4) 1312(3) 1865(3) C2C3(3) C4C5(3) C5OH(2) C2OH(2) 1756(2) 1421(2)	DIAGONAL- HCC (53) COH (32) HCO (19) CC (6) CO (4) CCO (1) OFF-DIAG- BB28(5) BB29(3) BB23(1) BB30(1) BB19(-1) SB14(-1) SB12(-3) SB13(-4) BB18(-6) SB15(-7)
1336 (M)	1336 (M)	1336.	1352.	A	1534(20) 1643(20) C2OH(8) C5OH(8) HC3O(5) HC4O(5) 1532(4) 1645(4) 1316(3) 1861(3) HC1O(3) HC6O(3) C3C4(3) 1756(2) 1421(2) C1O7(2) C6O2(2) C3OH(2)	DIAGONAL- HCC (63) COH (22) HCO (16) CO (6) CC (6) CCO (2) OFF-DIAG- BB28(7) BB29(1) SB14(-2) SB13(-2) SB12(-3) BB18(-6) SB15(-9)
1309 (LT,W)	1313 (M)	1313.	1334.	B	C6OH(13) C1OH(13) 1312(12) 1865(12) 1645(5) 1532(5) C5OH(5) C2OH(5) 1316(5) 1861(5) 1643(2) 1534(2)	DIAGONAL- HCC (50) COH (38) HCO (5) CCO (2) CO (1) OFF-DIAG- BB23(4) SB15(2) BB29(1) SB13(-2) BB18(-2)
1302 (VW,SH)	1297 (M)	1297.	1309.	B	1756(16) 1421(16) HC6O(12) HC1O(12) 1316(6) 1861(6) 1645(5) 1532(5) HC2O(3) HC5O(3) 1534(3) 1643(3) C6O2(3) C1O7(3) 1423(3) 1754(3)	DIAGONAL- HCC (68) HCO (32) CO (8) CCO (4) CCC (2) OFF-DIAG- BB23(5) SB13(2) BB25(1) BB29(-1) SB15(-1) SB14(-2) BB28(-3) BB19(-3) SB12(-5) BB18(-9)
1285 (SH)	1282 (LT,SH)	1285.	1307.	A	1312(20) 1865(20) HC1O(13) HC6O(12) 1532(6) 1645(6) HC4O(6) HC3O(6) C3OH(2) C4OH(2) 1421(2) 1756(2) HC2O(2) HC5O(2)	DIAGONAL- HCC (57) HCO (41) COH (5) CC (3) CCO (3) CO (2) TOCC(2) OFF-DIAG- BB23(4) SB15(2) BB26(1) SB16(-1) SB12(-2) BB18(-15)

Conventional symbolism indicating relative intensity: s = strong, m = medium, w = weak, sh = shoulder, b = broad, v = very, lt = low temperature band

TABLE XLIX (Continued)

EXPERIMENTAL FREQUENCY (CM-1) RAMAN	EXPERIMENTAL FREQUENCY (CM-1) INFRARED	ASSIGNED FREQUENCY (CM-1)	CALCULATED FREQUENCY (CM-1)	CALCULATED SYMMETRY SPECIE	SPECTRAL INTERPRETATION --- POTENTIAL ENERGY DISTRIBUTIONS INTERNAL COORDINATES	FORCE CONSTANTS
1279 (M)	1272 (M)	1276.	1275.	A	HC6O (16) HC1O (16) 1421 (14) 1756 (14) HC5O (5) HC2O (5) 1316 (4) 1861 (4) HC3O (4) HC4O (4) C3OH (3) C4OH (3) C1C2 (3) C5C6 (3) 1423 (3) 1754 (3) C2O8 (2) C5O1 (2) 1865 (2) 1312 (2) 1532 (2) 1645 (2)	DIAGONAL- HCO (50) HCC (49) COH (11) CC (6) CO (4) CCO (2) TOCC (1) OFF-DIAG- BB23 (2) SB13 (2) BB28 (-1) SB12 (-2) SB15 (-6) BB18 (-14)
1266 (M)		1266.	1262.	B	HC1O (31) HC6O (31) 1421 (7) 1756 (7) 1316 (6) 1861 (6) 1865 (4) 1312 (4) 1754 (2) 1423 (2) C2O8 (2) C5O1 (2) HC5O (2) HC2O (2) C1OH (2) C6OH (2)	DIAGONAL- HCO (67) HCC (43) CO (5) COH (4) CC (2) CCO (2) OFF-DIAG- BB23 (2) SB14 (-1) BB29 (-2) SB15 (-2) SB12 (-2) BB18 (-19)
1245 (M)		1245.	1251.	B	HC2O (21) HC5O (21) 1534 (9) 1643 (9) C2OH (9) C5OH (9) 1423 (8) 1754 (8) HC4O (6) HC3O (6) C4OH (2) C3OH (2)	DIAGONAL- HCO (53) HCC (39) COH (23) CCO (2) TOCC (2) OFF-DIAG- BB23 (4) SB12 (-1) BB28 (-4) BB29 (-4) BB18 (-15)
1225 (W)		1225.	1226.	A	HC2O (24) HC5O (24) HC4O (11) HC3O (11) C2OH (8) C5OH (8) 1423 (6) 1754 (6) C4OH (4) C3OH (4) 1645 (3) 1532 (3) 1421 (3) 1756 (3)	DIAGONAL- HCO (70) HCC (29) COH (24) CC (2) OFF-DIAG- BB28 (-2) BB29 (-5) BB18 (-19)
1192 (W)	1194 (M)	1193.	1222.	B	HC3O (29) HC4O (29) C3OH (12) C4OH (12) 1532 (5) 1645 (5) 1534 (5) 1643 (5) HC2O (4) HC5O (4) 1423 (3) 1754 (3) C2OH (2) C5OH (2)	DIAGONAL- HCO (69) COH (30) HCC (28) CCC (3) CO (2) OFF-DIAG- BB25 (3) SB13 (2) BB30 (-2) BB23 (-2) BB19 (-3) BB28 (-3) SB12 (-3) BB29 (-5) BB18 (-19)
1137 (S)	1138 (SH)	1137.	1139.	B	C3O9 (20) C4OO (20) C2O8 (9) C5O1 (9) C1C2 (7) C5C6 (7) CC3C (7) CC4C (7) C1O7 (7) C6O2 (7) C4C5 (5) C2C3 (5) O934 (3) 1043 (3) O823 (3) 1154 (3) CC2C (3) CC5C (3) 1045 (2) O932 (2)	DIAGONAL- CO (71) CC (25) CCC (20) CCO (16) COH (2) OFF-DIAG- BB22 (2) SB16 (-2) SB13 (-4) CCCO (-5) SB17 (-6) SB14 (-21)
1129 (M)	1130 (S)	1129.	1117.	A	C6C1 (24) C5C6 (15) C1C2 (15) C2O8 (12) C5O1 (12) O716 (6) 1261 (6) HC1O (5) HC6O (5) C3C4 (5) CC2C (4) CC5C (4) C1O7 (3) C6O2 (3) C1OH (2) C6OH (2) C3O9 (2) C4OO (2) 1154 (2) O823 (2) O932 (2) 1045 (2)	DIAGONAL- CC (59) CO (35) CCO (22) HCO (12) CCC (11) COH (5) HCC (3) OFF-DIAG- SB12 (1) BB22 (1) SB13 (-2) BB23 (-2) CCCO (-4) SB15 (-5) SB16 (-10) SB17 (-10) SB14 (-14)
1102 (M)	1104 (S)	1103.	1107.	B	C1C2 (13) C5C6 (13) C1O7 (11) C6O2 (11) C5O1 (8) C2OH (8) CC6C (6) CC1C (6) C4C5 (6) C2C3 (6) O821 (5) 1156 (5) C1OH (4) C6OH (4) HC2O (3) HC5O (3) HC1O (2) HC6O (2) C3O9 (2) C4OO (2) 1421 (2) 1756 (2) 1316 (2) 1861 (2)	DIAGONAL- CO (43) CC (18) CCC (13) HCC (11) HCO (11) CCO (10) COH (9) OFF-DIAG- BB26 (1) BB23 (-1) CCCO (-1) BB25 (-2) SB14 (-6) SB17 (-6) SB15 (-7) SB13 (-8) SB16 (-8)
1094 (M)	1090 (VS)	1092.	1102.	A	C3C4 (17) C3O9 (15) C4OO (15) C6C1 (12) C1O7 (8) C6O2 (8) C4C5 (3) C2C3 (3) HC2O (3) HC5O (3) O716 (3) 1265 (3) 1045 (2) O932 (2) C5O1 (2) C2O8 (2) HC4O (2) HC3O (2)	DIAGONAL- CO (49) CC (36) CCO (11) HCO (9) COH (7) CCC (6) OFF-DIAG- SB12 (5) BB19 (1) SB16 (-1) SB17 (-3) SB13 (-3) CCCO (-4) SB14 (-15)
1082 (LT,S)	1081 (SH)	1081.	1085.	A	C6C1 (15) C3O9 (15) C4OO (15) C4C5 (11) C2C3 (11) C1O7 (9) C6O2 (9) C5O1 (7) C2O8 (7) C3C4 (6)	DIAGONAL- CO (63) CC (44) CCO (5) CCC (1) HCC (1) HCO (1) OFF-DIAG- SB15 (2) SB16 (-2) SB17 (-6) CCCO (-11)
1078 (LT,S)	1075 (SH)	1077.	1075.	A	C3C4 (45) C2O8 (6) C5O1 (6) HC3O (5) HC4O (5) C6C1 (5) C4C5 (4) C2C3 (4) 1312 (4) 1865 (4) C1O7 (4) C6O2 (4) O716 (3) 1261 (3) CC3C (3) CC4C (3) 1043 (2) O934 (2) C5C6 (2) C1C2 (2) 1154 (2) O823 (2) 1316 (2) 1861 (2) C3OH (2) C4OH (2)	DIAGONAL- CC (63) CO (19) CCO (17) HCC (13) HCO (11) CCC (6) COH (5) OFF-DIAG- SB12 (2) BB30 (1) BB22 (1) SB13 (-2) BB23 (-4) SB15 (-6) SB17 (-6) SB14 (-10) SB16 (-11)
1056 (W)	1065 (VS)	1061.	1071.	B	C2C3 (14) C4C5 (14) C3O9 (14) C4OO (14) C6O2 (13) C1O7 (13) C5O1 (12) C2O8 (12) O934 (4) 1043 (4) CC3C (2) CC4C (2)	DIAGONAL- CO (78) CC (30) CCO (10) CCC (6) HCO (4) HCC (3) OFF-DIAG- BB23 (-1) SB16 (-1) SB17 (-8) CCCO (-9) SB14 (-10)
1024 (W)	1032 (S)	1028.	1031.	A	C6C1 (25) C4C5 (15) C2C3 (15) C2O8 (12) C5O1 (12) C4OO (8) C3O9 (8) C3C4 (5) O823 (2) 1154 (2)	DIAGONAL- CC (61) CO (41) CCO (8) HCO (1) HCC (1) COH (2) CCC (2) OFF-DIAG- SB13 (-3) SB17 (-4) SB16 (-12)
1016 (SH)	1017 (VS)	1017.	1014.	B	C2O8 (13) C5O1 (13) C1O7 (10) C6O2 (10) C3O9 (9) C4OO (9) C1C2 (8) C5C6 (8) C4C5 (7) C2C3 (7) O712 (4) 1265 (4)	DIAGONAL- CO (65) CC (29) CCO (12) HCC (7) COH (3) HCO (2) CCC (1) OFF-DIAG- CCCO (4) SB12 (4) SB17 (-1) SB15 (-2) SB13 (-3) SB16 (-9) SB14 (-13)
997 (M)	998 (M)	997.	967.	A	C1O7 (12) C6O2 (12) C3C4 (10) C5O1 (7) C2O8 (7) C3O9 (6) C4OO (6) C2C3 (6) C4C5 (6) 1312 (4) 1865 (4) C1C2 (4) C5C6 (4) 1756 (3) 1421 (3) 1316 (3) 1861 (3) O934 (3) 1043 (2) HC3O (2) HC4O (2) 1754 (2) 1423 (2) O823 (2) 1154 (2) O821 (2) 1156 (2) CC6C (2) CC1C (2)	DIAGONAL- CO (51) CC (31) HCC (28) CCO (16) CCC (8) HCO (6) COH (3) OFF-DIAG- BB30 (1) BB18 (1) BB22 (1) BB25 (-1) BB26 (-2) SB13 (-4) BB23 (-4) SB15 (-5) SB17 (-10) SB16 (-10) SB14 (-10)
903 (M)	898 (S)	900.	912.	B	C2C3 (14) C4C5 (14) C1C2 (10) C5C6 (10) C1O7 (9) C6O2 (9) O932 (7) 1045 (7) 1043 (3) O934 (3) C4OO (3) C3O9 (3) 1421 (2) 1756 (2) HC2O (2) HC5O (2) CC6C (2) CC1C (2)	DIAGONAL- CC (48) CO (23) CCO (23) HCC (8) CCC (7) HCO (4) COH (2) OFF-DIAG- CCCO (5) SB15 (3) BB19 (2) SB12 (1) SB14 (-4) SB16 (-13) SB17 (-13)
864 (S)	864 (S)	864.	894.	A	C1C2 (19) C5C6 (19) O821 (6) 1156 (6) C1O7 (5) C6O2 (5) 1045 (4) O932 (4) C6C1 (4) 1421 (2) 1756 (2) O716 (2) 1261 (2) 1316 (2) 1861 (2) C3C4 (2)	DIAGONAL- CC (44) CCO (27) CO (14) HCC (12) HCO (3) CCC (1) OFF-DIAG- SB15 (6) CCCO (5) BB19 (4) BB18 (2) SB12 (1) SB14 (-4) SB17 (-5) SB16 (-14)

TABLE XLIX (Continued)

EXPERIMENTAL FREQUENCY (CM-1) RAMAN	INFRARED	ASSIGNED FREQUENCY (CM-1)	CALCULATED FREQUENCY (CM-1)	CALCULATED SYMMETRY SPECIE	SPECTRAL INTERPRETATION --- POTENTIAL ENERGY DISTRIBUTIONS INTERNAL COORDINATES	FORCE CONSTANTS
761 (VVW)	761 (W)	761.	767.	B	CC6C(6) CC1C(6) C2C8(5) C5C1(5) CC2C(5) CC5C(5) 1312(4) 1865(4) 1316(4) 1861(4) C400(3) C3C9(3) 0712(3) 1265(3) 1021(3) 1756(3) C2C3(2) C4C5(2) C1C2(2) C5C6(2)	DIAGONAL- HCC (25) CCC (23) CO (18) CCO (11) CC (9) COH (2) HCO (1) OFF-DIAG- BB19(8) BB26(4) SB14(3) SB17(3) SB16(3) BB24(-1) SB12(-1) SB13(-2) BB25(-3) BB23(-3)
	732 (M,B)					
665 (M)	665 (S)	665.	666.	B	0712(7) 1265(7) 1534(6) 1643(6) 1154(6) 0823(6) 0934(5) 1043(5) 1156(5) 0821(5) 0716(3) 1261(3) 1423(3) 1754(3) C2C8(2) C501(2) 1756(2) 1421(2) C1C2(2) C5C6(2) CC6C(2) CC1C(2)	DIAGONAL- CCO (51) HCC (25) CO (7) CC (5) CCC (5) OFF-DIAG- SB14(9) BB19(7) SB17(2) BB18(1) BB24(-1) SB15(-2) BB28(-2) BB23(-11)
656 (M)	657 (SH)	656.	652.	A	0712(11) 1265(11) C107(5) C602(5) C2C3(4) C4C5(4) CC2C(4) CC5C(4) 0716(3) 1261(3) 1312(2) 1865(2) C400(2) C309(2) 1645(2) 1532(2) 1754(2) 1423(2)	DIAGONAL- CCO (33) HCC (15) CO (13) CC (11) CCC (9) COH (3) HCO (1) OFF-DIAG- SB14(11) BB19(5) SB17(4) BB18(2) BB26(1) BB24(-1) SB12(-1) BB25(-1) SB13(-2) SB16(-2) BB30(-3)
	600 (W,B)					
554 (W)	553 (M)	554.	568.	B	0823(14) 1154(14) 0821(9) 1156(9) 0934(6) 1043(6) 1534(5) 1643(5) 0932(4) 1045(4) 0716(4) 1261(4) 1265(4) 0712(4) C1C2(4) C5C6(4) C4C5(3) C2C3(3)	DIAGONAL- CCO (82) HCC (18) CC (13) CCC (3) CO (5) OFF-DIAG- BB19(5) SB15(1) BB20(-1) BB25(-1) BB28(-2) SB17(-4) BB23(-16)
528 (VS)	528 (M)	528.	525.	A	C1C2(8) C5C6(8) C4C5(7) C2C3(7) 1532(6) 1645(6) C6C1(5) 0932(5) 1045(5) 0823(4) 1154(4) C3C4(2) 0934(2) 1043(2) 1423(2) 1754(2) C309(2) C400(2)	DIAGONAL- CC (36) CCO (24) HCC (18) CO (9) CCC (3) HCO (1) OFF-DIAG- SB16(6) SB14(5) CCCO(4) BB19(4) BB18(1) BB28(-2) SB15(-3) BB23(-7)
	509 (M)					
451 (M)	453 (W)	451.	450.	B	CC3C(15) CC4C(15) 0934(10) 1043(10) C2C3(4) C4C5(4) C309(3) C400(3) CC2C(3) CC5C(3) 1312(2) 1865(2) 0716(2) 1261(2)	DIAGONAL- CCC (37) CCO (28) CC (9) CO (9) HCC (6) OFF-DIAG- SB14(10) SB17(6) BB22(2) BB19(2) SB15(-1) BB30(-1) SB16(-1) BB23(-3)
446 (M)		446.	444.	A	0716(17) 1261(17) C6C1(5) 1265(5) 0712(5) 1532(5) 1645(5) 0823(4) 1154(4) 1043(3) 0934(3) 1421(3) 1756(3) C107(2) C602(2) 1754(2) 1423(2)	DIAGONAL- CCO (61) HCC (21) CC (7) CCC (6) CO (5) TOCC (2) HCO (1) OFF-DIAG- SB16(6) BB19(3) SB14(1) CCCO(1) BB22(1) BB24(-1) BB28(-2) BB25(-3) SB17(-3) BB23(-7)
425 (S)	430 (M)	425.	401.	A	C3C4(11) 0823(9) 1154(9) CC2C(6) CC5C(6) CC6C(5) CC1C(5) C6C1(5) 0821(3) 1156(3) 0932(3) 1045(3) 0716(3) 1261(3) 1316(3) 1861(3) C208(2) C501(2) CC4C(2) CC3C(2)	DIAGONAL- CCO (37) CCC (28) CC (17) HCC (9) CO (5) OFF-DIAG- SB17(9) SB14(8) BB22(2) BB25(2) BB26(-2) SB15(-3) SB16(-4) BB23(-7)
379 (W)	381 (W)	380.	375.	B	0932(18) 1045(18) 0712(10) 1265(10) 1534(6) 1643(6) C1C2(5) C5C6(5) 1532(3) 1645(3) 0716(2) 1261(2) 1423(2) 1754(2)	DIAGONAL- CCO (62) HCC (21) CC (10) CCC (3) TOCC (2) HCO (1) OFF-DIAG- SB16(9) BB19(5) SB14(-1) SB15(-2) BB25(-2) SB17(-2) BB28(-3) BB23(-6)
343 (W)	343 (VVW)	343.	308.	A	0821(19) 1156(19) 1154(13) 0823(13) C6C1(9) C3C4(9) CC2C(3) CC5C(3) 1312(2) 1865(2) TC20(2) TC50(2) CC4C(2) CC3C(2)	DIAGONAL- CCO (70) CC (21) CCC (9) HCC (8) TOCO(5) TOCC(1) OFF-DIAG- SB16(4) BB20(-1) BB26(-1) BB25(-1) SB15(-2) SB17(-3) BB23(-10)
	315 (M)	315.	293.	A	0934(23) 1043(23) 0932(22) 1045(22) 0823(4) 1154(4) TC30(3) TC40(3) 1265(2) 0712(2) 1534(2) 1643(2)	DIAGONAL- CCO (106) HCC (10) TOCO(6) CC (5) CCC (1) OFF-DIAG- BB28(1) BB20(-1) SB15(-3) BB19(-4) SB16(-8) BB23(-14)
303 (M)	305 (SH)	303.	291.	B	1156(17) 0821(17) 1154(8) 0823(8) 0716(8) 1261(8) 1045(7) 0932(7) 1043(4) 0934(4) 0712(3) 1265(3) TC20(2) TC50(2) 1312(2) 1865(2)	DIAGONAL- CCO (95) TOCO(7) HCC (7) CCC (3) CC (3) OFF-DIAG- BB19(-1) BB20(-1) BB22(-2) BB23(-11)
272 (M)	277 (W)	274.	266.	B	0716(15) 1261(15) CC3C(7) CC4C(7) 0934(7) 1043(7) 1534(6) 1643(6) 1154(5) 0823(5) 1532(4) 1645(4) 1423(3) 1754(3) CC6C(3) CC1C(3) TC12(2) TC56(2)	DIAGONAL- CCO (56) HCC (32) CCC (21) TOCC(6) CO (5) TOCO(4) CC (2) OFF-DIAG- BB19(9) SB16(2) BB22(-3) BB28(-4) BB25(-6) SB14(-9) BB23(-17)
255 (W)	257 (W)	255.	244.	A	0712(21) 1265(21) CC2C(6) CC5C(6) 1423(4) 1754(4) 1156(4) 0821(3) CC6C(3) CC1C(3) 0716(2) 1261(2) TC61(2) CC3C(2) CC4C(2)	DIAGONAL- CCO (57) CCC (22) HCC (15) TOCC(5) CO (3) TOCO(2) CC (1) OFF-DIAG- BB19(3) BB24(2) SB16(2) BB18(1) SB15(-1) BB25(-3) BB23(-4) SB14(-5)
			194.	B	TC10(23) TC60(23) CC6C(7) CC1C(7) 0712(6) 1265(6) 0716(6) 1261(6) 1316(3) 1861(3) 1754(2) 1423(2) 0934(2) 1043(2) 1532(2) 1645(2) 0932(2) 1045(2)	DIAGONAL- TOCO(46) CCO (36) HCC (19) CCC (16) CO (5) OFF-DIAG- BB19(3) BB22(-1) BB28(-1) BB26(-2) BB25(-3) BB23(-9) SB14(-10)
			183.	A	TC60(45) TC10(45)	DIAGONAL- TOCO(92) CCC (3) TOCC(3) CCO (1)
			177.	B	TC40(28) TC30(28) TC50(21) TC20(21)	DIAGONAL- TOCO(98) CCO (2)
			172.	A	TC20(38) TC50(38) TC30(9) TC40(9)	DIAGONAL- TOCO(94) CCO (5)
			170.	B	TC20(26) TC50(26) TC30(20) TC40(19)	DIAGONAL- TOCO(91) CCO (7) HCC (1) CCC (1) OFF-DIAG- BB23(-1)

TABLE XLIX (Continued)

EXPERIMENTAL FREQUENCY (CM-1) RAMAN	INFRARED	ASSIGNED FREQUENCY (CM-1)	CALCULATED FREQUENCY (CM-1)	CALCULATED SYMMETRY SPECIE	SPECTRAL INTERPRETATION --- POTENTIAL ENERGY DISTRIBUTIONS
					INTERNAL COORDINATES / FORCE CONSTANTS
			169.	A	TC40(37) TC30(36) TC50(9) DIAGONAL- TOCO(92) CCO (9) TC20(9) 1045(2) 0932(2) OFF-DIAG- BB23(-1) 1043(2)
			162.	B	TC10(26) TC60(26) 0716(12) DIAGONAL- TOCO(52) CCO (39) CCC (14) 1261(12) CC6C(6) CC1C(6) HCC (14) CO (5) 1265(4) 0712(4) 1316(3) OFF-DIAG- BB19(1) BB22(-1) BB25(-2) 1861(3) C107(2) C602(2) BB26(-2) BB23(-8) SB14(-10) 0823(2) 1154(2)
			130.	A	CC2C(8) CC5C(8) TC61(7) DIAGONAL- CCC (40) TOCC(39) CCO (21) TC45(7) TC23(7) TC56(6) CO (6) TOCO(6) HCC (4) CC (3) TC12(6) TC34(6) CC3C(6) HCO (2) CC4C(6) CC1C(5) CC6C(5) OFF-DIAG- SB16(4) BB19(1) BB23(-1) 0823(3) 1154(3) 0821(3) BB26(-2) BB22(-3) SB14(-9) SB17(-9) 1156(3) TC10(3) TC60(3) 0934(2) 1043(2) 0932(2) 1045(2) 1312(2) 1865(2)
			91.	A	TC34(17) TC61(14) CC3C(11) DIAGONAL- TOCC(46) CCC (39) CCO (9) CC4C(11) CC6C(9) CC1C(9) HCC (2) HCO (2) CO (2) TOCO(1) TC23(4) TC45(4) TC56(3) OFF-DIAG- SB17(3) BB19(1) BB22(-1) TC12(3) 0934(3) 1043(2) BB25(-1) SB14(-3) 0932(2) 1045(2)
			88.	B	CC2C(14) CC5C(14) TC45(12) DIAGONAL- TOCC(48) CCC (39) CCO (14) TC23(12) TC12(12) TC56(12) HCC (3) CO (3) CC4C(3) CC3C(3) 0821(3) OFF-DIAG- SB17(2) BB22(-1) BB26(-2) 1156(3) 1154(2) 0823(2) BB23(-2) SB14(-5) CC1C(2) CC6C(2)

TABLE L. MUCO-INOSITOL

EXPERIMENTAL FREQUENCY (CM-1) RAMAN	INFRARED	ASSIGNED FREQUENCY (CM-1)	CALCULATED FREQUENCY (CM-1)	CALCULATED SYMMETRY SPECIES	SPECTRAL INTERPRETATION --- POTENTIAL ENERGY DISTRIBUTIONS INTERNAL COORDINATES	FORCE CONSTANTS
	3355 (VS)		3357.		O8H0(98) O9H1(2)	DIAGONAL- OH (100)
	3300 (VS)		3357.		O12H(98) O11H(2)	DIAGONAL- OH (100)
	3270 (VS)		3357.		O10H(43) O11H(36) O9H1(19)	DIAGONAL- OH (100)
	3220 (VS)		3357.		O9H1(50) O11H(46) O10H(2)	DIAGONAL- OH (100)
			3357.		O7H9(46) O10H(33) O9H1(14) O11H(7)	DIAGONAL- OH (100)
			3357.		O7H9(53) O10H(21) O9H1(16) O11H(9)	DIAGONAL- OH (100)
	2970 (W)		2948.	A'	C4H6(51) C5H7(22) C3H5(22)	DIAGONAL- CH (98)
	2938 (W)		2940.	A'	C1H3(46) C2H4(26) C6H8(26)	DIAGONAL- CH (99)
			2940.	A''	C3H5(45) C5H7(45) C6H8(4) C2H4(4)	DIAGONAL- CH (99)
2928 (VS)			2938.	A'	C1H3(52) C2H4(22) C6H8(22) C4H6(3)	DIAGONAL- CH (99)
2915 (VS)			2936.	A''	C6H8(45) C2H4(45) C5H7(4) C3H5(4)	DIAGONAL- CH (99)
2893 (S)	2893 (W)		2933.	A''	C4H6(45) C3H5(27) C5H7(27)	DIAGONAL- CH (100)
	1500 (W)	1500.	1494.	A''	C2OH(21) C6OH(21) 1316(12) 1312(12) 1423(4) 1865(4) CCO (3) HCO (2) 1421(3) 1861(3) C2C3(3) C5C6(3)	DIAGONAL- COH (44) HCC (43) CC (5) OFF-DIAG- EB23(3) SB13(2) BB19(-1) SB15(-2)
	1461 (M)	1461.	1435.	A'	C3OH(25) C5OH(25) 1643(10) 1645(10) HC3O(7) HC5O(7)	DIAGONAL- COH (46) HCC (35) HCC (5) CCO (4) CO (1) CCC (1) OFF-DIAG- EB23(4) SB13(2) BB25(2) SB15(1) BB3O(-3)
	1451 (SH)	1451.	1427.	A''	C4OH(31) 1754(11) 1534(11) C2OH(6) C6OH(6) 1756(4) 1532(4) HC4O(3) 1423(2) 1865(2)	DIAGONAL- COH (51) HCC (31) HCO (14) CC (2) CCO (1) OFF-DIAG- BB29(3) BB23(2) BB25(1) SB15(-2) EE18(-2) SB13(-2) BB3O(-2)
	1423 (SH)	1423.	1416.	A'	C2OH(18) C6OH(18) C1OH(15) C4OH(14) HC1O(6) 1861(6) CC (8) CO (3) CCO (2) CCC (2) 1421(6) HC4O(3) C1C2(3) OFF-DIAG- BB29(2) BB26(1) SB16(-1) C6C1(3) C1O7(3) 1865(2) SB12(-2) EE18(-2) SB17(-2) SB13(-5) 1423(2) CC1C(2) SB15(-5)	DIAGONAL- COH (67) HCC (19) HCC (11)
			1414.	A'	C5OH(24) C3OH(24) HC3O(10) HC5O(10) C1OH(6) HC1O(5) CC (5) CCC (2) C4OH(4) 1861(3) 1421(3) OFF-DIAG- BB29(5) SB17(-1) SB15(-3) HC4O(3) 1756(2) 1532(2) SB12(-4) SB13(-5) BB18(-7) C1O7(2) 1865(2) 1423(2)	DIAGONAL- COH (58) HCO (29) HCC (17)
	1406 (W)	1406.	1407.	A'	C1OH(42) HC1O(19) C2OH(9) C6OH(9) C5OH(4) C3OH(4) CC (4) CO (2) CCO (1) C4OH(3) 1312(3) 1316(3) OFF-DIAG- BB29(4) BB23(3) BB3C(-1) C5C6(2) C2C3(2) SB15(-2) SB12(-2) SB13(-3) BB18(-5)	DIAGONAL- CCH (71) HCO (22) HCC (9)
1380 (VW)	1389 (M)	1385.	1368.	A''	1643(9) 1645(9) 1421(8) 1861(8) 1423(8) 1865(8) HCC (7) CCO (3) CO (2) 1534(7) 1754(7) C2OH(7) OFF-DIAG- BB28(4) BB23(3) SB14(-1) C6OH(7) C3C4(5) C4C5(5) SB12(-1) SB16(-2) EE18(-2) SB15(-6) HC3O(3) HC5O(3)	DIAGONAL- HCC (66) COH (16) CC (13)
	1367 (W,LT)	1367.	1364.	A'	HC4O(14) C4OH(13) 1754(9) 1534(9) C6OH(6) C2OH(6) CO (7) CC (6) CCO (3) CCC (2) 1865(5) 1423(5) 1645(4) OFF-DIAG- BB23(4) BB28(3) BB29(1) 1643(4) HC5O(3) HC3O(3) SB14(-3) SB12(-4) SB15(-5) BB18(-8) C1OH(3) 1861(3) 1421(3) C4OO(3) C3C4(2) C4C5(2) C5O1(2) C3O9(2)	DIAGONAL- HCC (44) COH (31) HCO (22)
1345 (VW)	1345 (M)	1345.	1359.	A'	C4OH(10) C1OH(10) 1861(9) 1421(9) C3OH(7) C5OH(7) CC (8) CCO (4) CCC (2) HC4C(6) HC6O(5) HC2O(5) OFF-DIAG- BB23(4) SB16(2) SB13(2) 1534(4) 1754(4) 1532(3) BB28(1) BB26(1) CCCC(-1) SB17(-2) 1756(3) C1O7(3) C6C2(2) BB3O(-2) SB15(-3) SB12(-4) SB14(-4) C2O8(2) C1C2(2) C6C1(2) BB18(-6)	DIAGONAL- HCC (38) COH (36) HCC (19)
1337 (SH)	1338 (SH)	1337.	1347.	A''	1421(12) 1861(12) C3OH(10) C5OH(10) 1645(7) 1643(7) CO (3) CCO (2) HC2O(7) HC6O(7) 1754(6) OFF-DIAG- EB28(3) EB23(3) SB12(-2) 1534(6) 1756(3) 1532(3) BB18(-5) C2O8(2) C6O2(2)	DIAGONAL- HCC (57) COH (22) HCO (17)
1327 (W)	1322 (VW)	1327.	1338.	A''	C2OH(11) C6OH(11) 1643(9) 1645(9) 1532(9) 1756(9) CO (10) CCO (4) CC (1) HC2O(9) HC6O(9) 1316(6) OFF-DIAG- EB23(4) BB29(3) BB3O(2) 1312(6) C2O8(5) C6O2(5) BB25(1) BB28(-1) BB19(-2) SB15(-3) 1423(3) 1865(3) HC5O(2) SB14(-3) SB12(-5) SB13(-6) EE18(-8) HC3O(2) 1421(2) 1861(2)	DIAGONAL- HCC (57) COH (23) HCC (22)
1319 (SH)	1312 (SH)	1312.	1312.	A'	1865(15) 1423(15) HC4O(13) HC2O(13) HC6O(13) HC5O(4) CC (6) CCO (3) CCC (2) HC3O(4) 1643(4) 1645(4) HC1O(4) 1756(3) 1532(3) C2OH(3) C6OH(3) C4OH(2) C1OH(2) C2O8(2) C6O2(2) C4OO(2) 1316(2) 1312(2)	DIAGONAL- HCO (50) HCC (48) CCH (10) CC (1) 1CCC(1) OFF-DIAG- EB23(3) BB26(1) SB15(1) BB25(1) SB14(-3) SB12(-5) BB18(-18)
1296 (W)	1297 (W)	1296.	1289.	A''	1316(22) 1312(22) C2OH(8) C6OH(8) 1643(5) 1645(5) CC (4) CCO (2) HC2C(4) HC6O(4) 1423(4) OFF-DIAG- BB23(4) SB13(-1) BB19(-1) 1865(4) 1754(3) 1534(3) SB15(-1) BB29(-2) BB28(-2) EE18(-3) 1756(2) 1532(2)	DIAGONAL- HCC (73) COH (17) HCC (9)
1280 (W)	1284 (M)	1282.	1276.	A'	HC1O(17) 1756(14) 1532(13) C1OH(11) HC5O(9) HC3C(9) CC (7) CCO (3) CCC (1) HC4C(5) C4OH(4) C5OH(4) OFF-DIAG- SB13(4) BB23(2) SB14(-2) C3OH(4) 1316(4) 1312(4) BB29(-4) SB15(-4) SB12(-5) BB18(-15) HC6C(3) HC2O(3) C5O1(2) C3O9(2) C1O7(2)	DIAGONAL- HCO (47) HCC (41) CCH (23) 1CCC(1)
1264 (VW)	1265 (M)	1265.	1275.	A''	HC2O(19) HC6O(19) 1532(13) 1756(13) 1423(7) 1865(7) CO (5) CCO (4) CCH (1) 1534(4) 1754(4) C3O9(2) OFF-DIAG- EB23(4) EB27(3) SB16(-1) C5C1(2) HC3O(2) HC5O(2) BB28(-1) SB17(-1) SB14(-2) SB15(-4) C2C3(2) C5C6(2) 1421(2) BB18(-13) 1861(2) C1C2(2) C6C1(2)	DIAGONAL- HCC (55) HCO (43) CC (9)

TABLE L (Continued)

EXPERIMENTAL FREQUENCY (CM-1) RAMAN	EXPERIMENTAL FREQUENCY (CM-1) INFRARED	ASSIGNED FREQUENCY (CM-1)	CALCULATED FREQUENCY (CM-1)	CALCULATED SYMMETRY SPECIES	SPECTRAL INTERPRETATION --- POTENTIAL ENERGY DISTRIBUTIONS INTERNAL COORDINATES	FORCE CONSTANTS
1252 (W)	1258 (SH)	1252.	1257.	A'	HC1O(30) HC2O(23) HC6O(23) C1OH(8) 1421(7) 1861(7) 1316(6) 1312(6) C1O7(2)	DIAGONAL- HCO (77) HCC (33) COH (11) CO (4) CCO (2) OFF-DIAG- SB13(2) BB29(-3) SB12(-5) BB18(-21)
1225 (W)	1221 (SH)	1225.	1236.	A''	HC3C(32) HC5O(32) C3OH(11) C5OH(11) 1534(9) 1754(9) 1532(3) 1756(3)	DIAGONAL- HCO (64) HCC (32) CCH (22) CC (2) TOCC(1) OFF-DIAG- BB23(2) SB15(1) BB28(-2) BB29(-5) BB18(-18)
1214 (W)	1216 (W)	1215.	1223.	A'	HC4C(42) C4OH(17) HC5O(12) HC3O(12) 1643(7) 1645(7) C3OH(5) C5OH(5) 1534(4) 1754(4)	DIAGONAL- HCO (68) COH (29) HCC (27) CCC (2) CO (1) OFF-DIAG- EB25(2) SB13(2) BB3O(-1) BB23(-2) BB19(-2) SB12(-2) BB28(-3) BB29(-5) BB18(-18)
	1144 (S)	1144.	1137.	A'	C4OO(25) C3O9(11) C5O1(11) C5C6(11) C2C3(11) C2O8(10) C6O2(10) CC4C(7) CC3C(5) CC5C(5) 0934(3) 1154(3) 1045(3) 1043(3) C4C5(2) C3C4(2) HC1O(2)	DIAGONAL- CO (68) CC (27) CCC (18) CCC (16) HCO (4) COH (3) OFF-DIAG- BB22(2) SB12(1) SB16(-1) SB13(-4) CCCO(-6) SB17(-7) SB14(-20)
1136 (M)		1136.	1127.	A''	C1C2(41) C6C1(41) HC2O(7) HC6C(7) CC2C(3) CC6C(3) C3O9(3) C5O1(3) 0716(3) 0712(3) 0932(3) 1156(3) 0821(3) 1261(3) C4C5(2) C3C4(2)	DIAGONAL- CC (86) CCO (19) HCO (15) CCC (10) CO (9) HCC (8) OFF-DIAG- BB22(1) CCCC(-1) SB12(-2) BB23(-2) SB14(-3) CCCO(-3) SB15(-7) SB17(-12) SB16(-19)
1112 (M)	1115 (S)	1114.	1109.	A'	C1O7(20) C3O9(15) C5O1(15) C5C6(5) C2C3(5) C2O8(4) C6O2(4) C3C4(4) C4C5(4) HC3O(3) HC5O(3) CC1C(3) 0932(3) 1156(3) CC2C(3) CC6C(3) C2OH(2) C6OH(2) C5OH(2) C3OH(2) C1C2(2) C6C1(2)	DIAGONAL- CO (59) CC (21) HCC (10) CCC (10) COH (7) CCO (6) HCC (4) OFF-DIAG- SB12(3) BB19(2) BB26(1) SB15(-2) CCCO(-2) SB17(-2) SB16(-2) SB13(-6) SB14(-8)
1089 (M)	1088 (VS)	1089.	1096.	A'	C1O7(30) C2O8(7) C6O2(7) HC4O(6) C3O9(5) C5O1(5) HC1O(5) CC4C(4) C3C4(4) C4C5(4) 0821(3) 1261(3) 0776(3) 0712(3) 1154(3) 0934(3) 1423(2) 1865(2) C1OH(2) C4OH(2) CC1C(2) HC3C(2) HC5O(2) CC6C(2) CC2C(2) 1265(2) 0823(2)	DIAGONAL- CO (55) CCC (22) HCO (16) CC (10) CCC (10) COH (7) HCC (7) OFF-DIAG- SB12(7) BB19(3) BB3O(2) SB15(1) BB22(1) BB29(-1) CCCO(-2) BB23(-3) SB13(-5) SB17(-7) SB14(-26)
1085 (M)		1085.	1081.	A''	C2O8(21) C6O2(21) C5O1(16) C3O9(16) C3C4(9) C4C5(9) C2C3(3) C5C6(3) CC3C(3) CC5C(3) C1C2(3) C6C1(3) 1043(3) 1045(3)	DIAGONAL- CO (73) CC (31) CCO (11) CCC (6) HCO (4) HCC (2) OFF-DIAG- SB16(2) SB17(-9) CCCO(-9) SB14(-12)
1075 (M)	1073 (S)	1074.	1077.	A'	C4OO(57) C6O2(7) C2O8(7) C4C5(7) C3C4(7) C5O1(6) C3O9(6) C1O7(4) C2C3(4) C5C6(4)	DIAGONAL- CO (87) CC (22) CCH (2) CCC (2) CCC (2) OFF-DIAG- SB15(1) SB17(-2) SB14(-4) SB13(-4) CCCO(-9)
1054 (M)	1050 (SH)	1054.	1054.	A''	C3C4(32) C4C5(32) C2C3(17) C5C6(17) 1316(4) 1312(4) 1421(3) 1861(3) 1865(3) 1423(3) C2O8(2) C6O2(2) C5O1(2) C3O9(2)	DIAGONAL- CC (100) HCC (22) CCO (8) CO (8) COH (3) HCC (1) CCC (1) OFF-DIAG- SB14(1) BB19(-1) CCCC(-2) SB13(-2) SB17(-2) BB23(-5) SB15(-14) SB16(-17)
	1042 (VS)	1042.	1040.	A'	C1O7(25) C5C6(11) C2C3(11) C4C5(6) C3C4(6) HC1O(5) C4OO(5) C6O2(4) C2O8(4) 1265(4) 0823(4) C1OH(4) C1C2(3) C6C1(3) HC4O(3) 1756(2) 1532(2) CC1C(2) 0934(2) 1154(2) 1861(2) 1421(2) C4OH(2)	DIAGONAL- CC (41) CO (38) CCC (16) HCC (9) HCC (9) CCH (8) CCC (7) OFF-DIAG- SB12(6) CCCO(4) BB18(1) BB19(1) BB24(-1) BB23(-1) SB13(-3) SB17(-6) SB15(-7) SB14(-9) SB16(-14)
1035 (VW)	1029 (W,SH)					
	1013 (S)	1013.	1005.	A''	C3O9(28) C5O1(28) C2O8(15) C6O2(15) C1C2(5) C6C1(5) 1423(3) 1865(3) 0716(3) 0712(3) 1316(3) 1312(3) 0821(2) 1261(2) 1754(2) 1534(2) 1643(2) 1645(2)	DIAGONAL- CO (87) HCC (21) CCO (15) CC (10) COH (2) CCC (2) OFF-DIAG- CCCO(3) SB12(2) SB17(1) SB13(-4) SB15(-5) BB23(-6) SB16(-6) SB14(-21)
949 (M)	950 (M)	949.	935.	A'	C1C2(11) C6C1(11) C2O8(11) C6O2(11) C4C5(11) C3C4(11) 1532(5) 1756(5) HC4O(4) 1154(3) 0934(3) CC5C(3) CC3C(3) CC4C(2) 1043(2) 1045(2) C5C6(2) C2C3(2) CC1C(2)	DIAGONAL- CC (48) CO (25) HCC (19) CCO (10) CCC (10) HCO (8) COH (2) OFF-DIAG- SB15(5) BB18(2) BB19(2) BB23(-1) SB12(-1) BB26(-1) CCCC(-2) SB16(-9) SB17(-16)
881 (VW)	885 (M)	885.	905.	A''	C2C3(21) C5C6(21) 1043(8) 1045(8) C4C5(7) C3C4(7) C2O8(6) C6O2(6) 0932(3) 1156(3) C5O1(2) C3O9(2)	DIAGONAL- CC (56) CCO (27) CC (16) HCC (8) CCC (4) HCC (3) COH (2) OFF-DIAG- CCCO(6) SB15(3) BB19(2) SB12(2) SB14(-4) SB17(-10) SB16(-14)
866 (VS)	872 (M)	869.	884.	A'	C1C2(20) C6C1(20) 1156(6) 0932(6) 0821(4) 1261(4) C2O8(3) C6O2(3) C5C6(3) C2C3(3) 1421(3) 1861(3) HC1O(2) 1045(2) 1043(2) C1O7(2) CC6C(2) CC2C(2)	DIAGONAL- CC (46) CCO (25) CC (11) HCC (11) CCC (4) HCC (4) OFF-DIAG- SB15(7) BB19(5) BB18(1) BB23(1) SB14(-1) SB17(-3) SB16(-15)
794 (VW)	802 (S)	802.	800.	A'	CC1C(12) C4OO(10) C5O1(4) C3O9(4) C3C4(4) C4C5(4) C2C3(4) C5C6(4) 1423(4) 1865(4) 1316(4) 1312(4) CC6C(4) CC2C(4)	DIAGONAL- CCC (23) CO (20) HCC (19) CC (19) CCO (10) COH (2) HCC (1) OFF-DIAG- BB19(7) BB26(3) SB14(3) CCCC(2) SB17(2) BB25(-1) SB12(-3) SB16(-1) SB15(-2) SB13(-2) BB23(-4)
719 (VW,B)	705 (SH)					
692 (VW)	667 (SH)					
662 (W,B)	659 (S)	659.	683.	A''	0823(14) 1265(14) CC3C(4) CC5C(4) 1532(4) 1756(4) 1754(3) 1534(3) 1643(3) 1645(3) 1156(3) 0932(3) C2O8(3) C6O2(3) 1423(3) 1865(3) 0934(2) 1154(2)	DIAGONAL- CCO (38) HCC (30) CCC (9) CO (6) CC (4) COH (3) OFF-DIAG- BB19(9) SB14(7) SB17(3) BB18(2) SB16(1) BB26(1) SB15(-1) BB3O(-2) SB13(-2) BB28(-2) BB25(-2) BB24(-3) EB23(-4)

TABLE L (Continued)

EXPERIMENTAL FREQUENCY (CM-1) RAMAN	INFRARED	ASSIGNED FREQUENCY (CM-1)	CALCULATED FREQUENCY (CM-1)	CALCULATED SYMMETRY SPECIES	SPECTRAL INTERPRETATION --- POTENTIAL ENERGY DISTRIBUTIONS INTERNAL COORDINATES	FORCE CONSTANTS
	622 (M)		624.	A'	0823(7) 1265(7) 0716(6) 0712(6) C3C4(4) C4C5(4) C107(4) C5C6(4) C2C3(4) C208(3) C602(3) C400(3) CC2C(3) CC6C(3) 1156(2) 0932(2) 1316(2) 1312(2) C501(2) C309(2)	DIAGONAL- CCO (33) CO (16) CC (16) CCC (7) HCC (7) HCO (2) COH (2) OFF-DIAG- SB14 (13) SB17 (4) BB19 (3) CCCO (1) BB18 (1) BB26 (1) EB3C (-1) SB13 (-1) SB12 (-1) SB16 (-3)
	600 (M,B)					
531 (S)		531.	545.	A'	C107(10) C6C1(8) C1C2(8) C821(6) 1261(6) C2C3(6) C5C6(6) C4C5(3) C3C4(3) CC1C(2) C400(2) 0823(2) 1265(2) C208(2) 0716(2) 0712(2) C602(2)	DIAGONAL- CC (33) CCO (29) CO (17) CCC (4) HCC (4) HCC (2) OFF-DIAG- SB16 (10) SB14 (9) CCCO (6) BB19 (1) SB12 (-2) SB15 (-2) SB17 (-4)
	526 (M)	526.	528.	A''	0934(20) 1154(20) 1045(5) 1043(5) CC2C(5) CC6C(5) 1643(4) 1645(4) 1534(4) 1754(4) C3C4(4) C4C5(4) 1421(3) 1861(3) C1C2(2) C6C1(2)	DIAGONAL- CCO (55) HCC (24) CC (13) CCC (12) CO (1) OFF-DIAG- BB19 (7) SB14 (4) SB17 (4) BB25 (2) BB18 (1) SB15 (-1) EB2E (-2) SB16 (-4) EB23 (-15)
490 (W)	490 (M)	490.	503.	A''	0932(11) 1156(11) 0716(11) C712(11) C1C2(6) C6C1(6) 1154(5) 0934(5) 0821(5) 1261(5) 1421(5) 1861(5) C5C6(4) C2C3(4) CC3C(4) CC5C(4) 1045(3) 1043(3) 1645(2) 1643(2)	DIAGONAL- CCO (72) CC (20) HCC (16) CCC (8) CO (2) TOCC (1) OFF-DIAG- EB19 (4) SB16 (1) BB2E (-1) BB22 (-1) SB15 (-3) SB17 (-3) EB23 (-15)
449 (M)	450 (M)	450.	445.	A'	CC4C(19) CC3C(6) CC5C(6) C4C5(6) C3C4(6) CC1C(5) 0821(5) 1261(5) C309(4) C501(4) 1154(4) 0934(4) 1265(3) 0823(3) 1316(2) 1312(2) 1643(2) 1645(2)	DIAGONAL- CCC (36) CCC (24) CC (12) CC (10) HCC (9) OFF-DIAG- SB14 (6) SB17 (5) EB19 (3) SB16 (2) EB22 (1) EB26 (-1) SB15 (-2) BB25 (-3)
418 (W)	417 (VW)	418.	413.	A'	1043(15) 1045(15) 0823(11) 1265(11) 1643(6) 1645(6) C2C3(4) C5C6(4) 0932(4) 1156(4) 1534(3) 1754(3)	DIAGONAL- CCO (65) HCC (21) CC (9) CCC (2) CO (1) TOCC (1) OFF-DIAG- SB16 (4) EB19 (4) SB14 (3) BB25 (2) SB17 (1) SB15 (-1) BB28 (-2) BB23 (-12)
390 (W)	390 (VW)	390.	399.	A''	0716(25) 0712(25) 0821(8) 1261(8) CC2C(3) CC6C(3) C208(2) C602(2) 1532(2) 1756(2) C2C3(2) C5C6(2) 1045(2) 1043(2) 1316(2) 1312(2)	DIAGONAL- CCO (71) HCC (10) CCC (8) CC (6) CO (4) HCC (1) OFF-DIAG- SB16 (8) SB14 (3) BB22 (2) BB26 (-1) BB19 (-1) BB25 (-2) SB17 (-3) BB23 (-8)
331 (W)	332 (W)	331.	312.	A''	0821(26) 1261(26) 1265(5) 0823(5) 0932(5) 1156(3) 1045(5) 1043(5) 1316(2) 1312(2) CC2C(2) CC6C(2) C716(2) 0712(2)	DIAGONAL- CCO (86) HCC (8) CCC (7) CC (4) TOCO (3) OFF-DIAG- SB16 (2) SB17 (1) EB20 (-1) EB26 (-1) EB23 (-10)
308 (W)	303 (W)	306.	297.	A'	1156(18) 0932(18) 1154(18) 0934(18) CC4C(5) C4C5(3) C3C4(3) TC30(3) TC50(3) C6C1(2) C1C2(2) 1421(2) 1865(2) 0821(2) 1261(2) 1265(2) 0823(2)	DIAGONAL- CCO (77) CC (11) CCC (9) HCC (7) TOCO (7) TOCC (1) OFF-DIAG- SB16 (4) BB20 (-1) EB22 (-2) SB17 (-3) EB23 (-10)
	294 (W)	294.	292.	A''	1043(27) 1045(27) 0932(12) 1156(12) 0934(11) 1154(11) TC40(4) 0712(2) 0716(2) 1754(2) 1534(2) 1261(2) 0821(2) C5C6(2) C2C3(2)	DIAGONAL- CCO (108) HCC (11) TOCC (7) CC (5) OFF-DIAG- BB20 (-1) SB15 (-3) BB19 (-4) SB16 (-8) BB23 (-16)
269 (VW)	263 (W)	263.	252.	A'	0823(8) 1265(8) 1534(8) 1754(8) CC4C(7) 0821(7) 1261(7) 1645(6) 1643(6) 0932(4) 1156(4) CC3C(4) CC5C(4) 0716(4) 0712(4) 1045(3) 1043(3) C400(3) 1154(3) 0934(3) CC1C(2) TC23(2) TC56(2) C107(2) 1532(2) 1756(2)	DIAGONAL- CCO (56) HCC (33) CCC (17) TOCC (6) CC (5) CC (1) OFF-DIAG- BB19 (9) BB24 (1) BB18 (1) SB16 (1) BB22 (-2) BB2E (-4) EB25 (-6) SB14 (-9) EB23 (-12)
		230.	A''	0823(18) 1265(18) CC2C(9) CC6C(9) TC10(8) 0712(6) 0716(6) CC3C(5) CC5C(5) 1861(2) 1421(2) 1534(2) 1754(2)	DIAGONAL- CCO (53) CCC (28) HCC (11) TOCO (10) TOCC (6) CO (4) OFF-DIAG- SB16 (2) BB24 (2) BB19 (1) BB22 (-1) BB30 (-1) BB25 (-2) BB23 (-4) SB14 (-8)
		188.	A'	TC20(39) TC60(39) CC1C(6) C716(3) 0712(3) 1421(2) 1861(2) 1265(2) 0823(2)	DIAGONAL- TOCO (78) CCO (14) CCC (8) HCC (6) CO (2) TOCC (2) OFF-DIAG- EB26 (-2) EB23 (-4) SB14 (-4)
		179.	A''	TC6C(34) TC20(33) TC40(12) TC10(10) TC50(5) TC30(5)	DIAGONAL- TOCO (98) CCC (1)
		175.	A''	TC4C(26) TC30(26) TC50(26) TC20(8) TC60(8) TC10(3)	DIAGONAL- TOCO (97) CCC (2)
		171.	A'	TC1C(73) TC60(6) TC20(6) TC40(2) 0716(2) 0712(2)	DIAGONAL- TOCO (92) CCC (6)
		170.	A''	TC50(46) TC30(46) 1156(2) 0932(2)	DIAGONAL- TOCO (88) CCO (8) CCC (4) HCC (2) OFF-DIAG- BB23 (-1) SB14 (-1)
		170.	A''	TC40(55) TC30(17) TC50(16) TC1C(4) 1045(2) 1043(2)	DIAGONAL- TOCO (92) CCO (8)
		154.	A'	0716(15) 0712(15) CC2C(12) CC6C(12) 0821(11) 1261(11) TC20(6) TC60(6) 1316(5) 1312(5) CC1C(5) C107(4) 1265(4) 0823(4) 0934(3) 1154(3) TC12(3) TC61(3) 1421(2) 1861(2) C6C2(2) C208(2)	DIAGONAL- CCO (69) CCC (28) HCC (23) TCCC (12) CO (10) TOCC (7) HCO (2) OFF-DIAG- SB16 (1) SB12 (-1) EB30 (-1) SB17 (-1) EB18 (-2) BB25 (-2) BB22 (-3) BB26 (-4) BB23 (-16) SB14 (-20)

TABLE L (Continued)

EXPERIMENTAL FREQUENCY (CM-1) RAMAN	INFRARED	ASSIGNED FREQUENCY (CM-1)	CALCULATED FREQUENCY (CM-1)	CALCULATED SYMMETRY SPECIES	SPECTRAL INTERPRETATION --- POTENTIAL ENERGY DISTRIBUTIONS INTERNAL COORDINATES	FORCE CONSTANTS
			130.	A'	CC1C(11) CC5C(7) CC3C(7) TC23(7) TC56(7) CC4C(6) TC45(5) TC34(5) TC12(5) TC61(5) TC20(4) TC60(4) CC2C(3) CC6C(3) 1043(2) 1045(2) 0934(2) 1154(2) 0932(2) 1156(2) 1423(2) 1865(2) 0821(2) 1261(2) HC10(2) C400(2)	DIAGONAL- CCC (38) TOCC(35) CCO (20) TOCO(8) HCC (7) CO (5) HCC (2) CC (2) OFF-DIAG- SB16(2) BB19(2) BB18(1) BB22(-2) BB23(-3) BB26(-3) SB17(-7) SB14(-8)
			89.	A'	CC1C(14) CC4C(13) TC34(13) TC45(13) TC61(10) TC12(10) CC3C(4) CC5C(3) CC6C(3) CC2C(3) 1043(3) 1045(3)	DIAGONAL- TOCC(46) CCC (40) CCO (10) HCC (3) HCO (2) CO (2) OFF-DIAG- SB17(3) BB26(-2) SB14(-3)
			88.	A''	TC56(15) TC23(15) CC5C(12) CC3C(12) CC2C(8) CC6C(8) TC45(4) TC12(4) TC61(4) TC34(4) 1156(3) 0932(3) 1154(2) 0934(2)	DIAGONAL- TOCC(47) CCC (39) CCO (11) HCC (4) HCO (2) CO (2) TOCC(1) OFF-DIAG- SB17 (3) BB19(1) BB23(-2) BB26(-2) SB14(-3)

TABLE LI. DEUTERATED SCYLLO-INOSITOL

EXPERIMENTAL FREQUENCY (CM-1) RAMAN	INFRARED	ASSIGNED FREQUENCY (CM-1)	CALCULATED FREQUENCY (CM-1)	CALCULATED SYMMETRY SPECIES	SPECTRAL INTERPRETATION --- POTENTIAL ENERGY DISTRIBUTIONS INTERNAL COORDINATES	FORCE CONSTANTS
			2952.	A1G	C3H5(16) C2H4(16) C4H6(16) C1H3(16) C5H7(16) C6H8(16)	DIAGONAL- CH (98)
	2940 (W)		2946.	B2	C3H5(25) C6H8(25) C1H3(24) C4H6(24)	DIAGONAL- CH (98)
	2920 (W)		2946.	B1	C5H7(33) C2H4(33) C4H6(8) C1H3(8) C6H8(8) C3H5(8)	DIAGONAL- CH (98)
			2935.	E2G	C3H5(29) C6H8(29) C2H4(19) C5H7(19)	DIAGONAL- CH (99)
			2935.	E1G	C1H3(32) C4H6(32) C2H4(14) C5H7(14) C6H8(4) C3H5(4)	DIAGONAL- CH (99)
	2882 (M)		2931.	A2U	C5H7(17) C6H8(17) C1H3(17) C4H6(17) C3H5(17) C2H4(17)	DIAGONAL- CH (100)
	2550 (SH)		2448.		O12H(48) O7H9(22) O10H(21) O9H1(8)	DIAGONAL- OH (99)
	2535 (S)		2448.		O11H(69) O12H(9) O10H(7) O7H9(7) O8H0(5) O9H1(3)	DIAGONAL- OH (99)
	2445 (S)		2448.		O7H9(54) O10H(28) O12H(6) O9H1(5) O8H0(3) O11H(2)	DIAGONAL- OH (99)
			2448.		O9H1(58) O8H0(18) O12H(17) O10H(6)	DIAGONAL- OH (99)
			2448.		O8H0(46) O10H(23) O11H(19) O12H(11)	DIAGONAL- OH (99)
			2448.		O8H0(27) O9H1(25) O7H9(15) O10H(14) O11H(9) O12H(8)	DIAGONAL- OH (99)
	1416 (M)	1416.	1406.	B2	1643(12) 1316(12) 1645(11) 1312(11) 1423(8) 1756(8) 1532(6) 1865(6)	DIAGONAL- HCC (78) CCO (5) CO (3) COH (2) OFF-DIAG- BB23(10) BB25(3) SB13(1) BB30(-1) SB14(-3)
	1392 (M)	1392.	1406.	B1	1534(13) 1861(13) 1754(12) 1421(12) 1865(7) 1532(7) 1423(5) 1756(5) 1312(2) 1645(2)	DIAGONAL- HCC (78) CCO (5) CO (3) COH (2) OFF-DIAG- BB23(10) BB25(3) SB13(1) BB30(-1) SB14(-3)
1416 (M)		1416.	1389.	E2G	1534(12) 1861(12) 1865(11) 1532(11) 1421(10) 1754(10) 1423(9) 1756(9)	DIAGONAL- HCC (85) HCO (4) COH (2) CC (2) CCO (1) OFF-DIAG- BB28(5) BB23(4) SB15(-6)
1394 (M)		1394.	1389.	E1G	1316(14) 1643(14) 1312(14) 1645(14) 1756(5) 1423(5) 1754(4) 1421(4) 1532(3) 1865(3) 1534(2) 1861(2)	DIAGONAL- HCC (85) HCO (4) COH (2) CC (2) CCO (1) OFF-DIAG- BB28(5) BB23(4) SB15(-6)
1366 (M)		1366.	1374.	A1G	HC10(9) HC20(9) HC30(9) HC40(9) HC50(9) HC60(9) 1643(4) 1865(4) 1754(4) 1756(4) 1861(4) BB19(2) 1316(4) 1312(4) 1421(4) 1423(4) 1532(4) 1534(4) C1O7(3) C2O8(3) C3O9(3) C4O0(3) C5O1(3) C6O2(3)	DIAGONAL- HCO (52) HCC (45) CO (16) CCC (3) CCO (3) TOCC (2) OFF-DIAG- BB28(6) BB23(5) BB25(4) SB17(1) SB15(-3) SB14(-5) SB12(-9) BB18(-23)
			1358.	A1U	1532(8) 1534(8) 1643(8) 1645(8) 1316(8) 1312(8) 1421(8) 1423(8) 1754(8) 1756(8) 1865(8) 1861(8) C3C4(2) C4C5(2) C5C6(2) C1C2(2) C2C3(2) C6C1(2)	DIAGONAL- HCC (97) CC (13) OFF-DIAG- BB28(13) SB16(-1) BB23(-2) SB15(-19)
	1328 (VW)					
1315 (VW)						
			1305.	A2U	HC10(15) HC20(15) HC40(15) HC50(15) HC30(15) HC60(15) 1643(2) 1645(2) 1754(2) 1756(2) 1865(2) 1861(2) 1316(2) 1312(2) 1421(2) 1423(2) 1532(2) 1534(2)	DIAGONAL- HCO (87) HCC (26) CO (9) COH (8) CCC (7) CCO (1) OFF-DIAG- BB25(5) BB29(3) BB30(1) SB14(-3) BB23(-3) SB13(-3) BB28(-3) BB19(-5) SB12(-9) BB18(-23)
	1298 (W)	1298.	1294.	B1	HC10(29) HC40(29) HC30(15) HC60(14) 1312(5) 1645(5) 1643(4) 1316(4) 1532(3) 1865(-3) HC50(2) HC20(2)	DIAGONAL- HCO (91) HCC (30) CO (4) COH (4) TOCC (2) CC (1) OFF-DIAG- BB29(2) SB13(-2) SB15(-2) SB12(-6) BB18(-24)
	1273 (W)	1273.	1294.	B2	HC20(28) HC50(28) HC30(16) HC60(16) 1421(5) 1754(5) 1423(4) 1756(4) 1534(4) 1861(4) HC10(2) HC40(2) 1865(2) 1532(2)	DIAGONAL- HCO (91) HCC (30) CO (4) COH (4) TOCC (2) CC (1) OFF-DIAG- BB29(2) SB13(-2) SB15(-2) SB12(-6) BB18(-24)
			1279.	E2G	HC40(27) HC10(27) HC30(16) HC60(16) 1312(6) 1645(6) 1532(5) 1865(5) 1316(3) 1643(3) 1756(2) 1423(2) C1OH(2) C4OH(2)	DIAGONAL- HCO (89) HCC (34) COH (5) CO (4) CCC (2) CC (2) OFF-DIAG- BB29(3) BB28(1) SB13(-2) BB23(-2) BB19(-2) SB15(-3) SB12(-6) BB18(-24)
			1279.	E1G	HC50(28) HC20(28) HC30(14) HC60(14) 1421(5) 1754(5) 1534(5) 1861(5) 1756(4) 1423(4) HC10(3) HC40(3) 1643(2) 1316(2) C2OH(2) C5OH(2)	DIAGONAL- HCO (89) HCC (34) COH (5) CO (4) CCC (2) CC (2) OFF-DIAG- BB29(3) BB28(1) SB13(-2) BB23(-2) BB19(-2) SB15(-3) SB12(-6) BB18(-24)
			1276.	A2G	1312(8) 1421(8) 1532(8) 1645(8) 1754(8) 1865(8) 1423(8) 1316(8) 1756(8) 1534(8) 1861(8) 1643(8)	DIAGONAL- HCC (95) CCO (8) OFF-DIAG- BB23(14) BB19(-5) BB28(-12)
	1256 (VW)					
	1242 (VW)					
1194 (M)		1194.	1209.	A1G	HC10(6) HC20(6) HC30(6) HC40(6) HC50(6) HC60(6) C1OH(5) C2OH(5) C3OH(5) C4OH(5) C5OH(5) C6OH(5) C1C2(3) C2C3(3) C3C4(3) C4C5(3) C5C6(3) C6C1(3)	DIAGONAL- HCO (34) COH (30) CC (17) CCO (14) CCC (8) CH (1) OFF-DIAG- BB19(6) BB29(4) BB18(3) SP15(2) BB23(2) BB22(1) BB30(-6) SB16(-10) SB17(-11)

Conventional symbolism indicating relative intensity: s = strong, m = medium, w = weak, sh = shoulder, b = broad, v = very, lt = low temperature band

TABLE LI (Continued)

EXPERIMENTAL FREQUENCY (CM-1) RAMAN	INFRARED	ASSIGNED FREQUENCY (CM-1)	CALCULATED FREQUENCY (CM-1)	CALCULATED SYMMETRY SPECIES	SPECTRAL INTERPRETATION --- POTENTIAL ENERGY DISTRIBUTIONS INTERNAL COORDINATES	FORCE CONSTANTS
	1151 (M)	1151.	1147.	A2U	C1O7 (13) C2O8 (13) C3O9 (13) C4O0 (13) C5O1 (13) C6O2 (13) CC2C (4) CC3C (4) CC4C (4) CC5C (4) CC6C (4) CC1C (4)	DIAGONAL- CO (78) CCC (25) CCO (15) HCO (3) OFF-DIAG- SB12 (5) BB22 (2) BB19 (2) BB23 (2) BB25 (-2) SB13 (-3) SB14 (-27)
1139 (M)		1139.	1119.	EG	C6C1 (21) C3C4 (21) C2O8 (12) C5O1 (12) C5C6 (11) C2C3 (11) C4O0 (7) C1O7 (7) CC2C (4) CC5C (4) 0712 (3) 1045 (3) C2OH (3) C5OH (3) 0932 (3) 1265 (3) CC4C (2) CC1C (2) 1154 (2) 0821 (2) C4OH (2) C1OH (2)	DIAGONAL- CC (68) CO (40) CCO (20) CCC (14) COH (9) HCC (1) OFF-DIAG- BB30 (3) BB22 (2) BB25 (-1) SB15 (-4) CCCO (-7) SB13 (-8) SB16 (-8) SB17 (-14) SB14 (-15)
1121 (M)		1121.	1119.	EG	C4C5 (21) C1C2 (21) C6O2 (12) C3O9 (12) C2C3 (11) C5C6 (11) C4O0 (7) C1O7 (7) CC3C (4) CC6C (4) 0716 (3) 1043 (3) C6OH (3) C3OH (3) 0823 (3) 1156 (3) CC4C (2) CC1C (2) 0934 (2) 1261 (2) C3C4 (2) C6C1 (2) C4OH (2) C1OH (2)	DIAGONAL- CC (68) CO (40) CCO (20) CCC (14) COH (9) HCC (1) OFF-DIAG- BB30 (3) BB22 (2) BB25 (-1) SB15 (-4) CCCO (-7) SB13 (-8) SB16 (-8) SB17 (-14) SB14 (-15)
	1114 (S)	1114.	1111.	EU	C3C4 (15) C6C1 (15) C3O9 (11) C6O2 (11) C3OH (9) C6OH (9) C2C3 (9) C5C6 (9) C4O0 (6) C1O7 (6) C4OH (5) C1OH (5) 0823 (3) 1156 (3) 1154 (3) 0821 (3) 0716 (2) 1043 (2)	DIAGONAL- CC (50) CO (34) COH (29) CCO (18) HCC (5) CCC (5) OFF-DIAG- BB23 (4) SB12 (-1) CCCO (-9) SB16 (-10) SB17 (-12) SB13 (-12)
	1102 (M)	1102.	1111.	EU	C1C2 (16) C4C5 (16) C2O8 (11) C5O1 (11) C2OH (9) C5OH (9) C2C3 (8) C5C6 (8) C4O0 (6) C1O7 (6) C4OH (5) C1OH (5) 0932 (3) 1265 (3) 0934 (3) 1261 (3)	DIAGONAL- CC (50) CO (34) COH (29) CCO (18) HCC (5) CCC (5) OFF-DIAG- BB23 (4) SB12 (-1) CCCO (-9) SB16 (-10) SB17 (-12) SB13 (-12)
1096 (S)		1096.	1106.	A1G	C6O2 (13) C2O8 (13) C4O0 (13) C5O1 (13) C1O7 (13) C3O9 (13) C2C3 (3) C4C5 (3) C5C6 (3) C6C1 (3) C1C2 (3) C3C4 (3)	DIAGONAL- CO (75) CC (20) COH (5) HCO (5) HCC (1) OFF-DIAG- SB12 (6) SB15 (2) SB17 (2) BB18 (-1) SB13 (-8) CCCO (-10)
		1097.	A1U	C1C2 (19) C2C3 (19) C3C4 (19) C4C5 (19) C5C6 (19) C6C1 (19)	DIAGONAL- CC (111) CCO (4) OFF-DIAG- CCCC (-2) SB16 (-13)
	1083 (M)				
	1072 (W,SH)				
	1034 (VS)	1034.	1010.	EU	C2O8 (20) C5O1 (20) C6O2 (9) C3O9 (9) C2OH (6) C5OH (6) 1316 (3) 1643 (3) 1534 (3) 1861 (3) C3OH (3) C6OH (3) C1O7 (2) C4O0 (2)	DIAGONAL- CO (61) HCC (20) COH (18) CCO (6) OFF-DIAG- SB13 (13) BB28 (-3) BB30 (-3) SB14 (-14)
	1013 (VS)	1013.	1010.	EU	C1O7 (18) C4O0 (18) C3O9 (12) C6O2 (12) C4OH (5) C1OH (5) C6OH (3) C3OH (3) 1423 (3) 1756 (3) 1532 (3) 1865 (3) 1421 (2) 1754 (2) 1645 (2) 1312 (2)	DIAGONAL- CO (61) HCC (20) COH (18) CCO (6) OFF-DIAG- SB11 (13) BB28 (-3) BB30 (-3) SB14 (-14)
1042 (W)		1042.	1007.	EG	C5O1 (21) C2O8 (21) C3C4 (13) C6C1 (13) C3O9 (8) C6O2 (8) C4C5 (5) C1C2 (5) C1O7 (3) C4O0 (3) C5C6 (2) C2C3 (2)	DIAGONAL- CO (64) CC (41) CCO (5) COH (2) HCC (1) OFF-DIAG- CCCO (7) SB17 (3) SB12 (1) SB15 (-3) SB13 (-5) SB14 (-6) SB16 (-8)
1023 (M)		1023.	1007.	EG	C4O0 (18) C1O7 (18) C6O2 (13) C3O9 (13) C2C3 (12) C5C6 (12) C4C5 (8) C1C2 (8)	DIAGONAL- CO (64) CC (41) CCO (5) COH (2) HCC (1) OFF-DIAG- CCCO (7) SB17 (3) SB12 (1) SB15 (-3) SB13 (-5) SB14 (-6) SB16 (-8)
	990 (SH)	990.	986.	A2U	C4OH (16) C3OH (16) C5OH (16) C2OH (16) C1OH (16) C6OH (16) HC1O (2) HC2O (2) HC3O (2) HC4O (2) HC5O (2) HC6O (2)	DIAGONAL- COH (96) HCO (9) HCC (6) CCO (2) CCC (1) OFF-DIAG- BB19 (-1) BB23 (-2) BB18 (-3) BB29 (-4) BB30 (-5)
1003 (W)		1003.	977.	EG	C2OH (28) C5OH (28) C1OH (10) C4OH (10) C3OH (5) C6OH (5) HC2O (3) HC5O (3)	DIAGONAL- COH (84) HCC (8) HCO (8) CCO (6) CO (4) CC (3) CCC (2) OFF-DIAG- SB13 (8) BB25 (1) BB28 (-1) SB17 (-1) BB19 (-1) SB12 (-2) BB23 (-3) BB29 (-3) BB18 (-3) SB14 (-4) BB30 (-6)
994 (W)		994.	977.	EG	C6OH (23) C3OH (23) C1OH (19) C4OH (19) HC3O (2) HC6O (2) HC4O (2) HC1O (2)	DIAGONAL- COH (84) HCC (8) HCO (8) CCO (6) CO (4) CC (3) CCC (2) OFF-DIAG- SB13 (8) BB25 (1) BB28 (-1) SB17 (-1) BB19 (-1) SB12 (-2) BB23 (-3) BB29 (-3) BB18 (-3) SB14 (-4) BB30 (-6)
	926 (W)	926.	931.	EU	C3OH (16) C6OH (16) C2C3 (9) C5C6 (9) C3C4 (9) C6C1 (9) C5OH (4) C2OH (4) C1OH (4) C4OH (4) C3O9 (3) C6O2 (3) HC3O (3) HC6O (3) 0716 (2) 1043 (2) 0712 (2) 1045 (2) 0823 (2) 1156 (2) 1154 (2) 0821 (2)	DIAGONAL- COH (48) CC (35) CCO (19) CO (10) HCO (8) CCC (4) OFF-DIAG- CCCO (4) SB12 (3) SB15 (-2) BB29 (-3) SB16 (-8) SB13 (-8) SB17 (-10)
	885 (W)	885.	931.	EU	C1OH (12) C4OH (12) C1C2 (12) C4C5 (12) C2OH (12) C5OH (12) 0932 (3) 0934 (3) 1265 (3) 1261 (3) C3C4 (3) C6C1 (3) C5C6 (3) C2C3 (3) C1O7 (2) C4O0 (2) C2O8 (2) C5O1 (2) HC1O (2) HC4O (2) HC2O (2) HC5O (2)	DIAGONAL- COH (48) CC (35) CCO (19) CO (10) HCO (8) CCC (4) OFF-DIAG- CCCO (4) SB12 (3) SB15 (-2) BB29 (-3) SB16 (-8) SB13 (-8) SB17 (-10)
		912.	A1G	C1OH (11) C2OH (11) C3OH (11) C4OH (11) C5OH (11) C6OH (11) C1C2 (3) C2C3 (3) C3C4 (3) C4C5 (3) C5C6 (3) C6C1 (3) HC1O (2) HC2O (2) HC3O (2) HC4O (2) HC5O (2) HC6O (2)	DIAGONAL- COH (68) CC (19) HCO (9) CCO (4) CCC (1) OFF-DIAG- BB30 (5) PB19 (2) SB15 (2) BB18 (1) SB13 (-1) BB29 (-3) SB16 (-6) SB17 (-7)
	724 (M)				

TABLE LI (Continued)

EXPERIMENTAL FREQUENCY (CM-1) RAMAN	EXPERIMENTAL FREQUENCY (CM-1) INFRARED	ASSIGNED FREQUENCY (CM-1)	CALCULATED FREQUENCY (CM-1)	CALCULATED SYMMETRY SPECIES	SPECTRAL INTERPRETATION --- POTENTIAL ENERGY DISTRIBUTIONS INTERNAL COORDINATES	FORCE CONSTANTS
			667.	A2G	0716(8) 0712(8) 0821(8) 0823(8) 0932(8) 0934(8) 1043(8) 1045(8) 1154(8) 1156(8) 1265(8) 1261(8) 1316(2) 1312(2) 1421(2) 1423(2) 1532(2) 1534(2) 1643(2) 1645(2) 1754(2) 1756(2) 1865(2) 1861(2)	DIAGONAL- CCO (97) HCC (23) OFF-DIAG- BB19(8) BB20(-1) BB28(-3) BB23(-23)
	627 (S)	627.	628.	EU	1423(7) 1756(7) 1532(6) 1865(6) 0823(6) 1156(6) 1043(5) 0716(5) 0932(5) 1265(5) 0712(5) 1045(5) 1316(4) 1643(4) 1312(3) 1645(3)	DIAGONAL- HCC (42) CCO (41) CCC (4) COH (3) HCO (3) CO (1) OFF-DIAG- BB19(11) SB14(5) BB18(4) BB30(3) SB16(1) SB17(1) BB25(-1) BB28(-5) BB23(-15)
	627 (S)	627.	628.	EU	0821(7) 1154(7) 0934(7) 1261(7) 1421(7) 1754(7) 1534(6) 1861(6) 1312(4) 1645(4) 1643(3) 1316(3) 0712(2) 1045(2) 1265(2) 0932(2)	DIAGONAL- HCC (42) CCO (41) CCC (4) COH (3) HCO (3) CO (1) OFF-DIAG- BB19(11) SB14(5) BB18(4) BB30(3) SB16(1) SB17(1) BB25(-1) BB28(-5) BB23(-15)
	582 (M)					
			548.	A2U	CC2C(6) CC3C(6) CC4C(6) CC5C(6) CC6C(6) CC1C(6) C107(4) C208(4) C309(4) C400(4) C501(4) C602(4)	DIAGONAL- CCC (37) CO (27) CCO (17) HCC (1) HCO (1) OFF-DIAG- SB14(17) BB22(3) BB23(2) BB19(2) SB12(-2) BB25(-2)
	513 (M)					
451 (VS)		451.	447.	A1G	C2C3(8) C3C4(8) C5C6(8) C6C1(8) C1C2(8) C4C5(8) C107(3) C208(3) C309(3) C400(3) C501(3) C602(3)	DIAGONAL- CC (48) CO (16) CCC (2) CCO (2) HCO (2) HCC (1) OFF-DIAG- SB17(10) CCCO(7) SB16(6) SB14(5) BB19(1) SB13(1) SB12(-2) SB15(-5)
417 (M)		417.	403.	EG	CC4C(10) CC1C(10) CC6C(8) CC3C(8) 1534(5) 1861(5) 1643(4) 1316(4) 0823(4) 1156(4) 1154(4) 0821(4) 0932(3) 1265(3) 1754(2) 1421(2) 1045(2) 0712(2) C107(2) C400(2)	DIAGONAL- CCC (36) HCC (28) CCO (26) CO (7) TOCC(4) OFF-DIAG- BB19(5) BB22(3) SB16(2) SB17(2) BB18(2) BB23(1) SB14(-3) BB28(-4) BB25(-10)
400 (M)		400.	403.	EG	CC5C(12) CC2C(12) 0716(4) 1043(4) 1532(4) 1865(4) CC3C(4) CC6C(4) 0934(4) 1261(4) 1645(4) 1312(4) 1756(3) 1423(3) 1045(3) 0712(3) 1421(2) 1754(2) C208(2) C501(2) CC4C(2) CC1C(2) 1265(2) 0932(2)	DIAGONAL- CCC (36) HCC (28) CCO (26) CO (7) TOCC(4) OFF-DIAG- BB19(5) BB22(3) SB16(2) SB17(2) BB18(2) BB23(1) SB14(-3) BB28(-3) BB25(-10)
389 (M)		389.	371.	EG	0821(11) 1154(11) 0823(9) 1156(9) 0934(7) 1261(7) 1265(4) 0932(4) 1532(4) 1865(4) 1756(3) 1423(3) CC2C(3) CC5C(3) C3C4(3) C6C1(3) 1312(2) 1645(2) CC3C(2) CC6C(2) 0716(2) 1043(2) C4C5(2) C1C2(2)	DIAGONAL- CCO (65) HCC (22) CCC (10) CC (10) TOCC(1) OFF-DIAG- BB25(5) SB17(5) SB14(4) BB19(3) BB18(1) BB22(1) BB28(-3) SB16(-10) BB23(-16)
	387 (M)					
360 (M,B)		360.	371.	EG	0712(11) 1045(11) 1043(9) 0716(9) 0932(7) 1265(7) 0934(4) 1261(4) 1534(4) 1861(4) 1643(3) 1316(3) CC4C(3) CC1C(3) C2C3(3) C5C6(3) 1754(2) 1421(2) 0823(2) 1156(2) CC6C(2) CC3C(2) C4C5(2) C1C2(2) 1312(2) 1645(2)	DIAGONAL- CCO (65) HCC (22) CCC (10) CC (10) TOCC(1) OFF-DIAG- BB25(5) SB17(5) SB14(4) BB19(3) BB18(1) BB22(1) BB28(-3) SB16(-10) BB23(-16)
	329 (M)					
			306.	EU	0716(9) 1043(9) C2C3(8) C5C6(8) 0823(7) 1156(7) 1045(7) 0712(7) C3C4(6) C6C1(6) 1154(5) 0821(5)	DIAGONAL- CCO (57) CC (28) TOCC(3) CCC (2) HCC (1) OFF-DIAG- SB16(15) BB19(1) BB22(-1) BB23(-2) SB17(-6)
			306.	EU	0934(10) 1261(10) C1C2(9) C4C5(9) 1265(9) 0932(9) 0821(5) 1154(5) C3C4(3) C6C1(3) 1045(3) 0712(3) 0823(2) 1156(2) C2C3(2) C5C6(2)	DIAGONAL- CCO (57) CC (28) TOCC(3) CCC (2) HCC (1) OFF-DIAG- SB16(15) BB19(1) BB22(-1) BB23(-2) SB17(-6)
			287.	A1U	1043(10) 1045(10) 1154(10) 1156(10) 1261(10) 0712(10) 0821(10) 0823(10) 0932(10) 1265(10) 0934(10) 0716(10)	DIAGONAL- CCO (125) HCC (18) CC (9) TOCO(5) OFF-DIAG- BB28(2) BB20(-2) SB15(-7) BB19(-8) SB16(-21) BB23(-23)
			275.	EG	0932(12) 1265(12) 0934(10) 1261(10) 0712(9) 1045(9) CC2C(6) CC5C(6) 1043(5) 0716(5) CC4C(3) CC1C(3) 1423(2) 1756(2) 1754(2) 1421(2) TC30(2) TC60(2) 0821(2) 1154(2)	DIAGONAL- CCO (76) CCC (19) HCC (14) TOCO(6) TOCC(5) CO (1) OFF-DIAG- BB19(4) SB14(-1) BB25(-2) BB22(-4) BB23(-15)
			275.	EG	0823(13) 1156(13) 0821(11) 1154(11) 0716(8) 1043(8) CC6C(6) CC3C(6) 0712(4) 1045(4) CC4C(3) CC1C(3) 0934(2) 1261(2) 1532(2) 1865(2) TC20(2) TC50(2) 1534(2) 1861(2) 1112(2)	DIAGONAL- CCO (76) CCC (19) HCC (14) TOCO(6) TOCC(5) CO (1) OFF-DIAG- BB19(4) SB14(-1) BB25(-2) BB22(-4) BB23(-15)
			210.	A2U	1316(6) 1312(6) 1421(6) 1423(6) 1532(6) 1534(6) 1643(6) 1645(6) 1754(6) 1756(6) 1865(6) 1861(6) 0716(5) 0712(5) 0821(5) 0823(5) 0932(5) 0934(5) 1043(5) 1045(5) 1154(5) 1156(5) 1265(5) 1261(5) CC1C(3) CC2C(3) CC3C(3) CC4C(3) CC5C(3) CC6C(3)	DIAGONAL- HCC (71) CCO (58) CCC (17) CO (7) OFF-DIAG- BB19(19) BB20(2) BB22(-4) BB28(-9) BB25(-12) SB14(-17) BB23(-33)

TABLE LI (Continued)

EXPERIMENTAL FREQUENCY (CM-1) RAMAN	INFRARED	ASSIGNED FREQUENCY (CM-1)	CALCULATED FREQUENCY (CM-1)	CALCULATED SYMMETRY SPECIES	SPECTRAL INTERPRETATION --- POTENTIAL ENERGY DISTRIBUTIONS INTERNAL COORDINATES	FORCE CONSTANTS
			125.	A1G	CC2C (7) CC3C (7) CC4C (7) CC5C (7) CC6C (7) CC1C (7) TC23 (7) TC12 (7) TC34 (7) TC45 (7) TC61 (7) TC56 (7) 0716 (2) 0934 (2) 1045 (2) 0821 (2) 0823 (2) 1156 (2) 1265 (2) 0932 (2) 0712 (2) 1154 (2) 1261 (2) 1043 (2)	DIAGONAL- TOCO (99)
			129.	A2G	TC20 (17) TC40 (17) TC30 (17) TC10 (17) TC50 (17) TC60 (17)	DIAGONAL- CCC (42) TOCC (41) CCO (29) CO (8) CC (5) OFF-DIAG- SB16 (8) BB23 (1) BB20 (-1) BB25 (-1) CCCO (-2) BB22 (-4) SB14 (-12) SB17 (-13)
			123.	EU	TC40 (31) TC10 (31) TC30 (13) TC60 (13) TC20 (4) TC50 (4)	DIAGONAL- TOCO (96) CCO (3)
			123.	EU	TC50 (28) TC20 (28) TC60 (19) TC30 (19)	DIAGONAL- TOCO (96) CCO (3)
			121.	EG	TC60 (25) TC30 (25) TC10 (22) TC40 (22)	DIAGONAL- TOCO (94) CCO (6) HCC (1) OFF-DIAG- BB23 (-1)
			121.	EG	TC50 (31) TC20 (31) TC40 (9) TC10 (9) TC60 (7) TC30 (6)	DIAGONAL- TOCO (94) CCO (6) HCC (1) OFF-DIAG- BB23 (-1)
			121.	A1U	TC20 (16) TC50 (16) TC40 (16) TC30 (16) TC10 (16) TC60 (16)	DIAGONAL- TOCO (95) CCO (6) OFF-DIAG- SB16 (-1)
			87.	EU	TC23 (15) TC56 (15) CC6C (12) CC3C (12) TC61 (8) TC34 (8) CC5C (6) CC2C (6) 0932 (3) 1265 (3) 0934 (2) 1261 (2) 0823 (2) 1156 (2)	DIAGONAL- TOCC (47) CCC (40) CCO (16) CO (3) OFF-DIAG- BB22 (-2) SB14 (-6)
			87.	EU	TC12 (15) TC45 (15) CC4C (12) CC1C (12) TC34 (8) TC61 (8) CC5C (7) CC2C (7) 0712 (3) 1045 (3) 1043 (2) 0716 (2) 0821 (2) 1154 (2)	DIAGONAL- TOCC (47) CCC (40) CCO (16) CO (3) OFF-DIAG- BB22 (-2) SB14 (-6)

TABLE LII. DEUTERATED NEO-INOSITOL

EXPERIMENTAL FREQUENCY (CM-1) RAMAN	EXPERIMENTAL FREQUENCY (CM-1) INFRARED	ASSIGNED FREQUENCY (CM-1)	CALCULATED FREQUENCY (CM-1)	CALCULATED SYMMETRY SPECIES	SPECTRAL INTERPRETATION --- POTENTIAL ENERGY DISTRIBUTIONS INTERNAL COORDINATES	FORCE CONSTANTS
			2985.	AG	C6H8(23) C1H3(22) C3H5(22) C4H6(22) C5H7(4) C2H4(4)	DIAGONAL- CH (98)
	2965 (W)		2948.	AU	C3H5(25) C4H6(25) C6H8(25) C1H3(25)	DIAGONAL- CH (99)
	2943 (W)		2939.	BU	C2H4(49) C5H7(49)	DIAGONAL- CH (99)
			2938.	AG	C5H7(45) C2H4(45) C3H5(2) C1H3(2) C6H8(2) C4H6(2)	DIAGONAL- CH (99)
	2918 (S)		2934.	BU	C4H6(25) C3H5(25) C1H3(24) C6H8(24)	DIAGONAL- CH (99)
			2934.	BG	C1H3(25) C6H8(25) C4H6(24) C3H5(24)	DIAGONAL- CH (99)
	2530 (S)		2448.		O9H1(25) O8H0(25) O7H9(23) O11H(11) O10H(8) O12H(7)	DIAGONAL- OH (99)
	2480 (S)		2448.		O10H(26) O11H(26) O12H(21) O9H1(10) O7H9(9) O8H0(7)	DIAGONAL- OH (99)
	2390 (S)		2448.		O7H9(44) O9H1(43) O12H(7) O10H(6)	DIAGONAL- OH (99)
			2448.		O12H(46) O10H(41) O7H9(6) O9H1(6)	DIAGONAL- OH (99)
			2448.		O8H0(35) O11H(34) O12H(9) O10H(8) O7H9(7) O9H1(7)	DIAGONAL- OH (99)
			2448.		O8H0(33) O11H(29) O12H(10) O10H(9) O7H9(9) O9H1(9)	DIAGONAL- OH (99)
	1405 (M)	1405.	1403.	AU	1316(10) 1534(10) 1643(10) 1861(10) 1756(9) 1754(9) 1423(9) 1421(9) C3C4(4) C6C1(4) 1312(3) 1532(3) 1865(3) 1645(3)	DIAGONAL- HCC (86) CC (8) CCC (5) CO (3) HCO (1) OFF-DIAG- BB23(6) BB28(5) BB27(-1) BB18(-1) BB19(-2) SB14(-2) SB15(-9)
1396 (M)		1396.	1397.	AG	1316(10) 1861(10) 1643(10) 1534(10) 1865(8) 1865(8) 1312(8) 1532(8) HC20(5) HC50(5) C208(2) C501(2)	DIAGONAL- HCC (77) HCO (10) CO (4) COH (2) OFF-DIAG- BB28(5) BB23(3) BB25(2) SB12(-2) BB18(-2) SB15(-2)
1373 (S)		1373.	1386.	BG	1421(17) 1423(17) 1754(17) 1756(17) 1643(3) 1316(3) 1534(3) 1861(3) HC10(2) HC30(2) HC40(2) HC60(2)	DIAGONAL- HCC (83) HCO (10) CO (3) CCO (3) CC (3) CCC (2) OFF-DIAG- BB23(7) BB26(2) BB25(1) BB28(-2) SB12(-2) BB18(-2) BB19(-3) SB15(-5)
	1381 (W)	1381.	1364.	AU	1423(11) 1421(11) 1754(11) 1756(11) 1643(4) 1534(4) 1316(4) 1861(4) 1312(4) 1532(4) 1865(4) 1645(4) C3C4(2) C6C1(2) C1C2(2) C4C5(2) C5C6(2) C2C3(2)	DIAGONAL- HCC (77) CC (12) HCO (5) COH (3) CCC (2) CCO (2) OFF-DIAG- BB23(3) BB28(2) BB26(2) BB25(1) BB27(1) BB19(1) SB16(-2) SB17(-4) SB15(-6)
	1368 (M)	1368.	1354.	BU	1532(12) 1865(12) 1645(12) 1312(12) HC20(11) HC50(11) C208(5) C501(5) 1534(5) 1861(5) 1643(5) 1316(5) 1421(2) 1423(2) 1754(2) 1756(2)	DIAGONAL- HCC (77) HCO (23) CO (12) CCO (4) CCC (2) COH (2) OFF-DIAG- BB25(3) BB23(2) BB27(-1) BB24(-1) SB13(-2) BB19(-2) BB28(-3) SB14(-4) SB12(-5) BB18(-8)
1329 (M)		1329.	1329.	AG	HC10(19) HC30(19) HC40(19) HC60(19) 1316(6) 1534(6) 1861(6) 1532(4) 1643(6) 1865(4) 1645(4) 1312(4) C107(3) C309(3) C400(3) C602(3) C3C4(2) C6C1(2)	DIAGONAL- HCO (78) HCC (37) CO (15) CC (5) CCC (2) CCO (2) COH (2) TOCC(1) OFF-DIAG- BB28(3) BB25(2) BB29(1) CCCO(-1) SB13(-2) SB14(-3) SB15(-6) SB12(-10) BB18(-25)
	1326 (W)	1326.	1321.	BU	HC40(20) HC30(20) HC10(20) HC60(20) 1643(5) 1316(5) 1861(5) 1534(5) C107(2) C309(2) C400(2) C602(2) C10H(2) C30H(2) C40H(2) C60H(2)	DIAGONAL- HCO (79) HCC (28) CO (8) COH (7) CCC (7) CCO (1) OFF-DIAG- BB25(4) BB29(3) BB28(-3) BB19(-3) SB13(-3) SB12(-8) BB18(-20)
	1303 (VW)	1303.	1296.	AU	HC10(22) HC30(22) HC60(22) HC40(21) 1534(4) 1861(4) 1316(4) 1643(4) 1532(4) 1865(4) 1645(4) 1312(4)	DIAGONAL- HCO (86) HCC (33) CO (3) COH (3) TOCC(2) OFF-DIAG- BB28(2) BB29(2) SB15(-1) SB13(-1) SB12(-6) BB18(-24)
1265 (S)		1265.	1286.	BG	HC30(20) HC60(20) HC10(20) HC40(20) 1312(8) 1645(8) 1532(4) 1865(4) 1756(2) 1423(2) 1534(2) 1861(2) 1754(2) 1421(2) 1643(2) 1316(2) C10H(2) C40H(2) C30H(2) C60H(2)	DIAGONAL- HCO (81) HCC (31) COH (6) CCO (2) OFF-DIAG- BB29(3) BB28(-1) BB19(-1) SB12(-3) BB18(-20)
1265 (S)		1265.	1286.	AG	HC20(38) HC50(38) 1421(7) 1754(7) 1423(7) 1756(7) C3C4(2) C6C1(2)	DIAGONAL- HCO (76) HCC (35) CC (5) COH (4) CO (2) TOCC(2) OFF-DIAG- BB29(2) SB17(-1) SB12(-3) BB18(-22)
	1264 (W)	1264.	1274.	BU	HC50(34) HC20(34) 1754(5) 1756(5) 1421(5) 1423(5) 1312(3) 1865(3) 1645(3) 1532(3) 1316(2) 1861(2) 1534(2) 1643(2)	DIAGONAL- HCO (68) HCC (38) CO (5) COH (3) CCO (2) TOCC(2) CC (1) OFF-DIAG- BB23(2) BB29(2) BB28(-1) SB14(-2) SB15(-3) BB18(-17)
1246 (M)		1246.	1269.	BG	1532(13) 1645(13) 1312(13) 1865(13) 1534(9) 1643(9) 1316(9) 1861(9) C1C2(3) C2C3(3) C4C5(3) C5C6(3) 1754(3) 1756(3) 1421(3) 1423(3)	DIAGONAL- HCC (94) CC (13) CCO (7) CO (5) CCC (2) OFF-DIAG- BB23(2) BB27(1) CCCO(-1) BB24(-2) SB16(-2) BB25(-2) SB17(-2) SB14(-3) BB19(-3) BB28(-5) SB15(-14)
1172 (M)		1172.	1166.	AG	C208(14) C501(14) C4C5(8) C5C6(8) C1C2(8) C2C3(8) CC2C(5) CC5C(5) C20H(4) C50H(4) 1045(4) 1265(4) O712(4) O932(4) C3C6(4) C6C1(4) HC40(2) HC60(2) HC10(2) HC30(2) C30H(2) C40H(2) C10H(2) C60H(2)	DIAGONAL- CC (41) CO (31) CCO (18) HCO (12) CCC (10) HCC (1) OFF-DIAG- BB19(2) BB29(2) BB18(2) BB22(-2) BB30(-2) SB13(-4) CCCC(-5) SB16(-6) SB14(-10) SB17(-12)

Conventional symbolism indicating relative intensity: s = strong, m = medium, w = weak, sh = shoulder, b = broad, v = very, lt = low temperature band

TABLE LII (Continued)

EXPERIMENTAL FREQUENCY (CM-1) RAMAN	INFRARED	ASSIGNED FREQUENCY (CM-1)	CALCULATED FREQUENCY (CM-1)	CALCULATED SYMMETRY SPECIES	SPECTRAL INTERPRETATION --- POTENTIAL ENERGY DISTRIBUTIONS INTERNAL COORDINATES	FORCE CONSTANTS
	1145 (VS)	1145.	1149.	BU	C107 (13) C309 (13) C400 (13) C602 (13) CC3C (4) CC1C (4) CC6C (4) CC4C (4) C20H (4) C50H (4) C501 (3) C208 (3) CC2C (2) CC5C (2)	DIAGONAL- CO (57) CCC (20) CCO (9) HCO (8) COH (8) HCC (4) CC (2) OFF-DIAG- SB12 (7) BB19 (3) SB16 (2) BB23 (1) BB22 (1) BB25 (-2) CCCO (-2) SB14 (-18)
1138 (M)		1138.	1134.	AG	C3C4 (18) C6C1 (18) C20H (5) C50H (5) 1645 (5) 1865 (5) 1312 (5) 1532 (5) C40H (4) C10H (4) C60H (4) C30H (4) C501 (3) C208 (3) 1154 (3) 1156 (3) 0821 (3) 0823 (3) CC6C (3) CC1C (3) CC3C (3) CC4C (3) HC20 (2) HC50 (2)	DIAGONAL- CC (40) COH (28) HCC (23) CCO (17) CCC (11) CO (8) HCO (3) OFF-DIAG- BB19 (3) BB18 (2) SB13 (2) SB12 (1) BB26 (1) BB29 (1) BB25 (-2) BB24 (-3) BB30 (-5) SB15 (-5) SB14 (-6) SB17 (-11) SB16 (-13)
	1120 (SH)	1120.	1124.	AU	C1C2 (22) C4C5 (22) C2C3 (22) C5C6 (22) C3C4 (12) C6C1 (12) 0821 (4) 0823 (4) 1154 (4) 1156 (4)	DIAGONAL- CC (110) CCO (17) CO (6) HCC (6) OFF-DIAG- BB24 (-1) CCCC (-2) SB14 (-2) SB15 (-12) SB16 (-19)
	1112 (S)	1112.	1112.	BU	C208 (13) C501 (13) C5C6 (12) C2C3 (12) C1C2 (12) C4C5 (12) C20H (11) C50H (11) 1045 (3) 1265 (3) 0712 (3) 0932 (3) CC2C (3) CC5C (3) 0716 (2) 1261 (2) 1043 (2) 0934 (2)	DIAGONAL- CC (49) COH (29) CO (27) CCO (20) HCC (7) CCC (6) HCO (3) OFF-DIAG- BB23 (4) BB22 (1) SB15 (-1) SB12 (-1) BB25 (-2) CCCO (-8) SB13 (-11) SB16 (-11) SB17 (-13)
1095 (S)		1095.	1105.	BG	C4C5 (15) C2C3 (15) C1C2 (15) C5C6 (15) C107 (7) C400 (7) C309 (7) C602 (7) C10H (3) C30H (3) C40H (3) C60H (3) 0934 (3) 1043 (3) CC3C (3) CC4C (3) CC6C (3) CC1C (3) 0716 (3) 1261 (3)	DIAGONAL- CC (59) CO (27) CCO (15) COH (11) CCC (11) HCC (6) OFF-DIAG- SB15 (9) BB30 (2) BB19 (1) BB25 (1) BB26 (-1) BB23 (-2) CCCO (-5) SB13 (-7) SB16 (-7) SB14 (-10) SB17 (-12)
1095 (S)		1095.	1088.	AG	C107 (19) C309 (19) C400 (19) C602 (19) C1C2 (4) C2C3 (4) C4C5 (4) C5C6 (4) C501 (2) C208 (2)	DIAGONAL- CO (80) CC (17) HCO (4) COH (3) HCC (2) CCO (2) CCC (1) OFF-DIAG- SB12 (6) SB17 (3) SB13 (-5) SB14 (-5) CCCO (-7)
		1056.		AU	C10H (16) C30H (16) C40H (16) C60H (16) C3C4 (5) C6C1 (5) C107 (4) C309 (4) C400 (4) C602 (4) 1312 (4) 1532 (4) 1645 (4) 1865 (4)	DIAGONAL- COH (65) HCC (18) CO (18) CC (14) CCO (3) CCC (3) OFF-DIAG- SB14 (5) SB15 (2) SB16 (-3) BB30 (-3) CCCO (-3) SB17 (-5) SB13 (-13)
	1037 (VS)	1037.	1035.	AU	C107 (19) C309 (19) C400 (19) C602 (19) C3C4 (4) C6C1 (4) 1312 (2) 1532 (2) 1645 (2) 1865 (2)	DIAGONAL- CO (76) HCC (13) CC (10) CCO (7) COH (4) OFF-DIAG- SB13 (7) BB19 (2) SB12 (1) SB16 (1) BB30 (-2) BB23 (-2) CCCO (-3) SB14 (-17)
1018 (VS)		1018.	1008.	BG	C602 (14) C309 (14) C400 (14) C107 (14) C1C2 (9) C2C3 (9) C4C5 (9) C5C6 (9) C30H (4) C40H (4) C10H (4) C60H (4)	DIAGONAL- CO (57) CC (36) COH (15) CCO (5) HCC (2) HCO (1) OFF-DIAG- CCCO (4) SB12 (3) SB17 (2) SB14 (-3) SB15 (-4) SB16 (-8) SB13 (-11)
	999 (SH)	999.	997.	BU	C40H (20) C60H (20) C30H (20) C10H (20) C501 (10) C208 (10) HC40 (2) HC10 (2) HC60 (2) HC30 (2)	DIAGONAL- COH (81) CO (20) HCO (7) HCC (4) CCO (1) OFF-DIAG- SB12 (1) SB14 (-1) BB30 (-2) BB18 (-2) BB29 (-3) SB13 (-5)
986 (M)		986.	996.	AG	C50H (15) C20H (15) C208 (12) C501 (12) C30H (8) C10H (8) C40H (8) C60H (8) C3C4 (2) C6C1 (2) HC20 (2) HC50 (2)	DIAGONAL- COH (63) CO (24) HCC (9) CC (8) HCO (6) CCO (4) OFF-DIAG- SB13 (9) CCCO (-2) BB29 (-2) BB18 (-3) SB12 (-3) BB30 (-4) SB15 (-4) SB14 (-7)
961 (M)		961.	979.	BG	C10H (17) C40H (17) C30H (17) C60H (17) C309 (5) C400 (5) C602 (5) C107 (5) 1534 (2) 1643 (2) 1316 (2) 1861 (2) HC10 (2) HC30 (2) HC40 (2) HC60 (2)	DIAGONAL- COH (68) CO (18) HCC (13) HCO (8) CCO (7) CCC (3) OFF-DIAG- SB13 (14) BB25 (1) BB28 (-1) BB19 (-1) BB29 (-3) BB18 (-4) SB12 (-4) BB23 (-4) BB30 (-6) SB14 (-9)
	987 (S)	987.	977.	BU	C20H (23) C50H (22) C501 (10) C208 (10) C602 (5) C107 (5) C400 (5) C309 (5) HC20 (4) HC50 (4) 1316 (2) 1861 (2) 1643 (2) 1534 (2) CC2C (2) CC5C (2) 1156 (2) 0821 (2) 1154 (2) 0823 (2) 1756 (2) 1421 (2) 1423 (2) 1754 (2)	DIAGONAL- COH (46) CO (39) HCC (16) CCO (12) HCO (8) CCC (4) CC (3) OFF-DIAG- SB13 (13) BB28 (-1) BB19 (-2) SB17 (-2) BB29 (-2) SB15 (-2) BB23 (-3) BB18 (-3) SB12 (-4) BB30 (-6) SB14 (-16)
948 (M)		948.	977.	AG	C50H (22) C20H (21) C208 (11) C501 (11) C3C4 (9) C6C1 (9) C60H (5) C30H (5) C40H (5) C10H (5) HC50 (3) HC20 (3)	DIAGONAL- COH (63) CO (23) CC (23) HCO (7) CCO (4) CCC (1) OFF-DIAG- SB12 (4) CCCO (2) SB15 (-1) SB17 (-2) BB29 (-3) SB14 (-3) SB16 (-4) SB13 (-14)
	880 (M)	880.	915.	BU	C208 (17) C501 (17) C20H (9) C50H (9) C1C2 (7) C2C3 (7) C4C5 (7) C5C6 (7) 1043 (3) 1261 (3) 0716 (3) 0934 (3) C30H (2) C40H (2) C10H (2) C60H (2)	DIAGONAL- CO (34) CC (28) COH (27) CCO (20) HCC (7) HCO (4) OFF-DIAG- CCCO (5) SB15 (3) BB19 (2) SB12 (2) BB30 (2) BB29 (-1) BB23 (-3) SB17 (-3) SB13 (-8) SB14 (-9) SB16 (-10)
	856 (M)	856.	846.	AU	C6C1 (24) C3C4 (24) C10H (6) C30H (6) C40H (6) C60H (6) C1C2 (3) C4C5 (3) C5C6 (3) C2C3 (3) CC3C (3) CC4C (3) CC6C (3) CC1C (3) 1312 (2) 1532 (2) 1645 (2) 1865 (2) 0716 (2) 0934 (2) 1043 (2) 1261 (2) HC10 (2) HC30 (2) HC40 (2) HC60 (2)	DIAGONAL- CC (58) COH (25) HCC (15) CCC (10) CCO (10) HCO (6) OFF-DIAG- BB30 (3) SB15 (2) BB18 (2) CCCO (2) BB26 (-1) SB14 (-1) BB29 (-2) SB13 (-2) BB23 (-2) SB16 (-11) SB17 (-19)
824 (S)		824.	833.	AG	C208 (13) C501 (13) C3C4 (8) C6C1 (8) C10H (5) C30H (5) C60H (5) C40H (5) C5C6 (4) C2C3 (4) C1C2 (4) C4C5 (4) 1312 (2) 1532 (2) 1645 (2) 1865 (2)	DIAGONAL- CC (30) CO (26) COH (20) CCO (8) HCC (8) HCO (4) CCC (3) OFF-DIAG- SB15 (4) CCCO (4) BB30 (4) BB19 (3) BB18 (2) BB29 (-1) SB13 (-2) SB16 (-8) SB17 (-9)
	727 (VS)	727.	708.	AU	C3C4 (10) C6C1 (10) 1265 (7) 0932 (7) 1045 (7) 0712 (7) 1156 (5) 0823 (5) 0821 (5) 1154 (5) 1312 (2) 1532 (2) 1645 (2) 1865 (2) 1423 (2) 1754 (2) 1756 (2) 1421 (2)	DIAGONAL- CCO (47) CC (20) HCC (17) CO (4) COH (3) OFF-DIAG- SB14 (7) BB19 (5) BB30 (2) CCCO (2) SB13 (1) SB16 (1) SB17 (1) BB24 (-2) SB15 (-1) BB23 (-7)

TABLE LII (Continued)

EXPERIMENTAL FREQUENCY (CM-1) RAMAN	INFRARED	ASSIGNED FREQUENCY (CM-1)	CALCULATED FREQUENCY (CM-1)	CALCULATED SYMMETRY SPECIES	SPECTRAL INTERPRETATION --- POTENTIAL ENERGY DISTRIBUTIONS INTERNAL COORDINATES	FORCE CONSTANTS
	712 (SH)	712.	700.	BU	C309(5) C602(5) C400(5) C107(5) CC3C(5) CC4C(5) CC6C(5) CC1C(5) C20H(3) C50H(3) 1154(3) 1156(3) 0821(3) 0823(3) 1754(2) 1756(2) 1421(2) 1423(2) C501(2) C208(2)	DIAGONAL- CO (28) CCC (23) CCO (15) HCC (12) COH (6) HCO (3) CC (2) OFF-DIAG- SB14 (9) BB19 (6) BB26 (2) BB30 (2) SB16 (2) CCCO (1) BB23 (1) SB17 (-1) SB12 (-2) BB25 (-3)
660 (M)		660.	664.	BG	0712(9) 0932(9) 1045(9) 1265(9) 0823(8) 1154(8) 1156(8) 0821(8) 0934(5) 1043(5) 0716(5) 1261(5) 1421(2) 1423(2) 1754(2) 1756(2)	DIAGONAL- CCO (88) HCC (12) CCC (3) CO (2) COH (2) OFF-DIAG- BB19 (5) BB20 (-1) SB14 (-1) BB24 (-2) BB23 (-6)
646 (S)		646.	646.	AG	C3C4(13) C6C1(13) CC5C(3) CC2C(3) C20H(3) C50H(3) CC6C(3) CC1C(3) CC4C(3) CC3C(3) 1754(2) 1756(2) 1421(2) 1423(2) 1154(2) 1156(2) 0821(2) 0823(2)	DIAGONAL- CC (28) CCC (17) HCC (12) CCO (9) COH (6) CO (3) HCO (2) OFF-DIAG- SB17 (11) BB19 (5) SB14 (2) BB18 (2) BB30 (2) BB26 (2) SB13 (1) CCCO (1) BB25 (-1) SB16 (-3)
	577 (S)					
542 (M,B)						
	507 (M)	507.	512.	BU	0934(7) 1043(7) 0716(7) 1261(7) CC2C(6) CC5C(6) 0823(6) 1154(6) 1156(6) 0821(6) 1316(5) 1534(5) 1643(5) 1861(5) 0712(2) 0932(2) 1265(2) 1045(2)	DIAGONAL- CCO (57) HCC (23) CCC (13) CO (3) CC (1) OFF-DIAG- SB14 (10) BB19 (5) BB30 (1) BB25 (1) BB18 (1) BB22 (1) SB16 (1) SB17 (-3) BB28 (-3) BB23 (-13)
490 (M,B)						
			443.	BG	0716(12) 0934(12) 1043(12) 1261(12) 0823(6) 1154(6) 1156(6) 0821(6) 1316(5) 1534(5) 1643(5) 1861(5) CC3C(2) CC4C(2) CC6C(2) CC1C(2)	DIAGONAL- CCO (77) HCC (25) CCC (6) TOCC (3) CC (2) OFF-DIAG- BB19 (6) SB16 (5) SB15 (2) BB22 (-1) BB24 (-2) SB14 (-2) SB17 (-2) BB28 (-3) BB25 (-3) BB23 (-17)
	438 (M)					
423 (M,B)		423.	426.	AG	C1C2(8) C2C3(8) C4C5(8) C5C6(8) CC2C(6) CC5C(6) C400(3) C602(3) C107(3) C309(3) 0712(2) 0932(2) 1045(2) 1265(2)	DIAGONAL- CC (32) CCC (13) CO (11) CCO (10) HCC (2) HCO (2) OFF-DIAG- SB17 (10) SB14 (8) SB16 (6) CCCO (3) BB23 (2) BB19 (2) BB18 (1) BB22 (1) SB12 (-1) SB15 (-5)
	393 (W)					
349 (W)		349.	360.	BG	CC3C(11) CC4C(11) CC6C(11) CC1C(11) 0712(8) 0932(8) 1045(8) 1265(8) C1C2(2) C2C3(2) C4C5(2) C5C6(2) 1421(2) 1423(2) 1754(2) 1756(2) 1043(2) 0716(2) 0934(2) 1261(2)	DIAGONAL- CCC (45) CCO (42) HCC (10) CC (9) CO (3) OFF-DIAG- SB17 (9) SB14 (8) BB22 (2) BB25 (1) BB20 (-1) SB15 (-3) BB26 (-4) BB23 (-9) SB16 (-9)
	330 (M)	330.	322.	BU	0712(9) 0932(9) 1045(9) 1265(9) C1C2(6) C4C5(6) C2C3(6) C5C6(6) 0934(6) 0716(6) 1043(6) 1261(6)	DIAGONAL- CCO (65) CC (25) HCC (7) CCC (4) TOCO (3) CO (1) OFF-DIAG- SB16 (9) BB19 (3) SB15 (2) BB22 (-1) SB17 (-6) BB23 (-10)
			319.	AU	0821(11) 0823(11) 1154(11) 1156(11) 0716(6) 1043(6) 1261(6) 0934(6) C1C2(2) C2C3(2) C4C5(2) C5C6(2)	DIAGONAL- CCO (70) CC (7) HCC (3) TOCO (2) HCO (2) OFF-DIAG- SB16 (10) BB24 (2) BB18 (1) SB15 (-2)
326 (M)		326.	306.	AG	1043(15) 0934(15) 0716(15) 1261(15) 0932(8) 1045(8) 1265(8) 0712(8) 0823(3) 1154(3) 0821(3) 1156(3)	DIAGONAL- CCO (103) HCC (10) TOCO (2) CC (2) CCC (1) OFF-DIAG- BB24 (2) SB17 (-1) BB20 (-1) SB16 (-1) SB15 (-2) BB19 (-3) BB23 (-12)
	306 (M)	306.	288.	AU	0932(12) 1045(12) 1265(12) 0712(12) 1043(9) 0716(9) 0934(9) 1261(9) 1154(6) 1156(6) 0821(6) 0823(6) C1C2(2) C4C5(2) C2C3(2) C5C6(2) 1421(2) 1423(2) 1754(2) 1756(2)	DIAGONAL- CCO (110) HCC (13) CC (8) TOCO (5) OFF-DIAG- SB17 (-1) BB20 (-1) SB15 (-3) BB19 (-5) SB16 (-12) BB23 (-16)
294 (M)		294.	258.	BG	0821(9) 0823(9) 1154(9) 1156(9) 1316(5) 1534(5) 1861(5) 1643(5) 1045(4) 0712(4) 0932(4) 1265(4) CC3C(3) CC4C(3) CC6C(3) CC1C(3) TC20(2) TC50(2)	DIAGONAL- CCO (56) HCC (26) CCC (12) TOCO (5) TOCC (5) CO (3) HCO (1) OFF-DIAG- BB19 (6) BB18 (3) BB24 (2) BB28 (-3) BB25 (-4) SB14 (-6) BB23 (-7)
239 (W)		239.	246.	AG	CC2C(17) CC5C(17) 0821(8) 0823(8) 1154(8) 1156(8) TC34(4) TC61(4) 0932(3) 1265(3) 1045(3) 0712(3)	DIAGONAL- CCO (45) CCC (40) TOCC (8) HCC (6) TOCO (4) CC (2) CO (2) OFF-DIAG- SB16 (6) BB24 (2) BB19 (2) SB15 (-2) BB22 (-3) BB25 (-3) SB17 (-4) SB14 (-5)
			198.	BU	0821(6) 0823(6) 1154(6) 1156(6) CC2C(6) CC5C(6) 1316(5) 1534(5) 1643(5) 1861(5) CC4C(3) CC3C(3) CC6C(3) CC1C(3) 1043(3) 0716(3) 0934(3) 1261(3) 0712(3) 0932(3) 1265(3) 1045(3) 1532(2) 1645(2) 1865(2) 1312(2)	DIAGONAL- CCO (46) HCC (35) CCC (26) CO (7) CC (2) OFF-DIAG- BB19 (9) SB16 (6) BB24 (3) BB18 (1) BB26 (-1) BB22 (-2) BB28 (-3) SB15 (-3) BB23 (-5) BB25 (-8) SB14 (-14)
			122.	AG	TC60(10) TC40(10) TC30(9) TC10(9) CC3C(6) CC6C(6) CC4C(6) CC1C(6) TC12(5) TC23(5) TC45(5) TC56(5) TC34(3) TC61(3) 1043(3) 1261(2) 0934(2) 0716(2)	DIAGONAL- TOCO (99)
			128.	BG	TC40(24) TC60(24) TC10(24) TC30(24) TC50(2) TC20(2)	DIAGONAL- TOCO (97) CCO (2)
			123.	BU	TC10(25) TC40(24) TC30(24) TC60(23)	DIAGONAL- TOCO (96) CCO (3)

TABLE LII (Continued)

EXPERIMENTAL FREQUENCY (CM-1) RAMAN	INFRARED	ASSIGNED FREQUENCY (CM-1)	CALCULATED FREQUENCY (CM-1)	CALCULATED SYMMETRY SPECIES	SPECTRAL INTERPRETATION --- POTENTIAL ENERGY DISTRIBUTIONS INTERNAL COORDINATES	FORCE CONSTANTS
			124.	AU	TC20(39) TC50(39) TC60(5) TC30(5) TC10(5) TC40(4)	DIAGONAL- TOCO(37) CCC (25) TOCC(24) CCO (17) HCC (4) CO (3) CC (1) OFF-DIAG- SB16(1) BB19(1) BB22(-2) BB23(-2) BB26(-2) SB17(-5) SB14(-6)
			122.	BG	TC20(46) TC50(45)	DIAGONAL- TOCO(94) CCO (3)
			95.	BU	TC12(12) TC23(12) TC45(12) TC56(12) CC2C(11) CC5C(11) CC4C(4) CC3C(4) CC6C(4) CC1C(4)	DIAGONAL- TOCO(94) CCO (6)
			121.	AU	TC30(19) TC60(19) TC40(19) TC10(19) TC50(10) TC20(9)	DIAGONAL- TOCO(57) TOCC(18) CCC (16) CCO (14) HCC (3) CO (2) CC (1) OFF-DIAG- SB16(1) BB26(-1) BB22(-1) BB23(-3) SB17(-4) SB14(-4)
			121.	AG	TC60(14) TC10(14) TC30(14) TC40(14) TC61(3) TC34(3) 1265(3) 0712(3) 1045(3) 0932(3) TC56(3) TC23(3) TC12(3) TC45(3) CC1C(3) CC6C(3) CC4C(3) CC3C(3) CC5C(2) CC2C(2)	DIAGONAL- TOCC(48) CCC (38) CCO (7) HCC (5) HCO (2) CO (1) OFF-DIAG- SB17(4) BB19(2) BB18(1) BB23(-1) BB26(-1) BB25(-2) SB14(-2)
			84.	AU	TC61(16) TC34(16) CC6C(10) CC3C(10) CC1C(10) CC4C(10) TC56(4) TC45(4) TC23(4) TC12(4) 1043(2) 1261(2) 0716(2) 0934(2) 1265(2) 0712(2) 0932(2) 1045(2)	DIAGONAL- TOCC(48) CCC (39) CCO (16) CO (4) HCC (3) TOCO(1) OFF-DIAG- SB17(1) BB22(-2) BB26(-2) BB23(-2) SB14(-6)

TABLE LIII. DEUTERATED MYO-INOSITOL

EXPERIMENTAL FREQUENCY (CM-1) RAMAN	INFRARED	ASSIGNED FREQUENCY (CM-1)	CALCULATED FREQUENCY (CM-1)	CALCULATED SYMMETRY SPECIES	SPECTRAL INTERPRETATION --- POTENTIAL ENERGY DISTRIBUTIONS INTERNAL COORDINATES	FORCE CONSTANTS
	2955 (W)		2950.	A'	C5H7(33) C4H6(25) C6H8(25) C3H5(7) C1H3(7)	DIAGONAL- CH (98)
	2918 (M)		2945.	A''	C4H6(28) C6H8(28) C1H3(22) C3H5(22)	DIAGONAL- CH (98)
	2930 (M)		2940.	A'	C5H7(28) C2H4(25) C1H3(23) C3H5(23)	DIAGONAL- CH (99)
			2938.	A'	C2H4(73) C1H3(10) C3H5(10) C5H7(6)	DIAGONAL- CH (99)
	2900 (M)		2935.	A''	C3H5(28) C1H3(28) C4H6(22) C6H8(22)	DIAGONAL- CH (99)
	2875 (W)		2932.	A'	C5H7(32) C6H8(24) C4H6(24) C1H3(10) C3H5(10)	DIAGONAL- CH (100)
	2510 (VS)		2448.		C8H0(39) O7H9(31) O9H1(26) O11H(3)	DIAGONAL- OH (99)
	2400 (VS)		2448.		O11H(49) O10H(32) O12H(16)	DIAGONAL- OH (99)
	2360 (VS)		2448.		O12H(63) O10H(31) O7H9(3) O9H1(3)	DIAGONAL- CH (99)
			2448.		O9H1(49) O7H9(44) O12H(4) O10H(2)	DIAGONAL- CH (99)
			2448.		O11H(47) O10H(34) O12H(16) O8H0(2)	DIAGONAL- CH (99)
			2447.		O8H0(59) O9H1(21) O7H9(19)	DIAGONAL- OH (99)
	1427 (M)		1407.	A''	1316(14) 1534(14) 1754(13) 1756(13) 1423(9) 1421(9) 1532(3) 1312(3) 1643(2) 1861(2)	DIAGONAL- HCC (82) CCC (4) CO (3) HCC (3) CC (2) COH (2) OFF-DIAG- BB23 (6) BB28 (2) BB25 (2) BB18 (-1) SB14 (-2) SB15 (-3)
1400 (SH)	1398 (S,SH)		1397.	A'	1645(26) 1865(26) 1643(12) 1861(12) C5OH(2)	DIAGONAL- HCC (79) HCC (5) CCO (3) COH (2) CO (2) OFF-DIAG- BB23 (7) BB28 (3) BB25 (2) BB18 (-1) SB14 (-2) SB15 (-3)
1387 (M)	1390 (S)		1389.	A'	1316(18) 1534(18) 1532(12) 1312(12) HC2O(8) HC5O(5) C2O8(3) 1754(2) 1756(2) 1643(2) 1861(2)	DIAGONAL- HCC (73) HCO (15) CO (7) CCO (2) COH (2) CCC (1) OFF-DIAG- EE23 (5) BB28 (4) BB25 (3) SB15 (-1) SB14 (-3) SB12 (-3) BB18 (-6)
1379 (M)			1377.	A''	1421(23) 1423(23) 1754(19) 1756(19) C3C4(3) C6C1(3)	DIAGONAL- HCC (86) CC (10) CCO (3) CO (2) HCO (1) CCC (1) OFF-DIAG- BB23 (5) BB28 (3) BB26 (1) BB19 (-1) SB17 (-2) SB15 (-8)
1368 (S)	1372 (SH)		1369.	A''	1643(18) 1861(18) 1865(10) 1645(10) 1421(6) 1423(6) 1754(4) 1756(4) HC1O(2) HC3O(2) 1312(2) 1532(2) C1C2(2) C2C3(2)	DIAGONAL- HCC (85) HCO (6) CC (6) COH (2) OFF-DIAG- BB28 (6) BB23 (2) BB25 (1) BB18 (-1) SB15 (-9)
1362 (S)			1342.	A'	HC1O(18) HC3O(18) HC5O(13) 1532(12) 1312(12) 1861(6) 1643(6) HC4O(5) HC6O(5) C2O8(4) HC2O(4) C1O7(4) C3O9(4) CC2C(2) 1756(2) 1754(2) C5O1(2)	DIAGONAL- HCO (64) HCC (44) CO (15) CCC (3) CCO (2) CC (2) COH (2) TOCC (2) OFF-DIAG- EE25 (3) BB29 (1) BB28 (1) BB19 (-1) SB13 (-2) SB15 (-3) SB14 (-4) SB12 (-10) BB18 (-21)
1323 (W)	1319 (W)		1311.	A'	HC4O(27) HC6O(27) HC3O(13) HC1O(13) 1643(6) 1861(6) 1316(4) 1534(4) 1865(3) 1645(3) C4O2(2) 1602(2) HC2O(2) 1421(2) 1423(2) C4OH(2) C6OH(2)	DIAGONAL- HCO (82) HCC (30) CO (8) COH (6) CCC (5) CCO (1) OFF-DIAG- BB25 (3) BB29 (3) SB14 (-2) BB28 (-2) BB19 (-3) SB13 (-3) SB12 (-8) BB18 (-22)
1296 (W)	1297 (W)		1296.	A''	HC4O(22) HC6O(22) HC3O(22) HC1O(22) 1312(8) 1532(8) 1643(5) 1861(5) 1865(2) 1645(2)	DIAGONAL- HCO (88) HCC (33) CO (5) COH (3) TOCC (2) CC (2) OFF-DIAG- BB29 (2) BB28 (1) SB13 (-2) SB15 (-3) SB12 (-6) BB18 (-24)
1274 (W,SH)	1276 (VW)		1288.	A'	HC5O(47) HC2O(21) 1754(8) 1756(8) HC4O(6) HC6O(6) HC1O(5) HC3O(5) 1421(4) 1423(4) C5OH(2) C5O1(2) 1861(2) 1643(2) C3C4(2) C6C1(2)	DIAGONAL- HCO (89) HCC (31) CCH (5) CC (5) CC (4) CCC (2) OFF-DIAG- BB29 (3) BB23 (-1) BB19 (-1) SB13 (-2) SB15 (-3) SB12 (-6) BB16 (-24)
			1282.	A''	HC6O(23) HC4O(23) HC1O(19) HC3O(19) 1645(8) 1865(8) 1532(3) 1312(3) 1316(2) 1534(2) 1421(2) 1423(2)	DIAGONAL- HCO (84) HCC (34) COH (6) CO (2) CCC (1) CC (1) CCC (1) OFF-DIAG- EE29 (3) SB13 (-1) BB19 (-2) SB15 (-2) SB12 (-4) BB18 (-22)
			1280.	A'	HC2O(51) HC5O(21) 1423(8) 1421(8) 1534(5) 1316(5) 1754(2) 1756(2) C2OH(2) HC3O(2) HC1O(2) C5OH(2)	DIAGONAL- HCO (76) HCC (35) COH (4) CC (3) CO (2) TOCC (2) OFF-DIAG- BB29 (2) SB15 (-1) SB12 (-2) BB10 (-20)
1268 (M)	1261 (W)		1273.	A''	1534(13) 1316(13) 1532(11) 1312(11) 1754(7) 1756(7) 1645(7) 1865(7) 1643(5) 1861(5) C1C2(3) C2C3(3) 1421(3) 1423(3)	DIAGONAL- HCC (93) CCO (7) CC (7) HCC (2) CO (2) OFF-DIAG- BB23 (10) SB14 (-1) BB19 (-3) SB15 (-6) BB28 (-8)
1187 (M)	1187 (VW,SH)		1181.	A'	C2O8(13) C5OH(7) C4OH(5) C6OH(5) C4C5(5) C5C6(5) HC5O(4) HC6O(4) HC4O(4) C3OH(4) C1OH(4) HC1O(3) HC3C(3) CC2C(3) C1C2(3) C2C3(3) 1312(3) 1532(3) 1045(2) 1265(2) CC5C(2) C712(2) O932(2) O823(2) O821(2)	DIAGONAL- COH (26) HCC (18) CCO (17) CC (16) CO (15) CCC (9) HCC (8) OFF-DIAG- BB19 (5) BB18 (3) SB15 (3) BB29 (3) EE25 (2) SB12 (2) BB22 (1) BB23 (1) BB30 (-5) SB16 (-6) SB14 (-9) SB17 (-10)
1151 (S)	1153 (SH)		1148.	A'	C1O7(14) C3O9(14) C5O1(10) C4O2(10) C6O2(10) C2OH(6) CC1C(4) CC3C(4) CC2C(3) CC4C(3) CC6C(3) CC5C(2) C2O8(3) HC2O(2) HC3O(2) HC1C(2)	DIAGONAL- CO (61) CCC (21) CCC (11) HCC (7) COH (6) HCC (4) CC (1) OFF-DIAG- SB12 (6) BB19 (3) BB22 (2) BB23 (2) BB25 (-2) SB14 (-20)

TABLE LIII (Continued)

EXPERIMENTAL FREQUENCY (CM-1) RAMAN	INFRARED	ASSIGNED FREQUENCY (CM-1)	CALCULATED FREQUENCY (CM-1)	CALCULATED SYMMETRY SPECIES	SPECTRAL INTERPRETATION --- POTENTIAL ENERGY DISTRIBUTIONS INTERNAL COORDINATES	FORCE CONSTANTS
1140 (W,SH)	1144 (VS)		1137.	A'	C6C1(20) C3C4(20) C2OH(14) C1C2(13) C2C3(13) C6O2(5) C400(5) C501(4) C2O8(4) 0932(4) 0712(4) CC2C(4) 1532(4) 1312(4) 0716(3) CC4C(3) CC6C(3) 0934(3) C4OH(2) C6OH(2) HC2O(2) CC5C(2) 1154(2) 1156(2)	DIAGONAL- CC (67) CCO (19) COH (19) CO (19) CCC (11) HCC (11) HCO (4) OFF-DIAG- BB23 (2) BB22 (2) SB12 (-1) BB25 (-3) SB14 (-3) CCCO (-5) SB13 (-6) SB15 (-7) SB17 (-13) SB16 (-15)
1119 (S)	1123 (VS)		1129.	A''	C1C2(25) C2C3(25) C3C4(10) C6C1(10) C4O0(9) C6O2(9) C5C6(5) C4C5(5) 0716(4) 0934(4) C107(4) C309(4) C4OH(4) C6OH(4) CC4C(4) CC6C(4) 0823(3) 0821(3) 1154(2) 1156(2)	DIAGONAL- CC (79) CO (27) CCO (22) CCC (10) COH (8) HCC (3) OFF-DIAG- FB30 (1) BB22 (1) BB23 (1) SB15 (-5) SB13 (-5) CCCO (-5) SB14 (-10) SB17 (-12) SB16 (-13)
	1109 (VS)		1109.	A'	C501(37) C4C5(18) C5C6(18) C5OH(12) C2O8(8) 1265(4) 1045(4) CC5C(4) C1C2(3) C2C3(3) C400(2) C6O2(2) C3OH(2) C1OH(2) 1043(2) 1261(2)	DIAGONAL- CO (50) CC (46) COH (18) CCO (16) HCC (6) HCC (2) OFF-DIAG- BB23 (2) BB30 (1) SB16 (-6) SB14 (-6) CCCO (-10) SB17 (-11) SB13 (-11)
1103 (S)			1105.	A''	C5C6(34) C4C5(34) C2C3(9) C1C2(9) C400(6) C602(6) C3C4(5) C6C1(5) 1154(2) 1156(2) C4OH(2) C6OH(2)	DIAGONAL- CC (97) CO (12) CCO (9) CCH (4) CCC (2) HCC (1) OFF-DIAG- CCCC (-2) SB14 (-2) CCCO (-2) SB15 (-3) SB13 (-3) SB17 (-3) SB16 (-13)
1089 (M)	1087 (S)		1093.	A'	C602(21) C400(21) C107(12) C309(12) C1C2(7) C2C3(7) C208(7) C2OH(4) C3C4(2) C6C1(2) CC5C(2) C1OH(2) C3OH(2)	DIAGONAL- CO (74) CC (20) COH (8) HCO (4) CCO (2) CCC (2) HCC (2) OFF-DIAG- SB12 (5) SB15 (2) SB14 (-3) SB13 (-8) CCCO (-8)
1048 (SH)	1049 (VS)		1069.	A''	C1OH(18) C3OH(18) C107(13) C309(13) C3C4(11) C6C1(11) 1312(4) 1532(4) C4OH(4) C6OH(4) C1C2(3) C2C3(3) C400(2) C602(2) 1043(2) 1261(2) 1423(2) 1421(2) CC3C(2) CC1C(2)	DIAGONAL- COH (44) CO (30) CC (30) HCC (13) CCO (6) CCC (4) OFF-DIAG- SB15 (3) SB14 (1) SB16 (-4) CCCO (-6) SB17 (-7) SB13 (-14)
1035 (M)	1030 (VS)		1026.	A''	C400(21) C602(21) C107(10) C3O9(10) C1OH(6) C3OH(6) 1312(3) 1532(3) 1754(3) 1756(3) 1645(2) 1865(2)	DIAGONAL- CO (62) HCC (17) COH (15) CCO (8) CC (5) OFF-DIAG- SB13 (10) BB19 (1) BB23 (-1) BB28 (-1) BB30 (-3) SB14 (-15)
1024 (M)			1006.	A''	C107(23) C309(23) C4C5(9) C5C6(9) C2C3(9) C1C2(9) C400(9) C602(9) C4OH(2) C6OH(2)	DIAGONAL- CO (64) CC (37) COH (5) CCO (4) HCC (2) OFF-DIAG- CCCO (6) SB17 (2) SB12 (1) BB23 (-1) SB15 (-3) SB13 (-6) SB14 (-6) SB16 (-7)
			1005.	A'	C501(32) C1OH(11) C3CH(11) C6C1(6) C3C4(6) C2OH(6) C3O9(5) C107(5) C5C6(2) C4C5(2) 1861(2) 1643(2)	DIAGONAL- CO (43) COH (31) CC (18) HCC (8) CCO (6) HCC (1) OFF-DIAG- SB13 (8) CCCC (3) SB17 (1) BB30 (-2) SB15 (-3) SB16 (-5) SB14 (-8)
988 (SH)	986 (VS)		991.	A'	C208(26) C1OH(18) C3OH(18) C5OH(9) C501(7) C4OH(5) C6OH(5) C107(5) C3O9(5) HC3O(2) HC1O(2) C6C1(2) C3C4(2)	DIAGONAL- COH (56) CO (42) HCO (6) CC (4) HCC (4) CCC (3) CCC (1) OFF-DIAG- CCCO (1) SB12 (1) SB16 (-1) BB18 (-1) BB29 (-2) SB13 (-6) SB14 (-7)
972 (W)			986.	A'	C2OH(49) HC2O(7) C2O8(5) C4OH(4) C6OH(4) C107(3) C3O9(3) 1421(3) 1423(3) 1316(3) 1534(3) C3C4(2) C6C1(2) C400(2) C602(2) C5OH(2) 0823(2) 0821(2) CC2C(2) 0932(2) 0712(2)	DIAGONAL- COH (62) CO (18) HCC (14) CC (9) CCO (8) HCO (8) CCC (2) OFF-DIAG- SB13 (11) BB28 (-1) BB19 (-1) SB17 (-1) SB15 (-3) BB29 (-3) SB12 (-3) BB23 (-3) BB18 (-3) BB30 (-6) SB14 (-8)
			979.	A'	C5OH(40) C4OH(15) C6OH(15) C2O8(12) HC5O(4) C6C1(3) C3C4(3) C1OH(3) C3OH(3)	DIAGONAL- COH (77) CO (13) CC (9) HCO (7) HCC (6) CCO (5) CCC (2) OFF-DIAG- SB17 (-2) BB23 (-2) SB13 (-2) BB18 (-3) SB14 (-3) BB29 (-3) BB3C (-4)
	949 (S,SH)		977.	A''	C6OH(27) C4OH(27) C3OH(12) C1OH(12) C4O0(3) C6O2(3) HC6O(2) HC4O(2) C107(2) C3O9(2) 1643(2) 1861(2) 1316(2) 1534(2) HC3O(2) HC1O(2)	DIAGONAL- COH (79) HCC (10) CO (9) HCC (8) CCO (6) CCC (3) CC (2) OFF-DIAG- SB13 (10) BB25 (1) BB19 (-1) BB28 (-1) SB12 (-3) BB29 (-3) BB1E (-4) BB23 (-4) SB14 (-6) BB3C (-6)
923 (W)			930.	A'	C5OH(22) C5C6(11) C4C5(11) C4OH(11) C6OH(11) C2OH(10) C2O8(5) C2C3(4) C1C2(4) HC5O(3) C501(3) 0934(2) 0716(2) 1265(2) 1045(2) 1261(2) 1043(2) HC4O(2) HC6O(2) HC2O(2)	DIAGONAL- COH (53) CC (31) CCO (16) HCO (8) CO (8) CCC (3) OFF-DIAG- CCCO (3) SB12 (2) BB3C (1) SB14 (-1) BB29 (-3) SB13 (-7) SB17 (-8) SB16 (-8)
887 (W)	886 (W)		896.	A''	C3C4(18) C6C1(18) C3OH(10) C1OH(10) C4OH(7) C6OH(7) 1154(5) 1156(5) C1C2(4) C2C3(4) 1043(3) 1261(3) HC1C(2) HC3O(2) CC3C(2) CC1C(2) C400(2) C602(2) C5C6(2) C4C5(2) HC4O(2) HC6O(2)	DIAGONAL- CC (47) COH (33) CCO (15) HCO (8) HCC (7) CCC (7) CO (5) OFF-DIAG- CCCO (3) SB12 (2) SB14 (-1) BB23 (-2) FB29 (-2) SB13 (-5) SB16 (-9) SB17 (-14)
854 (M)	851 (S)		872.	A'	C2O8(22) C2C3(7) C1C2(7) C1OH(7) C3OH(7) C6C1(6) C3C4(6) C4OH(4) C6CH(4) C5OH(4) 1261(3) 1043(3) C2OH(3)	DIAGONAL- COH (29) CC (27) CO (23) CCO (11) HCC (7) HCC (5) CCC (2) OFF-DIAG- EB30 (4) SB15 (4) CCCO (4) BB19 (3) BB18 (1) BB29 (-1) SB14 (-3) SB13 (-3) SB17 (-6) SB16 (-8)
716 (M)	716 (VS)		698.	A''	0712(12) 0932(12) 0823(11) 0821(11) 1312(4) 1532(4) C3C4(3) C6C1(3) 1423(2) 1421(2) 1645(2) 1865(2) C1OH(2) C3OH(2) 1043(2) 1261(2)	DIAGONAL- CCO (54) HCC (20) CC (6) COH (4) CO (3) CCC (2) OFF-DIAG- EE19 (2) SB14 (5) BB30 (3) SB16 (2) SB17 (2) BB18 (1) SB15 (-2) BB24 (-2) EE23 (-7)
704 (VW,SH)	703 (SH)		686.	A'	CC1C(8) CC3C(8) C2OH(5) 0821(5) 0823(5) C6C2(4) C400(4) 1423(4) 1421(4) CC2C(3) C2O8(3) C6C1(3) C1CH(3) C107(2) C3O9(2) HC2O(2) 1312(2) 1532(2)	DIAGONAL- CCC (22) CO (16) HCC (16) CCC (13) COH (7) CC (6) HCO (3) OFF-DIAG- SB14 (7) BB19 (6) SB17 (2) BB30 (2) EE26 (2) EB18 (1) BB24 (-1) SB12 (-2) BB25 (-3)

TABLE LIII (Continued)

EXPERIMENTAL FREQUENCY (CM-1) RAMAN	EXPERIMENTAL FREQUENCY (CM-1) INFRARED	ASSIGNED FREQUENCY (CM-1)	CALCULATED FREQUENCY (CM-1)	CALCULATED SYMMETRY SPECIES	SPECTRAL INTERPRETATION --- POTENTIAL ENERGY DISTRIBUTIONS INTERNAL COORDINATES	FORCE CONSTANTS
605 (W)	607 (SH)		623.	A''	1045 (14) 1265 (14) 0716 (13) 0934 (13) 1156 (7) 1154 (7) 1645 (6) 1865 (6) 0932 (5) 0712 (5) 1756 (5) 1754 (5) 1043 (4) 1261 (4) C3C4 (2) C6C1 (2) 1421 (2) 1423 (2)	DIAGONAL- CCO (85) HCC (27) CC (3) CCC (2) OFF-DIAG- BB19 (7) SB16 (-2) SB17 (-2) BB28 (-3) BB23 (-21)
583 (W)	587 (M)		568.	A'	0716 (10) 0934 (10) CC5C (5) 1643 (5) 1861 (5) C2C3 (5) 1756 (4) 1754 (4) 1316 (4) 1534 (4) 1154 (4) 1156 (4) 1043 (4) 1261 (4) 0823 (2) 0821 (2) C400 (2) C602 (2) 1865 (2) 1645 (2)	DIAGONAL- CCO (42) HCC (31) CCC (11) CO (6) CC (3) HCO (2) CCH (2) OFF-DIAG- SB14 (8) BB19 (7) BB18 (2) BB30 (2) BB28 (-4) BB23 (-12)
500 (S,B)	497 (M)		484.	A'	C3C4 (8) C6C1 (8) C501 (8) CC4C (7) CC6C (7) CC5C (4) C1C7 (4) C309 (4) 1154 (4) 1156 (4) C1C2 (3) C2C3 (3) C5C6 (3) C4C5 (3)	DIAGONAL- CC (28) CCC (18) CO (16) CCC (13) HCC (3) HCO (1) OFF-DIAG- SB14 (8) SB17 (7) CCCC (4) BB19 (2) BB22 (1) SB16 (1) SB12 (-1) SB15 (-1)
	452 (M)		432.	A''	0821 (11) 0823 (11) 1643 (9) 1861 (9) 1043 (5) 1261 (5) 1156 (4) 1154 (4) CC4C (4) CC6C (4) CC3C (3) CC1C (3) 1265 (3) 1045 (3) 1316 (3) 1534 (3) C3C4 (2) C6C1 (2) 1756 (2) 1754 (2) 0716 (2) 0934 (2) 1865 (2) 1645 (2)	DIAGONAL- CCO (50) HCC (32) CCC (14) CC (6) TOCC (4) CO (2) OFF-DIAG- BB19 (7) SB16 (4) BB18 (1) BB30 (1) SB17 (-1) SB14 (-3) BB28 (-4) BB25 (-6) BB23 (-8)
417 (VS)	420 (M)		416.	A'	CC5C (11) CC2C (7) C5C6 (6) C4C5 (6) C1C2 (5) C2C3 (5) 1045 (4) 1265 (4) 1156 (4) 1154 (4) C400 (3) C602 (3) CC4C (2) CC6C (2)	DIAGONAL- CCC (23) CC (21) CCC (21) CO (9) HCC (3) HCC (1) OFF-DIAG- SB17 (9) SB14 (8) SB16 (2) BB12 (2) BB19 (2) CCCO (1) SB15 (-2)
375 (S)	377 (W)		371.	A''	CC3C (9) CC1C (9) CC6C (7) CC4C (7) 1261 (6) 1043 (6) 0716 (5) 0934 (5) 0932 (5) 0712 (5) 1265 (5) 1045 (5) C4C5 (3) C5C6 (3) C1C2 (2) C2C3 (2)	DIAGONAL- CCO (43) CCC (12) CC (11) HCC (6) CO (3) OFF-DIAG- SB14 (8) SB17 (8) BB25 (3) BB22 (3) SB15 (-1) BB26 (-1) SB16 (-5) BB23 (-8)
362 (M)			339.	A'	1043 (15) 1261 (15) 0821 (8) 0823 (8) 1645 (6) 1865 (6) 0716 (6) 0934 (6) 0932 (6) 0712 (6) CC2C (5) 1156 (4) 1154 (4) 1756 (4) 1754 (4) 1421 (2) 1423 (2) CC5C (2)	DIAGONAL- CCO (79) HCC (28) CCC (8) TOCC (2) CC (2) CO (1) OFF-DIAG- BB19 (2) BB22 (1) BB18 (1) SB15 (-2) SB17 (-2) SB16 (-2) BB28 (-3) BB25 (-4) SB14 (-4) BB23 (-11)
	320 (M)		310.	A'	0712 (10) 0932 (10) C5C6 (7) C4C5 (7) C1C2 (7) C2C3 (7) 1043 (7) 1261 (7) 1265 (6) 1045 (6) 0716 (5) 0934 (5)	DIAGONAL- CCO (59) CC (28) TOCC (3) CCC (3) HCC (2) OFF-DIAG- SB16 (14) BB19 (2) BB22 (-1) BB23 (-4) SB17 (-5)
298 (W)	292 (VW)		296.	A''	0716 (16) 0934 (16) 1045 (11) 1265 (11) 1043 (11) 1261 (11) 0932 (6) 0712 (6) C4C5 (4) C5C6 (4) C1C2 (3) C2C3 (3) 1643 (2) 1861 (2) 1756 (2) 1754 (2)	DIAGONAL- CCO (91) CC (15) HCC (13) TOCO (4) CCC (3) TOCC (1) OFF-DIAG- BB25 (-1) BB20 (-1) SB17 (-2) BB19 (-2) SB16 (-4) SB15 (-4) BB23 (-13)
282 (W)			295.	A''	1154 (23) 1156 (23) 0821 (11) 0823 (11) 0712 (7) 0932 (7) 1045 (4) 1265 (4) C3C4 (3) C6C1 (3) TC50 (2)	DIAGONAL- CCO (94) HCC (7) CC (6) TCCO (4) CCC (3) OFF-DIAG- BB22 (-1) SB17 (-1) BB20 (-1) SB16 (-2) BB19 (-3) BB23 (-8)
	274 (M)		270.	A'	1045 (13) 1265 (13) CC5C (9) CC2C (8) 0934 (7) 0716 (7) 0932 (6) 0712 (6) 1754 (5) 1756 (5) 1043 (3) 1261 (3) CC4C (2) CC6C (2) 0823 (2) 0821 (2) TC34 (2) TC61 (2) 1643 (2) 1861 (2) 1865 (2) 1645 (2)	DIAGONAL- CCO (65) CCC (24) HCC (17) TCCO (6) TCCC (5) CO (2) OFF-DIAG- BB19 (5) SB16 (2) SB17 (-1) BB28 (-1) SB14 (-3) BB25 (-3) BB22 (-4) BB23 (-13)
	250 (W)		267.	A''	0821 (13) 0823 (13) 1154 (8) 1156 (8) 1316 (7) 1534 (7) 0712 (6) 0932 (6) 1043 (6) 1261 (6) CC3C (3) CC1C (3) CC6C (3) CC4C (3) TC20 (3) 1865 (2) 1645 (2) TC50 (2)	DIAGONAL- CCO (68) HCC (23) CCC (14) TCCO (5) TOCC (5) CO (2) CC (1) OFF-DIAG- BB19 (5) BB18 (1) BB24 (1) SB15 (-1) BB28 (-1) BB22 (-2) SB16 (-3) BB25 (-3) SB14 (-4) BB23 (-13)
			195.	A'	CC2C (14) 0821 (10) 0823 (10) 1316 (6) 1534 (6) 1643 (4) 1861 (4) 1156 (4) 1154 (4) 0716 (4) 0934 (4) 1865 (4) 1645 (4) 1754 (4) 1756 (4) 1045 (4) 1265 (4) CC3C (4) CC1C (4) 1043 (3) 1261 (3) 1532 (3) 1312 (3) 0932 (3) 0712 (3) CC6C (2) CC4C (2)	DIAGONAL- CCO (54) HCC (43) CCC (25) CO (7) CC (1) OFF-DIAG- BB19 (11) SB16 (3) BB24 (2) SB17 (-1) SB15 (-2) BB22 (-3) BB28 (-5) BB25 (-9) BB23 (-14) SB14 (-15)
			128.	A''	TC50 (22) TC60 (20) TC40 (20) TC10 (18) TC30 (18)	DIAGONAL- TOCO (99)
			127.	A'	TC60 (8) TC40 (8) CC3C (7) CC1C (7) TC23 (6) TC12 (6) TC45 (5) TC56 (5) CC4C (5) CC6C (5) TC34 (5) TC61 (5) CC5C (4) CC2C (3) TC30 (3) TC10 (3) 1043 (3) 1261 (3) 0932 (3) 0712 (3) 1156 (2) 1154 (2) 0716 (2) 0934 (2)	DIAGONAL- TOCC (32) CCC (32) TOCO (23) CCO (21) CO (5) HCC (3) CC (3) OFF-DIAG- SB16 (4) BB26 (-1) BB23 (-1) BB22 (-3) SB17 (-8) SB14 (-8)
			124.	A''	TC20 (51) TC50 (19) TC10 (11) TC30 (11) TC40 (2) TC60 (2)	DIAGONAL- TOCO (96) CCO (3)
			122.	A'	TC30 (23) TC10 (23) TC40 (15) TC60 (14) TC23 (2) TC12 (2) CC3C (2) CC1C (2) 0716 (2) 0934 (2)	DIAGONAL- TOCO (76) CCC (9) TOCC (8) CCO (7) CC (1) CO (1) OFF-DIAG- SB16 (2) SB14 (-2) SB17 (-2)
			121.	A''	TC20 (42) TC30 (18) TC10 (18) TC50 (10) TC60 (3) TC40 (3)	DIAGONAL- TOCO (94) CCC (4)
			121.	A'	TC40 (25) TC60 (24) TC30 (21) TC10 (21) 1045 (2)	DIAGONAL- TOCO (92) CCC (6) CCC (2) TOCC (1)
			121.	A''	TC50 (45) TC60 (23) TC40 (22) TC10 (2) TC30 (2)	DIAGONAL- TOCO (95) CCO (6)

TABLE LIII (Continued)

EXPERIMENTAL FREQUENCY (CM-1) RAMAN	INFRARED	ASSIGNED FREQUENCY (CM-1)	CALCULATED FREQUENCY (CM-1)	CALCULATED SYMMETRY SPECIES	SPECTRAL INTERPRETATION --- POTENTIAL ENERGY DISTRIBUTIONS INTERNAL COORDINATES	FORCE CONSTANTS
			89.	A'	CC5C(15) TC45(12) TC56(12) TC12(12) TC23(11) CC2C(9) CC1C(4) CC3C(4) CC4C(3) CC6C(3) 1154(3) 1156(3)	DIAGONAL- TOCC(48) CCC (39) CCO (12) HCC (3) CO (2) OFF-DIAG- SB17(2) BB19(1) EB25(-1) BB22(-1) SB14(-4)
			86.	A''	TC61(16) TC34(16) CC1C(10) CC3C(10) CC6C(9) CC4C(9) TC56(4) TC45(4) TC12(4) TC23(4) 1261(2) 1043(2) 0716(2) 0934(2) 0932(2) 0712(2)	DIAGONAL- TOCC(47) CCC (39) CCC (16) CO (3) HCC (2) OFF-DIAG- SB17(1) BB26(-1) BB23(-1) BB22(-2) SB14(-6)

TABLE LIV. DEUTERATED EPI-INOSITOL

EXPERIMENTAL FREQUENCY (CM-1) RAMAN	INFRARED	ASSIGNED FREQUENCY (CM-1)	CALCULATED FREQUENCY (CM-1)	CALCULATED SYMMETRY SPECIES	SPECTRAL INTERPRETATION --- POTENTIAL ENERGY DISTRIBUTIONS INTERNAL COORDINATES	FORCE CONSTANTS
	2958 (VW)		2948.	A'	C4H6(51) C5H7(22) C3H5(22)	DIAGONAL- CH (98)
2945 (W)			2940.	A'	C1H3(36) C2H4(31) C6H8(30) C4H6(2)	DIAGONAL- CH (99)
			2939.	A''	C3H5(46) C5H7(46) C6H8(4) C2H4(4)	DIAGONAL- CH (99)
2930 (W,SH)			2937.	A'	C1H3(63) C2H4(18) C6H8(18)	DIAGONAL- CH (99)
	2917 (M)		2936.	A''	C6H8(46) C2H4(46) C5H7(4) C3H5(4)	DIAGONAL- CH (99)
	2905 (M)		2933.	A'	C4H6(46) C3H5(27) C5H7(27)	DIAGONAL- CH (100)
	2560 (VS)		2448.		O8H0(68) O12H(15) O9H1(13) O11H(3)	DIAGONAL- OH (99)
	2547 (SH)		2448.		O12H(67) O8H0(15) O11H(14) O9H1(3)	DIAGONAL- OH (99)
	2515 (VS)		2448.		O10H(95) O11H(2) O9H1(2)	DIAGONAL- OH (99)
2455 (VS)			2448.		O11H(51) O9H1(31) O12H(11) O8H0(6)	DIAGONAL- OH (99)
	2422 (VS)		2448.		O9H1(84)	DIAGONAL- OH (99)
			2448.		O9H1(51) O11H(29) O8H0(10) O12H(6) O10H(3)	DIAGONAL- CH (99)
1407 (W,SH)	1415 (M)		1405.	A'	1534(18) 1754(18) 1865(9) 1423(9) 1756(6) 1532(6) 1861(5) 1421(5) HC10(3)	DIAGONAL- HCC (80) HCC (7) CC (5) CCC (4) CC (3) COH (2) OFF-DIAG- BB23 (7) BB28 (2) BB25 (2) BB19 (-2) SB12 (-2) SB14 (-3) BB16 (-3) SB15 (-5)
	1395 (M)		1393.	A''	1421(16) 1861(16) 1865(14) 1423(14) 1316(5) 1312(5) 1534(4) 1754(4) 1645(4) 1643(4) C3C4(3) C4C5(3)	DIAGONAL- HCC (87) CC (6) CCO (4) CO (2) HCO (1) OFF-DIAG- BB23 (7) BB28 (2) SB14 (-1) BB27 (-1) EB19 (-2) SB15 (-4)
1383 (M)	1390 (S)		1385.	A''	1643(25) 1645(25) 1532(5) 1756(5) 1421(3) 1861(3) 1534(3) 1754(3) 1316(3) 1312(3) HC30(3) HC50(3) HC20(2) HC60(2)	DIAGONAL- HCC (81) HCC (9) CCH (2) CC (2) CO (1) OFF-DIAG- BB28 (5) BB23 (3) BB25 (2) BB18 (-1) SB15 (-5)
1375 (M)			1373.	A'	1421(15) 1861(15) HC10(9) 1534(8) 1754(8) 1423(8) 1865(8) C6C1(5) C1C2(5) C1O7(4) 1756(3) 1532(3) C5C6(2) C2C3(2) 1645(2) 1643(2)	DIAGONAL- HCC (76) CC (14) HCO (11) CC (6) CCC (3) CCO (3) COH (2) OFF-DIAG- BB23 (5) BB26 (3) BB28 (2) CCCO (-1) SB14 (-2) SB12 (-3) SB17 (-4) BB18 (-4) SB15 (-11)
1361 (S)	1367 (W)		1354.	A''	1316(17) 1312(17) 1643(8) 1645(8) HC60(8) HC20(8) 1532(7) 1756(7) 1423(6) 1865(6) C2O8(5) C6O2(5) 1754(2) 1534(2)	DIAGONAL- HCC (81) HCO (16) CC (10) CCO (3) CC (1) CCC (1) OFF-DIAG- EB25 (3) BB23 (2) BB19 (-1) BB24 (-1) BB28 (-2) SB14 (-3) SB12 (-4) BB18 (-5)
1341 (S)	1344 (VW)		1340.	A'	HC10(24) HC30(23) HC50(23) 1756(9) 1532(9) C5O1(5) C3O9(5) 1312(5) 1316(5) C1O7(3) CC6C(2) CC2C(2)	DIAGONAL- HCO (71) HCC (34) CO (15) CCC (6) COH (3) CC (3) CCO (2) TOCC (1) OFF-DIAG- BB25 (4) BB29 (2) BB19 (-2) SB13 (-3) SB15 (-3) SB14 (-3) SB12 (-10) BB18 (-20)
1306 (M)	1311 (VW)		1306.	A'	HC40(65) HC10(15) 1643(11) 1645(11) C4O0(5) C4OH(3) 1756(2) 1532(2) 1312(2) 1316(2)	DIAGONAL- HCO (85) HCC (32) CC (6) COH (4) CCC (2) TOCC (1) OFF-DIAG- BB29 (2) BB25 (1) SB15 (-2) SB13 (-2) SB12 (-7) BB18 (-23)
1287 (S)	1291 (VW)		1294.	A''	HC3O(39) HC50(39) 1532(7) 1756(7) 1754(6) 1534(6) HC2O(3) HC6O(3) C3O9(3) C5O1(3) 1421(2) 1861(2) C3OH(2) C5OH(2) 1645(2) 1643(2) C3C4(2) C4C5(2)	DIAGONAL- HCO (83) HCC (36) CC (5) CC (4) COH (4) CCC (2) CCO (1) OFF-DIAG- BB29 (2) BB28 (2) SB17 (-1) BB19 (-2) SB13 (-2) SB15 (-4) SB12 (-6) BB18 (-23)
			1291.	A'	HC10(35) HC50(15) HC30(14) HC40(13) 1316(5) 1312(5) 1861(3) 1421(3) 1756(3) 1532(3) 1643(2) 1645(2) C1OH(2) HC60(2) HC2O(2)	DIAGONAL- HCO (80) HCC (29) COH (6) CCO (2) CO (2) CCC (1) OFF-DIAG- BB29 (3) BB19 (-1) SB13 (-1) SB12 (-3) EB18 (-20)
	1261 (W)		1280.	A'	HC2O(38) HC6O(38) 1423(10) 1865(10) HC4O(5) 1861(5) 1421(5) C1O7(2) 1754(2) 1534(2)	DIAGONAL- HCO (83) HCC (34) CO (5) CC (4) COH (2) TOCC (1) OFF-DIAG- CCCO (-1) SB15 (-2) SB12 (-3) BB18 (-24)
1250 (W)			1269.	A''	1534(15) 1754(15) HC60(10) HC2O(10) 1532(9) 1756(9) 1423(7) 1865(7) 1316(4) 1312(4) C2C3(3) C5C6(3) 1645(3) 1643(3) HC5O(2) HC3O(2)	DIAGONAL- HCC (75) HCC (23) CC (9) CCC (4) CO (2) COH (1) OFF-DIAG- BB23 (5) SB12 (1) SB14 (-1) BB19 (-1) SB16 (-1) BB28 (-3) BB16 (-6) SB15 (-8)
1235 (W)			1261.	A''	HC60(20) HC2O(20) 1316(15) 1312(15) 1861(8) 1421(8) 1756(2) 1532(2) 1643(2) 1645(2)	DIAGONAL- HCC (57) HCO (42) CC (3) CCO (1) TOCC (1) CO (1) OFF-DIAG- EB23 (2) SB12 (2) SB15 (1) BB18 (-12)
1177 (M)	1175 (VW,SH)		1161.	A'	C2C3(22) C5C6(22) C2O8(11) C6O2(11) C4O0(4) C3OH(3) C5OH(3) C2OH(3) C6OH(3) CC2C(3) CC6C(3) O821(3) 1261(3) 1156(2) O932(2) O716(2) O712(2) 1043(2) 1045(2) C5SC(2) CC3C(2) HC3O(2) HC5O(2) C4C5(2) C1OH(2) C3C4(2)	DIAGONAL- CC (48) CO (28) CCO (19) COH (15) CCC (10) HCO (7) HCC (3) OFF-DIAG- SB13 (5) BB19 (2) EB22 (1) BB25 (1) SB12 (-2) BB3O (-3) CCCC (-5) SB16 (-6) SB14 (-10) SB17 (-13)
	1142 (VS)		1150.	A''	C5C6(23) C2C3(23) C6OH(11) C2OH(11) C1C2(11) C6C1(11) C4C5(8) C3C4(8) O823(3) 1265(3) 1261(2) O821(2)	DIAGONAL- CC (82) COH (22) CCC (12) CC (1) HCC (1) OFF-DIAG- CCCC (-2) BB3O (-2) SB16 (-14)

TABLE LIV (Continued)

EXPERIMENTAL FREQUENCY (CM-1) RAMAN	INFRARED	ASSIGNED FREQUENCY (CM-1)	CALCULATED FREQUENCY (CM-1)	CALCULATED SYMMETRY SPECIES	SPECTRAL INTERPRETATION --- POTENTIAL ENERGY DISTRIBUTIONS INTERNAL COORDINATES	FORCE CONSTANTS
			1149.	A'	C4OH(11) CC4C(10) C3C4(9) C4C5(9) C3O9(8) C5C1(8) O934(7) 1154(7) C4OO(6) C2C3(5) C5C6(5) 1756(5) 1532(5) 1265(3) O823(3) HC4C(3) C3OH(2) C5OH(2) C2OH(2) C6OH(2) C6O2(2) C2O8(2) C1OH(2) C1C2(2) C6C1(2) C1O7(2)	DIAGONAL- CC (31) CO (28) CCC (22) CCH (22) CCC (12) HCC (12) HCO (6) OFF-DIAG- BB18 (2) BB22 (2) BB19 (1) BB29 (1) SB12 (1) BB24 (-1) BB3C (-2) SB15 (-3) SB17 (-8) SB16 (-9) SB14 (-15)
1134 (S)			1133.	A'	C1O7(14) C3O9(10) C5O1(10) HC2O(6) HC6O(6) C4OO(5) CC1C(5) C6O2(4) C2O8(4) C2OH(4) C6OH(4) C5C(3) CC3C(3) 1532(3) 1756(3) CC6C(2) CC2C(2) C4C5(2) C3C4(2) HC1O(2) C1C2(2) C6C1(2)	DIAGONAL- CO (48) HCO (18) CCC (16) COH (11) CC (9) CCC (7) HCC (7) OFF-DIAG- SB12 (8) BB19 (3) SB16 (-1) CCCO (-1) BB29 (-2) SB17 (-2) BB18 (-2) BB25 (-2) SB13 (-6) SB14 (-13)
1115 (VS)			1121.	A''	C1C2(31) C6C1(31) C4C5(10) C3C4(10) HC2O(9) HC6O(9) 1316(5) 1312(5) O716(5) O712(5) CC2C(5) CC6C(5) 1156(4) O932(4) C2O8(3) C6O2(3) C5O1(2) 1756(2) C3O9(2) 1532(2) C5C6(2) C2C3(2)	DIAGONAL- CC (85) CCO (20) HCC (20) HCC (16) CCC (12) CO (9) OFF-DIAG- BB22 (2) SB14 (-1) BB19 (-1) SB12 (-2) CCCO (-4) BB25 (-4) SB15 (-14) SB17 (-15) SB16 (-20)
	1085 (VS)		1087.	A'	C4OO(59) C4OH(6) C3C4(6) C4C5(6) C5O1(5) C3O9(5) C1O7(5) C2OH(4) C6OH(4) C5C6(3) C2C3(3)	DIAGONAL- CO (74) CC (17) COH (15) CCC (3) CCC (3) HCO (2) HCC (1) OFF-DIAG- SB12 (4) SB15 (2) SB17 (1) SB14 (-6) CCCO (-7) SB13 (-8)
1071 (M)	1065 (SH)		1082.	A''	C3O9(16) C5O1(16) C3OH(12) C5OH(12) C3C4(10) C4C5(10) C2C8(8) C6O2(8) C1C2(5) C6C1(5) C5C6(4) C2C3(4) 1043(4) 1045(4) CC3C(3) CC5C(3) 1316(3) 1312(3) 1421(2) 1861(2)	DIAGONAL- CO (48) CC (38) CCH (25) HCC (12) CCO (12) CCC (5) OFF-DIAG- SB15 (-3) SB16 (-4) SB14 (-4) CCCO (-8) SB17 (-9) SB13 (-12)
1058 (M,SH)			1049.	A'	C1CH(34) C1O7(16) C3OH(9) C5OH(9) C5O1(5) C3O9(5) C1C2(4) C6C1(4) C6O2(3) C2O8(3) 1756(3) 1532(3) C4OH(2) C4OO(2) CC1C(2) 1316(2) 1312(2)	DIAGONAL- CO (75) COH (21) HCC (10) CCC (9) CCC (3) HCO (1) OFF-DIAG- SB13 (2) BB23 (-2) SB14 (-20)
1046 (S)	1049 (VS)		1034.	A'	C1O7(44) C3O9(9) C5O1(9) C2OH(8) C6OH(8) C4OO(5) C2O8(4) C6O2(4) C1OH(3) O712(3) O716(3) 1756(2) 1532(2) 1312(2) 1316(2) C4CH(2)	DIAGONAL- CO (75) COH (21) HCC (10) CCC (9) CCC (3) HCO (1) OFF-DIAG- SB13 (2) BB23 (-2) SB14 (-20)
	1025 (S)		1016.	A''	C6OH(15) C2OH(15) C5O1(14) C3O9(14) C3C4(10) C4C5(10) C5OH(6) C3OH(6) C6O2(5) C2C8(5)	DIAGONAL- COH (43) CO (39) CC (20) HCC (5) CCO (5) CCC (1) OFF-DIAG- CCCO (2) BB3O (-1) SB15 (-3) SB16 (-5) SB14 (-7)
1005 (M)			1003.	A'	C1OH(39) C6O2(17) C2O8(17) C3OH(8) C5OH(8) C2OH(5) C6OH(5) HC1O(5) C5O1(2) C3O9(2) C4OO(2)	DIAGONAL- COH (66) CO (40) HCO (6) HCC (6) CC (3) CCC (2) OFF-DIAG- CCCO (-1) BB3O (-1) SB15 (-1) BB18 (-2) BB29 (-2) SB14 (-3) SB13 (-10)
	977 (S)		989.	A''	C3O9(15) C5O1(15) C2OH(14) C6OH(14) C2O8(13) C6O2(13) C1C2(4) C6C1(4) 1423(3) 1865(3) C3OH(3) C5OH(3) 1754(2) 1534(2) 1643(2) 1645(2)	DIAGONAL- CO (57) COH (34) HCC (15) CC (12) CCO (8) CCC (1) OFF-DIAG- CCCO (1) SB12 (-2) SB16 (-2) BB23 (-3) SB13 (-6) SB14 (-17)
			984.	A'	C4OH(47) C5OH(14) C3OH(14) HC4O(4) C1O7(4) C4OO(2) C6OH(2) C2OH(2) 1534(2) 1754(2) HC5O(2) HC3O(2) 1645(2) 1643(2)	DIAGONAL- COH (81) HCC (10) CO (9) HCO (8) CCO (6) CCC (2) CC (1) OFF-DIAG- SB13 (6) BB25 (1) SB12 (-2) BB29 (-3) BB23 (-3) BB18 (-3) SB14 (-4) BB3O (-6)
969 (M)			975.	A''	C3OH(23) C5OH(23) C2O8(13) C6O2(13) C3C4(10) C4C5(10) HC5O(3) HC3O(3) C5C1(2) C3O9(2)	DIAGONAL- COH (48) CO (30) CC (21) CCO (6) HCC (5) HCO (5) CCC (2) OFF-DIAG- SB12 (2) BB23 (-1) BB18 (-1) SB15 (-1) SB16 (-2) BB3O (-2) BB29 (-2) SB13 (-2) SB17 (-3) SB14 (-5)
	934 (M)		946.	A'	C2OH(18) C6OH(18) C4OH(16) C4C5(8) C3C4(8) C5C6(5) C2C3(5) C1O7(5) C1OH(4) HC4O(2) C5OH(2) C3OH(2) C4OO(2) 1154(2) O934(2)	DIAGONAL- COH (59) CC (27) CO (9) CCO (8) HCC (4) HCC (3) CCC (2) OFF-DIAG- CCCO (2) BB23 (-1) SB14 (-1) BB3O (-2) SB15 (-2) SB17 (-3) SB16 (-5)
882 (W)	889 (M)		889.	A'	C1C2(22) C6C1(22) C4OH(6) 1261(4) O821(4) C3C4(3) C4C5(3) 1861(3) 1421(3) HC4O(3) C5C6(2) C2C3(2) C3OH(2) C5OH(2) CC3C(2) CC5C(2) 1156(2) O932(2) C5O1(2) HC1O(2) C3O9(2)	DIAGONAL- CC (56) COH (14) CCC (13) CCC (8) HCC (8) HCO (5) CO (5) OFF-DIAG- SB15 (4) BB19 (2) SB14 (1) BB25 (-1) SB17 (-8) SB16 (-8)
860 (W)	863 (M)		874.	A''	C2C3(13) C5C6(13) C6O2(10) C2O8(10) C2OH(8) C6OH(8) 1043(5) 1045(5) C4C5(4) C3C4(4) C5OH(3) C3OH(3) O934(2) 1154(2)	DIAGONAL- CC (33) CO (22) COH (21) CCC (21) HCC (6) HCO (2) CCC (1) OFF-DIAG- SB13 (6) CCCO (4) SB15 (3) BB19 (2) SB12 (1) BB3O (-1) BB23 (-2) SB17 (-4) SB14 (-6) SB16 (-8)
817 (M)	819 (W)		849.	A'	C3OH(7) C5OH(7) C4OH(6) C3C4(6) C4C5(6) C6O2(4) C2O8(4) C5C6(4) C2C3(4) C6C1(3) C1C2(3) O821(3) 1261(3) CC1C(3) C4OO(2) 1043(2) 1045(2) 1532(2) 1756(2) HC5O(2) HC3C(2) O932(2) 1156(2)	DIAGONAL- CC (25) COH (23) CCC (15) CO (13) HCC (12) CCC (6) HCO (5) OFF-DIAG- SB15 (5) BB19 (4) BB3O (3) SB13 (2) CCCO (2) BB18 (2) BB23 (1) BB29 (-1) SB17 (-4) SB14 (-4) SB16 (-10)
	771 (S)		784.	A'	CC1C(12) C1OH(9) C2OH(7) C6O2(7) C1C2(6) C6C1(6) 1261(5) O821(5) C4OO(4) 1312(3) 1316(3) C3C4(3) C4C5(3) 1865(2) 1423(2)	DIAGONAL- CO (21) CC (20) CCO (15) CCC (13) HCC (12) COH (10) OFF-DIAG- SB14 (9) CCCC (4) BB19 (4) SB16 (2) BB18 (1) SB15 (1) BB23 (-1) BB24 (-1) SB13 (-2) SB17 (-8)

TABLE LIV (Continued)

EXPERIMENTAL FREQUENCY (CM-1) RAMAN	EXPERIMENTAL FREQUENCY (CM-1) INFRARED	ASSIGNED FREQUENCY (CM-1)	CALCULATED FREQUENCY (CM-1)	CALCULATED SYMMETRY SPECIES	SPECTRAL INTERPRETATION --- POTENTIAL ENERGY DISTRIBUTIONS INTERNAL COORDINATES	FORCE CONSTANTS
686 (M)	688 (W)		686.	A''	1265(12) 0823(12) CC3C(5) CC5C(5) 1423(4) 1865(4) 1156(4) 0932(4) 1756(4) 1532(4) 0716(2) 0712(2) 1534(2) 1754(2) C3C4(2) C4C5(2) C30H(2) C5OH(2) 1645(2) 1643(2)	DIAGONAL- CCO (40) HCC (25) CCC (10) COH (6) CC (5) CO (2) OFF-DIAG- EB19 (7) SB16 (3) SB14 (3) SB17 (3) BB18 (2) BB26 (2) BB30 (1) SB13 (-1) BB25 (-2) BB23 (-2) BB24 (-2)
			681.	A'	C400(7) 0716(6) 0712(6) 0823(6) 1265(6) 0821(5) 1261(5) C3C4(4) C4C5(4) 0932(3) 1156(3) 1316(2) 1312(2) C10H(2) CC5C(2) CC3C(2) C107(2) 1865(2) 1423(2) 1532(2) 1756(2)	DIAGONAL- CCO (45) HCC (12) CO (9) CC (9) CCC (7) COH (6) OFF-DIAG- SE14 (6) EB19 (5) BB3C (3) SB13 (1) CCCO (1) BB24 (-2) BB23 (-3)
555 (W)			551.	A''	0934(15) 1154(15) 0716(13) 0712(13) 1045(6) 1043(6) 0932(5) 1156(5) 1643(4) 1645(4) 1421(4) 1861(4) 0821(3) 1261(3) 1754(2) 1534(2) C1C2(2) C6C1(2) C4C5(2) C3C4(2) CC3C(2) CC5C(2)	DIAGONAL- CCO (86) HCC (25) CC (10) CCC (4) TOCC (1) OFF-DIAG- BB19 (5) BB25 (-1) BB28 (-2) SB15 (-2) SB16 (-3) SB17 (-4) BB23 (-21)
	533 (M)		509.	A''	0934(9) 1154(9) 1421(5) 1861(5) C1C2(5) C6C1(5) 0821(4) 1261(4) CC2C(4) CC6C(4) 0716(4) 0712(4) 1156(4) 0932(4) 1754(2) 1534(2) 1643(2) 1645(2) C4C5(2) C3C4(2) CC5C(2) CC3C(2)	DIAGONAL- CCO (46) HCC (20) CC (14) CCC (12) CO (2) OFF-DIAG- BB19 (6) SB17 (6) SB14 (5) BB18 (2) EB25 (1) BB28 (-1) SB16 (-2) SB15 (-3) BB23 (-9)
494 (VS)	498 (M)		481.	A'	C3C4(7) C4C5(7) CC4C(7) C501(6) C309(6) C6C1(5) C1C2(5) C107(4) C5C6(4) C2C3(4) CC2C(2) CC6C(2) 0932(2) 1156(2)	DIAGONAL- CC (31) CO (17) CCC (14) CCO (12) HCC (2) HCC (2) OFF-DIAG- SE14 (9) SB17 (8) CCCO (4) SB16 (1) BB22 (1) SB15 (-1) SB12 (-2)
	427 (M)		415.	A'	0823(16) 1265(16) 1045(9) 1043(9) 1643(8) 1645(8) 1534(4) 1754(4) CC4C(3) CC2C(3) CC6C(3) 1156(2) 0932(2)	DIAGONAL- CCO (56) HCC (24) CCC (12) CC (5) TOCC (2) CO (1) HCC (1) OFF-DIAG- SE16 (6) BB19 (5) BB3C (1) SB17 (-1) BB28 (-3) BB25 (-3) BB23 (-7)
	380 (M)		385.	A'	CC4C(12) C5C6(7) C2C3(7) CC3C(6) CC5C(6) CC1C(6) 0716(6) 0712(6) 1043(6) 1045(6) C400(3) 0934(2) 1154(2) 1423(2) 1865(2) C107(2) CC6C(2) CC2C(2)	DIAGONAL- CCC (33) CCO (31) CC (15) HCC (6) CO (5) OFF-DIAG- SE14 (9) SB17 (9) BB22 (2) BB25 (1) BB26 (-2) SB16 (-2) SB15 (-3) BB23 (-4)
368 (M)			335.	A''	0821(20) 1261(20) 1156(11) 0932(11) CC2C(5) CC6C(5) 0716(4) 0712(4) CC5C(3) CC3C(3) 1423(2) 1865(2) 0934(2) 1154(2)	DIAGONAL- CCO (74) CCC (16) HCC (6) CC (5) TOCO (2) CO (1) OFF-DIAG- BB22 (2) SB15 (1) SB17 (1) BB20 (-1) EB19 (-1) BB23 (-7)
340 (M)	341 (M)		301.	A''	1043(29) 1045(29) C2C3(8) C5C6(8) 1154(8) 0934(8) 0716(6) 0712(6) 1532(2) 1756(2) TC40(2) 1156(2) 0932(2)	DIAGONAL- CCO (92) CC (16) HCC (10) TOCO (3) CCC (2) OFF-DIAG- BB20 (-1) SB16 (-1) BB19 (-3) SB17 (-4) SB15 (-5) BB23 (-10)
289 (W)			295.	A'	0934(18) 1154(18) 0932(18) 1156(18) CC4C(4) C4C5(4) C3C4(4) C6C1(2) C1C2(2) 0821(2) 1261(2) TC30(2) TC5C(2) 1423(2) 1865(2) 1265(2) 0823(2)	DIAGONAL- CCO (81) CC (12) CCC (6) HCC (6) TOCO (4) TOCC (1) OFF-DIAG- SB16 (4) BB20 (-1) BB22 (-2) SB17 (-3) EB23 (-10)
	280 (M)		289.	A''	0716(19) 0712(19) 0821(10) 1261(10) 0823(6) 1265(6) 1154(5) 0934(5) 1045(4) 1043(4) CC2C(2) CC6C(2) TC10(2) 1156(2) 0932(2)	DIAGONAL- CCO (91) CCC (6) CC (4) TOCO (4) HCC (4) OFF-DIAG- SB16 (2) BB20 (-1) SB17 (-1) BB22 (-2) BB19 (-2) BB23 (-7)
271 (W)			250.	A'	C821(13) 1261(13) 1265(6) 0823(6) CC4C(5) 1534(4) 1754(4) CC1C(4) 0712(3) 0716(3) 1645(3) 1643(3) 1316(3) 1312(3) 0934(2) 1154(2) 1156(2) 0932(2) CC5C(2) CC3C(2) TC23(2) TC56(2)	DIAGONAL- CCO (56) HCC (24) CCC (14) TCCC (5) CO (3) HCO (2) TOCO (2) OFF-DIAG- BB19 (7) BB24 (3) BB18 (2) BB28 (-2) BB25 (-4) SB14 (-5) BB23 (-7)
236 (VW)			245.	A''	0823(21) 1265(21) CC2C(9) CC6C(9) 1156(6) 0932(6) CC5C(6) CC3C(4) 1534(3) 1754(3) TC34(2) TC45(2) 1043(2) 1045(2)	DIAGONAL- CCO (59) CCC (26) HCC (12) TOCC (6) TOCO (2) CO (2) CC (1) OFF-DIAG- BB19 (2) BB24 (2) SB16 (1) BB18 (1) SB15 (-1) BB22 (-1) SB17 (-2) BB25 (-3) BB23 (-3) SB14 (-5)
			199.	A'	CC2C(8) CC6C(8) 0823(7) 1265(7) CC1C(7) 0821(6) 1261(6) 1534(5) 1754(5) 1645(4) 1643(4) 1043(4) 1045(4) 0934(3) 1154(3) 1316(3) 1312(3) 0932(3) 1156(3) TC20(2) TC60(2) 1532(2) 1756(2) CC3C(2) CC5C(2)	DIAGONAL- CCO (48) HCC (30) CCC (27) CO (6) TOCO (5) CC (2) OFF-DIAG- EB19 (8) SB16 (4) BB24 (3) BB26 (-1) BB22 (-2) BB28 (-2) SB15 (-2) BB23 (-5) BB25 (-7) SB14 (-13)
			139.	A'	TC2C(21) TC60(21) TC12(6) TC61(6) CC1C(6) CC2C(5) CC6C(5) 0716(5) 0712(5) TC56(4) TC23(4) CC4C(3) CC3C(2) CC5C(2) TC34(2) TC45(2) 1154(2) C107(2) 0934(2)	DIAGONAL- TOCO(42) TOCC(24) CCC (23) CCC (17) HCC (4) CO (4) CC (2) OFF-DIAG- SB16 (2) BB26 (-1) BB25 (-1) BB22 (-2) BB23 (-3) SB17 (-6) SB14 (-6)
			132.	A''	TC2C(35) TC60(35) TC10(16) TC40(6) TC50(2) TC30(2)	DIAGONAL- TOCO(94) TOCC(2) CCC (2)
			127.	A''	TC5C(28) TC30(28) TC40(27) TC20(6) TC60(6) TC10(3)	DIAGONAL- TOCO(97) CCC (2)
			122.	A'	TC5C(47) TC30(46)	DIAGONAL- TOCO(94) CCC (4) TOCC(1)
			122.	A''	TC10(45) TC40(43) TC30(3) TC50(2)	DIAGONAL- TOCO(96) CCC (4)

TABLE LIV (Continued)

EXPERIMENTAL FREQUENCY (CM-1) RAMAN	INFRARED	ASSIGNED FREQUENCY (CM-1)	CALCULATED FREQUENCY (CM-1)	CALCULATED SYMMETRY SPECIES	SPECTRAL INTERPRETATION --- POTENTIAL ENERGY DISTRIBUTIONS
					INTERNAL COORDINATES / FORCE CONSTANTS
			120.	A''	TC1C(33) TC40(21) TC30(17) TC50(16) TC60(4) TC20(4) DIAGONAL- TOCO(94) CCC (5) CCC (1)
			114.	A'	TC2C(22) TC60(22) CC4C(6) TC34(6) TC45(6) CC3C(5) CC5C(5) TC23(4) TC56(4) CC1C(3) 1043(2) 1045(2) 0934(2) 1154(2) DIAGONAL- TOCO(47) TOCC(21) CCC (21) HCC (14) CO (3) CC (1) OFF-DIAG- SB16(1) BB22(-1) BB23(-1) BB26(-1) SB17(-4) SB14(-5)
			87.	A''	TC56(15) TC23(15) CC5C(12) CC3C(12) CC2C(6) CC6C(6) TC12(4) TC61(4) TC45(4) TC34(3) 0932(3) 1156(3) TC2C(3) TC60(3) 1423(2) 1865(2) 1154(2) 0934(2) DIAGONAL- TOCC(45) CCC (36) CCO (10) TOCO(6) HCC (5) CO (1) HCO (1) OFF-DIAG- SB17(3) BB19(2) BB25(-1) BB26(-2) EB23(-2) SB14(-3)
			84.	A'	CC1C(16) TC61(12) TC12(12) CC4C(11) TC34(11) TC45(11) 0712(3) 0716(3) CC3C(3) CC5C(3) TC20(3) TC60(3) CC6C(2) CC2C(2) 1043(2) 1045(2) DIAGONAL- TOCC(45) CCC (37) CCO (13) TOCO(6) HCC (3) CO (2) OFF-DIAG- SB17(2) BB19(1) BB22(-1) BB23(-2) EB23(-2) SB14(-4)

TABLE LV. MYO-INOSITOL — X-RAY CRYSTAL STRUCTURE

EXPERIMENTAL FREQUENCY (CM-1) RAMAN	INFRARED	ASSIGNED FREQUENCY (CM-1)	CALCULATED FREQUENCY (CM-1)	CALCULATED SYMMETRY SPECIES	SPECTRAL INTERPRETATION --- POTENTIAL ENERGY DISTRIBUTIONS INTERNAL COORDINATES	FORCE CONSTANTS
	3380 (VS)		3357.			DIAGONAL- OH (100)
	3220 (VS)		3357.		O7H9(69) O8HO(30)	DIAGONAL- OH (100)
	3170 (VS)		3357.		O8HO(68) O7H9(30)	DIAGONAL- CH (100)
			3357.		O8HO(50)	DIAGONAL- OH (100)
			3357.		O8HO(00)	DIAGONAL- CH (100)
			3357.		O9H1(00)	DIAGONAL- OH (100)
2964 (M)			2949.		C5H7(32) C4H6(28) C6H8(22) C3H5(8) C1H3(7)	DIAGONAL- CH (98)
	2955 (W)		2945.		C6H8(30) C4H6(27) C1H3(24) C3H5(18)	DIAGONAL- CH (99)
2940 (M)	2935 (W)		2940.		C2H4(38) C5H7(24) C3H5(20) C1H3(17)	DIAGONAL- CH (99)
2925 (VS)	2920 (M)		2937.		C2H4(60) C3H5(15) C1H3(13) C5H7(10)	DIAGONAL- CH (99)
	2900 (W)		2934.		C3H5(30) C1H3(28) C6H8(22) C4H6(20)	DIAGONAL- CH (99)
2887 (M)	2880 (VW)		2931.		C5H7(32) C6H8(24) C4H6(23) C3H5(10) C1H3(10)	DIAGONAL- CH (100)
	1445 (M)	1445.	1455.		C4OH(33) 1754(18) 1756(10) 1534(9) C5OH(7) 1532(2) 1645(2)	DIAGONAL- HCC (44) COH (42) CCO (3) CO (1) CC (1) HCC (1) OFF-DIAG- EB23(5) EB30(2) BB25(2) BB28(1) SB14(-2) SB13(-2)
			1435.		C1OH(25) C6OH(12) 1865(11) HC1O(10) 1861(9) C2OH(7) C5OH(5) 1645(3) 1316(2) C3OH(2) 1643(2)	DIAGONAL- COH (52) HCC (30) HCO (11) CCO (3) OFF-DIAG- BB23(4) BB29(2) EB25(1) SB13(-1) EB18(-2)
1427 (VW)		1427.	1427.		C6OH(33) C2OH(15) 1316(7) C1OH(5) 1756(5) 1312(4) C4OH(4) C3OH(3) C6C1(2) 1865(2) HC2O(2) 1261(2) 1532(2)	DIAGONAL- COH (60) HCC (22) CC (4) HCC (3) CCO (3) CO (2) CCC (2) OFF-DIAG- BB23(3) BB3O(3) SB15(2) BB25(2) BB28(1) SB17(-1) SB16(-2) SB13(-2)
			1423.		C3OH(38) 1423(11) C1OH(11) 1421(8) HC3O(8) C3C4(3) C6OH(3) 1534(3) HC1O(3) C2OH(3) 1643(2) C6C1(2)	DIAGONAL- COH (55) HCC (28) HCO (11) CC (6) CCO (3) CO (2) OFF-DIAG- BB29(3) BB23(3) SB15(-1) SB12(-1) SB16(-2) BB18(-2) SB13(-4)
1418 (W)	1416 (M)	1417.	1411.		C5OH(43) C4OH(13) C1OH(10) 1756(4) HC5O(4) HC1O(4) 1645(4) C2OH(3) 1534(3) C4C5(3) HC4O(2) C5C6(2)	DIAGONAL- COH (70) HCC (16) HCO (11) CC (5) CCO (2) OFF-DIAG- BB29(2) SB16(-1) SB13(-1) BB18(-2) SB15(-3)
1406 (SH)		1406.	1389.		C2OH(45) C1OH(14) C3OH(9) C6OH(7) C4OH(6) HC2O(5) 1534(3) HC1O(3) 1423(2) 1532(2)	DIAGONAL- COH (82) HCC (10) HCC (8) CC (3) CCO (1) CO (1) OFF-DIAG- SB15(-1) BB29(-1) BB18(-2)
	1379 (W,SH)	1379.	1380.		1316(19) 1861(16) 1421(11) 1645(6) 1643(6) C6C1(5) C3OH(5) 1423(5) 1865(5) 1312(4) HC1O(3) C6OH(3) C1O7(2) O7I2(2)	DIAGONAL- HCC (75) COH (11) CC (8) HCC (7) CCO (4) CO (3) OFF-DIAG- EB28(6) BB23(3) SB13(1) BB3O(-1) SB12(-1) BB19(-1) SB14(-2) BB18(-3) SB15(-11)
1373 (SH)	1371 (M)	1371.	1363.		1645(19) C5OH(15) 1643(12) 1865(9) 1861(6) 1316(5) C2OH(5) 1534(4) C4OH(3) 1532(3) 1756(2) C6OH(2) C3C4(2) HC5O(2) 1423(2) HC1O(2) C1OH(2)	DIAGONAL- HCC (63) COH (27) HCC (6) CC (4) CO (2) CCO (2) OFF-DIAG- EB28(5) BB23(2) BB29(1) BB18(-2) SB13(-2) SB15(-6)
1360 (M)	1355 (W)	1357.	1358.		1754(27) C4OH(16) C6OH(12) 1756(12) C5OH(11) HC5O(8) HC4O(4) 1645(3) C4C5(2) 1865(2)	DIAGONAL- HCC (45) COH (41) HCO (13) CC (3) CO (2) CCO (1) OFF-DIAG- BB28(4) BB23(1) SB12(-2) BB18(-3) SB15(-4)
1344 (W)	1343 (W)	1343.	1349.		HC4O(14) C2OH(11) 1534(10) C6OH(10) 1865(7) HC6O(7) 1756(7) C3OH(6) 1532(5) 1643(5) C4OH(5) HC5O(5) 1645(3) C4OO(2) C1OH(2) C5O1(2) C6O2(2)	DIAGONAL- HCC (41) COH (33) HCC (27) CO (7) CC (2) CCO (1) OFF-DIAG- BB28(4) BB23(2) SB13(2) BB29(-2) SB14(-2) SB15(-4) SB12(-4) BB18(-10)
1328 (M)	1323 (W)	1323.	1338.		1421(26) 1423(14) C3OH(11) 1861(9) C1OH(5) HC1O(4) C4OH(4) 1643(4) HC6O(3) 1534(3) 1645(3) C2C3(3) 1316(2) 1532(2) HC2O(2)	DIAGONAL- HCC (65) COH (21) HCO (9) CC (5) CCO (2) CO (1) OFF-DIAG- EB23(4) BB28(2) SB13(1) BB18(-3) SB15(-5)
1305 (W)	1312 (SH)	1305.	1322.		1532(20) HC3O(17) 1643(14) 1312(12) HC2O(7) C2O8(7) HC6O(6) HC1O(5) HC4O(4) 1423(4) C2OH(3) C3O9(3) HC5O(3) 1645(2) 1861(2) C1O7(2) CC2C(2)	DIAGONAL- HCC (57) HCO (42) CO (12) COH (8) CCO (3) CCC (2) TOCC (1) OFF-DIAG- EB25(3) BB23(2) BB29(1) BB24(-1) BB19(-1) SB15(-2) SB13(-2) SB14(-4) SB12(-7) BB18(-15)
1282 (M)	1281 (VW,SH)	1282.	1282.		HC2O(32) HC4O(15) 1423(13) 1645(8) 1532(6) HC5O(5) 1865(5) 1534(4) C3O9(3) 1421(3) 1754(3) 1861(3) C1OH(2) C2C3(2)	DIAGONAL- HCO (55) HCC (48) CO (6) COH (3) CC (3) CCC (3) CCO (3) OFF-DIAG- BB23(3) BB19(-1) BB29(-2) SB15(-2) SB13(-2) SB14(-2) SB12(-3) BB18(-16)
1268 (VW)	1271 (W)	1271.	1276.		HC6O(36) HC4O(18) HC3O(14) HC2O(10) 1865(9) 1532(7) 1645(6) 1423(4) C3OH(3) HC5C(3) 1861(3) C3O9(3) 1754(2)	DIAGONAL- HCO (82) HCC (35) COH (4) CO (4) CC (2) TOCC (2) OFF-DIAG- SB15(-2) SB12(-4) BB18(-23)
	1258 (LT,W)	1258.	1261.		1312(26) HC2O(18) 1316(10) 1421(8) 1861(8) HC6O(7) C6OH(7) HC5O(5) 1532(4) C1O7(3) HC1O(3) 1645(2) C1C2(2) 1754(2) 1643(2) C2C3(2)	DIAGONAL- HCC (65) HCO (33) CCH (7) CC (5) CO (4) CCC (3) OFF-DIAG- EB23(4) SB14(-1) BB19(-1) SB15(-5) BB18(-9)

TABLE LV (Continued)

EXPERIMENTAL FREQUENCY (CM-1) RAMAN	EXPERIMENTAL FREQUENCY (CM-1) INFRARED	ASSIGNED FREQUENCY (CM-1)	CALCULATED FREQUENCY (CM-1)	CALCULATED SYMMETRY SPECIES	SPECTRAL INTERPRETATION --- POTENTIAL ENERGY DISTRIBUTIONS INTERNAL COORDINATES	FORCE CONSTANTS
1248 (W)	1245 (M)	1247.	1250.		HC4O(19) HC1O(18) HC6O(12) 1534(11) 1643(9) HC3O(9) C1OH(7) C3OH(7) 1312(7) HC2O(7) C4OH(3) 1861(2) 1316(2) C1O7(2)	DIAGONAL- HCO (64) HCC (35) COH (18) CC (4) CCC (4) CCO (2) CC (1) TOCC(1) OFF-DIAG- EB25(2) SB13(1) BB23(-1) SB14(-2) BB19(-3) BB28(-3) SB12(-4) BB18(-17)
1220 (W)	1217 (W)	1218.	1238.		HC3O(35) HC6O(18) HC5O(13) HC1O(12) C3OH(7) 1312(7) 1534(6) HC4O(5) 1532(5) C1OH(4) 1865(3) C5OH(3) 1756(2) 1861(2) 1643(2)	DIAGONAL- HCO (83) HCC (29) COH (15) CO (2) CCC (1) CC (1) CCC (1) OFF-DIAG- EB25(1) BB23(-1) BB26(-2) BB19(-2) SB12(-3) BB29(-3) BB18(-22)
1198 (VW)	1194 (M)	1196.	1235.		HC5O(42) HC1O(18) 1756(15) 1316(9) C5OH(8) C1OH(8) HC4O(5) 1865(3) 1643(2) 1861(2)	DIAGONAL- HCO (67) HCC (33) COH (18) CC (3) CO (1) CCC (1) CCO (1) OFF-DIAG- EB23(1) BB19(-1) SB12(-2) BB28(-3) BB29(-4) BB18(-17)
1143 (M)	1145 (S)	1144.	1152.		C6O2(15) C4OO(13) C5O1(11) C1O7(11) C2O8(10) C3O9(9) C1C2(8) CC5C(5) CC6C(4) CC1C(4) C2C3(3) CC4C(3) CC3C(3) O716(2) 1261(2) 1265(2) 1045(2) 1043(2)	DIAGONAL- CO (70) CCC (20) CCC (13) CC (13) HCO (4) COH (2) HCC (2) OFF-DIAG- SB12(5) BB19(2) BB23(2) BB22(2) BB25(-1) SB17(-4) SB13(-4) CCCO(-4) SB14(-21)
1131 (M)		1131.	1120.		C2C3(24) C1O7(17) C3C4(16) C4OO(9) HC5O(5) HC2C(5) C2O8(5) CC2C(4) C1C2(4) HC1O(3) HC3O(3) O821(3) O712(3) 1045(2) O932(2) C3O9(2) C1OH(2) CC5C(2) O716(2)	DIAGONAL- CC (47) CO (34) HCC (19) CCC (14) CCC (9) COH (4) HCC (3) OFF-DIAG- SB12(3) BB22(1) BB30(1) BB18(-1) EB23(-1) SB15(-2) CCCO(-3) SB13(-3) SB17(-6) SB16(-6) SB14(-13)
1122 (M)		1122.	1120.		C1C2(31) C3O9(20) C6C1(16) C2C3(13) C6O2(9) HC2O(4) C4C5(4) O823(3) O934(3) CC4C(3) HC1O(3) CC2C(3) CC3C(2) O716(2) O821(2) O932(2) HC4O(2) 1265(2) C2O8(2)	DIAGONAL- CC (64) CO (32) CCO (18) HCC (11) CCC (10) COH (4) HCC (3) OFF-DIAG- BB30(1) BB22(1) BB18(-1) BB23(-2) SB15(-2) CCCC(-4) SB13(-4) SB17(-9) SB16(-9) SB14(-12)
1112 (SH)	1111 (S)	1111.	1102.		C4C5(48) C5O1(21) C4OO(9) C1C2(8) C3C4(8) C2O8(6) C5C6(5) 1043(4) 1156(4) C6O2(4) C5OH(3) CC6C(2) CC3C(2) CC5C(2) O823(2) HC3O(2)	DIAGONAL- CC (68) CO (41) CCC (13) CCC (7) COH (5) HCO (3) HCC (2) OFF-DIAG- SB15(-3) SB13(-4) CCCC(-6) SB16(-7) SB17(-8) SB14(-9)
1107 (LT,M)	1107 (LT,SH)	1107.	1092.		C5C6(42) C5O1(28) C6C1(9) C6O2(8) C2O8(5) C4OO(5) 1154(5) C2C3(4) C1O7(4) 1261(4) CC4C(3) CC1C(3) CC5C(3) 1045(2)	DIAGONAL- CC (57) CO (51) CCO (15) CCC (10) HCO (4) HCC (2) COH (2) OFF-DIAG- SB13(-2) BB22(1) EB23(-1) SB12(-2) SB15(-3) SB16(-4) CCCO(-7) SB17(-9) SB14(-13)
1097 (M)	1096 (SH)	1097.	1087.		C4OO(23) C6O2(21) C2O8(19) C1C2(10) C2C3(10) C4C5(8) C5C6(8) C4OH(3) C3O9(3) C1O7(3) C2OH(2) C6OH(2)	DIAGONAL- CO (71) CC (36) COH (8) CCO (5) HCC (3) CCC (3) HCC (2) OFF-DIAG- SB12(-2) SB16(-4) SB17(-4) SB13(-9) CCCO(-10)
1066 (S)	1063 (SH)	1066.	1050.		C6C1(22) C3O9(22) C1O7(19) C6O2(13) C4OO(12) C2C3(4) 1423(3) C6OH(3) O712(2) C4C5(2) 1045(2) 1421(2) C934(2)	DIAGONAL- CO (67) CC (32) HCC (9) CCO (9) COH (5) HCO (5) CCC (3) OFF-DIAG- BB23(-1) SB13(-4) SB16(-5) SB17(-6) CCCO(-7) SB14(-7)
1053 (M)	1047 (VS)	1050.	1047.		C3C4(27) C1O7(8) C5C6(7) C1C2(7) C2C3(6) C6O2(5) O716(4) HC2O(4) C4OH(4) HC4O(3) 1265(3) C4OO(3) HC5C(3) C3O9(3) HC6O(3) 1532(3) O934(3) O932(3) C4C5(3) 1312(3) C2OH(2) CC5C(2) CC3C(2) C3OH(2) 1754(2)	DIAGONAL- CC (51) CO (20) CCO (18) HCO (14) HCC (11) COH (9) CCC (7) OFF-DIAG- BB18(2) BB19(2) EB22(1) BB23(1) SB13(-1) SB14(-3) CCCO(-2) SB15(-2) SB17(-12) SB16(-15)
1012 (M)	1012 (M)	1012.	1001.		C3O9(17) C6O2(16) C4OO(15) C1O7(15) C5C6(13) C4C5(11) C2C3(8) C1C2(7)	DIAGONAL- CO (63) CC (40) CCO (5) HCC (3) COH (2) OFF-DIAG- CCCO(6) SB17(3) BB23(-1) SB13(-3) SB15(-4) SB14(-6) SB16(-9)
1003 (SH)	999 (S)	999.	987.		C5O1(31) C2O8(14) C3O9(11) C1O7(9) C5C6(8) C3C4(8) C4C5(6) C6C1(5) 1045(3) 1265(3) CC2C(2) 1861(2) 1643(2) C5OH(2)	DIAGONAL- CO (65) CC (28) CCO (11) HCC (7) CCC (3) COH (3) HCO (2) OFF-DIAG- CCCO(6) SB12(3) SB15(-2) SB17(-3) SB13(-5) SB16(-8) SB14(-12)
936 (M)	927 (M)	932.	923.		C3C4(18) C6C1(14) 1043(7) 1532(7) C2C3(6) 1154(5) C2O8(4) 1312(4) 1156(3) 1261(3) C1O7(3) CC3C(3) CC1C(3) C4OO(2) C6C2(2) HC4O(2) CC4C(2) HC3O(2) CC6C(2) C5C6(2) HC1O(2) C1C2(2) C3O9(2)	DIAGONAL- CC (43) CCO (23) HCC (17) CO (13) CCC (10) HCC (7) CCH (4) OFF-DIAG- CCCO(5) SB15(3) SB12(3) BB18(3) BB19(2) BB23(2) BB22(1) SB14(-6) SB16(-13) SB17(-16)
902 (S)	896 (M)	899.	890.		C2O8(38) C1C2(11) C6C1(8) 1261(7) C2C3(6) 1312(4) C7I2(3) 1043(3) O932(3) C5O1(2) C4C5(2)	DIAGONAL- CO (41) CC (28) CCO (18) HCC (10) HCO (2) CCC (2) COH (2) OFF-DIAG- CCCO(5) SB15(4) BB19(3) BB18(1) SB14(-5) SB17(-5) SB16(-9)
738 (W)	730 (M)	730.	725.		O823(16) O932(11) O712(10) C3C4(8) 1532(6) 1423(5) O821(5) C4OO(3) 1645(3) 1154(3) C6C1(3) 1534(2) CC3C(2) 1312(2) 1265(2) 1045(2) 1865(2) 1754(2)	DIAGONAL- CCO (52) HCC (25) CC (11) CO (5) CCC (3) OFF-DIAG- BB19(7) SB14(5) SB16(2) SB17(2) CCCO(1) SB15(-2) BB24(-2) BB23(-7)
	711 (LT,M)	711.	719.		O821(14) CC1C(8) 1421(8) C6C1(7) CC3C(6) C6O2(6) 1312(4) C2OH(3) 1423(3) C3O9(3) C4OO(3) O823(2) C2O8(2) 1316(2) CC2C(2) C1O7(2) O712(2) 1156(2)	DIAGONAL- CCO (22) HCC (21) CCC (17) CO (15) CC (9) COH (3) HCO (1) OFF-DIAG- EB19(7) SB14(6) SB17(3) BB26(2) BB18(1) BB24(-1) SB13(-2) BB30(-2) BB25(-2)
617 (W)	608 (W,SH)	608.	623.		1045(16) 1265(14) O716(12) 0934(12) 1154(7) 1645(6) 1156(6) 1865(6) O712(6) 0932(5) 1756(5) 1754(5) 1043(3) 1261(3) 1423(2) C3C4(2) 0823(2)	DIAGONAL- CCO (86) HCC (27) CC (2) CCC (2) OFF-DIAG- BB19(7) SB17(-1) SB16(-1) BB28(-3) BB23(-21)

TABLE LV (Continued)

EXPERIMENTAL FREQUENCY (CM-1) RAMAN	INFRARED	ASSIGNED FREQUENCY (CM-1)	CALCULATED FREQUENCY (CM-1)	CALCULATED SYMMETRY SPECIES	SPECTRAL INTERPRETATION --- POTENTIAL ENERGY DISTRIBUTIONS INTERNAL COORDINATES	FORCE CONSTANTS
593 (VW)	584 (M)	584.	590.		0934 (11) 0716 (10) CC2C (5) 1643 (5) 1754 (5) 1861 (4) CC5C (4) 1756 (4) 1316 (4) 1534 (4) 1043 (4) 1154 (4) 1156 (3) 1261 (3) C400 (3) C602 (3) 0821 (3) 0823 (2) 1645 (2) 1865 (2)	DIAGONAL- CCO (43) HCC (31) CCC (12) CO (8) CC (3) HCC (1) OFF-DIAG- SB14 (9) BB19 (7) BB18 (2) BB28 (-4) BB23 (-12)
509 (VS)		509.	493.		C3C4 (10) C6C1 (9) C501 (7) CC4C (6) CC6C (6) 1154 (4) 1156 (4) C309 (4) C1C7 (4) C2C3 (4) C4C5 (4) C1C2 (4) CC5C (4) C5C6 (3) 1265 (2)	DIAGONAL- CC (33) CO (16) CCC (15) CCO (13) HCC (3) OFF-DIAG- SB14 (8) SB17 (6) CCCO (4) BB19 (1) SB16 (1) BB22 (1) SB12 (-1) SB15 (-1)
467 (M)	450 (W)	458.	444.		0821 (11) 1861 (10) 0823 (10) 1643 (9) 1043 (7) 1261 (7) 1265 (5) 1156 (5) 0716 (4) 1045 (4) 1316 (4) 1154 (4) 1534 (4) D934 (3) C6C1 (2) 1756 (2) C3C4 (2) 1754 (2) CC6C (2)	DIAGONAL- CCO (60) HCC (35) CC (7) CCC (6) TOCC (3) CO (2) CCH (1) OFF-DIAG- EB19 (7) SB16 (3) BB18 (1) BB30 (-1) SB17 (-2) SB14 (-4) BB25 (-4) BB28 (-4) BB23 (-12)
435 (VS)	432 (M)	434.	428.		CC5C (10) C5C6 (6) 1154 (6) C1C2 (6) C4C5 (6) CC2C (6) C2C3 (5) 1156 (5) 1265 (4) 1045 (3) CC4C (3) C400 (3) CC6C (3) C602 (3) 0716 (2)	DIAGONAL- CCO (24) CC (23) CCC (21) CO (8) HCC (5) OFF-DIAG- SB14 (8) SB17 (8) BB22 (2) BB19 (2) CCCO (1) BB25 (1) SB16 (1) BB23 (-1) SB15 (-3)
393 (M)	387 (W)	390.	386.		CC3C (10) CC1C (10) CC6C (9) CC4C (8) 0932 (7) 0712 (5) 0716 (5) 1265 (4) 0934 (4) 1045 (4) 1043 (4) C5C6 (3) C4C5 (3) 1261 (2) 1423 (2) C1C2 (2) 1421 (2) C2C3 (2)	DIAGONAL- CCO (40) CCC (38) CC (10) HCC (5) CO (3) OFF-DIAG- SB14 (9) SB17 (8) BB22 (3) BB25 (2) BB20 (-1) BB30 (-2) SB15 (-2) BB26 (-2) SB16 (-5) BB23 (-6)
378 (M)	367 (VW)	373.	349.		1043 (15) 1261 (13) 0823 (10) CC2C (7) 1645 (7) 0821 (7) 1154 (6) 1865 (6) 0712 (5) 1756 (5) 1754 (4) 0934 (4) C932 (3) 0716 (3) CC5C (3) 1156 (3) 1421 (2) CC4C (2)	DIAGONAL- CCO (70) HCC (30) CCC (13) TCCC (3) CO (2) CC (2) TOCC (1) OFF-DIAG- BB19 (3) BB22 (1) BB30 (-1) SB15 (-2) SB17 (-2) BB28 (-3) BB25 (-5) SB14 (-5) BB23 (-10)
327 (W)		327.	314.		0712 (16) 0716 (12) 1045 (12) 1043 (10) C5C6 (10) C2C3 (9) 0932 (6) C4C5 (4) C1C2 (3) TC1C (2) TC40 (2) 0934 (2)	DIAGONAL- CCO (62) CC (26) TOCC (6) HCC (4) CCC (3) OFF-DIAG- SB16 (11) EB19 (1) BB22 (-1) SB17 (-6) BB23 (-6)
312 (W)		312.	297.		1265 (20) 1261 (16) 0934 (11) 0823 (6) 0821 (6) 1156 (5) C4C5 (5) C1C2 (5) 1045 (4) 0716 (4) 1154 (4) 1043 (4) 0932 (3) 1756 (2) 1643 (2) 1312 (2) TC60 (2) 1861 (2)	DIAGONAL- CCO (84) HCC (12) CC (10) TOCO (5) CCC (3) TOCC (1) OFF-DIAG- BB24 (1) BB19 (-1) BB25 (-1) SB16 (-2) SB15 (-3) BB23 (-9)
296 (W)	294 (SH)	295.	294.		0932 (16) 1156 (14) 0821 (12) 0712 (11) 1154 (11) 0823 (8) 0934 (8) 0716 (4) C6C1 (3) C3C4 (3) 1423 (2) C4C5 (2) C1C2 (2) TC10 (2) TC20 (2)	DIAGONAL- CCO (86) CC (11) HCC (6) TCCO (5) CCC (2) OFF-DIAG- SB16 (2) BB22 (-1) BB20 (-1) BB19 (-2) SB17 (-3) BB23 (-7)
289 (SH)		289.	275.		1045 (16) 1265 (9) 0932 (9) CC5C (8) 0934 (8) 1043 (8) CC2C (7) 0716 (5) 1754 (5) 0712 (4) 1756 (4) TC40 (4) 1156 (3) 0823 (3) CC6C (3) 1261 (2) TC10 (2) 1865 (2) TC34 (2) TC30 (2) TC61 (2)	DIAGONAL- CCO (67) CCC (21) HCC (15) TCCO (9) TOCC (5) CC (2) OFF-DIAG- BB19 (4) SB14 (-2) BB25 (-3) BB22 (-4) BB23 (-13)
	280 (M)	280.	263.		1154 (15) 1156 (13) 1261 (11) 0823 (7) CC4C (6) 1316 (6) 1534 (6) 1265 (6) 0821 (6) CC1C (4) 1645 (4) 1043 (4) 0712 (3) CC3C (3) CC6C (3) TC5C (3) 1865 (2) TC20 (2) 0932 (2) 1643 (2) TC56 (2) 0934 (2)	DIAGONAL- CCO (68) HCC (22) CCC (17) TCCO (6) TOCC (5) CC (2) CO (2) OFF-DIAG- BB19 (5) BB28 (-1) SB15 (-1) BB22 (-3) SB14 (-3) SB16 (-3) BB25 (-3) BB23 (-15)
			207.		CC2C (12) 0821 (9) 0823 (8) 1156 (7) 1316 (7) 1261 (6) 1865 (5) 1534 (5) CC1C (4) 1861 (4) 1643 (4) 0934 (4) 1754 (4) 0716 (4) 1756 (3) 1045 (3) TC30 (3) CC3C (3) 1645 (3) 1312 (3) TC50 (3) 1043 (3) 1532 (2) 1154 (2) 1265 (2) TC60 (2) CC6C (2) 0712 (2)	DIAGONAL- CCO (50) HCC (42) CCC (23) TCCO (9) CO (6) OFF-DIAG- BB19 (10) BB24 (2) SB16 (2) BB30 (-1) EB22 (-2) BB28 (-5) BB25 (-8) SB14 (-13) BB23 (-15)
			183.		TC40 (60) TC10 (13) TC60 (8) TC50 (7) TC30 (4) TC20 (3) 1045 (3)	DIAGONAL- TOCO (95) CCO (5) HCC (1)
			178.		TC10 (52) TC40 (23) TC20 (9) TC3C (6) TC60 (3) 0712 (2)	DIAGONAL- TOCO (93) CCO (6) CC (1)
			175.		TC50 (63) TC60 (15) TC40 (7) TC1C (4) 1043 (2)	DIAGONAL- TOCO (91) CCO (5) CCC (2) HCC (2) TOCC (1)
			172.		TC20 (50) TC30 (18) TC10 (13) TC60 (7) 0821 (3) 0712 (2) TC50 (2)	DIAGONAL- TOCO (91) CCO (7) HCC (2) CCC (1) OFF-DIAG- EB23 (-2)
			171.		TC60 (58) TC50 (18) TC10 (9) TC30 (4) 1265 (2) 0716 (2)	DIAGONAL- TOCO (90) CCC (6) HCC (2) CCC (2)
			167.		TC30 (58) TC20 (30) 0823 (3) 0932 (2)	DIAGONAL- TOCO (90) CCC (7) HCC (2) CCC (1)
			126.		TC23 (8) CC3C (8) TC12 (8) CC1C (8) TC34 (7) TC61 (7) CC4C (6) TC56 (6) TC45 (6) CC6C (6) CC5C (5) CC2C (4) C932 (3) 1265 (3) 1045 (3) 0934 (3) 0712 (3) 0716 (2) 1159 (2) 1043 (2) 1261 (2) 1156 (2) TC60 (2) 1423 (2)	DIAGONAL- TOCC (42) CCC (38) CCO (24) CO (6) TOCO (4) HCC (3) CC (3) OFF-DIAG- SB16 (4) BB26 (-1) EB23 (-2) BB22 (-3) SB17 (-10) SB14 (-10)
			89.		TC56 (15) CC5C (13) TC23 (13) TC45 (12) TC12 (10) CC2C (9) CC3C (5) CC6C (4) 1156 (3) 1154 (3) CC1C (2) CC4C (2)	DIAGONAL- TOCC (50) CCC (36) CCO (11) HCC (3) CO (2) OFF-DIAG- SB17 (3) BB19 (1) BB25 (-1) BB22 (-1) SB14 (-4)

TABLE LV (Continued)

EXPERIMENTAL FREQUENCY (CM-1) RAMAN	INFRARED	ASSIGNED FREQUENCY (CM-1)	CALCULATED FREQUENCY (CM-1)	CALCULATED SYMMETRY SPECIES	SPECTRAL INTERPRETATION --- POTENTIAL ENERGY DISTRIBUTIONS
					INTERNAL COORDINATES / FORCE CONSTANTS
			86.		TC61(17) TC34(16) CC1C(11) DIAGONAL- TCCC(49) CCC (38) CCO (15) CC4C(10) CC3C(8) CC6C(8) CO (3) BCC (2) TC12(6) TC45(6) TC56(3) OFF-DIAG- SB17(2) BB26(-1) BB23(-1) TC23(2) 1043(2) 0716(2) BB22(-2) SB14(-5) 0712(2) 1261(2) 0934(2) 1045(2) 0932(2)

TABLE LVI. EPI-INOSITOL — X-RAY CRYSTAL STRUCTURE

EXPERIMENTAL FREQUENCY (CM-1) RAMAN	INFRARED	ASSIGNED FREQUENCY (CM-1)	CALCULATED FREQUENCY (CM-1)	CALCULATED SYMMETRY SPECIES	SPECTRAL INTERPRETATION --- POTENTIAL ENERGY DISTRIBUTIONS INTERNAL COORDINATES	FORCE CONSTANTS
	3450 (VS)		3357.		O10H(84) O9H1(9) O12H(6)	DIAGONAL- OH (100)
	3435 (SH)		3357.		O12H(92) O10H(6)	DIAGONAL- OH (100)
	3390 (VS)		3357.		O9H1(82) O10H(9) O8H0(8)	DIAGONAL- OH (100)
	3370 (VS)		3357.		O8H0(91) O9H1(8)	DIAGONAL- OH (100)
	3285 (VS)		3357.		O9H1(22)	DIAGONAL- OH (100)
	3235 (VS)		3357.		O7H9(99)	DIAGONAL- OH (100)
2964 (S)	2960 (SH)		2947.		C4H6(50) C3H5(24) C5H7(21) C2H4(2)	DIAGONAL- CH (98)
2951 (M)			2941.		C2H4(37) C6H8(36) C1H3(23) C4H6(2)	DIAGONAL- CH (99)
	2942 (W)		2939.		C5H7(45) C3H5(40) C6H8(8) C2H4(5)	DIAGONAL- CH (99)
2928 (VS)	2930 (VW)		2936.		C2H4(43) C6H8(43) C5H7(7) C3H5(6)	DIAGONAL- CH (99)
	2918 (M)		2936.		C1H3(76) C2H4(12) C6H8(12)	DIAGONAL- CH (99)
2913 (M)	2905 (M)		2933.		C4H6(47) C3H5(28) C5H7(24)	DIAGONAL- CH (100)
	1433 (SH)	1433.	1445.		C4OH(33) C3OH(19) 1534(9) 1643(8) 1532(4) 1754(4) C4C5(2) 1756(2) 1045(2)	DIAGONAL- COH (55) HCC (29) CC (3) CCO (3) HCO (2) CCC (1) OFF-DIAG- EB30(4) EB23(3) BB28(2) BB25(1) SB16(-1) SB17(-1) SB13(-2)
1428 (W,SH)		1428.	1432.		C5OH(36) HC5O(13) C6OH(10) 1645(10) 1756(8) 1643(6) C3OH(4) HC6O(2)	DIAGONAL- COH (51) HCC (27) HCO (16) CCC (1) CO (1) CCO (1) OFF-DIAG- BB29(2) BB25(1) BB23(1) BB28(1) SB13(-1) SB12(-1) BB18(-2)
	1418 (M)	1418.	1418.		C1OH(47) C2OH(14) HC1O(13) 1421(5) 1316(4) C6C1(3) 1423(3) C5OH(2) C4OH(2)	DIAGONAL- COH (66) HCC (14) HCO (14) CC (5) CCO (2) CCC (2) CO (1) OFF-DIAG- BB29(3) BB23(1) SB12(-1) SB16(-1) EB18(-2) SB13(-2)
1410 (SH)	1407 (SH)	1410.	1404.		1861(21) C2OH(20) 1865(12) C6OH(11) 1312(8) 1316(5) HC2C(3) 1421(3)	DIAGONAL- HCC (51) COH (35) HCO (6) CC (4) CCO (3) CO (2) CCC (2) OFF-DIAG- BB23(4) SB12(-1) BB18(-2) BB19(-2) SB15(-2)
1403 (M)		1403.	1401.		C6OH(35) C2OH(24) C5OH(8) C5C6(4) 1861(4) 1865(3) C1C2(3) 1316(3) HC2C(2) C3OH(2) 1421(2)	DIAGONAL- COH (71) HCC (15) CC (7) HCO (5) CCO (2) CO (2) CCC (2) OFF-DIAG- SB13(1) BB29(-1) SB16(-1) SB15(-2) SB17(-2)
1395 (M)	1386 (M)	1391.	1390.		C3OH(34) C4OH(21) C5OH(6) HC3C(5) HC5O(5) 1754(4) C2OH(4) 1423(4) C6OH(3) 1861(2) 1534(2) 1865(2) HC4O(2)	DIAGONAL- COH (69) HCC (19) HCO (13) CC (2) CCC (2) CO (1) OFF-DIAG- SB12(-1) SB15(-2) BB29(-2) BB18(-3)
	1379 (LT,W)	1379.	1385.		C6OH(21) 1861(14) C2OH(9) C5OH(8) 1865(8) C3OH(8) C1OH(7) HC1O(5) HC6O(4) 1312(3) C4OH(3) C6C1(3) C1C2(2) C1O7(2)	DIAGONAL- COH (57) HCC (29) HCO (11) CC (7) CO (2) CCC (2) OFF-DIAG- EB23(2) SB16(-1) SB12(-1) SB17(-1) BB18(-2) SB15(-3)
1366 (M)		1366.	1360.		1423(29) 1421(15) C1OH(14) 1534(12) C4OH(10) 1532(4) C3C4(3) HC1O(2) HC2O(2) C3O9(2) HC3O(2)	DIAGONAL- HCC (60) COH (25) HCO (7) CC (5) CCO (4) CO (3) OFF-DIAG- EB23(5) BB3O(-1) BB19(-2) BB18(-2) SB15(-4)
	1352 (M)	1352.	1348.		1645(29) 1643(18) C3OH(13) C5OH(8) 1754(7) HC5O(7) 1532(2) 1312(2) C3C4(2) 1316(2)	DIAGONAL- HCC (65) COH (24) HCO (8) CC (4) CCO (3) CO (3) OFF-DIAG- EB23(3) BB28(3) SB12(-1) SB14(-1) BB19(-1) BB18(-3) SB15(-6)
1344 (W)	1341 (M)	1342.	1345.		1312(18) C2OH(14) 1316(12) 1532(9) 1754(8) 1865(8) C6OH(7) 1756(6) HC2O(5) C2O8(5) 1421(3) C5CH(3) C6O2(3) 1534(3) C3OH(2) C4C5(2)	DIAGONAL- HCC (67) COH (27) CO (6) HCO (8) CC (3) CCO (2) OFF-DIAG- BB29(2) BB3O(2) BB26(1) BB24(-1) SB12(-2) SB14(-3) BB18(-3) SB15(-4) SB13(-5)
1322 (M)		1322.	1328.		1643(14) HC4O(13) C4OH(13) 1534(11) 1421(9) 1754(8) HC3O(8) C3OH(4) HC6O(4) 1423(3) 1756(3) C1OH(3) C4O2(2) C2OH(2) C4C5(2) 1865(2)	DIAGONAL- HCC (51) HCO (27) COH (22) CO (7) CC (5) CCO (1) OFF-DIAG- BB28(3) SB13(3) BB23(2) SB14(-1) BB29(-2) SB12(-4) SB15(-5) BB18(-10)
1306 (M)	1310 (M)	1308.	1314.		HC3O(20) 1756(19) 1532(18) HC5O(9) HC4O(9) C5CH(7) C6O2(4) 1645(3) C4OH(3) C3O9(3) HC1O(3) 1316(3) C5C1(2) C3OH(2) HC6O(2) C2O8(2) C1OH(2)	DIAGONAL- HCC (46) HCC (45) COH (17) CC (12) CCO (3) CCC (3) TOCC (1) CC (1) OFF-DIAG- EB25(3) EB24(-1) SB15(-2) SB14(-5) SB12(-7) BB18(-15)
1276 (M)	1280 (W)	1280.	1287.		HC2O(42) HC4O(15) 1423(11) 1421(9) HC6O(6) 1532(5) HC3O(4) 1645(4) C1O7(3) C3O9(3) C3OH(3) 1643(3) 1865(2) C6C1(2)	DIAGONAL- HCO (69) HCC (36) CC (8) COH (4) CC (3) CCC (2) CCC (1) OFF-DIAG- EB23(2) BB26(1) SB14(-2) SB12(-4) BB18(-22)
	1271 (W)	1271.	1279.		HC6O(16) 1865(12) 1532(11) 1756(10) HC3O(10) HC5O(10) 1312(8) HC4O(7) HC1O(7) C5OH(5) C5O1(4) HC2O(3) C1C2(3) 1643(2) 1423(2) C4C5(2)	DIAGONAL- HCO (54) HCC (47) CC (8) COH (7) CCC (3) CCO (3) OFF-DIAG- BB23(2) SB13(2) BB19(-3) SB17(-1) BB29(-1) SB14(-2) SB12(-4) SB15(-5) EB18(-17)
1258 (W)		1258.	1269.		HC6O(16) HC2O(16) 1316(15) 1312(13) HC3O(8) 1421(7) 1861(6) 1756(6) 1532(4) HC4O(4) 1645(3) HC5O(2)	DIAGONAL- HCC (57) HCO (46) COH (3) CC (1) TOCC (1) OFF-DIAG- SB15(1) BB23(1) BB18(-13)
1252 (W)	1251 (M)	1251.	1262.		HC4O(25) HC3O(24) 1534(21) HC6O(12) 1643(6) 1423(5) HC2C(4) HC5O(3) 1754(3) 1861(3) 1312(2) 1865(2) 1645(2)	DIAGONAL- HCO (69) HCC (46) COH (3) CC (2) CCO (1) CO (1) TOCC (1) OFF-DIAG- BB23(2) SB12(-2) SB15(-2) BB28(-3) EB18(-18)

TABLE LVI (Continued)

EXPERIMENTAL FREQUENCY (CM-1) RAMAN	EXPERIMENTAL FREQUENCY (CM-1) INFRARED	ASSIGNED FREQUENCY (CM-1)	CALCULATED FREQUENCY (CM-1)	CALCULATED SYMMETRY SPECIES	SPECTRAL INTERPRETATION --- POTENTIAL ENERGY DISTRIBUTIONS INTERNAL COORDINATES	FORCE CONSTANTS
1243 (W,SH)	1234 (W)	1239.	1243.		HC10 (48) C10H (15) HC60 (14) 1316 (12) HC30 (6) 1756 (6) 1312 (5) 1754 (4) 1865 (2) 1534 (2)	DIAGONAL- HCO (68) HCC (34) COH (17) CO (2) TOCC (2) CCO (1) OFF-DIAG- SB13 (1) BB19 (-1) SB12 (-3) BB29 (-3) EB18 (-18)
1204 (W)	1202 (M)	1203.	1230.		HC50 (34) 1754 (21) HC40 (15) C50H (12) 1645 (7) HC10 (6) 1865 (5) HC60 (4) C40H (3) 1312 (2) C5C6 (2)	DIAGONAL- HCO (60) HCC (38) COH (17) CC (3) CCO (1) OFF-DIAG- BB23 (2) SB15 (-1) BB29 (-2) BB28 (-3) BB18 (-16)
1147 (W)	1149 (M,SH)	1148.	1143.		C400 (21) C309 (15) C501 (14) C2C3 (12) CC4C (8) C208 (6) C5C6 (6) C107 (6) C602 (5) 0934 (5) C3C4 (4) CC5C (4) 1154 (4) CC3C (4) 1045 (3) 1043 (2) HC60 (2)	DIAGONAL- CO (67) CC (24) CCC (18) CCO (15) HCO (4) COH (2) HCC (2) OFF-DIAG- SB12 (3) BB22 (2) BB30 (1) SB16 (-1) SB13 (-4) SB17 (-5) CCCC (-6) SB14 (-19)
1130 (S)	1136 (S)	1133.	1129.		C1C2 (38) C6C1 (25) C2C3 (18) HC6C (7) C3C4 (6) C107 (4) C501 (4) 0821 (3) 0823 (3) 1316 (3) CC6C (3) C5C6 (3) 0716 (3) C10H (2) C602 (2) HC10 (2) 1156 (2) 1261 (2)	DIAGONAL- CC (90) CCO (15) CO (11) HCO (10) HCC (9) CCC (5) COH (3) OFF-DIAG- BB19 (-1) BB25 (-1) EB18 (-1) CCCC (-2) CCCO (-2) SB13 (-2) SB14 (-3) SB17 (-5) SB15 (-9) SB16 (-16)
1125 (SH)	1131 (S,SH)	1128.	1121.		C107 (17) C6C1 (15) HC20 (12) C3C4 (10) C5C6 (10) C400 (9) CC2C (7) C309 (6) C2C3 (6) 0712 (5) C208 (5) C4C5 (4) 0932 (4) C1C2 (3) HC50 (3) HC3C (3) 1261 (3) C20H (2) 1532 (2) CC1C (2) C501 (2) C50H (2) HC10 (2)	DIAGONAL- CC (88) CO (39) HCC (21) CCO (16) CCC (11) HCC (7) COH (5) OFF-DIAG- BB22 (1) BB25 (-1) BB19 (-1) BB23 (-2) BB18 (-3) SB13 (-3) CCCC (-4) SB15 (-6) SB16 (-7) SB17 (-8) SB14 (-11)
1085 (SH)	1086 (S)	1086.	1100.		C5C6 (30) C4C5 (24) C3C4 (18) C2C3 (12) C602 (11) HC60 (7) C60H (4) CC6C (4) 1156 (4) HC20 (4) 0716 (4) C208 (3) 1316 (3) C1C2 (2) 1312 (2) 0932 (2) C20H (2) C6C1 (2)	DIAGONAL- CC (88) CO (16) CCC (15) HCC (12) HCC (10) COH (7) CCC (6) OFF-DIAG- BB18 (-1) CCCC (-1) SB14 (-1) BB23 (-2) EB19 (-2) EB25 (-2) SB12 (-4) SB13 (-4) CCCO (-4) SB17 (-9) SB15 (-11) SB16 (-15)
1079 (S)	1076 (SH)	1079.	1085.		C208 (29) C602 (18) C501 (9) C1C2 (7) C6C1 (6) C3C4 (4) CC4C (4) C107 (4) 0823 (4) HC4C (4) 1265 (4) CC1C (3) HC10 (3) 1154 (3) HC30 (2) 1865 (2) 0934 (2) C3C9 (2) HC5C (2) C4C5 (2)	DIAGONAL- CO (62) CC (20) CCC (16) HCO (11) CCC (10) HCC (5) CCH (4) OFF-DIAG- EB19 (3) EB18 (2) SB15 (2) SB12 (1) SB13 (-1) SB16 (-1) CCCC (-4) SB17 (-10) SB14 (-21)
1066 (VW)	1062 (VS)	1062.	1073.		C400 (49) C2C3 (15) C309 (14) C208 (7) C5C6 (7) C107 (4) C3C4 (3) C501 (3) C40H (2) C30H (2) 0712 (2)	DIAGONAL- CO (77) CC (26) COH (6) CCO (6) HCC (5) CCC (3) HCC (2) OFF-DIAG- SB12 (1) SB17 (-1) SB16 (-2) SB14 (-7) CCCO (-7) SB13 (-7)
1050 (M)	1047 (VS)	1048.	1068.		C501 (32) C309 (27) C602 (16) C4C5 (12) C3C4 (5) C5C6 (5) C6C1 (4) C400 (4) CC3C (3) 1043 (3) CC5C (3) C208 (2) 1045 (2) 0934 (2) 1421 (2) 1861 (2) C1C2 (2)	DIAGONAL- CC (80) CC (28) HCC (9) CCO (9) CCC (6) COH (3) HCC (2) OFF-DIAG- SB12 (-2) SB15 (-2) BB23 (-2) SB13 (-4) SB17 (-6) CCCO (-9) SB14 (-12)
1023 (M)	1033 (S)	1028.	1018.		C107 (52) C501 (9) C5C6 (8) C309 (8) C4C5 (8) C3C4 (6) C2C3 (6) C400 (4) 1421 (3) 1861 (2)	DIAGONAL- CO (74) CC (28) HCC (9) CCO (8) COH (3) CCC (3) HCO (2) OFF-DIAG- CCCO (2) BB23 (-2) SB13 (-4) SB15 (-4) SB16 (-8) SB14 (-10)
988 (W)	984 (M)	986.	975.		C602 (21) C309 (17) C5C1 (16) C208 (16) C3C4 (10) C4C5 (9) C1C2 (3) 1261 (2) 1043 (2) C6C1 (2) 0821 (2)	DIAGONAL- CO (71) CC (26) CCO (11) HCC (7) CCC (3) CCH (1) HCC (1) OFF-DIAG- CCCO (5) SB12 (2) SB13 (-2) SB17 (-2) SB16 (-6) SB14 (-17)
919 (S)	919 (M)	919.	925.		C4C5 (11) C208 (9) C1C2 (7) 1532 (6) C3C4 (6) 1756 (6) C602 (6) C6C1 (6) C2C3 (5) C5C6 (4) HC40 (4) CC5C (4) CC4C (3) CC3C (3) 1154 (3) 0934 (3) 1045 (2) 1043 (2) HC50 (2) C40H (2)	DIAGONAL- CC (39) HCC (19) CO (12) CCO (11) CCC (11) HCO (9) CCH (5) OFF-DIAG- SB15 (6) BB19 (3) EB18 (3) CCCC (1) EB30 (-1) SB13 (-2) SB16 (-9) SB17 (-14)
910 (W)	902 (S)	902.	899.		C208 (17) C602 (14) C4C5 (10) C2C3 (10) C5C6 (9) C3C4 (8) 1043 (6) 1045 (6) 0712 (2) 0716 (2) C6C1 (2)	DIAGONAL- CC (41) CO (33) CCO (23) HCC (6) HCO (2) CCC (2) CCH (1) OFF-DIAG- CCCO (6) SB15 (3) EB19 (2) SB12 (2) SB17 (-6) SB14 (-7) SB16 (-12)
874 (M)	872 (M)	873.	845.		C1C2 (12) 1261 (11) 0821 (10) C6C1 (10) CC1C (5) 0932 (4) 1861 (4) 1156 (4) 1421 (3) C400 (3) 1312 (3) 1316 (3) C602 (3) C208 (3) C5C1 (2) C309 (2) CC2C (2) C20H (2)	DIAGONAL- CCO (32) CC (24) HCC (18) CO (13) CCC (9) COH (3) HCO (2) OFF-DIAG- BB19 (6) SB17 (3) BB26 (2) SB15 (1) BB30 (-2) BB24 (-2) SB14 (-4) SB16 (-10)
791 (M)	793 (S)	792.	786.		C6C1 (12) C1C2 (10) CC1C (10) C602 (9) C208 (8) 1312 (5) 1316 (5) 0821 (4) C4C5 (3) C3C4 (3) 1261 (3) C400 (3) 1423 (2) 1865 (2) 1156 (2) 0932 (2)	DIAGONAL- CC (30) CO (21) CCC (16) HCC (14) CCC (11) COH (2) OFF-DIAG- SB14 (8) CCCO (5) SB15 (4) BB19 (4) BB18 (3) BB24 (-1) BB23 (-2) SB13 (-2) SB17 (-12)
718 (M)	716 (S)	717.	706.		0823 (16) 0712 (10) C3C4 (8) 0932 (7) C400 (6) 1423 (6) 1532 (5) CC3C (5) 0821 (4) 1261 (2) 1312 (2) 1043 (2) C4C5 (2) 1154 (2) 1316 (2) CC2C (2)	DIAGONAL- CCO (45) HCC (18) CC (11) CC (9) CCC (8) COH (1) OFF-DIAG- SB14 (6) BB19 (5) SB17 (1) CCCO (1) EB24 (-2) EB23 (-3)
695 (VVW)	689 (W)	689.	699.		1265 (18) 0716 (9) 1156 (8) 1756 (7) 1865 (6) CC5C (6) C4C5 (5) 0823 (3) C400 (3) 1754 (2) 1261 (2) 1045 (2) 1643 (2)	DIAGONAL- CCO (46) HCC (23) CCC (9) CC (6) CO (5) COH (2) OFF-DIAG- EB19 (7) SB14 (5) SB17 (1) BB18 (1) BB26 (1) SB16 (1) BB30 (-1) BB25 (-1) BB24 (-1) BB23 (-3)
556 (M)	552 (M)	554.	569.		1154 (14) 0934 (14) 0712 (13) 0716 (13) 1261 (6) 1421 (6) 1861 (6) 0821 (5) 1043 (5) 1156 (5) 1643 (5) 1645 (4) 0932 (4) 1045 (4) C6C1 (3) 1534 (3) CC3C (2) 1754 (2) CC5C (2) C1C2 (2)	DIAGONAL- CCO (84) HCC (27) CC (9) CCC (5) TOCC (1) OFF-DIAG- EB19 (6) BB25 (-2) BB26 (-2) SB16 (-2) SB17 (-3) SB15 (-3) BB23 (-21)

TABLE LVI (Continued)

EXPERIMENTAL FREQUENCY (CM-1) RAMAN	INFRARED	ASSIGNED FREQUENCY (CM-1)	CALCULATED FREQUENCY (CM-1)	CALCULATED SYMMETRY SPECIES	SPECTRAL INTERPRETATION --- POTENTIAL ENERGY DISTRIBUTIONS INTERNAL COORDINATES	FORCE CONSTANTS
501 (M,SH)	501 (S)	501.	524.		0934 (13) 1154 (12) CC2C (5) 1261 (5) 1421 (4) 1861 (4) CC6C (4) C1C2 (4) 0821 (4) C6C1 (4) 1534 (3) C4C5 (3) 0932 (3) 1643 (3) 1754 (2) CC3C (2) 1043 (2) 1645 (2) C3C4 (2) 1156 (2) CC5C (2) 0712 (2) 1045 (2)	DIAGONAL- CCO (45) HCC (21) CCC (13) CC (13) CO (2) COH (1) HCC (1) OFF-DIAG- EE19 (6) SB17 (6) SB14 (5) BB18 (2) BB25 (2) BB28 (-1) BB30 (-2) SB16 (-2) SB15 (-2) BB23 (-9)
518 (VS)		518.	492.		C3C4 (8) C5C1 (7) C4C5 (6) C1C2 (6) C6C1 (6) C3C9 (6) C107 (5) CC4C (5) C2C3 (4) C5C6 (3) CC6C (3) 1265 (3) 1156 (2) 0932 (2) 1154 (2) CC2C (2) 0823 (2)	DIAGONAL- CC (33) CO (17) CCC (17) CCC (13) HCC (2) OFF-DIAG- SB14 (9) SB17 (6) CCCC (5) BB22 (1) BB30 (-1) SB12 (-1) EB23 (-2)
431 (M)		431.	430.		1043 (16) 0823 (13) 1045 (12) 1265 (12) 1645 (8) 1643 (7) C2C3 (7) C5C6 (5) 1534 (4) 1754 (4) 0932 (2)	DIAGONAL- CCO (58) HCC (25) CC (14) TOCC (2) COH (1) OFF-DIAG- SB16 (8) BB19 (5) EB30 (-2) SB15 (-3) EB28 (-3) BB23 (-10)
385 (M)	386 (M)	385.	392.		CC4C (14) CC1C (9) 0712 (7) CC5C (7) 0716 (6) CC3C (5) C823 (4) CC2C (4) 1265 (3) C2C3 (3) C5C6 (3) 0934 (3) CC6C (3) 1154 (3) C400 (2) C1C7 (2)	DIAGONAL- CCC (40) CCC (30) CC (10) HCC (6) CO (5) OFF-DIAG- SB17 (8) SB14 (8) BB22 (2) BB23 (-1) SB16 (-2) SB15 (-2) BB26 (-2)
367 (M)	350 (M)	358.	344.		1261 (22) 0821 (20) 1156 (13) 0932 (12) CC6C (4) CC2C (4) CC3C (3) CC5C (3) 1154 (3) 1865 (2) 1423 (2) C5C6 (2) C2C3 (2)	DIAGONAL- CCO (74) CCC (14) CC (7) HCC (6) TOCO (2) CO (1) OFF-DIAG- SB14 (2) BB22 (1) SB17 (1) SB15 (1) BB26 (-1) BB20 (-1) BB19 (-1) BB23 (-6)
321 (W)	313 (W)	317.	304.		0712 (28) 0716 (27) 0821 (9) C5C6 (7) C2C3 (6) 1261 (5) 0823 (4) TC10 (4) 1265 (3) 1043 (3) 1045 (3) CC2C (2) 1421 (2) 1861 (2)	DIAGONAL- CCO (83) CC (14) HCC (6) TOCO (6) CCC (4) OFF-DIAG- SB16 (3) BB20 (-1) BB22 (-1) BB19 (-1) SB17 (-4) BB23 (-8)
306 (W)	295 (SH)	306.	301.		1154 (22) 1156 (21) 0932 (15) 0934 (9) 1045 (4) CC4C (4) C3C4 (4) 0823 (3) 0821 (3) TC50 (3) C4C5 (3) C1C2 (2) 1865 (2) C6C1 (2) TC30 (2) 1261 (2) 1423 (2)	DIAGONAL- CCO (82) CC (12) TCCC (6) CCC (6) HCC (6) OFF-DIAG- SB16 (3) BB20 (-1) BB22 (-2) SB17 (-3) BB23 (-9)
285 (M)	285 (M)	285.	299.		1045 (26) 1043 (26) 0934 (17) 1265 (10) 0932 (7) 1154 (4) TC40 (3) 0823 (3) C5C6 (2) C2C3 (2) 1643 (2) TC30 (2)	DIAGONAL- CCO (96) HCC (8) TOCC (6) CC (6) CCC (1) OFF-DIAG- SB17 (-1) BB20 (-1) SB16 (-2) SB15 (-3) EE19 (-3) BB23 (-9)
252 (M)	243 (SH)	252.	264.		1261 (10) 0821 (8) CC4C (7) 0823 (6) 1534 (6) 1754 (4) 1643 (4) 0716 (4) 1645 (4) 1316 (3) 1265 (3) CC3C (3) 1312 (3) 0934 (3) CC1C (3) 1154 (3) TC20 (2) TC60 (2) 1045 (2) CC5C (2) C400 (2) CC6C (2) TC23 (2)	DIAGONAL- CCO (44) HCC (27) CCC (16) TCCC (6) TOCO (6) CO (3) HCO (2) CC (1) OFF-DIAG- BB19 (8) BB24 (3) SB16 (3) BB18 (2) EE22 (-1) BB28 (-2) BB25 (-5) SB14 (-5) BB23 (-7)
234 (VW,SH)	236 (M)	236.	254.		1265 (16) 0823 (14) CC2C (11) CC6C (9) 0932 (6) CC5C (6) CC3C (6) 1156 (6) 1045 (5) 1754 (4) 1043 (4) 1534 (3) TC34 (2) TC45 (2) 1756 (2)	DIAGONAL- CCO (52) CCC (31) HCC (13) TCCC (6) TOCO (4) CO (2) CC (1) OFF-DIAG- BB19 (3) BB24 (2) SB16 (2) BB18 (1) SB15 (-1) SB17 (-2) BB22 (-2) BB25 (-3) BB23 (-4) SB14 (-4)
			203.		1265 (7) CC6C (7) 0821 (7) CC2C (7) 1261 (6) 0823 (6) CC1C (5) 1754 (5) 1534 (4) 1643 (4) 1316 (4) 1045 (4) 1312 (4) 1645 (3) 0934 (3) 1156 (3) 1043 (2) TC60 (2) 1154 (2) 0716 (2) TC10 (2) 1756 (2) 1532 (2) CC5C (2) CC3C (2) 0932 (2) TC40 (2)	DIAGONAL- CCO (45) HCC (31) CCC (24) TOCO (7) CO (5) CC (2) OFF-DIAG- BB19 (8) SB16 (5) BB24 (3) BB18 (1) EE30 (-1) BB26 (-1) BB22 (-2) BB28 (-2) SB15 (-3) BB23 (-4) BB25 (-7) SB14 (-12)
			179.		TC4C (36) TC50 (24) TC30 (23) TC10 (6) TC20 (5) TC60 (2)	DIAGONAL- TOCO (95) CCC (2) CCC (1) HCC (1)
			173.		TC1C (52) TC20 (24) TC40 (15) TC50 (3)	DIAGONAL- TOCO (94) CCC (3)
			172.		TC6C (79) TC30 (6) TC50 (4) 1261 (3) TC40 (2)	DIAGONAL- TOCO (92) CCC (5) HCC (1)
			171.		TC5C (52) TC30 (24) TC60 (10) TC10 (4) TC40 (3) 1154 (2)	DIAGONAL- TOCO (93) CCC (6)
			169.		TC3C (37) TC40 (36) TC50 (10) TC10 (8) 1043 (3) 0932 (2)	DIAGONAL- TOCO (91) CCC (9) HCC (2) OFF-DIAG- EE23 (-1)
			168.		TC2C (64) TC10 (23) TC30 (4) 0821 (3) 0712 (2)	DIAGONAL- TOCO (92) CCC (7) HCC (2)
			124.		CC4C (9) TC34 (8) TC23 (8) CC3C (8) TC45 (8) TC56 (7) CC5C (7) TC61 (7) CC1C (7) TC12 (7) CC2C (4) CC6C (3) 1043 (3) 0934 (3) 1045 (3) 0932 (3) 0712 (2) 0716 (2) 1156 (2) 1154 (2) C400 (2)	DIAGONAL- TOCC (45) CCC (38) CCC (23) CC (6) HCC (5) CC (2) TOCO (2) HCO (1) OFF-DIAG- SB16 (3) BB19 (1) BB26 (-2) EB22 (-3) EB23 (-3) SE17 (-8) SB14 (-9)
			88.		TC56 (18) TC23 (15) CC3C (12) CC5C (10) CC6C (7) TC61 (7) CC2C (6) TC34 (5) TC45 (3) 0932 (3) TC12 (3) 1156 (2) 0934 (2)	DIAGONAL- TOCC (51) CCC (36) CCC (9) HCC (4) HCO (2) CO (1) OFF-DIAG- SE17 (3) BB19 (2) BB25 (-1) BB23 (-2) BB26 (-2) SB14 (-3)
			85.		TC12 (17) CC1C (14) TC61 (13) TC45 (12) CC4C (11) TC34 (9) CC5C (4) CC2C (3) 0712 (3) 0716 (3) 1045 (2) 1043 (2) CC3C (2) CC6C (2)	DIAGONAL- TOCC (52) CCC (35) CCC (13) HCC (3) CO (2) OFF-DIAG- SB17 (3) BB22 (-1) BB26 (-2) BB23 (-2) SE14 (-4)

APPENDIX VI

SYMMETRY COORDINATES FOR THE INOSITOLS

In this appendix, the definitions of the symmetry coordinates for the inositols are presented. The numbers in parentheses correspond to the internal coordinates defined in the tables in Appendix II and in Table XV for scyllo-inositol. The symmetry coordinates as defined represent the unnormalized U matrix. The U matrix is normalized by the computer programs GMAT and ZSYM.

Contents

TABLE LVII

DEFINITION OF SYMMETRY COORDINATES FOR SCYLLO-INOSITOL

A_{1g} Representation

S1 = 2(1) + 2(2) + 2(3) + 2(4) + 2(5) + 2(6)
S2 = 2(7) + 2(8) + 2(9) + 2(10) + 2(11) + 2(12)
S3 = 2(13) + 2(14) + 2(15) + 2(16) + 2(17) + 2(18)
S4 = 2(19) + 2(20) + 2(21) + 2(22) + 2(23) + 2(24)
S5 = 2(25) + 2(26) + 2(27) + 2(28) + 2(29) + 2(30)
S6 = (31) + (32) + (33) + (34) + (35) + (36) + (37) + (38) + (39) + (40) + (41) + (42)
S7 = (43) + (44) + (45) + (46) + (47) + (48) + (49) + (50) + (51) + (52) + (53) + (54)
S8 = 2(55) + 2(56) + 2(57) + 2(58) + 2(59) + 2(60)
S9 = 2(61) + 2(62) + 2(63) + 2(64) + 2(65) + 2(66)
S10 = 2(67) - 2(68) + 2(69) - 2(70) + 2(71) - 2(72)

A_{2g} Representation

S11 = (31) - (32) + (33) - (34) + (35) - (36) + (37) - (38) + (39) - (40) + (41) - (42)
S12 = (43) - (44) + (45) - (46) + (47) - (48) + (49) - (50) + (51) - (52) + (53) - (54)
S13 = 2(73) - 2(74) + 2(75) - 2(76) + 2(77) - 2(78)

E_g Representation

S14 = (1) - 2(2) + (3) + (4) - 2(5) + (6)
S15 = 2(7) - (8) - (9) + 2(10) - (11) - (12)
S16 = 2(13) - (14) - (15) + 2(16) - (17) - (18)
S17 = 2(19) - (20) - (21) + 2(22) - (23) - (24)
S18 = - (25) - (26) + 2(27) - (28) - (29) + (30)
S19 = 3(33) - 3(34) - 3(35) + 3(36) + 3(39) - 3(40) - 3(41) + 3(42)
S20 = -2(31) - 2(32) + (33) + (34) + (35) + (36) - 2(37) - 2(38) + (39) + (40) + (41) + (42)
S21 = 3(45) - 3(46) - 3(47) + 3(48) + 3(51) - 3(52) - 3(53) + 3(54)
S22 = -2(43) - 2(44) + (45) + (46) + (47) + (48) - 2(49) - 2(50) + (51) + (52) + (53) + (54)
S23 = 2(55) - (56) - (57) + 2(58) - (59) - (60)
S24 = 2(61) - (62) - (63) + 2(64) - (65) - (66)
S25 = - (67) - 2(68) - (69) + (70) + 2(71) + (72)
S26 = -3(74) - 3(75) + 3(77) + 3(78)

TABLE LVII (Continued)

DEFINITION OF SYMMETRY COORDINATES FOR SCYLLO-INOSITOL

A_{1u} Representation

S27 = 2(1) - 2(2) + 2(3) - 2(4) + 2(5) - 2(6)
S28 = (31) - (32) - (33) + (34) + (35) - (36) - (37) + (38) + (39) - (40) - (41) + (42)
S29 = (43) - (44) - (45) + (46) + (47) - (48) - (49) + (50) + (51) - (52) - (53) + (54)
S30 = 2(67) + 2(68) + 2(69) + 2(70) + 2(71) + 2(72)
S31 = 2(73) + 2(74) + 2(75) + 2(76) + 2(77) + 2(78)

A_{2u} Representation

S32 = 2(7) - 2(8) + 2(9) - 2(10) + 2(11) - 2(12)
S33 = 2(13) - 2(14) + 2(15) - 2(16) + 2(17) - 2(18)
S34 = 2(19) - 2(20) + 2(21) - 2(22) + 2(23) - 2(24)
S35 = 2(25) - 2(26) + 2(27) - 2(28) + 2(29) - 2(30)
S36 = (31) + (32) - (33) - (34) + (35) + (36) - (37) - (38) + (39) + (40) - (41) - (42)
S37 = (43) + (44) - (45) - (46) + (47) + (48) - (49) - (50) + (51) + (52) - (53) - (54)
S38 = 2(55) - 2(56) + 2(57) - 2(58) + 2(59) - 2(60)
S39 = 2(61) - 2(62) + 2(63) - 2(64) + 2(65) - 2(66)

E_u Representation

S40 = 3(1) - 3(3) - 3(4) + 3(6)
S41 = 2(7) + (8) - (9) - 2(10) - (11) + (12)
S42 = 2(13) + (14) - (15) - 2(16) - (17) + (18)
S43 = 2(19) + (20) - (21) - 2(22) - (23) + (24)
S44 = (25) - (26) - 2(27) - (28) + (29) + 2(30)
S45 = 3(33) - 3(34) + 3(35) - 3(36) - 3(39) + 3(40) - 3(41) + 3(42)
S46 = -2(31) - 2(32) - (33) - (34) + (35) + (36) + 2(37) + 2(38) + (39) + (40) - (41) - (42)
S47 = 3(45) - 3(46) + 3(47) - 3(48) - 3(51) + 3(52) - 3(53) + 3(54)
S48 = -2(43) - 2(44) - (45) - (46) + (47) + (48) + 2(49) + 2(50) + (51) + (52) - (53) - (54)
S49 = 2(55) + (56) - (57) - 2(58) - (59) + (60)
S50 = 2(61) + (62) - (63) - 2(64) - (65) + (66)
S51 = -3(67) + 3(69) - 3(70) + 3(72)
S52 = -3(74) + 3(75) - 3(77) + 3(78)

TABLE LVIII

DEFINITION OF SYMMETRY COORDINATES FOR NEO-INOSITOL

A_g Representation

$$
\begin{aligned}
S1 &= (1) + (2) + (4) + (5) \\
S2 &= 2(3) + 2(6) \\
S3 &= (7) + (9) + (10) + (12) \\
S4 &= 2(8) + 2(11) \\
S5 &= (13) + (15) + (16) + (18) \\
S6 &= 2(14) + 2(17) \\
S7 &= (19) + (21) + (22) + (24) \\
S8 &= 2(20) + 2(23) \\
S9 &= 2(25) + 2(28) \\
S10 &= (26) + (27) + (29) + (30) \\
S11 &= (31) + (36) + (37) + (42) \\
S12 &= (32) + (35) + (38) + (41) \\
S13 &= (33) + (34) + (39) + (40) \\
S14 &= (43) + (48) + (49) + (54) \\
S15 &= (44) + (47) + (50) + (53) \\
S16 &= (45) + (46) + (51) + (52) \\
S17 &= (55) + (57) + (58) + (60) \\
S18 &= 2(56) + 2(59) \\
S19 &= (61) + (63) + (64) + (66) \\
S20 &= 2(62) + 2(65) \\
S21 &= (67) - (68) - (70) + (71) \\
S22 &= 2(69) - 2(72) \\
S23 &= (73) - (75) - (76) + (78)
\end{aligned}
$$

B_g Representation

$$
\begin{aligned}
S24 &= (1) - (2) + (4) - (5) \\
S25 &= (7) - (9) + (10) - (12) \\
S26 &= (13) - (15) + (16) - (18) \\
S27 &= (19) - (21) + (22) - (24) \\
S28 &= (26) - (27) + (29) - (30) \\
S29 &= (31) - (36) + (37) - (42) \\
S30 &= (32) - (35) + (38) - (41) \\
S31 &= (33) - (34) + (39) - (40) \\
S32 &= (43) - (48) + (49) - (54) \\
S33 &= (44) - (47) + (50) - (53) \\
S34 &= (45) - (46) + (51) - (52) \\
S35 &= (55) - (57) + (58) - (60) \\
S36 &= (61) - (63) + (64) - (66) \\
S37 &= (67) + (68) - (70) - (71) \\
S38 &= (73) + (75) - (76) - (78) \\
S39 &= 2(74) - 2(77)
\end{aligned}
$$

TABLE LVIII (Continued)

DEFINITION OF SYMMETRY COORDINATES FOR NEO-INOSITOL

A_u Representation

$$
\begin{aligned}
S40 &= (1) - (2) - (4) + (5) \\
S41 &= 2(3) - 2(6) \\
S42 &= (7) - (9) - (10) + (12) \\
S43 &= (13) - (15) - (16) + (18) \\
S44 &= (19) - (21) - (22) + (24) \\
S45 &= (26) + (27) - (29) - (30) \\
S46 &= (31) - (36) - (37) + (42) \\
S47 &= (32) - (35) - (38) + (41) \\
S48 &= (33) - (34) - (39) + (40) \\
S49 &= (43) + (48) - (49) + (54) \\
S50 &= (44) - (47) - (50) + (53) \\
S51 &= (45) - (46) - (51) + (52) \\
S52 &= (55) - (57) - (58) + (60) \\
S53 &= (61) - (63) - (64) + (66) \\
S54 &= (67) + (68) + (70) + (71) \\
S55 &= 2(69) + 2(72) \\
S56 &= (73) + (75) + (76) + (78) \\
S57 &= 2(74) + 2(77)
\end{aligned}
$$

B_u Representation

$$
\begin{aligned}
S58 &= (1) + (2) - (4) - (5) \\
S59 &= (7) + (9) - (10) - (12) \\
S60 &= 2(8) - 2(11) \\
S61 &= (13) + (15) - (16) - (18) \\
S62 &= 2(14) - 2(17) \\
S63 &= (19) + (21) - (22) - (24) \\
S64 &= 2(20) - 2(23) \\
S65 &= 2(25) - 2(28) \\
S66 &= (26) - (27) - (29) + (30) \\
S67 &= (31) + (36) - (37) - (42) \\
S68 &= (32) + (35) - (38) - (41) \\
S69 &= (33) + (34) - (39) - (40) \\
S70 &= (43) + (48) - (49) - (54) \\
S71 &= (44) + (47) - (50) - (53) \\
S72 &= (45) + (46) - (51) - (52) \\
S73 &= (55) + (57) - (58) - (60) \\
S74 &= 2(56) - 2(59) \\
S75 &= (61) + (63) - (64) - (66) \\
S76 &= 2(62) - 2(65) \\
S77 &= (67) - (68) + (70) - (71) \\
S78 &= (73) - (75) + (76) - (78)
\end{aligned}
$$

TABLE LIX

DEFINITION OF SYMMETRY COORDINATES FOR MYO-INOSITOL

A' Representation

$S1 = (1) + (2)$
$S2 = (3) + (6)$
$S3 = (4) + (5)$
$S4 = (7) + (9)$
$S5 = 2(8)$
$S6 = (10) + (12)$
$S7 = 2(11)$
$S8 = (13) + (15)$
$S9 = 2(14)$
$S10 = (16) + (18)$
$S11 = 2(17)$
$S12 = (19) + (21)$
$S13 = 2(20)$
$S14 = (22) + (24)$
$S15 = 2(23)$
$S16 = 2(25)$
$S17 = (26) + (30)$
$S18 = (27) + (29)$
$S19 = 2(28)$
$S20 = (31) + (36)$
$S21 = (32) + (35)$
$S22 = (33) + (34)$
$S23 = (37) + (42)$
$S24 = (38) + (41)$
$S25 = (39) + (40)$
$S26 = (43) + (48)$
$S27 = (44) + (47)$
$S28 = (45) + (46)$
$S29 = (49) + (54)$
$S30 = (50) + (53)$
$S31 = (51) + (52)$
$S32 = (55) + (57)$
$S33 = 2(56)$
$S34 = (58) + (60)$
$S35 = 2(59)$
$S36 = (61) + (63)$
$S37 = 2(62)$
$S38 = (64) + (66)$
$S39 = 2(65)$
$S40 = (67) - (68)$
$S41 = (69) - (72)$
$S42 = (70) - (71)$
$S43 = (73) - (75)$
$S44 = (76) - (78)$

A'' Representation

$S45 = (1) - (2)$
$S46 = (3) - (6)$
$S47 = (4) - (5)$
$S48 = (7) - (9)$
$S49 = (10) - (12)$
$S50 = (13) - (15)$
$S51 = (16) - (18)$
$S52 = (19) - (21)$
$S53 = (22) - (24)$
$S54 = (26) - (30)$
$S55 = (27) - (29)$
$S56 = (31) - (36)$
$S57 = (32) - (35)$
$S58 = (33) - (34)$
$S59 = (37) - (42)$
$S60 = (38) - (41)$
$S61 = (39) - (40)$
$S62 = (43) - (48)$
$S63 = (44) - (47)$
$S64 = (45) - (46)$
$S65 = (49) - (54)$
$S66 = (50) - (53)$
$S67 = (51) - (52)$
$S68 = (55) - (57)$
$S69 = (58) - (60)$
$S70 = (61) - (63)$
$S71 = (64) - (66)$
$S72 = (67) + (68)$
$S73 = (69) + (72)$
$S74 = (70) + (71)$
$S75 = (73) + (75)$
$S76 = 2(74)$
$S77 = (76) + (78)$
$S78 = 2(77)$

TABLE LX

DEFINITION OF SYMMETRY COORDINATES FOR EPI-INOSITOL AND MUCO-INOSITOL

A' Representation

$$
\begin{aligned}
S1 &= (1) + (6) \\
S2 &= (2) + (5) \\
S3 &= (3) + (4) \\
S4 &= 2(7) \\
S5 &= (8) + (12) \\
S6 &= (9) + (11) \\
S7 &= 2(10) \\
S8 &= 2(13) \\
S9 &= (14) + (18) \\
S10 &= (15) + (17) \\
S11 &= 2(16) \\
S12 &= 2(19) \\
S13 &= (20) + (24) \\
S14 &= (21) + (23) \\
S15 &= 2(22) \\
S16 &= (25) + (29) \\
S17 &= (26) + (28) \\
S18 &= 2(27) \\
S19 &= 2(30) \\
S20 &= (31) + (32) \\
S21 &= (33) + (42) \\
S22 &= (34) + (41) \\
S23 &= (35) + (40) \\
S24 &= (36) + (39) \\
S25 &= (37) + (38) \\
S26 &= (43) + (44) \\
S27 &= (45) + (54) \\
S28 &= (46) + (53) \\
S29 &= (47) + (52) \\
S30 &= (48) + (51) \\
S31 &= (49) + (50) \\
S32 &= 2(55) \\
S33 &= (56) + (60) \\
S34 &= (57) + (59) \\
S35 &= 2(58) \\
S36 &= 2(61) \\
S37 &= (62) + (66) \\
S38 &= (63) + (65) \\
S39 &= 2(64) \\
S40 &= (67) - (72) \\
S41 &= (68) - (71) \\
S42 &= (69) - (70) \\
S43 &= (74) - (78) \\
S44 &= (75) - (77)
\end{aligned}
$$

A'' Representation

$$
\begin{aligned}
S45 &= (1) - (6) \\
S46 &= (2) - (5) \\
S47 &= (3) - (4) \\
S48 &= (8) - (12) \\
S49 &= (9) - (11) \\
S50 &= (14) - (18) \\
S51 &= (15) - (17) \\
S52 &= (20) - (24) \\
S53 &= (21) - (23) \\
S54 &= (25) - (29) \\
S55 &= (26) - (28) \\
S56 &= (31) - (32) \\
S57 &= (33) - (42) \\
S58 &= (34) - (41) \\
S59 &= (35) - (40) \\
S60 &= (36) - (39) \\
S61 &= (37) - (38) \\
S62 &= (43) - (44) \\
S63 &= (45) - (54) \\
S64 &= (46) - (53) \\
S65 &= (47) - (52) \\
S66 &= (48) - (51) \\
S67 &= (49) - (50) \\
S68 &= (56) - (60) \\
S69 &= (57) - (59) \\
S70 &= (62) - (66) \\
S71 &= (63) - (65) \\
S72 &= (67) + (72) \\
S73 &= (68) + (71) \\
S74 &= (69) + (70) \\
S75 &= 2(73) \\
S76 &= (74) + (78) \\
S77 &= (75) + (77) \\
S78 &= 2(76)
\end{aligned}
$$

TABLE LXI

DEFINITION OF SYMMETRY COORDINATES FOR CIS-INOSITOL

A_1 Representation

S1 = (1) + (2) + (3) + (4) + (5) + (6)
S2 = 2(7) + 2(9) + 2(11)
S3 = 2(8) + 2(10) + 2(12)
S4 = 2(13) + 2(15) + 2(17)
S5 = 2(14) + 2(16) + 2(18)
S6 = 2(19) + 2(21) + 2(23)
S7 = 2(20) + 2(22) + 2(24)
S8 = 2(25) + 2(27) + 2(29)
S9 = 2(26) + 2(28) + 2(30)
S10 = (31) + (32) + (35) + (36) + (39) + (40)
S11 = (33) + (34) + (37) + (38) + (41) + (42)
S12 = (43) + (44) + (47) + (48) + (51) + (52)
S13 = (45) + (46) + (49) + (50) + (53) + (54)
S14 = 2(55) + 2(57) + 2(59)
S15 = 2(56) + 2(58) + 2(60)
S16 = 2(61) + 2(63) + 2(65)
S17 = 2(62) + 2(64) + 2(66)
S18 = (67) - (68) + (69) - (70) + (71) - (72)

A_2 Representation

S19 = (1) - (2) + (3) - (4) + (5) - (6)
S20 = (31) - (32) + (35) - (36) + (39) - (40)
S21 = (33) - (34) + (37) - (38) + (41) - (42)
S22 = (43) - (44) + (47) - (48) + (51) - (52)
S23 = (45) - (46) + (49) - (50) + (53) - (54)
S24 = (67) + (68) + (69) - (70) + (71) + (72)
S25 = 2(73) + 2(75) + 2(77)
S26 = 2(74) + 2(76) + 2(78)

Symmetry Coordinates for the E representation were not constructed.

TABLE LXII

DEFINITION OF SYMMETRY COORDINATES FOR L-CHIRO-INOSITOL

A Representation

$$
\begin{aligned}
S1 &= (1) + (5) \\
S2 &= (2) + (4) \\
S3 &= 2(3) \\
S4 &= 2(6) \\
S5 &= (7) + (12) \\
S6 &= (8) + (11) \\
S7 &= (9) + (10) \\
S8 &= (13) + (18) \\
S9 &= (14) + (17) \\
S10 &= (15) + (16) \\
S11 &= (19) + (24) \\
S12 &= (20) + (23) \\
S13 &= (21) + (22) \\
S14 &= (25) + (28) \\
S15 &= (26) + (27) \\
S16 &= (29) + (30) \\
S17 &= (31) + (42) \\
S18 &= (32) + (41) \\
S19 &= (33) + (40) \\
S20 &= (34) + (39) \\
S21 &= (35) + (38) \\
S22 &= (36) + (37) \\
S23 &= (43) + (54) \\
S24 &= (44) + (53) \\
S25 &= (45) + (52) \\
S26 &= (46) + (51) \\
S27 &= (47) + (50) \\
S28 &= (48) + (49) \\
S29 &= (55) + (60) \\
S30 &= (56) + (59) \\
S31 &= (57) + (58) \\
S32 &= (61) + (66) \\
S33 &= (62) + (65) \\
S34 &= (63) + (64) \\
S35 &= (67) + (71) \\
S36 &= (68) + (70) \\
S37 &= 2(69) \\
S38 &= 2(72) \\
S39 &= (73) + (78) \\
S40 &= (74) + (77) \\
S41 &= (75) + (76)
\end{aligned}
$$

B Representation

$$
\begin{aligned}
S42 &= (1) - (5) \\
S43 &= (2) - (4) \\
S44 &= (7) - (12) \\
S45 &= (8) - (11) \\
S46 &= (9) - (10) \\
S47 &= (13) - (18) \\
S48 &= (14) - (17) \\
S49 &= (15) - (16) \\
S50 &= (19) - (24) \\
S51 &= (20) - (23) \\
S52 &= (21) - (22) \\
S53 &= (25) - (28) \\
S54 &= (26) - (27) \\
S55 &= (29) - (30) \\
S56 &= (31) - (42) \\
S57 &= (32) - (41) \\
S58 &= (33) - (40) \\
S59 &= (34) - (39) \\
S60 &= (35) - (38) \\
S61 &= (36) - (37) \\
S62 &= (43) - (54) \\
S63 &= (44) - (53) \\
S64 &= (45) - (52) \\
S65 &= (46) - (51) \\
S66 &= (47) - (50) \\
S67 &= (48) - (49) \\
S68 &= (55) - (60) \\
S69 &= (56) - (59) \\
S70 &= (57) - (58) \\
S71 &= (61) - (66) \\
S72 &= (62) - (65) \\
S73 &= (63) - (64) \\
S74 &= (67) - (71) \\
S75 &= (68) - (70) \\
S76 &= (73) - (78) \\
S77 &= (74) - (77) \\
S78 &= (75) - (76)
\end{aligned}
$$